UNIVERSITY OF ALBERTA

AN EXPERIMENTAL STUDY OF FLOW REGIMES IN POOL AND WEIR FISHWAYS

by

GREGORY J. SIKORA ©

A THESIS
SUBMITTED TO THE FACULTY OF GRADUATE STUDIES AND RESEARCH IN
PARTIAL FULFILLMENT OF THE REQUIREMENTS FOR THE DEGREE OF
MASTER OF SCIENCE

IN

WATER RESOURCES ENGINEERING

DEPARTMENT OF CIVIL ENGINEERING

EDMONTON, ALBERTA
FALL, 1997

National Library
of Canada

Acquisitions and
Bibliographic Services

395 Wellington Street
Ottawa ON K1A 0N4
Canada

Bibliothèque nationale
du Canada

Acquisitions et
services bibliographiques

395, rue Wellington
Ottawa ON K1A 0N4
Canada

Your file Votre référence

Our file Notre référence

The author has granted a non-exclusive licence allowing the National Library of Canada to reproduce, loan, distribute or sell copies of this thesis in microform, paper or electronic formats.

L'auteur a accordé une licence non exclusive permettant à la Bibliothèque nationale du Canada de reproduire, prêter, distribuer ou vendre des copies de cette thèse sous la forme de microfiche/film, de reproduction sur papier ou sur format électronique.

The author retains ownership of the copyright in this thesis. Neither the thesis nor substantial extracts from it may be printed or otherwise reproduced without the author's permission.

L'auteur conserve la propriété du droit d'auteur qui protège cette thèse. Ni la thèse ni des extraits substantiels de celle-ci ne doivent être imprimés ou autrement reproduits sans son autorisation.

0-612-22673-5

Canada

UNIVERSITY OF ALBERTA

RELEASE FORM

NAME OF AUTHOR: **Gregory J. Sikora**

TITLE OF THESIS: **An Experimental Study of Flow Regimes in Pool and Weir Fishways**

DEGREE: **Master of Science**

YEAR THIS DEGREE GRANTED: **1997**

Permission is hereby granted to the University of Alberta to reproduce single copies of this thesis and to lend or sell such copies for private, scholarly, or scientific research purposes only.

The author reserves all other publication and other rights in association with the copyright in the thesis, and excepts as hereinbefore provided, neither the thesis nor any substantial portion thereof may be printed or otherwise reproduced in any material form whatever without the author's prior written permission.

. . . .
Gregory J. Sikora

303 7021 Gray Drive
Red Deer, Alberta
Canada, T4P 2B1

Date: August 1, 1997

UNIVERSITY OF ALBERTA

FACULTY OF GRADUATE STUDIES AND RESEARCH

The undersigned certify that they have read, and recommended to the Faculty of Graduate Studies and Research for acceptance, a thesis entitled **An Experimental Study of Flow Regimes in Pool and Weir Fishways** by **Gregory J. Sikora** in partial fulfillment of the requirements for the degree of **Master of Science in Water Resources Engineering**.

N Rajaratnam

Dr. N. Rajaratnam

Dr. J. Leonnard

Gan Thian Yew

Dr. T. Gan

DATE: August 1, 1997

TO MY WIFE NATHALIE,
FOR HER UNDERSTANDING,
CARE AND UNYIELDING SUPPORT
AS WELL AS
TO MY FAMILY AND FRIENDS
WHO HAVE PROVIDED ME WITH
ENDLESS ENCOURAGEMENT

ABSTRACT

The aim of this model study was to expand the understanding of the plunging, transitional and streaming regimes which occur for different pool and weir geometrical arrangements and discharges. By studying the behaviour of the flow patterns for each of these regimes and by observing how one flow regime transforms into another due to an increase in discharge, insight has been gained so that flow regime predictions can be made with an increased degree of confidence.

In order to understand these complex systems, water surface profiles, velocity measurements, photographs and stability observations were recorded for a total of 435 different pool and weir arrangements. By measuring the water surface profiles the head over the weir (*h*) for plunging flows, and depth (*d*) for streaming flows were recorded and used to confirm the dimensionless discharge relationships proposed by Rajaratnam, Katopodis and Mainali (1987b). The findings presented in this study have refined the ranges of values of these dimensionless parameters.

The velocity measurements conducted on a few selected flows have provided valuable information with regards to the dominant flow patterns, magnitude of the velocity profiles as well as the energy dissipating process within the pool and weir arrangement.

In addition, the recorded stability observations have revealed windows of longitudinal surges and transverse waves which make some pool and weir designs unsteady and unacceptable for fish transport.

ACKNOWLEDGMENTS

At this time the author takes great pleasure in acknowledging all the key people who have participated directly and indirectly in the completion of this project.

It is truly not only a great pleasure but a rare privilege to work under the guidance of Dr. N. Rajaratnam. Over the past three years, Dr. N. Rajaratnam has not only provided considerable insight into this study but his uncompromising dynamic character has inspired the author personally as well as academically.

The author would like to recognize Mr. C. Katopodis as a key contributor to the completion of this thesis. Mr. Katopodis who is a active administrator with the Department of Fisheries and Oceans, provided the financial relief for this project and this support is duly noted.

In the laboratory, Mr. S. Lovell not only constructed and maintained the model used in this study but his invaluable practical experience has made all experimental operations run effortlessly. Mr. S. Lovell's assistance is greatly appreciated.

The author would like to acknowledge the efforts of Dr. S. H. Wu who had assisted by providing computer software to expedite the experimental computations.

The author would also like to recognize all his fellow graduate students, who have assisted in numerous occasions.

If recognition to anyone has per chance been omitted, this oversight is deeply regretted and author alone will take responsibility for this shortcoming.

TABLE OF CONTENTS

page

1.0 INTRODUCTION AND LITERATURE REVIEW 1

1.1 Introduction 1

1.2 Literature Review 4
1.2.1 History of Fishways 5
1.2.2 Design Objectives for Upstream Fish Passage Facilities 6
1.2.3 Design Practices for New Fishways 11
1.2.4 Upstream Passage Facilities 11
1.2.5 Examples of Standard Fishway Designs 20
1.2.6 Geometry of Pool and Weir Fishways 22
1.2.7 Prediction of Flow Regimes in Pool and Weir Fishways 24
1.3 Objectives 28

2.0 EXPERIMENTAL INVESTIGATION 29

2.1 Apparatus 29

2.2 Experimental Nomenclature 30

2.3 Experimental Procedure 31
2.3.1 General 31
2.3.2 Water Surface Profiles 35
2.3.3 Photographs 39
2.3.4 Velocity Measurements 40

2.4 Experimental Errors and Uncertainties 43
2.4.1 General 43
2.4.2 Sources of Error and Estimates of Uncertainties 43
2.4.3 Computational Methods for Error Propagation 52
2.4.4 Computed Errors 56
2.4.4 Error Analysis Summary 61

2.5 Experimental Observations 62
2.5.1 General 62
2.5.2 Flow Regime Classification 63
2.5.2.1 General 63

TABLE OF CONTENTS (continued)

page

2.5.2.2 Plunging Flow Regime (P) 64
2.5.2.3 Plunging-Transitional Flow Regime (Pt) 67
2.5.2.4 Transitional Flow Regime (T) 68
2.5.2.5 Transitional-Streaming Flow Regime (tS) 69
2.5.2.6 Streaming Flow Regime (S) 71
2.5.2.7 Transitional-Baffle Flow Regime (tB) 73
2.5.2.8 Baffle Flow Regime (B) 74
2.5.2.9 Plunging Supercritical Bed Flow Regime (*P*) 76
2.5.2.10 Baffle Supercritical Bed Flow Regime (*B*) 76

2.5.3 Transformation of Flow Regimes with Increasing Discharge 77
2.5.4 Stability 82
2.5.5 Weir Height Effects on Flow Regimes 87
2.5.6 Energy Dissipation 89

3.0 ANALYSIS AND EXPERIMENTAL RESULTS 90

3.1 General 90

3.2 Flow Equations for Pool and Weir Fishways 91
3.2.1 General 91
3.2.2 Plunging Flow 91
3.2.3 Streaming Flow 92
3.2.4 Transitional Flow 99

3.3 Velocity Measurements 100
3.3.1 General 100
3.3.2 Plunging Flow 101
3.3.3 Transitional Streaming Flow 105

3.4 Summary of Results 108
3.4.1 General 108
3.4.2 Graphical Illustrations 109
3.4.3 Non Dimensional Domains 110

TABLE OF CONTENTS (continued)

page

4.0 CONCLUSION AND RECOMMENDATIONS 112

4.1 Conclusion 112

4.2 Recommendations 115

TABLES 116

FIGURES 139

PLATES 187

REFERENCES 201

APPENDICES

A Water Surface Profiles

A.1 Full Weir Height

A.1.1 'A' Class Weir Spacing - 5,10, 15, 20 & 30% Slope 204
A.1.2 'B' Class Weir Spacing - 5,10, 15, 20 & 30% Slope 220
A.1.3 'C' Class Weir Spacing - 5,10, 15, 20 & 30% Slope 236
A.1.4 'D' Class Weir Spacing - 5,10, 15, 20 & 30% Slope 252

A.2 Three Quarter Weir Height

A.2.1 'A' Class Weir Spacing - 5,10, 15, 20 & 30% Slope 268
A.2.2 'B' Class Weir Spacing - 5,10, 15, 20 & 30% Slope 279
A.2.3 'C' Class Weir Spacing - 5,10, 15, 20 & 30% Slope 290

A.3 Half Weir Height

A.3.1 'A' Class Weir Spacing - 5,10, 15, 20 & 30% Slope 301
A.3.2 'B' Class Weir Spacing - 5,10, 15, 20 & 30% Slope 312
A.3.3 'C' Class Weir Spacing - 5,10, 15, 20 & 30% Slope 323

TABLE OF CONTENTS (continued)

page

B Stability Observations

B.1 Full Weir Height

B.1.1 'A' Class Weir Spacing - 5,10, 15, 20 & 30% Slope 335

B.1.2 'B' Class Weir Spacing - 5,10, 15, 20 & 30% Slope 341

B.1.3 'C' Class Weir Spacing - 5,10, 15, 20 & 30% Slope 351

B.1.4 'D' Class Weir Spacing - 5,10, 15, 20 & 30% Slope 360

B.2 Half Weir Height

A.2.1 'A' Class Weir Spacing - 5,10, 15, 20 & 30% Slope 366

C Pool and Weir Experimental Database 376

LIST OF TABLES

Table	Title	Page
1	Weir Height and Weir Spacing Data	116
2	Experimental and Computational Data for Plunging Flow	117
3	Experimental and Computational Data for Streaming Flow	122
4	Experimental and Computational Data for Transitional Flow	127
5	Discrepancies in Continuity for Plunging Flows	134
6	Discrepancy in Continuity for a Transitional Streaming Flow	135
7	Tabular Summary of Full Weir Height Experimental Data	136
8	Tabular Summary of Three Quarter Weir Height Experimental Data	137
9	Tabular Summary of Half Weir Height Experimental Data	138

LIST OF FIGURES

Figure **Title** **Page**

1 Pool and Weir Fishways 139
2 Definition Sketches for Plunging and Streaming Flows 140
3 Definition Sketch of Experimental Apparatus 141
4 Definition Sketch of Point Gauge and Yarn Indicators 142
5 Definition Sketch of Pitch Probe and Manometer 143
6 Predominant Flow Regimes in Pool and Weir Fishways 144
7 WB05 Flow Patterns for Multiple Discharges 145
8 WB10 Flow Patterns for Multiple Discharges 146
9 WB15 Flow Patterns for Multiple Discharges 147
10 WB20 Flow Patterns for Multiple Discharges 148
11 WB30 Flow Patterns for Multiple Discharges 149
12 WA05 Flow Patterns for Multiple Discharges 150
13 WA10 Flow Patterns for Multiple Discharges 151
14 WA15 Flow Patterns for Multiple Discharges 152
15 WA20 Flow Patterns for Multiple Discharges 153
16 WA30 Flow Patterns for Multiple Discharges 154
17 Longitudinal Surge Progression 155
18 Plunging Flow Analysis - Q versus h 156
19 Plunging Flow Analysis - Q+ versus h/p 157
20 Streaming Flow Analysis - Q versus d, for All Streaming Flow 158
21 Streaming Flow Analysis - Q versus d, for 'B' Class Weirs 159
22 Streaming Flow Analysis - Q versus d, for 'C' Class Weirs 160
23 Streaming Flow Analysis - Q versus d, for 'D' Class Weirs 161
24 Streaming Flow Analysis - Q* versus L/d 162

LIST OF FIGURES (continued)

Figure Title Page

25 Streaming Flow Analysis - Cf versus P/d 163

26 Cf versus P/d, with Transitional Streaming Data 164

27 Cf versus P/d, with R.K.M-87' Data 165

28 Determination of Coefficient of Fluid Friction , C_f 166

29 Determination of Mannings 'n' for Streaming Flow 167

30 Graphical Illustration of Domains for
Dimensionless Transitional Discharge, Q_t 168

31 WA10-035 Velocity Profiles 169

32 WA10-035 Velocity Profiles, Maximum Velocity and Continuity . . 170

33 3/4WA10-035 Velocity Profiles 171

34 3/4WA10-035 Velocity Profiles, Maximum Velocity and Continuity . 172

35 1/2WA10-035 Velocity Profiles 173

36 1/2WA10-035 Velocity Profiles, Maximum Velocity and Continuity . 174

37 Comparison of Velocity Fields for Full, Three Quarter and
Half Weir Heights 175

38 Comparison of Water Surface Profiles and Maximum Velocity for Full,
Three Quarter and Half Weir Heights 176

39 WB10-065 Velocity Vectors and Profiles 177

40 WB10-065 Velocity Profiles, Maximum Velocity and Continuity . . 178

41 Water Surface Corrections for a Transitional Streaming flow . . . 179

42 Discharge versus Depth Averaged Velocity for Streaming Flows . . 180

43 Histogram Illustrating Domains of Steady and Unsteady Flow Regimes 181

44 Histogram Illustrating the Domains of All Steady Flow Regimes . . 182

45 Histogram Illustrating the Domains of Preferred Steady Flow Regimes 183

LIST OF FIGURES (continued)

Figure	Title	Page
46	Mapping of Flow Regimes with Dimensionless Parameters	184
47	Flow Regime Boundaries for Dimensionless Parameters	185
48	Verifying Dimensionless Parameters.	186

LIST OF PHOTOGRAPHIC PLATES

Plate	Description	Page
1	Plunging Flow, (P) - WA10-015	187
2	Plunging Flow, (P) - WB15-010	187
3	Plunging Flow, (P) - 3/4WB30-010	188
4	Plunging Transitional Flow, (Pt) - WB10-015	188
5	Transitional Flow, (T) - WB10-025	189
6	Transitional Baffle Flow, (tB) - WA15-065	189
7	Baffle Flow, (B) - WA10-105	190
8	Baffle Flow, (B) - WA15-105	190
9	Baffle Flow, (B) - WA30-065	191
10	Baffle Flow, (B) - 1/2WB30-045	191
11	Transitional Streaming Flow, (tS) - WB10-035	192
12	Transitional Streaming Flow, (tS) - 3/4WB10-035	192
13	Streaming Flow, (S) - WC05 -165	193
14	Streaming Flow, (S) - 1/2WC05-015	193
15	Plunging Flow with a Section of Supercritical Bed Flow, (*P*) - 1/2WA10-020	194
16	Baffle Flow with a Section of Supercritical Bed Flow, (*B*) - 1/2WA30-020	194
17	Velocity Measurements: Plunging Flow - WA10-035	195
18	Velocity Measurements: Plunging Flow - WA10-035	195
19	Velocity Measurements: Plunging Flow - 3/4WA10-035	196
20	Velocity Measurements: Plunging Flow - 1/2WA10-035	196
21	Velocity Measurements: Plunging Flow - 1/2WA10-035	197
22	Velocity Measurements: Transitional Streaming Flow - WB10-065	197

LIST OF PHOTOGRAPHIC PLATES (continued)

Plate	Description	Page
23	Transverse Wave - WD15-001	198
24	Longitudinal Surge - 1/2WB10-035	198
25	Longitudinal Surge, Onset - 1/2WB10-025	199
26	Longitudinal Surge, Main Body - 1/2WB10-025	199
27	Longitudinal Surge, Onset - 3/4WB10-020	200
28	Longitudinal Surge, Main Body - 3/4WB10-020	200

LIST OF SYMBOLS

d	Depth of streaming Flow
B	Baffle flow
b	Pool width
C_d	Discharge coefficient
C_f	Coefficient of fluid friction
F_o	Frounde number
g	Acceleration due to gravity
h	Maximum head over the weir
H	Head drop per pool - difference in elevation between two adjacent weir crests
L	Pool length
L/s	Liters per second
long.	Longitudinal surge
n	Mannings 'n'
p	Weir height
P	Plunging flow
Pt	Plunging transitional flow
q	Discharge per unit width
Q	Discharge
Q_m	Model discharge
Q_p	Prototype discharge
Q_+	Dimensionless discharge for plunging flow
Q_*	Dimensionless discharge for streaming flow
Q_t	Dimensionless discharge for transitional flow
R	Hydraulic radius
S	Streaming flow

LIST OF SYMBOLS (continued)

Stdy	Steady flow
S_o	Bed slope of fishway - Sine slope
T	Transitional
t	Weir thickness
tB	Transitional baffle
tS	Transitional streaming flow
trans.	Transverse wave
UnStdy	Unsteady flow
u	velocity component along the x-axis
U	Depth averaged velocity
v	velocity component along the y-axis
V	Magnitude of resultant vector
V_{max}	Maximum velocity
V_{min}	Minimum velocity
WSP	Water surface profile
x	Longitudinal axis
y	Vertical axis
z	Transverse axis
P	Plunging flow pattern which has a section of supercritical bed flow
B	Baffle flow pattern which has a section of supercritical bed flow
α	Weir angle with respect to fishway bed
γ	The weight per unit volume of the fluid
Δx	Elemental length along the x-axis
ρ	The mass density of the fluid
τ_o	Boundary Shear Stress

1.0 INTRODUCTION AND LITERATURE REVIEW

1.1 Introduction

The journey that migratory fish enter upon in order to complete their life cycle can become quite difficult, strenuous, and if successful, is without a doubt the result of unstoppable persistence and stamina. These fish that possess an instinctual migratory response must endure predators, physical obstacles and disease in order to reach their spawning beds. Although predators and disease can reduce the populations of these migratory fish, physical barriers or flow obstructions can potentially deny the vast majority of the spawning population from reaching their prescribed destinations.

There are three main classifications of obstructions which exist that impede the movement of migratory fish. Chutes, falls, debris jams, avalanches, and rock slides are just a few of many obstacles that can be classified as natural obstructions. Man made interferences such as dams, culverts, bridges, weirs and log jams are categorized into the artificial classification. Thirdly, water quality obstructions such as adverse temperatures, low dissolved oxygen levels and pollutants also inhibit the progress of upstream migrations (Clay, 1961). These water quality obstructions are indeed factors that deter fish migrations, however, the findings as a result of this study are more applicable to natural and artificial obstructions that actually result in a physical barrier or accelerated flow.

In today's society there is an ever growing need for freshwater supply and one of the most economical means of attaining and storing large volumes of water is through river obstructions such as dams or weirs. Water is essential for agricultural irrigation, powering hydroelectric generators and for basic human consumption. These man made obstructions do indeed provide a much needed water supply; however, they subsequently produce an artificial barrier which obstructs the natural paths of these migratory fish. Likewise, natural barriers share this common thread for they ultimately produce adverse conditions not favorable to fish transport. For example, the Fraser River rock slide at Hell's Gate in 1914 changed the channel configuration sufficiently to produce a physical barrier that restricted the sockeye salmon migrations (Clay, 1961).

These obstructions, both natural and artificial, have the potential to jeopardize the continued success of freshwater and saltwater fish stocks. It is not only our moral obligation to ensure that the fish ecosystems are preserved, but in Canada the Federal Fisheries Act mandates that all artificial obstructions in free flowing waters must provide suitable passage for migratory fish (Collins and Gillis, 1985).

This issue of upstream fish passage is not a new concern, for fish passage structures more commonly known as fishways, fish passes, fish lifts and fish ladders have been deployed to ensure that there is a hydraulic link for fish to proceed upstream (Clay, 1961). Although over the years there have been many different types of fishways constructed to restore damaged pathways, this study will focus on the pool and weir fishway and the flow patterns, flow regimes and stabilities which occur for different geometrical configurations. The following section in this report addresses the different types of fishways which have been utilized and will discuss their designs, advantages and limitations.

The problem of fish transport is multifaceted and quite complex. In order to design a stable hydraulic structure which is flexible and possesses a wide range of a favorable flow regimes is one thing, but to build this structure to meet the demands of the migratory fish is quite another. The goal of achieving a suitable upstream fish transport design can actually be divided into two subsections: the hydraulics of the fishway and the biological constraints of the fish which truly dictate the overall design. It is essential to understand the users of the system, for it is only by being aware of the behavioural preferences, physiological limitations and biological parameters of the fish can a suitable structure be constructed (Clay, 1961; Collins and Gillis, 1985; Powers and Orsborn, 1986 and Katopodis, 1981).

The fish behaviour concerns in question encompass variables such as migrational motivation, individual or schooling preference and flow preferences. These parameters are also influenced by external effects such as water temperature, light, pollution and confinement which ultimately may lead to stress. Physiological parameters are very much dependent on the species intended to pass. Swimming ability is related to velocity and is subdivided into categories defined as sustained, prolonged and burst speeds. Rate of fatigue, orientation to flow (rheotaxis) and jumping capabilities are just a few other physiological parameters which need to be addressed (Clay, 1961, Collins and Gillis, 1985, Powers and Orsborn, 1986 and Katopodis, 1981). For example, salmonoids typically are proficient in the ability of jumping clear out of the water and landing upstream of an elevated obstruction. This behaviour is well suited for navigating small obstructions or strategically moving from hold to hold to pass larger barriers. This jumping action which salmonoids are so capable of is the fundamental concept behind pool and weir fishways; however, other migratory species such as shad or sturgeon rarely leave the free surface. Therefore, appropriate designs must be made to meet their individual requirements (Collins and Gillis, 1985). Collins and Gillis (1985) expressed that the engineering of the Cabot Station fishway at Turner Falls on the Conneticut river in Massachusetts was excellent, however, the design was not appropriate for the fish species to be passed. It was believed that non-satisfactory success was partially related to the inadequacies in biological information base. Many studies have focused on the biological, physical and behavioural constraints of fish and these intangible parameters were found not to be the same for all aquatic species. Clay (1961), Collins and Gillis (1985), Powers and Orsborn (1986) and Katopodis (1981) focus more closely on the biological parameters and provide essential design criteria for specific fresh and salt water species.

Assuming that all biological requirements are known, the understanding of the hydraulics of fishways and the ability to predict the flow patterns becomes the next logical step in determining an appropriate design. To gain this knowledge of the flow dynamics in pool and weir fishways, field measurements at prototype facilities can be achieved; however, this process can prove to be difficult, expensive and only applicable for a narrow range of design arrangements. To study a wider range of designs, scaled model studies are an effective means of obtaining valuable information that is required to satisfy the hydraulic demand for better fishways.

The aim of this model study is to provide design information so that flexible and cost effective pool and weir fishways can be constructed to meet the demands of the species intended to pass. This model study collected experimental observations, recording water surface profiles, photographs and velocity measurements for as many as 435 different pool and weir arrangements. Through these means it was possible to classify the different flow regimes which shared common characteristics. This study also observed the flow mechanics for these regimes and noted how the flow patterns changed while transforming from one regime to another for increasing discharges. Furthermore, stability observations were conducted and ranges where various instabilities occurred were outlined. This study also confirmed and expanded the domains of the dimensionless parameters set forth by Rajaratnam, et al (1987b). These dimensionless parameters can be used as guidelines to predict expected flow regimes for a particular pool and weir arrangement.

The advances which are the result of this study will ultimately provide valuable tools which can assist in the design of new pool and weir fishways. Even though the concept of fishways is based on the idea of transporting more fish, the insight gained from this study can also be applied to the opposite end of the spectrum, thus, designing a fishway that only permits the advancement of a select group of fish. This protective device concept may possibly prevent the infiltration of foreign aquatic species while selectively permitting native fish to proceed (Collins and Gillis, 1985). The Lamprey in the Great lakes which are reducing the commercial and sport fishing populations is an excellent example where these resources may possibly be applied.

1.2 Literature Review

In the following subsections, the history of fishways will be reviewed and this shall in turn set the stage for the advancements of upstream fish passage facilities. In addition, the design requirements, the design practice as well as the standard examples of pool and weir fishways which are in use today will be outlined. The final subsection reviews previously derived analytical and empirical equations which provide quantitative values and ranges for flow regimes which occur in pool and weir fishways.

1.2.1 History of Fishways

The use of hydraulic structures commonly known as fish passes, fish ladders or simply fishways to assist migratory fish are not new concepts since some facilities have been recorded in Europe during the 17 th century (Clay, 1961). Nemenyi, a hydraulic engineer discovered legal literature written in 1662 for a province in France requiring mandatory construction of fish passes (Collins and Gillis, 1985). These fishways were designed to be simple open channels lined with bundles of tree branches and placed in the centre of the stream. These bundles of branches would provide resistance, reduce the stream velocity in that section and ultimately produce flow conditions suitable for fish transport. This legal requirement may not have been the precedence of laws now instated, but today in Canada, the Federal Fisheries Act mandates that all artificial obstructions in free flowing waters must provide suitable and successful passageways for migratory fish (Collins and Gillis, 1985). Over the past three hundred years this idea of a hydraulic structure which dissipates energy and provides suitable flow conditions conducive to upstream fish transport has grown but the understanding of fundamental fluid mechanics of these structures is still limited.

1.2.2 Design Objectives for Upstream Fish Passage Facilities

Regardless of what hydraulic system is deployed, the goal of transporting migratory fish upstream past natural or artificial obstructions still remains the same. Of course this process has a multitude of parameters which are site specific, depending on the geography as well as the species intended to pass. Even though the process of selection may be difficult and indecisive questions may arise, the facility must be able to complete the intended goals or otherwise it may just hinder the progress of the upstream migrants. A report published by the Institution of Civil Engineers in 1942 best describes the three essentials for a fish pass: *The fish should be able to swim through it without undue effort, they should do so without risk of injury and the pass should be quickly and easily found* (Orsborn, 1986).

In order to design any suitable fishway system for one or a more species, it is essential to define all the design parameters and goals which must be met and still remain relatively cost effective. These criteria often stem from biological data and it is important to accurately determine the ranges of the physiological and behavioural parameters, for the efficiency and success of the structure depends on it. Although most of these criteria are intangible, burst velocity and maximum leaping ability are two concrete physiological parameters which engineers can readily apply to their designs. The velocity at which a fish travels can be subdivide into three main categories. These three subsets which have been classified as sustained, prolonged and burst are different for all species, for each category is defined by the time required for a fish to experience fatigue. Sustained swimming speed does not induce fatigue, prolonged swimming speed will cause fatigue anywhere from 15 sec to 200 minutes and burst velocity which is capable of transporting the fish away from predators or used for leaping shall cause fatigue in less then 15 second. It is this burst velocity which shall define the upper limit of the fishes physical capabilities. For example, the burst velocity of the Chinook salmon (6.83 m/s [22.4 ft/s]) is fairly quick where the Pink salmon is substantially slower (3.44 m/s [11.3 ft/s]). Trout, which are typically a smaller, remarkably exhibit comparable capabilities for Steelhead and Brown trout have burst speeds of 8.08 m/s (26.5 ft/s) and 3.87 m/s (12.7 ft/s) respectively (Orsborn, 1986).

Once the burst and prolonged velocities have been determined, a suitable fishway such as one of the pool and weir designs must not have velocity fields in the plunging jet greater than the fishes' burst velocity and the velocities in the pool must be maintained low enough in order to allow for resting and reorientation. These resting areas should have velocity fields which range from 0.15 to 0.6 m/s (0.5 to 2.0 ft/s) and 0.15 to 0.3 m/s (0.5 to 1.0 ft/s) for salmon and freshwater species respectively (Katopodis, 1981). This parameter of maximum velocity can be difficult to achieve for some fishway designs, such as the pool and weir fishways, the only possible means of maintaining suitable velocity field is through the use of flow regulating devices.

Since natural obstructions such as water falls, rock slides and debris jams have no discharge regulating devices and because there is no significant storage capability present, continuity is essentially maintained upstream and downstream. Seasonal discharge peaks from snow pack runoff and summer rain storms will cause fluctuations in the water levels through the system; thus, a suitable fishway for natural obstructions must be capable of handling a wide range of flows while still keeping the system velocities within the design requirements. Artificial obstructions such as weirs and dams can deploy mechanical devices that can control the discharge passing through the system as well as the water levels upstream and downstream; therefore, a larger spectrum of fishway designs can be utilized to meet the aquatic demand.

Although it is possible to design fishways which are operating at a maximum allowable velocity, the facility can be more effective if lower velocity fields, which will provide passage for younger and smaller migrating fish, are implemented. This flexibility inherent in a large velocity gradient will pass not only the strong fish but a broad cross section of the fish population. It is this diversity that will ensure the structure will not invoke any form of natural selection but enable smaller, weaker juveniles to proceed upstream. Collins and Gillis, (1985) suggest the juvenile salmon should endure maximum velocities in the order of 0.7 m/s where as the adults can proceed in velocities as great as 2.4 m/s (7.9 ft/s). This allowance for juveniles is a special consideration; however, Atlantic salmon which are anadromous do endure the annual migrations for more that one year unlike the Pacific salmon. Applying this criteria to pool and weir fishways, and by using the maximum velocity of 2.4 m/s in the energy equation or simply converting kinetic energy to potential energy, a maximum head between adjacent weirs can obtained. Completing this computation results in a maximum head of 300 mm (1 ft) for a maximum velocity of 2.4 m/s. For pool and weir fishways, a head drop of 300 mm is most common for if the drop is designed to be less, this will require a substantial increase in the overall length of the facility. Since freshwater species generally require slower velocities, Katopodis (1981) advises that the maximum head drop between adjacent weirs should be limited to 150 mm (6 in).

The second concrete parameter which can be applied and is a derivative of swimming velocity is the maximum leaping capability. This physiological parameter must be studied for each species and likewise applied accordingly. Powers and Orsborn (1986b) compiled jumping data for Steelhead, Chinook and pink salmon and developed empirical leaping curves. These trajectory curves which are simply based on initial velocity have been plotted to illustrate the maximum leaping height and distance for associated leaping angles for each specific species. With this information it is possible to utilize the fishes capabilities and in turn reduce capital expenditures by increasing the overall slope of the physical structure. This maximum jumping capability parameter can assist the design, but for fish which do not typically break free from the surface, chutes or orifices can be implemented to the design to provide suitable passage.

This now leads into the critical estimation of population, timing and required volume of stored water in order to accurately determine the size of the facility. If the migration is spread out over a long time interval, a smaller facility would be required; however, if the migration is rapid and within a narrow time span, the facility must be large enough to handle the demand. This is where it is crucial to design the facility properly, for a generic design with no fine tuning may impose delays and consequently will be undersized. Once an estimated maximum demand is established (i.e., number of fish approaching the structure per hour or minute) and assuming a required volume per fish and maximum residence time which is required for resting, the size of the structure can be determined.

Clay (1961) observed that the Sockeye salmon which utilizes the vertical slot fishway on the Fraser river at Hell's Gate requires at least 0.057 m^3 (2 ft^3) per fish. Concluding from the observations, Clay (1961) suggested that a design volume of 0.113 m^3 (4 ft^3) per individual fish would be conservative and suitable for all fishways that intend to pass fish which are approximately the same size as a seven pound sockeye salmon. This approximation can be converted to volume per mass and setting 0.11 m^3/fish based on a 9 kilogram fish, the estimate is approximately 0.012 m^3/kg of fish (Collins and Gillis, 1985).

Although the design process may indeed be difficult and large assumptions may be required with respect to biological parameters, suitable structures can and are constructed to efficiently assist in fish passage past physical obstructions. A pool and weir design conducted by the Collins and Gillis (1985) is an excellent example of an efficient design. This study was set forth to attempt to measure the maximum height a 0.5 m (20 inch) sockeye salmon could achieve under what was believed to be preferred conditions. The pool and weir fishway consisted of 15 pools with a bed slope of one to eight. When the fish reached the top of the prototype it entered a seven meter deep lock that would transport the fish back to the initial pool in the system. Over the following five days, day and night, the 1.47 kg (3 pound 4 ounce) sockeye salmon successfully ascended the fishway 415 times to achieve an accumulative elevation of 2026.3 m (6,648 ft) in 7, 947 minutes. The ascent which was greater than 2 km (1 mile) required the fish to swim horizontally for a distance greater than 16 km (10 miles). The average residence time was approximately 1.2 minutes per pool. Remarkably the fish was still ascending when the test was discontinued (Collins and Gillis, 1985).

New designs as submitted by Aaserude and Orsborn (1986) suggest that certain flow conditions can be used to entice fish to ascend up a pool and weir fishway. They observed that when fish that typically leap to pass obstructions, they initiate their airborne attempt from a specific location downstream of the plunging flow. Studying this principle more closely, it was assumed that the chum and coho salmon used in the study preferred to leap from a standing wave immediately downstream of the plunging jet. In fact the leap heights increased when the fish leaped from this location. It was believed that the air entrainment from the upstream plunging flow which boils to the surface at the standing wave provides the fish an additional forward velocity by the means of buoyancy. This concept has been experimentally incorporated into new designs which are believed to stimulate the fish to leap (Aaserude and Orsborn, 1986). By introducing a small sill downstream of the weir it was possible to redirect a portion of the flow to the surface in the experimental arrangement. This enhancement device which produced a well defined standing wave is a refinement to the problem of fish transport; however, it should be noted that this device, though seems suitable, may only be applicable for a narrow range of discharges.

The angle of the weir with respect to the bed also is another variable which has shown to produce adverse and favorable effects. For fish which do not orient themselves effectively to achieve a maximum height, or for fish which inherently exhibit flat trajectories, it is possible to slope the weir upstream aggressively into the flow. This weir sloping effect as studied by Orsborn (1986) may facilitate easier access for some fish species. This modification like others are mentioned to illustrate the many variables which can be modified to produce different effects and do not fall within the scope of this study.

By selectively fine tuning all the relevant parameters it is possible to produce a better fish passage facility. It should be noted that a highly refined fishway is not necessarily better, for it is possible to over design and essentially restrict the passing fish to a smaller select population. Efficient fishway facilities are ones which exhibit suitable flow patterns and a wide flexible range which will pass a diverse population. Although it is the goal of the designer to pass all the fish which approach the fishway, that range of flexibility is not always attainable and it is not practical or feasible to construct multiple structures to handle this task. Since fishways often do not perform as expected and because the flow patterns within the structure may not be suitable for all the fish, a fishway which can effectively advance 80% of the fish which intend to pass is considered successful (Collins and Gillis, 1985).

1.2.3 Design Practices for New Fishways

In order to design a new fishway facility it is critical to consider all the biological, physiological and behavioural parameters which control this problem. In fact it is not the considerations per se that is important but the accurate estimates of these parameters which is significant, for any mistakes can result in adverse effects on the rate of ascent. Since it is often difficult to estimate these parameters and there is limited diversity in designs, designers are cautious and possibly reluctant to deviate drastically away from known facilities which do work. "Design criteria have evolved slowly, frequently through trial and error, rather than through sophisticated hydraulic modeling" (Collins and Gillis, 1985). In most instances to prevent a complete failure by proposing new conceptual designs, new fishways are based on old effective designs and modified slightly to what the designer believes may enhance the performance of the facility (Collins and Gillis, 1985). As a consequence, fishways are typically restricted to a few proven designs. T.P. Vande Sande summarizes this process best by stating that " Fish passage is still somewhat of an art, not like cookbook engineering even though the principles are quite simple and old" (Collins and Gillis, 1985).

1.2.4 Upstream Fish Passage Facilities

With this idea or overtone of copy and modify a previous design, there are three major transport schemes that are in use today. Facilities known as fish locks which behave similarly to navigational locks are one of these methods of transport. Physical collection schemes such as capture and transport is the second possible mode and fish ladders or, more commonly, fishways constitute the third. The order presented here does not necessarily depict the logical order in which a suitable facility would be chosen; however, this sequence will allow for a quick review of the first two and a more detailed description of the last.

Fish locks which have been attempted in the U.S.S.R (Commonwealth of Independent States) have been used successfully for the transport of sturgeon whereas fishway designs for sturgeon have resulted in little success (Collins and Gillis, 1985). Fish locks are normally used at large hydro facilities where there is a great difference in the upstream and downstream water levels and the economic feasibility of fishways does not exist. A few drawbacks to the fish lock design is that large volumes of water must be flushed down in order to re-initiate the passage sequence. Secondly, fish inherently swim against the current and as a consequence resist the pour out action and remain in the cargo bay while the unloading cycle occurs. Subsequently, a portion of the transported population remain in the vertical shaft and are returned back down to their initial starting point for another attempt. This repeating process along with the confinement of the system can induce trauma from shock as well as injury. Generally, lifts are not cost effective (Collins and Gillis, 1985).

The second means of providing upstream transport can be achieved by physically capturing and removing the fish from downstream of the obstruction and lifting or trucking them upstream. This mode of transport is usually not a first run choice for any physical handling of fish will inevitably result in increased fatalities due to confinement stress and physical injuries. In addition, this method does not allow for a continuous migration to occur for time is required in loading and unloading as well as the limited number of transport vehicles.

The third possible alternative of providing upstream transport for migratory fish at physical obstruction is through the use of hydraulic structures commonly classified as fishways. There are many different types of fishways in use around the world today; however, most designs that are used at both natural and artificial obstructions can be classified or derived from three standard designs. This of course excludes devices deployed for site specific conditions such as culverts. Pool and weir fishways, which is the scope of this study are the first type, vertical slot and Denil constitute the second and third respectively. In addition to these three designs, the steep pass fishway can be considered a fourth; but, since this design is quite similar to the Denil fishway, and the purpose of this section is to provide a brief introduction to different types of fishways, it shall be grouped with the Denil design. Each one of these concepts can and do pass fish upstream; however, advantages and disadvantages do exist for each design and the selection of an appropriate facility is dependent on the type of obstruction and the species intended to pass.

A pool and weir fishway as seen in Figure 1(a) is simply the construction of regular spaced weirs in a channel of flume that distributes the total head drop over the length of the facility. It is this incremental decrease in head that produces pools in-between the weirs; thus, the name of this design, pool and weir fishway simply describes a dominant flow pattern. This design permits fish to proceed upstream by leaping from one downstream pool over a weir and into the upstream pool. Upstream advancements are carried out repetitively until the fish passes completely through the structure or otherwise the fish can temporarily stop and rest in one of the many pools before proceeding upstream. From the available literature it is believed that the fish will rest or re-orientate themselves in the circulating pools prior to jumping or swimming over the next weir. The time delay which varies for each design is defined as residence time and must be considered when determining the size of the facility. A distinct advantage of pool and weir fishways is that they can operate under a wide array of flow patterns (Collins and Gillis, 1985). Plunging and streaming or shooting flow patterns as described by Clay (1961) and Rajaratnam, et al. (1987a) are the two predominant flow patterns which exist in a pool and weir fishway. These patterns are typically at either end of the flow regime spectrum, for plunging flow occurs in most arrangements at low discharges whereas streaming flow will result for larger flows. These plunging and streaming flow regimes are graphically illustrated in

Figures 2(a) and 2(b). Additionally, the transitional range which resides between these two defining regimes can be modifications of either plunging or streaming flow or a combination of the two. Even though it is evident that these ranges exist, it is not as of yet possible to precisely predict the exact flow condition which will result for each physical arrangement. It is this uncertainty of flow prediction for a specific design and discharge that defines the weakness of pool and weir fishways. This inability to accurately define passable discharges for any pool and weir structure can seriously restrict the fish migrations at non regulated natural obstructions. Typically, pool and weir fishways are not constructed at natural obstructions for there is no reliable way to control the discharge entering the facility; thus, there is no means of controlling the flow regime in the fishway and instabilities such as longitudinal surges may result (Clay, 1961).

At artificial obstructions such as irrigation or hydroelectric dams, where the flow may vary drastically because of headwater fluctuations, regulating devices must be incorporated into the facility. Telescoping or angling weirs and the use of orifices are three such devices which can be used to control the flow through the structure (Clay, 1961). Since the flow through a fishway is controlled by the upstream weir, orifices which are less sensitive to fluctuations in the headwater are often incorporated into standard pool and weir designs (Clay, 1961). Hydraulically, the discharge passing through an orifice is proportional to the head raised to the power of one half, whereas the discharge passing over a weir is proportional to the head raised to the three halves (Clay, 1961). This regulating modification is usually done by introducing an orifice along with a horizontal bed for the first few upstream weirs and then returning back to a standard weir type flow for the remainder of the fishway (Clay, 1961). Figures 1(a) and 1(b) illustrate the standard pool and weir design as well as a weir and orifice design.

The pool and weir design alone is indeed an effective facility for passing fish that are capable of leaping over the weirs but for fish species which do not behave in this manner, orifice or chute like alterations as seen in Figures 1(b) and 1(c) have been devised. Even though the pool and orifice design does exhibit certain flow advantages, its implementation should also be suitable for the species intended to pass. Collins and Gillis (1985) expressed that alewives do not exhibit jumping behaviour, however, they do have a strong schooling behaviour. This schooling preference poses a problem with the orifice design for these fish find security in numbers and the single file motion which would be required to pass these fish through the orifices would not be suitable (Collins and Gillis, 1985). Solutions to this particular problem may be achieved by reducing the head drop over each successive weir, increasing the discharge so that streaming flow occurs or by providing horizontal slots or chutes thus enabling the alewives to pass. "When considering a pool and weir fishway design, various configurations including the 'chute type' with broad crested weirs and those incorporating orifices like the Ice Harbor design should be considered in addition to the overflow weir design, because significant differences in flow patterns are associated with these configurations (Collins and Gillis, 1985)."

The idea of selecting an appropriate design for the species intended to pass is essentially the aim of all fishways and since pool and weir fishways have such a broad range of flow patterns, tailor made facilities can be constructed if accurate flow predictions can be achieved. An advantage of the pool and weir fishway is that since the design is flexible, it is possible to vary the discharge in the facility thus providing suitable flow conditions for a specific species. Researchers at the Bonneville laboratory discovered that Pacific Salmon and Steelhead prefer high velocity flow compared to low velocity flows (Collins and Gillis, 1985). Since the salmon run only occurs for a particular window of time, the discharge in the facility can be increased to meet this demand. After sufficient time and assuming that the salmonoids have completed their ascent, the discharge can be reduced to allow smaller fish species such as trout to pass or simply turned off allowing for increased storage for hydroelectric power. Pool and weir fishways are excellent energy dissipaters, especially at slopes greater than 15%, and require little to no maintenance; however, since the range of bed slopes normally vary from 1 in 10 to 1 in 16, which is the shallowest of all fishway designs, the facility must be longer in total length.

The second standard fishway design, which is in some ways similar to the pool and weir fishway, is the vertical slot fishway. This fishway shares the same succession of pools as seen in the pool and weir fishway; but instead of the flow passing over the weirs, the flow descends downstream through a single vertical slot in the weir. Clay (1961) and Katopodis (1981) have excellent figures which demonstrate the design and flow patterns for this type of facility. An interesting facet of this design is that the flow proceeding through the vertical slot is assumed to produce a fairly uniform longitudinal velocity profile (Clay, 1961). This uniformity allows the fish to ascend through the vertical slot at any depth. Recent experimental measurements and observations conducted by Dr. S. Wu at the University of Alberta, T. Blench Hydraulics Laboratory suggest that this generalization does not necessarily occur and the longitudinal slot velocities which are highly three-dimensional typically increase with the depth. Some other advantages of this vertical slot fishway design is that it will operate at steeper slopes (1 in 8 to 1 in 10), it is a relatively maintenance free energy dissipater and, since the design incorporates pools, there are resting areas for the fish to regain their strength before advancing into the next upstream pool. Additionally, the flow structure in the vertical slot fishway, unlike the pool and weir fishway, is mainly the result of the physical design and not entirely dependent on the discharge. Since the flow patterns in the facility are less sensitive to the discharge, this structure will accommodate wide fluctuations of headwater and tailwater depths (Clay, 1961). It is this ability to operate favorably for multiple flows without manual regulating devices that makes this design suitable for installations at natural obstructions.

Even though the vertical slot fishway does exhibit some strong advantages over the pool and weir concept, there are also disadvantages inherent to this design. The first disadvantage of this design is that larger minimum volumes of water are required to produce suitable flow conditions compared to the pool and weir design. These larger volumes of water are required to provide sufficient depth for the fish to proceed upstream as well as to accommodate adequate cover to satisfy behavioural parameters. This requirement of larger flows translates directly into lost water, or more specifically lost revenue, especially at hydroelectric dams. Secondly, the narrower range of flow pattern flexibility may be an advantage for non-regulated natural obstructions, however, the only possible method of changing an undesirable flow pattern is by physically altering the geometric arrangement. Unlike the pool and weir fishway where the discharge can be altered, physical alteration are costly and require a shut down time to perform these changes. Another drawback to this design is that since the velocity profile in the vertical slot is believed to be uniform (Clay, 1961) or slightly increasing with depth (Wu, pers. comm. 1996), the velocity gradient is not large enough to pass smaller, weaker fish and consequently only the standard design fish or stronger can pass. Moreover, Collins and Gillis (1985) expressed that fish which enter the vertical slot fishway are subjected to a higher risk of injury than in the pool and weir fishway (Collins and Gillis, 1985). This risk may in part be the result of the physical restriction in which the fish must pass and the velocity of the vertical jet.

The third standard fishway design classified as a Denil fishway is an effective energy dissipater but this design does not incorporate resting pool as seen in the pool and weir or the vertical slot fishways. The Denil fishway is constructed from a series of thin baffles which line the sides as well as the bottom of the deep channel shaped fishway. These baffles which are orientated at an angle to the flow produce circulating cells and an energy dissipating turbulent shear layer which reduces the velocity of flow passing through the system. The steep pass fishway is fundamentally similar and behaves comparably to the Denil fishway with the exception that, the steep pass fishway is somewhat more complex in design. For the purpose of this paper the Denil will only be addressed since the issues being focused on apply for both of these designs. Clay (1961) and Katopodis (1981) have excellent figures which illustrate the design and flow patterns for these two structures. An advantage of the Denil design is that it is hydraulically capable of being constructed at much steeper slopes than the two previously discussed facilities (Collins and Gillis, 1985). Typically this fishway can operate at a 1 to 4 slope, hence, the overall length of the facility will be shorter and not as costly. In addition, the Denil fishway design is appealing for a wide range of discharges can pass through this system as well as operate effectively for several headwater and tailwater conditions without appreciable change in flow patterns in the structure. This ability to pass unregulated flows and remain stable makes this design highly favorable for natural obstructions (Clay, 1961). Furthermore, the longitudinal velocity profile in the Denil fishway is unlike the vertical slot fishway for the smallest and largest velocity components are near the bottom and top respectively. This velocity gradient which varies indirectly with depth is particularly beneficial for it has been observed that not only can large migratory fish pass through this facility, but, also small 50 mm (2 in.) perch can execute an upstream ascent by swimming near the bottom of the structure (Clay, 1961).

Although the Denil design does exhibit several strong characteristics, it, just like the pool and weir and the vertical slot fishways, has drawbacks and weaknesses. One of the disadvantages of this design is that it is constructed of thin baffles and maintenance expenditures can be very costly especially in locations where high sediment load and natural debris may clog or totally obstruct the inflow. Further maintenance problems may arise when this design is subject to harsh winter conditions where ice formations can potentially damage the thin baffle lining. One biological problem with this design is that since the flow is highly turbulent and there are many thin baffles lining the bed and walls, physical contact with the fish can cause abrasive injuries and stress if incorrect fish size estimates are made. The Denil fishway design is exceptional for handling large fluctuations in inflow. However, the operational flexibility or the range of different flow patterns is quite small (Clay, 1961). This restriction may become a problem if the flow is not suitable for the fish intended to pass, and subsequently retrofitting or physical modifications would have to be undertaken to achieve suitable passage conditions. Furthermore, this design does not incorporate resting areas, and the maximum length of any run is controlled by the fishes' burst velocity. The fish must be able to successfully pass upstream through the facility without experiencing fatigue. In cases where the elevation change of the obstruction is greater than one passable section, the facility must segment the overall length and incorporate resting pools into the design. These resting pools may indeed increase the overall expenditure of the design, but savings can be made by traversing or stacking the fishway to reduce the required construction area or by building around permanent physical barriers.

The previous listed weaknesses of the Denil fishway can be reduced if careful estimates of controlling parameters can be made. However, one drawback of this design that can not be understated is that large volumes of water are required to set up suitable flow conditions for fish to proceed upstream. Of all three designs, the Denil fishway requires the largest volume of water to operate (Clay, 1961). Because of this large requirement, this design is not suitable for locations where water storage is essential.

After examining these three different fishway concepts, it is obvious that each facility is best suited for particular applications and provided that all geographic and biological parameters are properly addressed, an appropriate design can be selected. Typically, for natural obstructions vertical slot or Denil fishways are chosen as fishway designs because of their capability of passing unregulated flows. Bear in mind that these designs have smaller ranges of operational flexibility, thus, precise physical designs are essential. On the other end of the scale, the pool and weir fishway is an excellent facility for artificial obstructions for it has a wide range of operational flexibility, but requires manual regulating devices to control the flow through the structure.

1.2.5 Examples of Standard Fishway Designs

Reflecting back on all the biological and hydraulic parameters and the complexity of defining suitable ranges, as well as selecting a standard design, it is very clear that the problem, or actually the solution, of providing upstream fish transport facilities is multifaceted. It is this degree of uncertainty which forces engineers to resort to proven standard designs as key guidelines when a new facility is required. Even though this design process has developed mainly from trial and error and limited hydraulic modeling, there are a few cornerstone designs that have been constructed in the last century which efficiently pass migratory fish upstream. The paired vertical slot fishway on the Fraser River at Hell's Gate that passes Sockeye Salmon and trout is one of these established designs. In addition, the fishway constructed in 1937-8 at the Ice Harbor Dam on the Snake River which is still accepted as a standard design, deploys a pool and orifice design in the headwater section and pool and weir for the remainder of the facility (Clay, 1961). There are other such facilities similar to Ice Harbor and Hell's Gate fishways, but their numbers are few.

Although it may first appear that a solution to upstream fish passage might be difficult to achieve, many fishways (pool and weir, vertical slot, Denil and steep pass) have been constructed across Canada and around the world with reasonable success. Here in Canada or more widely, North America, the vertical slot as well as the pool and weir fishway have become the preferred designs (Clay, 1961; Collins and Gillis, 1985). Generally the Denil or steep pass fishways have not been all that favorable for the regular maintenance expenditures that are needed to keep this facility operational has deterred their implementation. However, in Alaska the maintenance expenditures associated with Denil fishways must be overshadowed by the designs success for, since the 1950's, at last count 43 Denil fishways have be constructed. The Denil design is the most popular in Alaska, for the physical barriers which exist are mostly natural (Collins and Gillis, 1985).

In Canada, by far the majority of the fishways have been constructed in British Columbia or the Maritime provinces which consist of New Brunswick, Nova Scotia and Prince Edward Island. These sea front provinces understandably have the most to gain by ensuring that migratory fish complete their journeys to their head waters far inland and replenish the harvestable fish stocks. Throughout British Columbia from 1945 to 1960, a total of 60 fishways were constructed at natural barriers. Of these 60, 39 were vertical slot fishways and were modeled after the vertical slot fishway on the Fraser River at Hell's gate. Understandably, the vertical slot fishway has gained popularity in British Columbia from purely a geographical point of view (Collins and Gillis, 1985). Surprisingly, the vertical slot fishway at Seton Creek is the only fishway passage facility that was constructed at a hydroelectric development.

On the eastern shoreline of Canada, the Maritime provinces have 222 facilities and the pool and weir design is by far the favored arrangement. Of these 222 facilities, 170 are pool and weir designs, 40 are vertical slot and the remaining 12 are of the Denil design. Interestingly, a large number of these facilities that are constructed throughout the Maritimes are constructed at hydroelectric developments. This would substantiate the large number of pool and weir fishways for they are typically constructed at locations where flow regulation can be achieved (Collins and Gillis, 1985)

As for the remainder of Canada, the Prairie provinces, Ontario and Newfoundland have many upstream fish passage facilities that are mainly of the vertical slot and pool and weir design. The Denil fishway design has also been constructed but not near as many as in comparison to the other two. On average each of these provinces with the exception of Saskatchewan, has in the order of 20 facilities constructed at natural and artificial obstructions. Saskatchewan, being a province with mild geographical gradients has constructed only three upstream fishway facilities.

The preceding section has provided an insight into what facilities are constructed across Canada, as well as the distribution of each particular design. It should be noted that the values presented in this prior section were extracted from the Canadian Electrical Association Research and Development study by Collins and Gillis which was produced in 1985. There may indeed be discrepancies with actual figures to date, however, the intended purpose was to provide general estimates of what type as well as where are the majority of facilities being constructed.

1.2.6 Geometry of Pool and Weir Fishways

A wide range of upstream fish passage facilities have been previously described; However, it is the flow patterns, stability and the physical arrangement of pool and weir fishway design which is the focus of this study. In order to gain a better appreciation of the pool and weir fishway, it is important to have a general understanding of what size these facilities are actually constructed to, or at least what are the typical physical ranges can be expected.

The design for a pool and weir fishway is fundamentally based on allowable maximum velocity and preferred flow patterns. Typically, a head of 30 cm (1 ft) between adjacent weirs produces passable velocities and favorable conditions for a wide range of fish, however, large head drops can and do exist for particular situations. The Baker River dam in Washington state uses a pool and weir design with a head drop between weirs of 0.61 m (2 ft) and is suitable for the salmonoids which use it. Freshwater species which are usually smaller and slower require a smaller head drop in order to proceed upstream. Katopodis (1981) suggests that a head drop of 20 cm is more suitable for freshwater species and will ultimately reduce the number of fish from being washed back during a passing attempt. Pool lengths L and weir heights p for pool and weir fishways vary as well for each design, but typical representative sizes range from 3 to 3.65 m (10 to 12 ft) and 1.5 to 2.4 m (5 to 8 ft) respectively (Clay, 1961; Katopodis, 1981). As a guideline, the ratio of pool length over weir height L/p ranges from 1.25 to 2.0 depending on the preferred flow conditions over a range of discharges. Fishway widths are usually site specific for they are a function of the fish population which intends to pass and an average residence time in each pool.

It should also be noted that even though a pool and weir fishway can hydraulically operate for indefinite lengths, ultimately economics will dictate what design parameters are to be implemented to provide a suitable system at a reasonable cost. From 1950 to 1960 several large hydroelectric projects were undertaken in the Maritime provinces. In 1952 the Tobique hydro development erected an enormous pool and weir fishway that provided passage for upstream migrants for a total head difference of 23.8 m (78 ft) (Collins and Gillis, 1985). If a head difference of 30 cm (1 ft) was selected, approximately 80 pool and weir cells would have been constructed. Obviously, the value of the facility out-weighed the capital expenditure for the fishway was constructed.

With a better understanding of the pool and weir fishway design, it is now possible to continue with the recent advancements and approaches which have been developed to assist in designing new pool and weir fishways. As previously expressed, pool and weir fishways can possess a large array of flow patterns for any physical arrangement. Since the pool and weir system is sensitive to the discharge passing through it, all physical arrangements can exhibit many different flow patterns. It is this flow pattern flexibility which makes this design concept so attractive and at the same time so potentially disastrous. "Although Denil and vertical slot fishways work, different configurations of the pool and weir design, depending on the behaviour of the species to be passed, appear likely to provide the highest efficiency and conditions (flow patterns, water depths and passage widths) suitable for the broadest range of species. Provided regulating system mechanism to control the discharge is added to the structure (Collins and Gillis, 1985)." Unfortunately, the ability of predicting the flow pattern for a specific discharge and arrangement is still quite limited. This is undeniably the weakness of the pool and weir design, however, recent quantitative advancements are narrowing the gap of this prediction uncertainty. The following section shall address the analytical and empirical approaches by previous researchers which can be used to provide some insight into flow regime prediction.

1.2.7 Predicting Flow Regimes in Pool and Weir Fishways

The key to designing new pool and weir fishway facilities is the ability of accurately predicting the flow regime which will occur for any physical arrangement and discharge. Generally, plunging flow which is similar to flow over a sharp crested weir will initially occur in pool and weir fishways and as the discharge increases the flow regime will ultimately transform into a uniform streaming flow. In most arrangements the plunging and streaming flow regimes occur on either end of the flow regime spectrum, and a transitional regime which can be the combination of either one or both regimes divides the two. It is this transitional range which truly complicates the ability of predicting any flow regime, for the boundaries of these three domains partially overlap from one to another and are in no way distinct. In order to define the domains of these regimes, a study conducted by Rajaratnam, et al. (1987a) collected analytical and empirical relationships that could be used to represent the standard flow patterns in the pool and weir fishway and applied them with reasonable success. For each of the three characteristic flow regimes, plunging, transitional and streaming, dimensionless parameters were also devised and applied to set bounds for each respective flow regime.

The first flow regime and undoubtedly the most common to pool and weir fishways is classified as plunging flow. Plunging flow as seen in Figure 2(a) is quite similar to the flow patterns produced by a sharp crested weir. Although there is indeed a similarity between the two, plunging flow in pool and weir fishways is the result of the system of weirs rather than a single isolated weir. Even though the weirs in a pool and weir fishway act hydraulically together to produce the plunging flow regime, it is possible to apply equations derived for a sharp crested weir to this problem. Rajaratnam, et al. (1987) used the principles of unsubmerged sharp crested weirs as outlined by Lakshmana Rao (1975) and applied this discharge equation for plunging flows. The discharge relationship for a unsubmerged sharp crested weirs as derived from the Bernoulli equation is as follows:

$$Q = \frac{2}{3} b C_d \sqrt{2g}\, h^{3/2} \qquad 1)$$

where Q is the discharge; b is the flume width; C_d is the discharge coefficient; g is the acceleration due to gravity and h is the head over the weir as seen in Figure 2(a). This discharge relationship which has been established for sharp crested weirs can be applied to the slender weirs found in pool and weir fishways. Pool and weir fishway weirs are typically 10 cm thick while the flow over the weir is usually restricted to 30 cm. The ratio of head over weir thickness results in an acceptable value of 3 which is greater than the required minimum of approximately 1.5 to 1.9 (Surya Rao and Shukla, 1971). The Weir Coefficient, C_d, can be approximated by using the Rehboch equation for applicable flows where h/p values are less then 6 (Kandaswamy and Rouse, 1957). The Rehboch equation which considers the effects of approach velocities is as follows:

$$C_d = 0.605 + 0.08 \frac{h}{p} \qquad 2)$$

where p is the weir height, as illustrated in Figure 2. A dimensionless discharge relationship for plunging flow can be expressed by rewriting Equation 1 as:

$$Q_+ = \frac{Q}{b \sqrt{g}\, h^{3/2}} = \frac{2}{3} \sqrt{2}\, C_d \qquad 3)$$

where Q_+ is the dimensionless discharge for plunging flow. The pool and weir laboratory experiments conducted by Rajaratnam, et al. (1987a) yielded an average dimensionless discharge Q_+ value of 0.61 which is not substantially different from a value of 0.57 when the Rehboch equation is substituted into Equation 3. In addition it was deduced from studying the log Q versus log h plots that for all weir spacings the discharge Q can be assumed to be proportional to $h^{3/2}$. This relationship suggests that the equations established for sharp crested weirs can be applied to plunging flow conditions in pool and weir fishways.

The second predominant flow pattern in a pool and weir fishway is classified as streaming or skimming flow. The characteristics typically observed in streaming flow, as seen in Figure 2(b), consist of a plane turbulent surface jet of depth *d* passing over the weirs height *p*, while the flow in the cells between the weirs is rotating in a singular direction due to the entrained flow from the surface jet. The turbulent shear stress interface which resides between the rotating cells and the surface jet is a key component to this system. It is this shear stress that dissipates the potential energy, prevents the flow from accelerating and permits steady uniform flow to occur. Efforts to quantify the streaming flow regime by Rajaratnam, et al. (1987a) were achieved by equating a force balance equation between the inertial and shear stress components found in a control volume of depth *d* and width Δx. This equation can be expressed as:

$$\Delta x \; d \; \gamma \; S_o = \bar{\tau} \; \Delta x \qquad 4)$$

where γ is the weight per unit volume of the fluid, S_o is the sine bed slope of the fishway and $\bar{\tau}$ is the average shear stress acting between the surface jet and the circulating cell. The average shear stress component can be computed by the Von Kámán integral equation and written in a dimensionless form as:

$$C_f = \frac{\bar{\tau}}{1/2 \rho U^2} \qquad 5)$$

where C_f is the coefficient of fluid friction, ρ is the mass density of the fluid and U is depth-averaged velocity of the surface streaming flow. With the substitution of Equation 5, it is possible to rewrite Equation 4 as:

$$Q = b\, d^{3/2} \sqrt{g\, S_o} \sqrt{\frac{2}{C_f}} \qquad 6)$$

Equation 6 can be expressed in a dimensionless form as:

$$Q_* = \frac{Q}{b\, d^{3/2} \sqrt{g\, S_o}} = \sqrt{\frac{2}{C_f}} \qquad 7)$$

where Q_* is the dimensionless discharge for streaming flows.

From the pool and weir laboratory experiments conducted by Rajaratnam, Katopodis and Mainali (1987b) it was determined from log Q versus log d plots that the discharge Q was approximately proportional to $d^{3/2}$ and the analytical approach undertaken to quantify this flow was acceptable. The experimental data also revealed that Q_* was not a singular value but ranged from 3 to 20. After closer examination it appeared that Q_* varied mainly with L/d and the following equation which best describes this trend was determined.

$$Q_* = \frac{3}{2} \sqrt{\frac{L}{d}} \qquad 8)$$

By equating Equations 7 and 8 it is therefore possible to estimate the depth of the surface streaming flow for any physical pool and weir arrangement and discharge. In addition, the coefficient of fluid friction C_f can be approximated by the same equality and expressed as:

$$C_f = \frac{8}{9}\frac{d}{L} \qquad 9)$$

Rajaratnam, et al. (1987b) determined that for a typical L/d value of 10, the coefficient of fluid friction C_f was equal to 0.08.

Although the previous equations quantitatively describe each plunging and streaming flow regime, it is necessary to develop an equation which can be used to predict the transition from one flow to another. The laboratory experiments by Rajaratnam, et al.

(1987b) revealed that the transitional range between the plunging and streaming flow appeared to be a function of the pool length L, and the following equation was proposed:

$$Q_t = \frac{Q}{b\,L^{3/2}\,S_o\,\sqrt{g}} \qquad 10)$$

where Q_t is the dimensionless discharge for the transitional regime which exists between plunging and streaming flows. From the experimental measurements, the dimensionless discharge for transitional flows Q_t ranged from 0.22 to 0.31 and an average value of 0.25 was suggested for this parameter (Rajaratnam, et al., 1987b).

1.3 Objectives

The objective of this pool and weir fishway study is primarily to advance the ability of flow regime prediction so that different fishway arrangements can be constructed to better address the needs of the migratory fish. In addition, any information gained from this study regarding the flow patterns within the dominant flow regimes, the transformation process from a plunging to streaming state, as well as which physical parameters are significant for flow regime generation, will advance the science of pool and weir hydraulic structures.

To achieve these goals, an experimental study was conducted and water surface profiles, stability observations, and photographs were recorded for a total of 435 different pool and weir arrangements and discharges. Furthermore, velocity measurements for a select few arrangements provided insight into what velocity profiles and maximum velocities should be expected for plunging and streaming flows.

2.0 EXPERIMENTAL INVESTIGATION

2.1 Apparatus

This pool and weir experimental study was performed in a six meter long, 0.56 meter wide, and 0.6 meter deep adjustable slope flume. The entire experimental structure was supported at two points and by simply elevating the tail end of the flume the slope of the model fishway could be adjusted from a horizontal position to a maximum slope of 30 percent. The side walls and the weirs were constructed of clear plexiglass and the flume bed was made of smooth aluminum. The plexiglass weirs 8, 10 and 12 millimeters thick, were fastened to the side walls with sheet metal brackets and bolted at an angle which would result in a vertical weir at a 10 percent bed slope. This angle defined as alpha α was constant for all experimental test runs and is shown in Figures 1 and 2. After the weirs were firmly bolted in place, silicone caulking was applied to the upstream and downstream perimeter of the weir, effectively anchoring the base of the weir as well as ensuring that a water tight seal was in place. A vertical weir configuration for all bed slopes would have been preferred but it was felt that this minor angular deviation was small enough not to significantly effect or influence the flow patterns for each flow regime. The weirs that were used for this model study were no taller than 140 millimeters and even at a 30 percent bed slope, the difference in elevation was considered acceptable.

The water supply for this model study was pumped from the floor sump and into a pre-flume head tank located at the upstream end of the flume. Excessive air entrainment and wave formations which were produced by the incoming water were dissipated by installing a pervious filter at the entrance of the flume. Moreover, the curved bottom of the upstream head tank ensured that inlet conditions would not create unnecessary disturbances that would propagate down through the studied section. Figure 3 fully illustrates the experimental apparatus and physical arrangement. A total of four pumps were used to supply the water needed for this study. Each pumping system consisted of a pump, gate valve, magnetic flow meter and volt meter. Of the four utilized pumps two were capable of passing discharges of ten liters per second each, while the other two could supply of 35 and 120 liters per second. When all combined, a total steady discharge of 165 liters per second could be achieved.

The full weir height as well as the weir spacings were designed and constructed to conform to a 1 to 11 geometric scale model. Since the flow in the pool and weir model was highly turbulent, relaxation of the dynamic similarity or Reynolds criteria was considered acceptable and the kinematic or Froudian criteria was implemented. The velocity, discharge and time ratios for a model with a length ratio of 11 are 3.32, 401.31, and 3.32 respectively. Even though it is truly impossible to completely scale a prototype facility, numerous researchers have confirmed that hydraulic model studies of fishways have been found to accurately reflect general flow patterns in these facilities (Collins and Gillis, 1985).

2.2 Experimental Nomenclature

To fully classify and prevent confusion between each test arrangement, an abbreviated system of code was established. Every water surface profile, photograph and observation note displays this code which fully describes the physical arrangement as well as the discharge flowing through the system. For example, WA05-005 was one of many such designations and just so happens to be the first water surface profile illustrated in Appendix A. This abbreviated code can be subdivided into five categories which describe the weir height, fishway type, weir spacing, bed slope and discharge. Starting from the left and proceeding to the right, the first designation corresponds to the weir height and will be either 1, 3/4 or 1/2. These numerals explain that the weirs for each respective arrangement were typically full, three quarter or one half the 1 to 11 scale size. For the full weir height the numeral one which precedes all other categories has been dropped for reasons of simplicity. The second designation 'W' indicates that the experiment was conducted on weirs only and no orifices or chutes were incorporated into the design. The next single letter defines what weir spacing was used. The letters A, B, C, and D were used in this third designation and correspond to a maximum through minimum pool length respectively. The fourth designation consisting of two numerals defines the sine slope of the bed. Continuing across, the dash simply separates the following three or four numerals which constitute the last designation that describe the discharge, in liters per second. The example listed above, WA05-005, when deciphered describes the arrangement as a full weir height pool and weir fishway with an 'A' class weir spacing, five percent bed slope and a discharge of five liters per second.

In addition to this code which categorizes the physical arrangements and discharges, other abbreviations were devised to classify the flow regimes as well as stability for each arrangement. For example the abbreviations for steady and unsteady flow are Stdy and Unstdy and the letters, P, T and S signify plunging, transitional and streaming flow respectively. The five previously listed abbreviations are indeed the most common; however, others do exist and shall be introduced when the associated flow regimes are described later on in this section. Complete abbreviation listings are always included in a legend accompanying the table or figure for quick referencing. The first page of Appendix C lists all the flow regime abbreviations and fully describes them.

2.3 Experimental Procedure

2.3.1 General

The aim of this pool and weir model study was to expand the understanding of the different flow regimes which occur for several physical arrangements and discharges. In order to understand these complex systems qualitative stability observations, photographs as well as water surface profiles and velocity measurements were recorded for several model arrangements and discharges.

This pool and weir model study which recorded data from several arrangements was performed in a quite systematic and sequential approach. In an overview, there was a total of four parameters which were altered to produce greater than 435 different modeling arrangements. These four variables were the discharge Q, the bed slope S_O, the spacing between the weirs L, and the weir height p. They have been ordered in this fashion to represent the sequence of which the variables were modified. Understandably the discharge was the easiest parameter to alter followed by the slope, weir spacing and finally the weir height which was changed after all other combinations were exhausted. Initially this pool and weir experimental study focused on the full weir height arrangement and then alterations were made to observe the flow patterns produced by half and three quarter heights in this order.

Starting with the full weir height, the largest weir spacing classified as the 'A' class spacing and a bed slope of five percent, several discharges varying from one liter per second to 165 liters per second were passed through the model. For each incremental change in discharge a time span of ten minutes was allowed to pass before any measurements or observations were recorded. This time period was felt to be necessary for it was required to ensure that the flow was fully developed and not in any way influenced from the previous discharge. After recording all pertinent information for the multiple discharges, the full weir height, the 'A' class weir spacing and a slope of five percent, this sequential process was repeated in a similar fashion keeping all the physical parameters the same except for changing the slope to 10, 15, 20 and 30 percent. Once these five cycles were completed the weir spacings were modified to one half the original length by introducing additional weirs at the midpoints. Again this entire combination process was repeated for the new 'B' class weir spaces for the several slopes and discharges which was followed by another bisection producing the 'C' class spacing. Similarly the 'C' class measurements and photographs were recorded, as well as for the 'D' class which represented the smallest weir spacing. Once the 'D' class weir spacing measurements and observations were noted, this would conclude the full weir height experimental subset. It should be noted that the standard length of a pool and weir fishway would correspond to this experiments' 'B' class weir spacing ($L/p \approx 2$). Generally a pool and weir fishway will be constructed to have a pool length to pool depth ratio ranging from approximately 1.25 to 2. Therefore, this model study observed and recorded flows for twice (A class), one half (C class) and one quarter (D class) the standard weir spacing or $L/p \approx 4$, $L/p = 1$ and $L/p \approx 1/2$ respectively.

This entire process of altering the discharge, slope and weir spacing to produce several experimental arrangements as outlined for the full weir height section was repeated twice more, with some modifications and exceptions, for the half and three quarter height weirs. After reviewing the full weir height data, it was possible to select a narrower range of the half and three quarter experimental arrangements and discharges which would still provide valuable information about the transition from plunging to streaming flow.

For both half and three quarter weir height groups of experiments, the closely spaced 'D' class weir spacing were omitted. The reason for excluding this smallest spacing was because the transition from plunging to streaming flow for the full weir height experiments occurred for very small discharges and over an even narrower range. When plunging flow did occur for this 'D' class spacing, it was present only for extremely low discharges for which surface tension effects appeared to become important. It was felt that the half and three quarter weir height experiments would behave similarly, and subsequently little practical information regarding the transformation from plunging to streaming flow would be gained. For these reasons the 'D' class weir spacings were no longer constructed.

From the previous full weir height experiments it was also found to be more convenient to start with the smallest weir spacing then remove select weirs as required. This process was much more time effective for instead of repetitively drying and caulking the weirs, they were simply unbolted and extracted. Although this reverse construction process decreased the shut down time of the flume, it also introduced a small discrepancy with regard to the spacing of the weirs for the half and three quarter weir height experiments. The weir spacings for the half and three quarter weir heights were based on distances computed for a full weir height. Now instead of introducing weirs which would decrease the length of the pools by one half of the weir thickness, the pool lengths were increased by one full weir thickness for each experimental set. The maximum weir thickness introduced a discrepancy of 6 millimeters and it was considered to be note worthy for calculation purposes but acceptable for observational comparisons. Even though this minor variation occurred, the standard nomenclature devised to describe the weir spacings, A through C class weir spacings, effectively describe the approximate lengths between the weirs. Table 1 catalogues all the designed and exact weir spacings and weir heights for this experimental model study.

In addition to the deletion of one weir spacing, the supply pumps were not always readily available, thus, reducing the maximum modeled discharge from 165 liters per second to 45 and 35 liters per second for the half and three quarter weir heights respectively. This reduction was due to the limited availability of the laboratory pumps. Fortunately, these smaller discharges were sufficiently large to induce at least transitional flows in the vast majority of the remaining experimental arrangements. Although fully developed streaming flow was not always possible, especially for steep slopes with large weir spacings, relevant data were still collected for the plunging and transitional regimes.

For all of the previously listed arrangements the flow supplied to the experimental flume was routed through as many as three pumping configurations. There were a total of four pumps used in this study; however, only one of the two smaller pumps that were capable of a discharge of 10 liters per second were attainable at a point in time. Initially there were three different size pumps available, each capable of maximum discharges of 10, 36 and 120 liters per second and when all three were operational, they could produce a maximum discharge of 165 liters per second. Generally the underlining objective in providing the flow to the flume was to keep the pumps operating within the center two thirds of their capable ranges. It was found that a stable flow supply as well as less instances of the pumps stalling due to overheating would occur if the pumps remained within this mid supply range. When the experimental flow demand was less than ten liters per second, the smallest pump was used. As the discharge demand increased, the first pump would be turned off and the next largest pump capable of 37 liters per second would be staged on to provide discharges in excess of ten liters per second. Flows ranging from 35 to 45 liters per second could be achieved by combining the flow from the first pump with the second. For discharges greater than 45 liters the main pump capable of 120 liters per second was utilized and was used alone or in combination of the first two.

2.3.2 Water Surface Profiles

For this experimental study, several water surface profiles were measured, recorded and plotted in order to provide insight into what type of flow regime was present for each and every geometrical configuration and discharge. By measuring and recording a total of 435 different water surface profiles two significant goals were achieved. Firstly, a valuable visual reference of all these modeled water surface profiles was created. Not only is it possible to view how the water surfaces change for different discharges and arrangements, but this catalog of water surface profiles can be used as a supplemental design tool. For example the height of the side walls for a pool and weir fishway can be determined for a range of flows by referring to these plots. Secondly, quantitative values for the plunging head *h* and the streaming depth *d* were determined from these records and used to confirm as well as expand the dimensionless discharge parameters proposed by Rajaratnam, et al. (1987).

The setup procedure undertaken to obtain these water surface profiles was described in part in the previous sections. Once a particular arrangement and flow was established, a point gauge positioned along the centerline of the flume and fitted with a vernier capable of measuring the water surface accurately to one thousandth of a foot (0.31 mm) was used to map the water surface profile. This point gauge was supported from a railing system constructed along the top of the flume and parallel to the bed. For each individual water surface profile ideally the point gauge measurements would start and end approximately at a stationing point one half the weir spacings upstream and downstream of the studied pool and weir cell. This method would therefore map the water surface profile over two weirs as well as half a cell in either upstream and downstream directions.

A standard steel pointer was originally used to measure the water surfaces and was found to be acceptable for low flow conditions where the water surface was unbroken and continuous. By increasing either the discharge, slope and weir spacings the water surface eventually became so highly air entrained and discontinuous that the steel pointer was no longer effective for it was difficult to discern exactly where the tip of the gauge was positioned. Several types of pointers such as rods with dye drips and painted pointers were made in an attempt to make this measurement less tedious and time consuming.

After numerous creative attempts, a pointer that incorporated two pieces of yarn was finally devised that made recording water surface profiles for broken surface flows readily achievable. This pointer system shown in Figure 4 was actually a combination of a steel pointer and two offset thin aluminum tubes that had yarn indicators attached at the ends. The two additional parallel pointers, supported in place with a piece of wood, were identical except for their lengths. The innermost yarn indicator was constructed to be equal in total length to the main steel pointer. The second or furthermost yarn indicator had a tube length equal to the steel pointer and a 20 millimeter yarn segment attached to the end. This arrangement was effective in measuring all steady water surface profiles for the original steel pointer easily measured the water surface for smooth surfaces while the two yarn indicators could be used for large more turbulent surface flows. By lowering the two yarn indicators into the turbulent surface flow the water surface measurement was recorded when the inner most (first) indicator was twitching due to the surface spray and the outermost (second) yarn indicator was submerged and orientated parallel to the surface flow streamlines. If the yarn indicators were not positioned far enough into the broken water surface, there would be little or no movement observed in the first indicator, where as the second indicator would not be in any way parallel to the surface flow. Although this method may appear to unconventional, it is far simpler to observe movement in two red yarn indicators rather than estimating where a chrome plated steel pointer comes in contact with a broken water surface. This dual yarn indicator system not only increased the accuracy of measuring the water surface profiles but gave a much higher degree of repeatability and consistency between each turbulent water surface profile was achieved.

For the full weir height set of experiments, a combination of four weir spacing (A, B, C and D), 12 discharges (5, 10, 15, 20, 25, 35, 45, 65, 85, 105, 135 and 165 liters per second) as well as five sine slopes (5, 10, 15, 20, 30 percent) resulted in a total of 240 water surface profiles. The water surface profiles for the half weir height class was somewhat smaller since the maximum discharge was only 45 liters per second. This set of 120 water surface profiles was the result of combining the same five slopes but only three weir spaces (A, B and C) and eight discharges (2.5, 5 10, 15, 20, 25, 35 and 45 liters per second). The three quarter weir height section was the last set of experiments performed for it was thought that these water surface profiles would provide insight into how the flow conditions changed from the full to half weir heights. The combination of only five discharges (10, 15, 20, 25 and 35 liters per second), the same five slopes and the three weir spacing (A, B and C) produced an additional 75 water surface profiles. In total 435 different water surface profiles were careful measured, recorded and plotted.

Appendix A fully illustrates all the water surface profiles measured during this experimental study. It is important to note that the water surface profiles illustrated in Appendix A and throughout this thesis are not sketches but actual measured data points plotted to scale. Viewing more closely, the water surface profiles within Appendix A were organized in the same sequential order in which they were recorded. Typically the first page of each set was a mosaic of all the slopes and discharges for a single weir spacing and height. Proceeding to the following page this plot will illustrate a superposition of several discharge water surface profiles for one slope, weir spacing and weir height. These pages showing several water surface profiles are particularly interesting for it is visually possible to observe how the water surface and flow patterns transform to reflect increases and decreases in discharge. The following page or pages illustrate each individual water surface profile plotted separately instead of all together as in the previous pages. This cycle of superimposed and individual water surface profiles repeats itself several times for different slopes, spacings and finally weir heights.

For some of the individual water surface profiles, there was more that one line plotted. The reasoning behind these multiple lines was as follows. For lower discharge ranges, the flow was typically plunging and was not difficult to measure. However, as the discharge increased and transformed into a transitional flow, the water surface often became discontinuous and turbulent waves developed. For these cases, the maximum and minimum water surface was measured as accurately as possible and an averaged water surface was computed. Water surface profile WC20-010 is an example of one of these cases. Referring to this water surface profile, the top, bottom and centre dashed lines illustrate the maximum, minimum and average water surface profiles respectively. These multiple lines simply shows that, although the flow maybe globally steady, the water surface can be considered to be within these outer boundaries. After closer examination the water surface computed by the mathematical average of the maximum and minimum measurements did not accurately depict the visual time averaged water surface profile. An additional fourth water surface profile illustrated with circles and a continuous line was visually time averaged and measured using the point gauge with the two yarn indicators. This fourth line best illustrates the true water surface profile for each arrangement.

For highly turbulent flow regimes, such as some baffle flows and large-discharge, wide-spaced weir streaming flows, another method other than the point gauge was used to measure and record the discontinuous water surface profiles. Plates 9 and 10 illustrate what types of flows were recorded by this method. For these situations, the water surface profiles were recorded by tracing the water surface on the clear plexiglass sidewalls of the flume with a marker. Unconventional as it may seem, this method was far more practical than the point gauge for errors or deviations from the time averaged water surface could be easily adjusted and corrected. The intent of this approach was not to produce extremely accurate water surface profiles but to provide a graphical display and record of what type of profile occurred. The water surface profiles generated from this method can be considered accurate to within ±5 millimeters.

2.3.3 Photographs

In addition to the water surface profile measurements and stability observations recorded during this model study, another parallel study, in which several flow arrangements were photographed, was conducted simultaneously. This photographic study by Sikora, Rajaratnam and Katopodis (1996) captured all of the 435 flow arrangements listed in the fourth paragraph of the previous section. The aim for this independent study was to develop a photographic diary to provide flow visualization of the mechanisms which interact to produce any flow regimes in a pool and weir fishway. Since the means of predicting flow regimes in pool and weir fishways is still quite limited, this photographic study can be used as a supplement to ensure that flow regime predictions are correct.

For this independent photographic research study two photographs were taken for each experimental arrangement and discharge. The first photograph was captured from as far away as possible to illustrate how the interaction of several weirs influences the overall water surface profiles. The second photograph was intended to be a close up, to show more closely the flow pattern in one cell. A tuft grid which was comprised of fine stainless steel wire and yarn, was used to show the two dimensional flow patterns in at least one pool and weir cell. The grid was positioned along the centre line of the flume unless exceedingly high concentrations of air entrainment obscured the photograph and forced a one third or one quarter flume width placement. The dimensions of the tufting grids were all 20 millimeter square with the exception of the 'A' class weir spacing for all weir heights and the full weir height 'B' class weir spacing. For these exceptions a 25 millimeter square wire grid was used. Each yarn indicator was securely glued to the wire intersections and was approximately either 20 or 25 mm long, depending on the grid spacing (Sikora, et al., 1996).

2.3.4 Velocity Measurements

In order to gain a better appreciation of what flow patterns exist in a pool and weir fishways, it was felt that velocity measurements of select flows would provide valuable insight and reveal specific characteristic that are the basis of these fundamental flows. By measuring several vertical velocity profiles in one pool and weir cell, maximum velocities as well as velocity distributions could shed light on how the flow patterns become established as well as how velocity dissipation occurs. Ideally, velocity measurements for all the flow arrangements and discharges would have provided volumes of information; however, this task would have required much more time to complete than was available for it took minimally two weeks to collect the experimental data for each flow arrangement. With this in mind, velocity profiles for only a few select arrangement and discharges were measured. It was felt that since the greater majority of pool and weir fishways are designed to behave in a plunging flow manner, an arrangement that exhibited this flow structure should be selected. To gain the most information from these velocity measurements, within the limited time frame, one configuration with three different weir heights was measured. By altering the weir height for one discharge, slope and weir spacing, this approach would provide far more information about maximum velocity paths and energy dissipation than for three or four randomly selected configurations. Initially, the velocity profiles for the full weir height case were measured and as the weirs were reduced in size, the half and three quarter weir height installations were measured in a similar fashion. The plunging arrangements measured were, WA10-035, 3/4WA10-035 and 1/2WA10-035. Section 3.3 looks more closely at the similarities and differences of these three cases. In addition to the plunging flow, velocity measurements for one transitional streaming flow regime were recorded. This second regime was of interest for it was almost a uniform streaming flow and any information regarding the velocity distributions in the rotating cell as well as the surface streaming flow would be beneficial. The velocity measurements of this transitional streaming flow, WB10-065, were performed as an independent study by Mrs. K. McKay and the author of this thesis (McKay and Sikora, 1994), and the findings that are presented here and in Section 3.3.2 have been done so with consent of both researchers. Photographic Plates 17 through 22 illustrate the four studied experimental arrangements and flow patterns.

For all four experimental arrangements and discharges the velocity measurements were recorded with the use of a pitch probe and manometer. The standard configuration of the pitch probe and manometers is illustrated in Figure 5. For the first set of measurements on the WA05-035 configuration, the velocity profiles as well as the velocity point measurements were widely spaced. After gaining confidence in the experimental apparatus and refinements to the method of which velocity measurements were made, the velocity profiles for the following arrangements contained several more point measures and were spaced more closely together. For the vast majority of all velocity measurements, the inlet of the pitch probe was positioned in a plane parallel to the bed and directed either upstream or downstream. These two configurations were suitable for recording flow velocities with approach magnitudes less than 65° with respect to the pitch probe inlet axis. Even though a pitch probe is capable of measuring approach angles as great as 65°, the maximum measured approach angle was not permitted to exceed 45°. With the use of a dye tracer extruded form a long thin needle, the approach angle, stagnation points, and the locations where flow reversals occurred were easily observed and appropriate alterations to the pitch probe were made. For any particular flow situation where the approach angle was identified to be greater than 45°, the pitch probe was simply angled into the flow either at a 30° or 45° angle with respect to the flume bed. This simple and effective alteration ensured that accurate measurements could be achieved even in areas where steep approach angles and flow fluctuations occurred.

Once the pitch probe was correctly positioned and setting the center entrance point of the middle tube as the physical coordinate location, the elevations of the water levels in the three manometer tubes were read as quickly and accurately as possible. When the flow entering the pitch probe was directly in line with the inlet axis, the first and third (top and bottom) manometer tubes had equal water levels and the second (center) tube manometer reading was understandably greater than the rest. For this situation, all three manometer water levels as well as all three differences in water levels were constant and stable making experimental recordings effortless. When the pitch probe was positioned in an area where the approach angle was rather steep the variability in the manometers became more significant. In most situations, the manometer water levels were rarely stable and fluctuating cycles or trends made instantaneous measurement recordings difficult to achieve. Even though the water levels in the manometer tubes did fluctuate, the difference in water levels between each manometer tube did not vary considerably and measurements could be made by watching for re-occurrences of previously observed water levels. Therefore, the task of measuring three manometer water levels for each point in each velocity profile was possible but required considerable lengths of time. Once the manometer tube measurements were recorded, the magnitude and direction of the velocity vector could be computed by applying the empirical calibration curves established by Rajaratnam and Muralidar (1967). The time required to convert this raw data with the calibration curves to velocity magnitudes and directional angles was drastically reduced by applying an in-house software package created by Dr. S. Wu at the University of Alberta hydraulics laboratory. The results of the velocity measurements conducted on the four experimental arrangements will be illustrated and reviewed in Section 3.3.

2.4 Experimental Errors and Uncertainties

2.4.1 General

For all experimental research projects, the end results or products of any study are only as accurate and reliable as the degree of accuracy in which the experimental measurements were recorded. It is important to understand that even though careful experimental practices may have been followed, the differential between true values and measured values must be anticipated and expected. In all instances, the merit of any experimental work is a function of all the possible errors that can occur during any one of many measuring instances. In order to determine the accuracy or degree of experimental uncertainly, all possible errors must be addressed, quantified and through a propagation of error analysis, only then will the true reliability and value of the experimental work be known. For this pool and weir study the propagation of error for the dimensionless parameters Q_*, C_f, Q_t will be determined by establishing confidence intervals for the experimentally measured values such as plunging head h and streaming depth d.

2.4.2 Sources of Error and Estimates of Uncertainties

In all experimental research projects errors that do result can be identified and classified as either random, systematic or mistakes (Dept. of Physics, 1982). The first type of experimental error known as random error, can be considered to be simply the deviation from a true value due to accidental or precision error. This type of error generally behaves in a statistical manner and the fluctuation from the true value for every repetitive measure would be best represented by a Gaussian or normal distribution. The second type of error known as systematic error can be very difficult to detect for it is the result of incorrect timing devices, misalignments and physical limitations. A stop watch that does not keep perfect time introduces a form of systematic error. This particular scenario can be corrected if substantial deviations are visible; however, typical fading or a slow deviation from true are often so slight that detection of errors only occur after long periods of time. For this reason it is really questionable whether all systematic errors are truly accounted for. The third possible type of error classified as mistakes usually can be easily identified for they are not representative and produce values that are often separated greatly from all other data points. Incorrect readings of scales, poorly written records and human error all fall within the mistake classification of errors. Any experimental data that can be determined to be influenced by a mistake is carefully examined and discarded and the following error analysis is conducted on the purely random data.

By understanding what types of errors can occur, it is now possible to outline and identify the sources of error in this specific experimental investigation. For this pool and weir fishway study, error in linear length measurements and discharge setting were the two main categorical sources. To determine confidence ranges for the dimensionless parameters Q_*, C_f and Q_t, the pool length, plunging head, streaming depth and bed slope data was required. Data for these four parameters were in turn achieved by numerous other measurements and as a result, the bed slope, flume width, weir height, pool length, point gauge stationing, and the point gauge vernier were the seven sources of linear measurement error in this experiment. One additional error that is of lesser concern is the result of the angling of attack of the weirs with respect to the flume bed. This error shall be addressed further on in this chapter.

Although the potential sources of error have been outline, the true task at hand is not only to determine what error could have occurred but to define accurately the interval that would encompass the deviation from the measured data and the true value with a certain degree of confidence. There are two standard approaches to determine the deviation intervals, however, the degree of confidence for each method is a function of what data collection approach was undertaken.

Data collection for experimental research can be achieved either by single or multiple sample techniques. The first method of data collection is based on single sample collection for each data point where as the second approach obtains experimental data by processing multiple measurements for each data point.

The error and confidence intervals that result from this multiple sample approach are based on statistical theory of probability and a normal frequency or Gaussian distribution accurately represents the random generated data (Dept. of Physics, 1982). This statistical approach establishes a mean value as well as a 68% confidence limit by assuming that the true value lies within one standard deviation either side of the computed mean value. The obvious difference between the two data collection methods is that multiple sample measurements for one data point can be statistically analyzed where as a single sample can not.

If a single data point collection approach was adopted, no statistical evaluation of that point could result and a artificial or 'limit' confidence interval is assigned. This approach commonly referred to as a limit error technique, calls upon the expertise of the researcher to evaluate and assign a suitable interval that would encompass all other possible data points within a 99% degree of confidence (Dept. of Physics, 1982). In fact the limit error technique can be considered to be more like a guarantee by the researcher that the true value will be within this confidence interval. Physical length measurements are therefore written as a nominal length and followed by a plus minus deviation which is commonly set to one half the of the smallest measurable scale. Although this holistic approach can be considered to be fairly conservative, the fundamental weakness woven into this technique is that the accuracy of the imposed permissible error intervals are only as good as the researcher who defines them.

For this experimental research project, much like many other hydraulic research studies, the vast number of data point needed to be collected did not permit for multiple measurement data sampling for all test runs and flow scenarios. Subsequently, the limit error approach shall be conducted to estimate the error intervals for all measurements and propagation of error analysis shall proceed there after.

Throughout this study a total of eleven potential error sources were identified and recorded. With the exception of the manometer readings and pitch probe alignment, the slope, flume width b, weir height p, weir angle α, pool length L, discharge Q, point gauge venire y and longitudinal stationing x measurements were required to determine the streaming depth d, plunging head h and the dimensionless parameters Q_+, C_f and Q_t. The eleventh source of error is quite different than that of the previous ten, for it is the result of approximating what would be the free surface when measuring the water surface profiles. This was truly a difficult task to achieve, for this non rigid boundary never remained placid or continuous for a complete range of discharges. To make situations more complex, the resulting error due to assuming a point elevation to represent the water surface was also influenced by the slope of the flume, the weir height and the weir spacings or more specifically the flow regime of the model. As a result, the uncertainty estimates for placid plunging flow of small discharges and slopes varied substantially for large discharge, steep sloped streaming flows. The following portion of this error analysis chapter shall address the eleven sources of error and assign estimated intervals to them.

The first form of error in computing the dimensionless parameters was from setting the correct bed slope. The sine slope was determined by measuring a four meter flume bed section and the corresponding vertical section. The error incurred due to these linear measurements, δy and δz was set as ± 0.5 millimeter and under a worst case situation the overall error in slope was computed to be in the order of 0.03%. Since the slopes were set at nominal percent slopes, this computed variance shall be considered to be trivial.

The weir height p for the full, three-quarter and half settings was initially measured and constructed with the use of a physical tape measure. Once in place, the point gauge which was suspended from the top of the flume was used to measure the perpendicular difference in elevation between the weir crest and the flume bed. The manufactures tolerance for the point gauge was set at ±0.0005 feet (0.15 millimeter) and was conservatively rounded up to ±0.25 millimeter.

The attack angle of the plexiglass weirs was considered to be a third possible source of error. However, since the weir heights were not excessively tall, and with a maximum angular deviation of approximately ±1°, the resulting difference in crest elevation was not large enough to warrant any correction.

The fifth source of error in this experimental study was the result of the inaccuracies in setting a definitive discharge. For this research project, a total of four different pumps were used to provide the required flows. In all four pumping arrangements, magnetic flow meters (Model No., Foxboro, City, State; Model No., Foxboro, City, State; Model No., Foxboro, City, State; Model No., Foxboro, City, State) were accurate to one quarter percent of the maximum full scale deflection, or in other words one quarter percent of the maximum output discharge. The two smaller pumps, referenced as pumps one and four, they were capable of supplying approximately 10 liters per second, thus a discharge error of ±0.025 liters per second could exist. The mid range pump, classified as pump number two, could produce a maximum discharge of approximately 36 liters per second and the associated discharge deviation was ±0.09 liters per second. The last pump of the four, was capable of supplying a discharge of 120 ±0.3 liters per second.

The water surface profiles for this experimental study were recorded by measuring the water surface elevation with a point gauge and the longitudinal stationing to the closest millimeter with respect to the flume bed. It should be noted that error due to incorrect stationing does not present any uncertainty to the computation of plunging head *h* and could be removed from this section of possible errors. However, this issue was introduced here in the aim of being thorough and to present the slight possibility of incorrect flow classification. The problem that could potentially occur is that some baffle flows, a sub domain of the transitional regime, are quite similar to plunging flows except that the maximum water surface, or plunging head, occurs downstream of each weir structure. It is remotely possible that a problem could arise when the maximum water surface is located near the crest of the downstream weir, and subsequently a plunging flow pattern may be incorrectly represented as a baffle flow condition. The likelihood of this occurring is very small for rarely did the maximum water elevation occur within one millimeter of the centerline of the crest of the weir.

The previous six illustrated error sources can be classified as discrepancies or deviations due to physical measuring inadequacies. The following two sources of error are unlike this previous types for they are the result of attempting to set a static point that would best represent a non rigid dynamic water surface. Since the water surface was not always stationary and turbulence affected its shape and stability, errors incurred by measuring a plunging and streaming flow water surface shall be addressed separately. Water surface profiles for plunging flows as observed in this study ranged from being tranquil and continuous to turbulent discontinuous and everywhere in-between. Because of this diversity it would be a quite simple to mask all plunging flows with one error interval; however, this average method would introduce enormously conservative errors to the calm low discharge water surface profile measurements. Viewing this problem from an other angle, ideally it would be convenient to assign an error interval to a definitive range of discharges; however, other parameters such as slope, weir height and spacing directly influence the shape of the water surface profile. After careful consideration the discharge was determined to be a representative indicator, but instead of developing concrete numerical ranges, only qualitative discharge domains were established. As a result three descriptive sub ranges of low, medium and high turbulence were established. Even though the plunging flow regimes were recorded for discharges within the range of 1 to 45 liters per second, the three sub ranges do not reflect equal portions of this discharge domain since other pertinent factors must be taken into consideration. By viewing the photographic Plates 1 through 3 presented in the this study as well as the many illustrated in 'A Photographic Study of Pool and Weir Fishways' by Sikora, Rajaratnam and Katopodis

(1996), a better understanding of what key indicators are present for each classification can be achieved. Section 2.5.2 and 2.5.3 shall describe generally how the flow transforms and the key indicators that define each flow classification. As a result of this divisional scheme, error intervals for plunging head *h* for low, medium and high discharges were set to reflect the stability of the water surface and are ±0.25, ±1.0 and ±2.5 millimeters respectively for plunging flows.

It is relevant to note that no corrections or correlation's were attempted in order to accommodate plunging head data for fully submerged weir flows with head data collected from fully supported unsubmerged plunging flows.

The approach and underlying rationale previously described for determining error intervals for plunging flows has also been adopted for streaming flows. In a similar fashion, the accuracy in determining or estimating the water surface for streaming flows was directly related to the discharge, slope, weir spacings and weir height. Even though the discharge was a strong indicator of what type of streaming flow pattern would occur, the slope and weir spacing proved to be equally as important. Hydraulically, as the slope increased also did the energy as well as the turbulence within the flow. Subsequently as the turbulence increased also did the deviations in the water surface; therefore, three sub domains that were introduced for plunging flow were likewise incorporated for streaming flows. Photographic Plates 13 and 14 illustrate the wide range or diversity of physical arrangements and discharges that can produce streaming flows.

The first class of streaming flows can be described as flows that are the result of shallow slopes, high discharges, and small weir spacings. Generally for this type of arrangement the water surface profile reflected uniform streaming flow conditions and a water surface elevation could be easily measured within ±0.5 millimeters. This calm streaming flow pattern was not frequently observed and was only present for shallow slopes and narrow weir spacings. As the slope and weir spacings increased even for a maximum discharge of 165 liters per second, the error in measuring the water surface increased to reflect these changes and was set at ±1.0 millimeter. The vast majority of all well defined streaming flows were within this range. Proceeding into the last streaming flow sub domain, when the experimental arrangement was set up with a steep slope and large weir spacings, barring all baffle flow conditions, the flow throughout the flume was substantially more turbulent and subsequently the water surface could only be measured accurately within ±2.5 millimeters.

Another issue that should not be neglected and does indeed effect the measurement records of only a few plunging and streaming water surface profiles, is the issue of distorted water surface profiles due to highly turbulent, air-entrained flows. The effect of air entrainment is not a simple issue to approach for even if it was possible to accurately measure the concentration of the air in the flow at one point, it could not be applied throughout the entire flow structure since air entrainment concentrations are not constant throughout the entire length of the pool. In addition, what true effects air entrainment has on elevating the water surface has not yet been resolved. For these reasons the issue of air entrainment has been presented here to confirm that it did occur for select flows but no attempts have been made to adjust any water surface profiles to reflect these altering conditions. In this research study, there were only a few streaming flows that had significant volumes of air entrainment which could have introduced inflated water surface elevations. Typically, this bulking effect occurred for baffle flows where large weir spacings and steep slopes were constructed. Photographic Plates 9 and 10 as well as the investigative study by Sikora, et al. (1996) can be viewed to gain a better appreciation of this effect.

Shifting away from the errors and uncertainties attributed to water surface profiles, there were an additional two errors that occurred during the velocity data collection portion of this study. This section of this study also had error sources previously addressed such as longitudinal station error and point gauge vernier error; however, the remaining two sources of error are due to discrepancies in manometer readings and pitch probe alignment.

In keeping this section as brief as possible the data collection method for velocity profiles has been previously described in section 2.3.4. The three manometer tubes were read to the closest millimeter and subsequently a possible error of ±0.5 millimeters did result for each tube reading. Nevertheless even though these errors did occur, they were considered to be negligible with respect to the natural fluctuations in the flow. The rationale supporting this statement is that flow at any point is not truly steady and the velocity fluctuations that were present in this highly turbulent flow would undoubtedly encompass a 0.5 millimeter misread deviation. This idea of error dismissal due to a larger fluctuation does not truly represent the situation, for manometer readings or better yet the differentials were observed and a mental, time-averaging approach was deployed for each point measured. As a result the collected velocity data from this study was as accurate as possible considering that the size and crudeness of the experimental apparatus being used to record this data. Section 3.3 will present the velocity profiles and the computed continuity errors for the flows that were measured.

This leads directly into the last identified error source and it was attributed to pitch probe alignment and size. The pitch probe as illustrated in Figure 5 was constructed from three 3 millimeter tubes and had an overall sampling point height of 9.3 millimeters. It was this overall height of the pitch probe that presents the problem or issue of what velocity point was really being measured. The centerline elevation of the middle tube was for all intents and purposes the location at which the velocity was measured. However, it is quite possible if the point being measured was located in a region of a large velocity gradient or unsteady flow reversals, subsequently the velocity of the flow entering the top tube could be drastically different than the velocity in the bottom tube, thus, adversely skewing the final computed magnitude and direction. This concept of error due to a definitive probe height can not be neglected but what corrective measures that should be implemented for this situation have not been determined. Even though there was error due to this effect, the velocity measurement obtained during this study have produced some very interesting and proportionate velocity profiles. These findings will be presented in Section 3.3.

2.4.3 Computational Methods for Error Propagation

Now that the probable error for each measurement has been addressed, the methods to determine how these errors propagate in mathematical computations will be outlined. There are two methods that can be used to determine the how to quantitatively account for error propagation. The first being the limit error approach is only applicable for single sample data collection methods and the associated 99% confidence intervals. The following rules and operations for singular data samples are as follows:

Addition and Subtraction

eg. $z = x \pm y$

$$\delta z = \delta x + \delta y \qquad 11)$$

Multiplication by integer:

eg. $z = kx$

$$\delta z = |k|\delta x \qquad 12)$$

Multiplication and Division

eg. $z = xy$ or $z = x/y$

$$\delta z = |z|\left(\frac{\delta x}{|x|} + \frac{\delta y}{|y|}\right) \qquad 13)$$

Power

eg. $z = x^n$

$$\delta z = |z|\frac{|n|\delta x}{|x|} \qquad 14)$$

Function of n varaibles

eg. $z = f(x,y,z)$

$$\delta z = \left|\frac{\delta f}{\delta x}\right|\delta x + \left|\frac{\delta f}{\delta y}\right|\delta y + \left|\frac{\delta f}{\delta z}\right|\delta z \qquad 15)$$

where:

δx = the assigned limit error interval for x

δy = the assigned limit error interval for y

δz = the assigned limit error interval for z

The second method known as the standard error method utilizes statistical computations, 68% confidence intervals and is therefore applicable for multiple data collections only. The following propagation rules apply to the standard error approach and the multiple data collection technique.

Addition and Subtraction

eg. $z = x \pm y$

$$\delta z = \sqrt{(\delta x)^2 + (\delta y)^2} \qquad 16)$$

Multiplication by integer:

eg. $z = kx$

$$\delta z = |k|\delta x \qquad 17)$$

Multiplication and Division

eg. $z = xy$ or $z = x/y$

$$\delta z = |z|\sqrt{\left(\frac{\delta x}{x}\right)^2 + \left(\frac{\delta y}{y}\right)^2} \qquad 18)$$

Power

eg. $z = x^n$

$$\delta z = |z|\frac{|n|\delta x}{|x|} \qquad 19)$$

Function of n varaibles

eg. $z = f(x,y,z)$

$$\delta z = \sqrt{\left(\frac{\delta f}{\delta x}\delta x\right)^2 + \left(\frac{\delta f}{\delta y}\delta y\right)^2 + \left(\frac{\delta f}{\delta z}\delta z\right)^2} \qquad 20)$$

where:

δx = the standard error interval for x

δy = the standard error interval for y

δz = the standard error interval for z

It is not within the scope of this paper to derive the previously listed equations; however, it is important to reflect on noteworthy differences in each of these propagation techniques. The principal variation between these two approaches or sets of rules is in the weighting of each error source prior to their summation.

The first or limit error approach simply assumes each error is to be equally weighted and the final propagated error is the summation of all potential error sources. This technique which assumes a confidence interval of 99% is indeed conservative and does provide valid propagation of error values for occasions where only a few sources of error are encountered (Dept. of Physics, 1982). The problem that presents itself with this limit error method is that if a single data point is a function of several measurements and subsequently equally as many potential error sources, the propagated error interval may be considerably large. Subsequently, it is quite possible that the final propagated error can easily overshadow or diminish the significance of the final data point for measurements that encounter multiple error sources.

The second approach or standard error technique is different from the limit error method for the final propagated error which is only applicable for a 68% confidence interval is the result of taking the root of the sum of the squared errors. This procedure essentially weights the magnitudes of each error source and the final propagated error interval prioritizes the effects of the significant errors and places less weight on the smaller ones. As a result this approach produces more realistic error intervals but is only applicable to statistically gathered data (Dept. of Physics, 1982).

Reflecting on both of these propagation of error approaches it is evident that the standard error method has an advantage over the limit error technique for more realistic error intervals are produced. Even though each of these methods are only applicable for each associated confidence interval, the standard error method for computing error propagation along with assigned limit errors is generally accepted practice within the fluid mechanics community (Ahmed, 1995). Further in this chapter calculations using both methods, limit and standard error approaches, for computing the error interval for plunging head *h* shall demonstrate the variances in each methods results. The following equations provided by Kline and McClintock (1953) are the standard error propagation equations listed above but written in an different form.

$$R = f\left(V_1^{m_1}, V_2^{m_2} \ldots V_n^{m_n}\right) \tag{21)}$$

and

$$\frac{\Delta_R}{R} = \left[\left(m_1 \frac{\Delta V_1}{V_1}\right)^2 + \left(m_2 \frac{\Delta V_2}{V_2}\right)^2 + \ldots + \left(m_n \frac{\Delta V_n}{V_n}\right)^2\right] \tag{22)}$$

Where R is a function of variables $V_1^{m_1}, V_2^{m_2} \ldots V_n^{m_n}$, $\Delta V_1, \Delta V_2, \Delta V_n$ are the individual error intervals for the variables V_1, V_2, V_3 respectively and ΔR is the propagated error interval for R.

2.4.4 Computed Errors

By applying Equation 22 or the Equations 16 through 20, the propagated error intervals for the plunging head ***h***, streaming depth ***d***, depth averaged velocity ***U***, dimensionless flow parameters Q_+, C_f and Q_t can be determined.

To compute the plunging head ***h*** for all plunging flows, a total of four physical measurements were required. Three of the four measurements were made with the point gauge to determine the perpendicular height of the weir, the bed elevation and the estimated water surface elevation. The weir height and the bed elevation both could be measured to ± 0.25 millimeter where as the water surface error intervals were either ± 0.25, ± 1.0 or ± 2.5 millimeters depending on the turbulent nature of the plunging flow. The stationing of the point gauge at the maximum water depth as well as above the downstream weir was accurate to ± 0.5 millimeters. It is possible to express plunging head ***h*** as:

$$h = \frac{\text{Elev.}_{\text{water surface}} - \text{Elev.}_{\text{weir}}}{\cos\alpha} + \left[\left(\text{Sta.}_{\text{weir}} - \text{Sta.}_{\text{water surface}}\right) - \left(\text{Elev.}_{\text{water surface}} - \text{Elev.}_{\text{weir}}\right)\tan\alpha\right]\sin\alpha \qquad 23)$$

where:
α = the sine slope of the flume bed

By neglecting the error associated to the slope and applying the limit error approach to determine the error of propagation for plunging head ***h***, the following results were computed. For the three subclasses of plunging flow as previously described by discharge and turbulent guidelines, the maximum calculated error intervals δh were ± 2.0, ± 3.5 and ± 6.5 millimeters. These values are based on limit errors and limit error propagation formulas. Reflecting on the calculated results, the limit error approach computed a water surface error interval for undisturbed placid flow conditions to be ± 2.0 millimeters. It is obvious from this calculation and from the other two subclasses that the limit error propagation formulas are much too conservative, for a placid water surface profile can be confidently measured to within ±1 millimeter.

When substituting the limit error intervals into the standard error equations to determine the error of propagation for plunging head *h*, the following values were computed. For the three subclasses of plunging flow, the propagated error intervals δh are ± 1.23, ± 1.62 and 3.62 millimeters. These error intervals reflect more accurately the degree of accuracy in locating the water surface and the plunging head *h* for plunging flow regimes.

In a similar fashion, the streaming depth *d* was determined with a point gauge by finding the difference in elevations between the estimated water surface and the crest of the downstream weir. The elevation of the rigid weir crest could be measured to the closest 0.25 millimeter whereas the water surface limit error intervals being functions of discharge, weir spacings and slope were assigned values of ± 0.5, ± 1.0 and ± 2.5 millimeters. The propagated error intervals for streaming depths δd, for each increasingly turbulent streaming flow subclass were ± 0.56, ± 1.12 and ± 2.55 millimeters.

With the propagation of error intervals for the plunging head *h* and streaming depth *d*, it is possible to determine the error interval for the dimensionless parameters that are used to describe the three distinct flow regimes in pool and weir fishways. The first dimensionless parameter which expresses the initial plunging flow regime can be written as:

$$Q_{+} = \frac{141\sqrt{2}}{300} + \frac{4\sqrt{2}}{75}\frac{h}{p} \qquad 24)$$

by substituting Equation 2, the Rehboch equation, into Equation 3. By applying Equation 18, the propagation of error for the dimensionless plunging flow parameter Q_{+} can be expressed by the following equation:

$$\delta Q_{+} = \frac{4\sqrt{2}}{75}\frac{h}{p}\sqrt{\left(\frac{\delta h}{h}\right)^2 + \left(\frac{\delta p}{p}\right)^2} \qquad 25)$$

where:

δh = the head error interval for punging flows

δp = the error interval for the weir height

In order to obtain a range of how large or small this propagated error interval can be, values for two flow conditions one being a low discharge placid flow and the other being a highly turbulent large discharge flow were computed. The first flow, WA05-005 was considered to be a tranquil plunging flow that did not exhibit any water surface discontinuities or a vigorously turbulent flow. The water surface profile for WA05-005 which can be referred to in Appendix A, had a plunging head of 27.3 millimeters over a 140.8 millimeter high weir produced a Q_+ equal to 0.6793. Since this flow was relatively calm the smallest error interval for plunging head *h* was applied, $\delta h = \pm 1.13$ millimeters, and a computed value of δQ_+ resulted in a minor error of ± 0.0006.

The second computed plunging flow was selected with intent to define the maximum possible propagated error interval or worst case scenario. For this case, WA30-045 was selected to reflect a highly turbulent flow structure and a head of 139.2 millimeters over a 140.8 millimeter high weir crest was recorded. Computations performed in a similar manner to the previous calculations, with the exception of $\delta h = \pm 3.62$ millimeters to reflect the highly turbulent flows, produced values of $Q_+ = 0.7392 \pm 0.0019$. From these computed results it is evident that for the modeled plunging flows and the data collection methods, the values of dimensionless parameter Q_+ are accurate to at least three decimal places.

The second dimensionless parameter, which has been derived to quantify streaming flow regimes, can be rewritten from Equation 7 as:

$$C_f = \frac{2gS_o}{U^2}d \qquad 26)$$

where:

C_f = coefficient of fluid friction

U = depth averaged velocity

To determine the propagation of error for the coefficient of fluid friction C_f, a propagation of error analysis for the depth-averaged velocity must first be determined. Since the intent of this exercise is to determine the maximum and minimum error interval associated with C_f, two vastly different streaming flows that will produce very small and very large error intervals with respect to the depth averaged velocity were selected. Flows WD05-165 and WD30-015 were chosen to reflect the best and worst cases respectively.

The first streaming flow, WD05-165, was the result of very narrowly spaced weirs, a flat slope and large discharge. This arrangement and discharge produced a fairly smooth water surface and a relatively uniform streaming flow. From the experimental measurements, a streaming depth *d* was recorded to be equal to 155.1 millimeters. By setting $\delta Q = \pm 0.31\ L/s$, $\delta b = \pm 0.50\ mm$, $\delta d = \pm 0.56\ mm$ and performing an propagation of error analysis, the depth averaged velocity

U = 1.90 ± 0.0079 m/s.

The second flow, WD30-015, was selected for this steep experimental arrangement produced a shallow streaming flow and highly turbulent water surface. For this situation a streaming depth of 20.7 millimeters was measured. By setting $\delta Q = \pm 0.09\ L/s$, $\delta b = \pm 0.50\ mm$ and $\delta d = \pm 2.55\ mm$ the depth averaged velocity for this flow was equal to 1.29 ± 0.16 m/s. It is evident form these two different streaming flows that the range of permissible error for the depth averaged velocity ranges from approximately ± 0.0079 to ± 0.16 m/s.

With the probable velocity error intervals determined for the two framing flows, these values were then used to determine the expected maximum and minimum error intervals for the coefficient of fluid friction C_f. For the best case scenario, (i.e. flow WD05-165) the coefficient of fluid friction $C_f = 0.042 \pm 0.0004$ was determined by setting

$d = 155.14 \pm 0.56$ mm, $U = 1.90 \pm 0.008$ m / s and $S_o = 0.05$. Likewise, for the worst case streaming flow WD30-015, the input variables $d = 20.73 \pm 2.55$ mm, $U = 1.29 \pm 0.159$ m/s and $S_o = 0.30$ yielded a coefficient of fluid friction $C_f = 0.0731 \pm 0.0201$.

From this propagation of error analysis, the error for the coefficient of fluid friction C_f can at worst only influence the value of the second decimal place of the computed fluid friction value. Since these error intervals are not significantly large, the physical methods used to collect the experimental data was acceptable for all the streaming flows.

The third and last dimensionless parameter, expressed earlier as Equation 10, has been proposed to quantify the transitional flows that occurs between the plunging and streaming regimes. For this experimental study there were many flows that were classified as a transitional flow but no two were identically alike. Fundamentally, the transitional flow regime was not one distinct flow structure but encompasses many different flow patterns and variations. The following section in this chapter will address the complexities and sub domains of the transitional flow regime. For the purpose of error propagation in Equation 10, the experimental arrangement WB15-035 was selected. By setting $b = 560 \pm 0.5$mm, $L = 335 \pm 0.5$mm, $Q = 35 \pm 0.09$L/s and $S_o = 0.15$ the dimensionless parameter Q_t and error interval was determined to be 0.686 ± 0.005. For the majority of the transitional cases the experimental discharges were within the 15 to 45 liter per second range, and WB15-035 does accurately represent this case. Error propagation analysis for two different flows WB15-010 and WB15-165 were computed in addition to the typical transitional flow for the following two reasons. One was to set a range of the error intervals for this physical arrangement even though the flows were plunging and streaming respectively. The second was to determine what errors should be expected when Equation 10 was solved for all experimental flows. For WB15-010 and WB15-165, the dimensionless parameters were computed and the results were $Q_t = 0.196 \pm 0.002$ and $Q_t = 3.235 \pm 0.021$ respectively. The error intervals associated with these three flows do not significantly effect the values of computed dimensionless discharges and since a large range was addressed this suggests that all other error intervals should not deviate drastically from these results.

The last portion of this section shall address the propagation of error and error intervals that occur when the pitch probe and manometer apparatus were used to determine the centerline vertical velocity profiles in the studied pool and weir arrangements. The task of quantify the error in measuring a velocity is unlike the previous situations for there are not only many sources of errors, but the error intervals associated to these errors are difficult to determine if at all. The size of the pitch probe, the horizontal and vertical configuration, the manometer readings and the angle of attack were four sources of error that were undoubtedly present but very difficult to quantify. Another source of error equally as difficult to estimate was the location of the zero shear line or the elevation of zero velocity. This point was difficult to locate for the pitch probe would straddled the rapidly oscillating and fluctuating flow at the center of a flow cell. It was this continually changing flow that directly alters the velocity profile and introduces a continuity error in all bi-directional vertical velocity profiles.

Even though the sources of error presented here were indeed evident, the limitation that exists was not only in determining what values should be assigned to the associated error intervals but how to determine the weight of each error and the binding relationship that will result in an overall propagated error interval. It is because of these restricting limitations and until future studies define these bounds and relationships, nothing more than mentioning this problem shall be presented in section.

2.4.5 Error Analysis Summary

The error analysis revealed that the physical methods used to collect the data for this experimental study did introduce measurable errors. However, the propagated errors were not significant enough to drastically influence the values of the computed dimensionless parameters used to quantify pool and weir flow regimes.

In review, the propagation of error analysis for plunging head *h* and streaming depth *d*, resulted in the following low, medium and high turbulence error intervals:

Low Turbulence:	$\delta h = \pm 1.2$ mm	$\delta d = \pm 0.6$ mm
Medium Turbulence:	$\delta h = \pm 1.6$ mm	$\delta d = \pm 1.2$ mm
High Turbulence:	$\delta h = \pm 3.6$ mm	$\delta d = \pm 2.6$ mm

These plunging head and streaming depth error intervals were then in turn used along with other physical and geometrical confidence intervals to compute the propagated errors for the plunging, streaming and transitional parameters. For the three regimes, plunging, streaming and transitional, the maximum calculated errors, δQ_+, δC_f and δQ_t were ±0.002, ±0.02 and ±0.02 respectively.

2.5 Experimental Observations

2.5.1 General

From this experimental study of pool and weir fishways a significant quantity of physical data were collected, studied and analyzed, and will be presented in the following chapter. Although the quantitative values resulting from this research project will ultimately provide designers with construction guidelines and references, the true essence or feel of the non tangible flow characteristics and patterns for each flow regime has not been fully expressed. By conducting the many different experimental arrangements in a continuous progression for a range of discharges, the transformation of the water surface, generally from a plunging to a streaming state, not only revealed significant sub-regimes and flow patterns but also regions of longitudinal and transverse flow instabilities.

The aim of this section is to reflect on the many observations made during this experimental study and to present the predominant and distinguishing flow patterns and characteristics that have been identified and used as flow regime classification criteria. In addition to focusing on flow structure and the transformation process from one regime to another, issues such as flow instabilities and the effects of weir height on flow regimes will also be addressed. It is felt that by expressing these qualitative observations it will be possible to convey more than just quantitative design values for pool and weir fishways.

The following six subsections will provide informative insight into what flow patterns exist in each pool and weir flow regime. However, it is highly recommended that a copy of the photographic study by Sikora, et al. (1996) should be viewed in conjunction with the following sections, for the sometimes subtle traits which are quite often difficult to describe can be more easily identified within the photographic plates.

2.5.2 Flow Regime Classification

2.5.2.1 General

Pool and weir fishways are interesting hydraulic structures, for any one of the three predominant flow regimes can occur with any particular physical arrangement and discharge. Clay (1961) was one of the first researchers to define the plunging, transitional and streaming or shooting flow regimes that may exist for this fishway design. Since then other individuals have studied the hydraulics of pool and weir fishways and have likewise arrived at the same findings. Rajaratnam, et al. (1987a) confirmed the works of Clay (1961) by observing that the entire flow spectrum can be sectioned into either plunging, transitional or streaming flows. These three regimes, plunging, transitional and streaming are indeed the major classifications of flow regimes found in pool and weir fishways. however, the study presented here has focused not only on the bounding plunging and streaming flows but the sub regimes that fall within and define the transitional flow domain. It was observed that the transitional flow regime actually encompasses several flows that can not be considered purely plunging or streaming. In an attempt to define the flows within this transitional domain more accurately, five new sub-regimes or sub-classifications have been devised based on the predominant flow patterns and water surface profiles that occur for each situation. Figure 6b through 6f graphically illustrate these sub domains. In addition to the five sub classifications of transitional flow, one additional regime which can occur prior to plunging flows was identified and termed a supercritical bed flow. The nine flow regime classifications and their abbreviations, which do not necessarily occur in this order, are as follows: Plunging (P), Plunging-Transitional (Pt), Transitional (T), Transitional-Streaming (tS), Streaming (S), Transitional-Baffle (tB), Baffle (B), Plunging Supercritical Bed Flow (*P*) and Baffle Supercritical Bed Flow (*B*). These listed flow regime classifications will be addressed separately and the predominant flow patterns which exist as well as when they are likely to occur shall be outlined in the following subsections.

2.5.2.2 Plunging Flow Regime (P)

The first regime and undoubtedly the most common has been classified as plunging flow due to the plunging jet which passes the flow from the upstream pool down over a weir and into the adjacent downstream pool. For this weir-like type of flow there are three significant flow patterns which occur in every pool or cell. In viewing Figure 6a it is evident that the plunging jet is the predominant feature and because of this diving action, two fully encompassing circulating cells have developed. The first rotating cell was located in the nape directly beneath the plunging jet. Regardless of whether the nape was self supported and air entrained or fully submerged, the cell within always maintained a clockwise rotation. The second significant cell was positioned near the surface immediately downstream of the point where the plunging jet poured into the pool. This counterclockwise surface rotating cell behaved similarly and closely resembled the flow patterns and structure found in a hydraulic jump. For low discharge conditions the length of the surface circulating cell, as shown in Figure 15a, tends initially to be fairly small and isolated. Both of the two rotating cells were typically uniform across the width of the flume and varied in length depending on the physical dimensions of the pool, the discharge and the slope. Figure 6a and Plates 1 through 3, accurately illustrate the flow patterns and structure as well as the water surface profile typically found in a plunging flow regime.

Besides the three significant flow patterns, plunging jet and two rotating cells, there were other subtle less obvious flow characteristics that are equally as important. The point where the plunging jet impinges against the bed of the flume was one of these less pronounced characteristics. This quasi-stationary point, as referenced by a hollow arrow on Figure 6a, alone has little importance but to designate a point of positive and negative flow. However, by observing where this point was with relation to the length of the pool *L*, insight into how the flow patterns will change to accommodate a variation in discharge can result.

Another interesting feature was the point of bifurcation located at the surface immediately upstream of the downstream weir. This point of surface bifurcation, denoted also by a hollow arrow on Figure 6, does not remain stationary for a range of discharges but assumes a constant position depending on the state of the regime. For all plunging flows the location of the point of bifurcation must reside upstream of the weir. This criteria was set forth because in some instances the only difference between a baffle flow and a distorted plunging flow, was that the point of bifurcation. The point of surface bifurcation (maximum water elevation) for a baffle flow can occur downstream of the weir. Figure 13e illustrates this situation.

By focusing on this surface disturbance, it is obvious that the plunging jet entering the pool is redirected initially along the bed of the flume and then upward towards the surface. This upward flow can and often does elevate the water surface just prior to spilling over the weir, but in either case the maximum head elevation h, always occurs at or near the point of bifurcation. In addition, the boil-like surface disturbance was not only a quick reference for the point of surface bifurcation, but a real indicator that the flow being passed over the weir or back upstream does not support a two dimensional flow assumption. Section 2.5.3

will shed more light on this issue of surface and bed bifurcation points of flow and their transformation with increased discharge.

As for when plunging flows are most likely to occur, the four parameters, discharge, pool length, slope and weir height do indeed influence what type of flow regime will occur, but it is the discharge, pool length and slope, in this order that influence the plunging flow regime most significantly. It is important to note that not any one of these parameters will produce a plunging state but it is the combination of these three parameters that will determine if and to what extent a plunging flow will exist. For this experimental study plunging flows were commonly observed for lower end discharges, 5 to 45 liters per second, A, B and C weir spacings and for all five slopes, 5, 10, 15, 20 and 30 percent. As a general rule, plunging flows can be expected to occur for small slopes and narrow weir spacings if the discharge was likewise reduced to prevent the transformation of a transitional flow. The corollary to this statement also holds true for if a larger flow was to be displaced and a plunging regime was desired, the weir spacing and or the slope must also be increased. It was observed from this experimental study that although the increased slope of the fishway does prevent the transition from plunging to a transitional flow, it was much less effective than increasing the length of the pool. Generally the rate of which the flow transformed from a plunging to a transitional state was indirectly proportional to the weir spacing. Plates 1 and 2 both illustrate a plunging regime, however, it was evident that the distance between the weirs directly effects the structure within the pool and subsequently the rate of change. An excellent example to emphasize this point was that, for a WA05-005 arrangement, a plunging flow was observed whereas for a narrower weir spacing, WD05-005, there was no evidence of a plunging flow and fully developed streaming state existed. Tables 7, 8 and 9 summarize the range over which plunging flows existed for each of the four geometrical parameters.

2.5.2.3 Plunging-Transitional Flow Regime (Pt)

The second flow regime was classified as plunging-transitional flow, a sub-set of the transitional regime classification, and shares some resemblance to the plunging regime. However, there are significant differences in the flow structure and the water surface profiles. The deviations from the true plunging state are as follows. The surface roller, unlike previously observed for plunging flows, was relatively quite small and was drawn closer to the surface. The second predominant roller located in the nape expands downstream to a point of approximately one half the weir spacing. If this circulating cell did exceed the mid point between the weirs the flow became unsteady and the plunging jet no longer capable of penetrating to the bottom of the pool was diverted back upward and confined to the surface strata. Subsequently a full pool length clockwise circulation occurred. Figure 9d illustrates the unsteady flow patterns that exist at this point of transformation. After closer observations it was evident that this plunging-transitional regime occurs at, or shortly after, weir submergence.

Another significant difference attributed to the plunging-transitional state and a direct result of the elevated plunging flow was the deviation from the flat water surface profiles typical of plunging flows, to an undulated and curved water surface. Furthermore, the point of surface bifurcation, if it existed, had been forced downstream to a location just before where the approaching flow spills over the weir crest. It can be deduced from the photographs and observations that the redirected plunging jet was the major contributor and influenced these new water disturbances and undulated water surface profiles. Figure 6b and Plate 4 illustrates the typical flow patterns and water surface profiles for plunging-transitional flows.

In all observed instances the plunging-transitional regime occurred sequentially after a true plunging flow and was directly the result of an increase in discharge. Although this was indeed the observed progression trend, not all geometrical arrangements initiated a plunging flow and transformed into a transitional state or what has been termed a plunging-transitional flow. For this experimental study the plunging-transitional state did not occur for the 'A' class weir spacing, L/p = 4, but did follow the plunging regime for the 'B' and 'C' class weir spaces, L/p = 2 and L/p = 1 respectively. Explanation for the absence of the 'A' class plunging transitional flow was due to the exceedingly long pool length and the development of a transitional-baffle or baffle flow regime. This divergence of flow patterns strongly emphasizes that the pool length was an important variable for flow regime development in pool and weir fishways and can be as significant as the discharge.

2.5.2.4 Transitional Flow Regime (T)

The third flow regime category deemed as a transitional flow gained this classification because it does not strongly resemble the preceding plunging flow characteristics or the streaming attributes of a fully developed streaming flow. It a true sense, this flow or the flow patterns observed for this situation, reflect a transitional state and can be described as a superposition of the two extremes. The dominant flow patterns for a transitional regime were the large full cell counterclockwise rotating cell, the elevated, once plunging, jet and the absence of the surface bifurcation point. Figure 6c and Plate 5 both illustrate the general flow patterns and water surface profiles for this transitional regime classification. Generally, a transitional flow was the result of an increase in discharge and the stepwise progression from a plunging-transitional flow regime. As a result of this increase in discharge, the flattened trajectory of the plunging jet as identified in a plunging-transitional flow now introduces a significant wave formation to the water surface. Figure 11c accurately illustrates this wavy surface strata flow and the potential for momentum transfer into the underlying cell. Focusing on this figure it is interesting to note that the sinusoidal water surface reflects the separated surface flow and a predominant, fully supported, air-filled nape.

Another important characteristic with regards to the wavy water surface is that it was not restricted to one set profile and, as a consequence, this transitional state was often highly unsteady and non uniform across the width of the flume. The stability observations outlined in Appendix B for the experimental arrangement WB05-010 accurately detail and provide insight into the three dimensional flow patterns for steady transitional flow regimes.

For this experimental study it was observed that the transitional flow regime was generally restricted to the three shallowest slopes, 5, 10 and 15% and occurred for weir spacings that were narrow enough to resist baffle flow patterns but spaced sufficiently to prevent the initiation of a transitional-streaming or streaming flow. Generally transitional flow were the result of a 'B' or 'C' class weir spacing or smaller, L ≈ 2p and L ≈ 1p respectively. Because of these geometrical parameters an increase in discharge or decrease in slope would therefore initiate a transitional streaming flow and ultimately a streaming flow regime. The transitional flow regime did not occur for the 'A' class weir spacing, for this geometrical arrangement provided suitable conditions for the dominant baffle like flow characteristics to exist immediately after the initial plunging state.

2.5.2.5 Transitional-Streaming Flow Regime (tS)

Transitional-streaming flow, as the name suggests, was a transitional flow regime that in part resembles and reflects the flow patterns of a fully developed streaming flow. In a general sense, a transitional-streaming flow regime posses the clockwise circulating cell and the overriding surface flow similar to the streaming regime. However, influences from the transitional state still exist and are unmistakably present. The dominant flow characteristics of this classification are as follows.

Even though the overriding streaming flow and the fully rotating cell exist for this regime classification they are not fully developed and as a result the water surface remains in a discontinuous state and displays standing wave formations. The significant difference in particular from a transitional flow and the transitional-streaming flow was that the boundary or separation line between the coarsely streaming flow and the circulating cell can now be visually discerned. In addition, the bifurcation point due to the plunging jet had progressed downstream and, if it occurred at all, this point of impingement was positioned against the upstream face of the downstream weir. The absence of this feature indicates that the flow passing from one pool to another did not penetrate the flow between the weirs but passed overhead and reasonably parallel to the bed. Figure 6f as well as Plates 11 and 12 illustrate these dominant flow patterns and characteristics.

An interesting trait with regards to the clockwise rotating cell located between the weirs was that the center of this cell did not necessarily occur at the geometric centre of the pool. Photographs taken of this transitional-streaming state reveal that the center of the circulating cell was initially forced downstream and parallel to the bed due to the driving surface jet. With an increase in discharge the overriding flow follows more closely a parallel path with respect to the bed of the flume and the origin of the rotating cell migrated upstream to the geometric centre between the weirs. Typically, when the centre of rotation reached this end state and the water surface streamlines become parallel and continuous, this signified the onset of the fully developed streaming flow regime. Figures 10d, 10e and 10f illustrate the location of the center of rotation and its position with an increase in discharge.

Experimental observations revealed that transitional-streaming flows occurred favorably for weir spacing B, C and D ($2 > L/p > 0.5$) but not for 'A' class spacing because the available discharge and flume depth were insufficient to proceed past the 'A' class baffle-like flows. As for the discharge required to produce a transitional-streaming flow, this was highly dependent on the weir spacing and slope. Generally, transitional-streaming flows occurred for smaller discharges if either the slope or the weir spacing were also reduced. Likewise, if the slope and or the weir spacing were increased, the discharge required to produce a transitional-streaming flow would also be greater. For the 'B', 'C' and 'D' class spacing and for 5 and 30 percent bed slopes, transitional-streaming flows occurred for discharges ranging from 25 to 65, 10 to 25 and 2.5 to 5 liters per second respectively.

The height of the weir was one experimental variable that did not appear to have a substantial influence on the occurrence of the transitional-streaming flow for any one comparable slope and weir spacing. This observation was considered reasonable for although the weir height varied from approximately 140 to 70 millimeters (full and 1/2 weir heights respectively) no small sill-like obstructions, or conversely no tall weirs were studied. Tables 7, 8 and 9 can be viewed for tabular information with regards to the occurrence of the transitional-streaming flow with respect to the four geometrical parameters, discharge, weir spacing, slope and weir height.

2.5.2.6 Streaming Flow Regime (S)

The fifth flow regime to be identified has been classified as a fully developed streaming flow. This flow regime, perhaps the second most common flow condition other than plunging flows, has gained its description because the predominant streaming overhead flow that transports the majority of incoming water over the underlying weirs. For all streaming flows encountered in this experimental study, calculations have revealed and confirmed that the surface streaming flows are supercritical.

The second dominant flow pattern observed for this flow regime was the fully uni-rotational cell that encompasses all area between the weirs. This rotating cell of water can be compared to or described as a horizontally aligned vortex that has sufficient rotational velocity to trap and contain air entrainment. Photographic Plate 13 shows quite clearly the two distinct and dominant flow patterns as well as the air entrainment that is captured within the streaming flow and the underlying circulating cell. With regard to the centre of rotation within the rotating cell, there appeared to be some variance to the exact locations as expressed in the previous section describing transitional-streaming flows. From experimental observations, the origin of rotation appears to be initially located within the proximity of one quarter the pool length upstream of the downstream weir. As the discharge increases, this point of central rotation progressed upstream to roughly the geometric centre between the two weirs. In addition, the slope of the fishway appears to influence the location of this origin of rotation. Observations revealed that as the slope of the fishway was increased, the centre of the cell was forced further downstream and larger discharges were required in comparison to smaller slopes to cause a shift to the geometric centre. Figures 8e and 8f illustrate this initial offset of the origin of rotation and the final central location.

As for when streaming flows are expected to occur, this was dependent on the discharge, the slope and the weir spacing. Fundamentally, streaming flows occurred after all other flow regimes and for all weir arrangements and slopes if sufficient discharge was available. Generally the discharge required to initiate a streaming flow was indirectly proportional to the combination of the length between the weirs and the slope of the arrangement. For example, it was virtually impossible to produce any flow regime other than that of streaming flows for 'D' class weir spacings, $L = 0.5p$, and 5 through 30 percent slopes. Whereas, on the other end of the spectrum, massive volumes of water would be required to produce a streaming flow for a 'WA30' arrangement. Figure 12f illustrates one of few 'A' class experimental arrangements, WA05-165, that was conducive to a streaming flow regime. As a rule of thumb, streaming flows were best suited for narrow weir spacings, for 5 to 30 percent slopes and for discharges ranging from 65 to 165, 15 to 45 and 5 to 15 liters per second for 'B', 'C' and 'D' class weir spacings, respectively. Figure 6g as well as Plates 13 and 14 illustrate the flow patterns and diversity of streaming flows observed in this experimental study.

Reflecting on the reasoning for conducting this research, which was to further the understanding of pool and weir fishways, the question of practicality also must be addressed when selecting a suitable streaming flow design. Although 'D' class weir spacings gave essentially exclusively streaming flows, the limited space between the weirs produces mainly vertical flow conditions within the cells and minimal rest areas for the staging fish. As a result only weir spacings within the range of $2 > L/p > 1$, or nominally

'B' and 'C' class weir spacings, should be considered for streaming flows. Another fundamental problem that might occur with the streaming flow regime is the issue of flow direction and fish orientation. Collins and Gillis (1985) addressed this issue of fish orientation and postulated that the streaming flow regime, with its uni-directional rotating cell, may cause the fish to face downstream when residing in the lower portions of the cell and thus directing the fish downstream rather than upstream. These concerns may not be significant for slopes less than 15% and for larger more robust fish such as Sturgeon. However, for smaller fish and steeper slopes this issue becomes apparent and merits consideration.

2.5.2.7 Transitional-Baffle Flow Regime (tB)

The transitional-baffle flow regime as shown in Figure 6d shares some resemblance to the transitional-plunging flow regime: However, the maximum spacing between the weirs and the increased discharge produced a distinct flow regime. For this experimental study, transitional-baffle flows occurred exclusively for full weir height 'A' class, $L/p \approx 4$, weir spacings and discharges greater than that required to maintain plunging or plunging-transitional flows. Like other flow regimes, the slope of the flume directly influenced the required discharge needed to initiate or overcome the threshold of this regime. To provide a simple relationship, larger discharges would be required to initiate a transitional-baffle flow for steeper experimental arrangements. For this experimental study, discharges ranging from 35 to 65 liters per second were required to produce this transitional-baffle flow.

The dominant flow patterns observed for the transitional-baffle flows were as follows. The circulating cell located within the nape or beneath the plunging jet was substantially larger than what would be found in preceding plunging or transitional-plunging flows. The point of jet impingement or flow bifurcation located on the bed of the flume was extended downstream to the midpoint between the weirs. As a result, the now subsurface plunging jet proceeded downstream parallel to the bed and, as it approached the downstream weir, it was immediately redirected upward, thus, distorting and elevating the water surface. The slope as well as the discharge controlled the severity of this vertical motion and likewise the boil-like deformations visible in the water surface. For the vast majority of transitional-baffle flows, unlike plunging flows, the maximum water surface elevation was recorded downstream of each weir. In addition to the elevated and displaced water surface, transitional-baffle flows were characterized by the extension of the plunging jet downstream into the receiving pool. This point of plunging jet re-entry, as designated by a hollow arrow on Figure 6d, generally occurs within the central region of the pool and was the result of the arrangement geometry or more specifically the substantial approach velocities and the reduced angle of trajectory. Another significant flow characteristic of the transitional-baffle flows and also the direct result of the elongated plunging jet was the size and location of the surface roller. The surface roller as seen in Figures 6d, 14d and 15d was considerably smaller in size compared to a preceding plunging flow and in addition it was forced further downstream and closer to the surface. Experimental arrangement WA15-065, as captured in Plate 6, was an excellent example of a transitional streaming flow for two circulating cells, the large plunging jet and the vertical directed flow were easily discerned and identified.

2.5.2.8 Baffle Flow Regime (B)

With an increase in discharge, the transitional-baffle flows as previously described, transformed into what were classified as fully developed baffle flows. Since this regime was essentially the next progression step after the transitional-baffle regime, the dominant flow patterns were essentially slight deviations of the previous state. One significant difference with regards to the flow patterns, was the location of the plunging flow bed impingement point. This point as illustrated in Figure 6e was positioned downstream of the midpoint between the weirs. This differs from the transitional flows and 'B' class weir spacings for flow stability could be achieved instead of the plunging jet being directed upward and over the weir. In addition, the development of a large clockwise rotating cell had formed and completely encompassing the area in-between the weirs. Another distinct flow characteristic was the reduction and / or the deletion of the surface roller. As illustrated in Figure 6e and Plate 7 the surface roller, if it existed at all, was isolated to the tail end of the pool and was often nothing more than a small reversal of flow due to the steep inclination of the water surface.

Generally all baffle flows as illustrated in Plates 7 and 8 were comprised of a highly turbulent body of water that proceeded downstream in a continuous curved or serpentine like fashion. In a broad sense, the observed baffle flows were really nothing more than supercritical flows that were contorted and reshaped by the widely spaced weirs. Plates 7 through 10 illustrate that the baffle like flows had significant approach velocities and as a consequence the flows were deflected off the weirs, through the air, and back into the downstream pools. In some instances where steeper slopes or large discharges were studied, the baffle flow was observed to leap completely free from one weir, over the adjacent downstream pool and come into contact within the second downstream pool. Plate 10 and Figure 16f illustrates this leaping effect.

It was also observed that not all baffle flows were uniform throughout the width of the flume. Situations have occurred where the flume width appeared to be divided almost equally into four parallel sub channels or longitudinal lanes. In each one on these four sections the water surface profile and flow patterns appeared to be identical, however, the first and third lane were in phase while the second and the fourth were out of phase or transposed downstream by one pool length. This non uniformity has been graphically illustrated in Figure 15f.

*2.5.2.9 Plunging Supercritical Bed Flow Regime (*P*)*

Plunging supercritical flows as the name suggests were simply plunging flows that have short sections of supercritical bed flow immediately downstream of the plunging jet. This flow regime was not common in this experimental study for it occurred for situations where the head drop between two adjacent weirs was greater than the weir height. Or, in other words, the backwater curve from each weir could not reach the base of the upstream weir, thus, this structure was not able to provide a pool for the plunging jet to diffuse into. Supercritical plunging flows were observed during this experimental study for only one full weir height arrangements, Figure 16a, and for the entire 3/4WA20 and 1/2WA10 geometric arrangements. The dominant flow patterns for this regime, other than the supercritical bed flow, was the distinct hydraulic jump at the toe of the pool as well as the accompanying surface roller. Figure 6h and Plate 15 illustrate this flow regime and the flow patterns within.

An interesting note with regards to the length of the supercritical flow was that it was dependent on the approach velocity of the plunging jet as well as the slope of the flume or more specifically the point where the downstream water level intersects the with the flume bed. By studying the mosaic of the water surface profiles of the 1/2WA10 and 3/4WA20 arrangements, located in Appendix A, it was obvious that the toe of the hydraulic jump for all modeled discharges occurs at or near this point of intersection. It was therefore the discharge, or more specifically the horizontal component of the plunging jet, that determines the length of the supercritical flow.

*2.5.2.10 Baffle Supercritical Bed Flow Regime (*B*)*

Supercritical baffle flows are very similar to the previously-described plunging supercritical regime and for all intents and purposes they both can be lumped into one supercritical regime classification. The reason why this class was proposed was because, as the slope of the flume was increased, the pools perched by the downstream weirs had become significantly smaller and the initial length of the supercritical flow was greater than half the pool length. In addition, as the discharge was increased, the observed flow patterns such as the length of the nape and the trajectory angle of the plunging jet, were more representative of baffle, or sill-like flows, rather than plunging flows.

Photographic Plate 16 illustrates the long reach of supercritical bed flow as well as the baffle-like ramping effect which forced the supercritical flow over the short weirs. The water surface profiles for experimental arrangements 1/2WA15, 1/2WA20 and 1/2WA30 as well as 3/4WA30 (which are illustrated in Appendix A) reflect the same characteristics with regards to the length of supercritical flow and the positioning of the toe of the hydraulic jump as expressed in the previous section.

2.5.3 Transformation of Flow Regimes with Increasing Discharge

The previous section of this thesis addressed what flow regimes and dominant flow patterns were observed for many different pool and weir geometric arrangements. The order in which these flow regimes were presented reflects, more or less, the overall progression of the initial plunging flow regime passing through a transitional phase and into a final state of streaming flow. However, there was little reference to the key indicators or flow patterns that provide insight into not only what will be the following regime but when, in a general sense, it will occur. The aim of this section is to outline the significant charges in flow patterns as one regime transforms into another as well as the order of observed flow regimes in response to an increase in discharge.

This experimental study confirmed that all geometrical arrangements will essentially proceed from a plunging regime to a streaming state, and it was the physical parameters such as discharge, pool length, slope and sometimes weir height that effect the rate of transformation as well as what flow regimes will occur within the transitional range. From this research project it was evident that the discharge and pool length were the two significant parameters that influenced what type of flow regimes were to occur. It is important to note that, although the slope was a critical parameter, its function was not necessarily influential on what type of flow regime would occur. However, it affected the rate of which one regime transformed to another. Figures 7 through 16 show the effects of the slope on both 'A' and 'B' class weir spacings.

This experimental study revealed that there are essentially two different routes or schematic paths that can be taken to transform a plunging flow into a fully developed streaming flow. These paths were characteristically different, for the sub-flow regimes within in the transitional regime were controlled by the pool length. For 'A' class weir spacing, $L/p \approx 4$, baffle like flows were observed whereas for 'B', 'C' and 'D', $L/p \leq 2$, a transitional flow as illustrated in Figure 6c proceeded after the plunging-transitional state. To summarize, for 'A' class weir spacings the observed flow regime progression started with a Plunging regime and then transformed into Plunging-Transitional, Transitional-Baffle, Baffle, Transitional-Streaming and, ultimately, into a fully-developed Streaming flow, in this order. For experimental arrangements 'B' through 'D' the observed flow regimes in order of occurrence were; Plunging, Transitional-Plunging, Transitional, Transitional-Streaming and, finally, Streaming. Figure 6a through 6h illustrate the dominant regimes that were observed for both of these cases.

Aside from the two distinct paths of regime transformation listed above, the issue of supercritical bed flow as described in sections 2.5.2.9 and 2.5.2.10 should be addressed. From this experimental study it was revealed that for geometric arrangements where the length was approximately eight times the length of the weir height, $L/p \approx 8$, and the slope was sufficient to prevent the receiving pool from reaching the base of the upstream weir, supercritical bed flows occurred. For these situations, experimental observations suggest that the flow patters would slowly transform from the supercritical state, through a highly turbulent baffle-like regime and ultimately to a state of streaming flow. Since these flow patterns are the result of extreme geometric arrangements and the flows observed would be in no possible way suitable to fish transport, little more than identifying their existence shall occur within this section. The remainder of this section will address the significant flow patterns for the full weir height, (L/p ≤ 4) arrangements and provide insight of how these regimes change to accommodate an increase in discharge and a change in slope .

After studying the many photographs and diagrams produced from this experimental study the progression from plunging to streaming flows initially appeared to quite complex and the result of many different flow patterns. By observing these flow patterns in a macro field of view, instead of at a micro scale, it became evident that all the identified flow regimes, different as they may be, share one common flow pattern. This characteristic, the jet of water passing over the weir, initially starts out as a plunging jet and in response to an increase in discharge its curvature will transform until it approaches its final linear state as a streaming surface flow. In fact, the point where the plunging jet impinges against the bed of the flume, the point of flow bifurcation or point of stagnation, was a key indicator of how advanced or at what stage the observed flow regime was in. Explanation to this concept is as follows.

Initially, for plunging flows, the point of jet impingement (as indicated by the hollow arrow beneath the bed in Figure 6a) was within the upstream one quarter of the pool length. As the discharge was increased, the upstream head and approach velocity became greater therefore transposing the point of impingement further downstream and increasing the size of the nape. The rate at which the point progresses downstream was influenced, not only by the discharge but, also, by the slope of the channel. When the slope was increased, the bifurcation point migrated upstream. Thus, larger discharges would be required to remain at the same stage of plunging flow as for a milder slope arrangement.

With another increase in discharge the curvature of the plunging jet was reduced and the point of impingement was forced further downstream. It was observed that when the point of jet impingement was within the second upstream quarter, the elongated nape and reduced surface roller was representative of the plunging-transitional flows. Plunging-transitional flows generally occurred until the point of jet bifurcation was transported downstream to roughly the mid point between the weirs. It was at this central location where the pool length became an important parameter, for either transitional flows or baffle-like flows would occur depending on the weir spacing.

For 'B' class or smaller weir spacings, the advancement of the plunging jet, with only a few exceptions, resulted in what was deemed as a transitional flow. It was observed that as the point of bifurcation entered the lower half of the pool, the plunging jet now had an extended alignment that resulted in the reduction of the surface roller as well as the rapid increase of the roller located in the nape. With an additional increase in discharge it was observed that the plunging jet was unable to constantly penetrate the pool and as a consequence the backwater effects and the altered flow structure elevated the plunging jet upward. Figure 9d illustrates this transitional range where the flow structure was unsteady and continually changing from the transitional flow regime to the initiation of a transitional-streaming regime.

As a result of another increase in discharge the now elevated plunging jet no longer divided the pool into two equal circulating cells. The surface roller ceased to exist whereas the cell originally located in the nape of the plunging flow now encompassed the entire pool length. Figures 6c and 6f illustrate this transformation from the transitional to the transitional-streaming flow regime. From this point forward additional increases in discharge transformed the transitional-streaming flow into a fully developed streaming flow regime. Figures 7 through 11 illustrate and summarize this shift from plunging to streaming flows for 'B' class and narrower weir spacings.

For 'A' class weir spacings, unlike the narrower spaced arrangements, the longer pool length provided sufficient distance to initiate baffle-like flows. When the point of bifurcation of the plunging jet reached the centre of the pool, the circulating cell within the nape had extended downstream to roughly the mid pool length. Figure 6d illustrates the growth of the nape roller as well as the reduction of the surface roller. An additional significant observation at this stage was that the flow passing through the pool has considerable momentum and the structured energy dissipating pool typical of plunging flows did not truly exist. As result there were essentially no low velocity holding areas suitable for fish staging and rest other than the area within the nape.

With another incremental increase in discharge the point of jet impingement progressed downstream to within the half and three quarter pool length portion of the pool. The flow structure observed for this situation was drastically different than the 'B' class and smaller weir spacing experimental arrangements, because flow stability as a baffle flow could be achieved. This stability was attributed to the fact that sufficient pool length was available. Consequently the plunging jet did not impinge against the downstream weir causing a flow reversal and a full pool length circulating cell. As the discharge was increased once again the point of impingement of the plunging jet moved further downstream. Once the point of impingement proceed past roughly the three quarter pool length mark, instabilities, flow reversals and regime transformations occurred as described for the 'B' class and smaller weir spacing arrangements. Typically, the flow became highly turbulent and unsteady for this condition and marked the transition from the baffle regime to the transitional-streaming flow regime. Examples of this change in state have been captured in Figures 13f, 14g and 15f.

Once the transitional-streaming regime became established it was only a matter of increasing the discharge sufficiently to produce the fully developed streaming regime as shown in Figure 12f. Figures 12 through 16 have been constructed to illustrate the progression of plunging flow through the baffle flow regime and onto the final streaming flow regime. In addition, these figures captured the rate of change of these flow regimes due to the different modeled slopes for the 'A' class weir spacings.

An interesting note with regard to the transformation of flow regimes for different geometric experimental arrangements was that the transformation process for scaled versions of test runs produced identical flow transformation processes. For instance, the arrangement classes WA05 to WA30 and 1/2WB05 to 1/2WB30, both shared L/p ratios equal to 4, however, the scale that they were constructed to were truly 1:11 and 1:22 respectively. By reviewing the recorded water surface profiles as well as the photographs for these two arrangement classes, it was apparent that the same flow regime progressions occurred. The only difference between the two of these arrangements was the scaled discharge required to produce the associated flow. Based on Froudian modeling criteria the 1:11 size arrangement would require 5.66 times the discharge as for the 1:22 model in order to produce similar flow regimes. This discharge ratio appeared to be representative of the rate of transformation.

Before closing this section on flow transformation, it is important to note that the transformation processes as a result of changing the discharge was observed for both increasing and decreasing flow rates. A test conducted for repeatability revealed that, even though some flow regimes were sensitive to increasing or decreasing flow set up conditions, after sufficient lengths of time, it was irrelevant which approach was taken for regime convergence eventually occurred.

2.5.4 Stability

In addition to recording observations focusing on flow regime classifications and transformation characteristics, stability observations, or more specifically, flow regime instabilities were also noted. The stability observation portion of this study was conducted in parallel with the data collection of water surface profiles and photographs. The only difference was that the discharges monitored were not only those which were recorded for the water surface profiles and photographs. For all intends and purposes, if only the set 10 or 12 discharges were observed for each arrangement, only singular points of flow instabilities would be recorded. In order to conduct a more thorough investigation, the discharge through the flume was increased initially in small steps so that the regions of unsteady flow could be determined rather than just isolated to one point. Generally, the flow instabilities detected in this study were the result of longitudinal surges or transverse waves and were typically isolated to discharges less than 35 liters per second. Therefore 35 liters per second was roughly the limit of fine incremental increases in discharge and the remaining, larger increases in discharge, mirrored the water surface profile data collection portion of this study.

For each experimental arrangement and discharge being observed a time allowance of ten minutes was required so that instabilities could generate or dissipate from previous runs. This time allowance was critical since flow instabilities were observed to occur not only with respect to time but also with distance. For example, it was not uncommon for the upstream half of the experimental arrangement to be completely steady, whereas the downstream half showed evidence of longitudinal surge or transverse waves. As a result, the stability observations were a rather lengthy task to complete. Subsequently only the WA, WB, WC, WD and 1/2WA, 5 to 30 percent slope, arrangements were studied for flow instabilities. For each weir class, slope and discharge, the stability of the flow as well as detailed notes depicting the source of the instability were recorded and are presented in Appendix B. In addition to this listing, flow instabilities for all the recorded water surface profiles have been noted and added into Tables 7, 8 and 9.

From this pool and weir experimental study, observations revealed that if instabilities were to occur they were the direct result of either longitudinal surges, transverse waves or a weighted combination of the two. Explanations of why these instabilities occurred can be attributed to surface tension effects, initial flow patterns, weir height uniformity across the width of the flume as well as the shape of the weir crest (Collins and Gillis, 1985).

It is important to note that this section on flow stability does not constitute new flow regimes or flow classifications. The point being made is that flow instabilities such as longitudinal surges and transverse waves are simply flow disturbances that may be superimposed onto any one of the nine previously identified flow regimes. The following portion of this section will focus on the mechanisms and structure of both longitudinal surges and transverse waves as well as the sequences in which they occurred.

The first of the two noted causes of flow instabilities was the result of longitudinal surges. In most instances longitudinal surges initially appeared as small flushing disturbances that occur in regular periodic cycles. As the discharge was increased the return period of these surges became smaller and the severity and amplitude of these surges increased. It was only by increasing the discharge that the return period of the surges converged to zero and a steady flow was achieved or at some point in time the second transverse waves dominated the flow.

These longitudinal surges were not the result of an unsteady water supply, but it appeared that the physical geometry of the experimental arrangement permitted water to be stored within a few initial upstream weirs. When the maximum available storage was achieved this retained water was then released as a longitudinal surge. As this longitudinal surge proceeded downstream the flow structure within each passing cell changed dramatically in response to localized influx of water. Plate 24 illustrates the rapid change in flow structure that can occur in response to a longitudinal surge. Moreover, photographic plates 25 through 28 capture the effects, before and during of a longitudinal surge for both 1/2WB10-025 and 3/4WB10-020 experimental arrangements. An interesting observation with regard to the progression of a longitudinal surge was that the defining flow characteristic or mechanisms detected within the surge were constant and independent, to some degree, of the rate of return as well as the discharge being passed. Viewing Figure 17, typically what occurred was that, as the stored volume of water passed through an observed pool, the transformation process from a plunging to a streaming and back to a plunging regime occurred. The notable characteristics of this process were attributed to the ascent or straightening of the plunging jet and the downstream progression of the point of plunging jet impingement as the bulk of the surge passed by. This transformation process was remarkably similar if not identical to the process of flow regime transformation described in the previous section 2.5.3. Figures 17a through 17h graphically illustrate the reoccurring longitudinal surge cycle along with the dominant flow characteristics.

The second observed source of flow instabilities was the result of transverse waves. These transverse waves were rather unique for the progression of the two mirror image source waves were carried downstream; thus, producing the criss-cross patterns as captured in Plate 23. In Plate 23 this wave formation appeared to be similar to the standing waves observed in supercritical flows; however, this photograph only captured a instant in time and the wave formations were actually being displaced downstream. Similar to the longitudinal surge, the discharge influenced the amplitude and frequency of this transverse wave formation. With an increase in discharge the transverse wave grew in amplitude until a point where it appeared to grow dramatically or resonate. The superposition effect at the intersection of the two crossing waves would produce substantial crests or troughs. Often the troughs were large enough to expose the weirs, whereas the transverse thrust produced by the elevated crests would test the structural stability of the side walls. After this maximum wave generation point was achieved, increases in discharge would result in a decline in the amplitude until steady flows were approached or the longitudinal surges would evolve and dominate the flow.

From this experimental study longitudinal surges and transverse waves were identified as sources of regime instabilities; however, the sequence with which these surges and waves occurred was observed to be not highly structured. For some arrangements longitudinal surges initiated the unsteady flow conditions. As the discharge was incrementally increased the return period of these surges decreased to a point that the following surge occurred instantaneously. It was at this instant return period that appeared to be the limit of the longitudinal surge and initial threshold of the transverse wave. In other instances the transverse wave would be apparent for discharges less than 5 liters per second and as the discharge was increased, this wave formation would dissipate and steady flows would exist for a limited range of discharges before the initiation of longitudinal surges. It was not uncommon for a range of discharges producing transverse waves to exist within a larger set of longitudinal surges or vice versa. To complicate this attempt to define general trends of instabilities, the slope of the flume would also influence the progression and existence of these surges and waves. In a very general sense, WA experimental arrangements only experienced windows of longitudinal surges whereas the WB, WC, and WD classes encountered ranges of transverse waves and longitudinal surges for lower end discharges and discharges up to and including 35 liters per second, respectively.

In addition to the full weir height WA, WB, WC, and WD arrangements, flow instabilities were also observed for the 1\2WA set. These observations were recorded in Appendix B. The motivation behind observing this particular arrangement was to determine if longitudinal surges or transverse waves would occur for an arrangement constructed with a pool length approximately eight times the height of the weir, (i.e. L/p ≈ 8). Observations revealed that no substantial ranges of instability existed for this arrangement at any slope. A possible explanation to why no instabilities were observed can be attributed to the fact that these arrangements produced supercritical bed flows. Or quite possibly, since the half weir height arrangement was actually a 1 to 22 scale model, the range of discharges that would produce any instabilities would be scaled down 5.7 times smaller then that required for a full weir height, 1 to 11 scale model. As a result, the unsteady flows would be generated for discharges less then 6.5 liters per second and significant surface tension effects common in low discharge situations would have most likely effected or diffused the longitudinal surges or transverse waves.

Reflecting back on all the instability observations there does not appear to be any fixed sequences that can be used as a guideline or template to discern when unsteady flow windows could be expected. As a result the best that can be offered at this point is to refer to Appendix B which maps out the unsteady flows as well as the causes and severity of the instabilities.

2.5.5 Weir Height Effects on Flow Regimes

From this experimental study it was determined that the discharge, pool length and slope were three-significant physical parameters that influenced what flow regime would occur as well as the stability of the flow. In addition to these three parameters a fourth, the weir height, was also altered in attempts to determine if notable changes would result. This section addresses the alterations that occurred to the water surface profiles, flow regimes, flow regime transformation process and ranges of instabilities for all three (full, three-quarter and one-half) weir heights.

The first and most apparent observation with regards to reducing the height of the weir was the changes to the water surface profiles. When the weir height was reduced by one quarter its full height, i.e., from full to three-quarter weir height, the shape of the observed water surface profiles for similar discharges and spacings seemed to be nearly identical. Likewise as the weir height was reduced from the three quarter to half weir height, the water surface profiles remained similar with exception of being lowered vertically in response to the drop in the weir height. From the many plotted water surface profiles it was apparent that this parallel offset did in fact occur for all three weir heights.

The only exception to this observation was for the half weir height arrangements where the slope or pool length was large enough to permit supercritical bed flows and an unsubmerged hydraulic jump did form. For this case, the water surface profiles were realigned throughout the supercritical flow reaches. Figure 38 illustrates the similarities of the superimposed water surface profiles for WA10-035, 3/4WA10-035 and 1/2WA10-035 arrangements.

As for the distance that the parallel water surface profiles were transposed, it initially appeared that the unit reduction in weir height simply lowered the water surface profiles down by the same unit. However, by comparing plunging head and streaming depth data for full, three quarter and half weir height arrangements, the vertically transposed distances were found not to be all equal. From the streaming depth data, the values of the data collected tended to increase with a decrease in weir height. For example, the streaming depths for a discharge of 35 liters per second resulted in streaming depths 10 to 15 millimeters shallower for a full weir height arrangement in comparison to the half weir height arrangement. This variation in depth was fairly constant for other slopes and may possibly be attributed to errors caused by the fact that the water surface profiles for half weir height arrangements tended to be more turbulent.

On the other hand, this claim of error due to increased turbulence was not support by the plunging head data because plunging heads for three quarter and half weir height arrangements were remarkably similar. As for the full weir height, the plunging head values were roughly 25 to 35 percent larger than those required for the half and three quarter weir heights respectively. This increase in values for plunging head can be attributed to the fact that some of the full weir height arrangements were actually submerged weir flows.

After examining all the recorded data, factors such as turbulent water surface profiles and submerged weir effects appear to contribute to the variance in plunging head and streaming depth data. As for definitive answer to whether the difference in water surface elevation was equal to the reduction in weir height, from the collected data this correlation appeared to be the case.

The second objective was to determine if the weir height parameter influenced what flow regime would develop as well as if measurable changes to the flow regime transformation process would occur. By comparing the flow regimes produced for arrangements with common physical parameters, it was conclusive that the weir height was not a principle parameter in determining which flow regime would occur. In addition, for experimental arrangements that were identical with exception of the weir height, each set of experiments experienced similar flow regimes and flow regime transformation processes for comparable discharges. The only exception to this blanket statement was for arrangements that experienced supercritical flows due to half weir heights and insufficient pool depths.

The third and final issue being addressed was to determine if alterations in weir heights would effect the stability of flow. For this experimental study, detailed stability observations were made for only five groups or sets (WA, WB, WC, WD and 1/2WA). Unfortunately, since only one half weir height class was observed, comparisons revealing stability alterations for different weir heights was quite limited. By comparing the stability observations for WA and 1/2WA, no instabilities occurred for the half weir height arrangements, unlike the full weir height arrangements. This does not automatically suggest the half weir height arrangement was immune to flow instabilities, for supercritical bed flows occurred for many of the arrangements as well as the half weir height arrangement was really a half scale (1 to 22) of the WB class. This issue of a smaller scale and its effects on required flows have been presented in Section 2.5.4. As a result the effect of weir height and flow stability will remain inconclusive for there were limited comparable stability observation notes.

2.5.6 Energy Dissipation

This section on energy dissipation has been added not to analytically compute energy losses but to emphasize the effectiveness of pool and weir fishway designs as energy dissipaters. For several of the experimental arrangements unfavorable baffle and streaming flows regimes developed. These adverse flow regimes are definitely not suitable as solutions for fish transport; however, the ability of these arrangements to efficiently diffuse potential energy and remain as a steady uniform flow makes then desirable devices for energy dissipating applications. Since these observed steep slope arrangements with various weir spacings are not all that different to stepped spillway designs, it is possible that the data and photographs collected from this study could be used to enhance these such structures.

3.0 ANALYSIS AND EXPERIMENTAL RESULTS

3.1 General

This study comprised of measured water surface profiles, velocity measurements, photographs and stability observations has provided a great deal of qualitative insight into the dominant flow regimes that exist in pool and weir fishways. In addition, the order of which these flow patterns would transpose in response to an increase in discharge was studied and significant flow discerning characteristics were recorded. Besides these intangible characteristics, the physical measurements collected during this research project can be used as input data to quantitatively advance the accuracy of predicting what flow regime will occur for a range of physical structures.

The first section of this chapter will address the analytical and empirical relationships derived by Rajaratnam, et al. (1987b) that are used to predict and discern the ranges of plunging, transitional and streaming flow regimes for pool and weir fishways. The values, or more specifically the domains, of these dimensionless parameters will then be confirmed or redefined based on the data collected from this study.

The following section will address and discuss the associated finding of the velocity measurements recorded for the three plunging flows as well as the one transitional-streaming flow. Even though only four pool and weir arrangements were selected for velocity measurements, the results of this exploration has provided unprecedented insight into the shape of the velocity profiles, the regions or maximum and minimum velocities, and the direction of flow within a pool and weir cell.

The final section of this chapter will reflect on all the data collected during this research project and the findings, both qualitative and quantitative, will be presented in both tabular and graphical formats.

3.2 Flow Equations for Pool and Weir Fishways

3.2.1 General

This section addresses the dimensionless relationships presented by Rajaratnam, et al. (1987b), and confirms their applicability as well as presents and compares the computed values of these parameters based on this study's data collection.

3.2.2 Plunging Flows

Rajaratnam, et al. (1987b) proposed that plunging flows within pool and weir arrangements appeared to share similar characteristics to those observed for flows over sharp crested weirs. By combining a sharp crested weir discharge relationship (Equation 1) with the Rehboch equation (Equation 2) the dimensionless parameter for plunging flows was introduced as Equation 3.

$$Q = \frac{2}{3} b C_d \sqrt{2g}\, h^{3/2} \tag{1}$$

$$C_d = 0.605 + 0.08 \frac{h}{p} \tag{2}$$

$$Q_+ = \frac{Q}{b \sqrt{g}\, h^{3/2}} = \frac{2}{3} \sqrt{2}\, C_d \tag{3}$$

The restrictions to Equations 1 and 2 were that the ratio of plunging head over weir thickness was greater than 1.5 and the plunging head over weir height was less than 6, respectively. These parameters were met by this experimental study.

In order to confirm the applicability of Equation 3 to plunging flows in pool and weir fishways, the data collected must reflect the discharge to plunging head relationship, $Q \propto h^{3/2}$. Studying Figure 18, log Q versus log h, the discharge was proportional to the plunging head raised to the power of 1.401 for all plunging flows, slopes and weir spacings. This best fit line was computed by the method of least squares and the coefficient of determination was equal to 94.2 percent. By grouping all the large, medium and small weir spacings (A, B and C classes) and computing each individual best fit line, the values of the exponent ranged from 1.02 to 1.45, 1.21 to 1.64 and 1.40 respectively. These computed values were similar to the data computations produced by Rajaratnam, et al. (1987b) and, as a result, it is reasonable to assume that the discharge head relationship is approximately defined by $Q \propto h^{3/2}$. Therefore the dimensionless parameter, Equation 3, is a valid approximation for plunging flows within pool and weir arrangements.

For the observed plunging flows, the average dimensionless parameter Q_+ was equal to 0.68 and varied from 0.43 to 1.07 with a maximum error interval of ± 0.002. Unlike the narrow range observed by Rajaratnam, et al. (1987b), Figure 19 illustrates the variance experienced in the plot of log Q_+ versus log h/p.

By superimposing the data set collected by Rajaratnam, et al. (1987b) it appears that the previously collected data is a subset of the wider range collected from this study. It is therefore suggested that the value assigned for the dimensionless parameter Q_+ be the average of the complete data set and as a result $Q_+ = 0.65$ rather than equal to 0.61 as previously determined. Table 2 lists all the plunging flows and computed values used for this plunging flow analysis.

3.2.3 Streaming Flows

Streaming flows, unlike plunging flows, are the final flow regime to occur within a pool and weir fishway as discharge is increased. For these flow regimes which are comprised of a streaming jet passing over a circulating cell, an analytical approach was undertaken by Rajaratnam, et al. (1987b) in an attempt to derive a dimensionless parameter that could be used to define this streaming flow state. Equation 6 is the proposed discharge relationship for streaming flows, and Equation 7 is the dimensionless equivalent of Equation 6.

$$Q = b\,d^{3/2}\sqrt{g\,S_o}\sqrt{\frac{2}{C_f}} \qquad 6)$$

$$Q_* = \frac{Q}{b\,d^{3/2}\sqrt{g\,S_o}} = \sqrt{\frac{2}{C_f}} \qquad 7)$$

The data collected from the study performed by Rajaratnam, et al. (1987b) found that the discharge was proportional to the depth raised to the power of 1.5 for large weir spacings and the exponent varied from 0.72 to 1.68 with a mean of 1.2 for the smaller weir spacings. The streaming depth data collected from this experimental study as illustrated by the log Q versus log d plots in Figures 20, 21, 22 and 23 supports the previous finding of discharge to streaming depth proportionality. For the entire set of streaming flows as listed in Table 3 and illustrated in Figure 20, the discharge was computed to be proportional to the depth raised to the power of 1.4 ($Q \propto d^{1.4}$) with a coefficient of determination of 88.3 percent. For each individual weir spacing (B, C and D classes) Figures 21, 22 and 23 have been plotted to illustrate the linearity of the log Q versus log d relationship. The computed exponent for each of the three weir spacings (Figures 21, 22 and 23) was 1.62, 1.50 and 1.49 with coefficients of determination equal to 92.5, 89.1 and 93.8 percent respectively. As a result, the data collected from this study confirms that the discharge is approximately proportional to the streaming depth raised to the power of 1.5 ($Q \propto d^{3/2}$). Therefore, Equations 6 and 7 are applicable relationships suitable for streaming flows within pool and weir fishways.

In evaluating the dimensionless discharge (Q_*) for streaming flows, with the data collected from this experimental study, it was found that Q_* varied from 3 to 12. The findings produced by Rajaratnam, Katopodis and Mainali observed a larger range that spanned from 3 to 20. It was proposed that the dimensionless discharge Q_* varied with respect to L/d and Equation 8 was derived to describe this relationship.

$$Q_* = \frac{3}{2}\sqrt{\frac{L}{d}} \qquad 8)$$

By superimposing the data collected by Rajaratnam, et al. (1987b) along with the data gathered from this study it is evident by viewing Figure 24 that Equation 8 does not apply for the entire data set. It is possible that the complete set of data may be defined by two equations such that Equation 8 applies for L/d ratios greater than 5 and by another equation for the remainder of the data. This bimodal approach may work, but, the spread in the L/d data which lies over two orders of magnitude suggest that the parameter L/d may not be as significant as initially thought. Indeed, L/d may not be the appropriate parameter. From the experimental observations conducted during this study, the pool length was the most significant parameter that influenced the discharge required to produce a streaming flow regime. Therefore the idea of incorporating a length variable has validity but the combination with the streaming depth does not provide a narrow relationship. In either case, Equation 8 does not accurately represent the entire set of dimensionless streaming discharge data and as a consequence Equation 9 proposed by Rajaratnam, et al. (1987b) does not apply for streaming flows with L/d ratios < 5.

$$C_f = \frac{8}{9}\frac{d}{L} \qquad 9)$$

Another approach or attempt to create order out of the collected streaming flow data was undertaken by solving for the coefficient of fluid friction for streaming flows. Equation 6 can be rewritten as:

$$C_f = \frac{2gS_o}{U^2}(d) \qquad 27)$$

where U is the depth-averaged velocity and So is the sine slope. The underlying assumptions to Equation 27 are that the turbulent shear stress contribution to C_f, due to the interface between the circulating cell and the over riding streaming flow is much greater than the side wall friction components estimated as $C_f = f / 4$ (where f is the friction factor) and the hydraulic radius can be approximated by the streaming depth *d*. Table 3 lists the streaming flows as well as the associated computed values of coefficient of friction, C_f. In plotting C_f versus p/d , as illustrated in Figure 25, the coefficient of friction occupied a much narrower range, from 0.0173 to 0.2202, with the average C_f equal to 0.0642. For the most part, Figure 25 suggests that the coefficient of friction appears to be approximately equal to 0.6 with the addition of some larger values for p/d ratios ranging from 1 to 2. These deviating values were the result of some WB and 1/2WC arrangements and they were possibly more typical of transitional streaming flows rather than true streaming flows. Figure 26 was generated by computing the coefficients of friction for the collected set of steady transitional streaming flows and superimposing these points over the streaming flow data. The steady transitional streaming flows (tS), illustrated as the smaller solid black circles do deviate in a similar fashion from the narrow grouping, thus, suggesting that the elevated coefficient of friction points for values of p/d less than 2 may not be true streaming flows. Furthermore, by viewing the photographs taken of the flow arrangements producing the 4 maximum coefficient of friction values, the flows WB30-135, WB30-165, 1/2WC30-035 and 1/2WC30-045 appeared to be influenced by excessive levels of air entrainment. It is possible that the larger percentages of air entrainment may have increased the streaming flow depth, thus, positively skewing the computed coefficient of friction values. Due to these listed reasons, the mean coefficient of friction was computed without these four points and was equal to 0.0606 with a maximum error interval of $\pm 0.02 (\pm 0.0004 \text{ to } \pm 0.02)$.

The values of coefficient of friction for the streaming data collected by Rajaratnam, et al. (1987b) were likewise computed and the complete data set, with the exception of a few streaming flows which had p/d values greater than 20, was plotted with the data collected from this study. Figure 27 illustrates the streaming flow data sets collected from both studies. Viewing Figure 27, the streaming data collected from this study produced p/d ratios ranging from 0.7 to 9 whereas the data of Rajaratnam, et al. (1987a) data yielded p/d ratios ranging from 3 to 20. This variation in p/d, which spans over one order of magnitude, illustrates the diversity of the experimental arrangements studied. Also, the computed coefficient of friction (C_f) ranged over one order of magnitude, from 0.0173 to 0.322 with a mean of 0.0703. This average value does provide a quantitative value for the coefficient of fluid friction; however, the variation being greater than one order of magnitude does not conclusively support a singular mean value.

In attempt to determine if there are sub-ranges within the domain of the coefficients of friction, Equation 27 can be rewritten as:

$$C_f = \frac{2gS_o d^3}{q^2} \qquad 28)$$

Moreover Equation 28 can be rewritten as:

$$\frac{q^2}{2gS_o} = \frac{1}{C_f} d^3 \qquad 29)$$

and by plotting $q^2/2gS_o$ versus d^3, the inverse value of the slope which is equal to the coefficient of friction, C_f, could be determined. The aim of constructing this plot was to establish a more definitive value for C_f or to possibly discern ranges for C_f with respect to different weir spacings or physical parameters. Figure 28 illustrates the plotted results of Equations 29 for the data collected from this study. From the collected data, two distinct groups have developed. One best fit line defines the coefficient of friction for 'C' and 'D' class weir spacings ($L/p \cong 1 \& 0.5$) to be equal to be 0.047 with a coefficient of determination equal to 98.2 percent. The second best fit line, constructed with the 'B' class ($L/p \cong 2$) weir spacings, yielded a coefficient of friction equal to 0.099 with a coefficient of determination equal to 89.5 percent. The results of this plot suggest that depending on the physical structure, the value of the coefficient of friction , C_f will vary. It is interesting to note that for the entire data set collected from Rajaratnam, et al. (1987a) as well as from this study, the computed mean value for the coefficient of friction, 0.0703, falls within these two values.

By substituting the computed values for C_f into Equation 7, the dimensionless discharge Q_* ranged from 4.50 to 6.52 with the mean value equal to 5.29. The mean dimensionless discharge value does bisect the data cluster on Figure 24 ; however, the variance does not support a single value. It is therefore recommended that for physical arrangements with a pool length to weir height ratios less than or equal to one, the coefficient of friction, C_f, is equal to 0.047. Whereas for longer pool lengths with ratios $L/p \cong 2$, the value of the coefficient of friction shall be 0.099. This approach of applying different coefficients of friction for different physical arrangements is supported by the study conducted by Chimani and Rajaratnam (1996). Chimani and Rajaratnam observed that the coefficient of fluid friction, C_f, varied from 0.005 to 1 depending on the physical structure. To check this approach of dual valued coefficients of friction, Equation 27 can be rewritten as:

$$d = \left(\frac{Q}{b}\right)^{\frac{2}{3}} \left(\frac{C_f}{2gS_o}\right)^{\frac{1}{3}} \qquad 30)$$

and the streaming depth can be computed and checked with the measured data. For example, experimental arrangements WD05-025 and WB05-165 produced streaming flows with measured depths equal to 38.4 and 199 millimeters. Computed streaming depths via equation 30, with coefficient of friction values equal to 0.046 and 0.099, resulted in values of 46 and 206 millimeters respectively. Although these test results really only confirm Equation 27 or Equation 30 with calibrated data, the point being illustrated is that this approach can provide reasonable approximations for streaming depths when the appropriate coefficient of friction is applied.

From this portion of the study on streaming flows it appears that the physical arrangement influences the value of the coefficient of fluid friction. Another approach to this problem of streaming depth prediction for different physical arrangements, can be addressed by determining the Mannings 'n' instead of coefficients of friction for each set of pool length to weir height ratios. By combining Mannings discharge equation with the continuity equation

$$\frac{q}{S_o^{1/2}} = \frac{1}{n} d^{5/3} \qquad 31)$$

and by plotting $q/S_o^{1/2}$ versus $d^{5/3}$ from Equation 31, values for Mannings 'n' can be determined. Figure 29 illustrates the results for both physical arrangement groups, $L/p \leq 1$ and $L/p \cong 2$. For the 'C' & 'D' classes weir spacings ($L/p \leq 1$), and the 'B' class weir spacings ($L/p \cong 2$) the Mannings 'n' was approximated to be equal to 0.034 and 0.054 with coefficients of determination equal to 98.1 and 88.6 percent respectively. From Figure 29, it is conclusive that the two different pool and weir groupings have distinct Mannings n's; therefore, it is not possible to simply group all pool and weir designs together under one design parameter or coefficient.

Attempts to determine a relationship between Mannings 'n' and the coefficient of fluid friction, C_f, for pool and weir fishways was undertaken but no constructive results were achieved.

3.2.4 Transitional Flow

Having formulated dimensionless parameters that can be used to describe and predict plunging and streaming flows, it would now be advantageous to develop a dimensionless equation that would positively define the midrange transitional flows. Rajaratnam, et al. (1987a) recognized that the pool length was a significant design parameter and proposed the following dimensionless equation.

$$Q_t = \frac{Q}{b\,L^{3/2}\,S_o\,\sqrt{g}} \tag{10)}$$

The findings of this study likewise confirm and support the fact that the pool length is a influential parameter whereas the slope and weir height were less important. For all transitional flows, the values for the dimensionless parameter (Q_t in Equation 10) were computed and have been tabulated in Table 4. Rajaratnam, et al. (1987a) observed that the values of the dimensionless parameter fell within a narrow range, from 0.22 to 0.31 and an average value of 0.25 was proposed. From the transitional flows experienced during this experimental study, the domain of values for Q_t was significantly larger than the proposed 0.25 and the range varied from 0.25 to 1.75 with a maximum error interval of ±0.02.

In an attempt to determine if the transitional dimensionless discharge parameter (Q_t) was a valid defining equation, Equation 10 was computed for all Plunging, Plunging-transitional, Transitional, Transitional-streaming and Streaming flows. The computational results have been grouped in Figure 30 to illustrate the ranges of the Plunging, Plunging-transitional, Transitional, Transitional-streaming and Streaming flows. From this figure it is possible to identify the three dominant plunging, transitional and streaming ranges and also to define ranges for which each flow regime will occur. For transitional flows, Q_t varied from 0.25 to 1.75. However, by viewing the range for which Transitional-plunging and Transitional-streaming flows are likely to occur, it is reasonable to widen the transitional range to $0.20 \leq Q_t \leq 2.00$. As a result plunging flows were observed to occur for $Q_t \leq 0.20$ and streaming flows will dominate for $Q_t \geq 2.00$.

These findings not only define a range for transitional flows but mark cornerstones for which plunging and streaming flows are likely to dissipate or generate, respectively. Another significant point with regard to these ranges is that it is now possible, via Equation 10, to predict what flow regime will likely occur, based only on physical geometry and discharge. Then by using Equation 1 or Equation 6 the plunging head *h* or streaming depth *d* can be computed.

3.3 Velocity Measurements

3.3.1 General

The previous section of this chapter addressed flow regime prediction from an empirical approach. The results of this quantitative analysis have advanced the capabilities of predicting what flow regimes are likely to occur for a wide array of pool and weir structures. However, they have not provided any definitive insight into what velocities or velocity profiles will exist within plunging, transitional or streaming flows. By reviewing Section 2.5.2 which addresses flow structure, along with the many recorded photographs, it would be possible to estimate what flow patterns will occur. Nevertheless, the magnitude of the flows would still remain unknown. In all reality there is little to gain from a fishway which produces favorable flow patterns but velocities greater than what the intended fish can sustain.

The primary aim of this section is to develop a basis for understanding what velocities and velocity profiles should be expected for plunging and streaming flows. To achieve this goal, measured centerline velocity profiles will be plotted and analyzed for a select group of plunging and streaming flows. The plotted results illustrate the regions of maximum and minimum velocities as well as the longitudinal path of maximum velocity. The relationship between weir height and maximum velocity and energy dissipation within the pool will likewise be addressed.

Velocity profiles for a total of four pool and weir structures were recorded, three of which were plunging flows and the remainder was a transitional-streaming flow. Since the process to collect the velocity data via pitch probe and manometer was rather time consuming, the flows selected best represent the idealized flow patterns found in plunging and streaming flows.

3.3.2 Plunging Flows

The experimental arrangement WA10-035, (full weir height, L/p = 4, 10% bed slope, 35 L/s) was the first plunging flow selected for velocity measurements. This structural arrangement and discharge produced all of the typical plunging flow attributes such as a plunging jet, a large surface roller, surface and bed bifurcation points and a circulating flow within the plunging nape. Although the 'A' class weir spacing was twice as long (L/p=4) as a standard pool and weir arrangement (L/p=2), this pool length was selected because more vertical profiles could be measured with the pitch probe.

Instead of selecting other unrelated plunging flows for the following sets of velocity measurements, modifications to the weir height were made to incorporate three-quarter and half weir heights with the present arrangement. By modifying only the weir height parameter insight into the relationship between the weir height and velocity profiles, as well as changes to flow structure and water surface profiles can be achieved. Plates 17 through 21 illustrate the WA10-035, 3/4WA10-035 and 1/2WA10-035 plunging flows. The values presented in this section reflect modeled velocities and discharges. Prototype discharges and velocities can be computed by applying the following prototype to model ratios, $Q_r = 401$ and $V_r = 3.32$ respectively.

During the collection of the velocity data for the three plunging flows, the observed flow patterns were not unlike the characteristics described in section 2.5.2.2. However, after collecting, processing and plotting the velocity profiles, information with regard to the location of the maximum velocities, stagnation points and velocity gradients as well as how these characteristics change with response to different weir heights, resulted. For all three plunging flows, the plotted vertical velocity profiles were similar in shape and vector direction. The locations of maximum velocity or, more specifically, the path of maximum velocity from one section to the next was also common for all three arrangements, as illustrated in Figures 31, 33 and 35. Figure 37 represents all three plunging flows in a vertical alignment to assist in a visual comparison. Typically, the point of maximum velocity would occur just above the weir crest, continue upward for the following section, and then dive within the centre of the plunging jet to the bottom of the pool. After traveling along the bottom of the pool this imaginary maximum velocity path would ascend until it reached the crest of the downstream weir where it would continue on into the following pool in a continuous cyclic fashion. Figures 32, 34 and 36 illustrate these paths as well as the magnitudes of maximum section velocities. The maximum velocities recorded at each section for each pool and weir arrangement have been superimposed for comparison on Figure 38. For both full and three-quarter weir heights (WA10-035 and 3/4WA10-035) the maximum model velocity, located at the weir crests, were approximately 1.35 and 1.5 meters per second, respectively. Proceeding downstream, the flow structure which was similar to a submerged hydraulic jump dissipated the energy thus lowering the measured downstream velocities. For the half weir height arrangement, 1/2WA10-035, the reduced weir height permitted a section of supercritical flow to develop and maximum velocities exceeded 1.75 meters per second and remained higher than for the previous two arrangements. Further downstream the free surface hydraulic jump dissipated the energy and reduced the maximum velocities as illustrated in Figure 38.

For all three plunging flow arrangements, the head drop between two adjacent weirs was approximately 34.5 millimeters. Converting this head drop to a prototype scale, and applying a standard velocity calculation , $V = \sqrt{2gh}$, the resulting 380 millimeter elevation difference in weir crests would produce a mean velocity of 2.75 meters per second. Comparing this value to the measured maximum velocities for the full and three-quarter weir heights, the resulting converted prototype velocities would be 4.48 and 4.95 meters per second or 64 and 82 percent greater. In fact the estimated prototype velocity of 2.75 meters per second, converted to a model velocity of 0.83 meters per second, is relatively low even for a mean average value. The mean model / prototype velocity for both full and three-quarter weir heights was approximately 1.0 / 3.32 meters per second. Generally the maximum velocities that should be expected within a pool and weir arrangement are approximately 75 percent greater than estimation calculations based on $V = \sqrt{2gh}$.

The region of the minimum velocities within all three pool and weir designs were generally confined to the nape as well as the surface circulating cell. Figure 37 illustrates the shallow velocity gradients within the circulating surface cells of all three plunging flows. The apparent disadvantage to this flow regime or, more specifically, the inherent velocity profiles, are that the maximum velocities are for the most part located near the bottom of the pool where most fish are behaviorally conditioned to reside. As a result, this forces the fish to position themselves in the mid to upper strata of the pool and as a consequence there may not be sufficient pool length for the fish to accelerate to a required pool jumping velocity.

The velocity profiles for all three arrangements were piece-wise integrated as a check to confirm continuity. In order to compute an integrated discharge through each vertical section, three assumptions or approximations were required. Theoretically, the velocity at the bed and at the crest of the weir is zero. Since the pitch probe could not measure the velocity immediately outside of the boundary layer, the velocity at the bed and weir crest was assumed to be equal to the magnitude of the horizontal component of the adjacent vector directly above. Likewise the velocity vector at the water surface was not measurable with the pitch probe and the assumed velocity was equal to the horizontal component of the adjacent vector directly below. The third assumption was that the zero velocity intersect or point of flow reversal could be linearly interpolated from the horizontal components of the magnitude of the two adjacently opposite vectors.

Figures 32, 34 and 36 illustrate the measured values of the forward and reverse flows as well as the overall integrated continuity at each vertical section. Continuity calculations listed in Table 5 reveal that some sections, primarily in the upstream section of the pool, produced large discrepancies in continuity, whereas at other sections closure was achieved within a 5 percent discrepancy interval. Generally the downstream sections produced the smallest discrepancies in continuity. The possible explanations for large discrepancies within the plunging jet region can be apart attributed to the natural instability in the flow reversal within the nape. However, the magnitude of the velocity reversal within the nape is relatively small, hence, the large discrepancy or inadequacy of the return discharge could not be totally compensated even if the zero velocity point was actually closer to the underside of the plunging jet.

After reviewing the discrepancies within this plunging jet region for all three flow arrangements, the large positive deviations for two arrangements and the large negative discrepancies for the other were actually not errors but confirming evidence that the flow within a plunging regime is highly three dimensional. Observations of lateral shifts in the tufting grids, which were installed within the pool to assist in the photographic section of this report, reinforce the claim of three dimensional flow. Supporting this statement, often in plunging flow arrangements, surface disturbances termed as 'boils' occurred upstream of the weir and were often transported in part downstream within the plunging jet. These surface disturbances appeared to be the result of the wall jet being deflected upward immediately upstream of the weir. This deflected flow was not transversely uniform and as a result the water surface reflected regions of radial surface bifurcation, or what has been classified as 'boils'. From these points of surface bifurcation, the flow was either routed upstream or passed downstream producing transverse variations in the water surface. The maximum deflection of the transverse water surface was approximately 5 millimeters.

Other general qualitative observations with regard to the measured velocity profiles are as follows. The rotating surface cell immediately downstream of the plunging jet was for the most part consistent in length. However, with each decrease in weir height, this rotating cell became proportionally vertically shallower. Likewise the length of the nape became proportionally shorter.

The bell shaped velocity profiles within the latter half of the pool were similar in shape to the velocity profiles produced by a plane turbulent jet. A jet analysis to determine the shape and velocity distribution of these velocity profiles was not conducted for it was not within the scope of this project.

The water surface profiles produced by the three plunging flows were similar in shape with the exception of the section of supercritical flow for the half weir height arrangement. Figure 38 illustrates the parallel offset of the water surface profiles as the weir height was decreased. An interesting note with regard to the plunging head measurements for all three flows, was that they were not all equal. For the full weir height the plunging head was 113 millimeters, whereas for the three-quarter and half weir heights, the plunging head was equal to 85 and 88 millimeters. Closer inspection of all three arrangements reveal that the full weir height is the only arrangement that produces a submerged weir flow. This submergence characteristic would explain the additional 25 millimeters.

3.3.3 Transitional Streaming Flow

The experimental arrangement WB10-065 (full weir height, L/p = 2, 10% bed slope, 65 L/s) was the fourth and final arrangement for which velocity measurements were recorded. This physical arrangement actually produced an advanced transitional-streaming flow, but, the flow patterns within were characteristic and representative of a fully developed streaming flow. The only real difference was that the water surface was discontinuous and was not completely without fluctuating disturbances. Plate 22 shows the recorded flow regime.

The dominant flow characteristics observed for this flow regime were the unidirectional circulating cell with the overriding streaming flow. Other subtle attributes have been outlined in section 2.5.2.6. Figure 39 illustrates these characteristics by plotting both vector and velocity envelope profiles. The minimum velocities measured within the transitional-streaming flow were located within the central core of the rotating cell. Theoretically a line of zero shear stress exists at this divisional strata; however, the natural fluctuating direction of flow near this element makes this line difficult to locate precisely. The maximum velocity path or maximum velocities for all vertical sections were typically located at or near the water surface. The solid line constructed on Figure 39 illustrates this maximum velocity path. The maximum model velocities ranged from 1.70 to 1.95 meters per second with an average maximum model velocity for all cross sections approximately equal to 1.75 meters per second. This average maximum velocity of 1.75 meters per second was not considerably different than the depth averaged model velocity of 1.55 metes per second. The variance in the maximum velocities for this arrangement is displayed in Figure 40. It is interesting to note that the velocity vectors at an elevation roughly equal to the height of the weir and at the bed of the flume, were approximately the same magnitude. This congruency confirms that the flow within the circulating cell is propelled by the turbulent shear layer along the underside of the over-riding streaming flow. As a result there is a residency period of time before the water within the cell is transported downstream. A slug of dye which was injected into the central core of the circulating cell confirmed this flow interaction for the colour concentration of the dye remained for a significant period of time before it was diluted and washed downstream.

The piece wise integration of the velocity profiles for the flow arrangement WB10-065 was carried out in a similar fashion as for the three previously computed plunging flows. Likewise, the assumptions required to assign the magnitude of the horizontal velocity components at the surface, weir crest and bed were unchanged and are listed in the previous section. Initially, the model water surface elevation was assumed to be 226 millimeters above the bed of the flume or a streaming depth of 83 millimeters. After integrating each velocity profile, the average error in discharge continuity was approximately 15.05 percent. The first plot in Figure 41 illustrates the forward and return flows for each vertical section as well as the sum of the two for the assumed water surface elevation equal to 226 millimeters. After closer review it was felt that the errors were moderately high and by lowering the water surface elevation down to 218 millimeters, a difference of 8 millimeters, a minimum continuity error of 3.53 percent resulted. This approach of decreasing the streaming depth to minimize the average error was done not to alter the test results but to determine an explanation for the significant errors. Figure 40 as well as the second plot in Figure 41 illustrates the forward and reverse flows as well as the continuity calculations for the water surface elevation of 218 millimeters.

Since the maximum error in measuring the water surface for streaming flows with the point gauge was ±2.5 millimeters, as outlined in section 2.4.4, this suggests that the errors from the apparatus and velocity measuring device as well as human error produced a total error interval of approximately 5.5 millimeters for this turbulent type of transitional-streaming flow. In reality, the cause of the error is truly not important, but the main point here is that the error as a result of the apparatus and recording methods was approximately constant for all vertical sections. Table 6 indexes the computed errors at each complete vertical section. As a result, the uniformity in error for each cross section confirms the assumption of two dimensional flow for streaming flows. Hence, the analytical approach undertake to determine the streaming flow dimensionless parameter Q_* is valid.

Another aspect that was investigated with regards to the streaming flow was the computation of the mean average velocity. From the velocity measurements on the WB10-065 experiment arrangement, the depth averaged velocity was computed to be 1.55 meters per second. This computed velocity was approximately 10 to 26 percent less than the measured maximums. This variance in velocity raised the question of how the depth averaged velocity changes with an increase in discharge. From section 3.2.3 it was determined that the Mannings n varied with respect to the spacing of the weirs, therefore, the proportional relationship of Mannings discharge relationship was not straight forward. By plotting the model discharge versus the depth-averaged velocity Figure 42 was generated. For all streaming flows the computed depth-averaged velocities revealed that all the skimming flows of depth d were supercritical flows. The curved lines plotted in Figure 42 illustrate that an equal increase in discharge will result in a smaller increase in depth averaged velocity for shallower slopes compared to steeper ones, especially for longer weir spacings ('B' class weir spacing). The results presented here are certainly not ground breaking. However, they have been included here to emphasize that the variation in velocity for a slope is critical especially if no discharge regulating device is to be installed with a pool and weir fishway.

3.4 Summary of Results

3.4.1 General

This pool and weir experimental study consisted of 435 different geometric arrangements and discharges. For each one of these arrangements, the flow was classified as either a plunging, plunging-transitional, transitional, transitional-streaming, streaming, transitional-baffle, baffle or supercritical bed flow. Section 2.5.2 describes the dominant flow characteristics for each of these regimes. Also, stability observations were conducted and the 435 arrangements were classified as steady or unsteady flows. In addition, measured water surface profiles produced plunging heads and stream depths for the plunging and streaming flows, respectively. With all this resulting data the objective at hand was to determine a means to present the results in a relatively simple and concise format. The two different approaches undertaken have been classified as the 'Graphical Presentation of Results' and 'Non Dimensional Domains'.

3.4.2 Graphical Illustrations

To graphically illustrate the data collected from this study as well as the many physical parameters, tables and histograms have been used to convey this information. The data collected for the full, three-quarter and half weir height experiments were compiled and tabulated in Tables 7, 8 and 9 respectively. These three tables which act as 'road maps' are arranged with the model discharge on the vertical axis and the physical model variables along the horizontal axis. By selecting the weir height, discharge, weir spacing and slope, in this order, information regarding to stability, flow regime and plunging head or streaming depth can be determined. A legend located below each table provides an explanation for all of the abbreviations used within each designated cell. The advantage to this tabular method is that all the recorded data are presented in a concise and rigid format. However, the only drawback to this approach is that the flow regime trends or, more specifically, the limits of each flow regime are restricted to the set discharges for which water surface profiles were recorded.

To overcome this problem of ranges of flow regime uncertainty, the histograms constructed in Figures 43, 44 and 45 illustrate the flow regime ranges recorded within the stability observations section of Appendix B. These noted ranges were observed for smaller incremental increases in discharge and, hence, a more accurate illustration of flow regime domains is produced. Figure 43 shows all the recorded flow regimes regardless of whether the flows were steady or unsteady. In contrast, the histogram in Figure 44 only illustrates steady uniform flows. The third and final histogram, Figure 45, was constructed to illustrate the preferred steady plunging and streaming flow regimes suitable for pool and weir fishways. In viewing Figure 45, it is apparent that the range of plunging flows for 'A' class weir spacings is significantly larger than that produced for 'B' class weir spacings. On the other end of the histogram, Figure 45 reveals that the vast majority of the flows for ' D' class weir spacings and all five slopes were classified as streaming flows.

3.4.3 Non Dimensional Domains

This section has been created in attempt to devise dimensionless parameters which can be plotted and in turn the ranges and domains for each plunging, transitional, baffle, streaming and supercritical bed flow regime can be visually discerned and classified. During this pool and weir study the most significant parameters influencing the flow regime were the discharge, pool length, slope and weir height, in this order. The last parameter, the flume width , was really a constant for its measure did not change. By conducting a dimensional analysis, the dimensionless parameters $Q/\sqrt{g}bL^{3/2}$ and S_0L/p were derived. Of these two parameters, the first was similar to the dimensionless discharge parameter for transitional flows, Q_*, with the exception of the absence of the slope within the denominator. Figure 46 reveals that by plotting these two dimensionless parameters there appears to be distinct ranges and domains for each flow regime. Perimeter lines or divisional boundaries have been added to the dimensionless plot, as illustrated in Figure 47, in order to better define the flow regime domains. In viewing these constructed regime boundaries on Figure 47, it appears that the progression from supercritical bed flow, through plunging and transitional regimes and onto streaming flows properly represents the true order of flow regime transformation.

Before setting definitive numeric boundaries for these dimensionless parameters, the effectiveness or accuracy of these parameters must be confirmed. The data collected from the study undertaken by Rajaratnam, et al. (1987a), was used to critique the dimensionless parameters and the values of the dimensionless domains illustrated in Figure 46 and 47. By superimposing the computed parameters based on the data collected by Rajaratnam, et al. (1987a), it is evident that the proposed dimensionless parameters do not positively group all common regimes. In viewing Figure 48 both studies have produced sequential data but the regimes within both sets do not occupy common ranges. As a result, this attempt to discern ranges of flow regimes with dimensionless parameters has produced inconclusive results. Perhaps future pool and weir studies may construct order out of these dimensionless parameters or use this data with other defining techniques to establish flow regime domains.

4.0 CONCLUSION AND RECOMMENDATIONS

4.1 Conclusion

Pool and weir fishways are hydraulic structures that have been developed to assist in upstream fish transport by creating passable flow regimes. These hydraulic structures can produce a wide array of flow patterns by simply altering one of the physical parameters such as discharge, weir spacing or slope. It is of this diversity or, more specifically, the lack of ability to predict which flow regime will occur for any one physical design, that restricts the construction of these hydraulic structures to a select group of proven arrangements.

The aim of this pool and weir fishway study was primarily to advance the ability of flow regime prediction so that different fishway arrangements can be constructed to better address the needs of the migratory fish. In addition, any information gained from this study regarding the flow patterns within the dominant flow regimes, the transformation process from a plunging to streaming state, as well as which physical parameters are significant for flow regime generation, will advance the science of pool and weir hydraulic structures.

To achieve these goals, water surface profiles, stability observations, and photographs were recorded for a total of 435 different experimental pool and weir arrangements and discharges. Furthermore, velocity measurements for a select few arrangements provided insight into what velocity profiles and maximum velocities should be expected for plunging and streaming flows.

The transformation process from plunging to streaming flows, designated as transitional flows, was observed and can be best described as a range which is comprised of many sub-transitional flow regimes. Plunging-transitional, transitional, transitional-streaming, transitional-baffle and baffle flows were the five regimes observed to occur within the range of the transitional regime. For many of the experimental arrangements, only a few of these noted sub-regimes occurred, thus, suggesting that certain physical parameters controlled or were influential of what regime would occur. It was observed that for physical arrangements in which the pool length to weir height ratio was approximately equal to 4 ($L/p \cong 4$), transitional-baffle and baffle flow regimes occurred after plunging flows and before streaming flows in response to an increase in discharge. For pool length to weir height ratios approximately equal to or less than 2 ($L/p \leq 2$), baffle flow did not form and the plunging, transitional and streaming progression occurred.

In addition to the regime transformation process, stability observations identified longitudinal surges, transverse waves or the combination of the two disturbances as being two predominant instabilities within the pool and weir arrangements. These longitudinal surges or transverse waves did not appear to be generated for any particular physical reason or at any set discharge. Generally the longitudinal surges would occur in a cyclic fashion. However, as the discharge was increased, so also did the frequency of surges. Upon convergence of the longitudinal surge (an instantaneous return period), the transitional waves would appear. With additional increases in discharge the transverse waves would increase in amplitude and then reduce down in size only to give way to a reoccurring longitudinal surge. This instability pattern was not common for all experiments nor was it observed for the same range of discharges. If instabilities were to occur, they would develop in the initial plunging stages and would rarely exist for model discharges greater than 35 liters per second.

From the measured water surface profiles, the plunging head and streaming depth values were used to confirm the applicability of the dimensionless parameters derived by Rajaratnam, et al. (1987b) as well as to redefine the values that represent them.

For plunging flows the value of the dimensions parameter Q_+ from this study's data was determined to be equal to 0.68. Combining and averaging the values present from both studies, a dimensionless discharge value of 0.65 resulted.

For streaming flows, the computed values for the dimensionless parameter, Q_*, resulted in a mean value equal to 5.29. However, by plotting Q_* versus L/d, the data collected from this study did not support the equation $Q_* = 1.5\sqrt{L/d}$ as proposed by Rajaratnam, et al. (1987b). Another approach to define streaming flows was undertaken by rearranging the dimensionless discharge equation and solving for the coefficient of fluid friction, C_f. It was determined that the physical arrangement influenced the value of the coefficient of fluid friction and subsequently, C_f was determined to be equal to 0.099 for 'B' class weir spacings ($L/p \cong 4$), and equal to 0.047 for 'C' and 'D' class weir spacings ($L/p \leq 2$). Since these results support the concept of different energy loss values for different weir spacings, this initiated the undertaking to determine the Mannings n for each weir spacing classification. From the data collected from this study, pool and weir arrangements constructed with a smooth bed and sharp crested weirs, resulted in Mannings n equal to 0.054 for 'B' class weir spacings ($L/p \cong 4$), and equal to 0.034 for 'C' and 'D' class weir spacings ($L/p \leq 2$).

For transitional flows, the computed values of the dimensionless parameter derived for the transitional flows, Q_t, ranged from 0.25 to 1.75. After computing the dimensions parameters set forth for transitional flows for all plunging, transitional and streaming flows, distinct ranges for each regime developed. It was determined that the transitional flow regime domain occurred for the dimensionless parameter ranging from $0.2 < Q_t < 2.0$, whereas plunging and streaming flows occurred for $Q_t < 0.2$ and $Q_t > 2.0$ respectively. As a result Q_t can be used as a guide to flow regime prediction.

The velocity measurements recorded during this experimental study have provided insight into the flow structure within both plunging and streaming flows. The quantitative results of this portion of the study revealed that the maximum flows within a plunging flow regime occurred immediately downstream of the weir, within the plunging flow, and were approximately 75 percent greater than uniform flow velocity approximations. In addition, the path of maximum velocity for plunging flows traverses the entire vertical section where as for streaming flows the path of maximum velocities is confined to the supercritical surface streaming flow.

4.2 Recommendations

Even though this experimental study of flow regimes within pool and weir fishways has expanded our understanding of these structures, as well as advanced the art of predicting flow regimes, several other questions have come forth. The unresolved issues of predicting flow instabilities and the velocity distributions within plunging flows are two of these questions that have been selected to be recommendations for future independent studies.

It is recommended that the stability data collected from this experimental study should be further reviewed and a quantitative analysis should also be attempted. Ultimately, the development of empirical relationships would assist in the design of new pool and weir fishways by predicting and preventing the construction of unstable regimes.

The second experimental recommendation, addresses the uncertainty of flow patterns and velocity profiles within plunging flows. The results presented within Section 3.3.2 confirm that the flow structure within a plunging regime is highly three dimensional. It was observed that centerline velocity profiles were representative of the flow structure; however, there were instances where large discrepancies in continuity occurred. The recommendation presented here is to select a few typical plunging flows and map the velocities within the pool and weir structure by collecting longitudinal and transverse velocity profiles. By conducting both longitudinal and transverse profiles, a more complete understanding of the flow patterns, maximum and minimum velocities would result.

Further recommendations as a result of this study are aimed at the methods undertaken to collect experimental data. For future experimental works of this magnitude, it is highly suggested that electronic water surface measuring devices as well as pressure transducers be integrated into the data collection process. Due to the limitations of the physical devices as well as the dynamic action of the water surface within the pool and weir fishway, electronic devices would have reduced the time required for data collection.

Table 1: Weir Height and Weir Spacing Data

Weir Heights (p)		
Type	Design (mm)	Actual (mm)
Full (1)	140	140.8
0.75	105	119.1
0.5	70	74.1

Weir Spacings (L)				
Type	Design (mm) / Actual (mm)			
	A	B	C	D
Full (1)	/ 685	/ 335	/ 166	/ 77
0.75	696 / 694	342 / 342	165 / 164	-
0.5	696 / 703	342 / 348	165 / 169	-

Flume Width = 560mm

Table 2: Experimental and Computational Data for Plunging Flow

Legend

P = Plunging Flow
Pt = Plunging Transitional Flow (slight deviation from plunging flow conditions)
P = Plunging Flow pattern which has a section of supercritical bed flow

h = Maximum head over weir (mm)

Italics indicate that the flow is not in a true plunging or streaming state

Experimental Arrangement	Weir Spacing (L) (mm)	Weir Height (p) (mm)	Slope (%)	Discharge (Qm) (l/s)	Stability d/dt	Type of Flow Pattern	Plunging Head (h) (mm)	Cd	Preliminary Q+=f(Cd)	Q+ Q+=f(Q,b,g,h)	h/p
WA05-005	685	140.8	5	5	Steady	P	27.3	0.62	0.59	0.63	0.2
WA05-010	685	140.8	5	10	Steady	P	47.0	0.63	0.60	0.56	0.3
WA05-015	685	140.8	5	15	Steady	P	65.6	0.64	0.61	0.51	0.5
WA05-020	685	140.8	5	20	Steady	P	80.4	0.65	0.61	0.50	0.6
WA10-005	685	140.8	10	5	Steady	P	27.3	0.62	0.59	0.63	0.2
WA10-010	685	140.8	10	10	Steady	P	44.3	0.63	0.59	0.61	0.3
WA10-015	685	140.8	10	15	Steady	P	55.1	0.64	0.60	0.66	0.4
WA10-035	685	140.8	10	35	Steady	P	114.5	0.67	0.63	0.51	0.8
WA10-045	685	140.8	10	45	Steady	P	135.7	0.68	0.64	0.51	1.0
WA15-005	685	140.8	15	5	Steady	P	29.1	0.62	0.59	0.58	0.2
WA15-010	685	140.8	15	10	Steady	P	45.8	0.63	0.59	0.58	0.3
WA15-020	685	140.8	15	20	Steady	P	71.2	0.65	0.61	0.60	0.5
WA15-025	685	140.8	15	25	Steady	P	84.1	0.65	0.62	0.58	0.6
WA15-035	685	140.8	15	35	Steady	P	106.2	0.67	0.63	0.58	0.8
WA15-045	685	140.8	15	45	Steady	P	112.6	0.67	0.63	0.68	0.8
WA20-005	685	140.8	20	5	Steady	P	28.1	0.62	0.59	0.61	0.2
WA20-010	685	140.8	20	10	Steady	P	45.4	0.63	0.59	0.59	0.3
WA20-015	685	140.8	20	15	Steady	P	67.2	0.64	0.61	0.49	0.5
WA20-020	685	140.8	20	20	Steady	P	73.6	0.65	0.61	0.57	0.5
WA30-010	685	140.8	30	10	Steady	P	42.9	0.63	0.59	0.64	0.3

Experimental Arrangement	Weir Spacing (L) (mm)	Weir Height (p) (mm)	Slope (%)	Discharge (Qm) (l/s)	Stability d/dt	Type of Flow Pattern	Plunging Head (h) (mm)	Cd	Preliminary Q+=f(Cd)	Q+ Q+=f(Q,b,g,h)	h/p
WA30-015	685	140.8	30	15	Steady	P	73.9	0.65	0.61	0.43	0.5
WA30-020	685	140.8	30	20	Steady	P	75.6	0.65	0.61	0.55	0.5
WA30-025	685	140.8	30	25	Steady	P	90.5	0.66	0.62	0.52	0.6
WA30-035	685	140.8	30	35	Steady	P	114.1	0.67	0.63	0.52	0.8
WA30-045	685	140.8	30	45	Steady	P	139.2	0.68	0.64	0.49	1.0
WA10-020	685	140.8	10	20	Unsteady	P	68.8	0.64	0.61	0.63	0.5
WA10-025	685	140.8	10	25	Unsteady	P	83.1	0.65	0.61	0.60	0.6
WA15-015	685	140.8	15	15	Unsteady	P	58.3	0.64	0.60	0.61	0.4
WA20-025	685	140.8	20	25	Unsteady	P	82.4	0.65	0.61	0.60	0.6
WA20-035	685	140.8	20	35	Unsteady	P	107.3	0.67	0.63	0.57	0.8
WA20-045	685	140.8	20	45	Unsteady	P	130.1	0.68	0.64	0.55	0.9
WA30-005	685	140.8	30	5	Unsteady	P	27.1	0.62	0.58	0.64	0.2
WA05-025	685	140.8	5	25	Steady	Pt	*100.0*	0.66	0.62	0.45	0.7
WA10-065	685	140.8	10	65	Steady	Pt	*168.8*	0.70	0.66	0.53	1.2
3/4WA05-010	694	119.1	5	10	Steady	P	31.8	0.63	0.59	1.01	0.3
3/4WA05-015	694	119.1	5	15	Steady	P	50.0	0.64	0.60	0.76	0.4
3/4WA05-020	694	119.1	5	20	Steady	P	63.8	0.65	0.61	0.71	0.5
3/4WA05-025	694	119.1	5	25	Steady	P	78.7	0.66	0.62	0.65	0.7
3/4WA05-035	694	119.1	5	30	Steady	P	102.1	0.67	0.64	0.52	0.9
3/4WA10-010	694	119.1	10	10	Steady	P	31.1	0.63	0.59	1.04	0.3
3/4WA10-015	694	119.1	10	15	Steady	P	39.9	0.63	0.60	1.07	0.3
3/4WA10-12	694	119.1	10	20	Steady	P	53.6	0.64	0.60	0.92	0.4
3/4WA10-13	694	119.1	10	25	Steady	P	66.7	0.65	0.61	0.83	0.6
3/4WA10-14	694	119.1	10	30	Steady	P	86.0	0.66	0.62	0.68	0.7
3/4WA15-010	694	119.1	15	10	Steady	P	30.5	0.63	0.59	1.07	0.3
3/4WA15-015	694	119.1	15	15	Steady	P	43.2	0.63	0.60	0.95	0.4
3/4WA15-020	694	119.1	15	20	Steady	P	53.9	0.64	0.60	0.91	0.5
3/4WA15-025	694	119.1	15	25	Steady	P	65.4	0.65	0.61	0.85	0.5
3/4WA15-035	694	119.1	15	30	Steady	P	82.0	0.66	0.62	0.73	0.7
3/4WA20-010	694	119.1	20	10	Steady	*P*	*31.2*	0.63	0.59	1.03	0.3
3/4WA20-015	694	119.1	20	15	Steady	*P*	*40.8*	0.63	0.60	1.04	0.3
3/4WA20-020	694	119.1	20	20	Steady	*P*	*54.5*	0.64	0.60	0.90	0.5
3/4WA20-025	694	119.1	20	25	Steady	*P*	*66.4*	0.65	0.61	0.83	0.6
3/4WA20-035	694	119.1	20	30	Steady	*P*	*86.5*	0.66	0.63	0.67	0.7

Experimental Arrangement	Weir Spacing (L) (mm)	Weir Height (p) (mm)	Slope (%)	Discharge (Qm) (l/s)	Stability d/dt	Type of Flow Pattern	Plunging Head (h) (mm)	Cd	Preliminary Q+=f(Cd)	Q+ Q+=f(Q,b,g,h)	h/p
1/2WA05-002.5	703	74.1	5	2.5	Steady	P	16.3	0.62	0.59	0.69	0.2
1/2WA05-005	703	74.1	5	5	Steady	P	24.4	0.63	0.60	0.75	0.3
1/2WA05-010	703	74.1	5	10	Steady	P	37.4	0.65	0.61	0.79	0.5
1/2WA05-015	703	74.1	5	15	Steady	P	54.8	0.66	0.63	0.67	0.7
1/2WA05-020	703	74.1	5	20	Steady	P	64.8	0.67	0.64	0.69	0.9
1/2WA05-025	703	74.1	5	25	Steady	P	78.8	0.69	0.65	0.64	1.1
1/2WA05-035	703	74.1	5	35	Steady	P	98.6	0.71	0.67	0.64	1.3
1/2WA05-045	703	74.1	5	45	Steady	P	115.6	0.73	0.69	0.65	1.6
1/2WA10-002.5	703	74.1	10	2.5	Steady	*P*	15.7	0.62	0.59	0.73	0.2
1/2WA10-005	703	74.1	10	5	Steady	*P*	23.3	0.63	0.59	0.80	0.3
1/2WA10-010	703	74.1	10	10	Steady	*P*	35.0	0.64	0.61	0.87	0.5
1/2WA10-015	703	74.1	10	15	Steady	*P*	47.6	0.66	0.62	0.82	0.6
1/2WA10-020	703	74.1	10	20	Steady	*P*	59.7	0.67	0.63	0.78	0.8
1/2WA10-025	703	74.1	10	25	Steady	*P*	70.3	0.68	0.64	0.77	0.9
1/2WA10-035	703	74.1	10	35	Steady	*P*	88.5	0.70	0.66	0.76	1.2
1/2WA10-045	703	74.1	10	45	Steady	*P*	106.9	0.72	0.68	0.73	1.4
WB10-005	335	140.8	10	5	Steady	P	27.1	0.62	0.58	0.64	0.2
WB15-005	335	140.8	15	5	Steady	P	31.0	0.62	0.59	0.52	0.2
WB15-010	335	140.8	15	10	Steady	P	45.4	0.63	0.59	0.59	0.3
WB20-005	335	140.8	20	5	Steady	P	31.6	0.62	0.59	0.51	0.2
WB20-015	335	140.8	20	15	Steady	P	61.2	0.64	0.60	0.57	0.4
WB30-005	335	140.8	30	5	Steady	P	30.8	0.62	0.59	0.53	0.2
WB30-015	335	140.8	30	15	Steady	P	59.6	0.64	0.60	0.59	0.4
WB15-015	335	140.8	15	15	Unsteady	P	64.1	0.64	0.60	0.53	0.5
WB15-020	335	140.8	15	20	Unsteady	P	59.1	0.64	0.60	0.79	0.4
WB20-010	335	140.8	20	10	Unsteady	P	48.1	0.63	0.60	0.54	0.3
WB30-010	335	140.8	30	10	Unsteady	P	44.4	0.63	0.59	0.61	0.3
WB05-005	335	140.8	5	5	Steady	Pt	28.7	0.62	0.59	0.59	0.2
WB10-010	335	140.8	10	10	Steady	Pt	49.2	0.63	0.60	0.52	0.3
WB10-015	335	140.8	10	15	Unsteady	Pt	54.7	0.64	0.60	0.67	0.4
WB10-020	335	140.8	10	20	Unsteady	Pt	59.4	0.64	0.60	0.79	0.4
WB20-020	335	140.8	20	20	Unsteady	Pt	71.0	0.65	0.61	0.60	0.5
WB30-020	335	140.8	30	20	Unsteady	Pt	-	-			

Experimental Arrangement	Weir Spacing (L) (mm)	Weir Height (p) (mm)	Slope (%)	Discharge (Qm) (l/s)	Stability d/dt	Type of Flow Pattern	Plunging Head (h) (mm)	Cd	Preliminary Q+=f(Cd)	Q+ Q+=f(Q,b,g,h)	h/p
3/4WB10-010	342	119.1	10	10	Steady	P	42.1	0.63	0.60	0.66	0.4
3/4WB15-010	342	119.1	15	10	Steady	P	34.0	0.63	0.59	0.91	0.3
3/4WB15-015	342	119.1	15	15	Steady	P	50.6	0.64	0.60	0.75	0.4
3/4WB15-020	342	119.1	15	20	Steady	P	66.8	0.65	0.61	0.66	0.6
3/4WB20-010	342	119.1	20	10	Steady	P	35.5	0.63	0.59	0.85	0.3
3/4WB20-015	342	119.1	20	15	Steady	P	50.4	0.64	0.60	0.76	0.4
3/4WB20-020	342	119.1	20	20	Steady	P	62.1	0.65	0.61	0.74	0.5
3/4WB30-010	342	119.1	30	10	Steady	P	36.7	0.63	0.59	0.81	0.3
3/4WB30-015	342	119.1	30	15	Steady	P	51.1	0.64	0.60	0.74	0.4
3/4WB30-020	342	119.1	30	20	Steady	P	62.0	0.65	0.61	0.74	0.5
3/4WB10-015	342	119.1	10	15	Unsteady	P	-	-	-	-	-
3/4WB10-020	342	119.1	10	20	Unsteady	Pt	-	-	-	-	-
3/4WB10-025	342	119.1	10	25	Unsteady	Pt	-	-	-	-	-
3/4WB15-025	342	119.1	15	25	Unsteady	Pt	-	-	-	-	-
3/4WB20-025	342	119.1	20	25	Unsteady	Pt	-	-	-	-	-
3/4WB30-025	342	119.1	30	25	Unsteady	Pt	-	-	-	-	-
1/2WB05-002.5	348	74.1	5	2.5	Steady	P	17.6	0.62	0.59	0.61	0.2
1/2WB05-005	348	74.1	5	5	Steady	P	27.4	0.63	0.60	0.63	0.4
1/2WB10-002.5	348	74.1	10	2.5	Steady	P	16.6	0.62	0.59	0.66	0.2
1/2WB10-005	348	74.1	10	5	Steady	P	23.0	0.63	0.59	0.82	0.3
1/2WB10-010	348	74.1	10	10	Steady	P	44.6	0.65	0.62	0.61	0.6
1/2WB10-015	348	74.1	10	15	Steady	P	62.4	0.67	0.63	0.55	0.8
1/2WB15-002.5	348	74.1	15	2.5	Steady	P	15.9	0.62	0.59	0.71	0.2
1/2WB15-005	348	74.1	15	5	Steady	P	22.9	0.63	0.59	0.83	0.3
1/2WB15-010	348	74.1	15	10	Steady	P	40.9	0.65	0.61	0.69	0.6
1/2WB15-015	348	74.1	15	15	Steady	P	52.1	0.66	0.62	0.72	0.7
1/2WB20-002.5	348	74.1	20	2.5	Steady	P	16.7	0.62	0.59	0.66	0.2
1/2WB20-005	348	74.1	20	5	Steady	P	25.4	0.63	0.60	0.70	0.3
1/2WB20-010	348	74.1	20	10	Steady	P	41.5	0.65	0.61	0.68	0.6
1/2WB20-015	348	74.1	20	15	Steady	P	53.7	0.66	0.63	0.69	0.7
1/2WB20-020	348	74.1	20	20	Steady	P	61.5	0.67	0.63	0.75	0.8
1/2WB30-010	348	74.1	30	10	Steady	P	42.0	0.65	0.61	0.66	0.6
1/2WB10-020	348	74.1	10	20	Steady	Pt	74.2	0.69	0.65	0.56	1.0
1/2WB15-020	348	74.1	15	20	Steady	Pt	67.7	0.68	0.64	0.65	0.9
1/2WB20-025	348	74.1	20	25	Steady	Pt	68.4	0.68	0.64	0.80	0.9

Experimental Arrangement	Weir Spacing (L) (mm)	Weir Height (p) (mm)	Slope (%)	Discharge (Qm) (l/s)	Stability d/dt	Type of Flow Pattern	Plunging Head (h) (mm)	Cd	Preliminary Q+=f(Cd)	Q+ Q+=f(Q,b,g,h)	h/p
1/2WB30-005	348	74.1	30	5	Steady	*P*	*27.7*	0.63	0.60	0.62	0.4
1/2WB30-002.5	348	74.1	30	2.5	Unsteady	*P*	*19.1*	0.63	0.59	0.54	0.3
1/2WB05-010	348	74.1	5	10	Unsteady	Pt	-	-	-	-	-
1/2WB05-015	348	74.1	5	15	Unsteady	Pt	-	-	-	-	-
WC10-005	166	140.8	10	5	Steady	P	24.8	0.62	0.58	0.73	0.2
WC15-005	166	140.8	15	5	Steady	P	24.3	0.62	0.58	0.75	0.2
WC05-005	166	140.8	5	5	Steady	Pt	*21.0*	0.62	0.58	0.94	0.1
WC20-005	166	140.8	20	5	Unsteady	Pt	22.9	0.62	0.58	0.82	0.2
WC30-005	166	140.8	30	5	Unsteady	Pt	*24.3*	0.62	0.58	0.75	0.2
1/2WC10-002.5	169	74.1	10	2.5	Steady	P	18.9	0.63	0.59	0.55	0.3
1/2WC10-005	169	74.1	10	5	Steady	P	24.7	0.63	0.60	0.74	0.3
1/2WC15-002.5	169	74.1	15	2.5	Steady	P	19.2	0.63	0.59	0.54	0.3
1/2WC15-005	169	74.1	15	5	Steady	P	28.0	0.64	0.60	0.61	0.4
1/2WC20-002.5	169	74.1	20	2.5	Steady	P	19.5	0.63	0.59	0.52	0.3
1/2WC20-005	169	74.1	20	5	Steady	P	31.5	0.64	0.60	0.51	0.4
1/2WC30-002.5	169	74.1	30	2.5	Steady	P	20.8	0.63	0.59	0.47	0.3
1/2WC30-005	169	74.1	30	5	Steady	P	32.2	0.64	0.60	0.49	0.4
1/2WC15-010	169	74.1	15	10	Unsteady	Pt	-	-	-	-	-
1/2WC30-010	169	74.1	30	10	Unsteady	P	-	-	-	-	-

Table 3: Experimental and Computational Data for Streaming Flow

Legend

tS = Transitional Streaming Flow (slight deviation from classical streaming flow conditions)
S = Streaming Flow

d = depth of streaming flow (mm)

Italics indicate that the flow is not in a true plunging or streaming state
** Signifies that there was more than one flow present.
This was typically found in an unsteady flow

Experimental Arrangement	Weir Spacing (L) (mm)	Weir Height (p) (mm)	Slope (%)	Discharge (Qm) (l/s)	Stability d/dt	Type of Flow Pattern	Streaming Depth (d) (mm)	$Q_* = \frac{Q}{bd^{3/2}\sqrt{gS_o}}$	L/d	U=Q/A (m/s)	$C_f = \frac{2gS_o}{U^2}(R)$	p/d	$d^{5/3}$ (m^(5/3))	$\frac{q}{\sqrt{S_o}}$ (m^2/s)	d^3 (m^3)	$\frac{q^2}{2gS_o}$ (m)
WB05-135	335	140.8	5	135	Steady	S	176.6	4.64	1.9	1.36	0.093	0.8	0.056	1.078	5.51E-3	5.92E-2
WB05-165	335	140.8	5	165	Steady	S	199.0	4.74	1.7	1.48	0.089	0.7	0.068	1.318	7.88E-3	8.85E-2
WB10-085	335	140.8	10	85	Steady	S	108.8	4.27	3.1	1.39	0.110	1.3	0.025	0.480	1.29E-3	1.17E-2
WB10-105	335	140.8	10	105	Steady	S	120.4	4.53	2.8	1.56	0.097	1.2	0.029	0.593	1.75E-3	1.79E-2
WB10-135	335	140.8	10	135	Steady	S	145.7	4.38	2.3	1.65	0.104	1.0	0.040	0.762	3.09E-3	2.96E-2
WB10-165	335	140.8	10	165	Steady	S	151.7	5.04	2.2	1.94	0.079	0.9	0.043	0.932	3.49E-3	4.42E-2
WB15-105	335	140.8	15	105	Steady	S	116.8	3.87	2.9	1.60	0.134	1.2	0.028	0.484	1.60E-3	1.19E-2
WB15-135	335	140.8	15	135	Steady	S	129.5	4.26	2.6	1.86	0.110	1.1	0.033	0.622	2.17E-3	1.97E-2
WB15-165	335	140.8	15	165	Steady	S	149.1	4.22	2.2	1.98	0.112	0.9	0.042	0.761	3.31E-3	2.95E-2
WB20-165	335	140.8	20	165	Steady	S	138.1	4.10	2.4	2.13	0.119	1.0	0.037	0.659	2.63E-3	2.21E-2
WB30-135	335	140.8	30	135	Steady	S	119.0	3.42	2.8	2.03	0.171	1.2	0.029	0.440	1.69E-3	9.87E-3
WB30-165	335	140.8	30	165	Steady	S	148.1	3.01	2.3	1.99	0.220	1.0	0.041	0.538	3.25E-3	1.47E-2
WC05-020	166	140.8	5	20	Steady	S	38.2	6.83	4.3	0.93	0.043	3.7	0.004	0.160	5.58E-5	1.30E-3
WC05-025	166	140.8	5	25	Steady	S	42.4	7.31	3.9	1.05	0.037	3.3	0.005	0.200	7.60E-5	2.03E-3
WC05-035	166	140.8	5	35	Steady	S	53.5	7.22	3.1	1.17	0.038	2.6	0.008	0.280	1.53E-4	3.98E-3
WC05-045	166	140.8	5	45	Steady	S	66.8	6.65	2.5	1.20	0.045	2.1	0.011	0.359	2.98E-4	6.58E-3
WC05-065	166	140.8	5	65	Steady	S	83.1	6.92	2.0	1.40	0.042	1.7	0.016	0.519	5.74E-4	1.37E-2
WC05-085	166	140.8	5	85	Steady	S	99.2	6.94	1.7	1.53	0.042	1.4	0.021	0.679	9.75E-4	2.35E-2
WC05-105	166	140.8	5	105	Steady	S	114.1	6.94	1.5	1.64	0.041	1.2	0.027	0.839	1.49E-3	3.58E-2
WC05-135	166	140.8	5	135	Steady	S	132.9	7.10	1.2	1.81	0.040	1.1	0.035	1.078	2.35E-3	5.92E-2
WC05-165	166	140.8	5	165	Steady	S	168.0	6.11	1.0	1.75	0.054	0.8	0.051	1.318	4.74E-3	8.85E-2
WC10-035	166	140.8	10	35	Steady	S	49.6	5.72	3.3	1.26	0.061	2.8	0.007	0.198	1.22E-4	1.99E-3

Experimental Arrangement	Weir Spacing (L) (mm)	Weir Height (p) (mm)	Slope (%)	Discharge (Qm) (l/s)	Stability d/dt	Type of Flow Pattern	Streaming Depth (d) (mm)	$Q_* = \frac{Q}{bd^{3/2}\sqrt{gS_o}}$	L/d	U=Q/A (m/s)	$C_f = \frac{2gS_o}{U^2}(R)$	p/d	$d^{5/3}$ (m^(5/3))	$\frac{q}{\sqrt{S_o}}$ (m^2/s)	d^3 (m^3)	$\frac{q^2}{2gS_o}$ (ms)
WC10-045	166	140.8	10	45	Steady	S	54.4	6.39	3.1	1.48	0.049	2.6	0.008	0.254	1.61E-4	3.29E-3
WC10-065	166	140.8	10	65	Steady	S	69.9	6.34	2.4	1.66	0.050	2.0	0.012	0.367	3.41E-4	6.87E-3
WC10-085	166	140.8	10	85	Steady	S	82.5	6.46	2.0	1.84	0.048	1.7	0.016	0.480	5.62E-4	1.17E-2
WC10-105	166	140.8	10	105	Steady	S	93.2	6.65	1.8	2.01	0.045	1.5	0.019	0.593	8.10E-4	1.79E-2
WC10-135	166	140.8	10	135	Steady	S	110.7	6.61	1.5	2.18	0.046	1.3	0.026	0.762	1.36E-3	2.96E-2
WC10-165	166	140.8	10	165	Steady	S	129.6	6.38	1.3	2.27	0.049	1.1	0.033	0.932	2.17E-3	4.42E-2
WC15-035	166	140.8	15	35	Steady	S	41.4	6.11	4.0	1.51	0.054	3.4	0.005	0.161	7.12E-5	1.33E-3
WC15-045	166	140.8	15	45	Steady	S	48.8	6.14	3.4	1.65	0.053	2.9	0.007	0.207	1.16E-4	2.19E-3
WC15-065	166	140.8	15	65	Steady	S	58.8	6.71	2.8	1.97	0.044	2.4	0.009	0.300	2.03E-4	4.58E-3
WC15-085	166	140.8	15	85	Steady	S	65.7	7.44	2.5	2.31	0.036	2.1	0.011	0.392	2.83E-4	7.83E-3
WC15-105	166	140.8	15	105	Steady	S	81.5	6.64	2.0	2.30	0.045	1.7	0.015	0.484	5.42E-4	1.19E-2
WC15-135	166	140.8	15	135	Steady	S	94.0	6.89	1.8	2.56	0.042	1.5	0.019	0.622	8.31E-4	1.97E-2
WC15-165	166	140.8	15	165	Steady	S	112.6	6.43	1.5	2.62	0.048	1.3	0.026	0.761	1.43E-3	2.95E-2
WC20-045	166	140.8	20	45	Steady	S	45.3	5.96	3.7	1.78	0.056	3.1	0.006	0.180	9.27E-5	1.65E-3
WC20-065	166	140.8	20	65	Steady	S	56.5	6.17	2.9	2.05	0.053	2.5	0.008	0.260	1.81E-4	3.43E-3
WC20-085	166	140.8	20	85	Steady	S	68.7	6.01	2.4	2.21	0.055	2.0	0.012	0.339	3.25E-4	5.87E-3
WC20-105	166	140.8	20	105	Steady	S	73.9	6.66	2.2	2.54	0.045	1.9	0.013	0.419	4.04E-4	8.96E-3
WC20-135	166	140.8	20	135	Steady	S	87.6	6.64	1.9	2.75	0.045	1.6	0.017	0.539	6.73E-4	1.48E-2
WC20-165	166	140.8	20	165	Steady	S	98.6	6.80	1.7	2.99	0.043	1.4	0.021	0.659	9.58E-4	2.21E-2
WC30-025	166	140.8	30	25	Steady	S	28.9	5.30	5.7	1.55	0.071	4.9	0.003	0.082	2.41E-5	3.39E-4
WC30-035	166	140.8	30	35	Steady	S	38.2	4.87	4.3	1.63	0.084	3.7	0.004	0.114	5.59E-5	6.64E-4
WC30-045	166	140.8	30	45	Steady	S	43.7	5.12	3.8	1.84	0.076	3.2	0.005	0.147	8.36E-5	1.10E-3
WC30-065	166	140.8	30	65	Steady	S	55.9	5.12	3.0	2.08	0.076	2.5	0.008	0.212	1.75E-4	2.29E-3
WC30-085	166	140.8	30	85	Steady	S	59.6	6.09	2.8	2.55	0.054	2.4	0.009	0.277	2.11E-4	3.91E-3
WC30-105	166	140.8	30	105	Steady	S	68.7	6.07	2.4	2.73	0.054	2.0	0.012	0.342	3.25E-4	5.97E-3
WC30-135	166	140.8	30	135	Steady	S	76.6	6.62	2.2	3.15	0.046	1.8	0.014	0.440	4.50E-4	9.87E-3
WC30-165	166	140.8	30	165	Steady	S	87.0	6.69	1.9	3.39	0.045	1.6	0.017	0.538	6.59E-4	1.47E-2
3/4WC05-015	164	119.1	5	15	Steady	S	23.3	10.74	7.0	1.15	0.017	5.1	0.002	0.120	1.27E-5	7.31E-4
3/4WC05-020	164	119.1	5	20	Steady	S	31.6	9.10	5.2	1.13	0.024	3.8	0.003	0.160	3.14E-5	1.30E-3
3/4WC05-025	164	119.1	5	25	Steady	S	45.9	6.49	3.6	0.97	0.048	2.6	0.006	0.200	9.65E-5	2.03E-3
3/4WC05-035	164	119.1	5	30	Steady	S	56.2	5.74	2.9	0.95	0.061	2.1	0.008	0.240	1.78E-4	2.93E-3
3/4WC10-035	164	119.1	10	30	Steady	S	42.5	6.17	3.9	1.26	0.053	2.8	0.005	0.169	7.69E-5	1.46E-3
3/4WC20-035	164	119.1	20	30	Steady	S	44.0	4.14	3.7	1.22	0.117	2.7	0.005	0.120	8.54E-5	7.31E-4
3/4WC30-020	164	119.1	30	20	Steady	S	-	-	-	-	- -	-				
3/4WC30-025	164	119.1	30	25	Steady	S	30.0	5.01	5.5	1.49	0.080	4.0	0.003	0.082	2.70E-5	3.39E-4
3/4WC30-035	164	119.1	30	30	Steady	S	40.0	3.90	4.1	1.34	0.131	3.0	0.005	0.098	6.40E-5	4.88E-4
1/2WC05-015	169	74.1	5	15	Steady	S	35.7	5.68	4.7	0.75	0.062	2.1	0.004	0.120	4.53E-5	7.31E-4
1/2WC05-020	169	74.1	5	20	Steady	S	40.8	6.18	4.1	0.87	0.052	1.8	0.005	0.160	6.81E-5	1.30E-3
1/2WC05-025	169	74.1	5	25	Steady	S	46.9	6.27	3.6	0.95	0.051	1.6	0.006	0.200	1.03E-4	2.03E-3
1/2WC05-035	169	74.1	5	35	Steady	S	62.4	5.73	2.7	1.00	0.061	1.2	0.010	0.280	2.43E-4	3.98E-3

Experimental Arrangement	Weir Spacing (L) (mm)	Weir Height (p) (mm)	Slope (%)	Discharge (Qm) (l/s)	Stability d/dt	Type of Flow Pattern	Streaming Depth (d) (mm)	$Q_* = \frac{Q}{bd^{3/2}\sqrt{gS_o}}$	L/d	U=Q/A (m/s)	$C_f = \frac{2gS_o}{U^2}(R)$	p/d	$d^{5/3}$ (m^(5/3))	$\frac{q}{\sqrt{S_o}}$ (m^2/s)	d^3 (m^3)	$\frac{q^2}{2gS_o}$ (m)
1/2WC05-045	169	74.1	5	45	Steady	S	66.9	6.64	2.5	1.20	0.045	1.1	0.011	0.359	2.99E-4	6.58E-3
1/2WC10-015	169	74.1	10	15	Steady	S	29.1	5.46	5.8	0.92	0.067	2.5	0.003	0.085	2.45E-5	3.66E-4
1/2WC10-020	169	74.1	10	20	Steady	S	34.1	5.72	5.0	1.05	0.061	2.2	0.004	0.113	3.98E-5	6.50E-4
1/2WC10-025	169	74.1	10	25	Steady	S	42.5	5.15	4.0	1.05	0.075	1.7	0.005	0.141	7.66E-5	1.02E-3
1/2WC10-035	169	74.1	10	35	Steady	S	51.2	5.45	3.3	1.22	0.067	1.4	0.007	0.198	1.34E-4	1.99E-3
1/2WC10-045	169	74.1	10	45	Steady	S	57.6	5.87	2.9	1.39	0.058	1.3	0.009	0.254	1.91E-4	3.29E-3
1/2WC15-020	169	74.1	15	20	Steady	S	34.4	4.61	4.9	1.04	0.094	2.2	0.004	0.092	4.08E-5	4.33E-4
1/2WC15-025	169	74.1	15	25	Steady	S	37.5	5.07	4.5	1.19	0.078	2.0	0.004	0.115	5.27E-5	6.77E-4
1/2WC15-035	169	74.1	15	35	Steady	S	45.1	5.38	3.7	1.39	0.069	1.6	0.006	0.161	9.18E-5	1.33E-3
1/2WC15-045	169	74.1	15	45	Steady	S	52.7	5.47	3.2	1.52	0.067	1.4	0.007	0.207	1.47E-4	2.19E-3
1/2WC20-020	169	74.1	20	20	Steady	S	30.8	4.72	5.5	1.16	0.090	2.4	0.003	0.080	2.92E-5	3.25E-4
1/2WC20-025	169	74.1	20	25	Steady	S	43.6	3.50	3.9	1.02	0.163	1.7	0.005	0.100	8.28E-5	5.08E-4
1/2WC20-035	169	74.1	20	35	Steady	S	50.6	3.92	3.3	1.24	0.130	1.5	0.007	0.140	1.30E-4	9.95E-4
1/2WC20-045	169	74.1	20	45	Steady	S	57.3	4.18	2.9	1.40	0.114	1.3	0.009	0.180	1.88E-4	1.65E-3
1/2WC30-035	169	74.1	30	35	Steady	S	48.2	3.45	3.5	1.30	0.168	1.5	0.006	0.114	1.12E-4	6.64E-4
1/2WC30-045	169	74.1	30	45	Steady	S	55.8	3.56	3.0	1.44	0.158	1.3	0.008	0.147	1.74E-4	1.10E-3
WD05-005	77	140.8	5	5	Steady	S	17.0	5.73	4.5	0.52	0.061	8.3	0.001	0.040	4.95E-6	8.13E-5
WD05-010	77	140.8	5	10	Steady	S	25.3	6.34	3.0	0.71	0.050	5.6	0.002	0.080	1.62E-5	3.25E-4
WD05-015	77	140.8	5	15	Steady	S	34.1	6.06	2.3	0.78	0.054	4.1	0.004	0.120	3.98E-5	7.31E-4
WD05-020	77	140.8	5	20	Steady	S	38.4	6.77	2.0	0.93	0.044	3.7	0.004	0.160	5.67E-5	1.30E-3
WD05-025	77	140.8	5	25	Steady	S	43.6	7.00	1.8	1.02	0.041	3.2	0.005	0.200	8.28E-5	2.03E-3
WD05-035	77	140.8	5	35	Steady	S	53.0	7.31	1.5	1.18	0.037	2.7	0.007	0.280	1.49E-4	3.98E-3
WD05-045	77	140.8	5	45	Steady	S	61.9	7.46	1.2	1.30	0.036	2.3	0.010	0.359	2.37E-4	6.58E-3
WD05-065	77	140.8	5	65	Steady	S	88.4	6.31	0.9	1.31	0.050	1.6	0.018	0.519	6.91E-4	1.37E-2
WD05-085	77	140.8	5	85	Steady	S	98.8	6.98	0.8	1.54	0.041	1.4	0.021	0.679	9.63E-4	2.35E-2
WD05-105	77	140.8	5	105	Steady	S	116.4	6.74	0.7	1.61	0.044	1.2	0.028	0.839	1.58E-3	3.58E-2
WD05-135	77	140.8	5	135	Steady	S	137.2	6.78	0.6	1.76	0.044	1.0	0.036	1.078	2.58E-3	5.92E-2
WD05-165	77	140.8	5	165	Steady	S	155.1	6.88	0.5	1.90	0.042	0.9	0.045	1.318	3.73E-3	8.85E-2
WD10-010	77	140.8	10	10	Steady	S	21.0	5.91	3.7	0.85	0.057	6.7	0.002	0.056	9.30E-6	1.63E-4
WD10-015	77	140.8	10	15	Steady	S	25.3	6.72	3.0	1.06	0.044	5.6	0.002	0.085	1.62E-5	3.66E-4
WD10-020	77	140.8	10	20	Steady	S	31.1	6.58	2.5	1.15	0.046	4.5	0.003	0.113	3.01E-5	6.50E-4
WD10-025	77	140.8	10	25	Steady	S	34.4	7.05	2.2	1.30	0.040	4.1	0.004	0.141	4.08E-5	1.02E-3
WD10-035	77	140.8	10	35	Steady	S	45.8	6.44	1.7	1.36	0.048	3.1	0.006	0.198	9.61E-5	1.99E-3
WD10-045	77	140.8	10	45	Steady	S	54.0	6.47	1.4	1.49	0.048	2.6	0.008	0.254	1.57E-4	3.29E-3
WD10-065	77	140.8	10	65	Steady	S	67.1	6.75	1.1	1.73	0.044	2.1	0.011	0.367	3.02E-4	6.87E-3
WD10-085	77	140.8	10	85	Steady	S	80.5	6.71	1.0	1.89	0.044	1.7	0.015	0.480	5.21E-4	1.17E-2
WD10-105	77	140.8	10	105	Steady	S	92.4	6.75	0.8	2.03	0.044	1.5	0.019	0.593	7.88E-4	1.79E-2
WD10-135	77	140.8	10	135	Steady	S	107.6	6.90	0.7	2.24	0.042	1.3	0.024	0.762	1.25E-3	2.96E-2
WD10-165	77	140.8	10	165	Steady	S	126.5	6.61	0.6	2.33	0.046	1.1	0.032	0.932	2.02E-3	4.42E-2
WD15-010	77	140.8	15	10	Steady	S	16.5	6.97	4.7	1.08	0.041	8.6	0.001	0.046	4.46E-6	1.08E-4
WD15-015	77	140.8	15	15	Steady	S	24.4	5.80	3.2	1.10	0.059	5.8	0.002	0.069	1.45E-5	2.44E-4

Experimental Arrangement	Weir Spacing (L) (mm)	Weir Height (p) (mm)	Slope (%)	Discharge (Qm) (l/s)	Stability d/dt	Type of Flow Pattern	Streaming Depth (d) (mm)	$Q_* = \frac{Q}{bd^{3/2}\sqrt{gS_o}}$	L/d	U=Q/A (m/s)	$C_f = \frac{2gS_o}{U^2}k(R)$	p/d	$d^{5/3}$ (m^(5/3))	$\frac{q}{\sqrt{S_o}}$ (m^2/s)	d^3 (m^3)	$\frac{q^2}{2gS_o}$ (m)
WD15-020	77	140.8	15	20	Steady	S	28.4	6.17	2.7	1.26	0.053	5.0	0.003	0.092	2.28E-5	4.33E-4
WD15-025	77	140.8	15	25	Steady	S	32.3	6.34	2.4	1.38	0.050	4.4	0.003	0.115	3.37E-5	6.77E-4
WD15-035	77	140.8	15	35	Steady	S	39.6	6.53	1.9	1.58	0.047	3.6	0.005	0.161	6.22E-5	1.33E-3
WD15-045	77	140.8	15	45	Steady	S	50.0	5.93	1.5	1.61	0.057	2.8	0.007	0.207	1.25E-4	2.19E-3
WD15-065	77	140.8	15	65	Steady	S	61.3	6.31	1.3	1.89	0.050	2.3	0.010	0.300	2.30E-4	4.58E-3
WD15-085	77	140.8	15	85	Steady	S	71.9	6.49	1.1	2.11	0.048	2.0	0.012	0.392	3.72E-4	7.83E-3
WD15-105	77	140.8	15	105	Steady	S	84.4	6.30	0.9	2.22	0.050	1.7	0.016	0.484	6.02E-4	1.19E-2
WD15-135	77	140.8	15	135	Steady	S	96.3	6.65	0.8	2.50	0.045	1.5	0.020	0.622	8.94E-4	1.97E-2
WD15-165	77	140.8	15	165	Steady	S	111.3	6.55	0.7	2.65	0.047	1.3	0.026	0.761	1.38E-3	2.95E-2
WD20-015	77	140.8	20	15	Steady	S	23.5	5.32	3.3	1.14	0.071	6.0	0.002	0.060	1.29E-5	1.83E-4
WD20-020	77	140.8	20	20	Steady	S	27.7	5.52	2.8	1.29	0.066	5.1	0.003	0.080	2.13E-5	3.25E-4
WD20-025	77	140.8	20	25	Steady	S	33.2	5.26	2.3	1.34	0.072	4.2	0.003	0.100	3.67E-5	5.08E-4
WD20-035	77	140.8	20	35	Steady	S	40.5	5.47	1.9	1.54	0.067	3.5	0.005	0.140	6.66E-5	9.95E-4
WD20-045	77	140.8	20	45	Steady	S	47.2	5.59	1.6	1.70	0.064	3.0	0.006	0.180	1.05E-4	1.65E-3
WD20-065	77	140.8	20	65	Steady	S	62.5	5.31	1.2	1.86	0.071	2.3	0.010	0.260	2.44E-4	3.43E-3
WD20-085	77	140.8	20	85	Steady	S	72.5	5.55	1.1	2.09	0.065	1.9	0.013	0.339	3.82E-4	5.87E-3
WD20-105	77	140.8	20	105	Steady	S	77.7	6.18	1.0	2.41	0.052	1.8	0.014	0.419	4.69E-4	8.96E-3
WD20-135	77	140.8	20	135	Steady	S	94.5	5.93	0.8	2.55	0.057	1.5	0.020	0.539	8.44E-4	1.48E-2
WD20-165	77	140.8	20	165	Steady	S	104.9	6.20	0.7	2.81	0.052	1.3	0.023	0.659	1.15E-3	2.21E-2
WD30-035	77	140.8	30	35	Steady	S	33.5	5.93	2.3	1.86	0.057	4.2	0.003	0.114	3.77E-5	6.64E-4
WD30-045	77	140.8	30	45	Steady	S	43.0	5.26	1.8	1.87	0.072	3.3	0.005	0.147	7.94E-5	1.10E-3
WD30-065	77	140.8	30	65	Steady	S	49.7	6.11	1.5	2.34	0.054	2.8	0.007	0.212	1.23E-4	2.29E-3
WD30-085	77	140.8	30	85	Steady	S	64.0	5.46	1.2	2.37	0.067	2.2	0.010	0.277	2.62E-4	3.91E-3
WD30-105	77	140.8	30	105	Steady	S	72.5	5.59	1.1	2.58	0.064	1.9	0.013	0.342	3.82E-4	5.97E-3
WD30-135	77	140.8	30	135	Steady	S	90.2	5.19	0.9	2.67	0.074	1.6	0.018	0.440	7.34E-4	9.87E-3
WD30-165	77	140.8	30	165	Steady	S	92.4	6.12	0.8	3.19	0.053	1.5	0.019	0.538	7.88E-4	1.47E-2
Transitional Streaming Flows																
WB15-045	335	140.8	15	45	Steady	tS	*64.7*	4.02	5.2	1.24	0.124	2.2	-	-	-	-
WB15-065	335	140.8	15	65	Steady	tS	*85.0*	3.86	3.9	1.36	0.134	1.7	-	-	-	-
WB15-085	335	140.8	15	85	Steady	tS	*100.0*	3.96	3.4	1.52	0.128	1.4	-	-	-	-
WB20-045	335	140.8	20	45	Steady	tS	*61.0*	3.81	5.5	1.32	0.138	2.3	-	-	-	-
WB20-065	335	140.8	20	65	Steady	tS	*90.8*	3.03	3.7	1.28	0.218	1.6	-	-	-	-
WB20-085	335	140.8	20	85	Steady	tS	*102.0*	3.33	3.3	1.49	0.181	1.4	-	-	-	-
WB20-105	335	140.8	20	105	Steady	tS	*113.7*	3.49	2.9	1.65	0.164	1.2	-	-	-	-
WB20-135	335	140.8	20	135	Steady	tS	*134.4*	3.49	2.5	1.79	0.164	1.0	-	-	-	-
3/4WB05-010	342	119.1	5	10	Steady	tS	30.0	4.91	11.4	0.60	0.083	4.0	-	-	-	-
3/4WB05-015	342	119.1	5	15	Steady	tS	35.0	5.84	9.8	0.77	0.059	3.4	-	-	-	-
3/4WB05-020	342	119.1	5	20	Steady	tS	46.0	5.17	7.4	0.78	0.075	2.6	-	-	-	-
3/4WB05-025	342	119.1	5	25	Steady	tS	64.0	3.94	5.3	0.70	0.129	1.9	-	-	-	-

Experimental Arrangement	Weir Spacing (L) (mm)	Weir Height (p) (mm)	Slope (%)	Discharge (Qm) (l/s)	Stability d/dt	Type of Flow Pattern	Streaming Depth (d) (mm)	$Q_* = \frac{Q}{bd^{3/2}\sqrt{gS_o}}$	L/d	U=Q/A (m/s)	$C_f = \frac{2gS_o}{U^2}(R)$	p/d	$d^{5/3}$ (m^(5/3))	$\frac{q}{\sqrt{S_o}}$ (m^2/s)	d^3 (m^3)	$\frac{q^2}{2gS_o}$ (ms)
3/4WB10-035	342	119.1	10	30	Steady	tS	-	-	-	-	-	-	-	-	-	-
3/4WB20-035	342	119.1	20	30	Steady	tS	-	-	-	-	-	-	-	-	-	-
1/2WB05-025	348	74.1	5	25	Steady	tS	*62.0*	4.13	5.6	0.72	0.117	1.2	-	-	-	-
1/2WB05-035	348	74.1	5	35	Steady	tS	*76.1*	4.25	4.6	0.82	0.111	1.0	-	-	-	-
3/4WC05-010	164	119.1	5	10	Steady	tS	*16.6*	11.91	9.9	1.08	0.014	7.2	-	-	-	-
3/4WC10-015	164	119.1	10	15	Steady	tS	*23.6*	7.45	6.9	1.13	0.036	5.0	-	-	-	-
3/4WC15-035	164	119.1	15	30	Steady	tS	*44.0*	4.78	3.7	1.22	0.088	2.7	-	-	-	-
3/4WC30-010	164	119.1	30	10	Steady	tS	-	-	-	-	-	-	-	-	-	-
3/4WC30-015	164	119.1	30	15	Steady	tS	-	-	-	-	-	-	-	-	-	-
1/2WC05-005	169	74.1	5	5	Steady	tS	*15.3*	6.73	11.0	0.58	0.044	4.8	-	-	-	-
1/2WC05-010	169	74.1	5	10	Steady	tS	*28.2*	5.39	6.0	0.63	0.069	2.6	-	-	-	-
1/2WC15-015	169	74.1	15	15	Steady	tS	*29.9*	4.28	5.7	0.90	0.109	2.5	-	-	-	-
1/2WC20-015	169	74.1	20	15	Steady	tS	*23.8*	5.22	7.1	1.13	0.073	3.1	-	-	-	-
1/2WC30-020	169	74.1	30	20	Steady	tS	*34.8*	3.21	4.9	1.03	0.194	2.1	-	-	-	-
1/2WC30-025	169	74.1	30	25	Steady	tS	*42.1*	3.02	4.0	1.06	0.220	1.8	-	-	-	-

Table 4: Experimental and Computational Data for Transitional Flow

Legend

P = Plunging Flow
Pt = Plunging Transitional Flow (slight deviation from plunging flow conditions)
T = Transitional Flow
tS = Transitional Streaming Flow (slight deviation from streaming flow conditions)
S = Streaming Flow
tB = Transitional Baffle Flow (flow is developing into baffle flow rather than streaming flow)
B = Baffle flow
B/S = Baffle Streaming Flow
P = Plunging Flow pattern which has a section of supercritical bed flow
B = Baffle Flow pattern which has a section of supercritical bed flow

Experimental Arrangement	Weir Spacing (L) (mm)	Weir Height (p) (mm)	Slope (%)	Discharge (Qm) (l/s)	Stability d/dt	Type of Flow Pattern	$Q_t = \frac{Q}{\sqrt{g} b S_o L^{3/2}}$
WB05-010	335	140.82	5	10	Steady	T	0.59
WB05-015	335	140.82	5	15	Steady	T	0.88
WB20-035	335	140.82	20	35	Steady	T	0.51
WC05-010	166	140.82	5	10	Steady	T	1.69
1/2WC05-002.5	169	74.07	5	2.5	Steady	T	0.41
1/2WC30-015	169	74.07	30	15	Steady	T	0.41
WB05-020	335	140.82	5	20	Unsteady	T	1.18
WB10-025	335	140.82	10	25	Unsteady	T	0.74
WB20-025	335	140.82	20	25	Unsteady	T	0.37
WB30-025	335	140.82	30	25	Unsteady	T	0.25
WC10-010	166	140.82	10	10	Unsteady	T	0.84
WC10-015	166	140.82	10	15	Unsteady	T	1.26
WC20-010	166	140.82	20	10	Unsteady	T	0.42
1/2WC20-010	169	74.07	20	10	Unsteady	T	0.41
3/4WC20-010	164	119.10	20	10	Unsteady	T	0.43
WA05-025	685	140.82	5	25	Steady	Pt	0.50
WA10-065	685	140.82	10	65	Steady	Pt	0.65
WB05-005	335	140.82	5	5	Steady	Pt	0.29
WB10-010	335	140.82	10	10	Steady	Pt	0.29
WC05-005	166	140.82	5	5	Steady	Pt	0.84
1/2WB10-020	348	74.07	10	20	Steady	Pt	0.56
1/2WB15-020	348	74.07	15	20	Steady	Pt	0.37
WB10-015	335	140.82	10	15	Unsteady	Pt	0.44
WB10-020	335	140.82	10	20	Unsteady	Pt	0.59
WB20-020	335	140.82	20	20	Unsteady	Pt	0.29
WB30-020	335	140.82	30	20	Unsteady	Pt	0.20
WC20-005	166	140.82	20	5	Unsteady	Pt	0.21
WC30-005	166	140.82	30	5	Unsteady	Pt	0.14
1/2WB05-010	348	74.07	5	10	Unsteady	Pt	0.56
1/2WB05-015	348	74.07	5	15	Unsteady	Pt	0.83
1/2WC15-010	169	74.07	15	10	Unsteady	Pt	0.55
3/4WB10-020	342	119.10	10	20	Unsteady	Pt	0.57
3/4WB10-025	342	119.10	10	25	Unsteady	Pt	0.71
3/4WB15-025	342	119.10	15	25	Unsteady	Pt	0.48
3/4WB20-025	342	119.10	20	25	Unsteady	Pt	0.36
3/4WB30-025	342	119.10	30	25	Unsteady	Pt	0.24
WB15-045	335	140.82	15	45	Steady	tS	0.88
WB15-065	335	140.82	15	65	Steady	tS	1.27
WB15-085	335	140.82	15	85	Steady	tS	1.67

Experimental Arrangement	Weir Spacing (L) (mm)	Weir Height (p) (mm)	Slope (%)	Discharge (Qm) (l/s)	Stability d/dt	Type of Flow Pattern	$Q_t = \frac{Q}{\sqrt{gbS_o}L^{3/2}}$
WB20-045	335	140.82	20	45	Steady	tS	0.66
WB20-065	335	140.82	20	65	Steady	tS	0.96
WB20-085	335	140.82	20	85	Steady	tS	1.25
WB20-105	335	140.82	20	105	Steady	tS	1.54
WB20-135	335	140.82	20	135	Steady	tS	1.98
WD15-005	77	140.82	15	5	Steady	tS	0.89
WD20-005	77	140.82	20	5	Steady	tS	0.67
1/2WB05-025	348	74.07	5	25	Steady	tS	1.39
1/2WB05-035	348	74.07	5	35	Steady	tS	1.94
1/2WC05-005	169	74.07	5	5	Steady	tS	0.82
1/2WC05-010	169	74.07	5	10	Steady	tS	1.64
1/2WC15-015	169	74.07	15	15	Steady	tS	0.82
1/2WC20-015	169	74.07	20	15	Steady	tS	0.62
1/2WC30-020	169	74.07	30	20	Steady	tS	0.55
1/2WC30-025	169	74.07	30	25	Steady	tS	0.68
3/4WB05-010	342	119.10	5	10	Steady	tS	0.57
3/4WB05-015	342	119.10	5	15	Steady	tS	0.86
3/4WB05-020	342	119.10	5	20	Steady	tS	1.14
3/4WB05-025	342	119.10	5	25	Steady	tS	1.43
3/4WB10-035	342	119.10	10	30	Steady	tS	0.86
3/4WB20-035	342	119.10	20	30	Steady	tS	0.43
3/4WC05-010	164	119.10	5	10	Steady	tS	1.72
3/4WC10-015	164	119.10	10	15	Steady	tS	1.29
3/4WC15-035	164	119.10	15	30	Steady	tS	1.72
3/4WC30-010	164	119.10	30	10	Steady	tS	0.29
3/4WC30-015	164	119.10	30	15	Steady	tS	0.43
WB05-025	335	140.82	5	25	Unsteady	tS	1.47
WB10-035	335	140.82	10	35	Unsteady	tS	1.03
WB10-045	335	140.82	10	45	Unsteady	tS	1.32
WB10-065	335	140.82	10	65	Unsteady	tS	1.91
WB15-035	335	140.82	15	35	Unsteady	tS	0.69
WB30-045	335	140.82	30	45	Unsteady	tB/tS	0.44
WB30-065	335	140.82	30	65	Unsteady	tS	0.64
WC15-010	166	140.82	15	10	Unsteady	tS	0.56
WC20-015	166	140.82	20	15	Unsteady	tS	0.63
WC20-020	166	140.82	20	20	Unsteady	tS	0.84
WC20-025	166	140.82	20	25	Unsteady	tS	1.05
WC20-035	166	140.82	20	35	Unsteady	tS	1.48
WC30-010	166	140.82	30	10	Unsteady	tS	0.28
WC30-015	166	140.82	30	15	Unsteady	tS	0.42
WC30-020	166	140.82	30	20	Unsteady	tS	0.56
WD10-005	77	140.82	10	5	Unsteady	tS	1.33
WD30-005	77	140.82	30	5	Unsteady	tS	0.44
1/2WB05-020	348	74.07	5	20	Unsteady	tS	1.11
1/2WB05-045	348	74.07	5	45	Unsteady	tS	2.50
1/2WB10-045	348	74.07	10	45	Unsteady	tS	1.25
1/2WB15-035	348	74.07	15	35	Unsteady	tS	0.65
1/2WB15-045	348	74.07	15	45	Unsteady	tS	0.83
1/2WB20-045	348	74.07	20	45	Unsteady	tS	0.62
1/2WB30-045	348	74.07	30	45	Unsteady	tS	0.42
1/2WC10-010	169	74.07	10	10	Unsteady	tS	0.82
3/4WB15-035	342	119.10	15	30	Unsteady	tS	0.57
3/4WB30-035	342	119.10	30	30	Unsteady	tS	0.29
3/4WC10-010	164	119.10	10	10	Unsteady	tS	0.86
3/4WC10-020	164	119.10	10	20	Unsteady	tS	1.72
3/4WC10-025	164	119.10	10	25	Unsteady	tS	2.15
3/4WC15-010	164	119.10	15	10	Unsteady	tS	0.57
3/4WC15-015	164	119.10	15	15	Unsteady	tS	0.86
3/4WC15-020	164	119.10	15	20	Unsteady	tS	1.14
3/4WC15-025	164	119.10	15	25	Unsteady	tS	1.43
3/4WC20-015	164	119.10	20	15	Unsteady	tS	0.64
3/4WC20-020	164	119.10	20	20	Unsteady	tS	0.86
3/4WC20-025	164	119.10	20	25	Unsteady	tS	1.07

Experimental Arrangement	Weir Spacing (L) (mm)	Weir Height (p) (mm)	Slope (%)	Discharge (Qm) (l/s)	Stability d/dt	Type of Flow Pattern	$Q_t = \frac{Q}{\sqrt{g} b S_o L^{3/2}}$
WA15-065	685	140.82	15	65	Steady	tB	0.44
WA20-065	685	140.82	20	65	Steady	tB	0.33
WA20-085	685	140.82	20	85	Steady	tB	0.43
1/2WB20-025	348	74.07	20	25	Steady	tB	0.35
1/2WB30-015	348	74.07	30	15	Steady	tB	0.14
1/2WB30-020	348	74.07	30	20	Steady	tB	0.19
WA05-035	685	140.82	5	35	Unsteady	tB	0.70
WA05-045	685	140.82	5	45	Unsteady	tB	0.91
WB30-035	335	140.82	30	35	Unsteady	tB	0.34
1/2WB10-025	348	74.07	10	25	Unsteady	tB	0.69
1/2WB10-035	348	74.07	10	35	Unsteady	Bt	0.97
WB30-045	335	140.82	30	45	Unsteady	tB/tS	0.44
Plunging Flow							
WA05-005	685	140.82	5	5	Steady	P	0.10
WA05-010	685	140.82	5	10	Steady	P	0.20
WA05-015	685	140.82	5	15	Steady	P	0.30
WA05-020	685	140.82	5	20	Steady	P	0.40
WA10-005	685	140.82	10	5	Steady	P	0.05
WA10-010	685	140.82	10	10	Steady	P	0.10
WA10-015	685	140.82	10	15	Steady	P	0.15
WA10-035	685	140.82	10	35	Steady	P	0.35
WA10-045	685	140.82	10	45	Steady	P	0.45
WA15-005	685	140.82	15	5	Steady	P	0.03
WA15-010	685	140.82	15	10	Steady	P	0.07
WA15-020	685	140.82	15	20	Steady	P	0.13
WA15-025	685	140.82	15	25	Steady	P	0.17
WA15-035	685	140.82	15	35	Steady	P	0.23
WA15-045	685	140.82	15	45	Steady	P	0.30
WA20-005	685	140.82	20	5	Steady	P	0.03
WA20-010	685	140.82	20	10	Steady	P	0.05
WA20-015	685	140.82	20	15	Steady	P	0.08
WA20-020	685	140.82	20	20	Steady	P	0.10
WA30-020	685	140.82	30	20	Steady	P	0.07
WA30-025	685	140.82	30	25	Steady	P	0.08
WA30-035	685	140.82	30	35	Steady	P	0.12
WA30-045	685	140.82	30	45	Steady	P	0.15
1/2WA05-002.5	703	74.07	5	2.5	Steady	P	0.05
1/2WA05-005	703	74.07	5	5	Steady	P	0.10
1/2WA05-010	703	74.07	5	10	Steady	P	0.19
1/2WA05-015	703	74.07	5	15	Steady	P	0.29
1/2WA05-020	703	74.07	5	20	Steady	P	0.39
1/2WA05-025	703	74.07	5	25	Steady	P	0.48
1/2WA05-035	703	74.07	5	35	Steady	P	0.68
1/2WA05-045	703	74.07	5	45	Steady	P	0.87
3/4WA05-010	694	119.1006	5	10	Steady	P	0.20
3/4WA05-015	694	119.1006	5	15	Steady	P	0.30
3/4WA05-020	694	119.1006	5	20	Steady	P	0.39
3/4WA05-025	694	119.1006	5	25	Steady	P	0.49
3/4WA05-035	694	119.1006	5	30	Steady	P	0.59
3/4WA10-010	694	119.1006	10	10	Steady	P	0.10
3/4WA10-015	694	119.1006	10	15	Steady	P	0.15
3/4WA10-12	694	119.1006	10	20	Steady	P	0.20
3/4WA10-13	694	119.1006	10	25	Steady	P	0.25
3/4WA10-14	694	119.1006	10	30	Steady	P	0.30
3/4WA15-010	694	119.1006	15	10	Steady	P	0.07
3/4WA15-015	694	119.1006	15	15	Steady	P	0.10
3/4WA15-020	694	119.1006	15	20	Steady	P	0.13
3/4WA15-025	694	119.1006	15	25	Steady	P	0.16
3/4WA15-035	694	119.1006	15	30	Steady	P	0.20

Experimental Arrangement	Weir Spacing (L.) (mm)	Weir Height (p) (mm)	Slope (%)	Discharge (Qm) (l/s)	Stability d/dt	Type of Flow Pattern	$Q_t = \frac{Q}{\sqrt{gbS_o L^{3/2}}}$
WB10-005	335	140.82	10	5	Steady	P	0.15
WB15-005	335	140.82	15	5	Steady	P	0.10
WB15-010	335	140.82	15	10	Steady	P	0.20
WB20-005	335	140.82	20	5	Steady	P	0.07
WB20-015	335	140.82	20	15	Steady	P	0.22
WB30-005	335	140.82	30	5	Steady	P	0.05
WB30-015	335	140.82	30	15	Steady	P	0.15
1/2WB05-002.5	348	74.07	5	2.5	Steady	P	0.14
1/2WB05-005	348	74.07	5	5	Steady	P	0.28
1/2WB10-002.5	348	74.07	10	2.5	Steady	P	0.07
1/2WB10-005	348	74.07	10	5	Steady	P	0.14
1/2WB10-010	348	74.07	10	10	Steady	P	0.28
1/2WB10-015	348	74.07	10	15	Steady	P	0.42
1/2WB15-002.5	348	74.07	15	2.5	Steady	P	0.05
1/2WB15-005	348	74.07	15	5	Steady	P	0.09
1/2WB15-010	348	74.07	15	10	Steady	P	0.19
1/2WB15-015	348	74.07	15	15	Steady	P	0.28
1/2WB20-002.5	348	74.07	20	2.5	Steady	P	0.03
1/2WB20-005	348	74.07	20	5	Steady	P	0.07
1/2WB20-010	348	74.07	20	10	Steady	P	0.14
1/2WB20-015	348	74.07	20	15	Steady	P	0.21
1/2WB20-020	348	74.07	20	20	Steady	P	0.28
1/2WB30-010	348	74.07	30	10	Steady	P	0.09
3/4WB10-010	342	119.1006	10	10	Steady	P	0.29
3/4WB15-010	342	119.1006	15	10	Steady	P	0.19
3/4WB15-015	342	119.1006	15	15	Steady	P	0.29
3/4WB15-020	342	119.1006	15	20	Steady	P	0.38
3/4WB20-010	342	119.1006	20	10	Steady	P	0.14
3/4WB20-015	342	119.1006	20	15	Steady	P	0.21
3/4WB20-020	342	119.1006	20	20	Steady	P	0.29
3/4WB30-010	342	119.1006	30	10	Steady	P	0.10
3/4WB30-015	342	119.1006	30	15	Steady	P	0.14
3/4WB30-020	342	119.1006	30	20	Steady	P	0.19
WC10-005	166	140.82	10	5	Steady	P	0.42
WC15-005	166	140.82	15	5	Steady	P	0.28
1/2WC10-002.5	169	74.07	10	2.5	Steady	P	0.21
1/2WC10-005	169	74.07	10	5	Steady	P	0.41
1/2WC15-002.5	169	74.07	15	2.5	Steady	P	0.14
1/2WC15-005	169	74.07	15	5	Steady	P	0.27
1/2WC20-002.5	169	74.07	20	2.5	Steady	P	0.10
1/2WC20-005	169	74.07	20	5	Steady	P	0.21
1/2WC30-002.5	169	74.07	30	2.5	Steady	P	0.07
1/2WC30-005	169	74.07	30	5	Steady	P	0.14
WA10-020	685	140.82	10	20	Unsteady	P	0.20
WA10-025	685	140.82	10	25	Unsteady	P	0.25
WA15-015	685	140.82	15	15	Unsteady	P	0.10
WA20-025	685	140.82	20	25	Unsteady	P	0.13
WA20-035	685	140.82	20	35	Unsteady	P	0.18
WA20-045	685	140.82	20	45	Unsteady	P	0.23
WB15-015	335	140.82	15	15	Unsteady	P	0.29
WB15-020	335	140.82	15	20	Unsteady	P	0.39
WB20-010	335	140.82	20	10	Unsteady	P	0.15
WB30-010	335	140.82	30	10	Unsteady	P	0.10
3/4WB10-015	342	119.1006	10	15	Unsteady	P	0.43
1/2WC30-010	169	74.07	30	10	Unsteady	P	0.27

Streaming Flow

WB05-135	335	140.82	5	135	Steady	S	7.94
WB05-165	335	140.82	5	165	Steady	S	9.70
WB10-085	335	140.82	10	85	Steady	S	2.50

Experimental Arrangement	Weir Spacing (L) (mm)	Weir Height (p) (mm)	Slope (%)	Discharge (Qm) (l/s)	Stability d/dt	Type of Flow Pattern	$Q_t = \frac{Q}{\sqrt{g}bS_oL^{3/2}}$
WB10-105	335	140.82	10	105	Steady	S	3.09
WB10-135	335	140.82	10	135	Steady	S	3.97
WB10-165	335	140.82	10	165	Steady	S	4.85
WB15-105	335	140.82	15	105	Steady	S	2.06
WB15-135	335	140.82	15	135	Steady	S	2.65
WB15-165	335	140.82	15	165	Steady	S	3.23
WB20-165	335	140.82	20	165	Steady	S	2.43
WB30-135	335	140.82	30	135	Steady	S	1.32
WB30-165	335	140.82	30	165	Steady	S	1.62
WC05-020	166	140.82	5	20	Steady	S	3.37
WC05-025	166	140.82	5	25	Steady	S	4.21
WC05-035	166	140.82	5	35	Steady	S	5.90
WC05-045	166	140.82	5	45	Steady	S	7.59
WC05-065	166	140.82	5	65	Steady	S	10.96
WC05-085	166	140.82	5	85	Steady	S	14.33
WC05-105	166	140.82	5	105	Steady	S	17.70
WC05-135	166	140.82	5	135	Steady	S	22.76
WC05-165	166	140.82	5	165	Steady	S	27.82
WC10-035	166	140.82	10	35	Steady	S	2.95
WC10-045	166	140.82	10	45	Steady	S	3.79
WC10-065	166	140.82	10	65	Steady	S	5.48
WC10-085	166	140.82	10	85	Steady	S	7.17
WC10-105	166	140.82	10	105	Steady	S	8.85
WC10-135	166	140.82	10	135	Steady	S	11.38
WC10-165	166	140.82	10	165	Steady	S	13.91
WC15-035	166	140.82	15	35	Steady	S	1.97
WC15-045	166	140.82	15	45	Steady	S	2.53
WC15-065	166	140.82	15	65	Steady	S	3.65
WC15-085	166	140.82	15	85	Steady	S	4.78
WC15-105	166	140.82	15	105	Steady	S	5.90
WC15-135	166	140.82	15	135	Steady	S	7.59
WC15-165	166	140.82	15	165	Steady	S	9.27
WC20-045	166	140.82	20	45	Steady	S	1.90
WC20-065	166	140.82	20	65	Steady	S	2.74
WC20-085	166	140.82	20	85	Steady	S	3.58
WC20-105	166	140.82	20	105	Steady	S	4.43
WC20-135	166	140.82	20	135	Steady	S	5.69
WC20-165	166	140.82	20	165	Steady	S	6.95
WC30-025	166	140.82	30	25	Steady	S	0.70
WC30-035	166	140.82	30	35	Steady	S	0.98
WC30-045	166	140.82	30	45	Steady	S	1.26
WC30-065	166	140.82	30	65	Steady	S	1.83
WC30-085	166	140.82	30	85	Steady	S	2.39
WC30-105	166	140.82	30	105	Steady	S	2.95
WC30-135	166	140.82	30	135	Steady	S	3.79
WC30-165	166	140.82	30	165	Steady	S	4.64
WD05-005	77	140.82	5	5	Steady	S	2.67
WD05-010	77	140.82	5	10	Steady	S	5.34
WD05-015	77	140.82	5	15	Steady	S	8.01
WD05-020	77	140.82	5	20	Steady	S	10.67
WD05-025	77	140.82	5	25	Steady	S	13.34
WD05-035	77	140.82	5	35	Steady	S	18.68
WD05-045	77	140.82	5	45	Steady	S	24.02
WD05-065	77	140.82	5	65	Steady	S	34.69
WD05-085	77	140.82	5	85	Steady	S	45.36
WD05-105	77	140.82	5	105	Steady	S	56.04
WD05-135	77	140.82	5	135	Steady	S	72.05
WD05-165	77	140.82	5	165	Steady	S	88.06
WD10-010	77	140.82	10	10	Steady	S	2.67
WD10-015	77	140.82	10	15	Steady	S	4.00
WD10-020	77	140.82	10	20	Steady	S	5.34
WD10-025	77	140.82	10	25	Steady	S	6.67
WD10-035	77	140.82	10	35	Steady	S	9.34

Experimental Arrangement	Weir Spacing (L) (mm)	Weir Height (p) (mm)	Slope (%)	Discharge (Qm) (l/s)	Stability d/dt	Type of Flow Pattern	$Q_* = \frac{Q}{\sqrt{g}bS_oL^{3/2}}$
WD10-045	77	140.82	10	45	Steady	S	12.01
WD10-065	77	140.82	10	65	Steady	S	17.34
WD10-085	77	140.82	10	85	Steady	S	22.68
WD10-105	77	140.82	10	105	Steady	S	28.02
WD10-135	77	140.82	10	135	Steady	S	36.02
WD10-165	77	140.82	10	165	Steady	S	44.03
WD15-010	77	140.82	15	10	Steady	S	1.78
WD15-015	77	140.82	15	15	Steady	S	2.67
WD15-020	77	140.82	15	20	Steady	S	3.56
WD15-025	77	140.82	15	25	Steady	S	4.45
WD15-035	77	140.82	15	35	Steady	S	6.23
WD15-045	77	140.82	15	45	Steady	S	8.01
WD15-065	77	140.82	15	65	Steady	S	11.56
WD15-085	77	140.82	15	85	Steady	S	15.12
WD15-105	77	140.82	15	105	Steady	S	18.68
WD15-135	77	140.82	15	135	Steady	S	24.02
WD15-165	77	140.82	15	165	Steady	S	29.35
WD20-015	77	140.82	20	15	Steady	S	2.00
WD20-020	77	140.82	20	20	Steady	S	2.67
WD20-025	77	140.82	20	25	Steady	S	3.34
WD20-035	77	140.82	20	35	Steady	S	4.67
WD20-045	77	140.82	20	45	Steady	S	6.00
WD20-065	77	140.82	20	65	Steady	S	8.67
WD20-085	77	140.82	20	85	Steady	S	11.34
WD20-105	77	140.82	20	105	Steady	S	14.01
WD20-135	77	140.82	20	135	Steady	S	18.01
WD20-165	77	140.82	20	165	Steady	S	22.01
WD30-035	77	140.82	30	35	Steady	S	3.11
WD30-045	77	140.82	30	45	Steady	S	4.00
WD30-065	77	140.82	30	65	Steady	S	5.78
WD30-085	77	140.82	30	85	Steady	S	7.56
WD30-105	77	140.82	30	105	Steady	S	9.34
WD30-135	77	140.82	30	135	Steady	S	12.01
WD30-165	77	140.82	30	165	Steady	S	14.68
1/2WC05-015	169	74.07	5	15	Steady	S	2.46
1/2WC05-020	169	74.07	5	20	Steady	S	3.28
1/2WC05-025	169	74.07	5	25	Steady	S	4.10
1/2WC05-035	169	74.07	5	35	Steady	S	5.74
1/2WC05-045	169	74.07	5	45	Steady	S	7.39
1/2WC10-015	169	74.07	10	15	Steady	S	1.23
1/2WC10-020	169	74.07	10	20	Steady	S	1.64
1/2WC10-025	169	74.07	10	25	Steady	S	2.05
1/2WC10-035	169	74.07	10	35	Steady	S	2.87
1/2WC10-045	169	74.07	10	45	Steady	S	3.69
1/2WC15-020	169	74.07	15	20	Steady	S	1.09
1/2WC15-025	169	74.07	15	25	Steady	S	1.37
1/2WC15-035	169	74.07	15	35	Steady	S	1.91
1/2WC15-045	169	74.07	15	45	Steady	S	2.46
1/2WC20-020	169	74.07	20	20	Steady	S	0.82
1/2WC20-025	169	74.07	20	25	Steady	S	1.03
1/2WC20-035	169	74.07	20	35	Steady	S	1.44
1/2WC20-045	169	74.07	20	45	Steady	S	1.85
1/2WC30-035	169	74.07	30	35	Steady	S	0.96
1/2WC30-045	169	74.07	30	45	Steady	S	1.23
3/4WB05-035	342	119.1006	5	30	Steady	S	1.71
3/4WC05-015	164	119.1006	5	15	Steady	S	2.58
3/4WC05-020	164	119.1006	5	20	Steady	S	3.43
3/4WC05-025	164	119.1006	5	25	Steady	S	4.29
3/4WC05-035	164	119.1006	5	30	Steady	S	5.15
3/4WC10-035	164	119.1006	10	30	Steady	S	2.58
3/4WC20-035	164	119.1006	20	30	Steady	S	1.29
3/4WC30-020	164	119.1006	30	20	Steady	S	0.57
3/4WC30-025	164	119.1006	30	25	Steady	S	0.72

Experimental Arrangement	Weir Spacing (L) (mm)	Weir Height (p) (mm)	Slope (%)	Discharge (Qm) (l/s)	Stability d/dt	Type of Flow Pattern	$Q_t = \frac{Q}{\sqrt{gbS_o}L^{3/2}}$
3/4WC30-035	164	119.1006	30	30	Steady	S	0.86
WB05-035	335	140.82	5	35	Unsteady	S	2.06
WB05-045	335	140.82	5	45	Unsteady	S	2.65
WB05-065	335	140.82	5	65	Unsteady	S	3.82
WB05-085	335	140.82	5	85	Unsteady	S	5.00
WB05-105	335	140.82	5	105	Unsteady	S	6.17
WB30-085	335	140.82	30	85	Unsteady	S	0.83
WB30-105	335	140.82	30	105	Unsteady	S	1.03
WC05-015	166	140.82	5	15	Unsteady	S	2.53
WC10-020	166	140.82	10	20	Unsteady	S	1.69
WC10-025	166	140.82	10	25	Unsteady	S	2.11
WC15-015	166	140.82	15	15	Unsteady	S	0.84
WC15-020	166	140.82	15	20	Unsteady	S	1.12
WC15-025	166	140.82	15	25	Unsteady	S	1.40
WD20-010	77	140.82	20	10	Unsteady	S	1.33
WD30-010	77	140.82	30	10	Unsteady	S	0.89
WD30-015	77	140.82	30	15	Unsteady	S	1.33
WD30-020	77	140.82	30	20	Unsteady	S	1.78
WD30-025	77	140.82	30	25	Unsteady	S	2.22

Table 5: Discrepancies in Continuity for Plunging Flows

WA10-035 Discharge Integration

Stationing (mm)	Forward Q (l/s)	Return Q (l/s)	Continuity (l/s)	Discrepancy (%)
-13.93	33.590	0.000	33.590	-4.03
50	47.280	-7.806	39.473	12.78
108	57.766	-12.578	45.188	29.11
175	57.777	-5.522	52.255	49.30
275	44.340	-8.955	35.384	1.10
325	45.574	-9.710	35.864	2.47
400	42.658	-8.815	33.842	-3.31
500	40.446	-11.880	28.566	-18.38
600	35.391	-4.355	31.036	-11.33
679	36.418	0.000	36.418	4.05

3/4WA10-035 Discharge Integration

Stationing (mm)	Forward Q (l/s)	Return Q (l/s)	Continuity (l/s)	Discrepancy (%)
-12	34.324	0.000	34.324	-1.93
63	39.401	-9.816	29.584	-15.47
103	38.978	-10.468	28.510	-18.54
138	38.779	-9.149	29.631	-15.34
188	40.103	0.000	40.103	14.58
238	37.248	-3.969	33.278	-4.92
288	41.346	-5.268	36.078	3.08
338	40.660	-5.897	34.763	-0.68
388	39.601	-5.325	34.275	-2.07
438	38.567	-6.132	32.435	-7.33
488	36.265	-5.010	31.255	-10.70
538	36.707	-4.426	32.281	-7.77
588	34.330	-1.711	32.619	-6.80
638	37.012	0.000	37.012	5.75
693	32.286	0.000	32.286	-7.75

1/2WA10-035 Discharge Integration

Stationing (mm)	Forward Q (l/s)	Return Q (l/s)	Continuity (l/s)	Discrepancy (%)
-7	39.824	0.000	39.824	13.78
53	40.665	-7.581	33.084	-5.47
93	42.246	-3.044	39.201	12.00
143	40.687	0.000	40.687	16.25
193	42.878	0.000	42.878	22.51
243	47.307	0.000	47.307	35.16
293	34.968	-3.117	31.851	-9.00
343	37.593	-3.569	34.024	-2.79
393	36.357	-2.546	33.810	-3.40
443	32.831	-2.928	29.903	-14.56
493	35.312	-1.936	33.376	-4.64
543	35.844	0.000	35.844	2.41
593	35.953	0.000	35.953	2.72
643	37.848	0.000	37.848	8.14
703	39.099	0.000	39.099	11.71

Table 6: Discrepancy in Continuity for a Transitional Streaming Flow

WB10-065 Discharge Integration

Stationing (mm)	Forward Q (l/s)	Return Q (l/s)	Continuity (l/s)	Error (%)
0	64.855	0.000	64.855	-0.22
50	69.425	not complete	69.425	
57	not complete	-12.837	-12.837	
100	70.746	-17.620	53.126	-18.27
150	82.922	-18.179	64.743	-0.40
200	87.618	-19.259	68.359	5.17
250	81.957	-17.367	64.590	-0.63
280	not complete	-13.348	-13.348	
335	68.861	not complete	68.861	

Table 7: Tabular Summary of Full Weir Height Experimental Data

Discharge Q (l/s)	Pool and Weir Study / Full Weir Height Spacing Class Designation Flume width = 560 mm																			
	A l = 685 mm					B l = 335 mm					C l = 166 mm					D l = 77 mm				
	Slope (%)					Slope (%)					Slope (%)					Slope (%)				
	5	10	15	20	30	5	10	15	20	30	5	10	15	20	30	5	10	15	20	30
5	Stdy P h = 27.3	Stdy P h = 27.3	Stdy P h = 29.1	Stdy *P* h = 28.1	UnStdy *P* h = 27.1	Stdy Pt _h = 28.7_	Stdy P h = 27.1	Stdy P h = 31.0	Stdy P h = 31.6	Stdy P h = 30.8	Stdy Pt _h = 21.0_	Stdy P h = 24.8	Stdy P h = 24.3	UnStdy Pt _h = 22.9_	UStdy Pt _h = 24.3_	Stdy S d = 17.0	UnStdy tS _d = 13.4_	Stdy tS _d = 11.7_	Stdy tS _d = 11.3_	UStdy tS _d = 12.4_
10	Stdy P h = 47.0	Stdy P h = 44.3	Stdy P h = 45.8	Stdy P h = 45.4	Stdy *P* h = 42.9	Stdy T	Stdy Pt _h = 49.2_	Stdy P h = 45.4	UnStdy P h = 48.0	UnStdy P h = 44.4	Stdy T	UnStdy T	UnStdy tS _d = 27.4_	UnStdy T	UnStdy tS _d = 20.4_	Stdy S d = 25.3	Stdy S d = 21.0	Stdy S d = 16.5	UnStdy S d = 17.7	UnStdy S d = 18.3
15	Stdy P h = 65.6	Stdy P h = 55.1	UnStdy P h = 58.3	Stdy P h = 67.8	Stdy *P* h = 73.9	Stdy T	UnStdy Pt _h = 54.7_	UnStdy P h = 64.1	Stdy P h = 61.2	Stdy P h = 59.6	UnStdy S d = 32.4	UnStdy T	UnStdy S d = 24.5	UnStdy tS _d = 24.0_	UnStdy tS _d = 23.0_	Stdy S d = 34.1	Stdy S d = 25.3	Stdy S d = 24.4	Stdy S d = 23.5	UnStdy S d = 20.7
20	Stdy P h = 80.4	UnStdy P h = 68.8	Stdy P h = 71.2	Stdy P h = 73.6	Stdy *P* h = 75.6	UnStdy T	UnStdy Pt _h = 59.4_	UnStdy P h = 59.1	UnStdy Pt _h = 71.0_	UnStdy Pt Surges	Stdy S d = 38.2	UnStdy S d = 38.0	UnStdy S d = 32.5	UnStdy tS _d = 28.6_	UnStdy tS _d = 23.7_	Stdy S d = 38.4	Stdy S d = 31.1	Stdy S d = 28.4	Stdy S d = 27.7	UnStdy S d = 23.8
25	Stdy Pt h = 100.0	UnStdy P h = 83.1	Stdy P h = 84.1	UnStdy P h = 82.4	Stdy P h = 90.5	UnStdy tS _d = 62.6_	UnStdy T	UnStdy Pt _h = 56.1_	UnStdy T Surges	UnStdy T	Stdy S d = 42.4	UnStdy S d = 41.1	UnStdy S d = 39.9	UnStdy tS _d = 32.2_	Stdy S d = 28.9	Stdy S d = 43.6	Stdy S d = 34.4	Stdy S d = 32.3	Stdy S d = 33.2	UnStdy S d = 26.2
35	UnStdy tB	Stdy P h = 114.5	Stdy P h = 106.2	UnStdy P h = 107.3	Stdy P h = 114.1	UnStdy S d = 71.3	UnStdy tS _d = 61.4_	UnStdy tS _d = 61.4_	Stdy T	UnStdy tB **	Stdy S d = 53.5	Stdy S d = 49.6	Stdy S d = 41.4	UnStdy tS _d = 41.0_	Stdy S d = 38.2	Stdy S d = 53.0	Stdy S d = 45.8	Stdy S d = 39.6	Stdy S d = 40.5	Stdy S d = 33.5
45	UnStdy tB	Stdy P h = 135.7	Stdy P h = 112.6	UnStdy P h = 130.1	Stdy P h = 139.2	UnStdy S d = 77.4	UnStdy tS _d = 67.0_	Stdy tS _d = 64.7_	Stdy tS _d = 61.0_	UnStdy tB/tS **	Stdy S d = 66.8	Stdy S d = 54.4	Stdy S d = 48.8	Stdy S d = 45.3	Stdy S d = 43.7	Stdy S d = 61.9	Stdy S d = 54.0	Stdy S d = 50.0	Stdy S d = 47.2	Stdy S d = 43.0
65	Stdy B	Stdy Pt h = 168.8	Stdy tB	Stdy tB	Stdy B	UnStdy S d = 102.2	UnStdy tS _d = 83.2_	Stdy tS _d = 85.0_	Stdy tS _d = 90.8_	UnStdy tS **	Stdy S d = 83.1	Stdy S d = 69.9	Stdy S d = 58.8	Stdy S d = 56.5	Stdy S d = 55.9	Stdy S d = 88.4	Stdy S d = 67.1	Stdy S d = 61.3	Stdy S d = 62.5	Stdy S d = 49.7
85	Stdy B	Stdy B	Stdy B	Stdy tB	Stdy B	UnStdy S d = 130.9	Stdy S d = 108.8	Stdy tS _d = 100.0_	Stdy tS _d = 102.0_	UnStdy tS **	Stdy S d = 99.2	Stdy S d = 82.5	Stdy S d = 65.7	Stdy S d = 68.7	Stdy S d = 59.6	Stdy S d = 98.8	Stdy S d = 80.5	Stdy S d = 71.9	Stdy S d = 72.5	Stdy S d = 64.0
105	Stdy B	UnStdy B	UnStdy B	UnStdy B	UnStdy B	UnStdy S d = 156.1	Stdy S d = 120.4	Stdy S d = 116.8	Stdy tS _d = 113.7_	UnStdy tS **	Stdy S d = 114.1	Stdy S d = 93.2	Stdy S d = 81.5	Stdy S d = 73.9	Stdy S d = 68.7	Stdy S d = 116.4	Stdy S d = 92.4	Stdy S d = 84.4	Stdy S d = 77.7	Stdy S d = 72.5
135	Stdy B	UnStdy B/S	UnStdy B	UnStdy B	UnStdy B	Stdy S d = 176.6	Stdy S d = 145.7	Stdy S d = 129.5	Stdy tS _d = 134.4_	Stdy tS d = 119.0	Stdy S d = 132.9	Stdy S d = 110.8	Stdy S d = 94.0	Stdy S d = 87.6	Stdy S d = 76.6	Stdy S d = 137.2	Stdy S d = 107.6	Stdy S d = 96.3	Stdy S d = 94.5	Stdy S d = 90.2
165						Stdy S d = 199.0	Stdy S d = 151.7	Stdy S d = 149.1	Stdy S d = 138.1	Stdy S d = 148.1	Stdy S d = 168.0	Stdy S d = 129.6	Stdy S d = 112.6	Stdy S d = 98.6	Stdy S d = 87.0	Stdy S d = 155.1	Stdy S d = 126.5	Stdy S d = 111.3	Stdy S d = 104.9	Stdy S d = 92.4

Legend

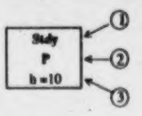

① Stdy =Steady Flow
UnStdy = Unsteady Flow

② P = Plunging Flow
Pt = Plunging Transitional Flow (slight deviation from plunging flow conditions)
T = Transitional Flow
tS = Transitional Streaming Flow (slight deviation from streaming flow conditions)
S = Streaming Flow
tB = Transitional Baffle Flow (flow is developing into baffle flow rather than streaming flow)
B = Baffle flow
B/S = Baffle Streaming Flow
P = Plunging Flow pattern which has a section of supercritical bed flow
B = Baffle Flow pattern which has a section of supercritical bed flow

③ h = Maximum head over weir (mm)
d = Depth of streaming flow (mm)

Italics indicate that the flow is not in a true plunging or streaming state
[96.05] indicates that the maximum head is downstream of the weir, i.e., baffle flow
** Signifies that there was more than one flow pattern present.
This was typically found in an unsteady flow.

Table 8: Tabular Summary of Three Quarter Weir Height Experimental Data

Discharge Q (l/s)	Pool and Weir Study / 3/4 Weir Height Spacing Class Designation Flume width = 560 mm - Avg. Weir Height = 119.1 mm														
	[A] l(design)=696mm l(actual)=694mm					[B] l(design)=342mm l(actual)=342 mm					[C] l(desing)=165mm l(actual)=164mm				
	Slope (%)					Slope (%)					Slope (%)				
	5	10	15	20	30	5	10	15	20	30	5	10	15	20	30
10	Stdy P h = 31.8	Stdy P h = 31.1	Stdy P h = 30.5	Stdy *P* *h = 31.2*	Stdy *B* *h = 28.3*	Stdy tS *d = 30*	Stdy P h = 42.1	Stdy P h = 34.0	Stdy P h = 35.5	Stdy P h = 36.7	Stdy tS *d = 16.6*	UnStdy tS *d = 15.1*	UnStdy tS *d = 16.6*	UnStdy T	Stdy tS -
15	Stdy P h = 50.0	Stdy P h = 39.9	Stdy P h = 43.2	Stdy *P* *h = 40.8*	Stdy *B* *h = 42.8*	Stdy tS *d = 35*	UnStdy P -	Stdy P h = 50.6	Stdy P h = 50.4	Stdy P h = 51.1	Stdy S d = 23.3	Stdy tS *d = 23.6*	UnStdy tS *d = 31.2*	UnStdy tS -	Stdy tS -
20	Stdy P h = 63.8	Stdy P h = 53.6	Stdy P h = 53.9	Stdy *P* *h = 54.5*	Stdy *B* *h = 56.1*	Stdy tS *d = 46*	UnStdy Pt -	Stdy P h = 66.8	Stdy P h = 62.1	Stdy P h = 62.0	Stdy S d = 31.6	UnStdy tS -	UnStdy tS -	UnStdy tS -	Stdy tS -
25	Stdy P h = 78.7	Stdy P h = 66.7	Stdy P h = 65.4	Stdy *P* *h = 66.4*	Stdy *B* *h = 69.2*	Stdy tS *d = 64*	UnStdy Pt -	UnStdy Pt -	UnStdy Pt -	UnStdy Pt -	Stdy S d = 45.9	UnStdy tS *d = 39.5*	UnStdy tS -	UnStdy tS -	Stdy S d = 30.0
35	Stdy P h = 102.1	Stdy P h = 86.0	Stdy P h = 82.0	Stdy *P* *h = 86.5*	Stdy *B* *h = 92.4*	Stdy S d = 54.2	Stdy tS -	UnStdy tS -	Stdy tS -	UnStdy tS -	Stdy S d = 56.2	Stdy S d = 42.5	Stdy tS *d = 44.0*	Stdy S d = 44.0	Stdy S d = 40.0

Legend

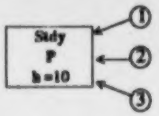

① Stdy = Stready Flow
UnStdy = Unsteady Flow

② P = Plunging Flow
Pt = Plunging Transitional Flow (slight deviation from plunging flow conditions)
T = Transitional Flow
tS = Transitional Streaming Flow (slight deviation from streaming flow conditions)
S = Streaming Flow
tB = Transitional Baffle Flow (flow is developing into baffle flow rather than streaming flow)
B = Baffle flow
B/S = Baffle Streaming Flow
P = Plunging Flow pattern which has a section of supercritical bed flow
B = Baffle Flow pattern which has a section of supercritical bed flow

③ h = Maximum head over weir (mm)
d = Depth of streaming flow (mm)

Italics indicate that the flow is not in a true plunging or streaming state
[96.05] indicates that the maximum head is downstream of the weir, i.e., baffle flow
** Signifies that there was more than one flow pattern present.
This was typically found in an unsteady flow.

Table 9: Tabular Summary of Half Weir Height Experimental Data

Pool and Weir Study / 1/2 Weir Height
Spacing Class Designation
Flume width = 560 mm

Discharge Q (l/s)	[A] L(design)=496mm L(actual)=783mm					[B] L(design)=342mm L(actual)=348 mm					[C] L(desing)=165mm L(actual)=169mm				
	Slope (%)					Slope (%)					Slope (%)				
	5	10	15	20	30	5	10	15	20	30	5	10	15	20	30
2.5	Stdy P h = 16.3	Stdy "P" h = 15.7	UnStdy "B" h = 16.4	UnStdy "B" h = 16.1	UnStdy "B" [h = 27.1]	Stdy P *h = 17.6*	Stdy P h = 16.6	Stdy P h = 15.9	Stdy P h = 16.7	UnStdy "P" h = 19.1	Stdy T	Stdy P h = 18.9	Stdy P h = 19.2	Stdy P h = 19.5	Stdy P h = 20.8
5	Stdy P h = 24.4	Stdy "P" h = 23.3	Stdy "B" h = 23.0	Stdy "B" h = 22.1	Stdy "B" h = 25.2	Stdy P *h = 27.4*	Stdy P h = 23.0	Stdy P h = 22.9	Stdy P h = 25.4	Stdy "P" h = 27.7	Stdy tS *d = 15.3*	Stdy P h = 24.7	Stdy P h = 28.0	Stdy P h = 31.5	Stdy P h = 32.2
10	Stdy P h = 37.4	Stdy "P" h = 35.0	Stdy "B" h = 38.7	Stdy "B" h = 35.6	Stdy "B" [h = 43.8]	UnStdy Pt	Stdy P h = 44.6	Stdy P h = 40.9	Stdy P h = 41.5	Stdy P h = 42.0	Stdy tS *d = 28.2*	UnStdy tS *d = 19.4*	UnStdy Pt	UnStdy T	UnStdy P
15	Stdy P h = 54.8	Stdy "P" h = 47.6	Stdy "B" h = 52.8	Stdy "B" h = 55.0	Stdy "B" [h = 56.0]	UnStdy Pt	Stdy P h = 62.4	Stdy P h = 52.1	Stdy P h = 53.7	Stdy tB *h = 61.8*	Stdy S d = 35.7	Stdy S d = 29.1	Stdy tS *d = 29.9*	Stdy tS *d = 23.8*	Stdy T
20	Stdy P h = 64.8	Stdy "P" h = 59.7	Stdy "B" h = 62.8	Stdy "B" h = 68.3	Stdy "B" [h = 73.8]	UnStdy tS	Stdy Pt *h = 74.2*	Stdy Pt *h = 67.7*	Stdy P h = 61.5	Stdy tB *h = 74.6*	Stdy S d = 40.8	Stdy S d = 34.1	Stdy S d = 34.4	Stdy S d = 30.8	Stdy tS *d = 34.8*
25	Stdy P h = 78.8	Stdy "P" h = 70.3	Stdy "B" h = 70.3	Stdy "B" [h = 74.0]	Stdy "B" [h = 80.7]	Stdy tS *d = 62.0*	UnStdy tB	Stdy tB *h = 78.2*	Stdy Pt *h = 68.4*	Stdy tB *h = 77.5*	Stdy S d = 46.9	Stdy S d = 42.5	Stdy S d = 37.5	Stdy S d = 43.6	Stdy tS *d = 42.1*
30	Stdy P h = 98.6	Stdy "P" h = 88.5	Stdy "B" h = 86.9	Stdy "B" [h = 93.0]	Stdy "B" [h = 99.6]	Stdy tS *d = 76.1*	UnStdy Bt	UnStdy tS	UnStdy tB *h = 85.4*	Stdy tB	Stdy S d = 62.4	Stdy S d = 51.2	Stdy S d = 45.1	Stdy S d = 50.6	Stdy S d = 48.2
40	Stdy P h = 115.6	Stdy "P" h = 106.9	Stdy "B" [h = 96.1]	Stdy "B" h = 111.8	Stdy "B" [h = 120.1]	UnStdy tS	UnStdy tS	UnStdy tS	UnStdy tS	UnStdy tB	Stdy S d = 66.9	Stdy S d = 57.6	Stdy S d = 52.7	Stdy S d = 57.3	Stdy S d = 55.8

Legend

Stdy ①
P ②
h =10 ③

① Stdy = Steady Flow
UnStdy = Unsteady Flow

② P = Plunging Flow
Pt = Plunging Transitional Flow (slight deviation from plunging flow conditions)
T = Transitional Flow
tS = Transitional Streaming Flow (slight deviation from streaming flow conditions)
S = Streaming Flow
tB = Transitional Baffle Flow (flow is developing into baffle flow rather than streaming flow)
B = Baffle flow
B/S = Baffle Streaming Flow
"P" = Plunging Flow pattern which has a section of supercritical bed flow
"B" = Baffle Flow pattern which has a section of supercritical bed flow

③ h = Maximum head over weir (mm)
d = Depth of streaming flow (mm)

Italics indicate that the flow is not in a true plunging or streaming state
[98.05] indicates that the maximum head is downstream of the weir, *i.e.*, baffle flow
** Signifies that there was more than one flow pattern present.
This was typically found in an unsteady flow.

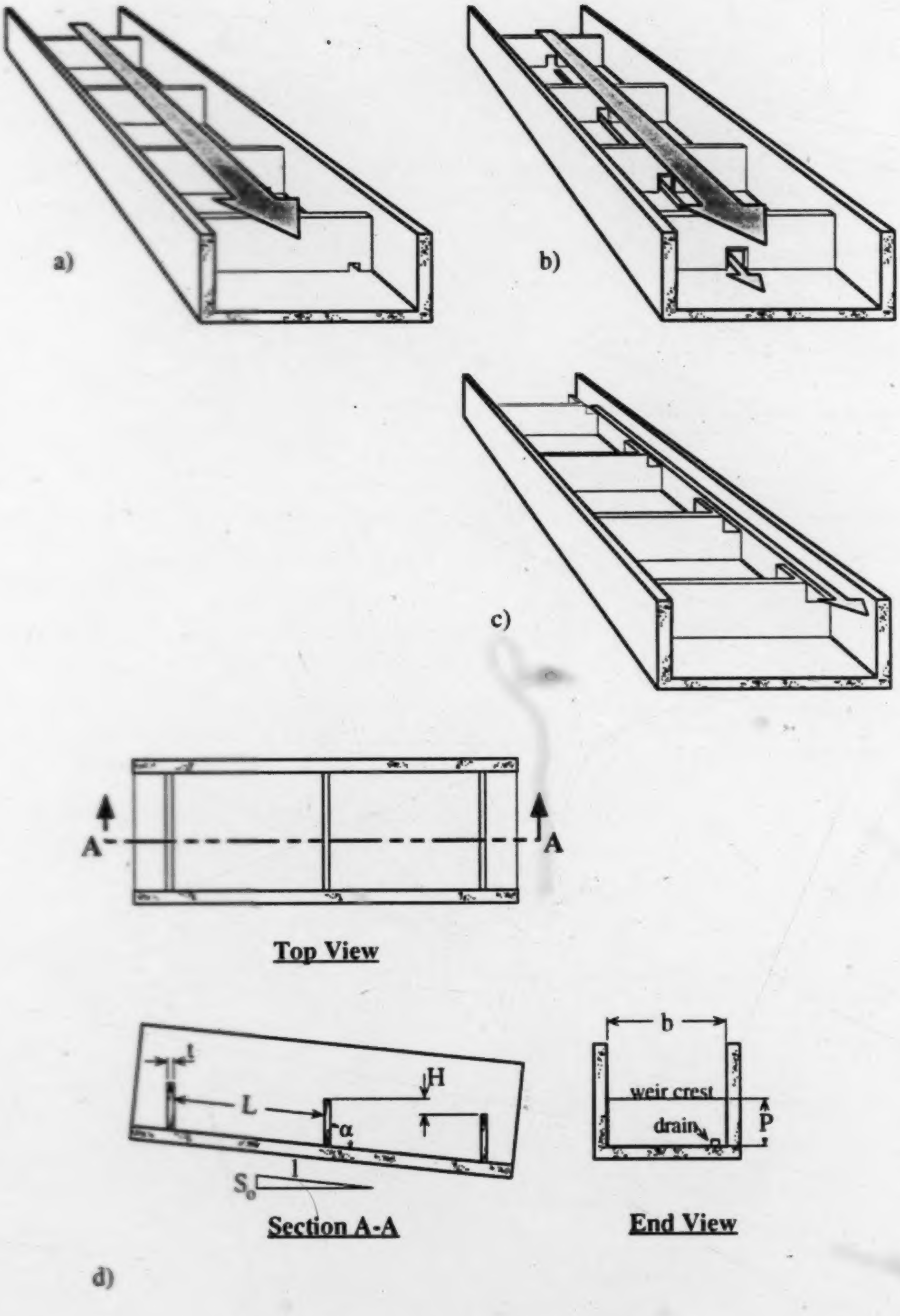

Figure 1(a-d): Pool and Weir Fishways

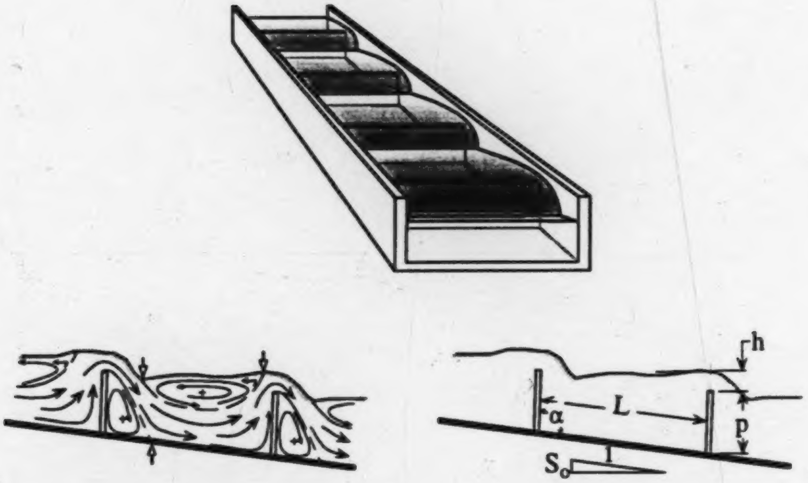

Typical Flow Patterns

Dimensions

a) Plunging Flow

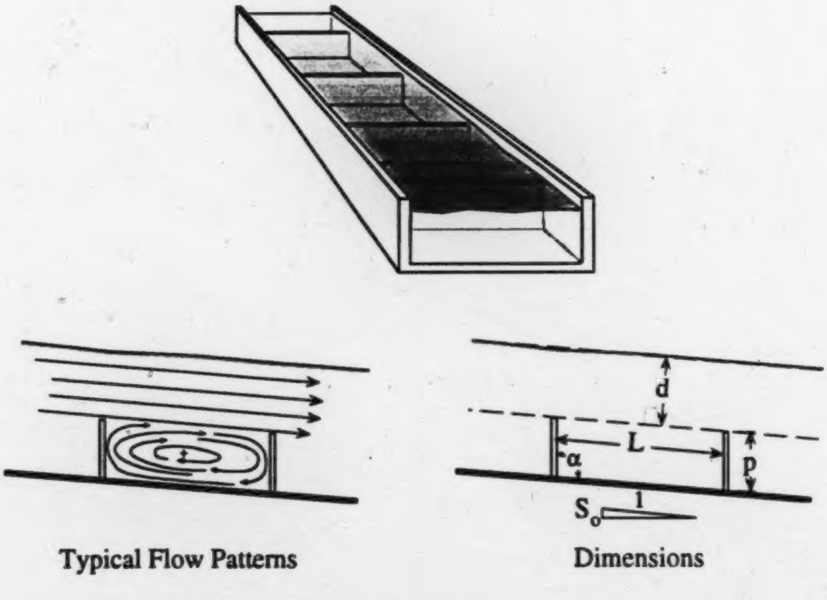

Typical Flow Patterns

Dimensions

b) Streaming Flow

Figure 2(a-b): Definition Sketches for Plunging and Streaming Flows

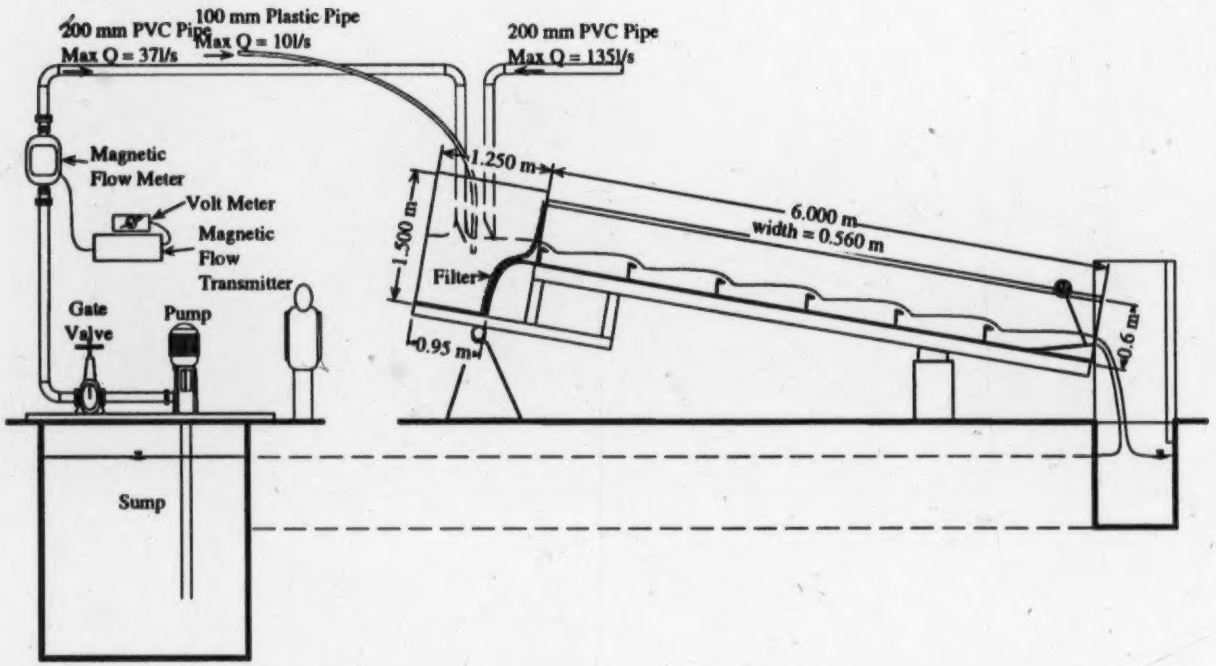

Figure 3: Definition Sketch of Experimental Apparatus - Pool and Weir Fishway Study

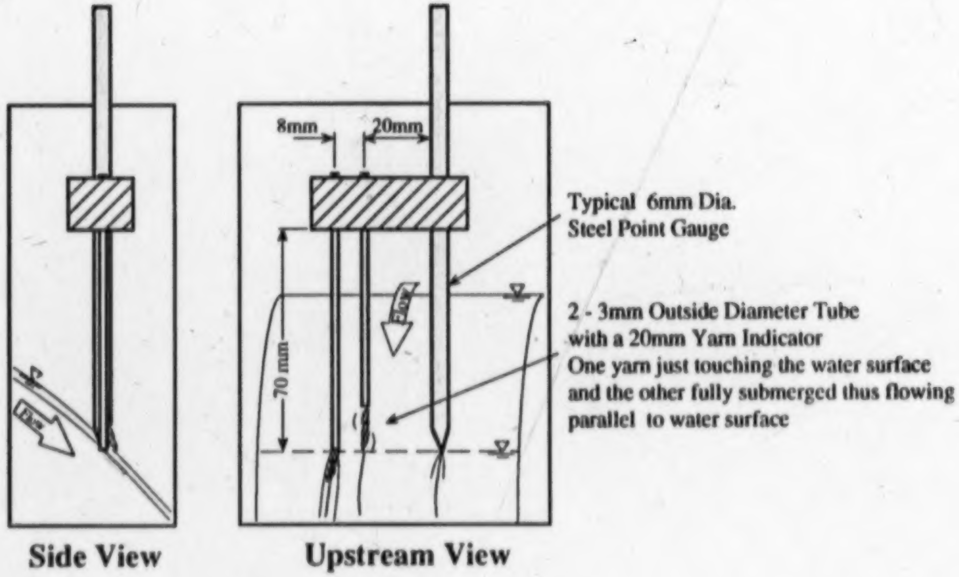
8mm
20mm
70 mm
Flow
Flow
Typical 6mm Dia.
Steel Point Gauge
2 - 3mm Outside Diameter Tube
with a 20mm Yarn Indicator
One yarn just touching the water surface
and the other fully submerged thus flowing
parallel to water surface

Side View **Upstream View**

Figure 4: Definition Sketch of Point Gauge and Yarn Indicators

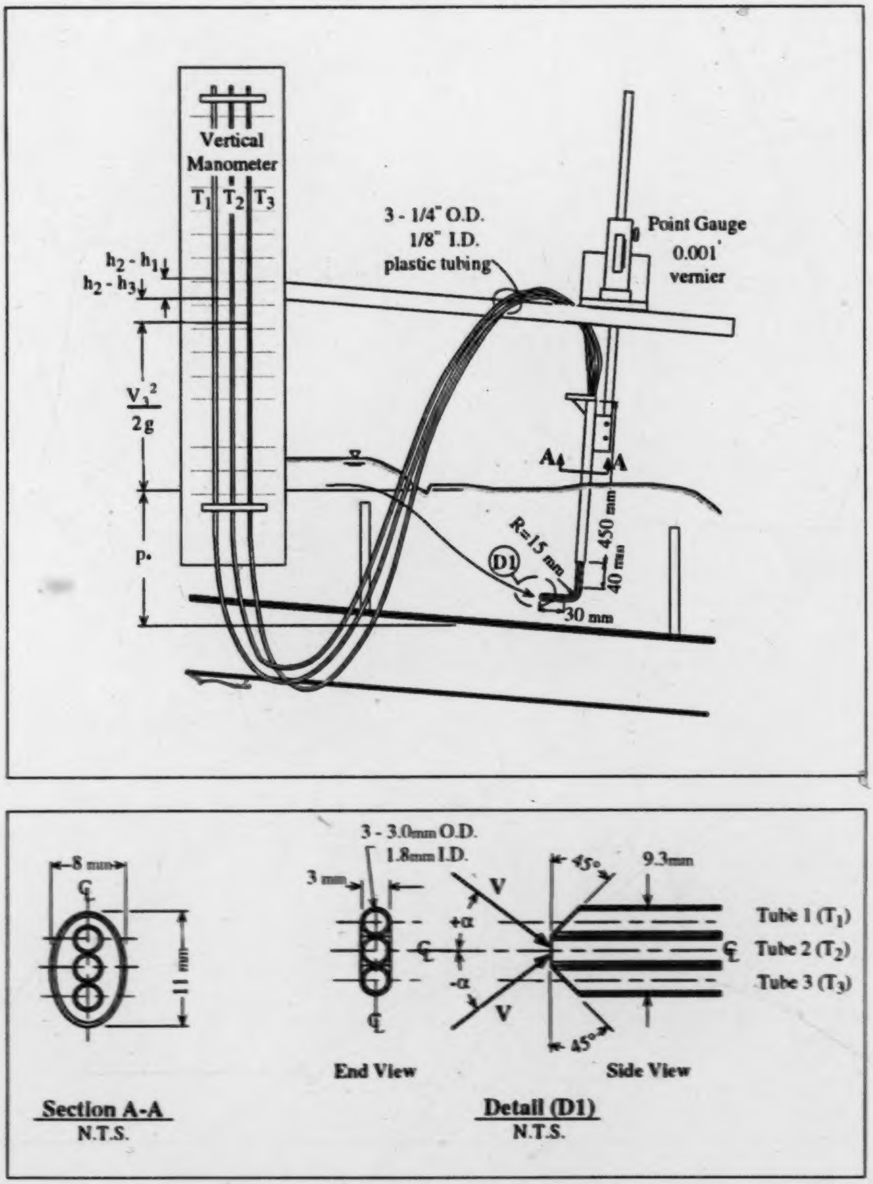

Figure 5: Definition Sketch of Pitch Probe and Manometer

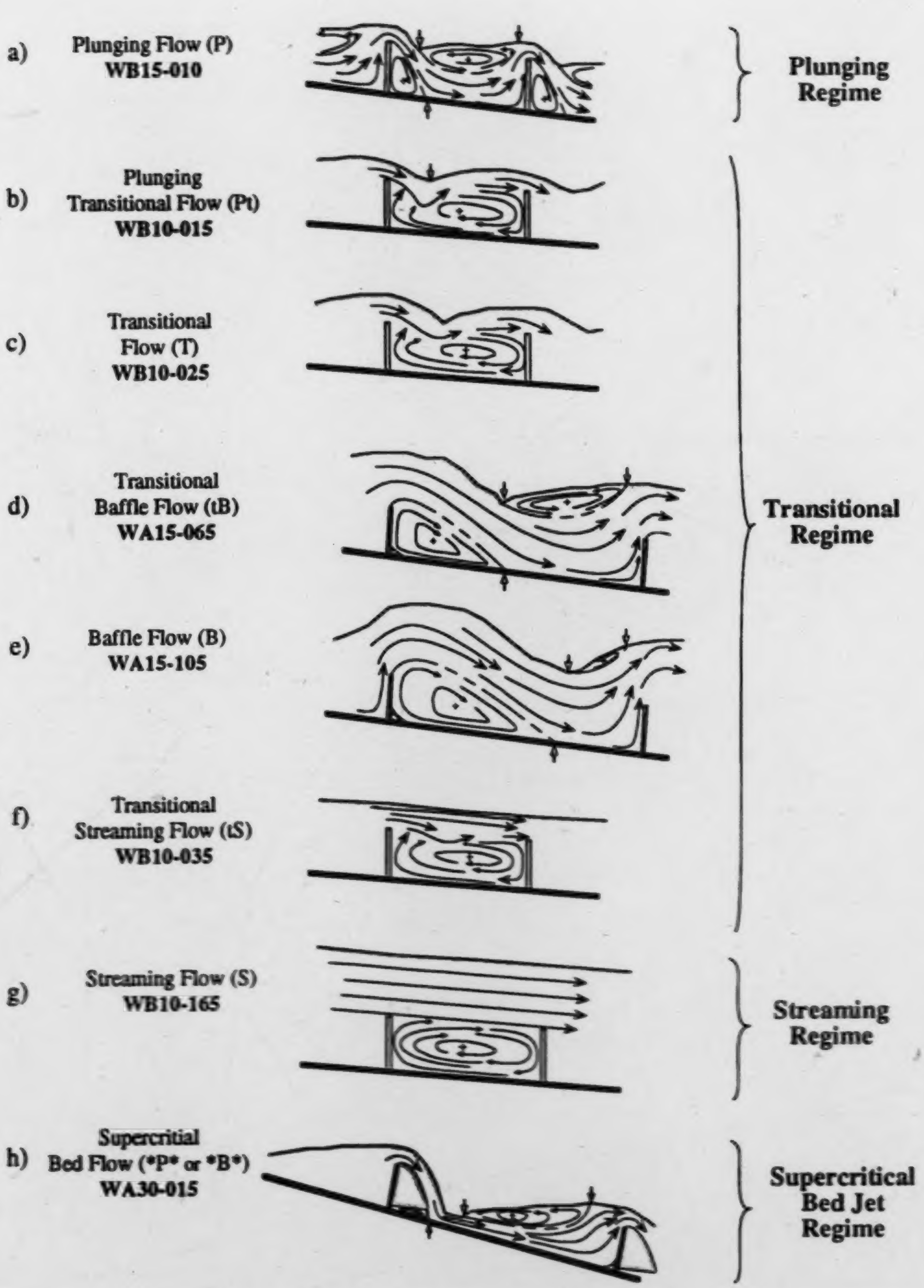

Figure 6(a-h): Predominant Flow Regimes in Pool and Weir Fishways (To Scale)

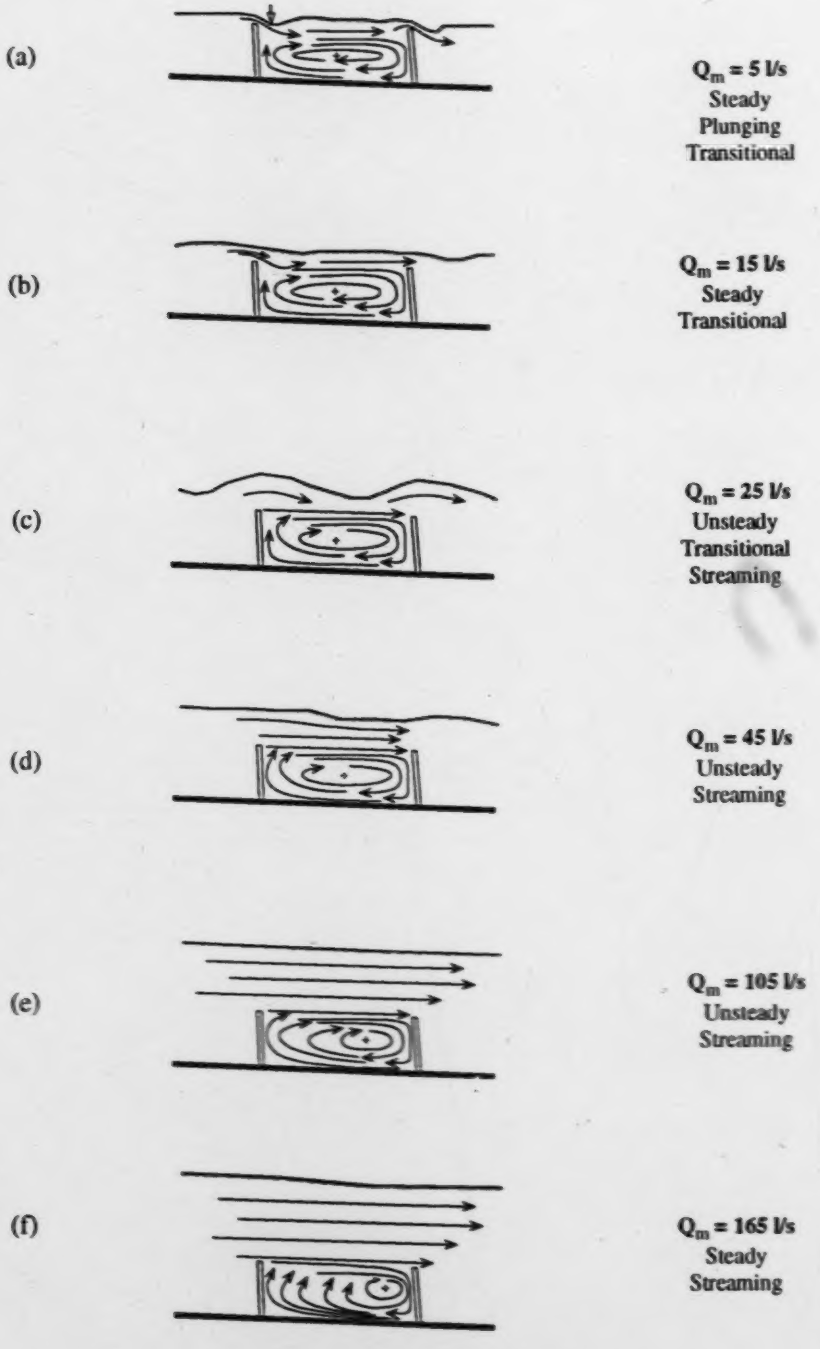

Figure 7(a-f): WB05 Flow Patterns for Multiple Discharges
(WB05: Full weir height, 'B' class weir spacings, 5% bed slope)

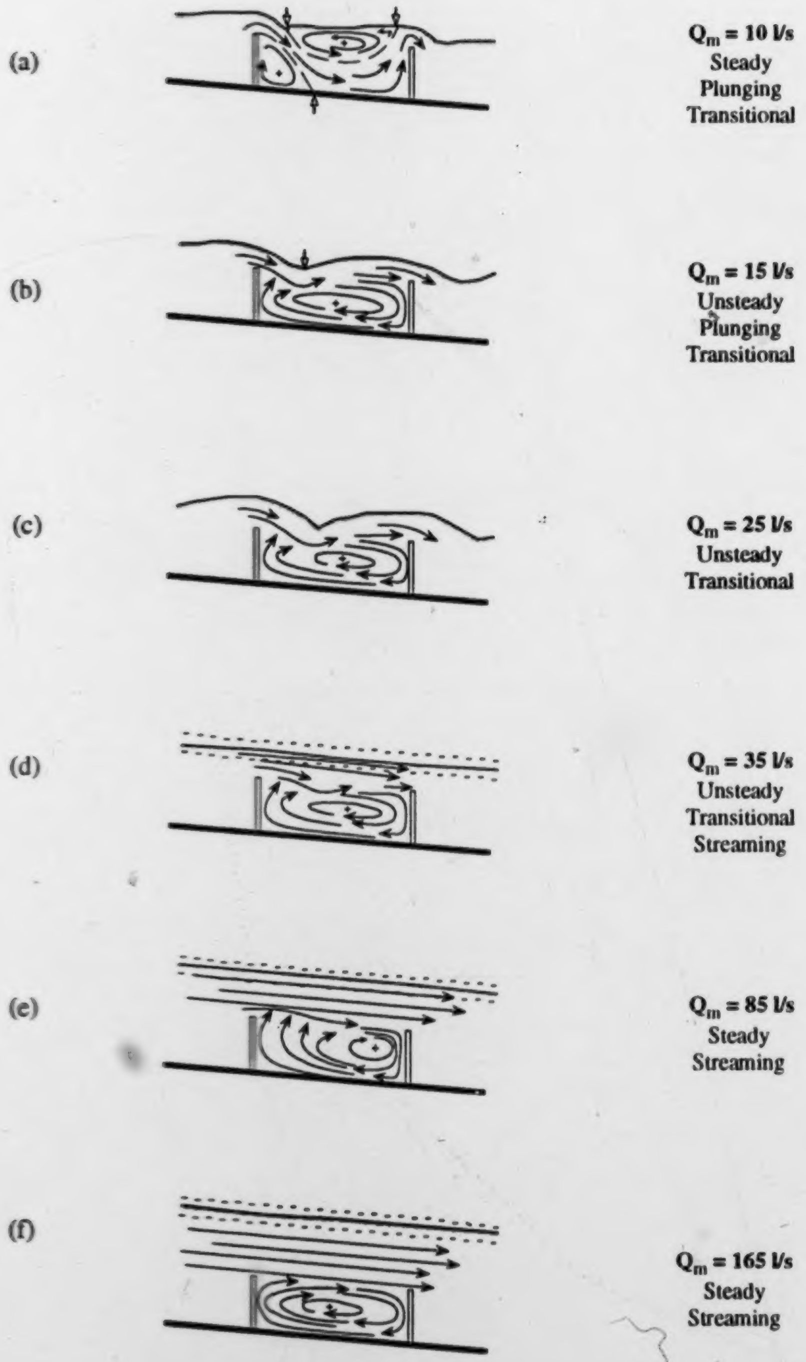

Figure 8(a-f): WB10 Flow Patterns for Multiple Discharges
(WB10: Full weir height, 'B' class weir spacings, 10% bed slope)

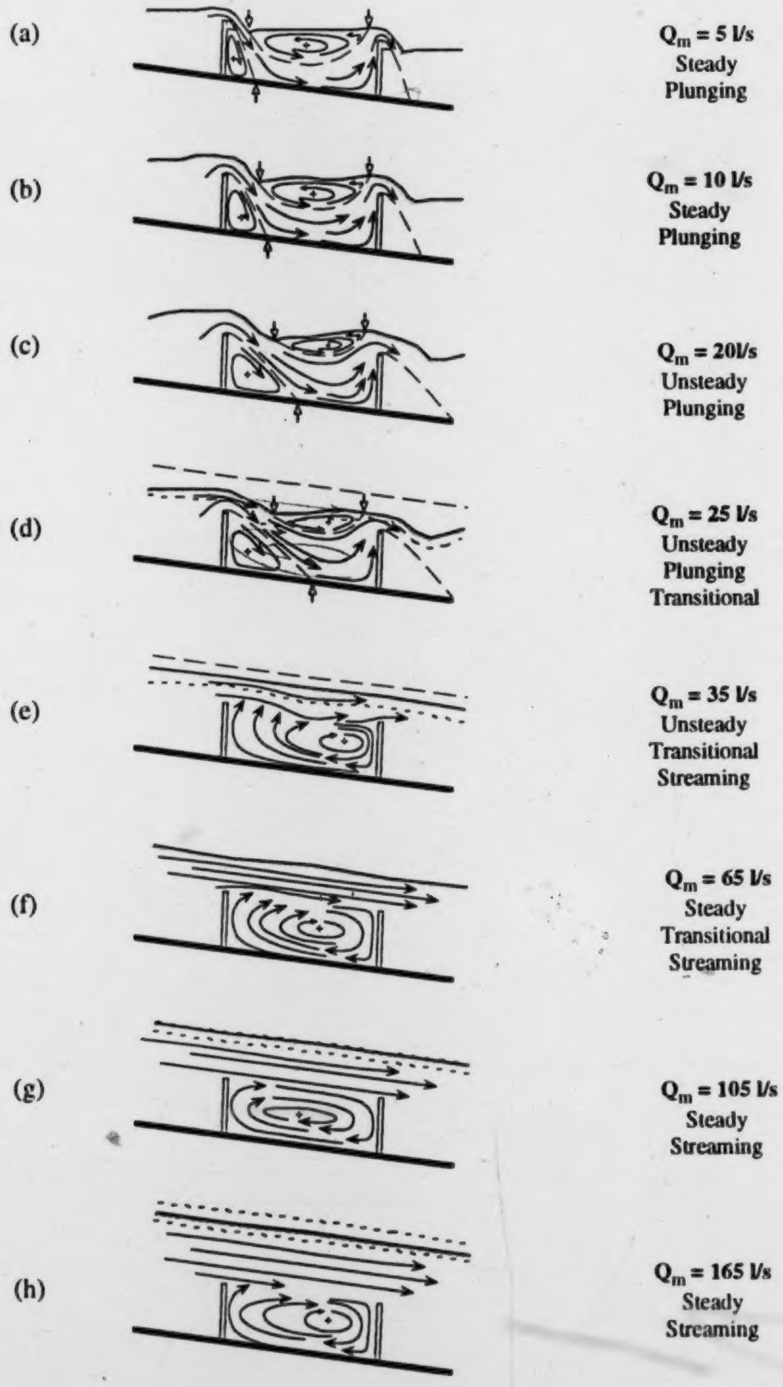

Figure 9(a-h): **WB15 Flow Patterns for Multiple Discharges**
(WB15: Full weir height, 'B' class weir spacings, 15% bed slope)

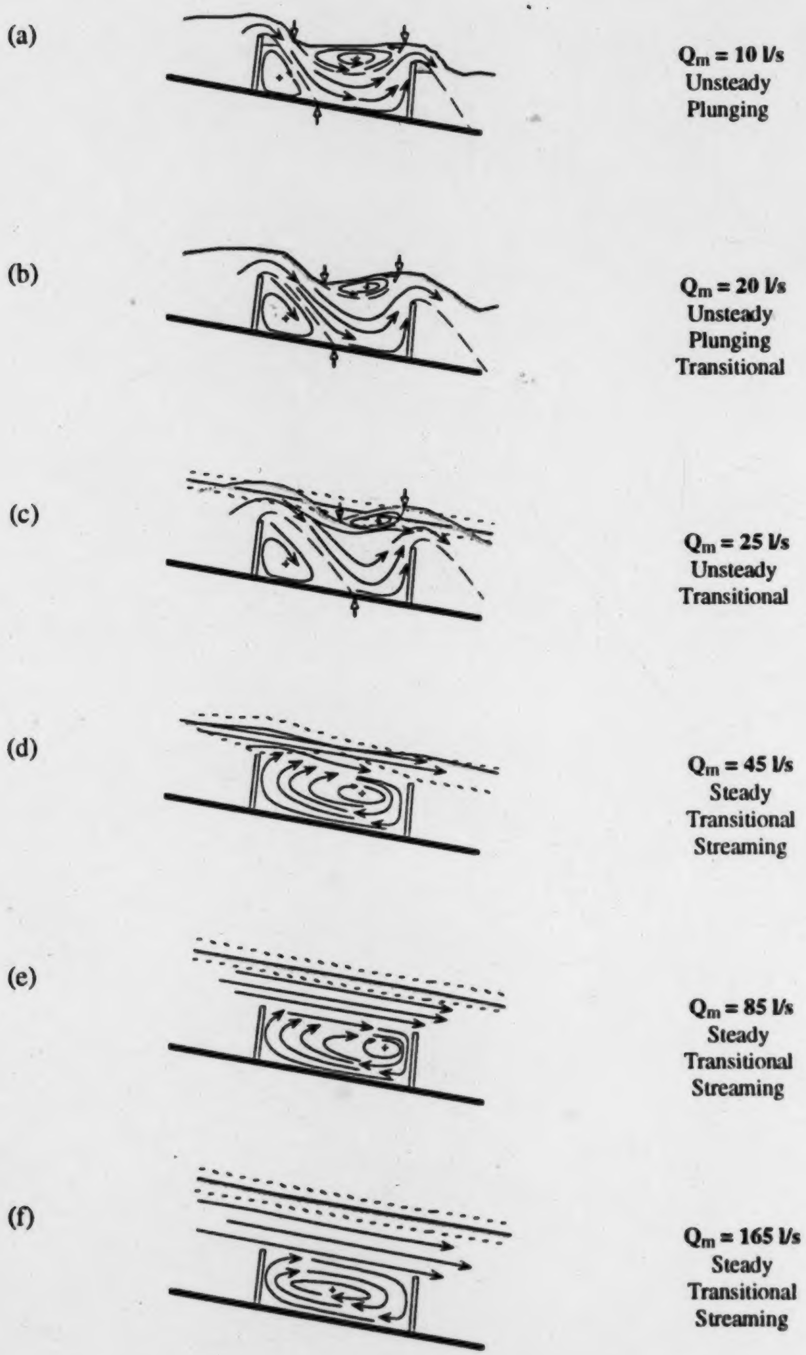

Figure 10(a-f): WB20 Flow Patterns for Multiple Discharges
(WB20: Full weir height, 'B' class weir spacings, 20% bed slope)

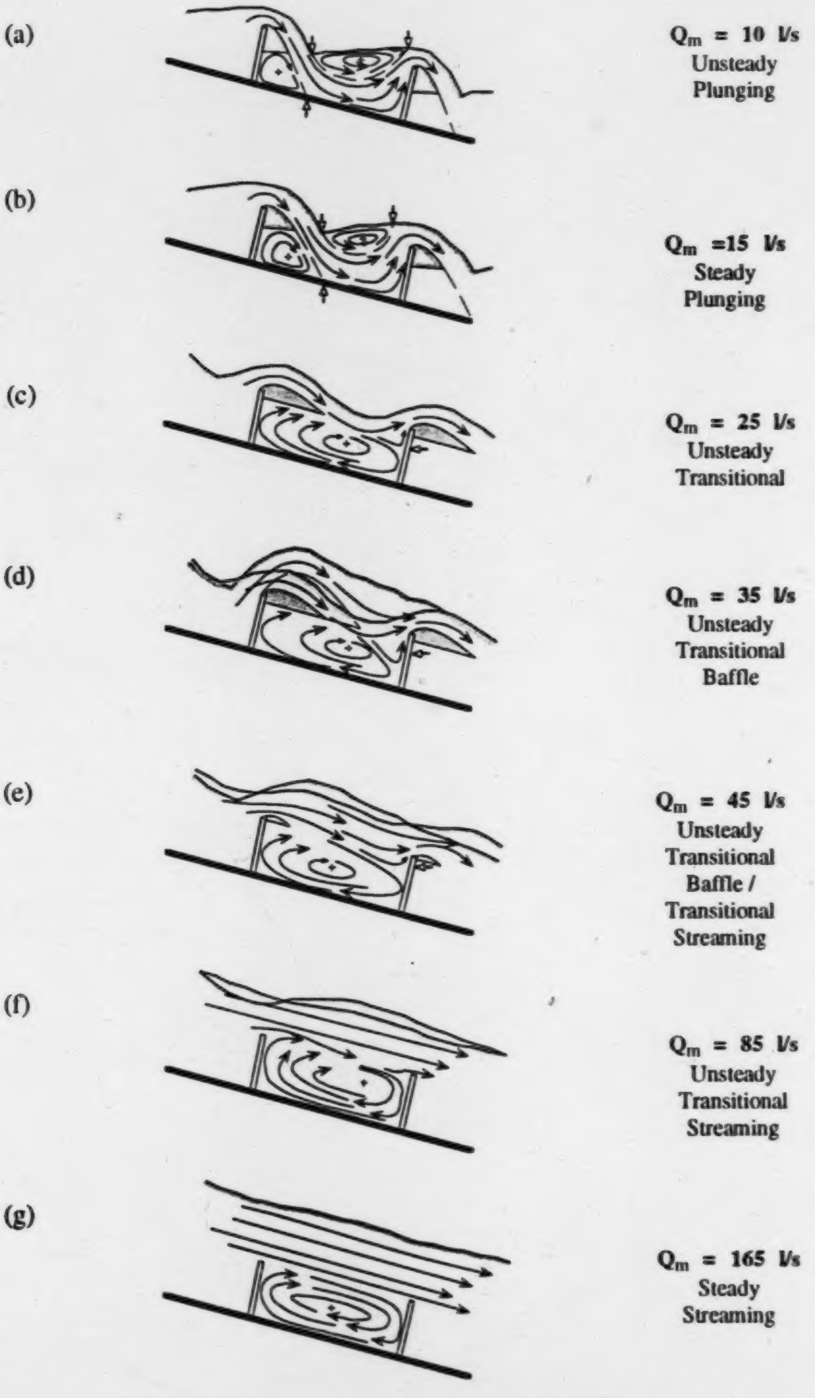

(a) Q_m = 10 l/s
Unsteady
Plunging

(b) Q_m =15 l/s
Steady
Plunging

(c) Q_m = 25 l/s
Unsteady
Transitional

(d) Q_m = 35 l/s
Unsteady
Transitional
Baffle

(e) Q_m = 45 l/s
Unsteady
Transitional
Baffle /
Transitional
Streaming

(f) Q_m = 85 l/s
Unsteady
Transitional
Streaming

(g) Q_m = 165 l/s
Steady
Streaming

Figure 11(a-g): WB30 Flow Patterns for Multiple Discharges
(WB30: Full weir height, 'B' class weir spacings, 30% bed slope)

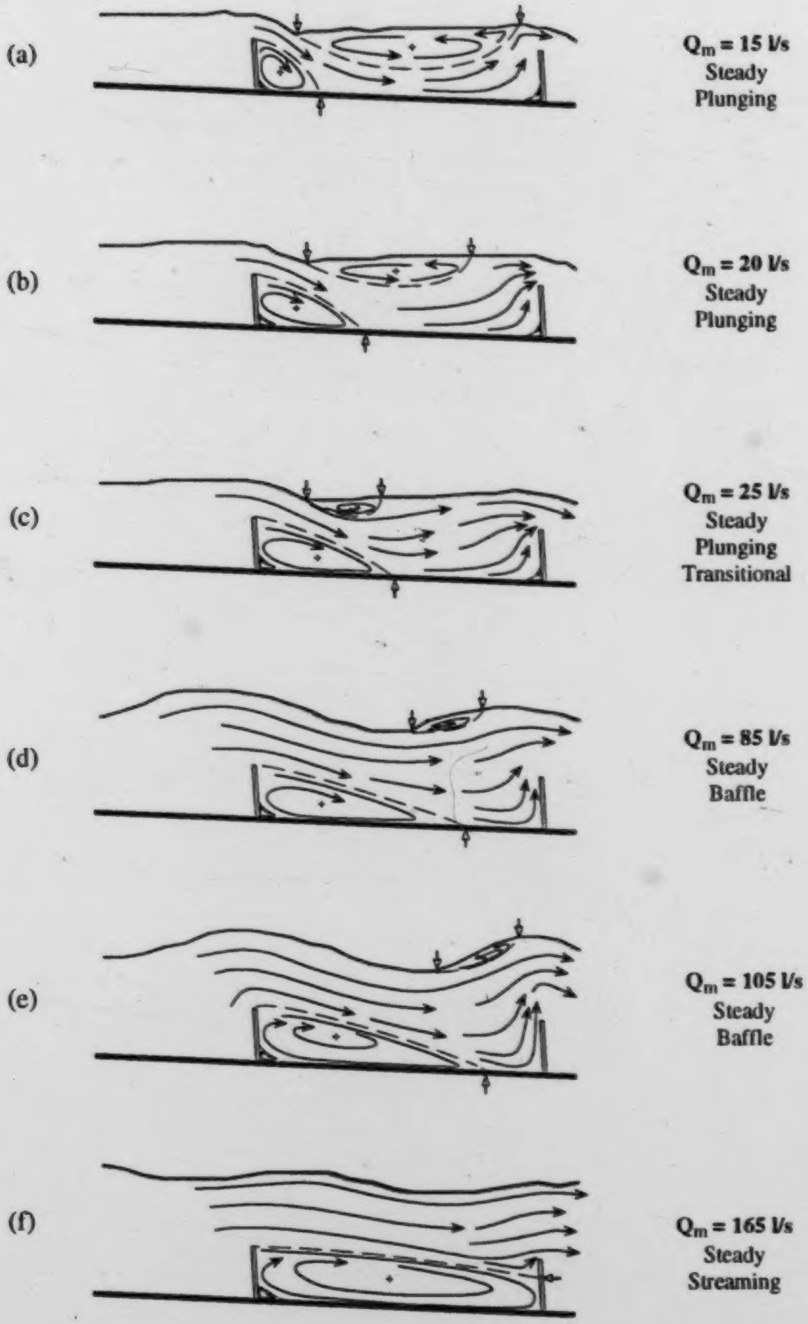

Figure 12(a-f): WA05 Flow Patterns for Multiple Discharges

(WA05: Full weir height, 'A' class weir spacings, 5% bed slope)

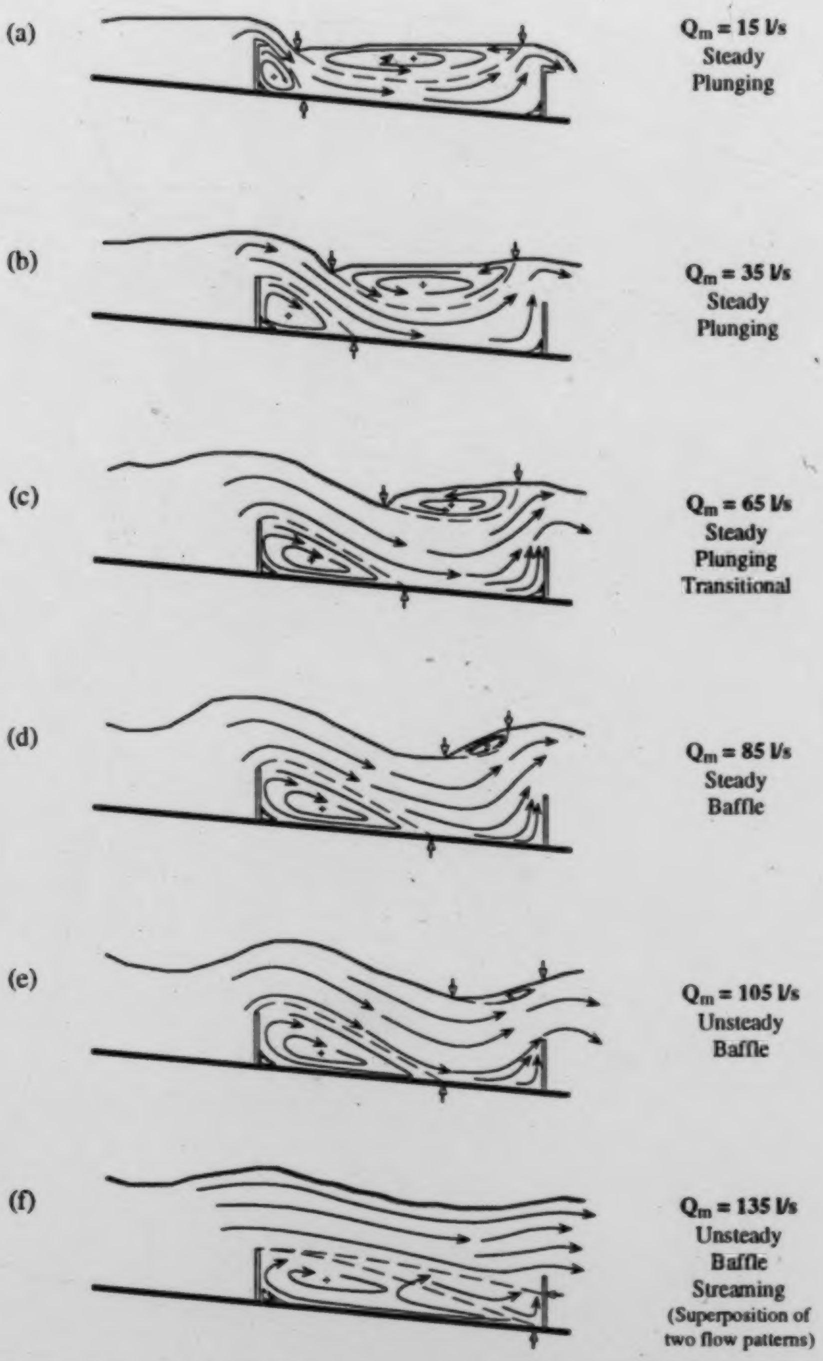

Figure 13(a-f): WA10 Flow Patterns for Multiple Discharges
(WA10: Full weir height, 'A' class weir spacings, 10% bed slope)

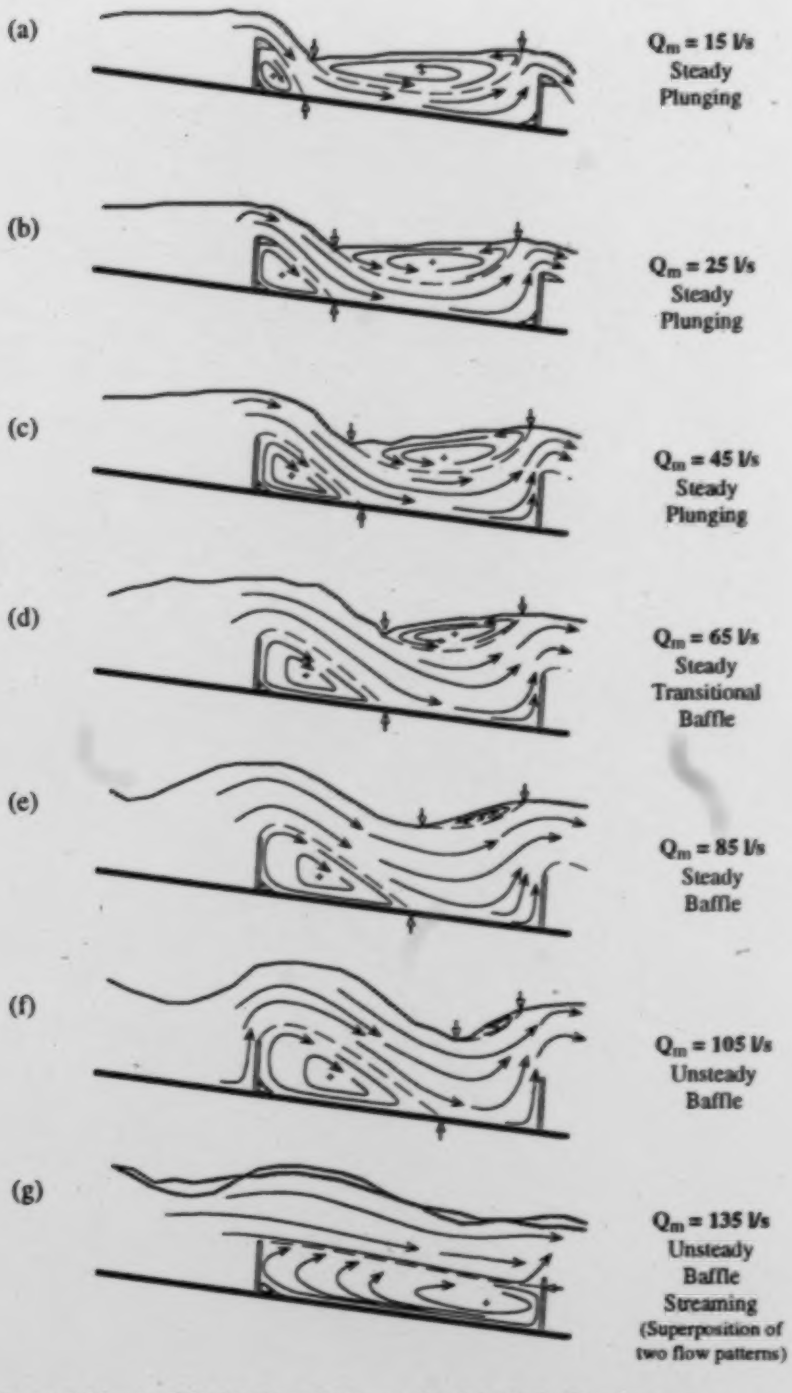

Figure 14(a-g): WA15 Flow Patterns for Multiple Discharges
(WA15: Full weir height, 'A' class weir spacings, 15% bed slope)

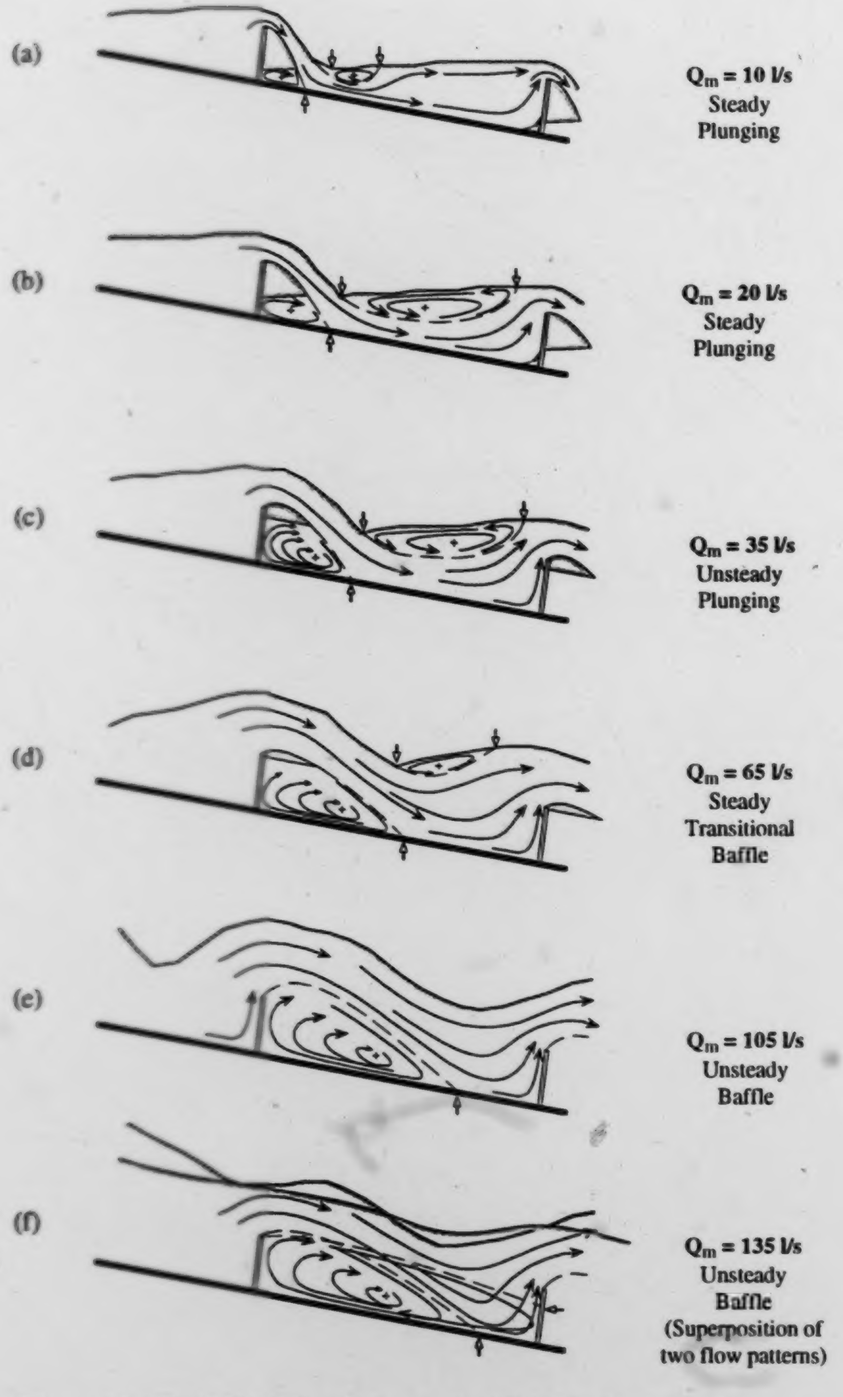

Figure 15(a-f): WA20 Flow Patterns for Multiple Discharges
(WA20: Full weir height, 'A' class weir spacings, 20% bed slope)

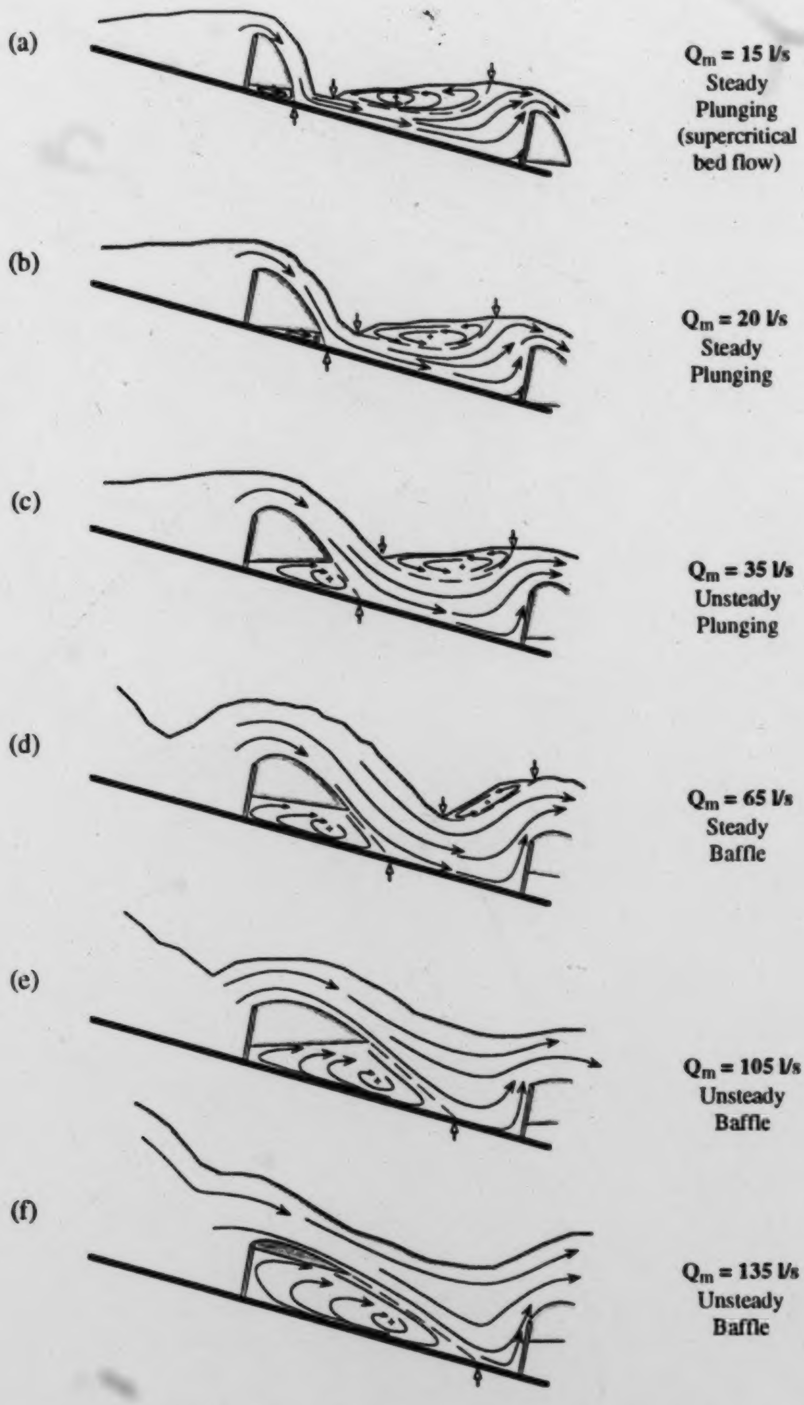

Figure 16(a-f): WA30 Flow Patterns for Multiple Discharges
(WA30: Full weir height, 'A' class weir spacings, 30% bed slope)

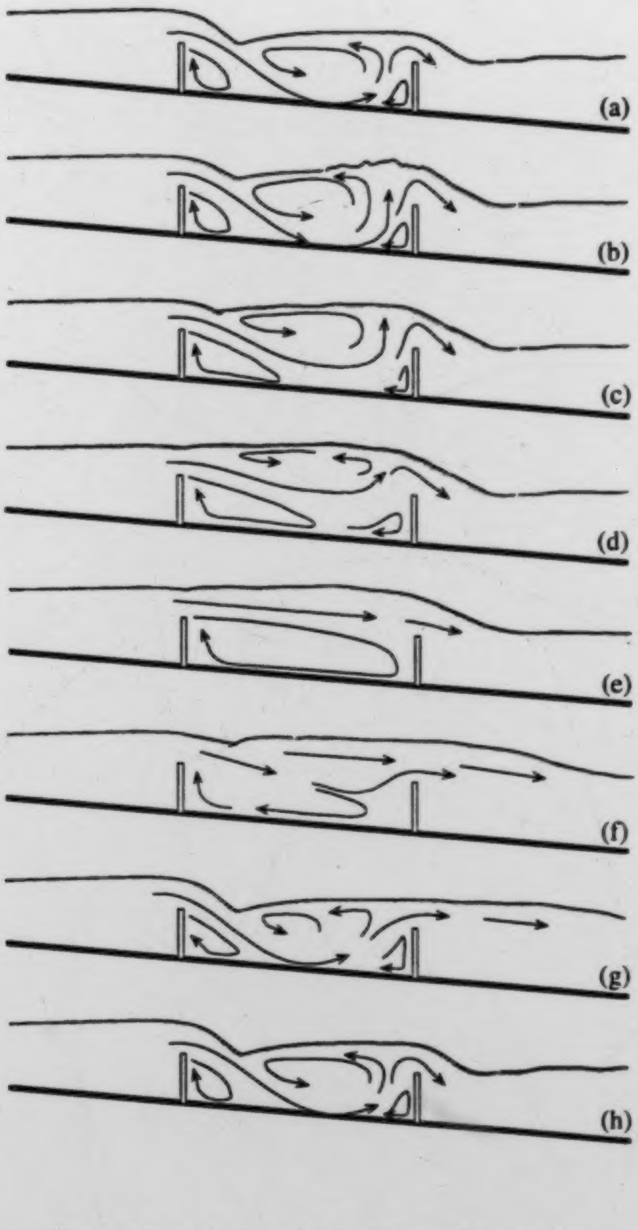

Figure 17(a-h): Longitudinal Surge Progression

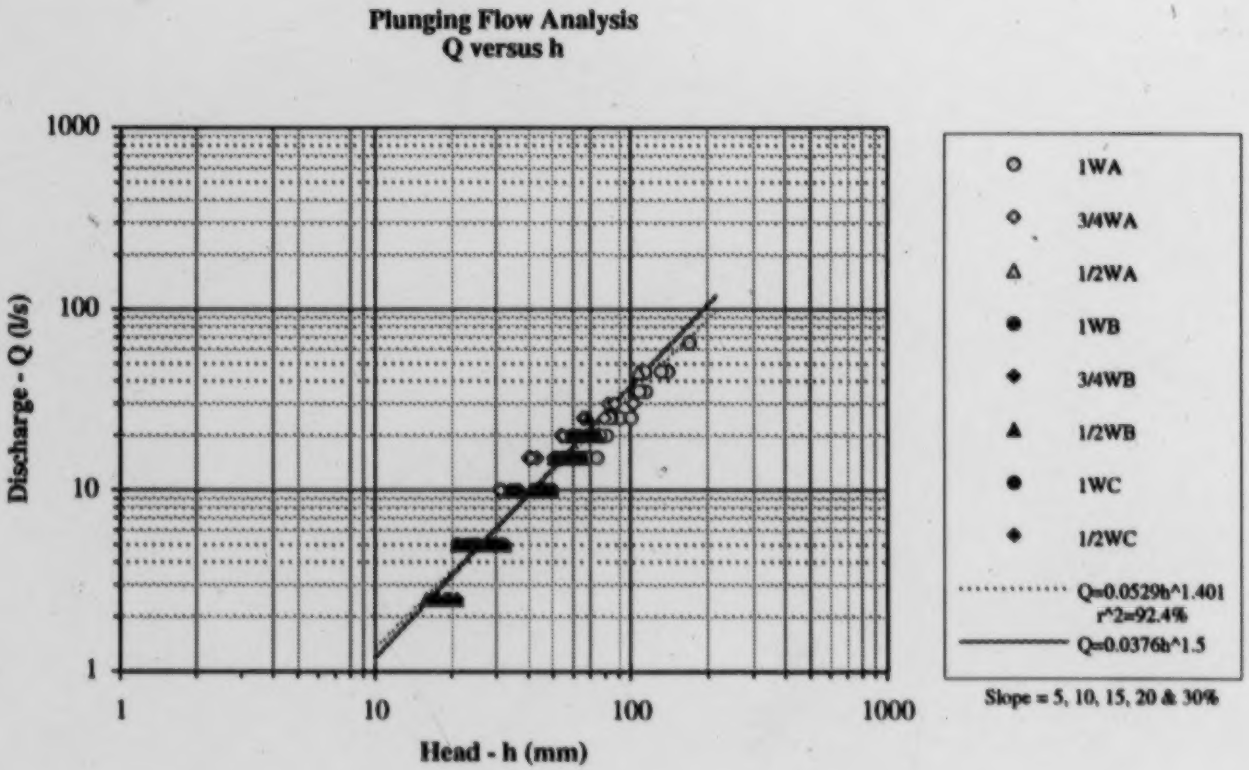

Figure 18: Discharge versus Plunging Head - Plunging Flow Analysis

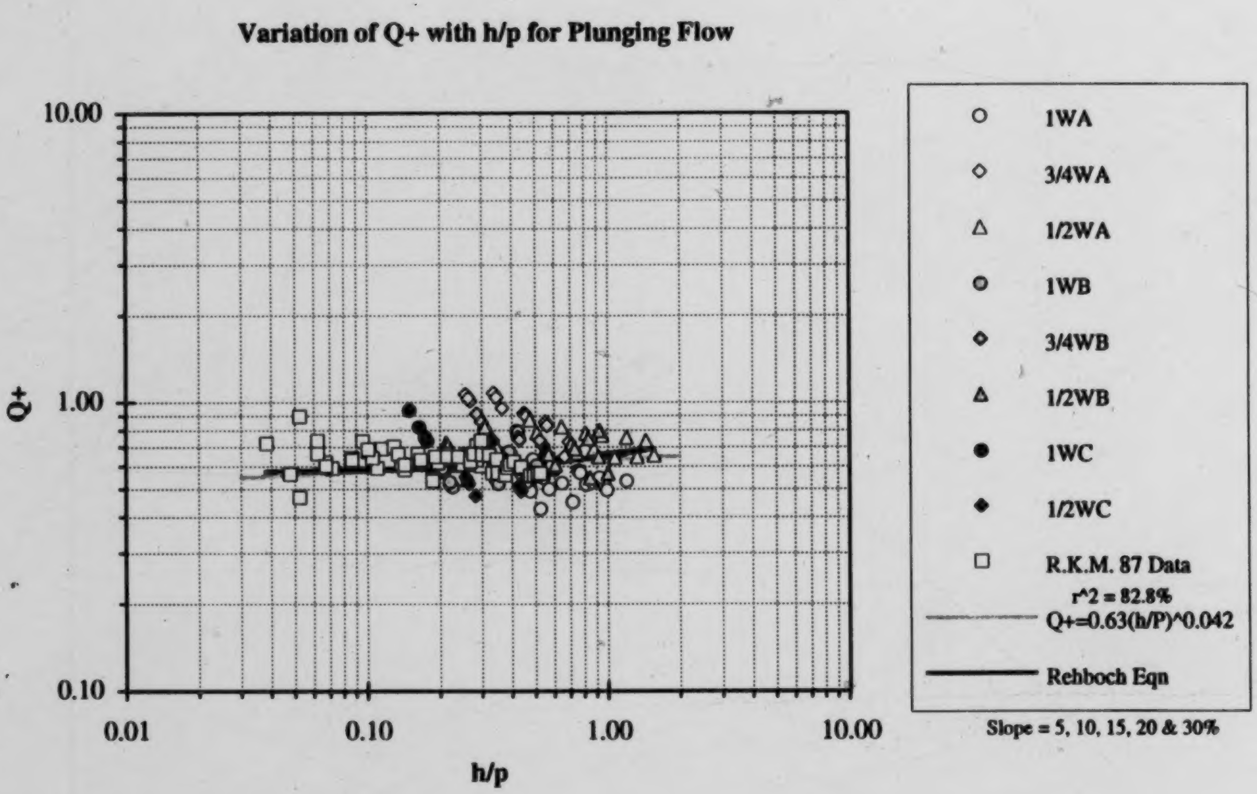

Figure 19: Dimensionless Discharge versus Plunging Head over Weir Height - Plunging Flow Analysis

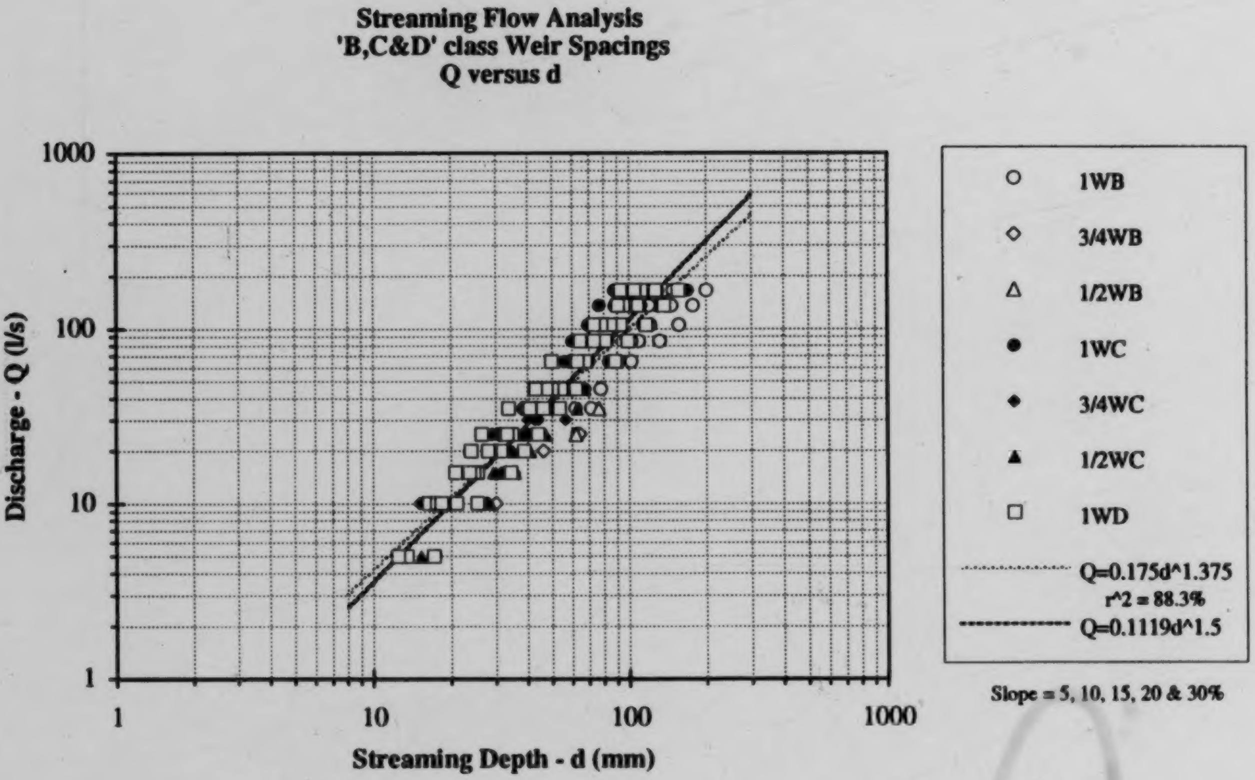

Figure 20: Discharge versus Streaming Depth for All Weir Arrangements - Streaming Flow Analysis

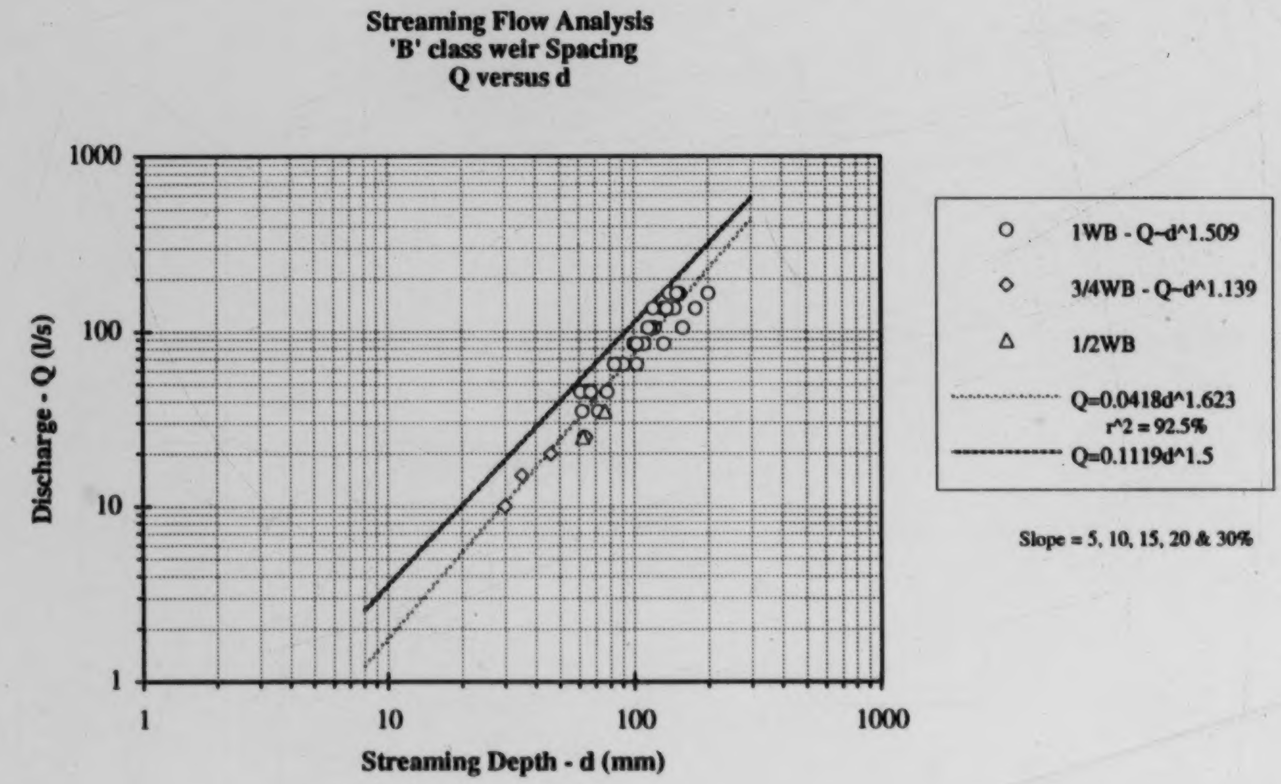

Figure 21: Discharge versus Streaming Depth for 'B' Class Weir Arrangement - Streaming Flow Analysis

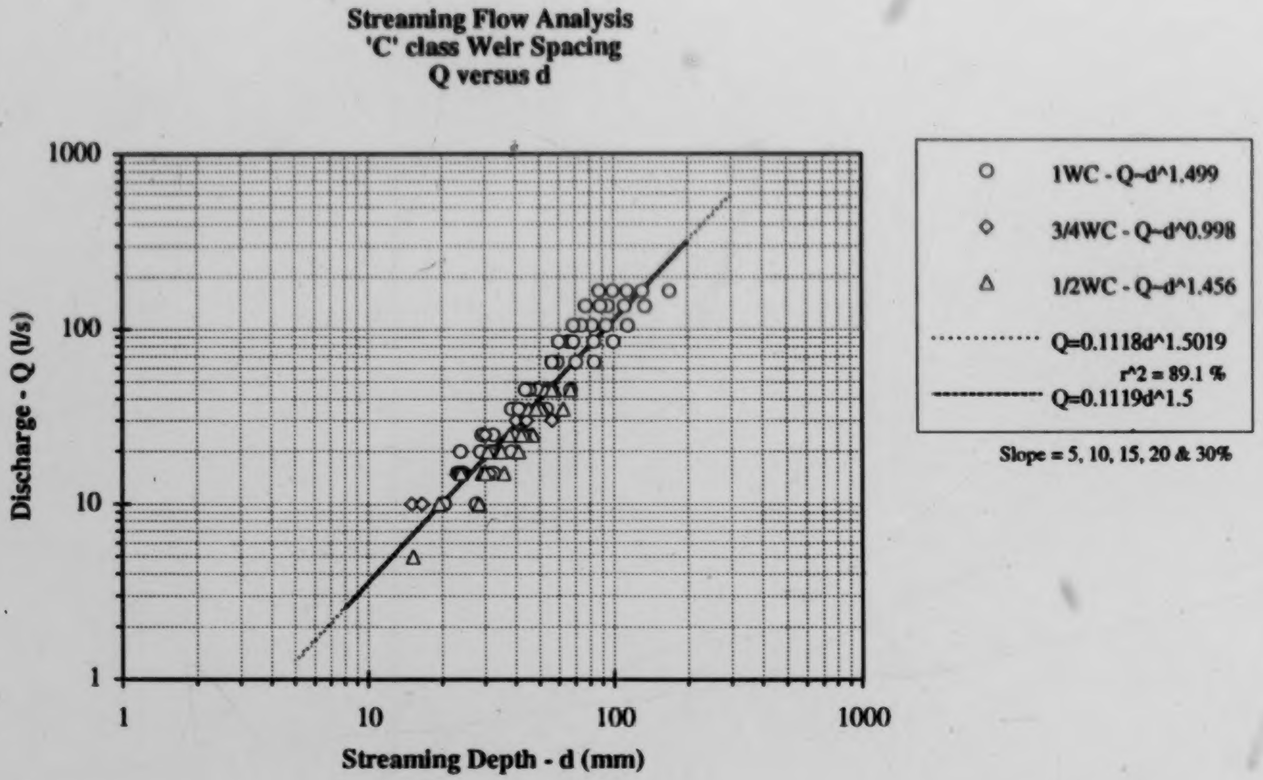

Figure 22: Discharge versus Streaming Depth for 'C' Class Weir Arrangement - Streaming Flow Analysis

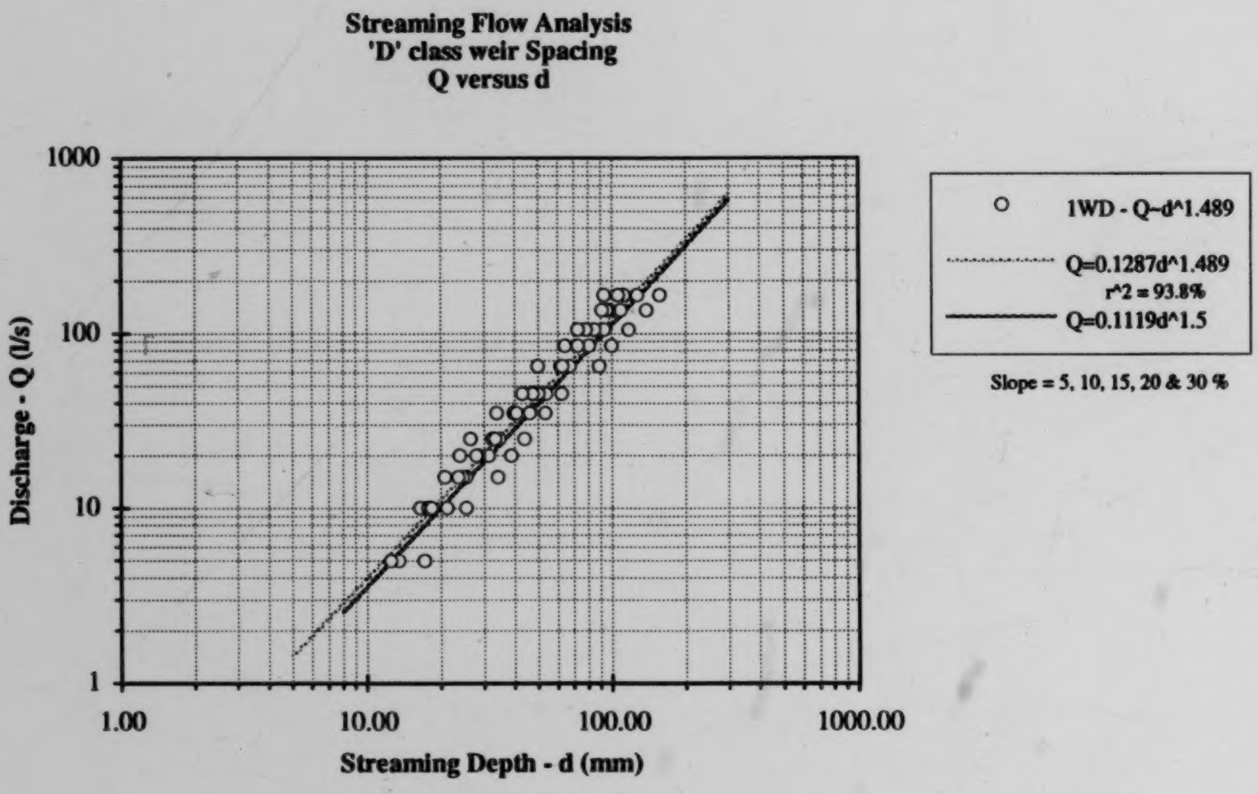

Figure 23: Discharge versus Streaming Depth for 'D' Class Weir Arrangement - Streaming Flow Analysis

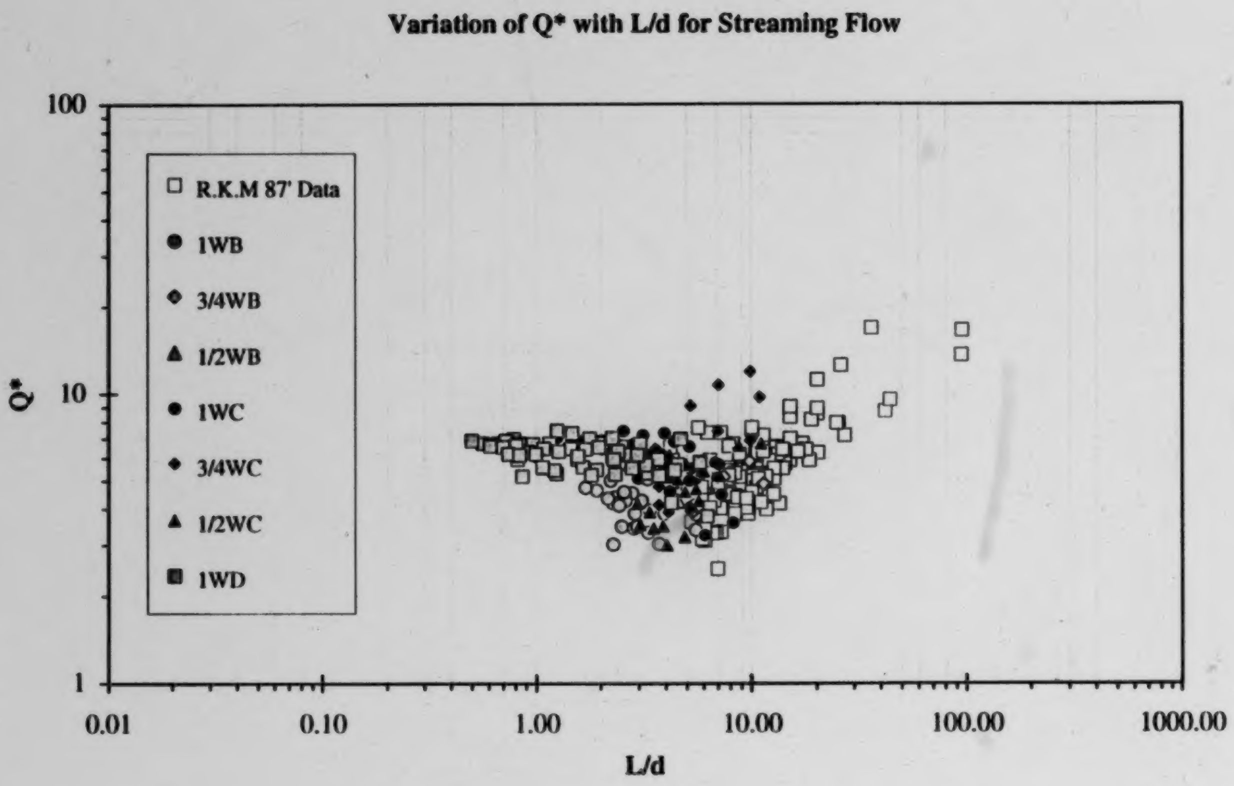

Figure 24: Dimensionless Discharge versus Pool Length over Streaming Depth - Streaming Flow Analysis

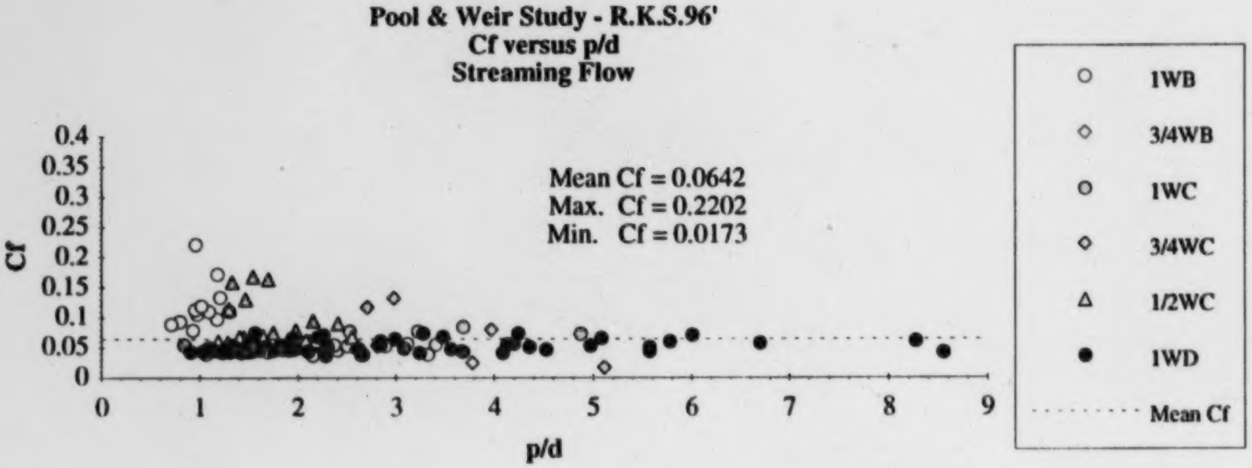

Figure 25: Coefficient of Fluid Friction versus Weir Height over Streaming Depth - Streaming Flow Analysis

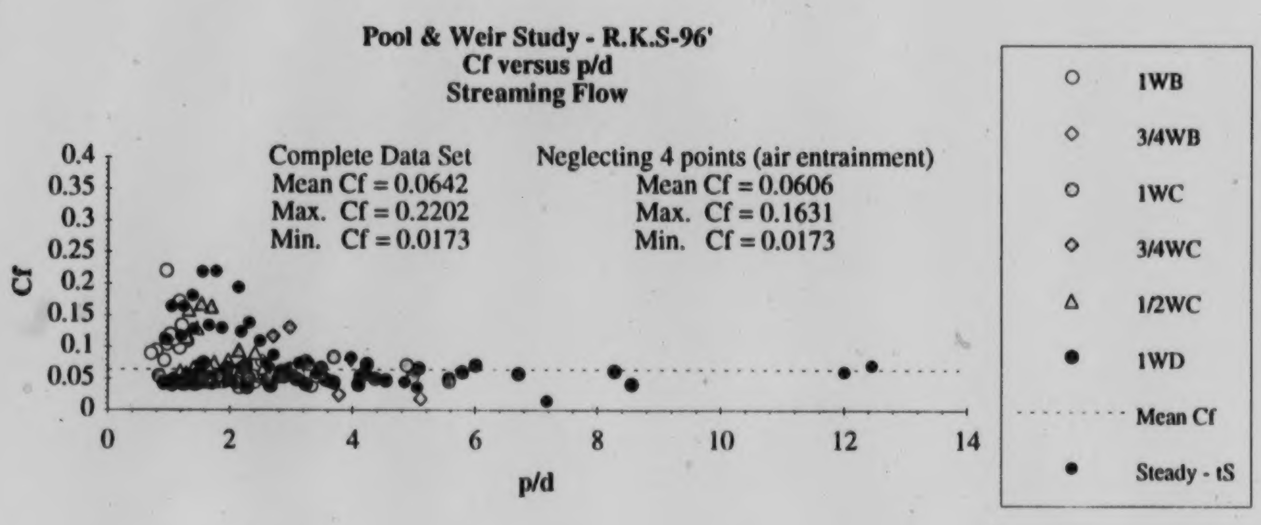

Figure 26: Coefficient of Fluid Friction versus Weir Height over Streaming Depth with Transitional Streaming Data

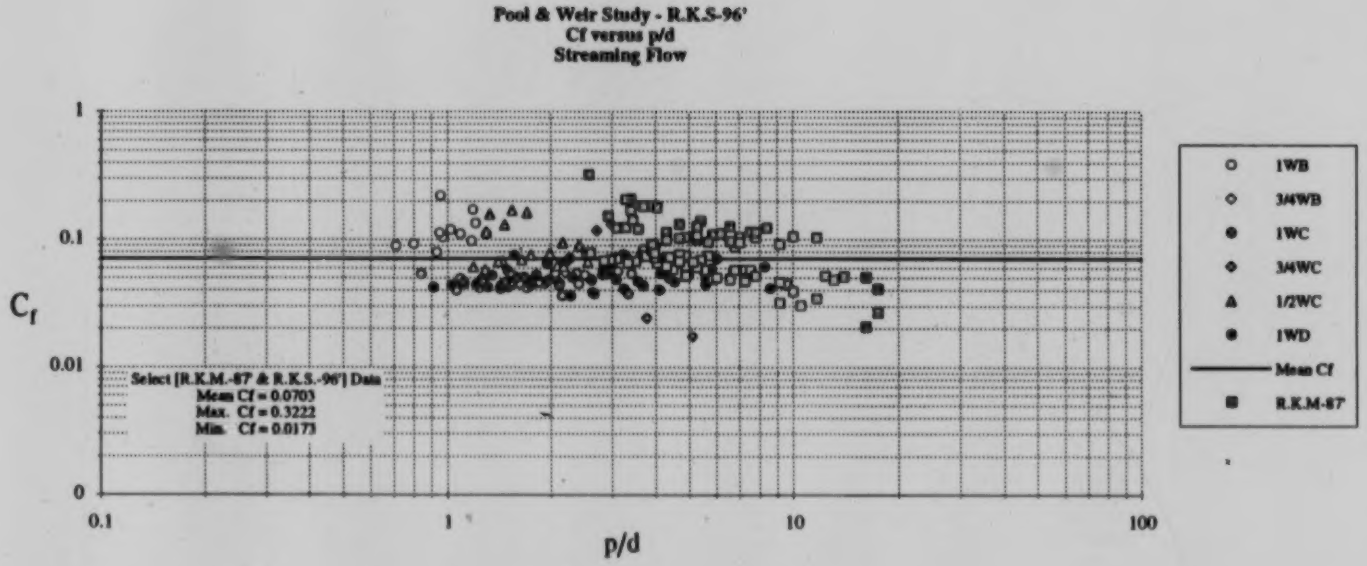

Figure 27: Coefficient of Fluid Friction versus Weir Height over Streaming Depth with R.K.M-87' Data - Streaming Flow Analysis

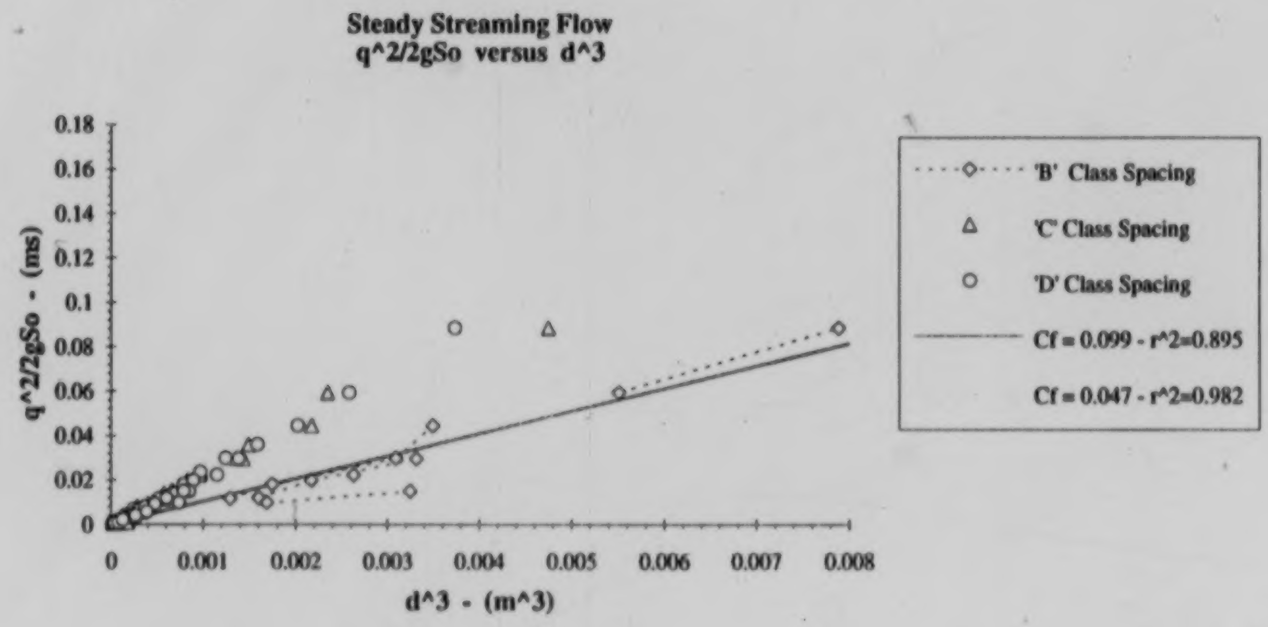

Figure 28: Determination of Coefficient of Fluid Friction,Cf - Streaming Flow Analysis

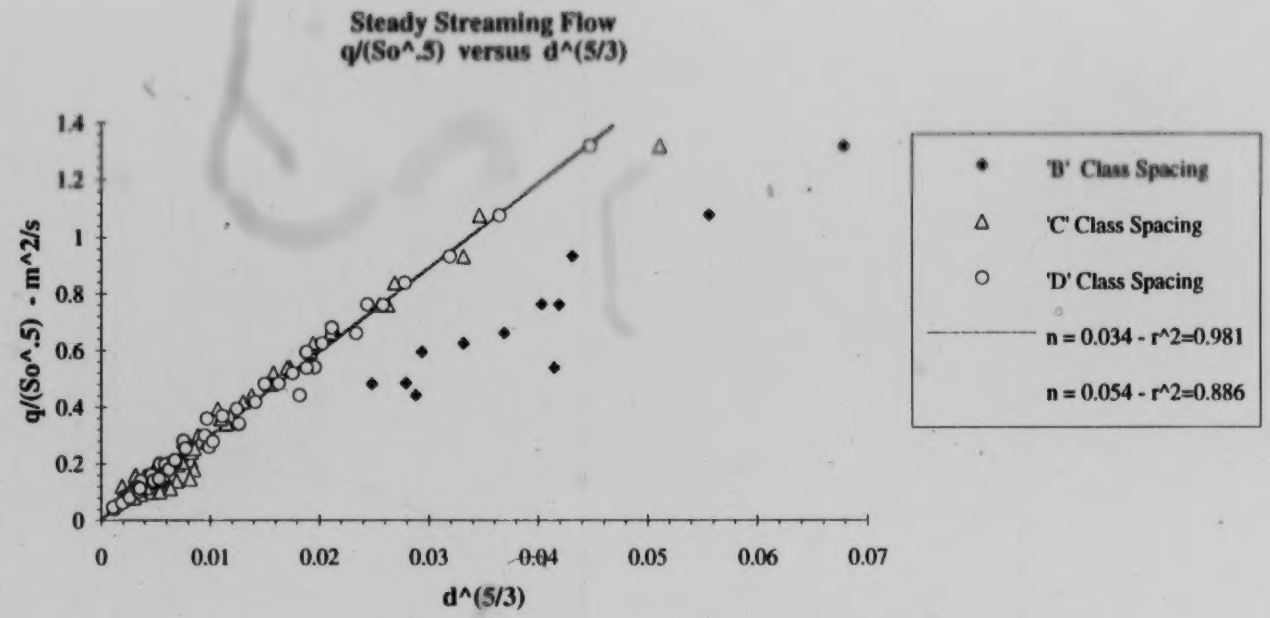

Figure 29: Determination of Mannings 'n' for Streaming Flow - Streaming Flow Analysis

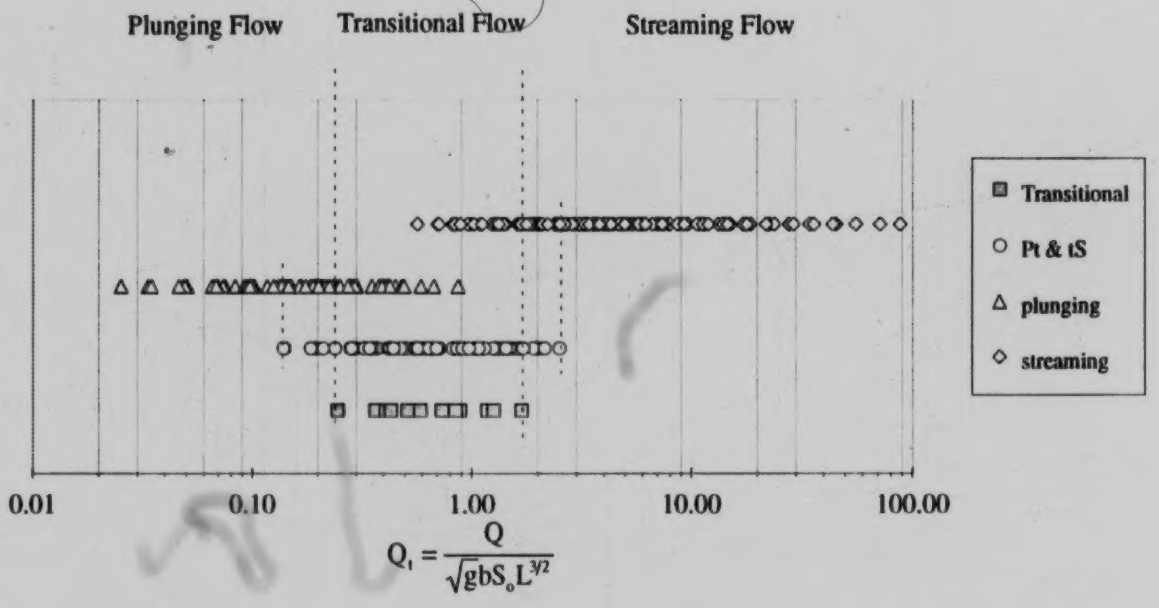

Figure 30: Graphical Illustration of Domains for Dimensionless Transitional Discharge, Qt

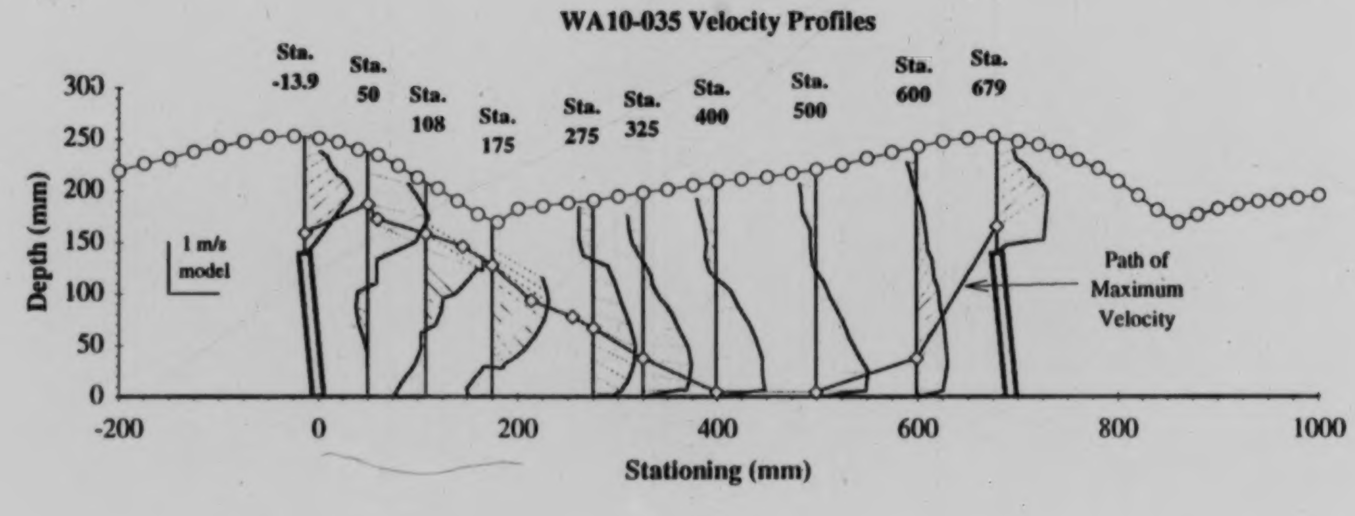

Figure 31: WA10-035 Velocity Profiles

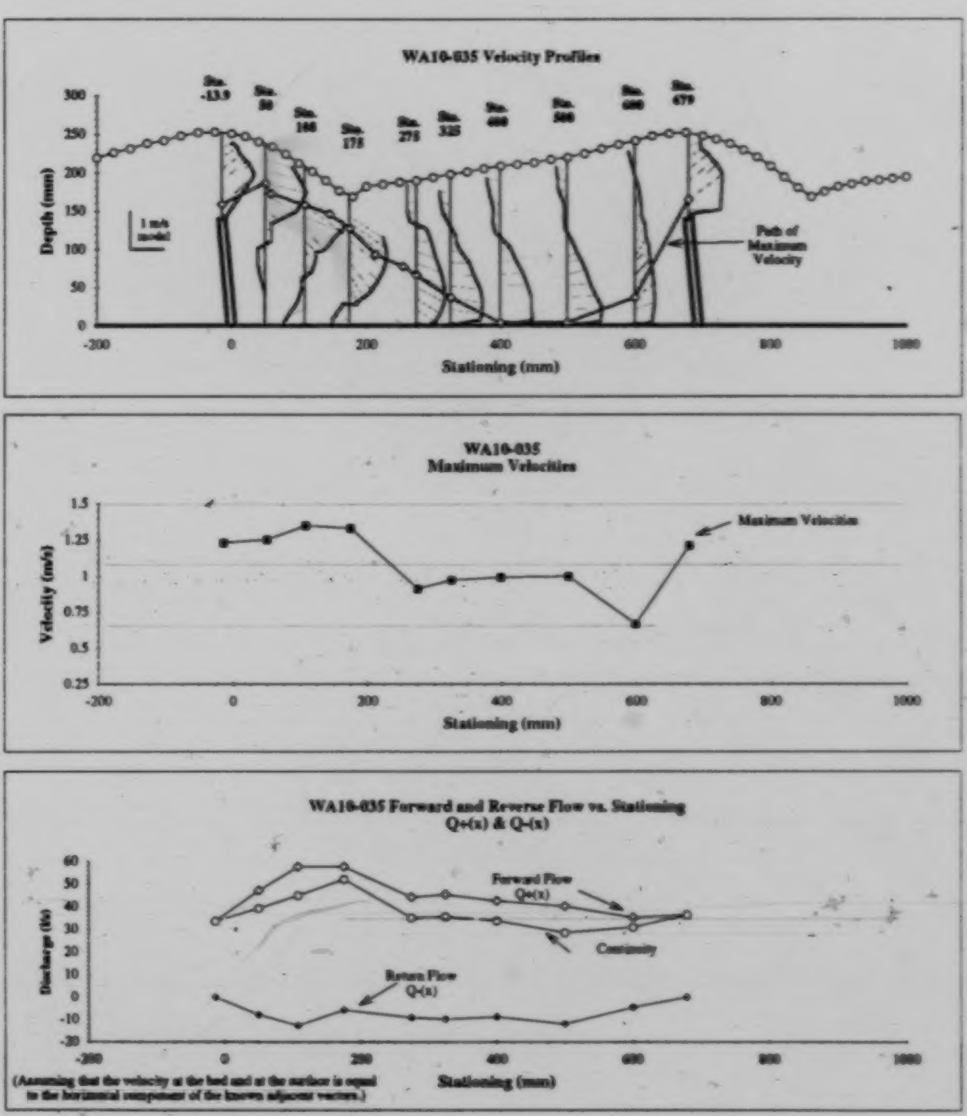

(Assuming that the velocity at the bed and at the surface is equal to the horizontal component of the known adjacent vectors.)

Figure 32: WA10-035 Velocity Profiles, Maximum Velocity and Continuity

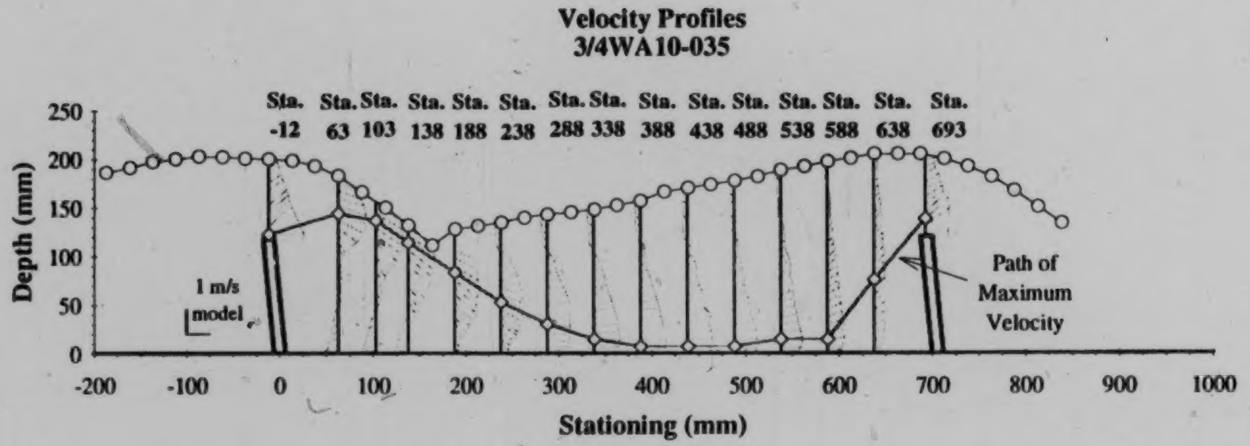

Figure 33: 3/4 WA10-035 Velocity Profiles

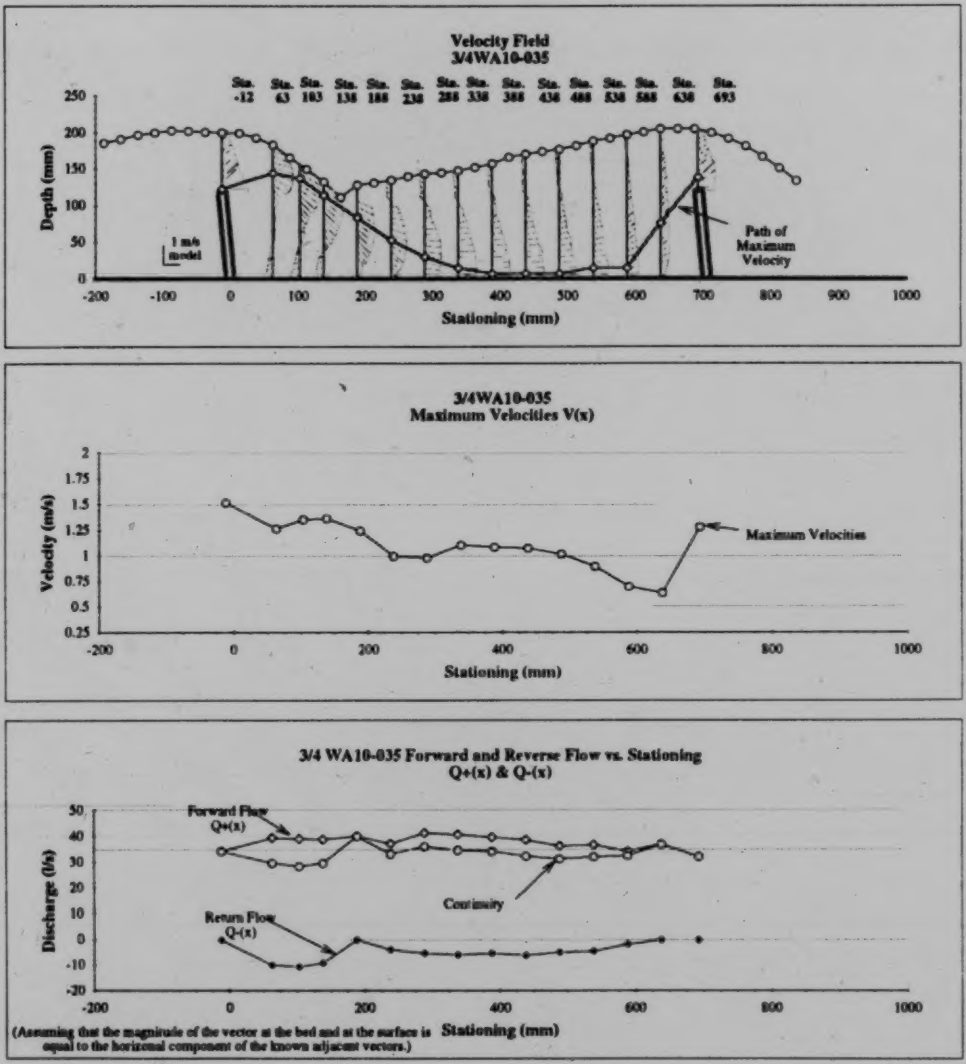

Figure 34: 3/4WA10-035 Velocity Profiles, Maximum Velocity and Continuity

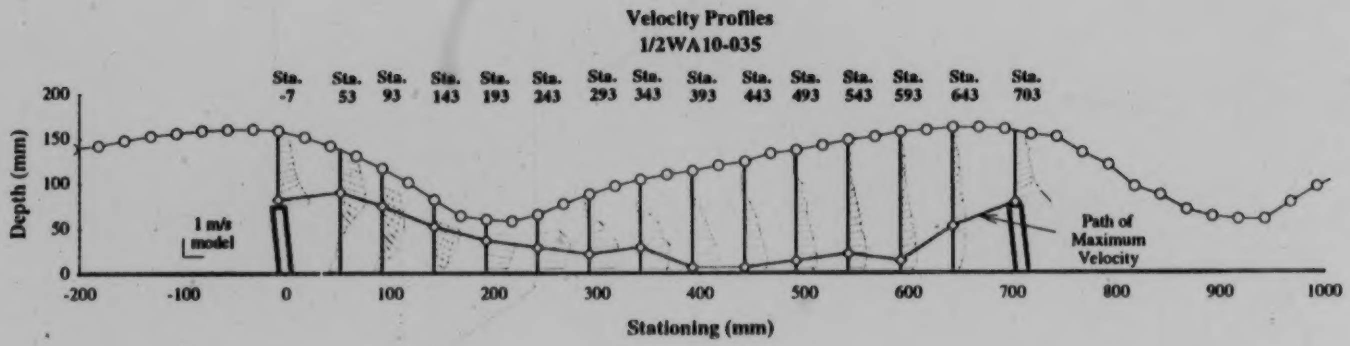

Figure 35: 1/2WA10-035 Velocity Profiles

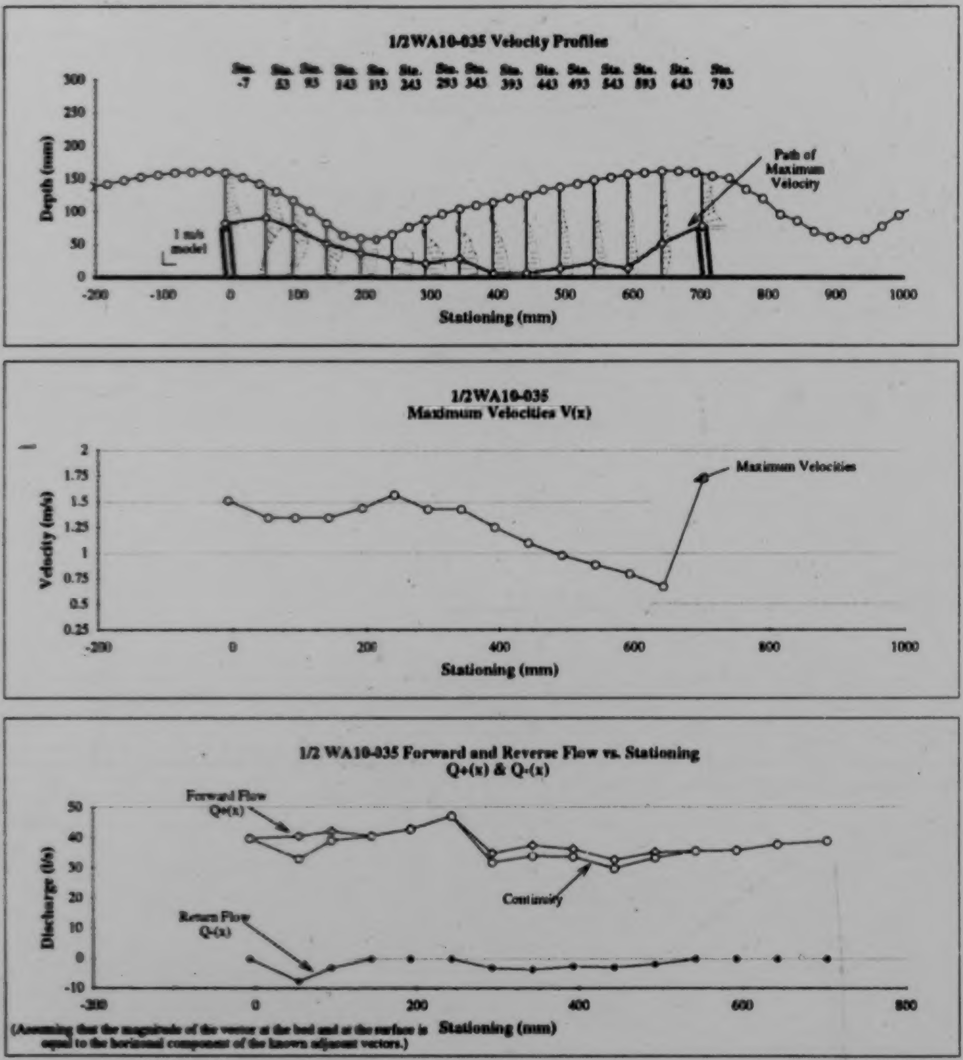

1/2WA10-035 Velocity Profiles

1/2WA10-035 Maximum Velocities V(x)

1/2 WA10-035 Forward and Reverse Flow vs. Stationing Q+(x) & Q-(x)

(Assuming that the magnitude of the vector at the bed and at the surface is equal to the horizontal component of the known adjacent vectors.)

Figure 36: 1/2WA10-035 Velocity Profiles, Maximum Velocity and Continuity

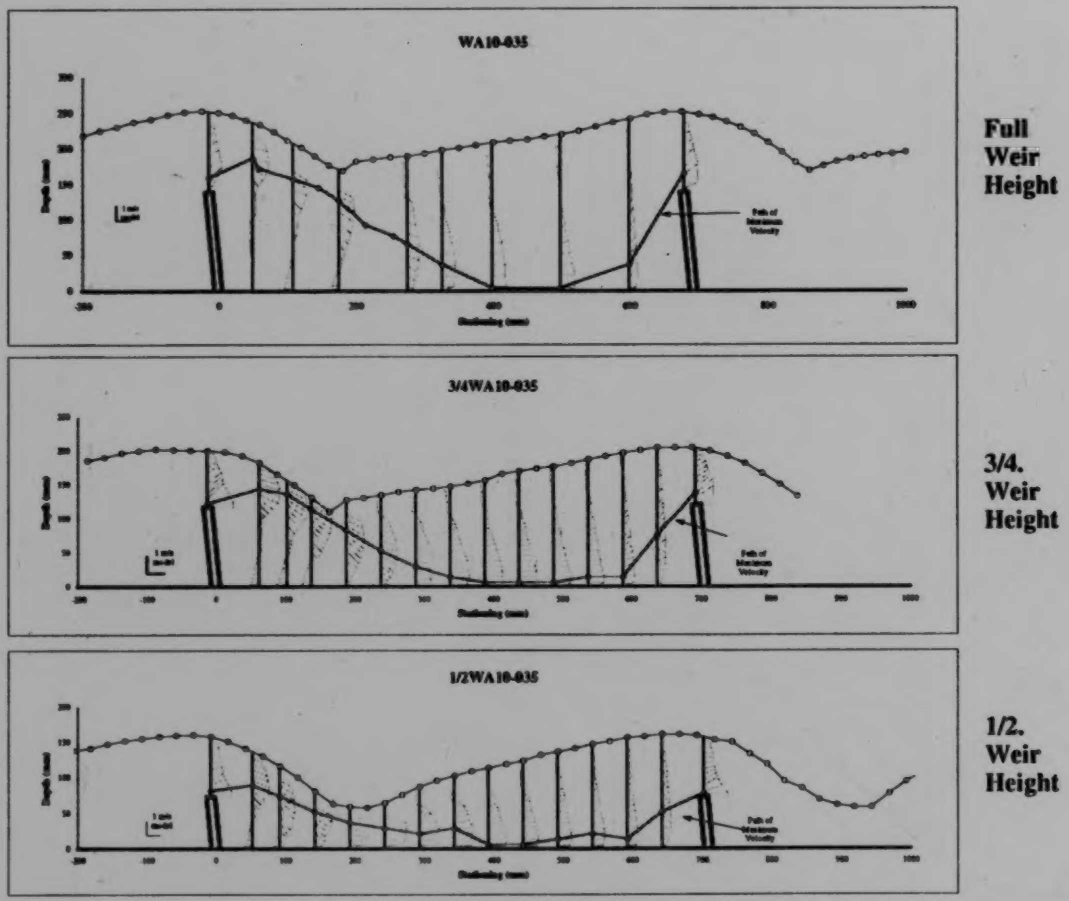

Figure 37: Comparison of Velocity Fields for Full, Three Quarter and Half Weir Heights

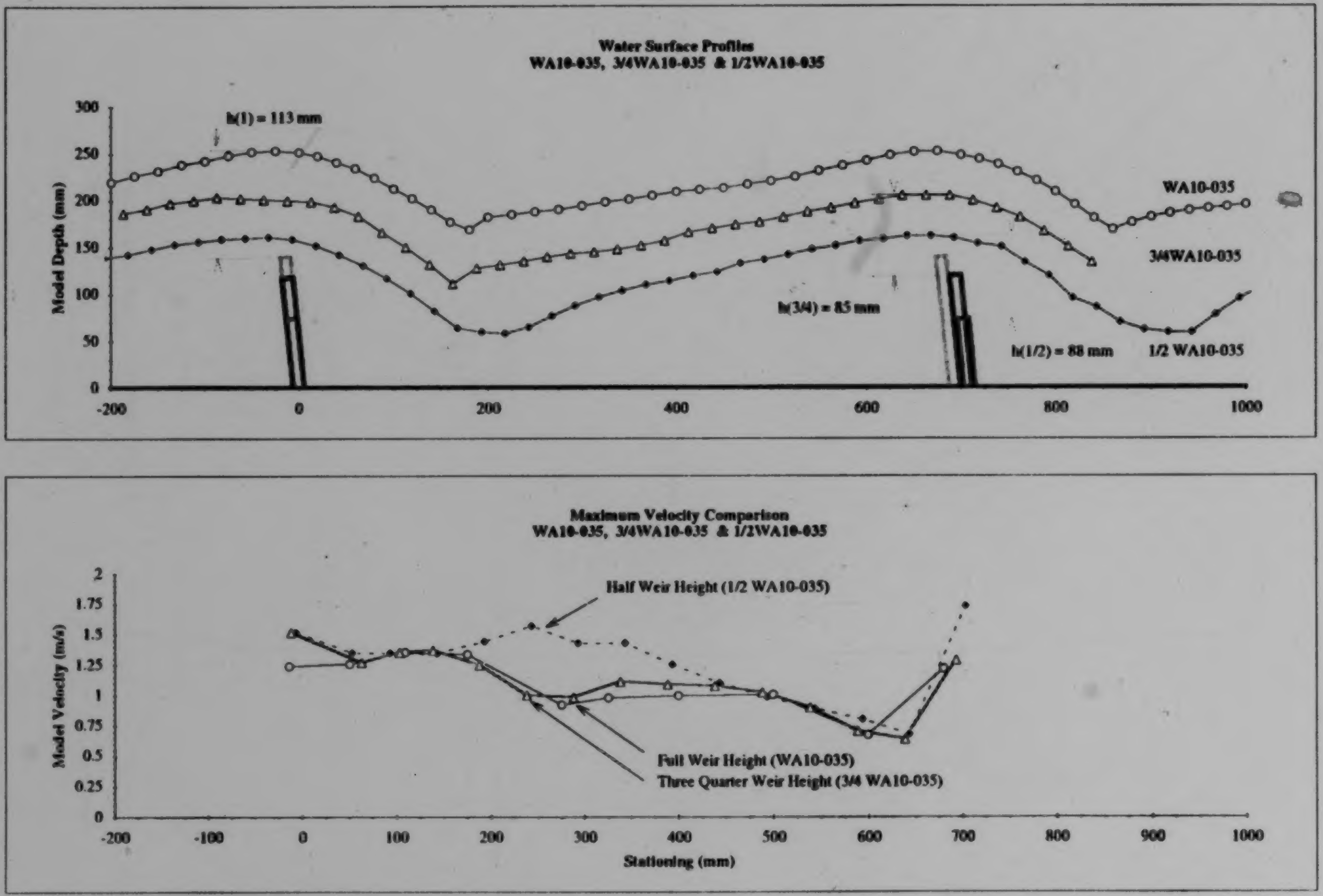

Figure 38: Comparison of Water Surface Profiles and Maximum Velocity for Full, Three Quarter and Half Weir Heights

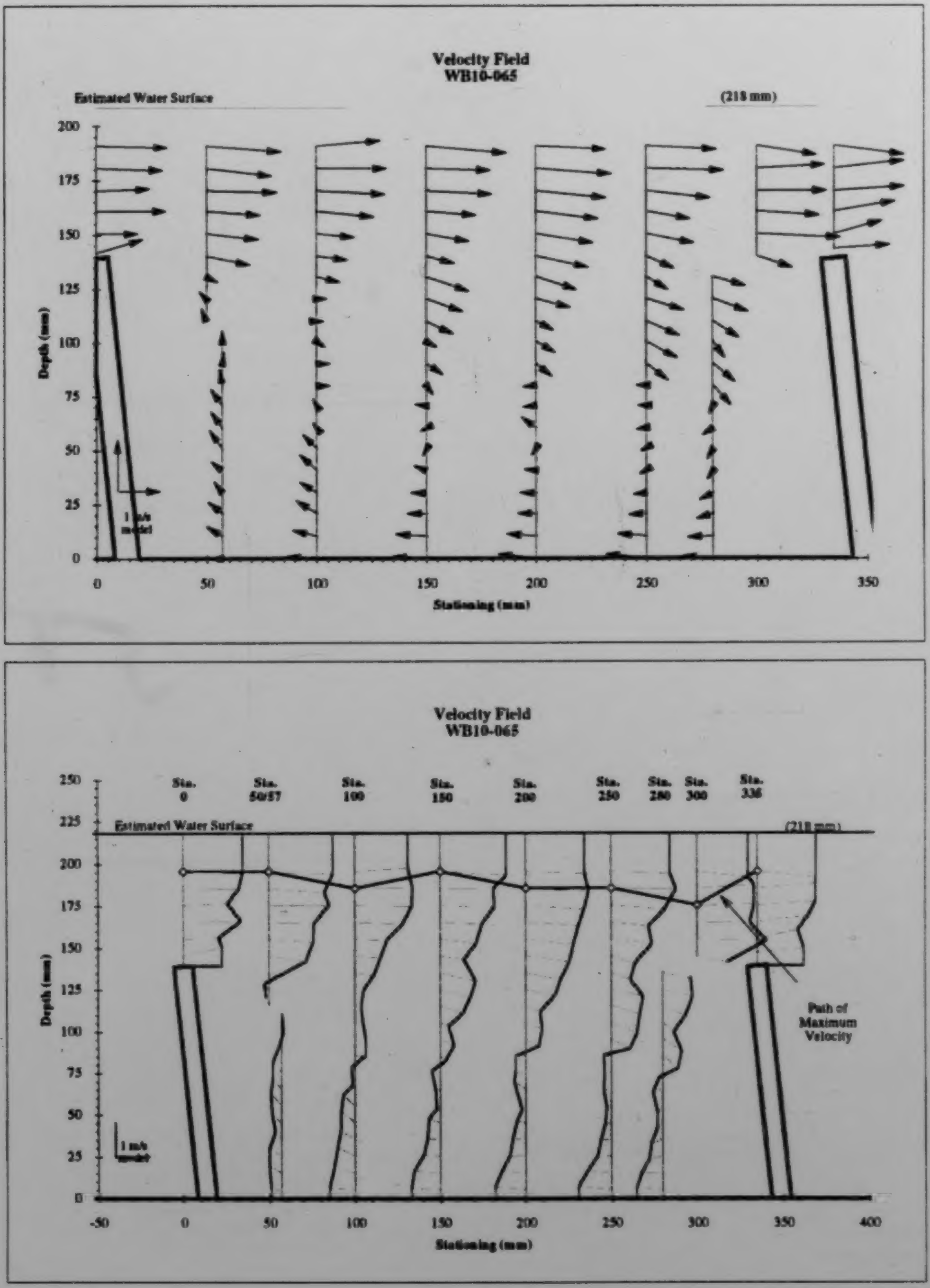

Figure 39: WB10-065 Velocity Vectors and Profiles

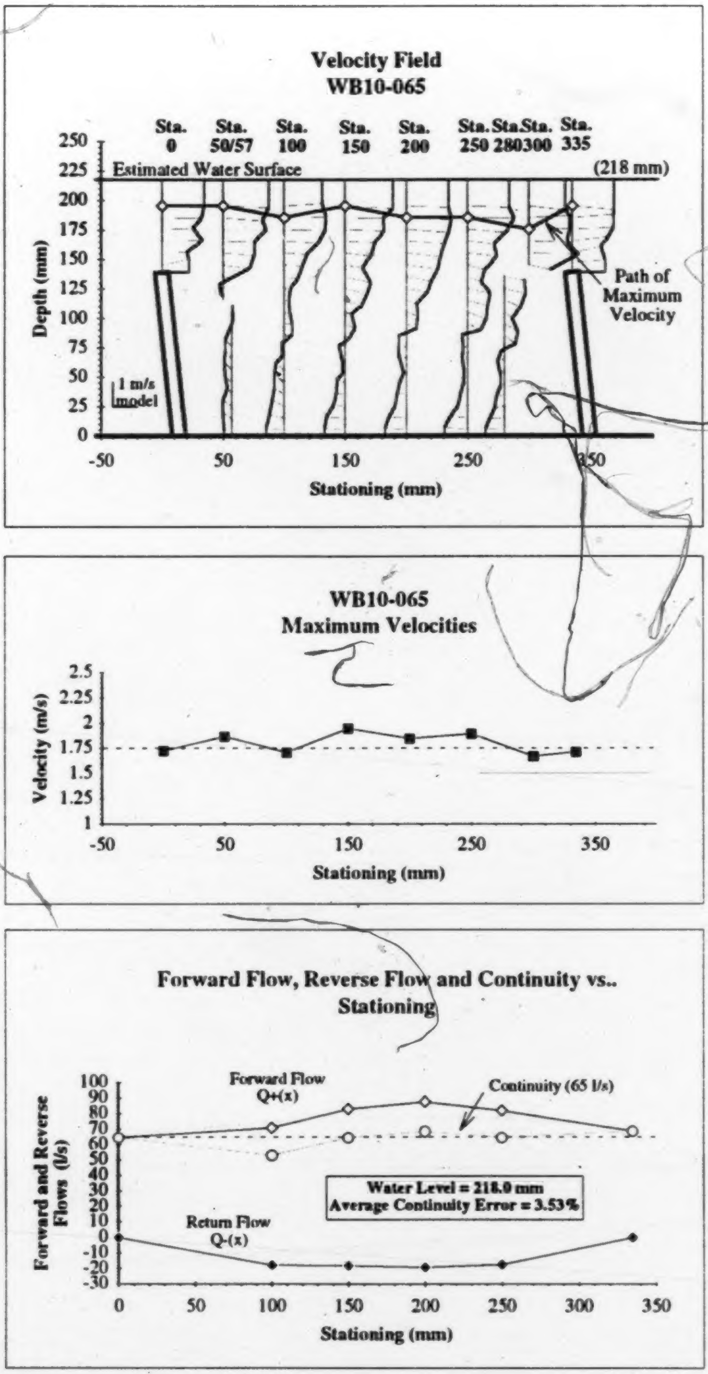

Figure 40: WB10-065 Velocity Profiles, Maximum Velocity and Continuity

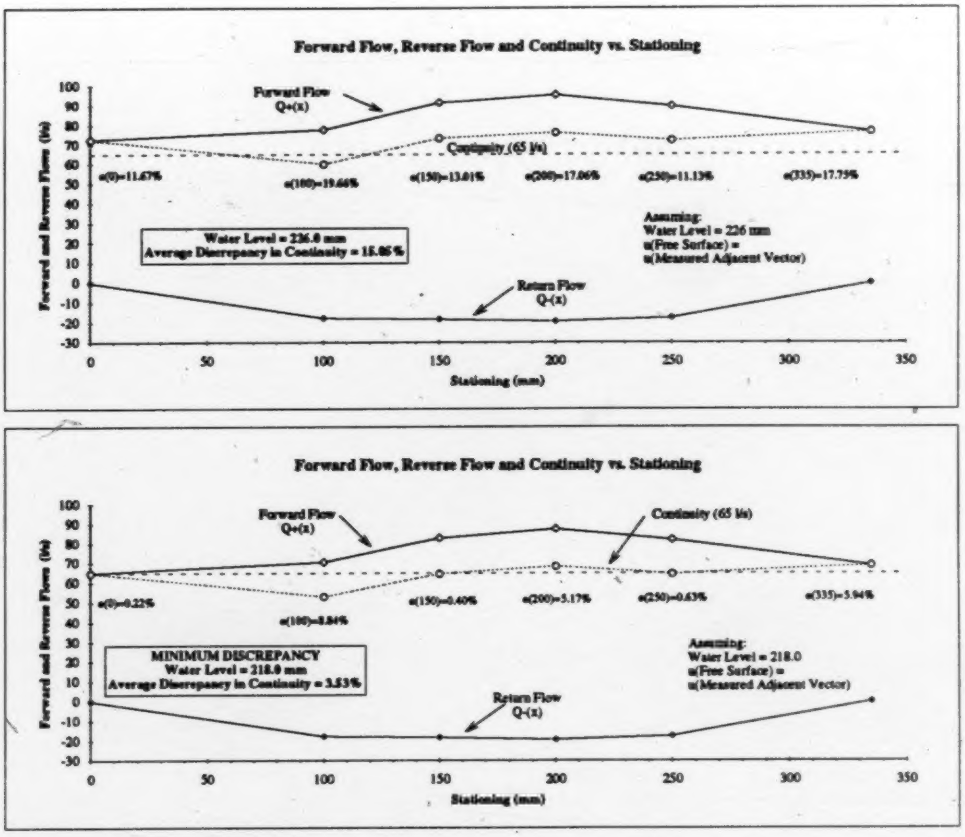

Assumption: u(free surface) = u(measured adjacent vector)

1st plot: This plot shows that by visually approximating the water surface to be = 226mm, the average discrepancy in continuity is 15.05%, ranging from 11.13% to 19.66%

2nd plot: This plot is the result of changing the water surface to achieve the minimal discrepancy in continuity. A water surface of 218mm (8mm lower than the original visual estimation of 226mm) produces an average discrepancy in continuity of 3.53%, ranging from 0.22% to 8.84%

Note: By minimizing the discrepancy in continuity, the water surface was found to be 218mm. Due to the turbulent nature of the flow, it is not unreasonable to assume this lower water surface elevation. This therefore shows that the transitional streaming flow (WB10-065) can be confidently approximated as TWO DIMENSIONAL FLOW.

Figure 41: Water Surface Correction for a Transitional Streaming Flow

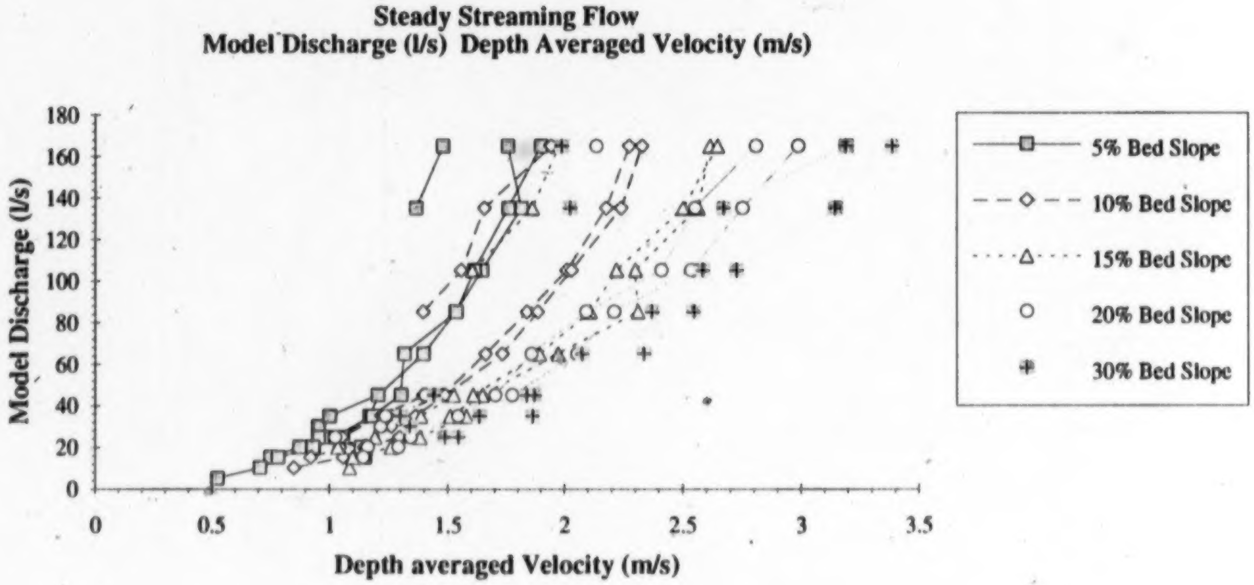

Figure 42: Discharge versus Depth averaged Velocity for Streaming Flows

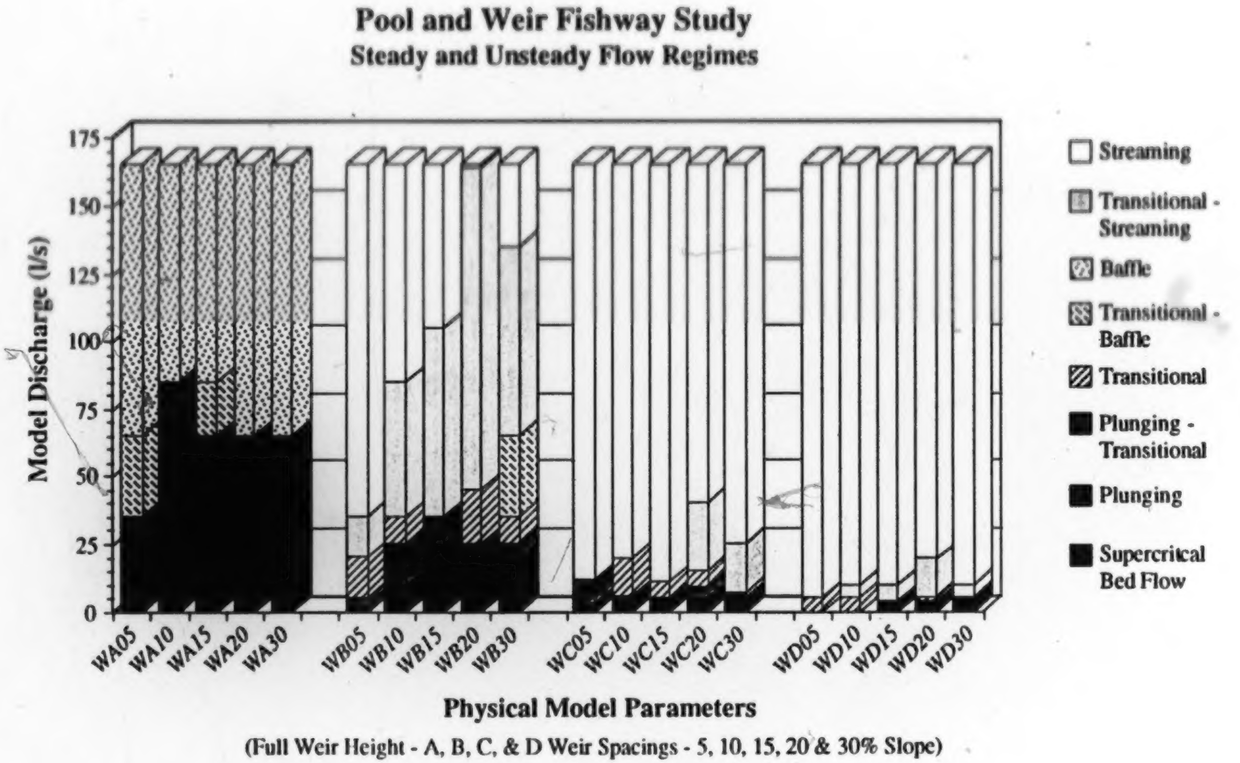

Figure 43: Histogram Illustrating the Domains of All Steady and Unteady Flow Regimes

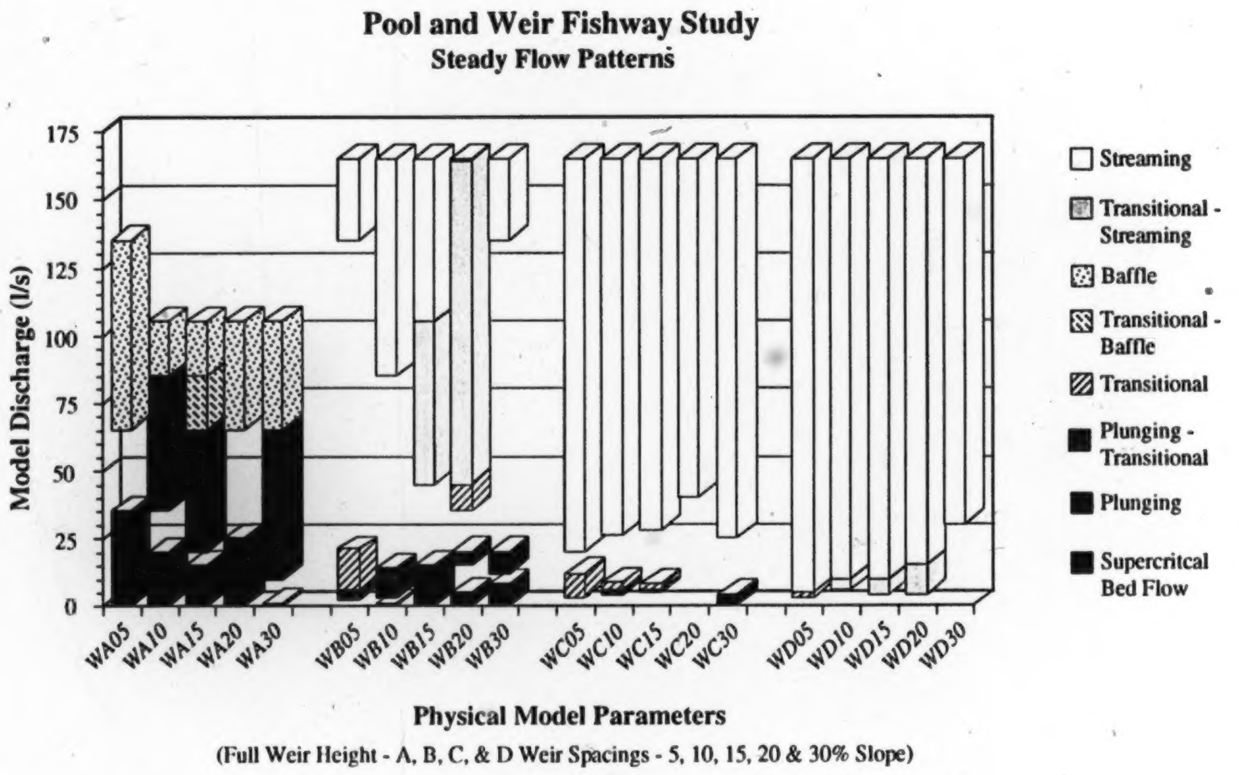

Figure 44: Histogram Illustrating the Domains of All Steady Flow Regimes

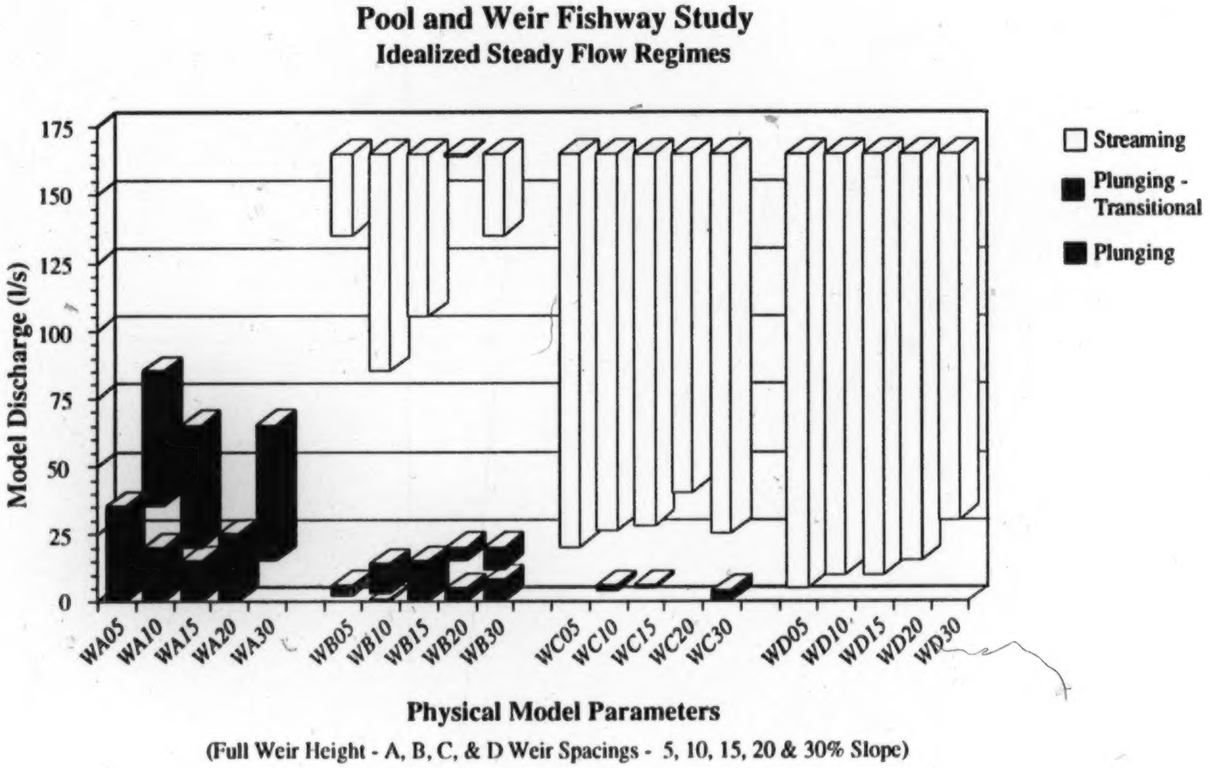

Figure 45: Histogram Illustrating the Domains of Preferred Steady Flow Regimes

Pool & Weir Fishway Study - R.K.S- 96 Data

$\frac{Q}{bL^{3/2}\sqrt{g}}$ versus $S_o\frac{L}{P}$

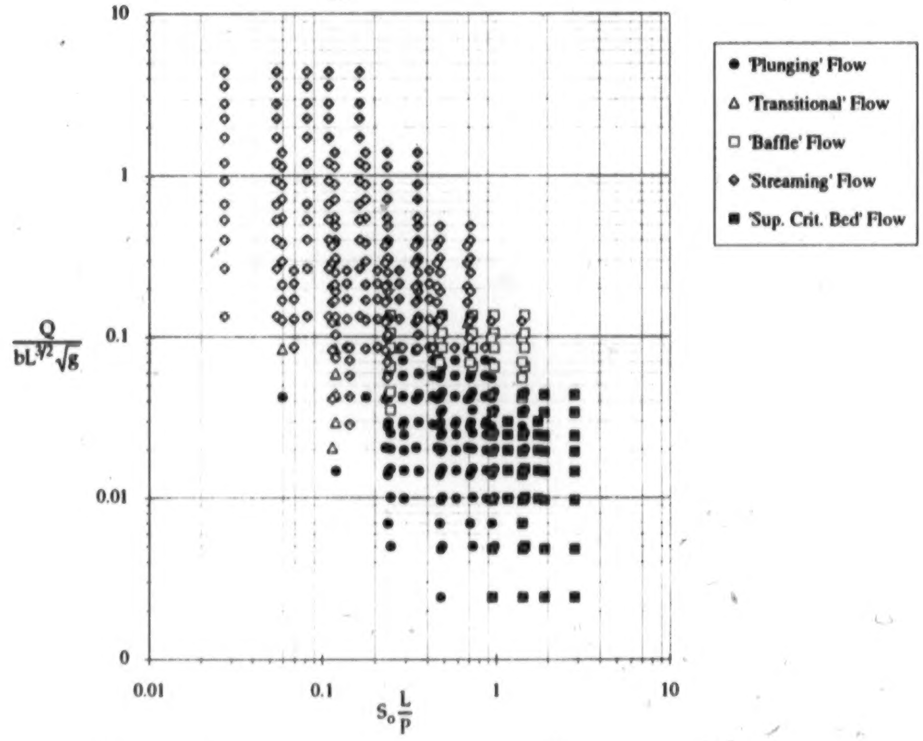

Figure 46: Mapping of Flow Regimes with Dimensionless Parameters

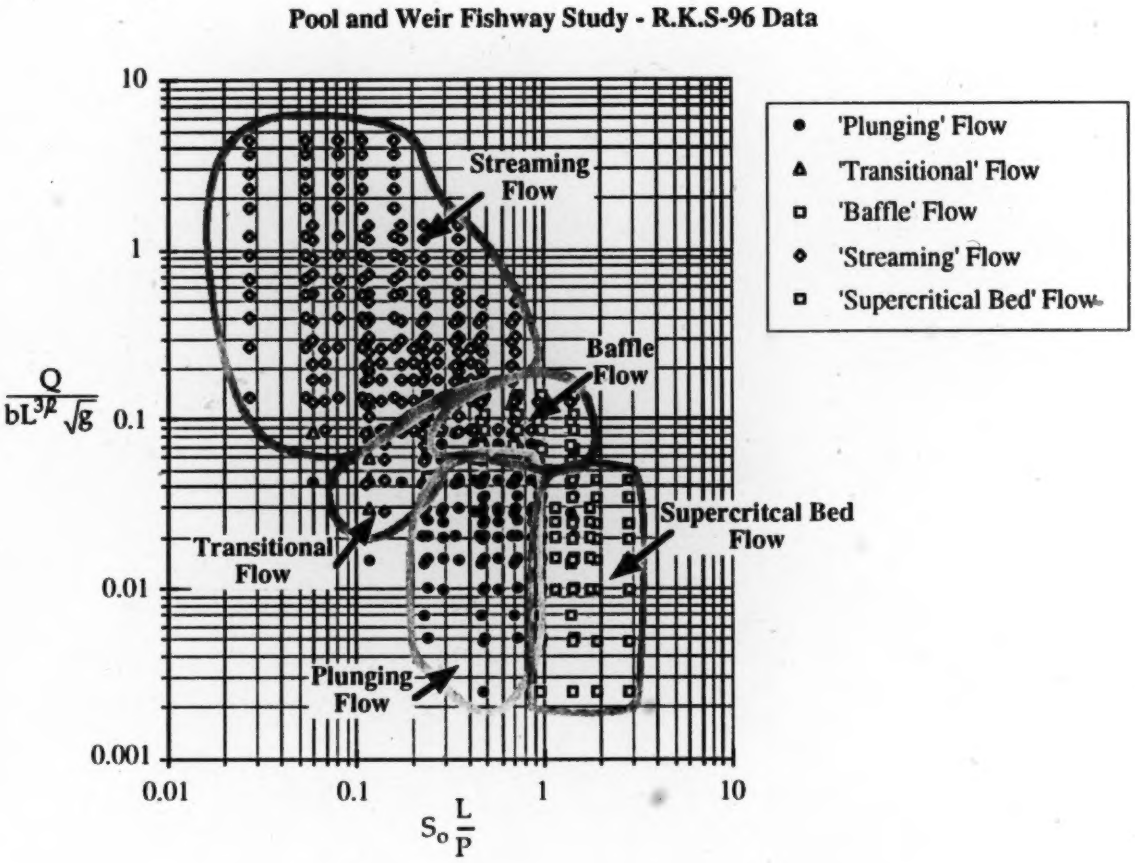

Figure 47: Flow Regime Boundaries for Dimensionless Parameters

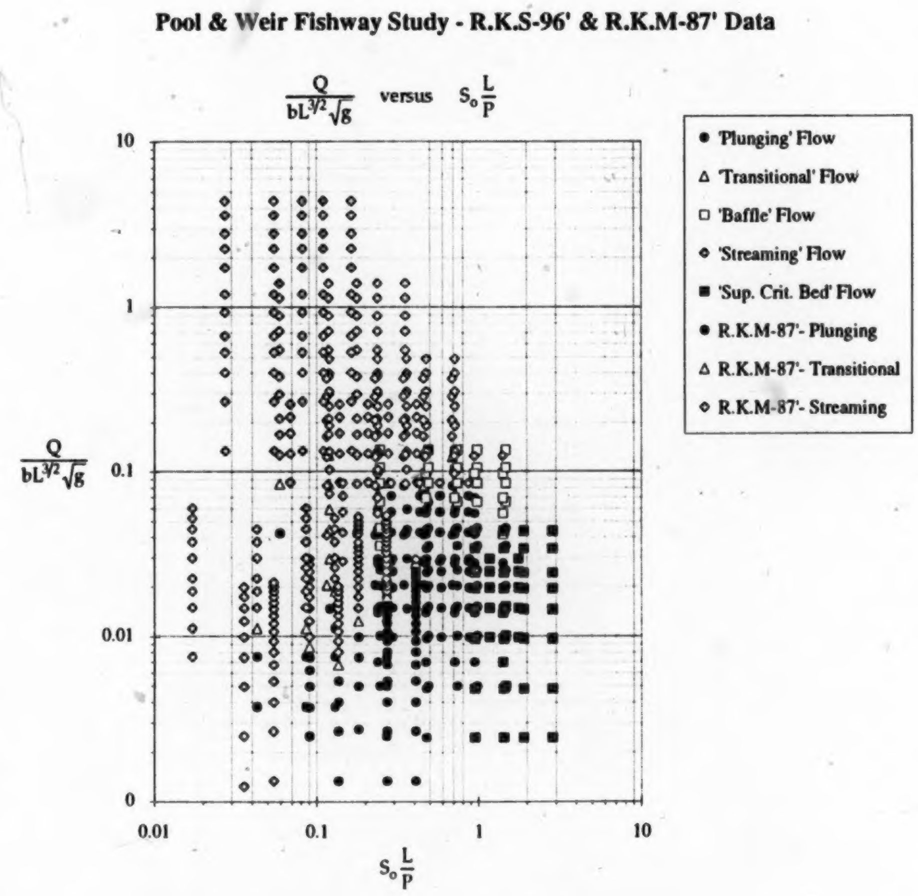

Figure 48: Verifying Dimensionless Parameters

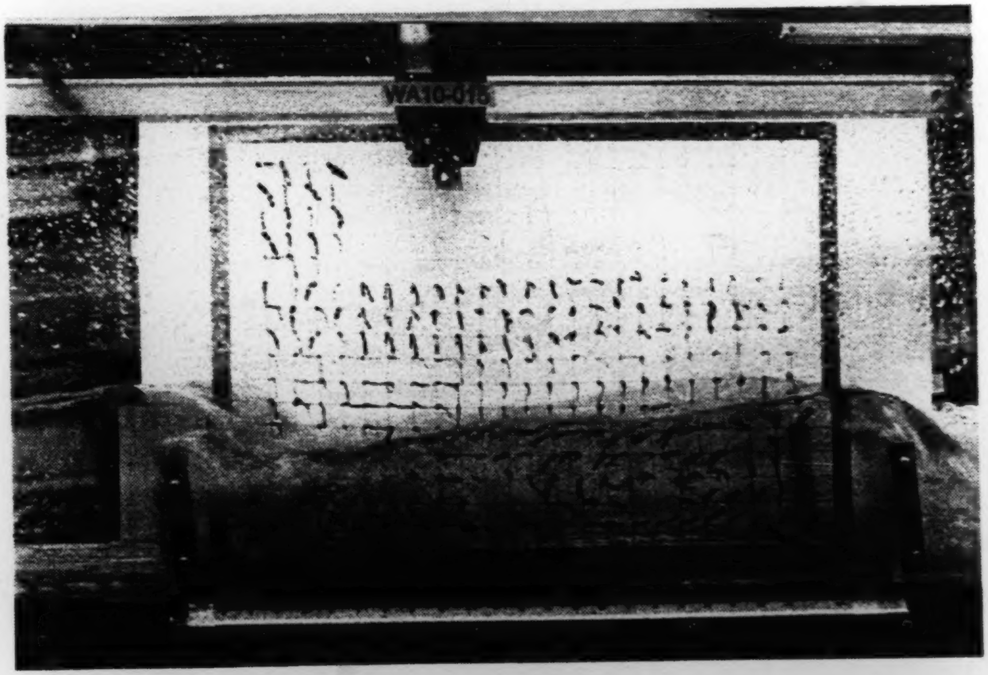

PLATE 1 Plunging Flow, (P) - WA10-015

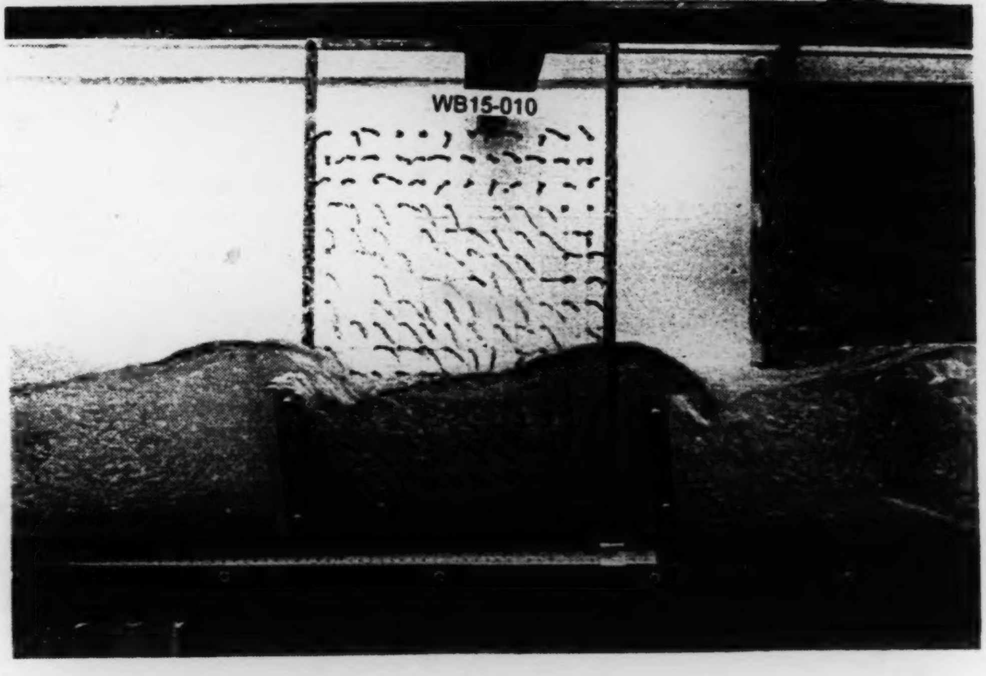

PLATE 2 Plunging Flow, (P) - WB15-010

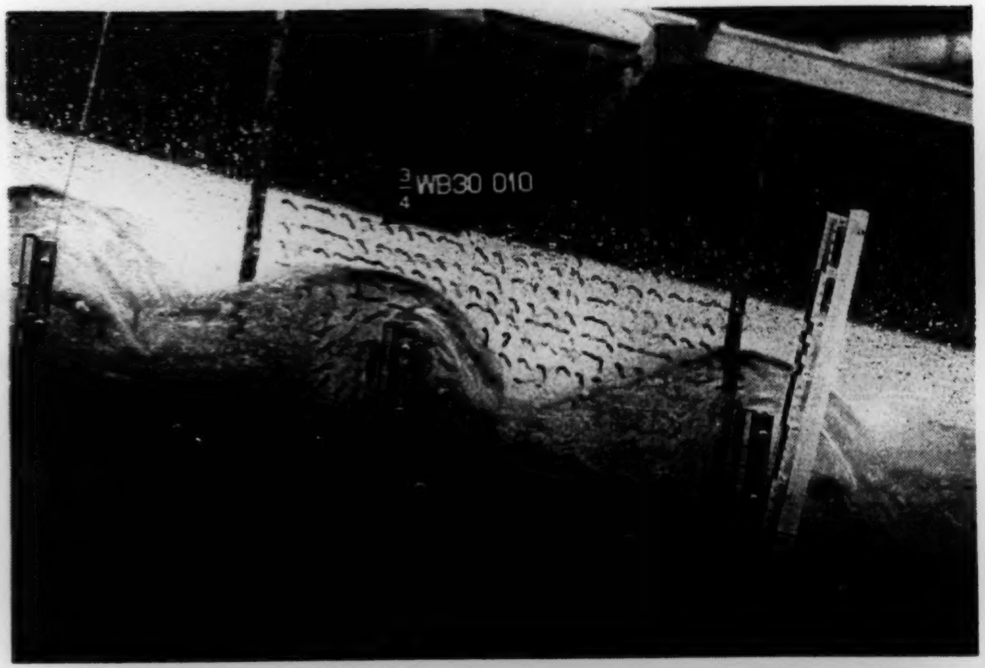

PLATE 3 Plunging Flow, (P) - 3/4WB30-010

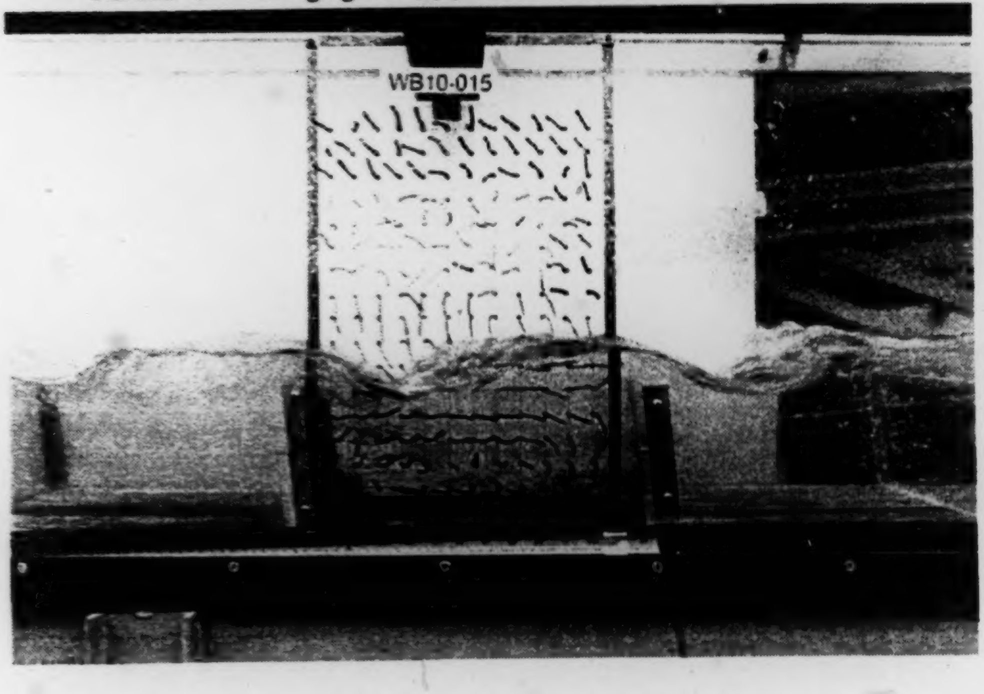

PLATE 4 Plunging Transitional Flow, (Pt) - WB10-015

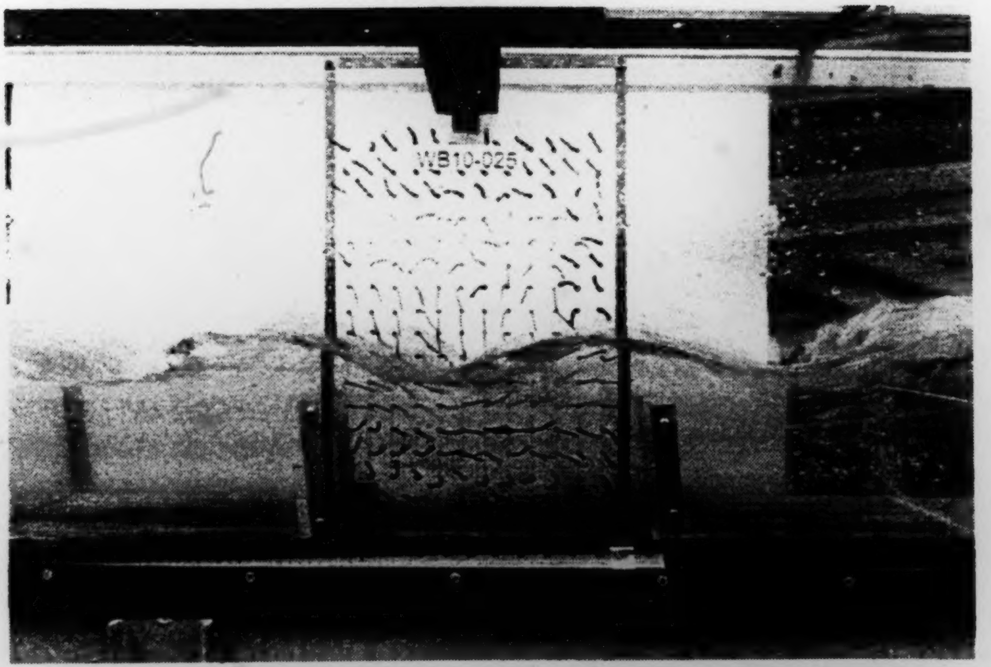

PLATE 5 Transitional Flow, (T) - WB10-025

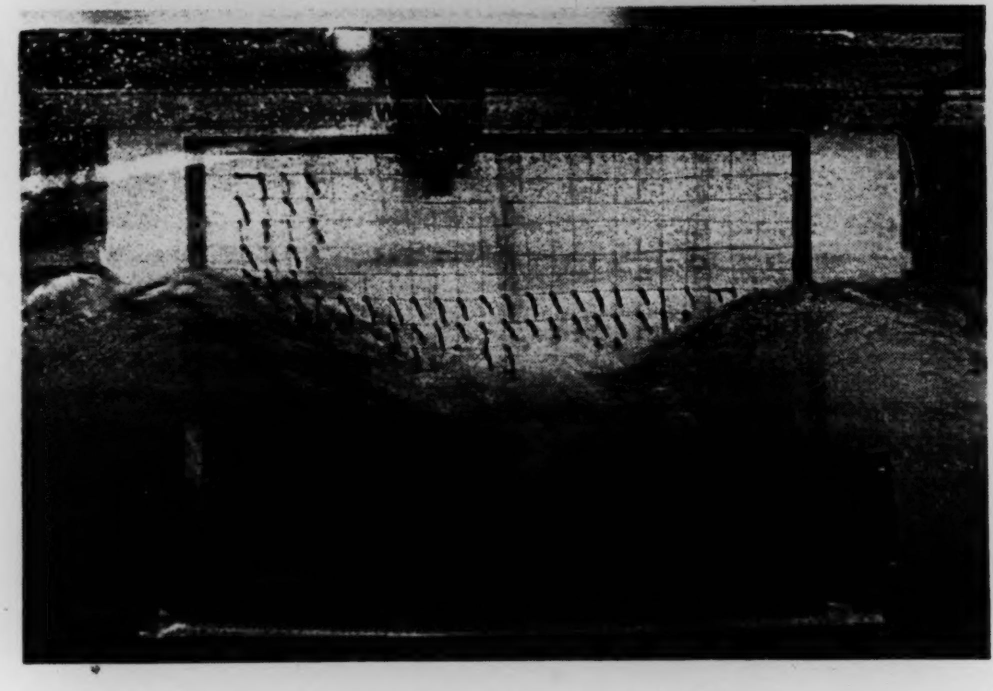

PLATE 6 Transitional Baffle Flow, (tB) - WA15-065

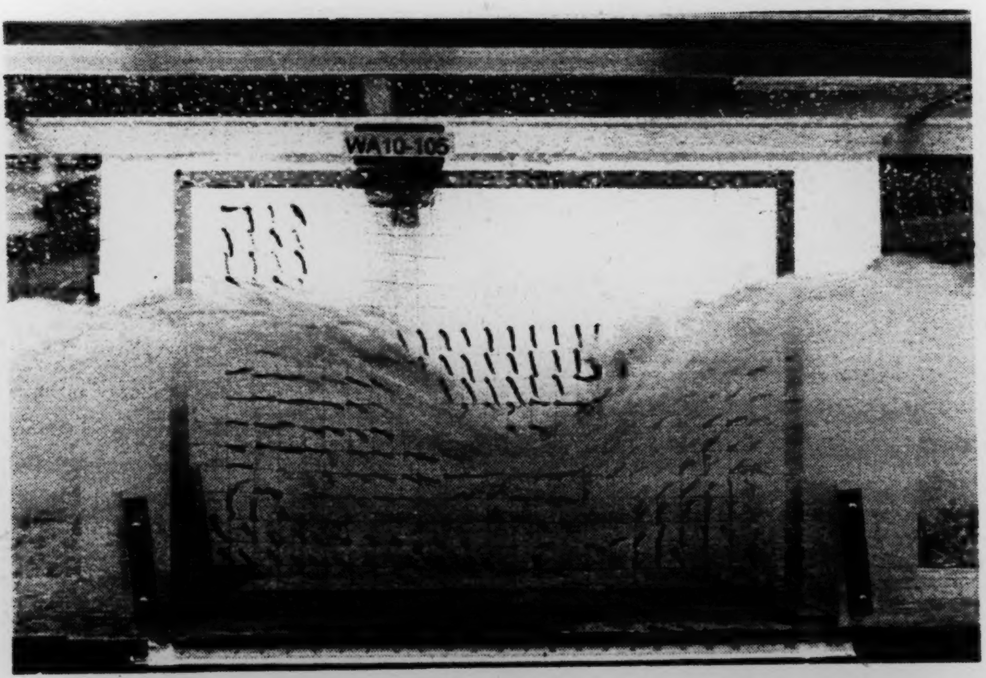

PLATE 7 Baffle Flow, (B) - WA10-105

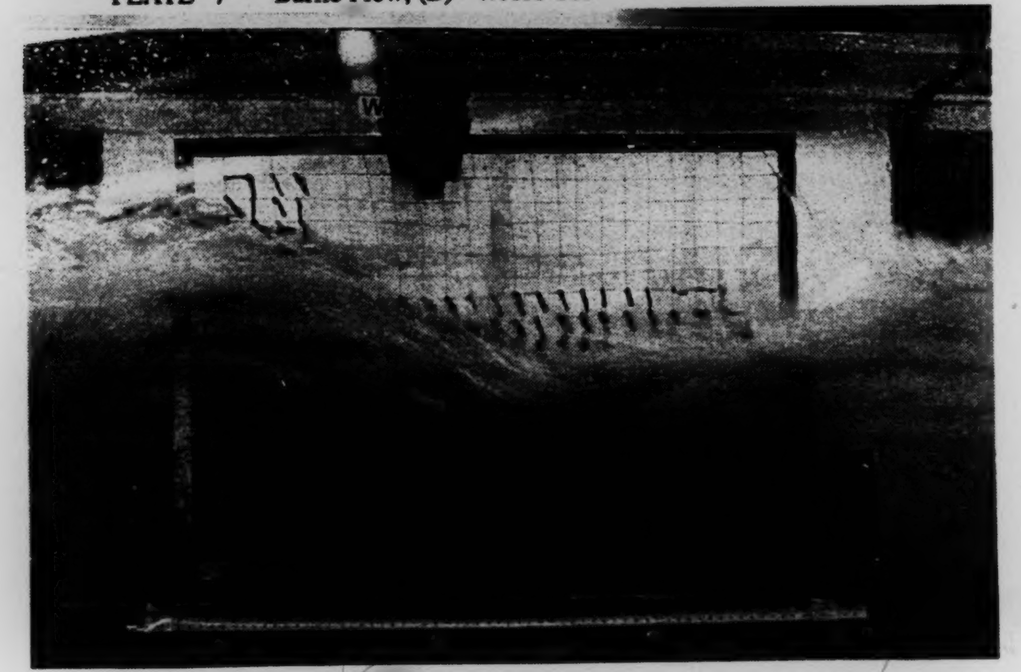

PLATE 8 Baffle Flow, (B) - WA15-105

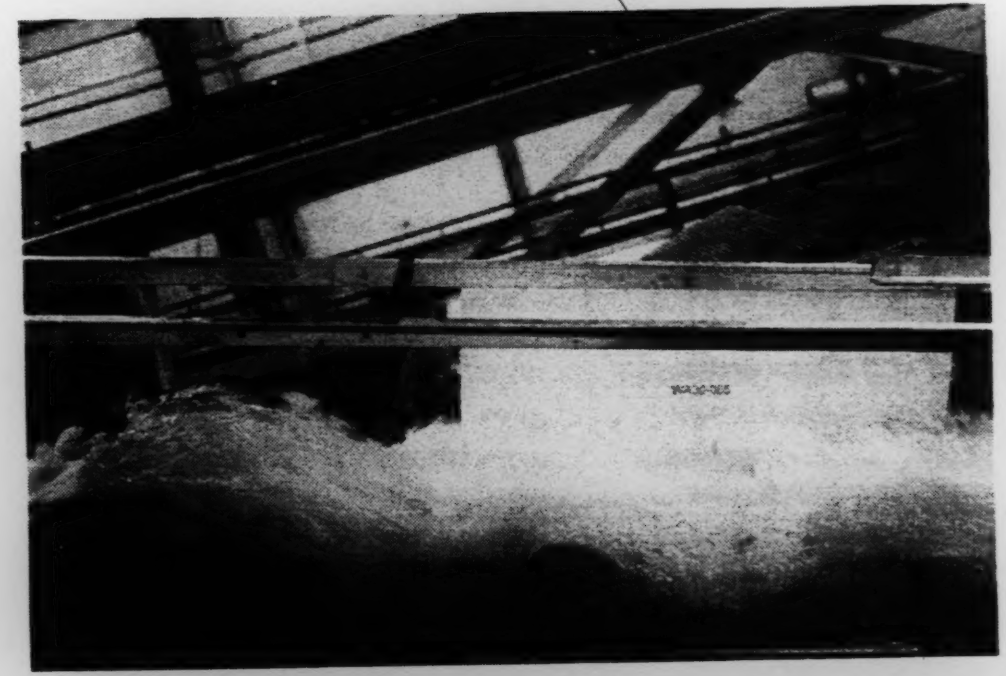

PLATE 9 Baffle Flow, (B) - WA30-065

PLATE 10 Baffle Flow, (B) - 1/2WB30-045

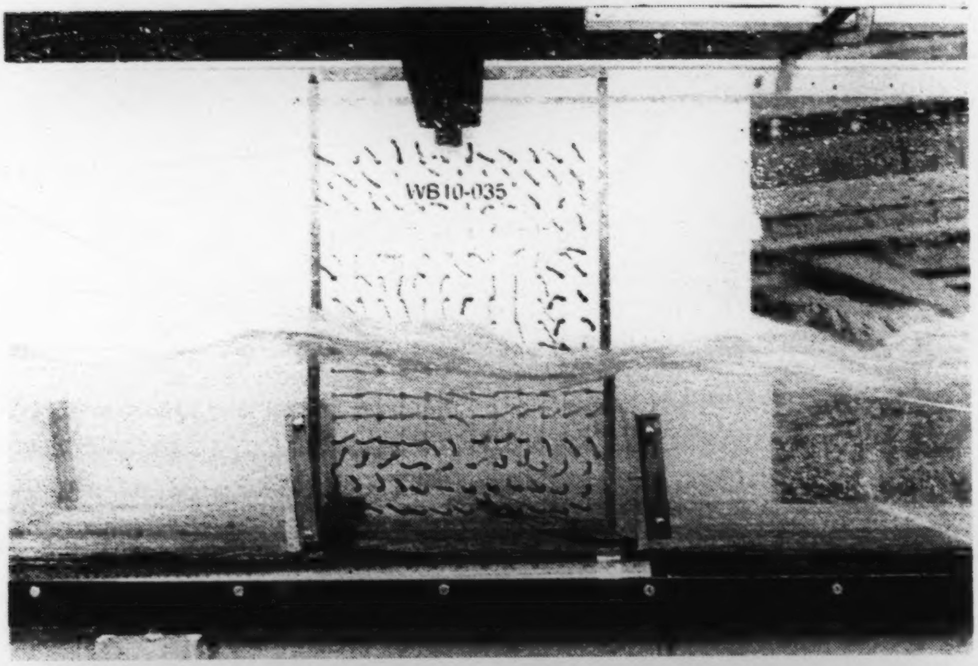

PLATE 11 Transitional Streaming Flow, (tS) - WB10-035

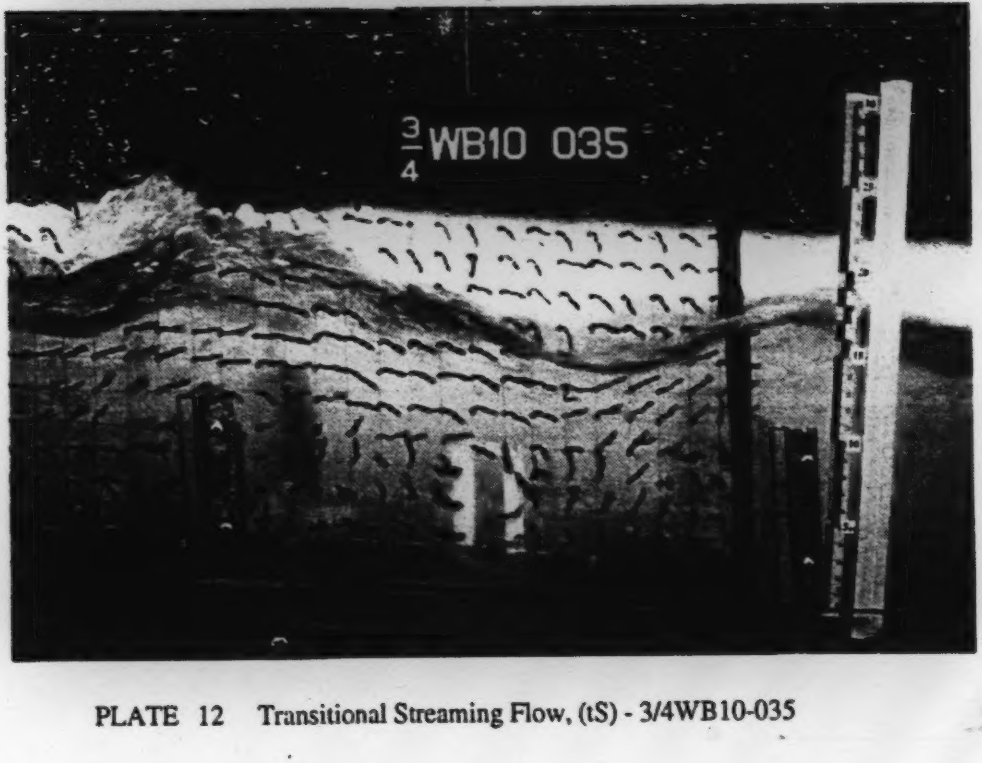

PLATE 12 Transitional Streaming Flow, (tS) - 3/4WB10-035

PLATE 13 Streaming Flow, (S) - WC05-165

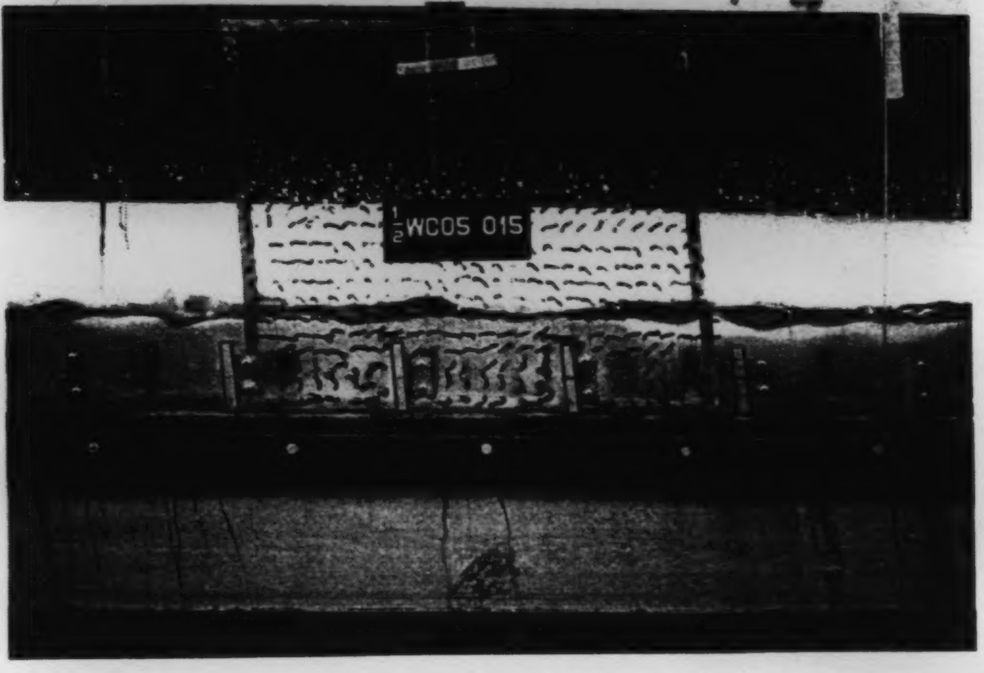

PLATE 14 Streaming Flow, (S) - 1/2WC05-015

PLATE 15 Plunging Flow with a Section of Supercritical Bed Flow, (*P*) - 1/2WA10-020

PLATE 16 Baffle Flow with a Section of Supercritical Bed Flow, (*B*) - 1/2WA30-020

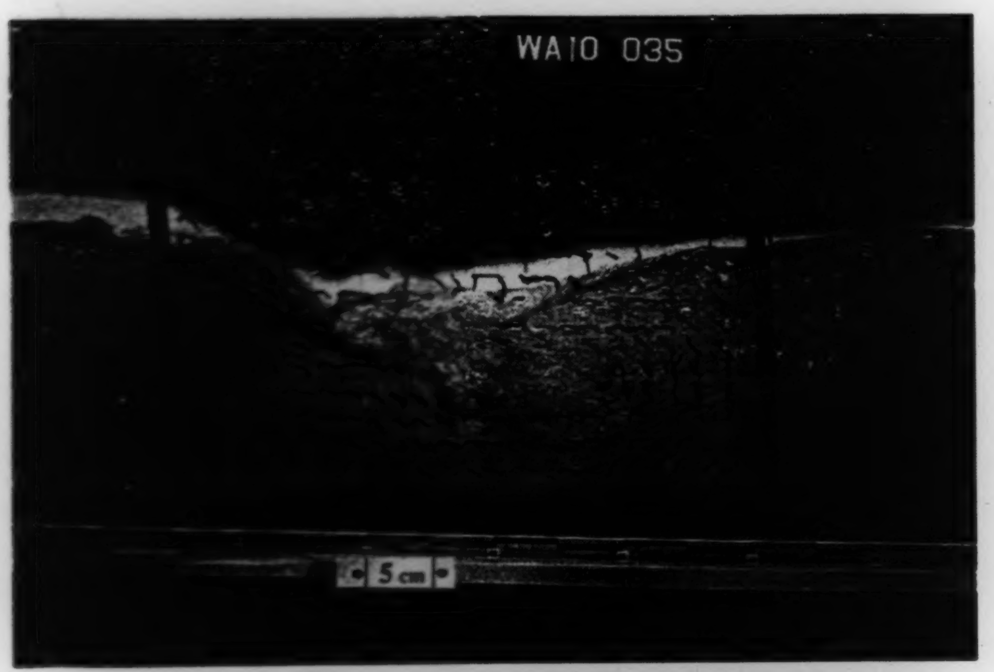

PLATE 17 Velocity Measurements: Plunging Flow - WA10-035

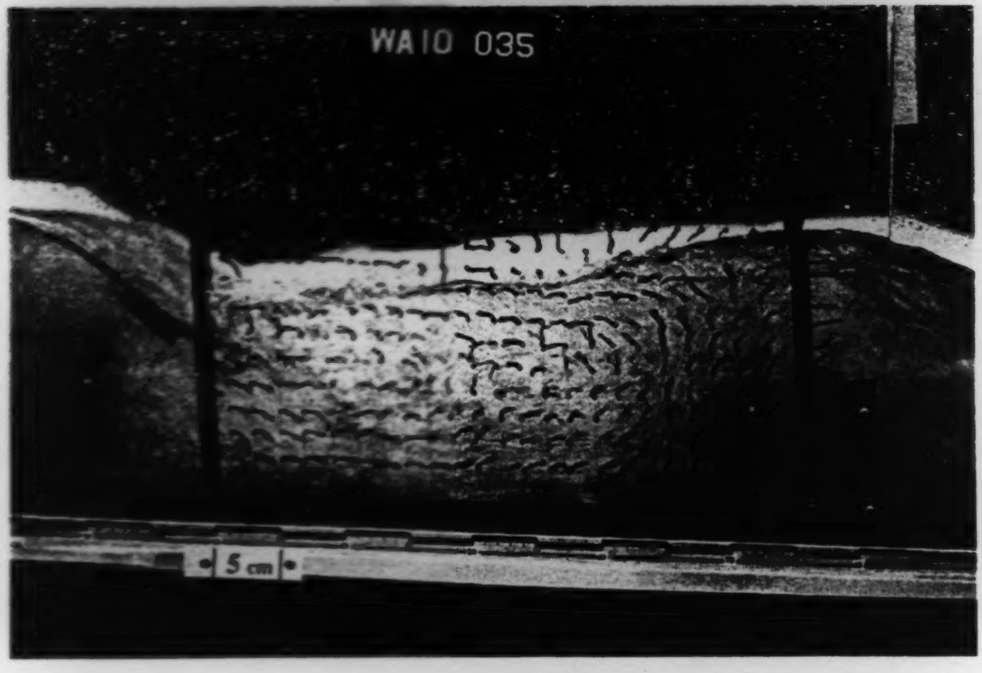

PLATE 18 Velocity Measurements: Plunging Flow - WA10-035

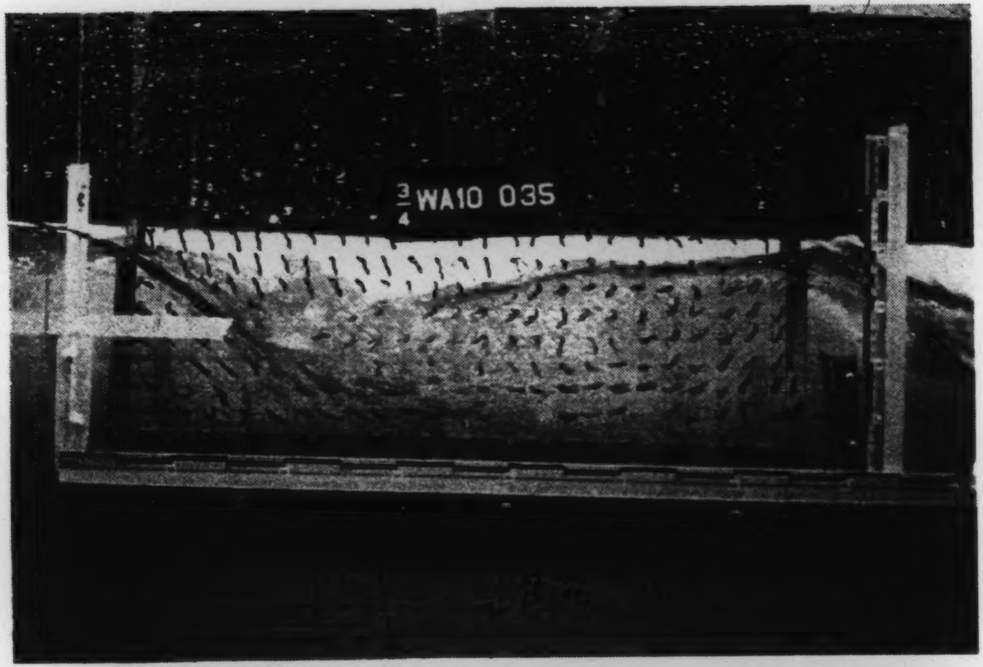

PLATE 19 Velocity Measurements: Plunging Flow - 3/4WA10-035

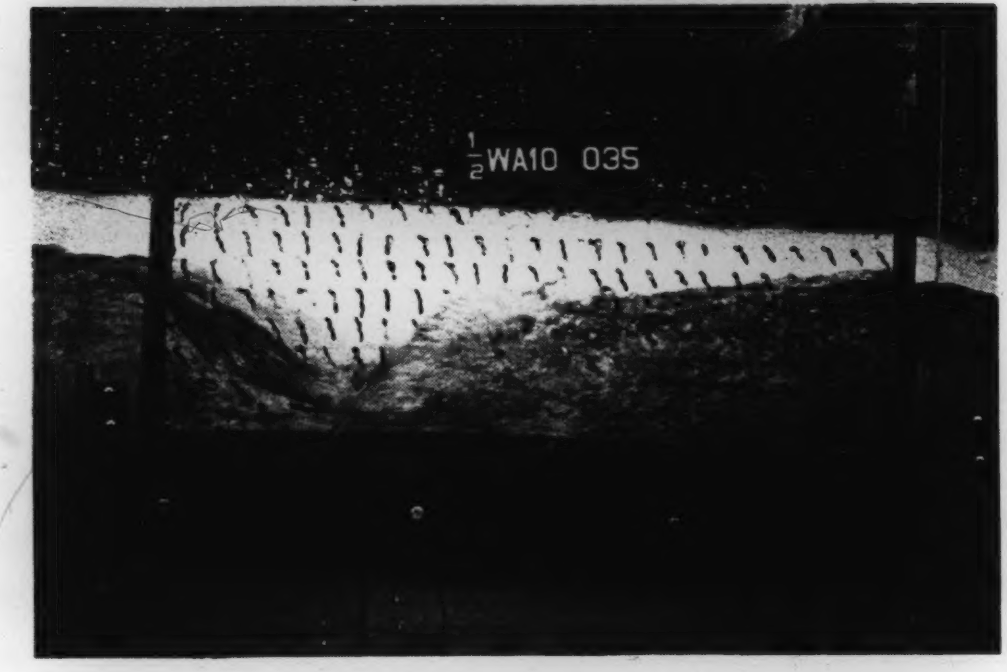

PLATE 20 Velocity Measurements: Plunging Flow - 1/2WA10-035

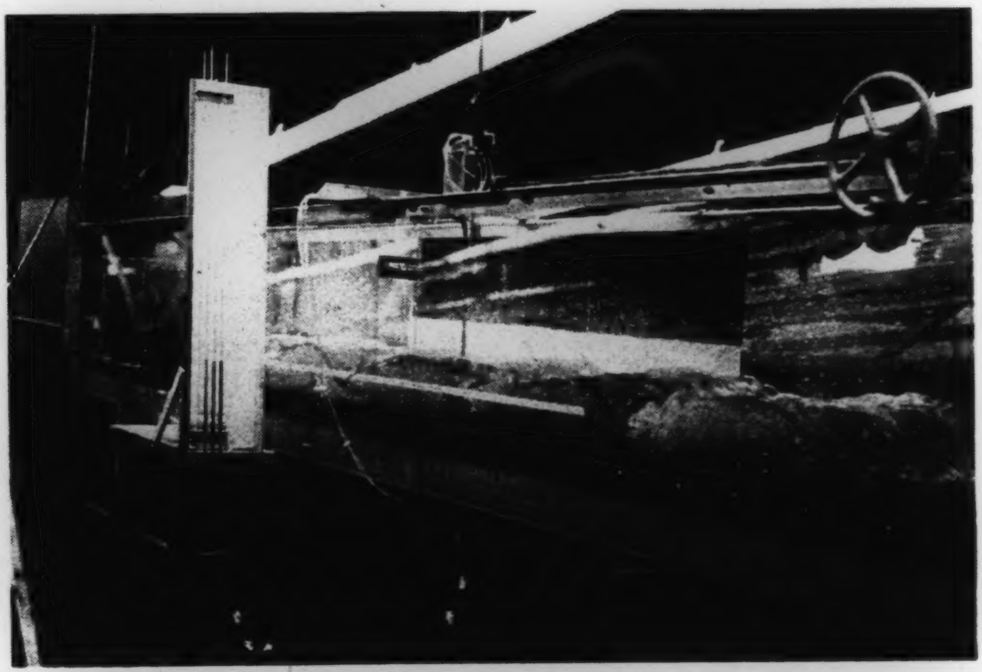

PLATE 21 Velocity Measurements: Plunging Flow - 1/2WA10-035

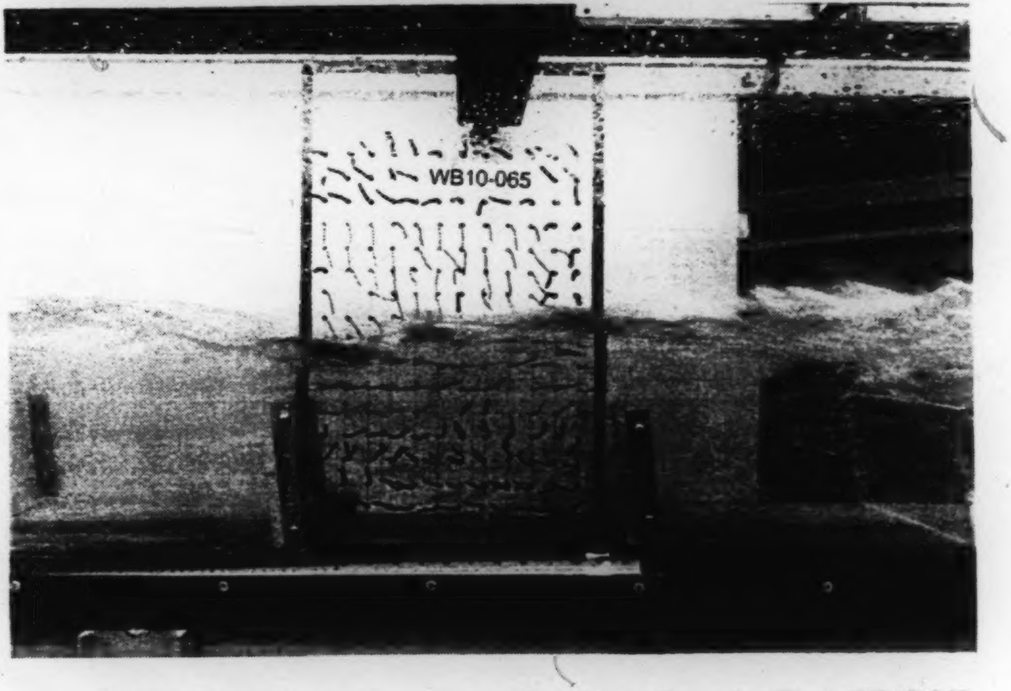

PLATE 22 Velocity Measurements: Transitional Streaming Flow - WB10-065

PLATE 23 Transverse Wave - WD15-001

PLATE 24 Longitudinal Surge - 1/2WB10-035

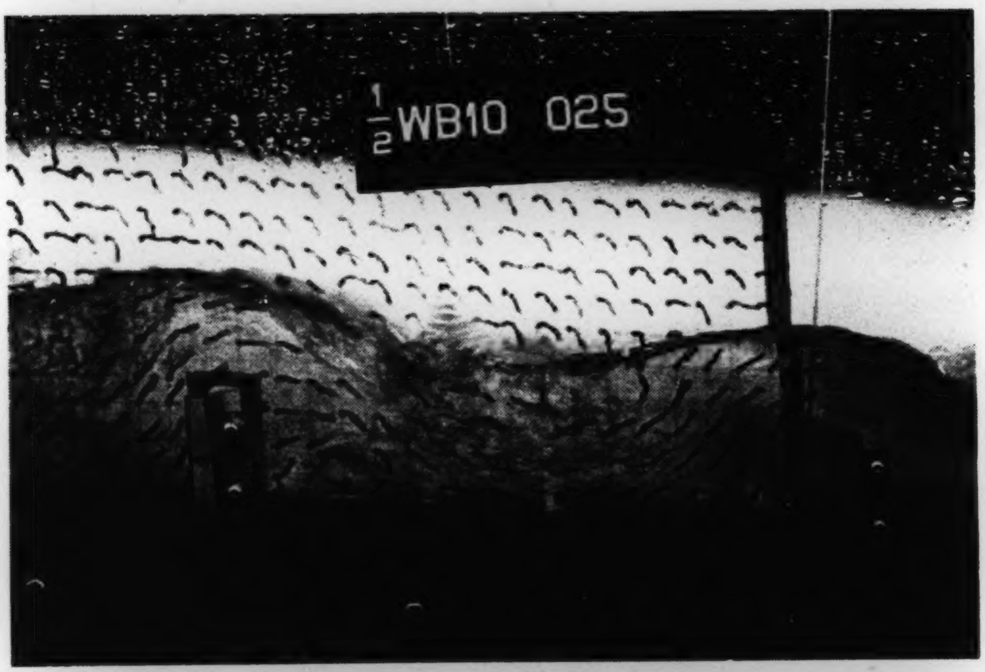

PLATE 25 Longitudinal Surge, Onset - 1/2WB10-025

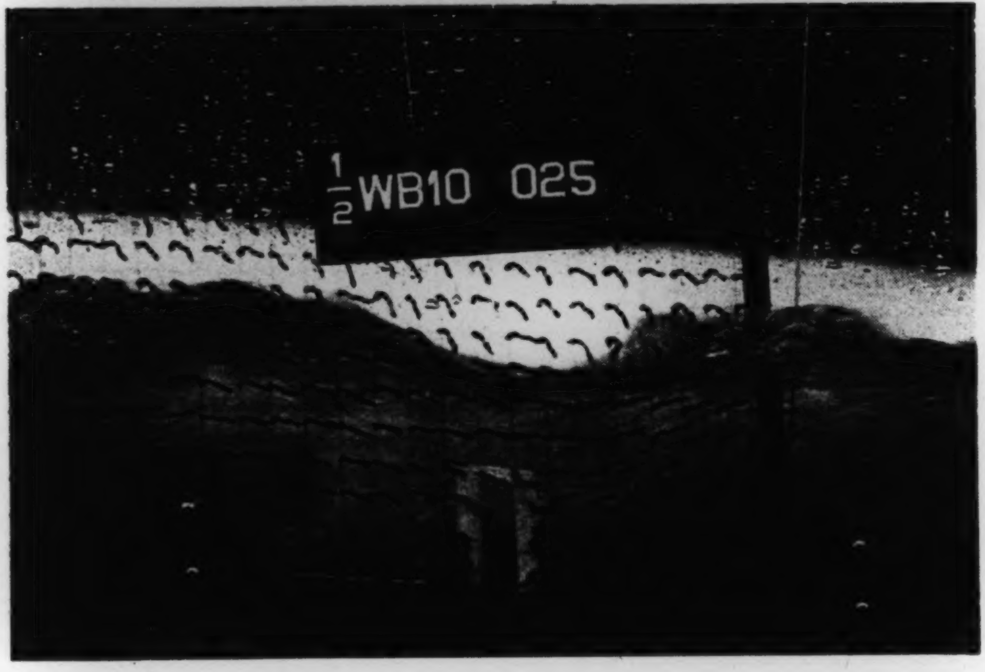

PLATE 26 Longitudinal Surge, Main Body - 1/2WB10-025

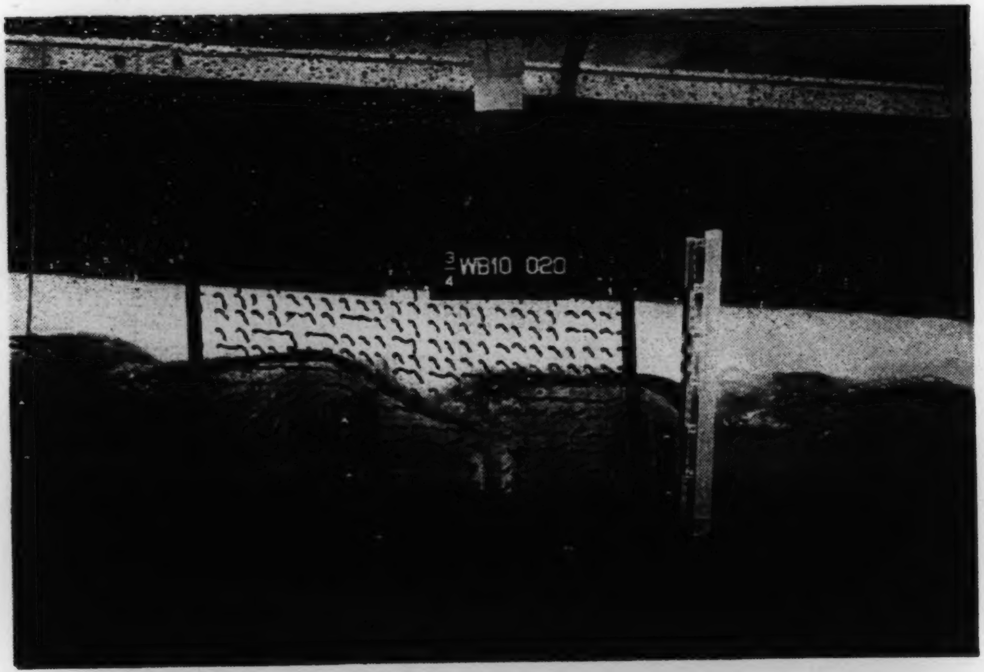

PLATE 27 Longitudinal Surge, Onset - 3/4WB10-020

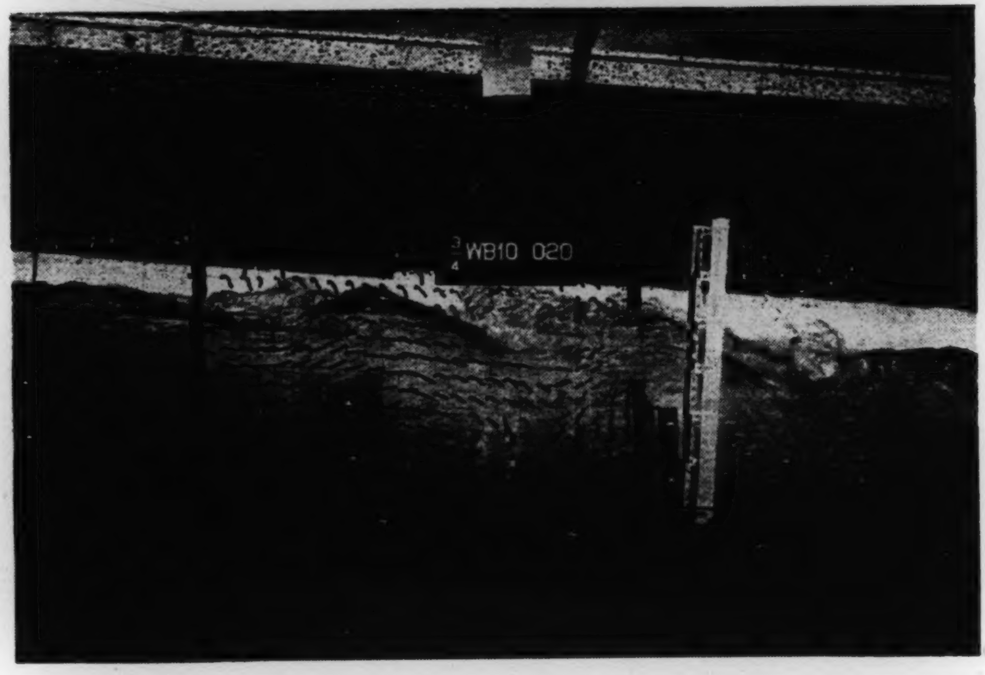

PLATE 28 Longitudinal Surge, Main Body - 3/4WB10-020

REFERENCES

Aaserude, R. and Orsborn, J.F., (1986). " ***Results of laboratory and Field Research on new concepts in Weir and Pool Fishways, Part 2 of Development of new concepts in Fishladder Design***", Albrook Hydraulics Laboratory, Washington State University, Pullman, Washington, USA

Ahmed, F., (1995). " ***Flow and Erosion Around Bridge Piers***", Ph.D. Thesis, Department of Civil Engineering, Water Resources Engineering, University of Alberta, Edmonton, Alberta, Canada

Clay, C.H., (1961). "***Design of fishways and other fish Facilities***", Department of Fisheries of Canada, Queen's Printer, Ottawa, Canada

Chamani, M.R. and Rajaratnam, N., (1996). "***An Experimental Study on Skimming Flow Over Stepped Spillways in the Developed Region***", Department of Civil Engineering, Water Resources Engineering, University of Alberta, Edmonton, Alberta, Canada

Collins, N.H. and Gillis, G.I., (1985). "***Upstream Fish Passage***", Canadian Electrical Association, Research and Development, 157 G 340

Dept. of Physics (1982)"***Error Analysis***", Undergraduate Physics Laboratory Manual, University of Alberta, Department of Physics, Edmonton, Alberta, Canada

Henderson, F. M., (1966) "***Open Channel Flow***", The Macmillian Company, New York Collier-Macmillian Canada Limited, Toronto, Ontario

Kandaswamy, P.K. and Rouse, H., (1957). "***Characteristics of Flow Over Terminal Weirs and Sills***", Proceedings of the American Society of Civil Engineers, Journal of the Hydraulics Division, vol. 83, No. Hy 4, 1-13

Katopodis, C., (1981). "***Considerations in the Design of Fishways for Freshwater Species***", 5 th Canadian Hydrotechnical Conference, Fredericton, New Brunswick, Canada, 857-878

Katopodis, C., (1990). "***Advancing the Art of Engineering Fishways for Upstream Migrants***", Proceedings of the International Symposium on Fishways '90 in Gifu, Japan, October, 19-28

Kline, S. L. and Mc Clintock, F.A., (1953) "***Describing Uncertainties in Single-Sample Experiments***", Mechanical Engineering, ASME, vol. 75, 3-8

Laksmana Rao, N. S., (1975). "***Theory of Weirs***", Advances in hydroscience, vol. 10, V.T. Chow, ed., Academic Press, New York, N.Y., 309-406

McKay, K and Sikora, G., (1994) "***Velocity Measurements in Pool and Weir Fishways***", Unpublished Technical Report, Department of Civil Engineering, University of Alberta, Edmonton, Alberta, Canada

REFERENCES (continued)

Orsborn, J.F., (1986). ***"Final Project Report, Part 1 of Development of New Concepts in Fishladder Design"***, Albrook Hydraulics Laboratory, Washington State University, Pullman, Washington, USA

Potter, M. and Wiggert, D., (1991). ***"Mechanics of Fluids"***, Prentice-Hall Inc. A Division of Simon and Schuster, Englewood Cliffs, New Jersey 07632 ISBN 0-13-572793-6

Powers, P. and Orsborn, J.F., (1986a). ***"Fishways - An Assessment of Their Development and Design, Part 3 of Development of new concepts in Fishladder Design"***, Albrook Hydraulics Laboratory, Washington State University, Pullman, Washington, USA

Powers, P. and Orsborn, J.F., (1986b). ***"Analysis of Barriers to Upstream Passage, Part 4 of Development of New Concepts in Fishladder Design"***, Albrook Hydraulics Laboratory, Washington State University, Pullman, Washington, USA

Rajaratnam, N., Katopodis, C. and Mainali, A., (1987a) ***"Pool and Weir Fishways"***, Report WRE 87-1, Department of Civil Engineering, University of Alberta, Edmonton, Alberta, Canada

Rajaratnam, N., Katopodis, C. and Mainali, A., (1987b) ***"Plunging and Streaming Flows in Pool and Weir Fishways"***, Journal of Hydraulic Engineering, vol. 114, No. 8, August 939-944

Rajaratnam, N., Katopodis, C. and Tovell, D., (1994) ***"An Investigation of Pool and Weir Fishways"***, Technical Report [94-R], Department of Civil Engineering, University of Alberta, Edmonton, Alberta, Canada

Rajaratnam, N., and Muralidar, D., (1967). ***"Yaw and Pitch Probes"***, Department of Civil Engineering, University of Alberta, Edmonton, Alberta, Canada

Sikora, G., Rajaratnam, N. and Katopodis, C., (1996) ***"A Photographic Study of Pool and Weir Fishways"***, Technical Report [August 1996-SRK1], Department of Civil Engineering, University of Alberta, Edmonton, Alberta, Canada

Surya Rao, S and Shukla, M.K., (1971)***"Characteristics of Flow Over Weirs of Finite Crest Widths"***, Journal of the Hydraulic Division, Proceedings of the American Society of Civil Engineers, vol. 97, No.Hy11, Proc. Paper 8515, November 1807-1816

APPENDIX A

Water Surface Profiles

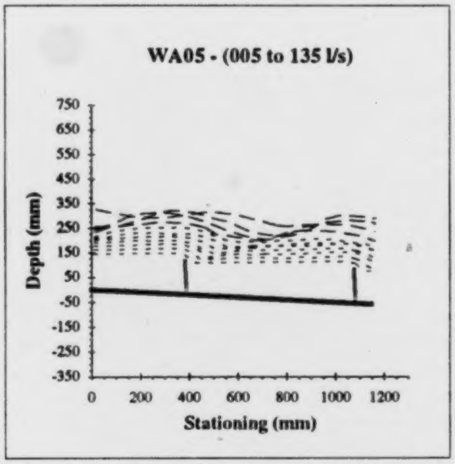
WA05 - (005 to 135 l/s)

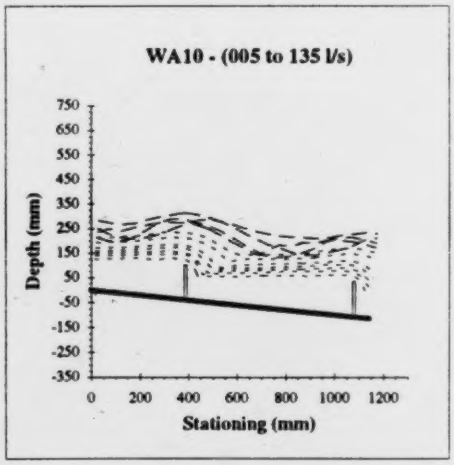
WA10 - (005 to 135 l/s)

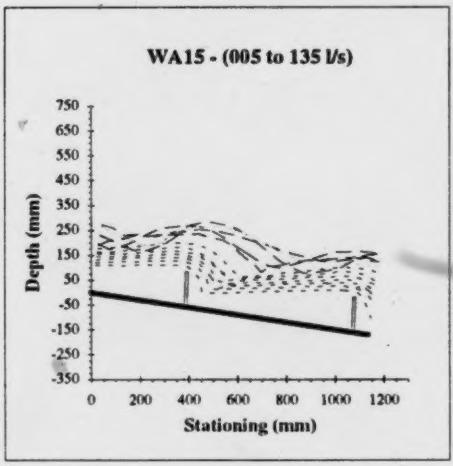
WA15 - (005 to 135 l/s)

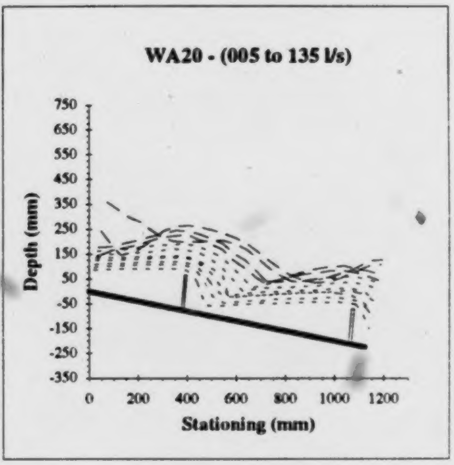
WA20 - (005 to 135 l/s)

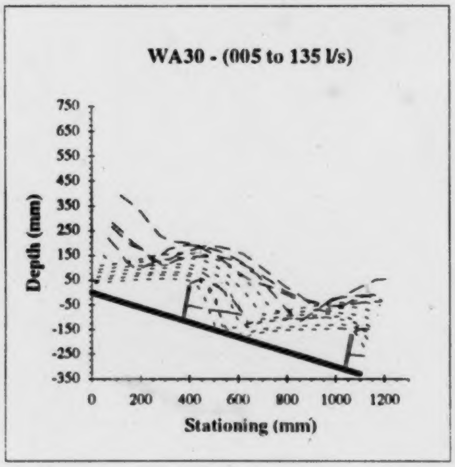
WA30 - (005 to 135 l/s)

Water Surface Profiles

Full Weir Height

Class 'A' Weir Spacing

5 to 30 % Slope, 5 to 135 l/s

WA05 - (005 to 135 l/s)

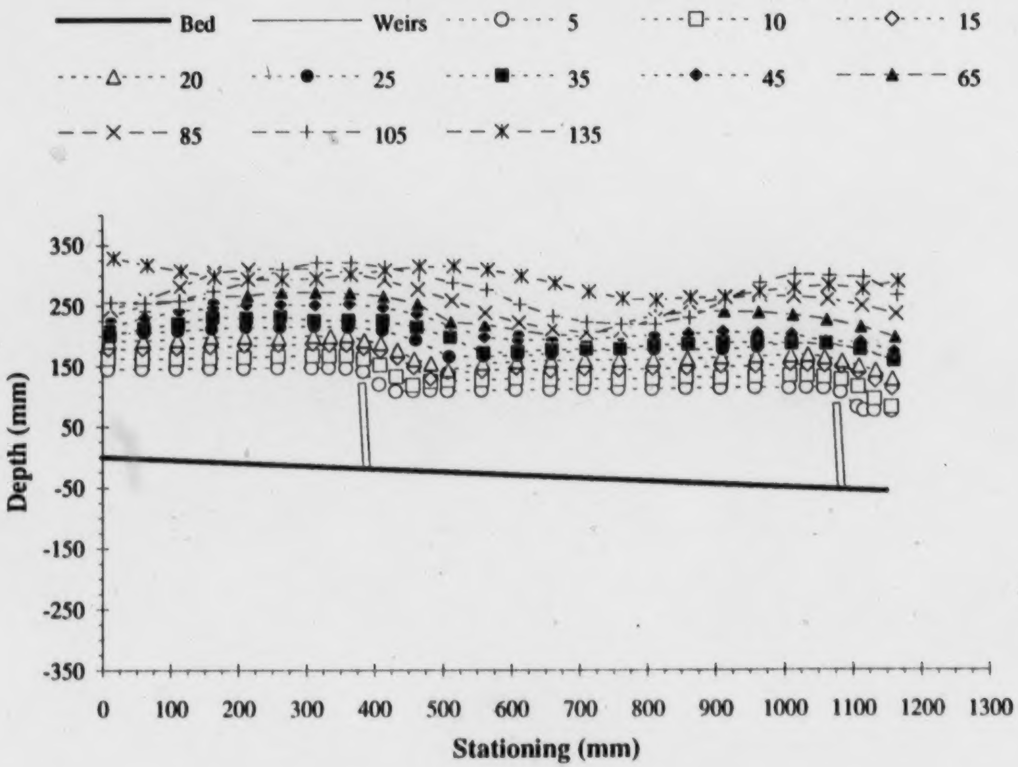

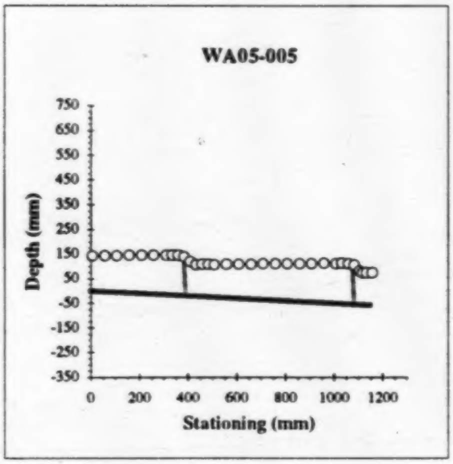
WA05-005
Depth (mm)
750
650
550
450
350
250
150
50
-50
-150
-250
-350
0
200
400
600
800
1000
1200
Stationing (mm)

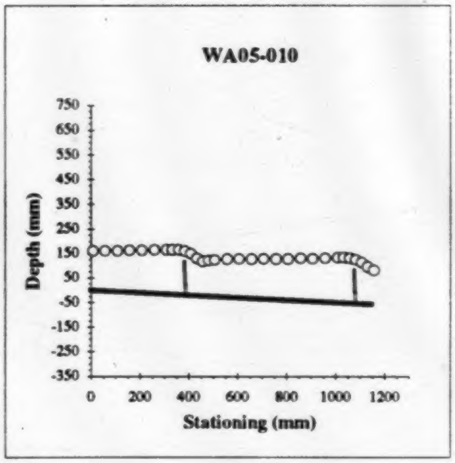
WA05-010
Depth (mm)
750
650
550
450
350
250
150
50
-50
-150
-250
-350
0
200
400
600
800
1000
1200
Stationing (mm)

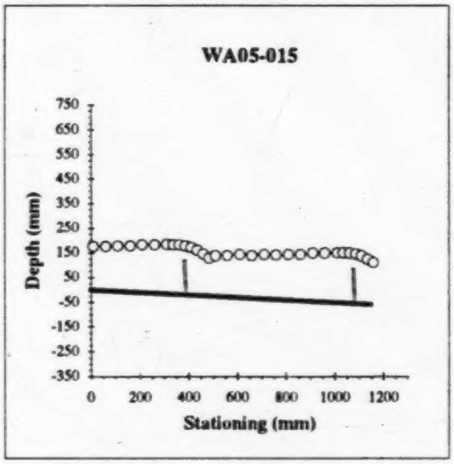
WA05-015
Depth (mm)
750
650
550
450
350
250
150
50
-50
-150
-250
-350
0
200
400
600
800
1000
1200
Stationing (mm)

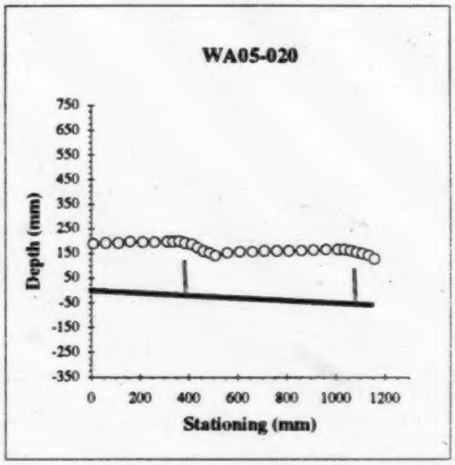
WA05-020
Depth (mm)
750
650
550
450
350
250
150
50
-50
-150
-250
-350
0
200
400
600
800
1000
1200
Stationing (mm)

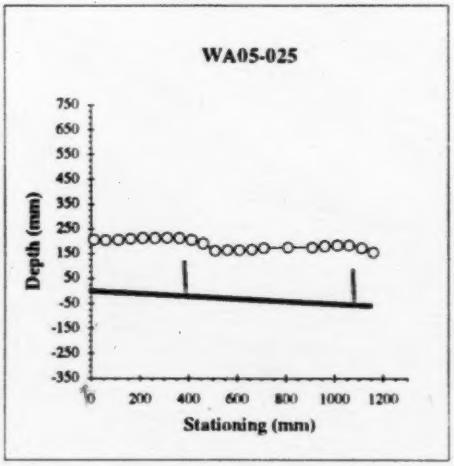
WA05-025
Depth (mm)
750
650
550
450
350
250
150
50
-50
-150
-250
-350
0
200
400
600
800
1000
1200
Stationing (mm)

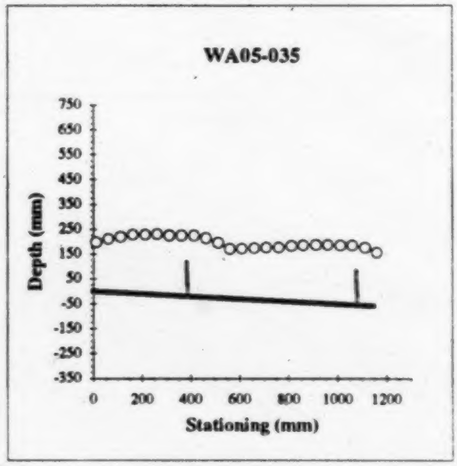
WA05-035
Depth (mm)
750
650
550
450
350
250
150
50
-50
-150
-250
-350
0
200
400
600
800
1000
1200
Stationing (mm)

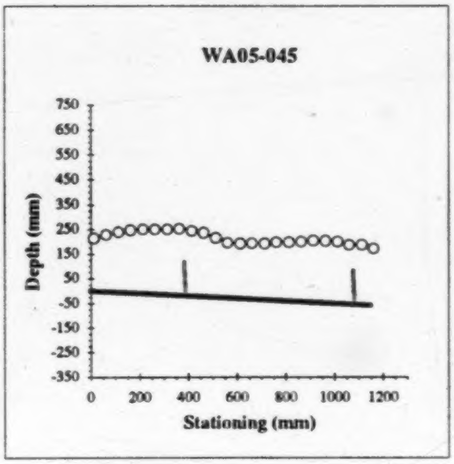
WA05-045

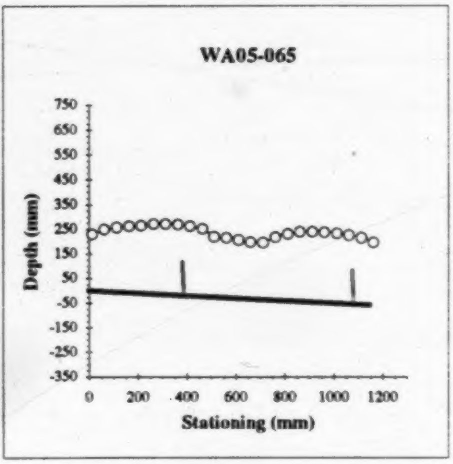
WA05-065

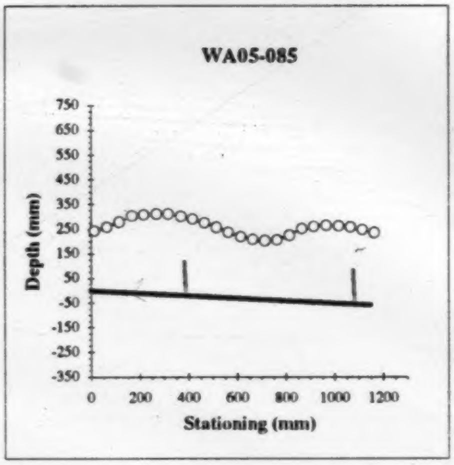
WA05-085

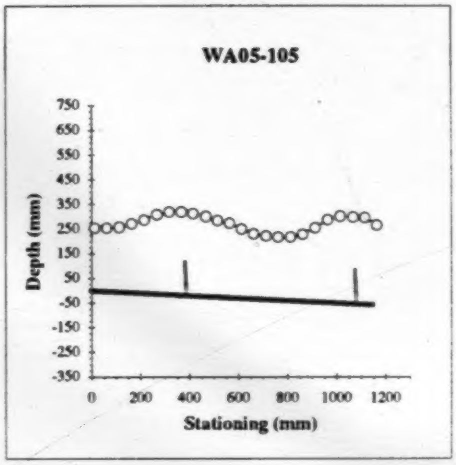
WA05-105

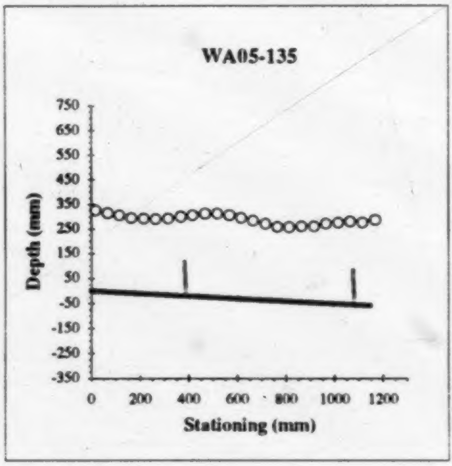
WA05-135

WA10 - (005 to 135 l/s)

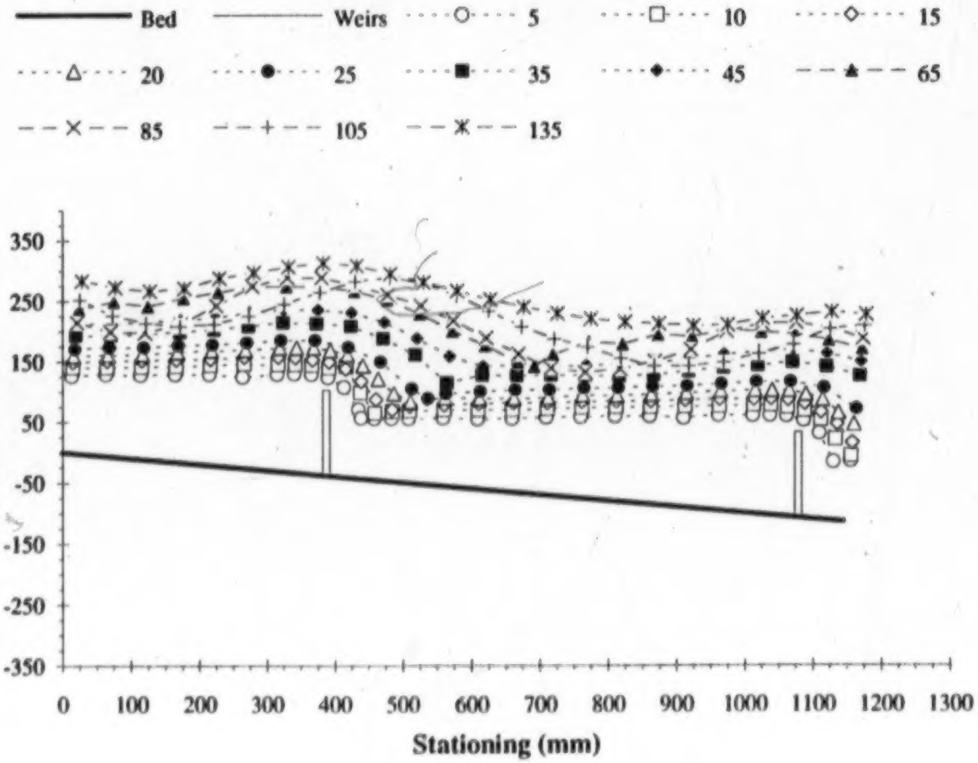

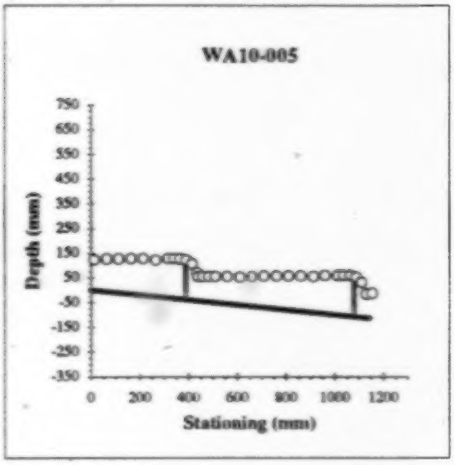
WA10-005
Depth (mm)
750
650
550
450
350
250
150
50
-50
-150
-250
-350
0
200
400
600
800
1000
1200
Stationing (mm)

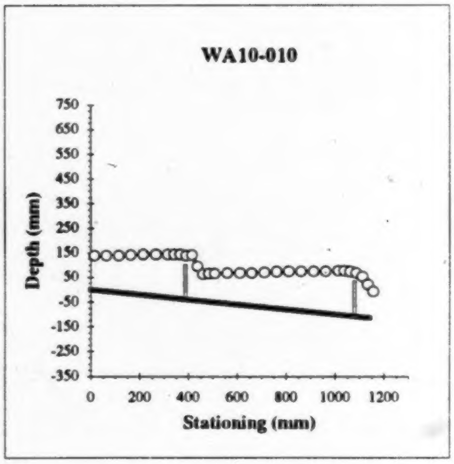
WA10-010
Depth (mm)
750
650
550
450
350
250
150
50
-50
-150
-250
-350
0
200
400
600
800
1000
1200
Stationing (mm)

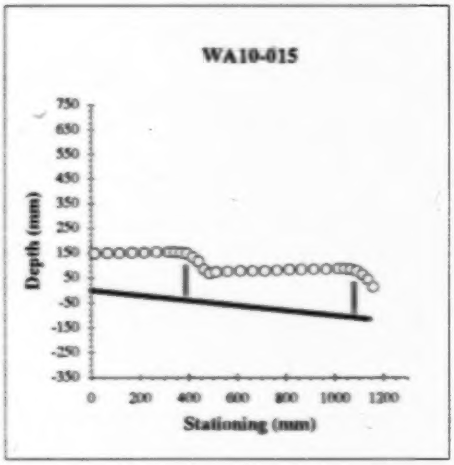
WA10-015
Depth (mm)
750
650
550
450
350
250
150
50
-50
-150
-250
-350
0
200
400
600
800
1000
1200
Stationing (mm)

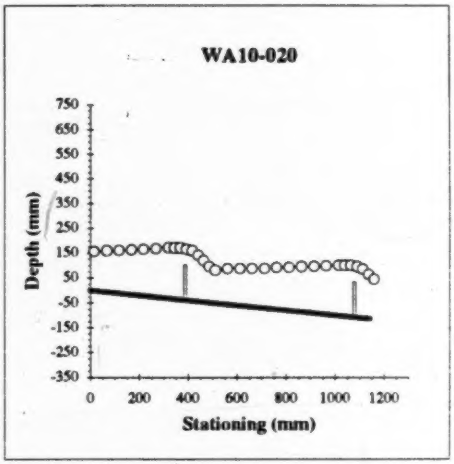
WA10-020
Depth (mm)
750
650
550
450
350
250
150
50
-50
-150
-250
-350
0
200
400
600
800
1000
1200
Stationing (mm)

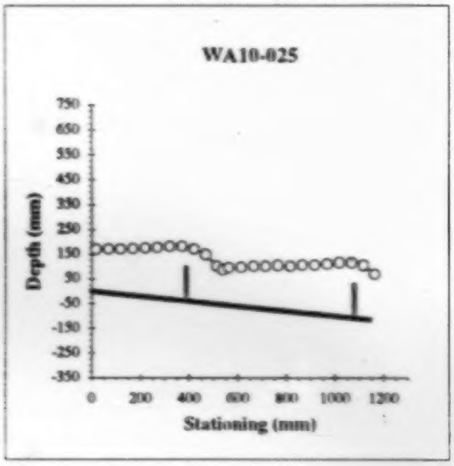
WA10-025
Depth (mm)
750
650
550
450
350
250
150
50
-50
-150
-250
-350
0
200
400
600
800
1000
1200
Stationing (mm)

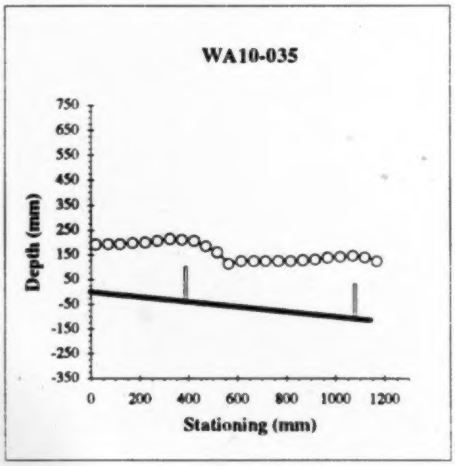
WA10-035
Depth (mm)
750
650
550
450
350
250
150
50
-50
-150
-250
-350
0
200
400
600
800
1000
1200
Stationing (mm)

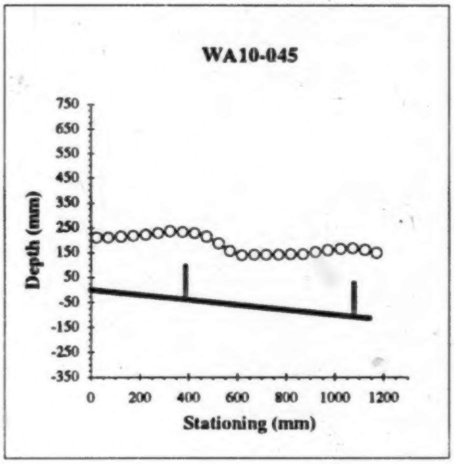
WA10-045

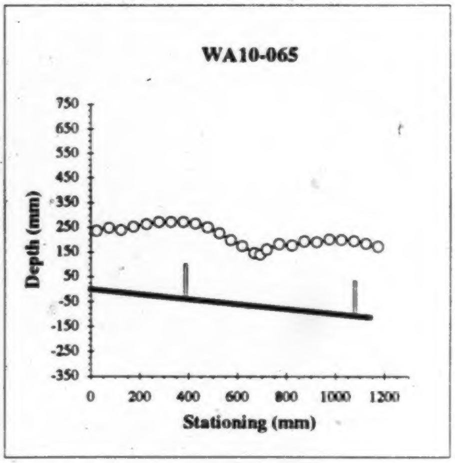
WA10-065

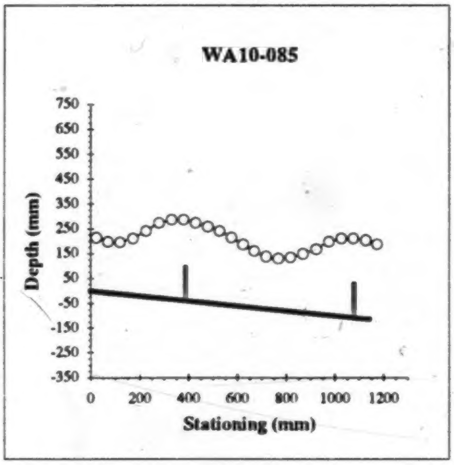
WA10-085

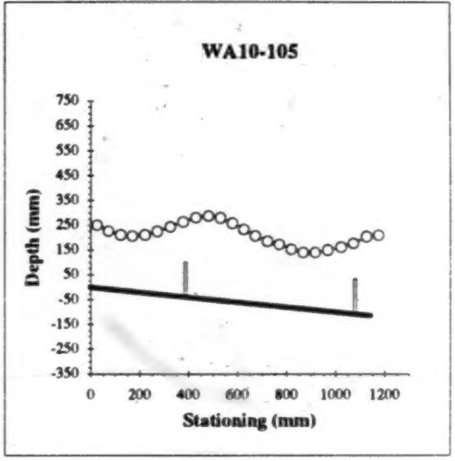
WA10-105

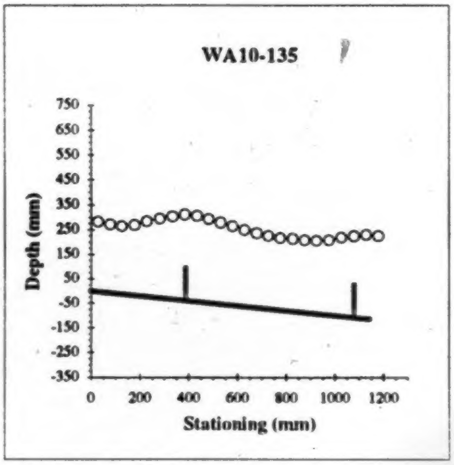
WA10-135

WA15 - (005 to 135 l/s)

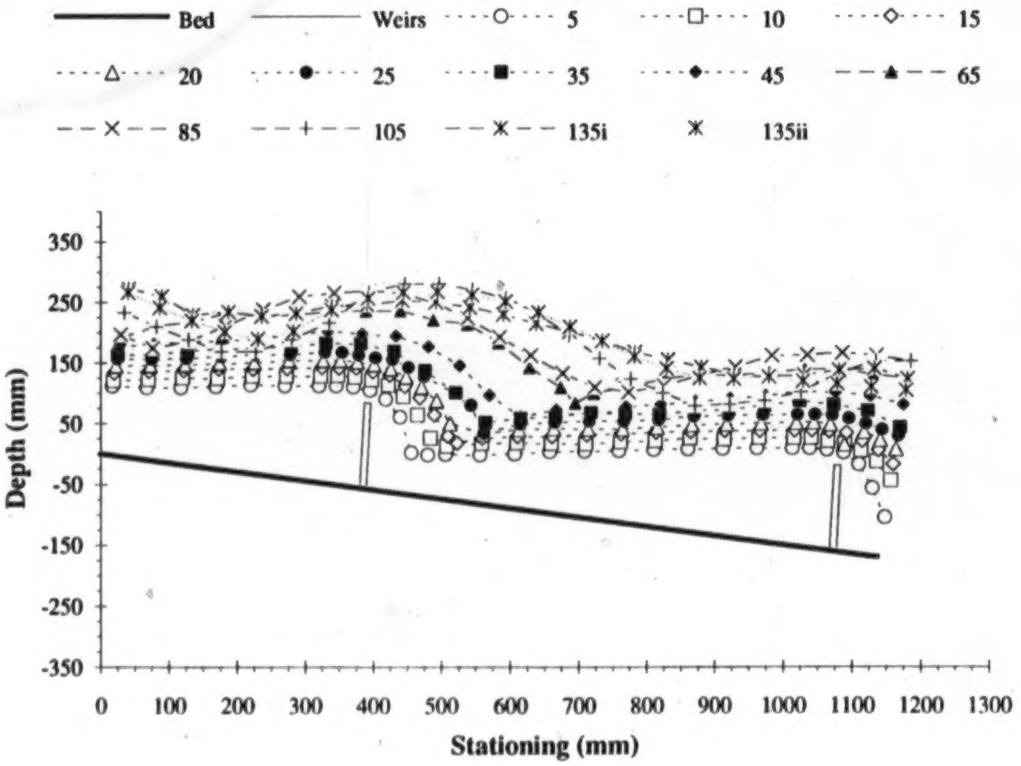

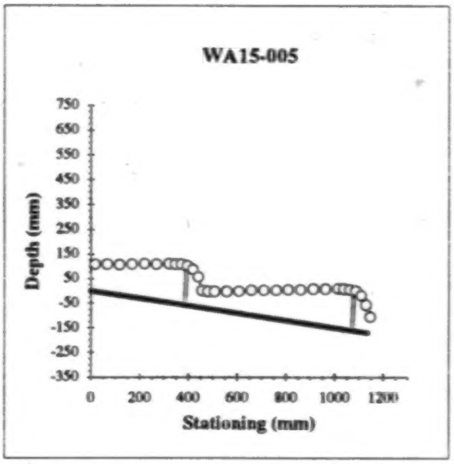
WA15-005
Depth (mm)
750
650
550
450
350
250
150
50
-50
-150
-250
-350
0
200
400
600
800
1000
1200
Stationing (mm)

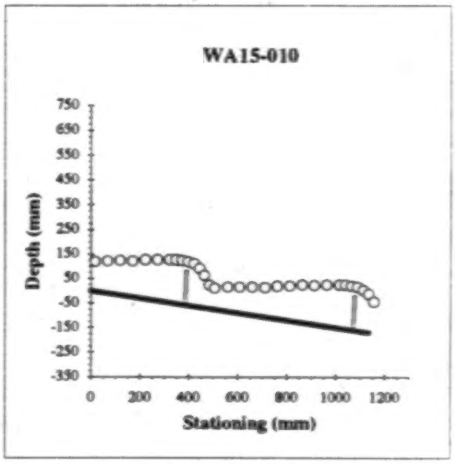
WA15-010
Depth (mm)
750
650
550
450
350
250
150
50
-50
-150
-250
-350
0
200
400
600
800
1000
1200
Stationing (mm)

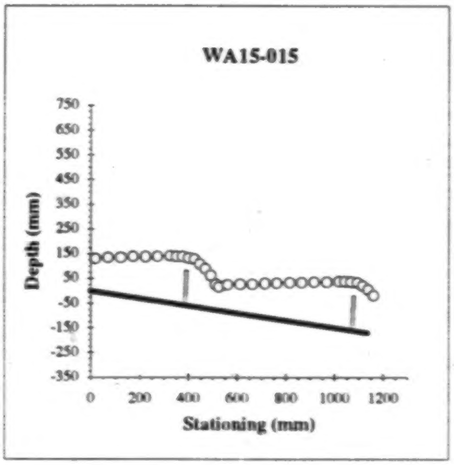
WA15-015
Depth (mm)
750
650
550
450
350
250
150
50
-50
-150
-250
-350
0
200
400
600
800
1000
1200
Stationing (mm)

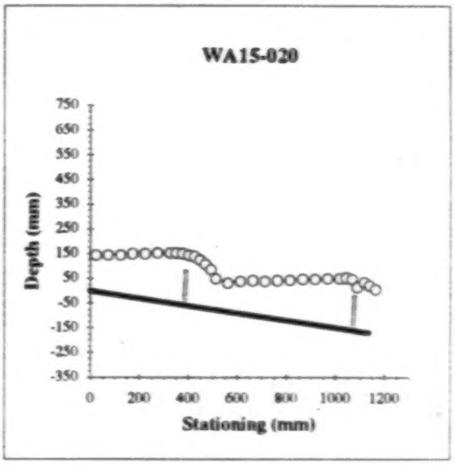
WA15-020
Depth (mm)
750
650
550
450
350
250
150
50
-50
-150
-250
-350
0
200
400
600
800
1000
1200
Stationing (mm)

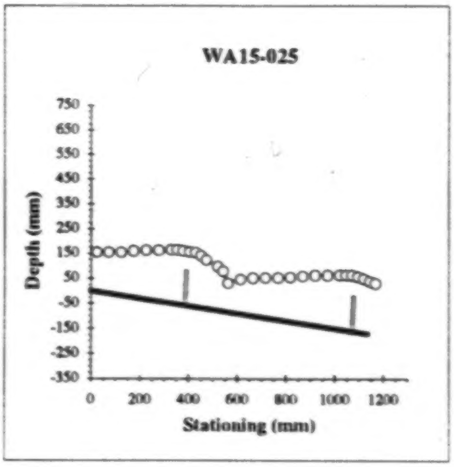
WA15-025
Depth (mm)
750
650
550
450
350
250
150
50
-50
-150
-250
-350
0
200
400
600
800
1000
1200
Stationing (mm)

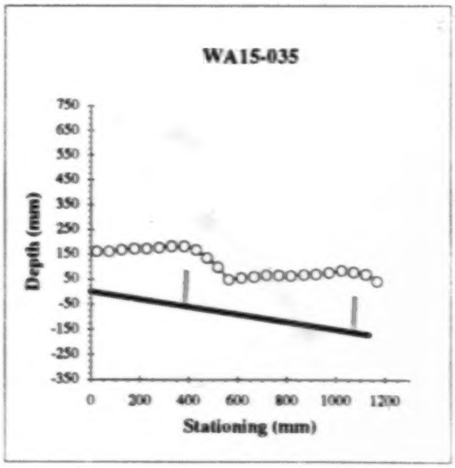
WA15-035
Depth (mm)
750
650
550
450
350
250
150
50
-50
-150
-250
-350
0
200
400
600
800
1000
1200
Stationing (mm)

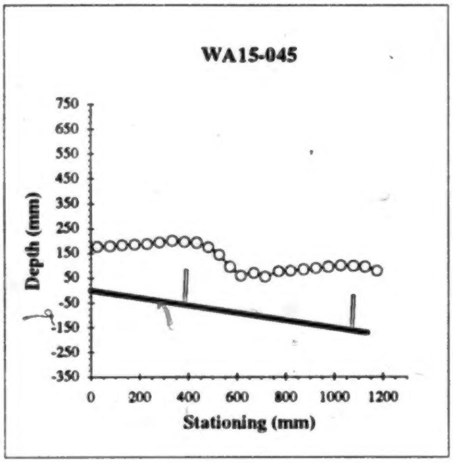
WA15-045

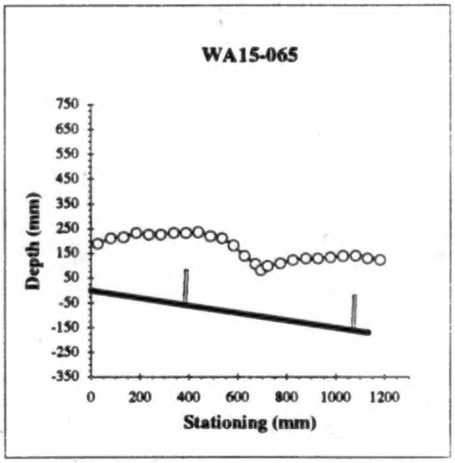
WA15-065

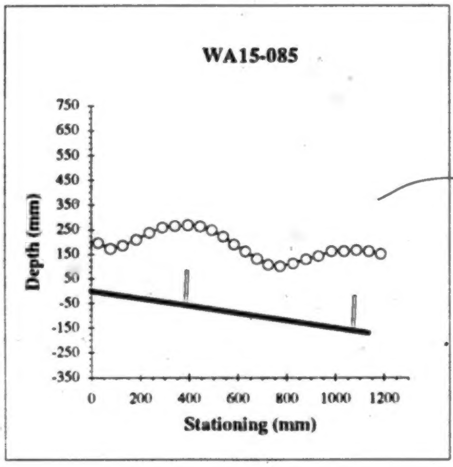
WA15-085

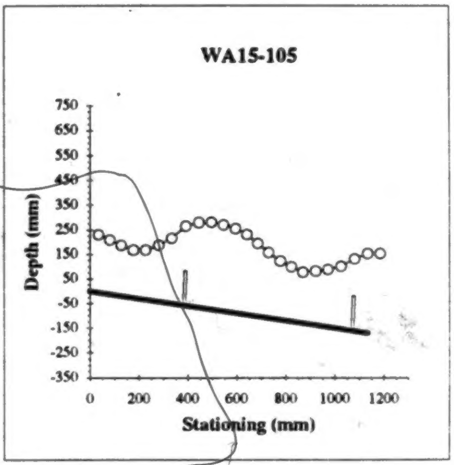
WA15-105

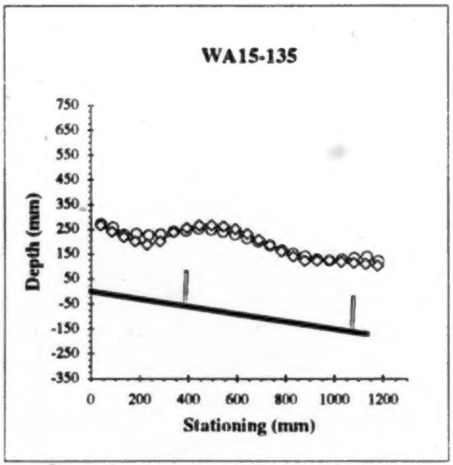
WA15-135

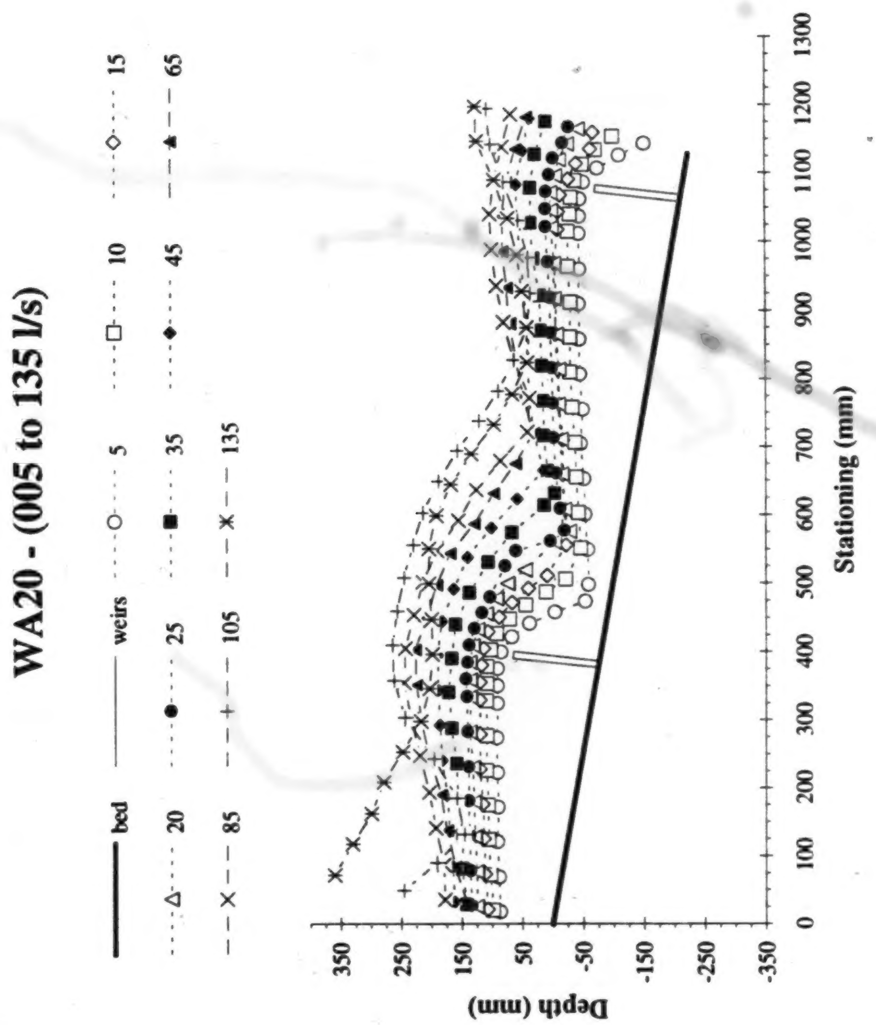
WA20 - (005 to 135 l/s)
bed
weirs
5
10
15
20
25
35
45
65
85
105
135
Depth (mm)
350
250
150
50
-50
-150
-250
-350
Stationing (mm)
0
100
200
300
400
500
600
700
800
900
1000
1100
1200
1300

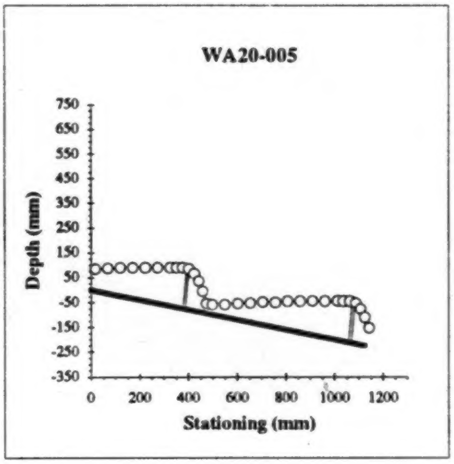
WA20-005
Depth (mm)
750
650
550
450
350
250
150
50
-50
-150
-250
-350
0
200
400
600
800
1000
1200
Stationing (mm)

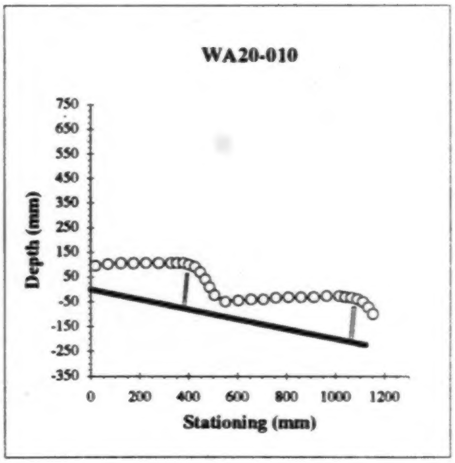
WA20-010
Depth (mm)
750
650
550
450
350
250
150
50
-50
-150
-250
-350
0
200
400
600
800
1000
1200
Stationing (mm)

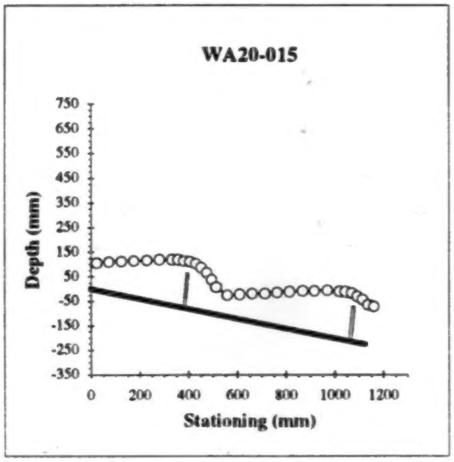
WA20-015
Depth (mm)
750
650
550
450
350
250
150
50
-50
-150
-250
-350
0
200
400
600
800
1000
1200
Stationing (mm)

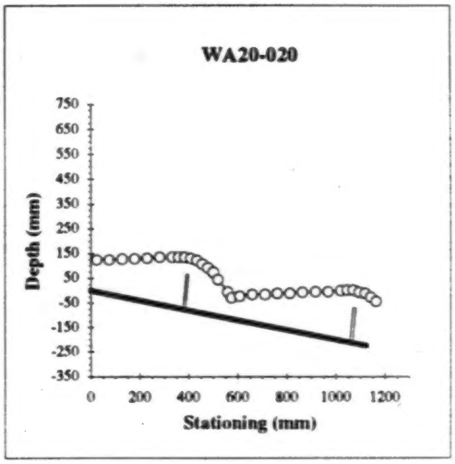
WA20-020
Depth (mm)
750
650
550
450
350
250
150
50
-50
-150
-250
-350
0
200
400
600
800
1000
1200
Stationing (mm)

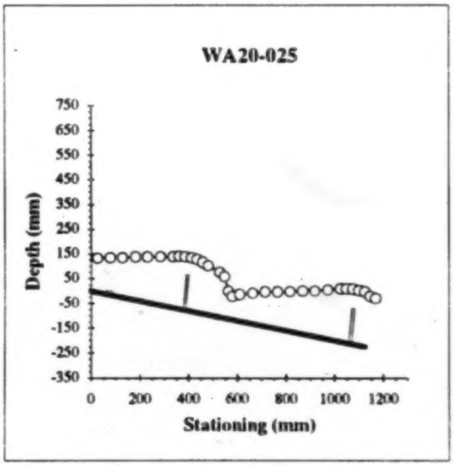
WA20-025
Depth (mm)
750
650
550
450
350
250
150
50
-50
-150
-250
-350
0
200
400
600
800
1000
1200
Stationing (mm)

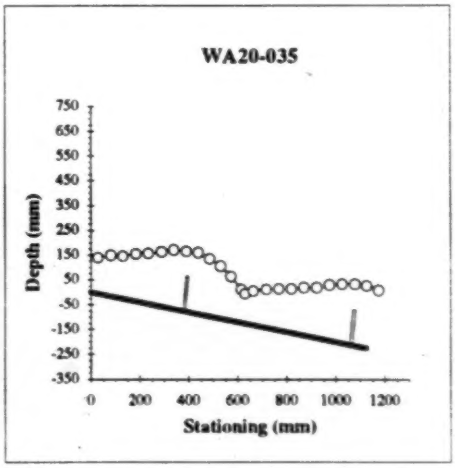
WA20-035
Depth (mm)
750
650
550
450
350
250
150
50
-50
-150
-250
-350
0
200
400
600
800
1000
1200
Stationing (mm)

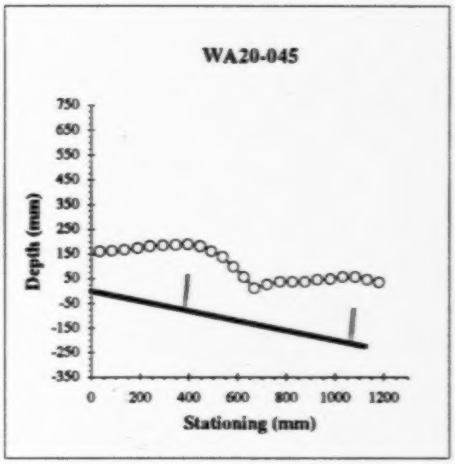
WA20-045
Depth (mm)
750
650
550
450
350
250
150
50
-50
-150
-250
-350
0
200
400
600
800
1000
1200
Stationing (mm)

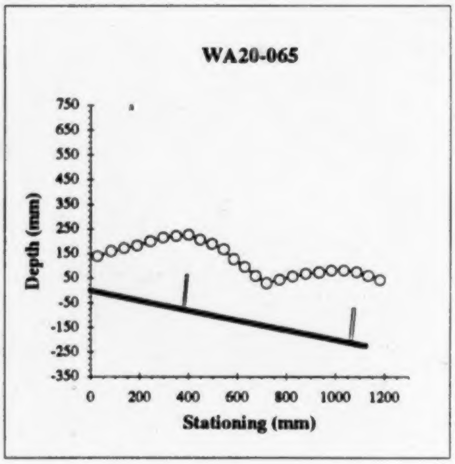
WA20-065
Depth (mm)
750
650
550
450
350
250
150
50
-50
-150
-250
-350
0
200
400
600
800
1000
1200
Stationing (mm)

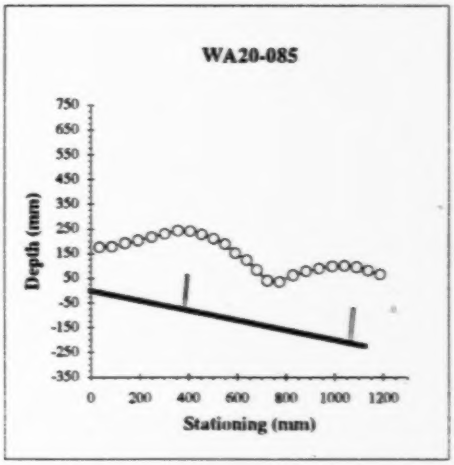
WA20-085
Depth (mm)
750
650
550
450
350
250
150
50
-50
-150
-250
-350
0
200
400
600
800
1000
1200
Stationing (mm)

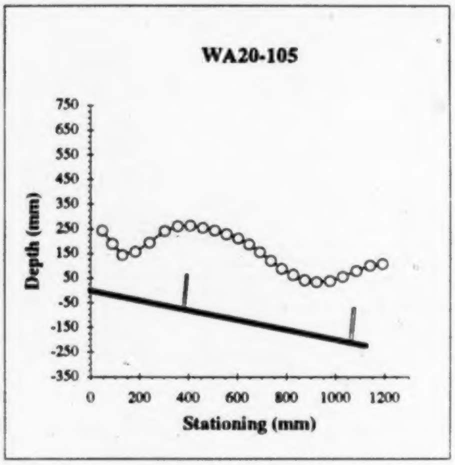
WA20-105
Depth (mm)
750
650
550
450
350
250
150
50
-50
-150
-250
-350
0
200
400
600
800
1000
1200
Stationing (mm)

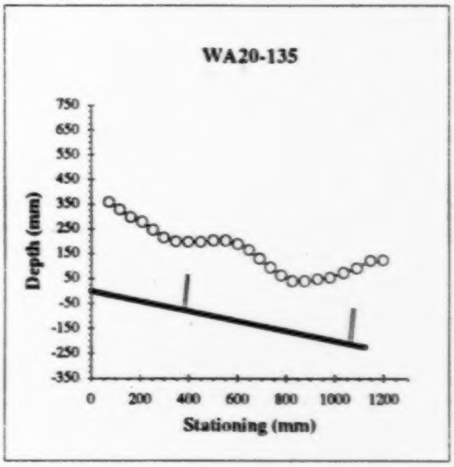
WA20-135
Depth (mm)
750
650
550
450
350
250
150
50
-50
-150
-250
-350
0
200
400
600
800
1000
1200
Stationing (mm)

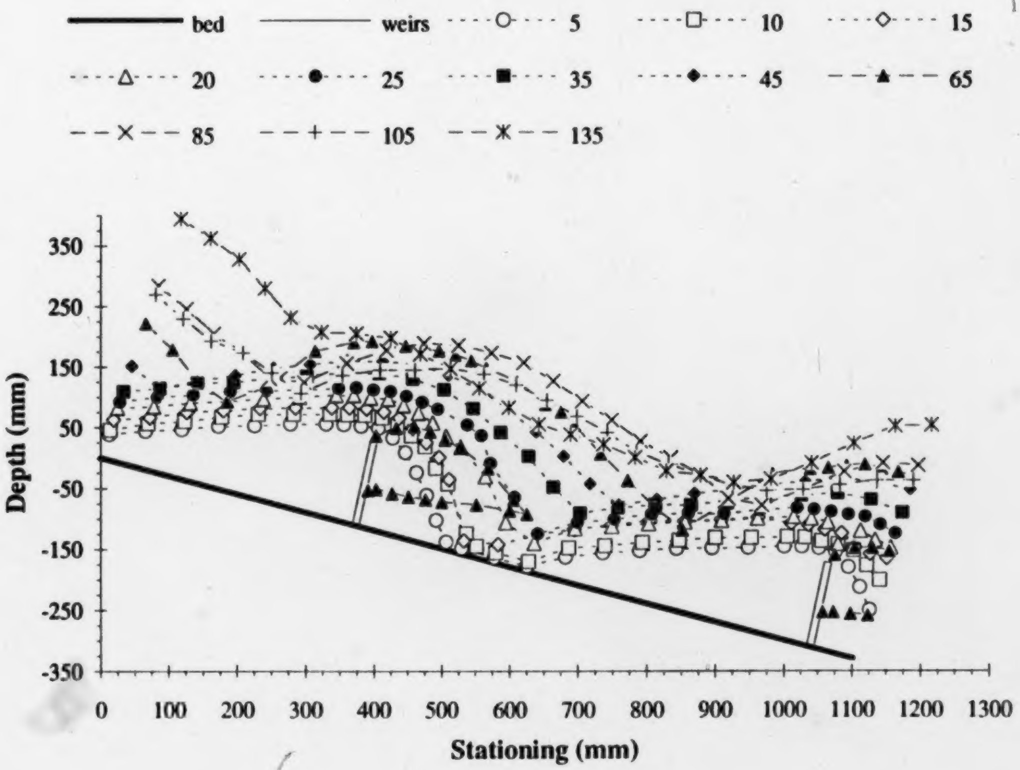
WA30 - (005 to 135 l/s)

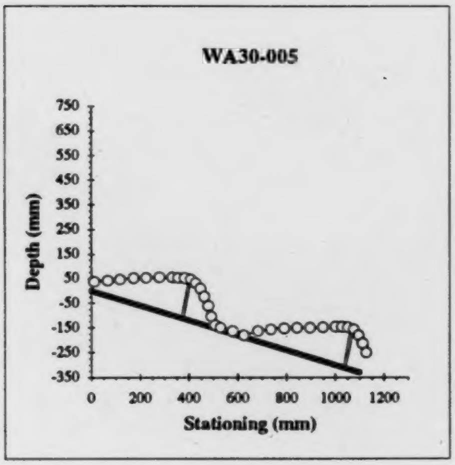
WA30-005

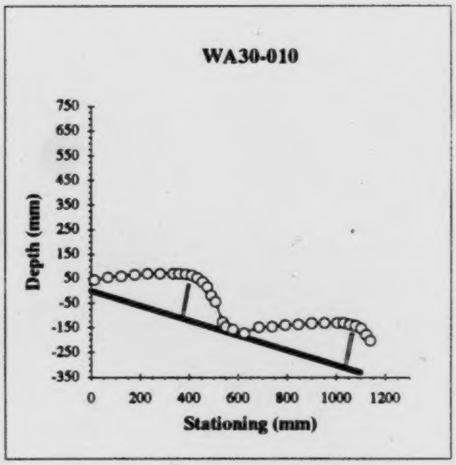
WA30-010

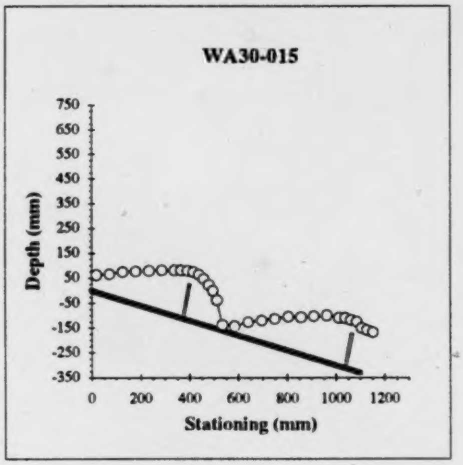
WA30-015

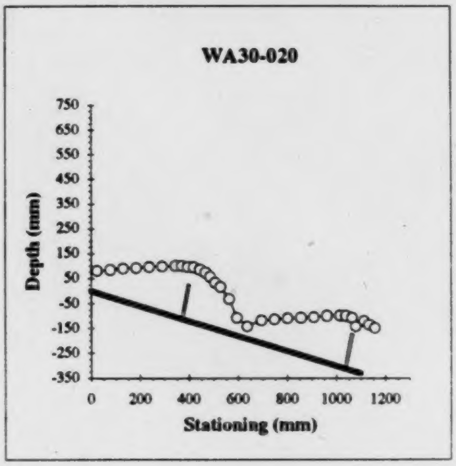
WA30-020

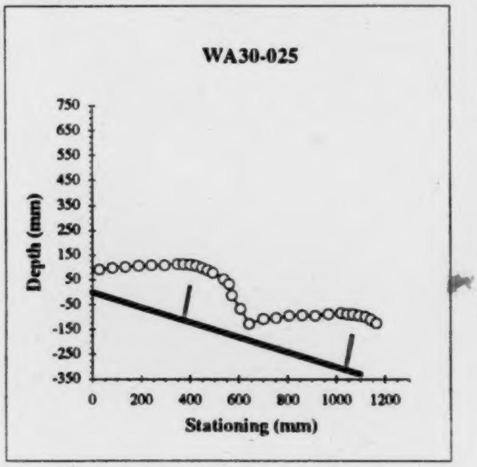
WA30-025

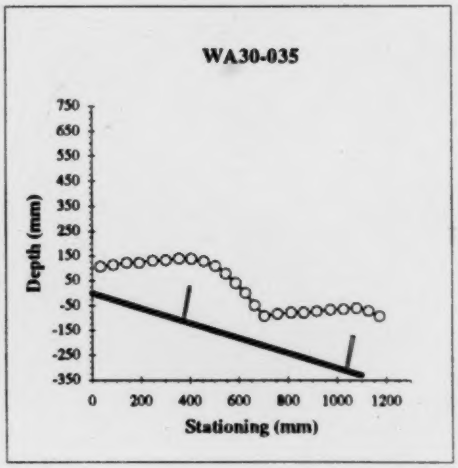
WA30-035

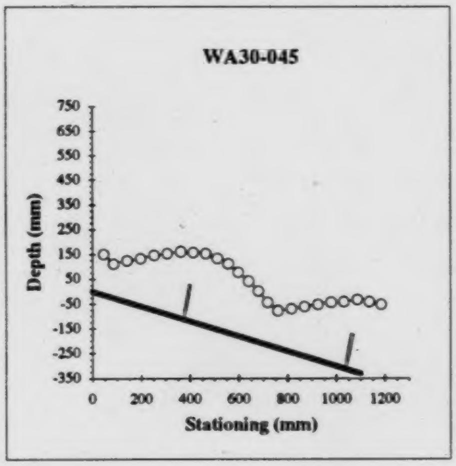
WA30-045

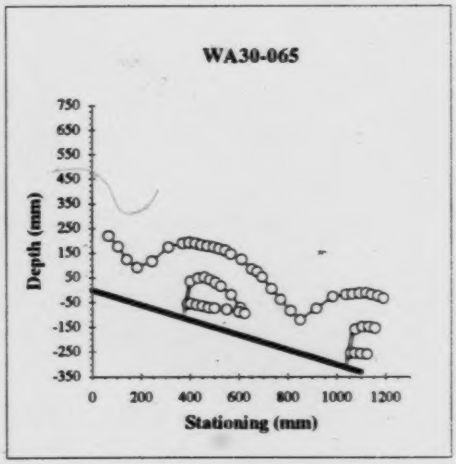
WA30-065

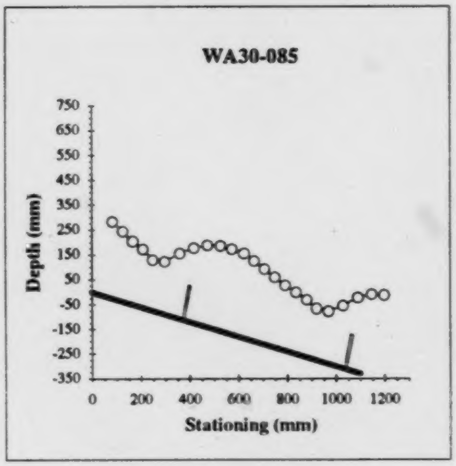
WA30-085

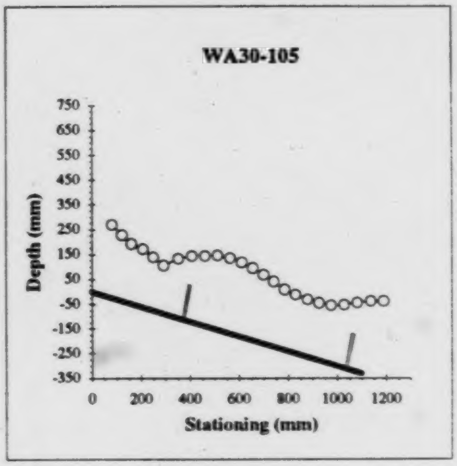
WA30-105

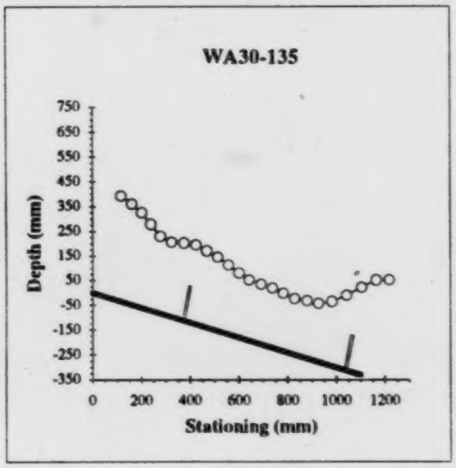
WA30-135

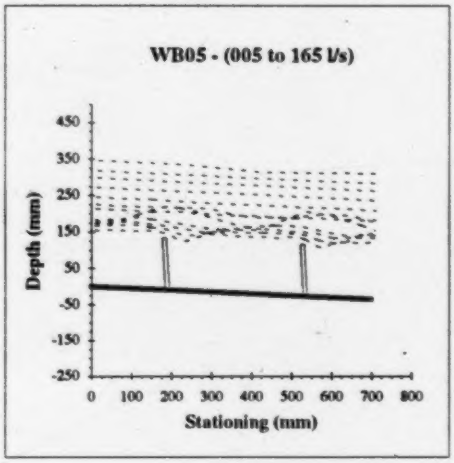

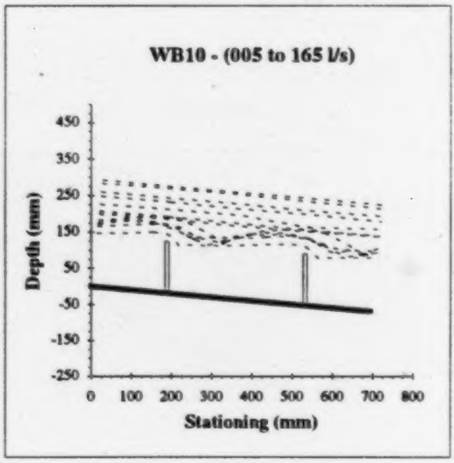

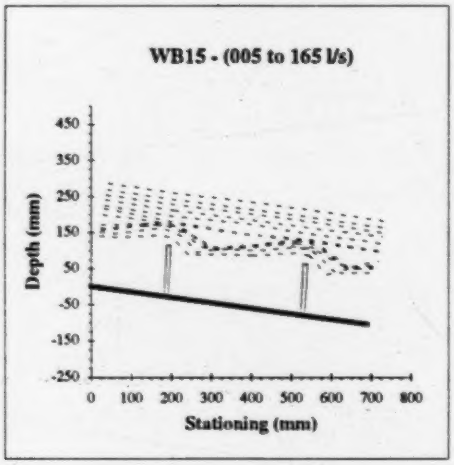

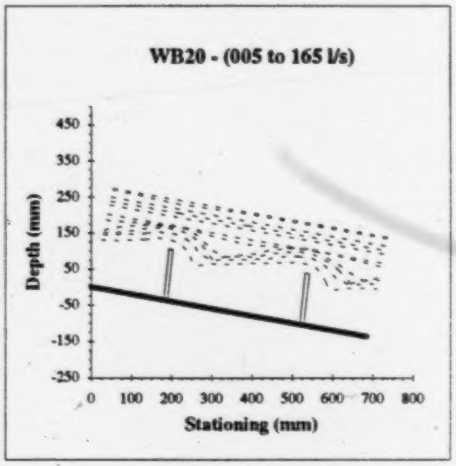

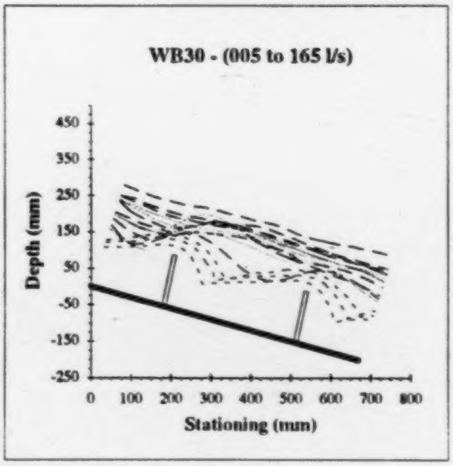

Water Surface Profiles

Full Weir Height

Class 'B' Weir Spacing

5 to 30 % Slope, 5 to 165 l/s

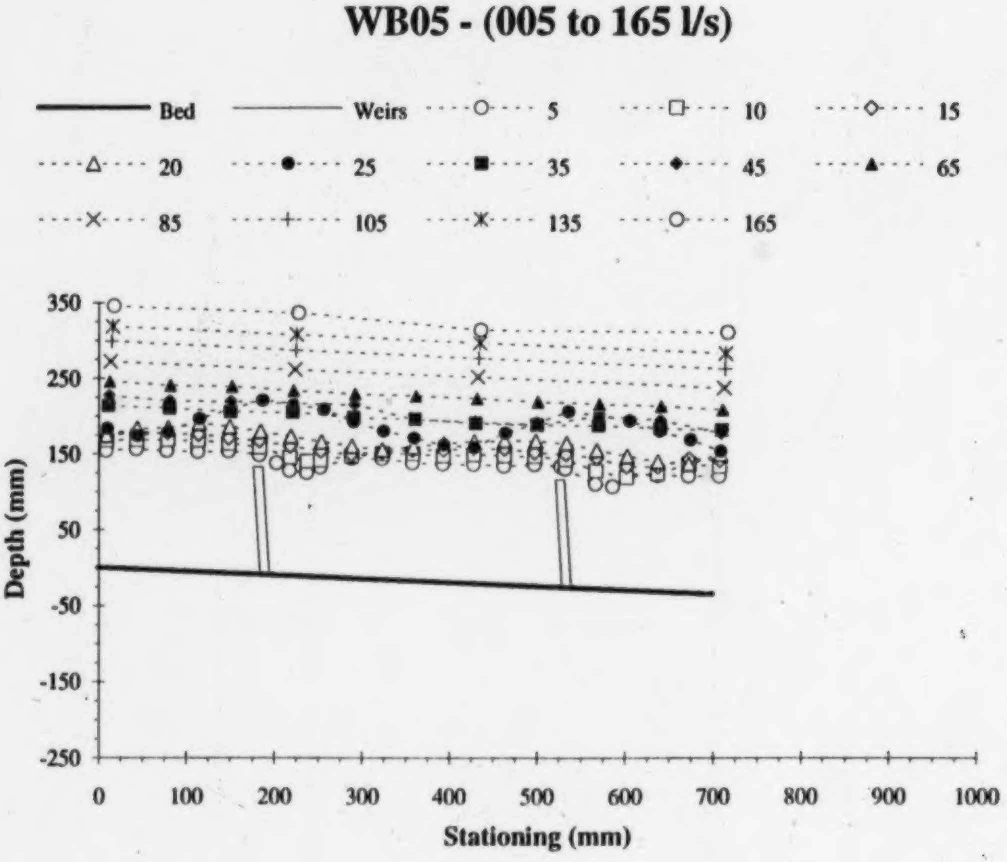
WB05 - (005 to 165 l/s)
Bed
Weirs
5
10
15
20
25
35
45
65
85
105
135
165
Depth (mm)
350
250
150
50
-50
-150
-250
0
100
200
300
400
500
600
700
800
900
1000
Stationing (mm)

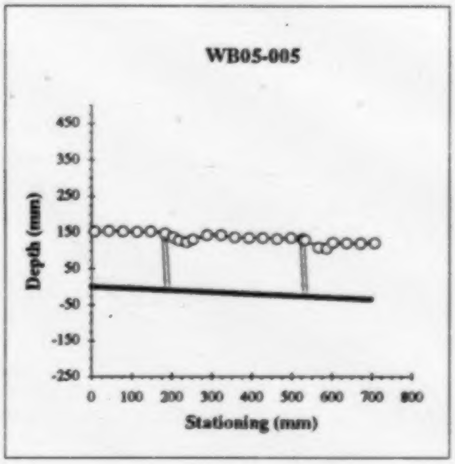
WB05-005
Depth (mm)
450
350
250
150
50
-50
-150
-250
0
100
200
300
400
500
600
700
800
Stationing (mm)

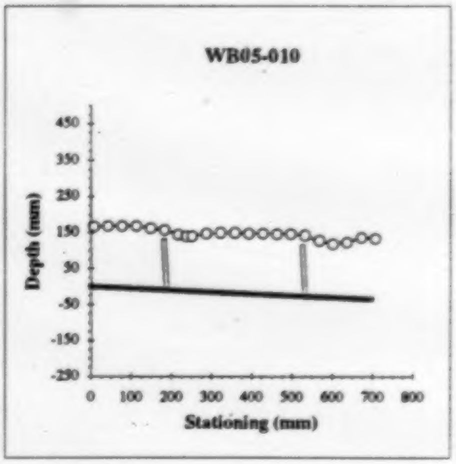
WB05-010
Depth (mm)
450
350
250
150
50
-50
-150
-250
0
100
200
300
400
500
600
700
800
Stationing (mm)

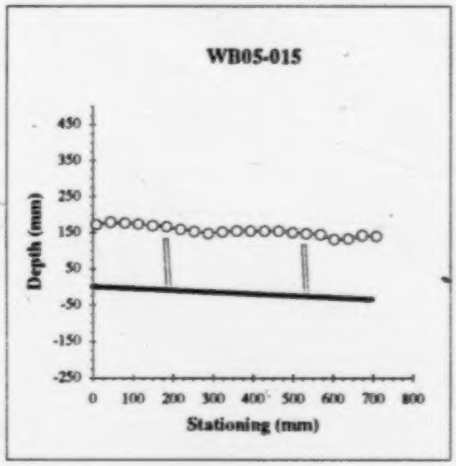
WB05-015
Depth (mm)
450
350
250
150
50
-50
-150
-250
0
100
200
300
400
500
600
700
800
Stationing (mm)

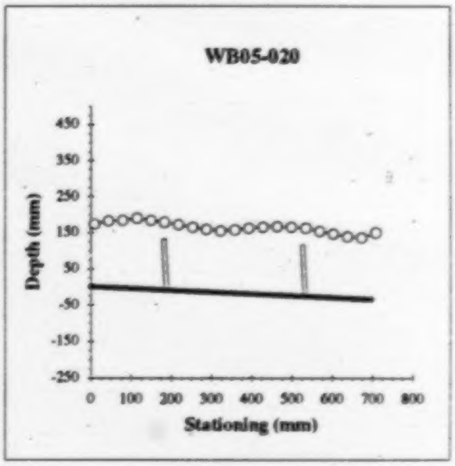
WB05-020
Depth (mm)
450
350
250
150
50
-50
-150
-250
0
100
200
300
400
500
600
700
800
Stationing (mm)

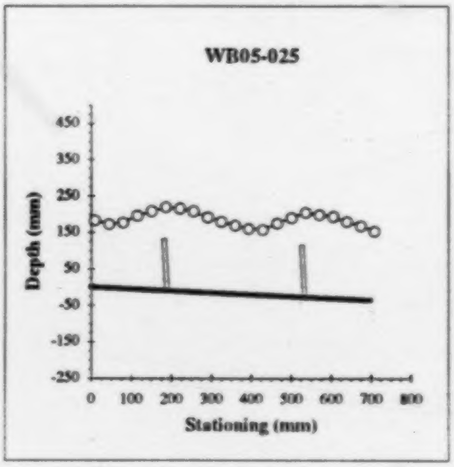
WB05-025
Depth (mm)
450
350
250
150
50
-50
-150
-250
0
100
200
300
400
500
600
700
800
Stationing (mm)

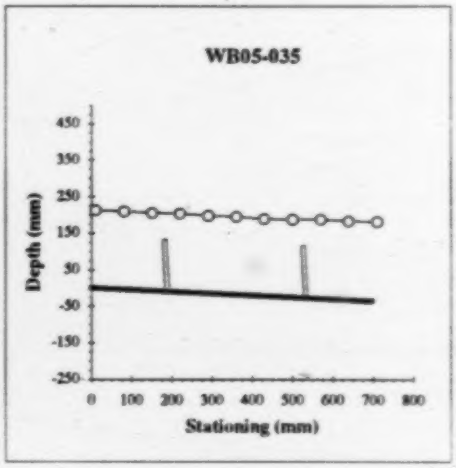
WB05-035
Depth (mm)
450
350
250
150
50
-50
-150
-250
0
100
200
300
400
500
600
700
800
Stationing (mm)

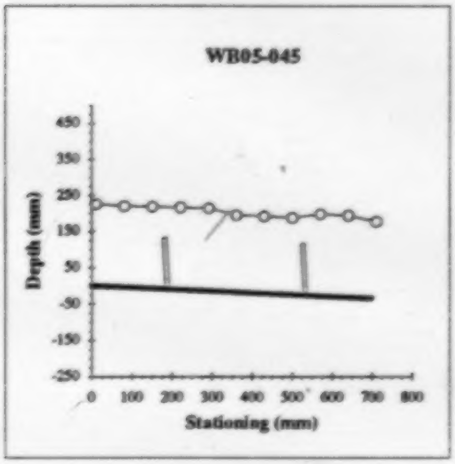
WB05-045

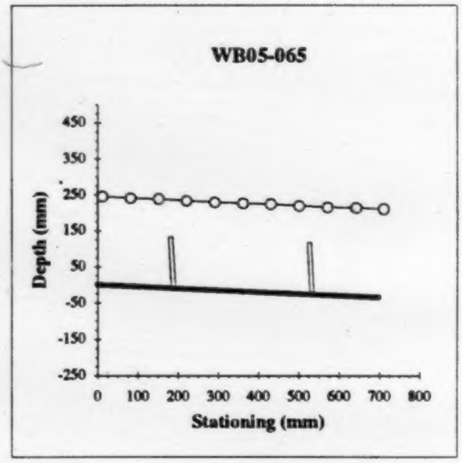
WB05-065

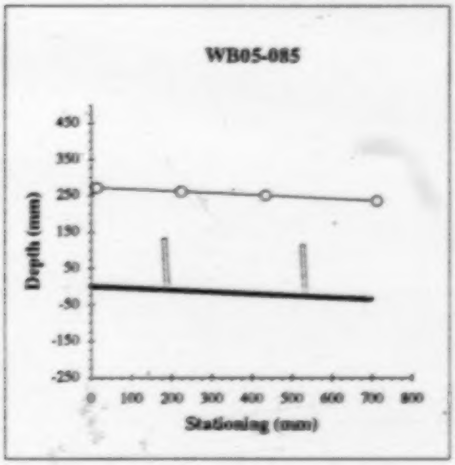
WB05-085

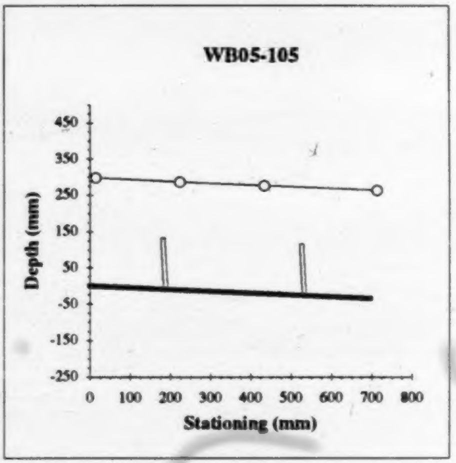
WB05-105

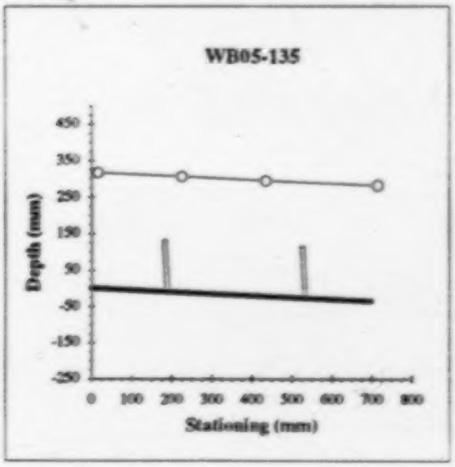
WB05-135

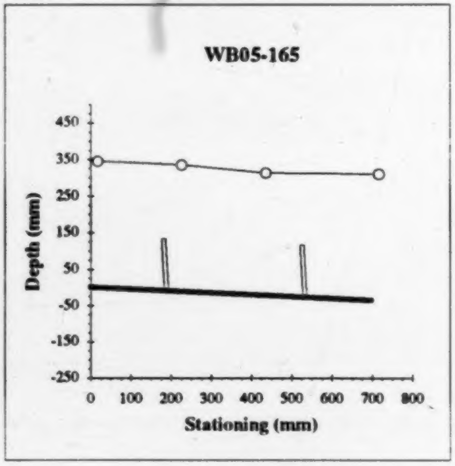
WB05-165

WB10 - (005 to 165 l/s)

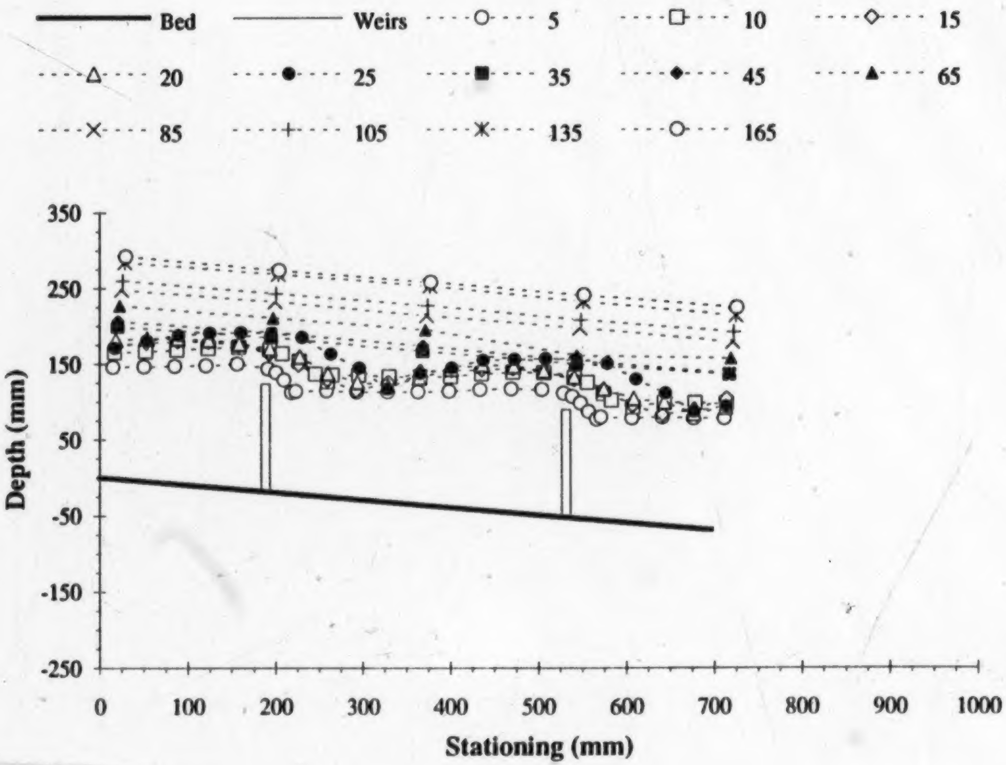

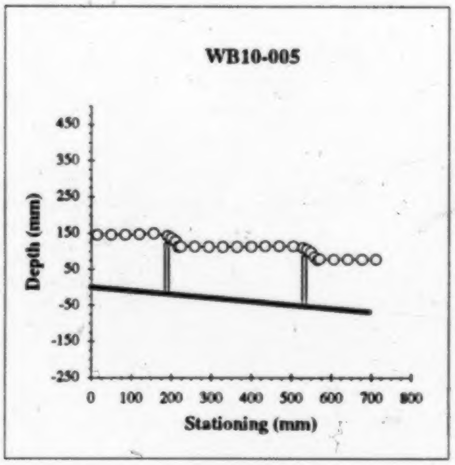
WB10-005

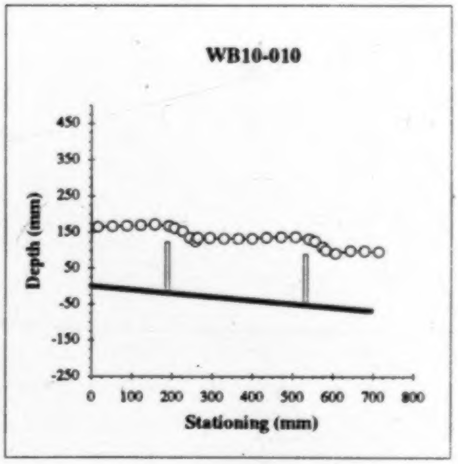
WB10-010

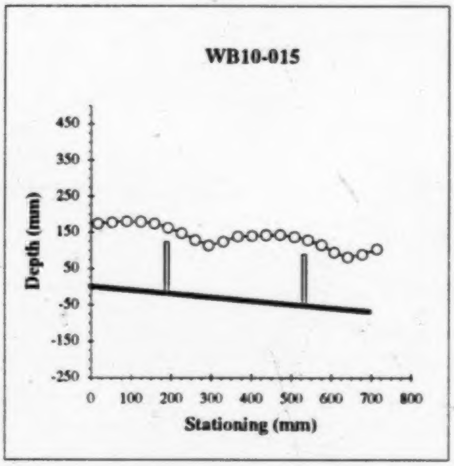
WB10-015

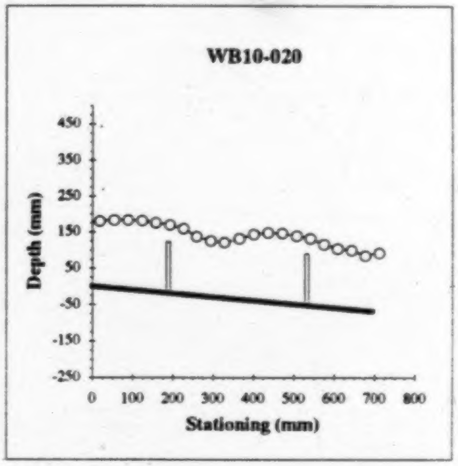
WB10-020

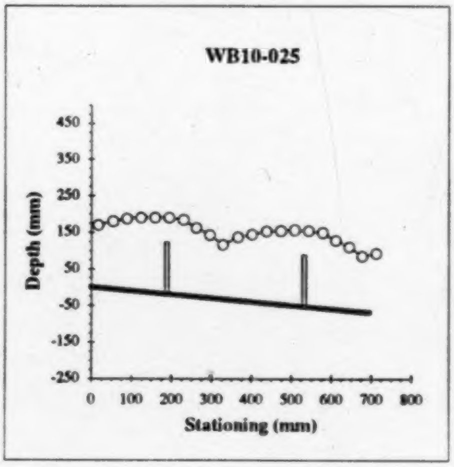
WB10-025

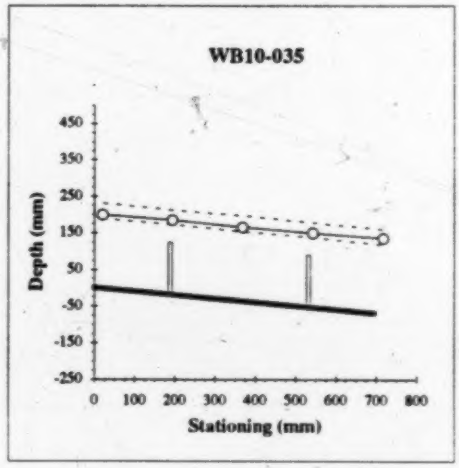
WB10-035

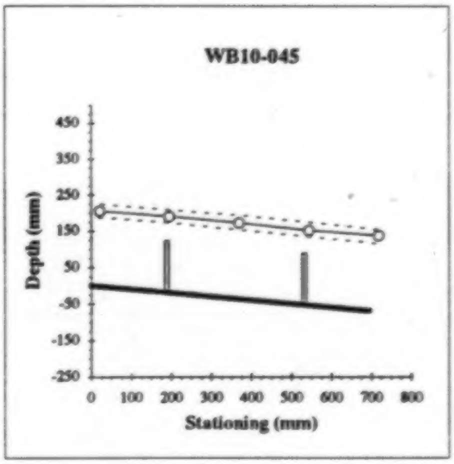
WB10-045
Depth (mm)
450
350
250
150
50
-50
-150
-250
0
100
200
300
400
500
600
700
800
Stationing (mm)

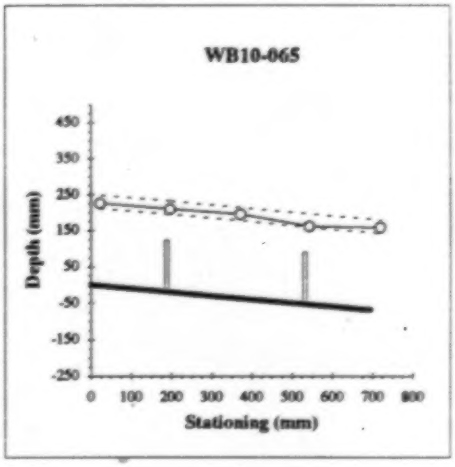
WB10-065
Depth (mm)
450
350
250
150
50
-50
-150
-250
0
100
200
300
400
500
600
700
800
Stationing (mm)

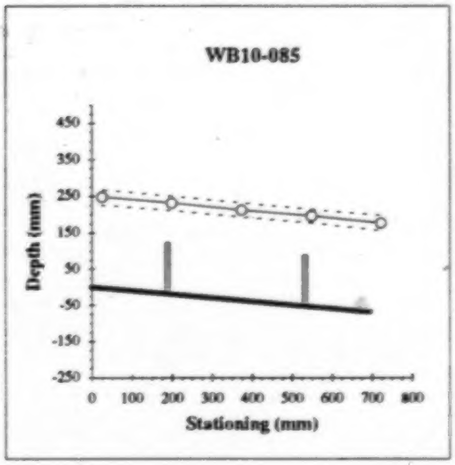
WB10-085
Depth (mm)
450
350
250
150
50
-50
-150
-250
0
100
200
300
400
500
600
700
800
Stationing (mm)

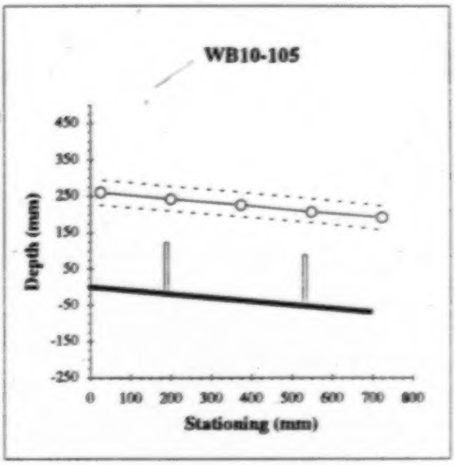
WB10-105
Depth (mm)
450
350
250
150
50
-50
-150
-250
0
100
200
300
400
500
600
700
800
Stationing (mm)

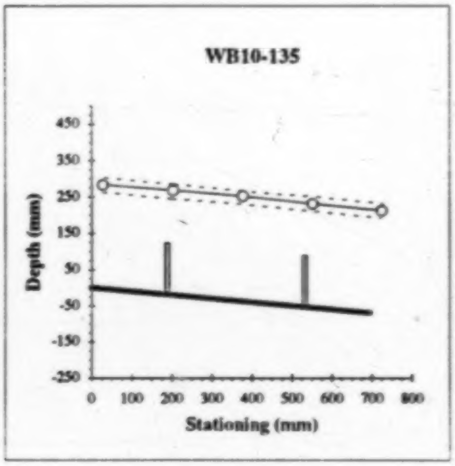
WB10-135
Depth (mm)
450
350
250
150
50
-50
-150
-250
0
100
200
300
400
500
600
700
800
Stationing (mm)

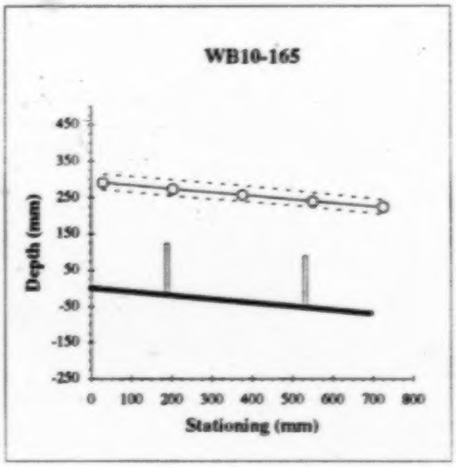
WB10-165
Depth (mm)
450
350
250
150
50
-50
-150
-250
0
100
200
300
400
500
600
700
800
Stationing (mm)

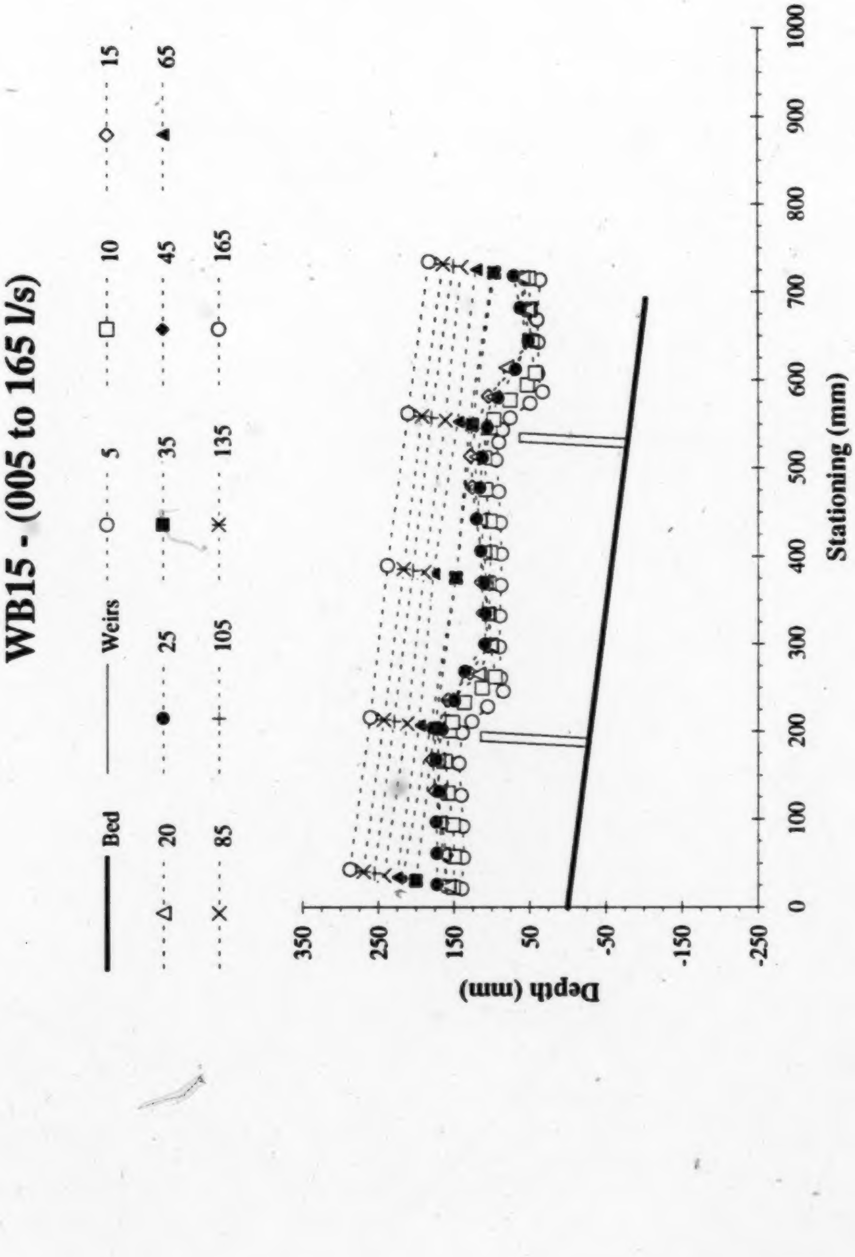
WB15 - (005 to 165 l/s)
Bed
Weirs
5
10
15
20
25
35
45
65
85
105
135
165
Depth (mm)
350
250
150
50
-50
-150
-250
Stationing (mm)
0
100
200
300
400
500
600
700
800
900
1000

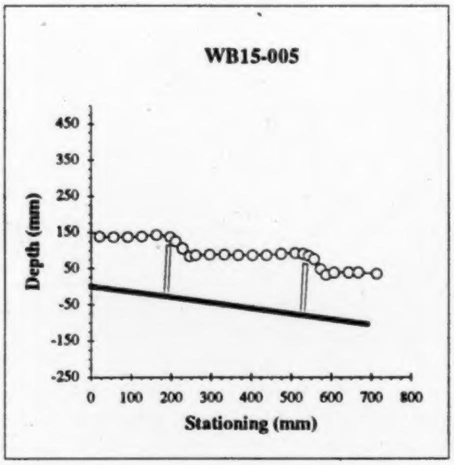

WB15-005

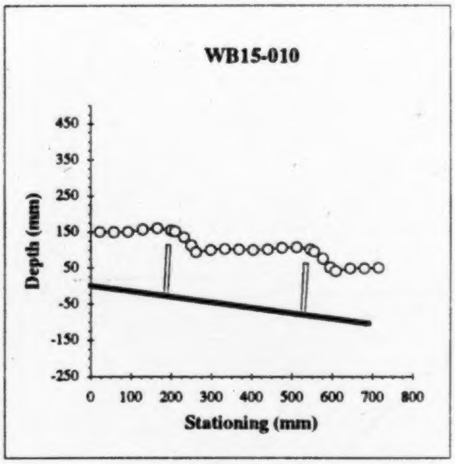

WB15-010

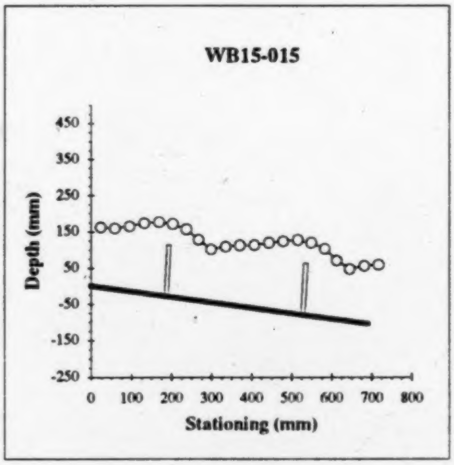

WB15-015

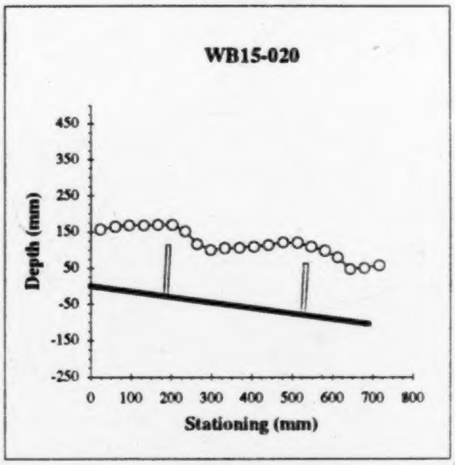

WB15-020

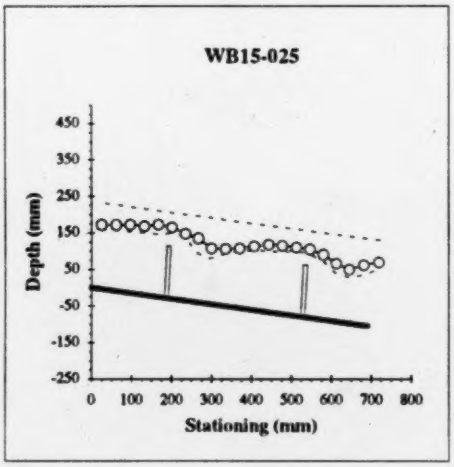

WB15-025

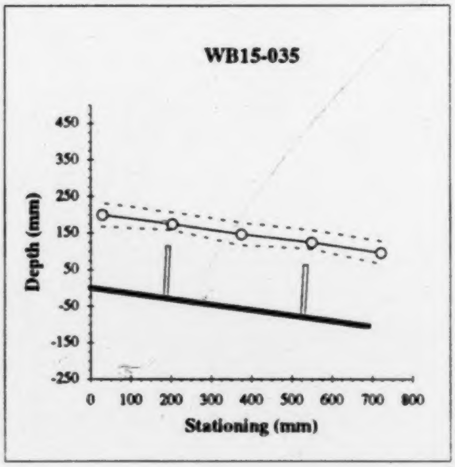

WB15-035

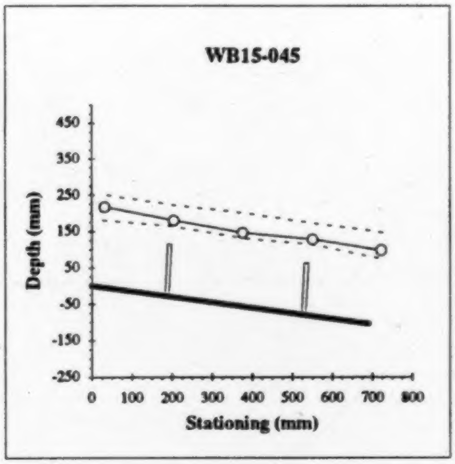
WB15-045

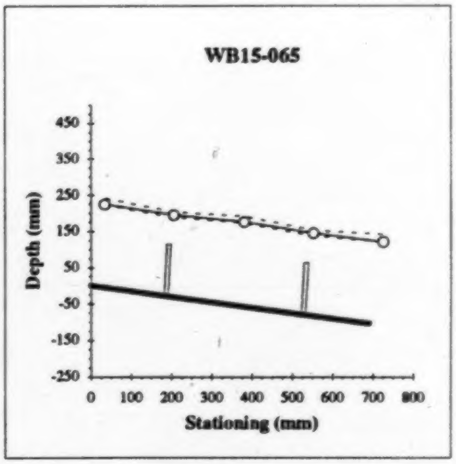
WB15-065

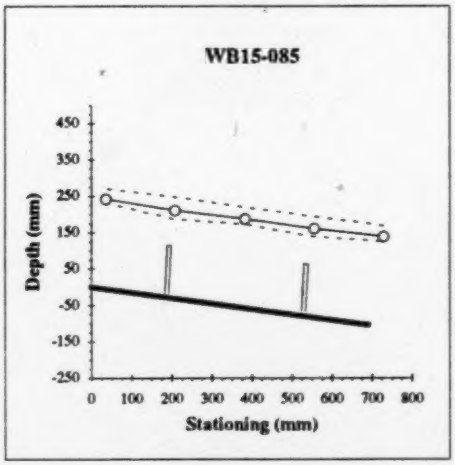
WB15-085

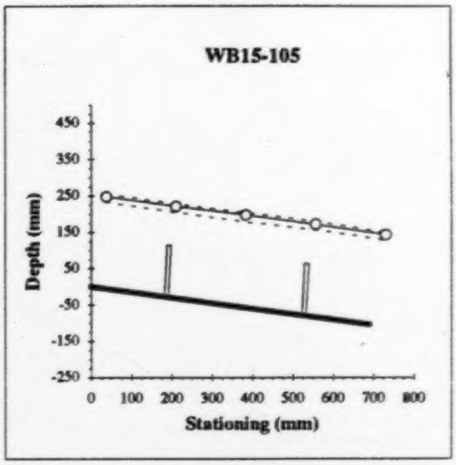
WB15-105

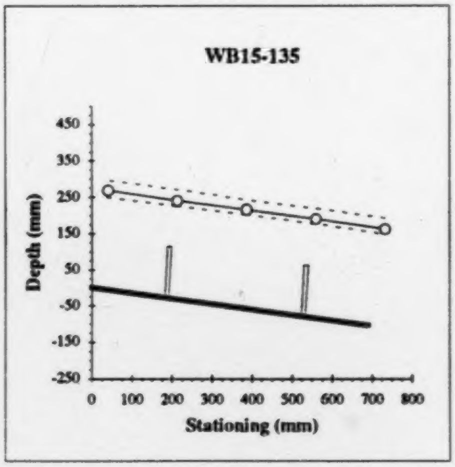
WB15-135

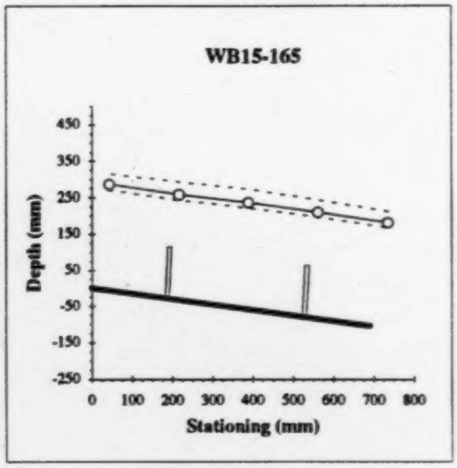
WB15-165

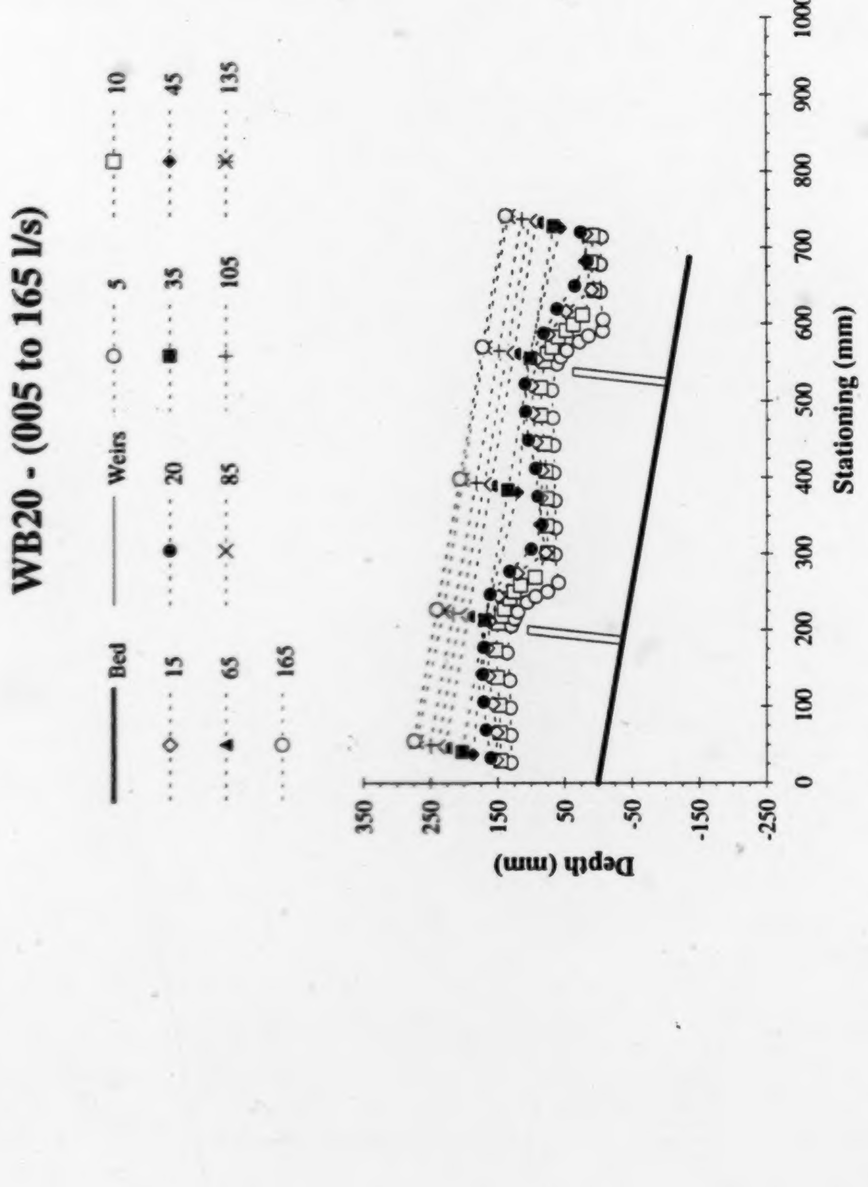
WB20 - (005 to 165 l/s)
Bed
Weirs
5
10
15
20
35
45
65
85
105
135
165
Depth (mm)
350
250
150
50
-50
-150
-250
0
100
200
300
400
500
600
700
800
900
1000
Stationing (mm)

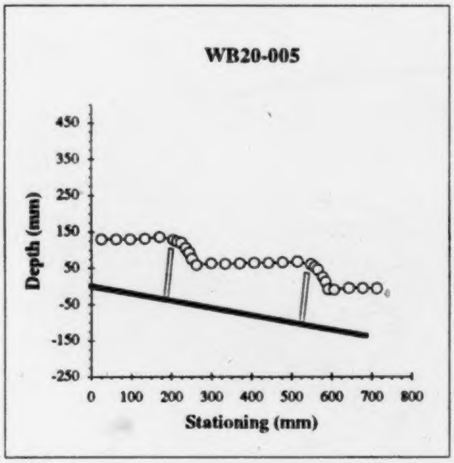
WB20-005

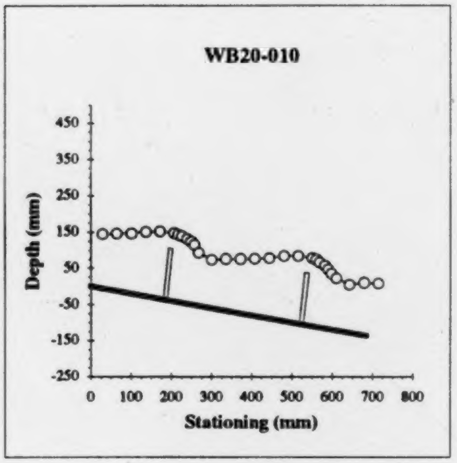
WB20-010

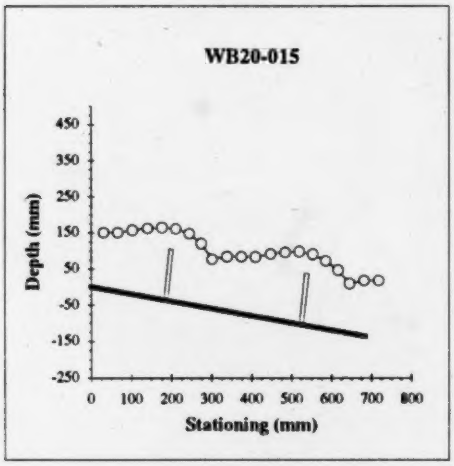
WB20-015

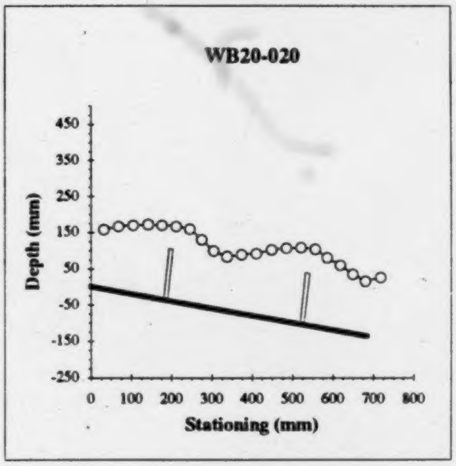
WB20-020

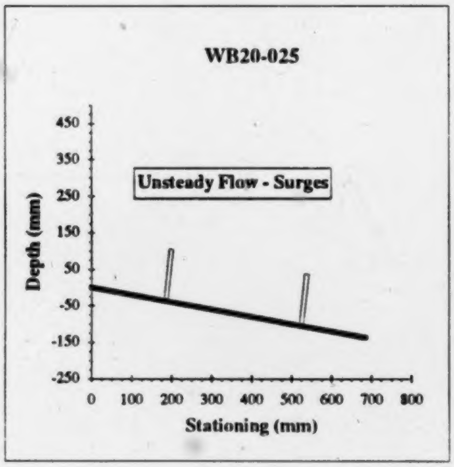
WB20-025

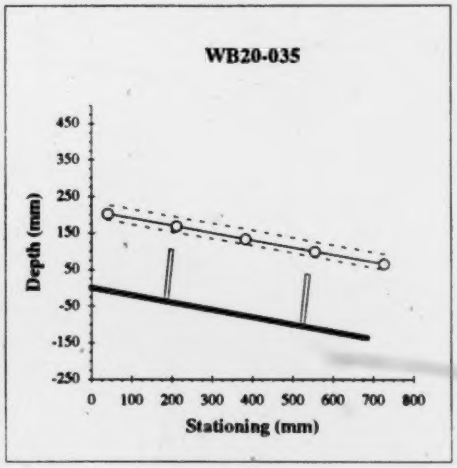
WB20-035

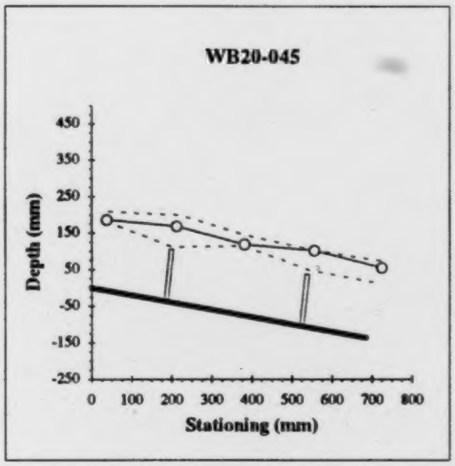
WB20-045
Depth (mm)
450
350
250
150
50
-50
-150
-250
0 100 200 300 400 500 600 700 800
Stationing (mm)

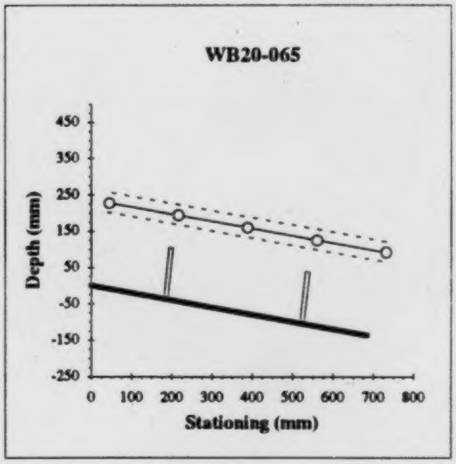
WB20-065
Depth (mm)
450
350
250
150
50
-50
-150
-250
0 100 200 300 400 500 600 700 800
Stationing (mm)

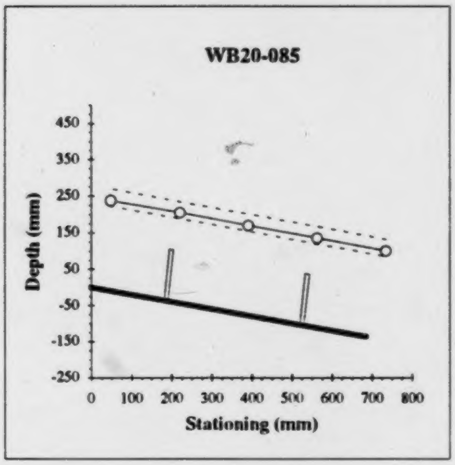
WB20-085
Depth (mm)
450
350
250
150
50
-50
-150
-250
0 100 200 300 400 500 600 700 800
Stationing (mm)

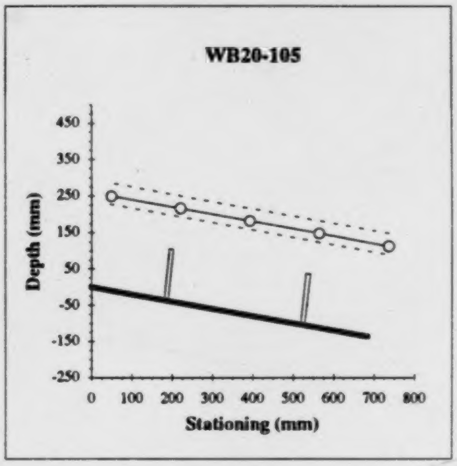
WB20-105
Depth (mm)
450
350
250
150
50
-50
-150
-250
0 100 200 300 400 500 600 700 800
Stationing (mm)

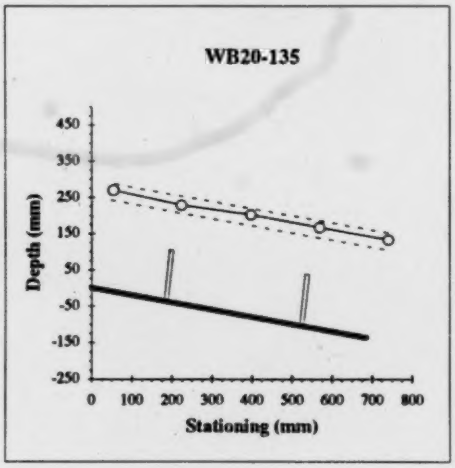
WB20-135
Depth (mm)
450
350
250
150
50
-50
-150
-250
0 100 200 300 400 500 600 700 800
Stationing (mm)

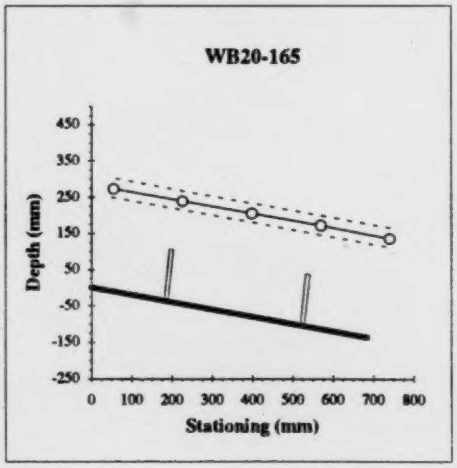
WB20-165
Depth (mm)
450
350
250
150
50
-50
-150
-250
0 100 200 300 400 500 600 700 800
Stationing (mm)

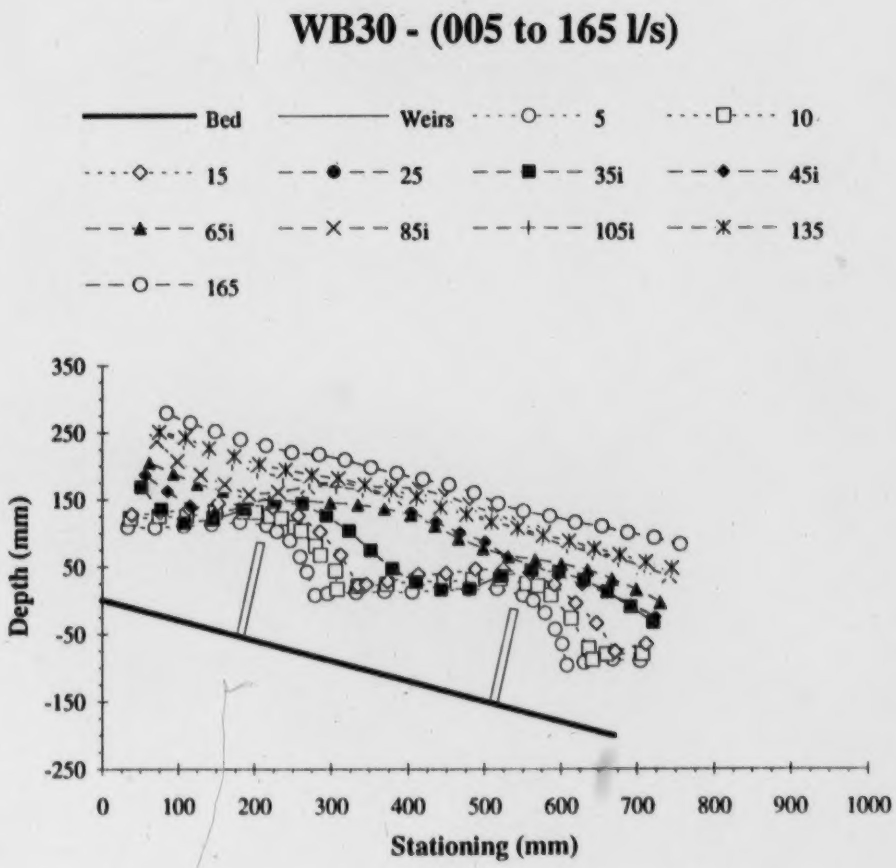
WB30 - (005 to 165 l/s)
Bed
Weirs
5
10
15
25
35i
45i
65i
85i
105i
135
165
350
250
150
50
-50
-150
-250
Depth (mm)
0
100
200
300
400
500
600
700
800
900
1000
Stationing (mm)

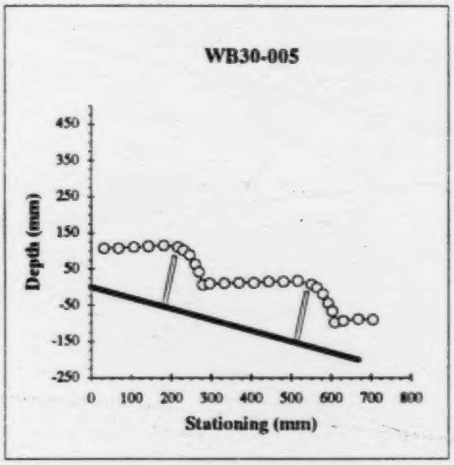
WB30-005
Depth (mm)
450
350
250
150
50
-50
-150
-250
0 100 200 300 400 500 600 700 800
Stationing (mm)

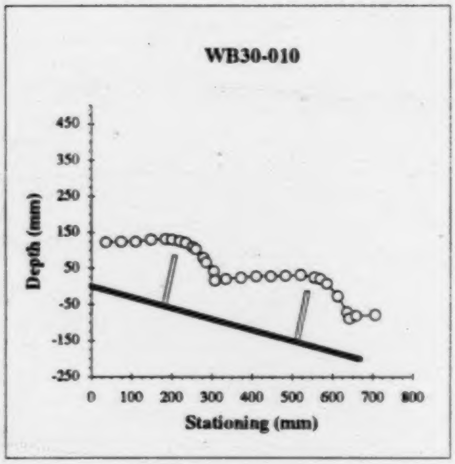
WB30-010
Depth (mm)
450
350
250
150
50
-50
-150
-250
0 100 200 300 400 500 600 700 800
Stationing (mm)

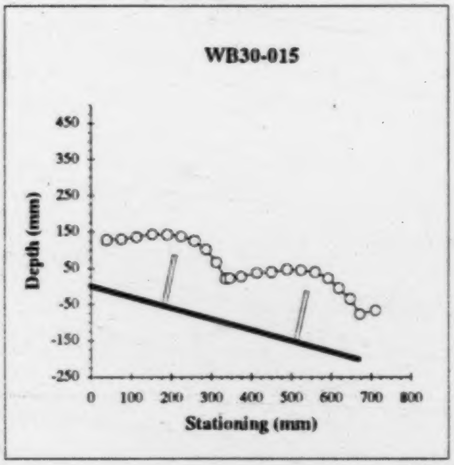
WB30-015
Depth (mm)
450
350
250
150
50
-50
-150
-250
0 100 200 300 400 500 600 700 800
Stationing (mm)

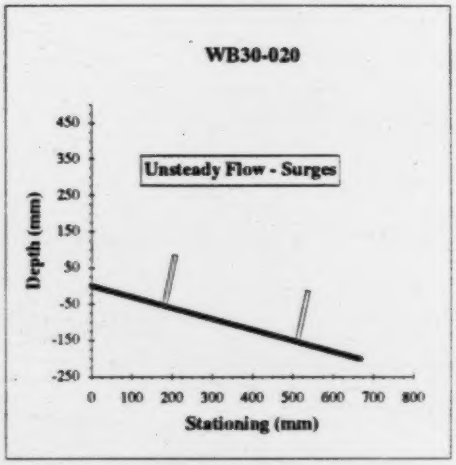
WB30-020
Unsteady Flow - Surges
Depth (mm)
450
350
250
150
50
-50
-150
-250
0 100 200 300 400 500 600 700 800
Stationing (mm)

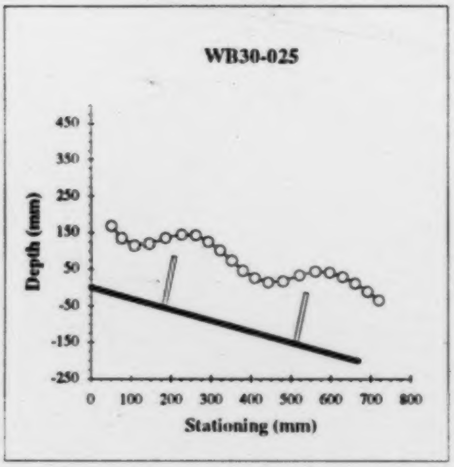
WB30-025
Depth (mm)
450
350
250
150
50
-50
-150
-250
0 100 200 300 400 500 600 700 800
Stationing (mm)

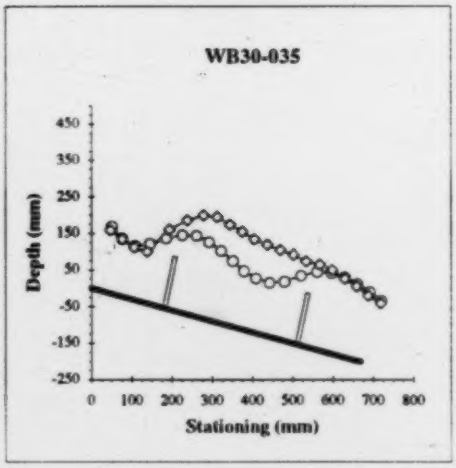
WB30-035
Depth (mm)
450
350
250
150
50
-50
-150
-250
0 100 200 300 400 500 600 700 800
Stationing (mm)

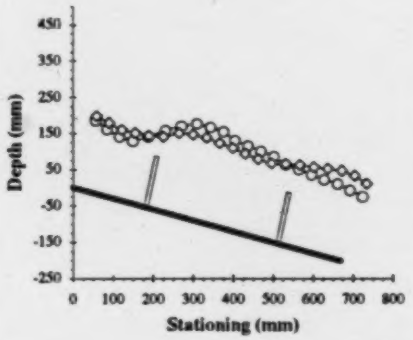

WB30-045

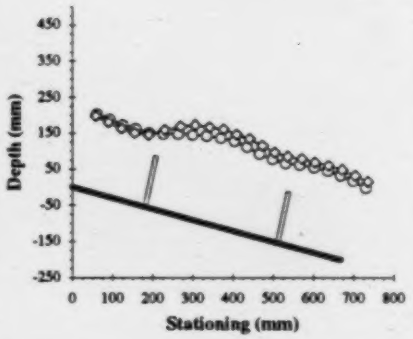

WB30-065

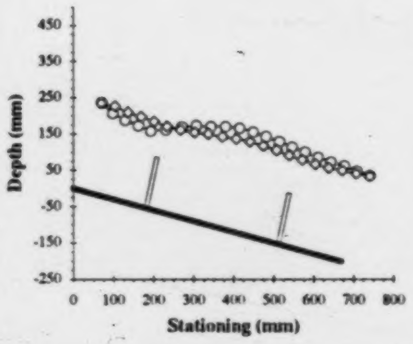

WB30-085

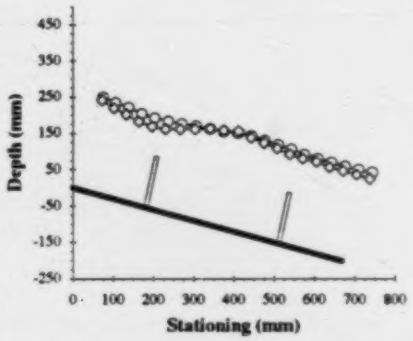

WB30-105

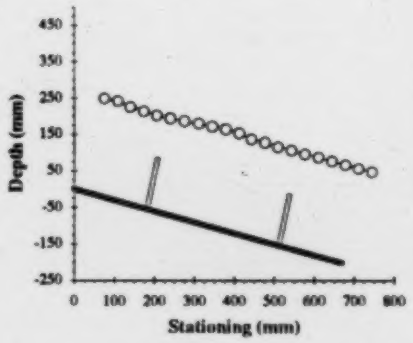

WB30-135

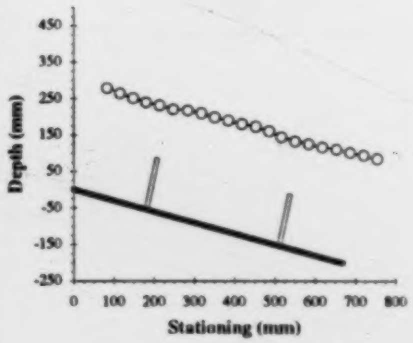

WB30-165

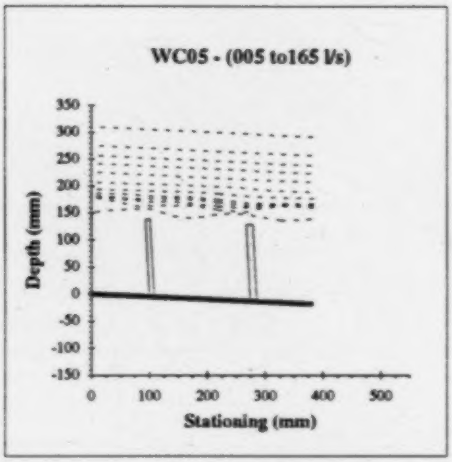
WC05 - (005 to165 l/s)

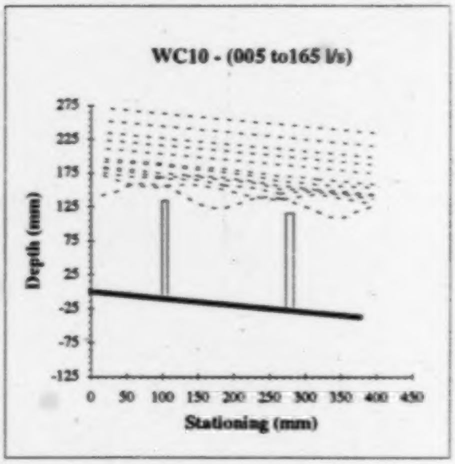
WC10 - (005 to165 l/s)

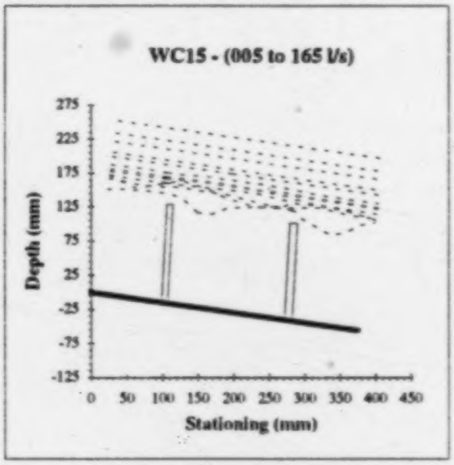
WC15 - (005 to 165 l/s)

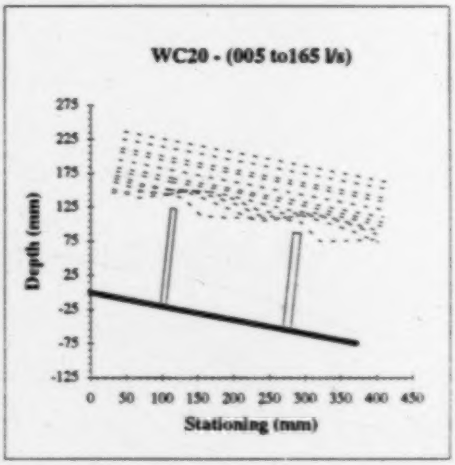
WC20 - (005 to165 l/s)

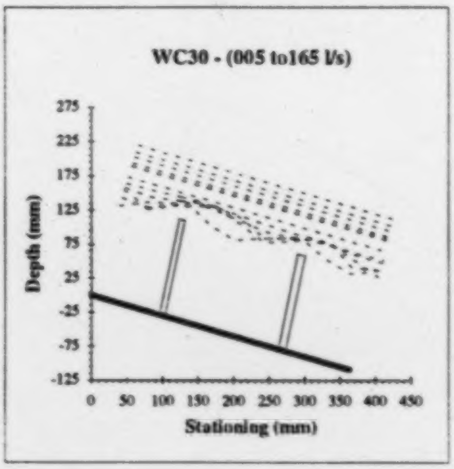
WC30 - (005 to165 l/s)

Water Surface Profiles

Full Weir Height

Class 'C' Weir Spacing

5 to 30 % Slope, 5 to 135 l/s

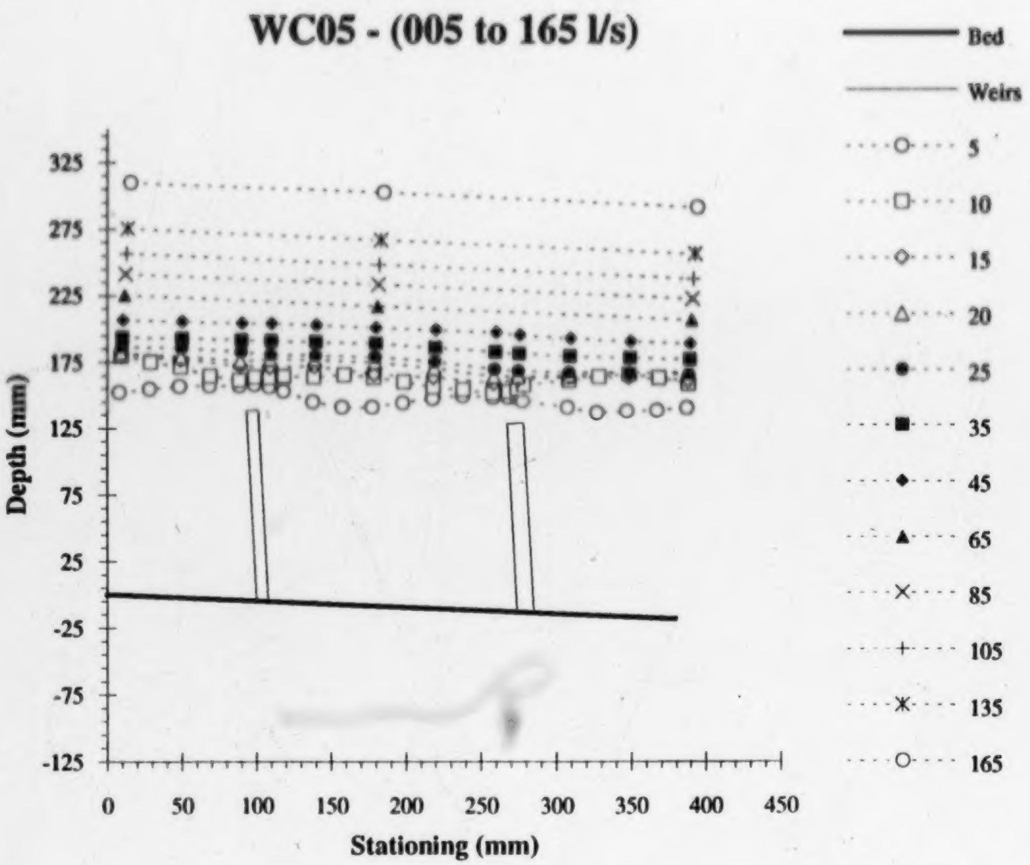
WC05 - (005 to 165 l/s)
Depth (mm)
325
275
225
175
125
75
25
-25
-75
-125
0
50
100
150
200
250
300
350
400
450
Stationing (mm)
Bed
Weirs
5
10
15
20
25
35
45
65
85
105
135
165

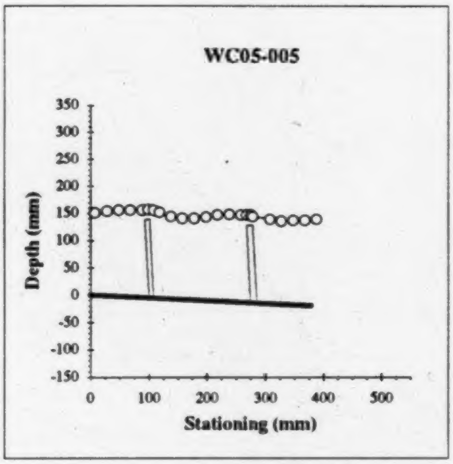
WC05-005

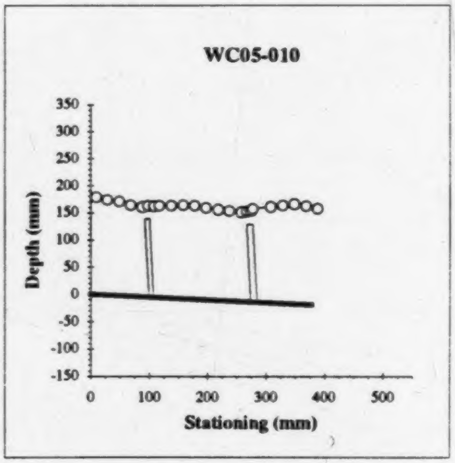
WC05-010

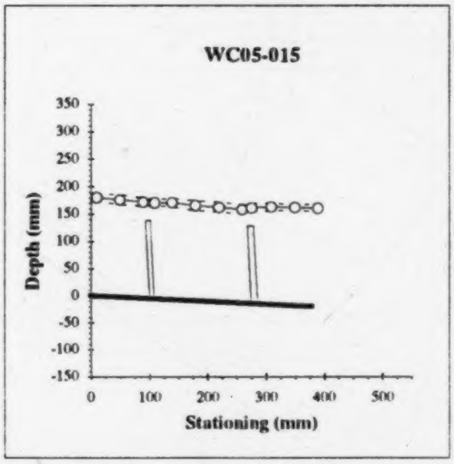
WC05-015

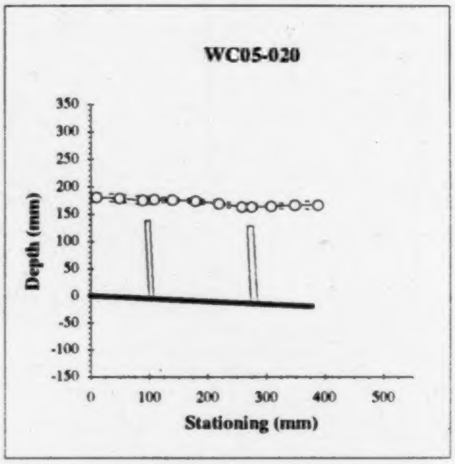
WC05-020

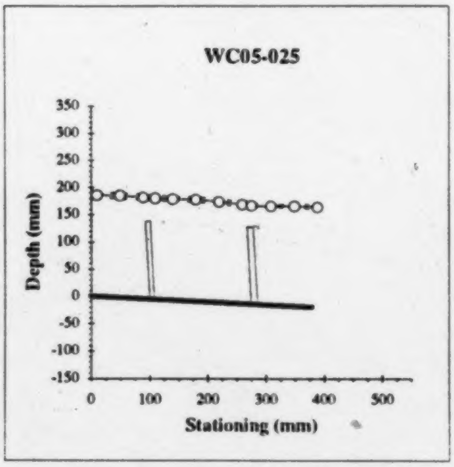
WC05-025

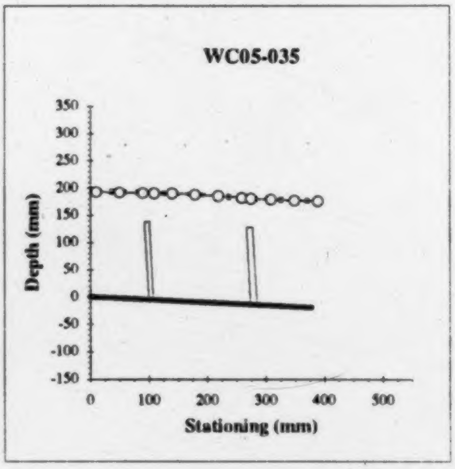
WC05-035

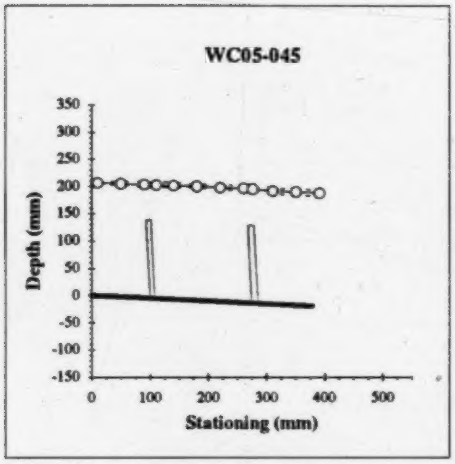
WC05-045

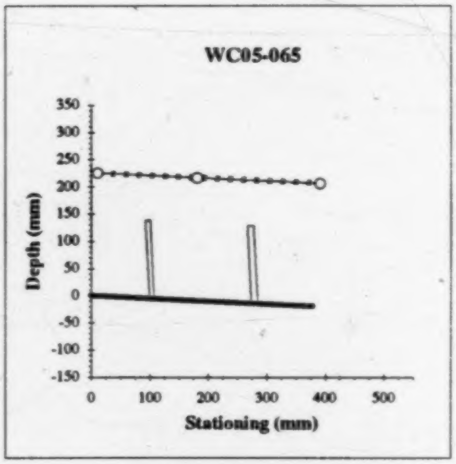
WC05-065

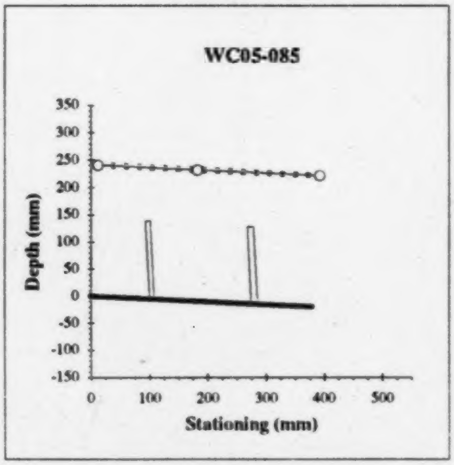
WC05-085

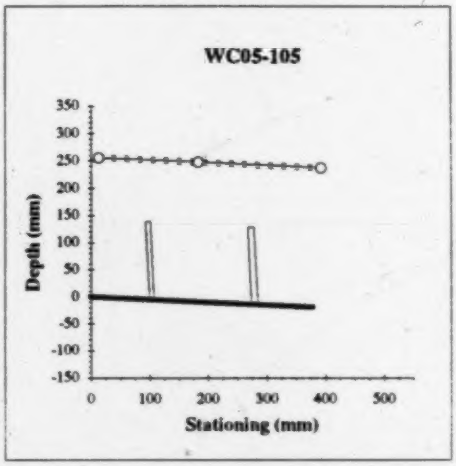
WC05-105

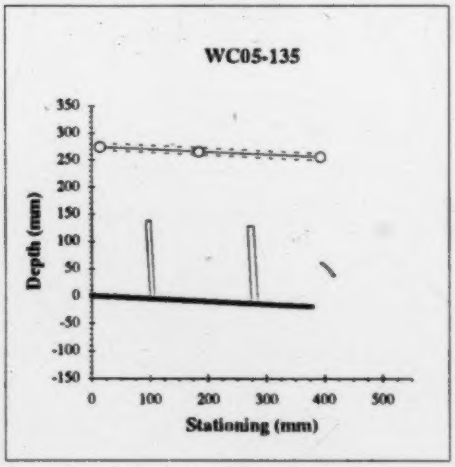
WC05-135

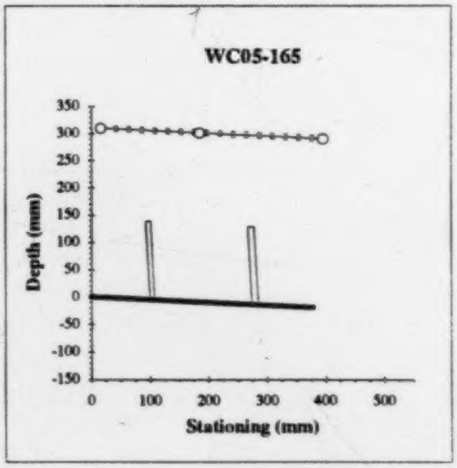
WC05-165

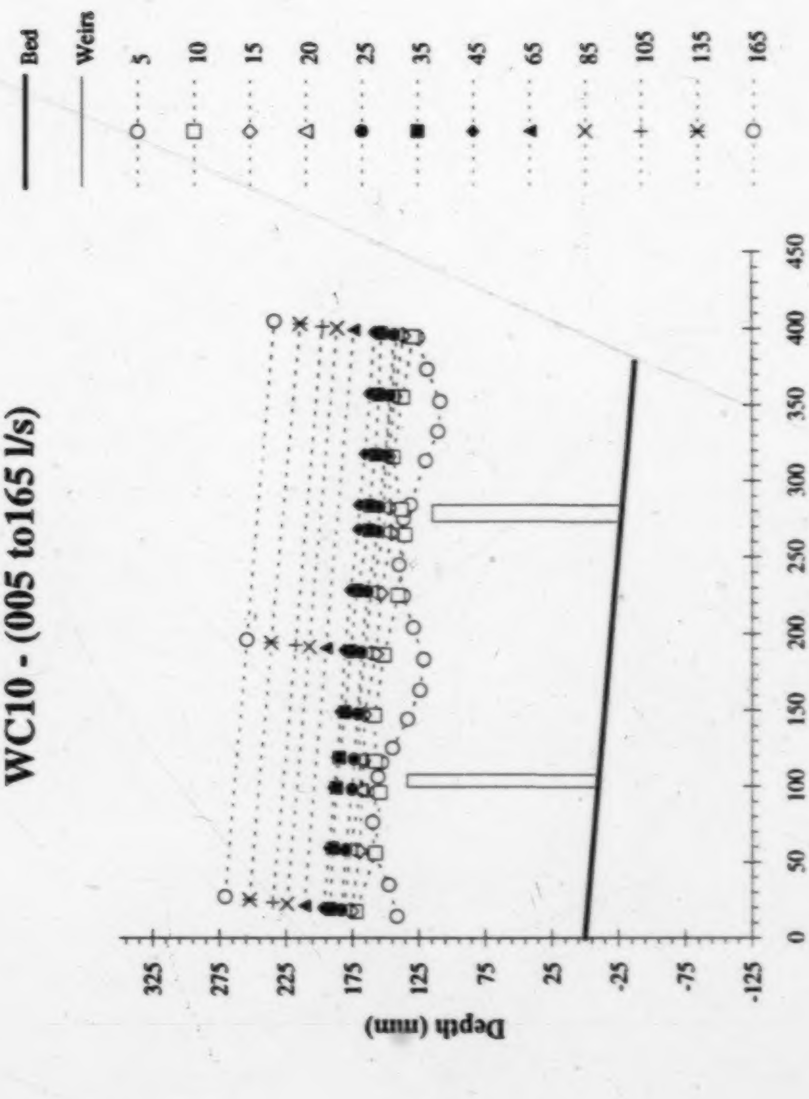

WC10 - (005 to165 l/s)

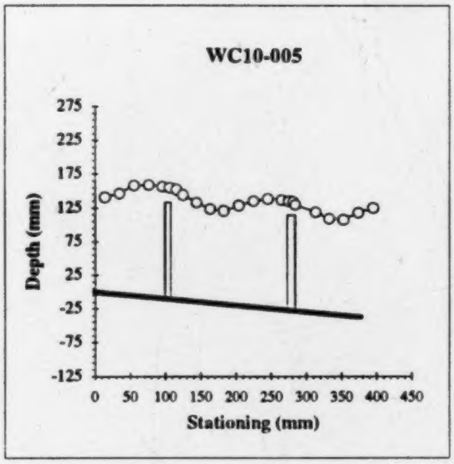
WC10-005
275
225
175
125
75
25
-25
-75
-125
Depth (mm)
0 50 100 150 200 250 300 350 400 450
Stationing (mm)

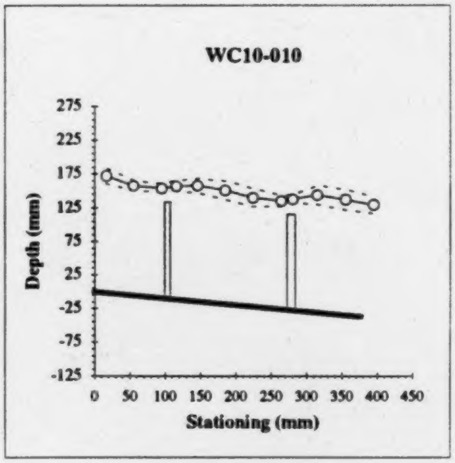
WC10-010
275
225
175
125
75
25
-25
-75
-125
Depth (mm)
0 50 100 150 200 250 300 350 400 450
Stationing (mm)

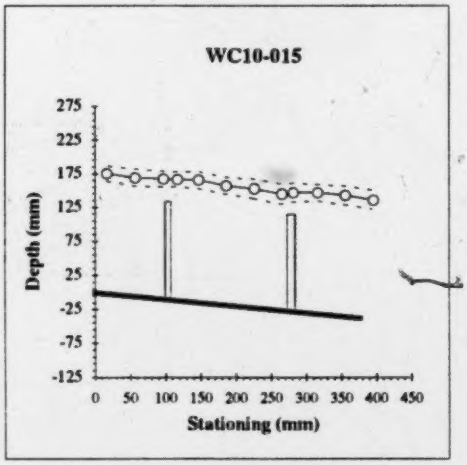
WC10-015
275
225
175
125
75
25
-25
-75
-125
Depth (mm)
0 50 100 150 200 250 300 350 400 450
Stationing (mm)

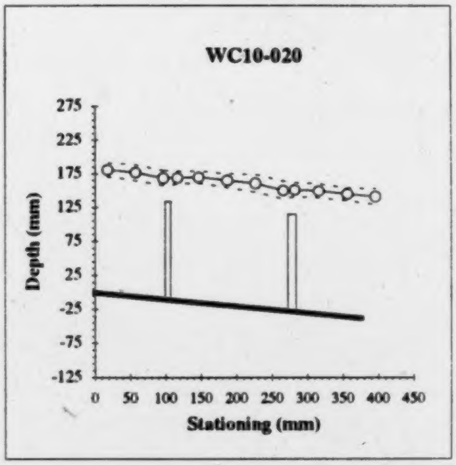
WC10-020
275
225
175
125
75
25
-25
-75
-125
Depth (mm)
0 50 100 150 200 250 300 350 400 450
Stationing (mm)

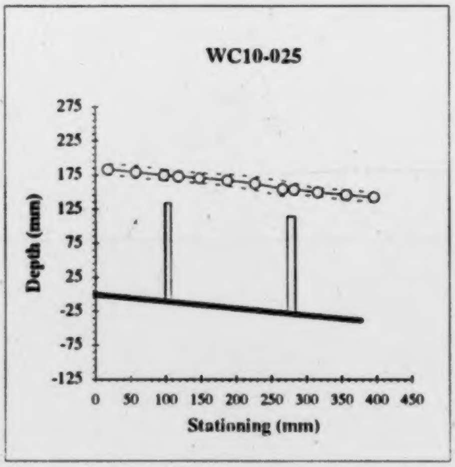
WC10-025
275
225
175
125
75
25
-25
-75
-125
Depth (mm)
0 50 100 150 200 250 300 350 400 450
Stationing (mm)

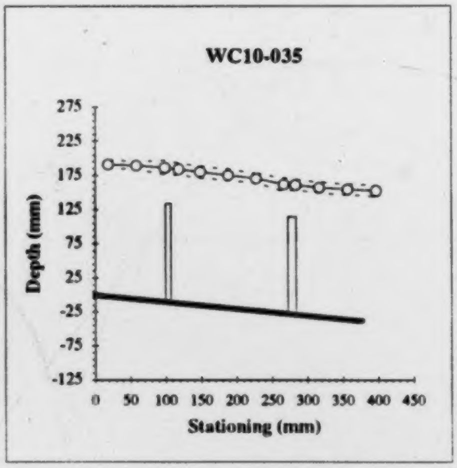
WC10-035
275
225
175
125
75
25
-25
-75
-125
Depth (mm)
0 50 100 150 200 250 300 350 400 450
Stationing (mm)

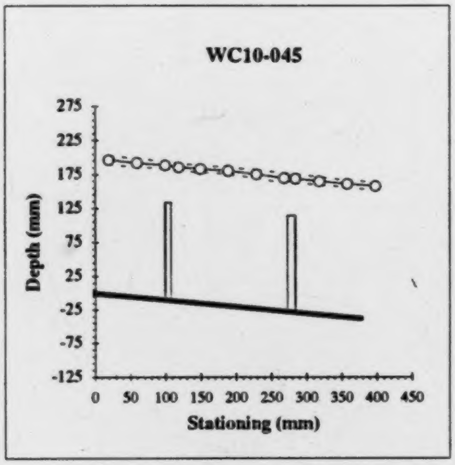
WC10-045
Depth (mm)
275
225
175
125
75
25
-25
-75
-125
0 50 100 150 200 250 300 350 400 450
Stationing (mm)

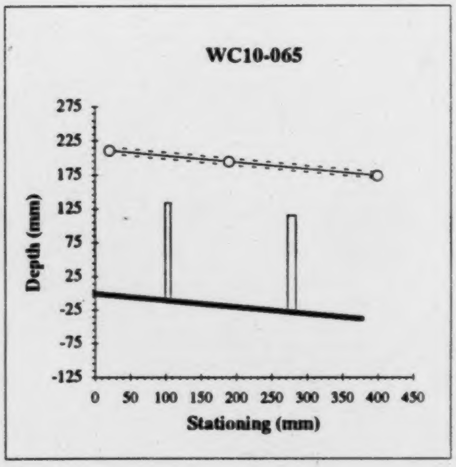
WC10-065
Depth (mm)
275
225
175
125
75
25
-25
-75
-125
0 50 100 150 200 250 300 350 400 450
Stationing (mm)

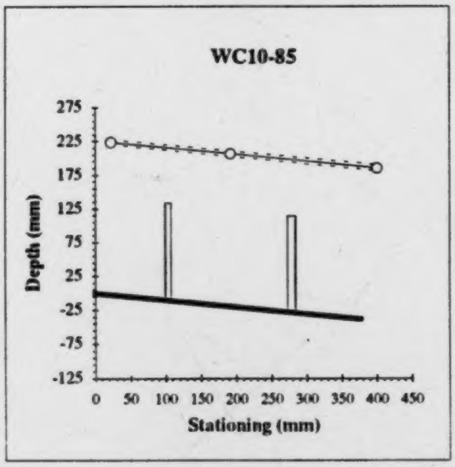
WC10-85
Depth (mm)
275
225
175
125
75
25
-25
-75
-125
0 50 100 150 200 250 300 350 400 450
Stationing (mm)

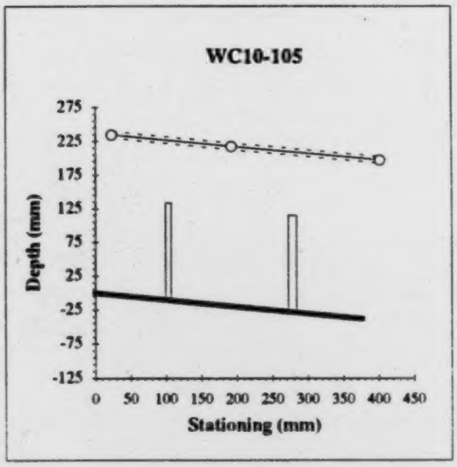
WC10-105
Depth (mm)
275
225
175
125
75
25
-25
-75
-125
0 50 100 150 200 250 300 350 400 450
Stationing (mm)

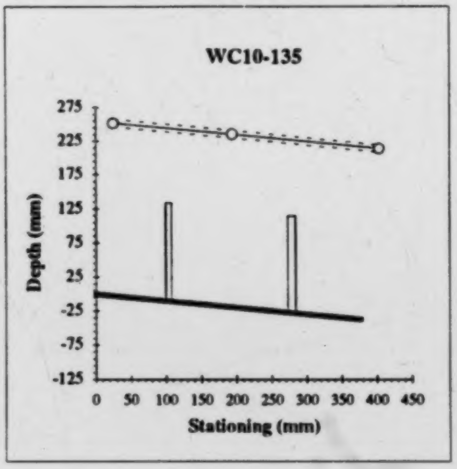
WC10-135
Depth (mm)
275
225
175
125
75
25
-25
-75
-125
0 50 100 150 200 250 300 350 400 450
Stationing (mm)

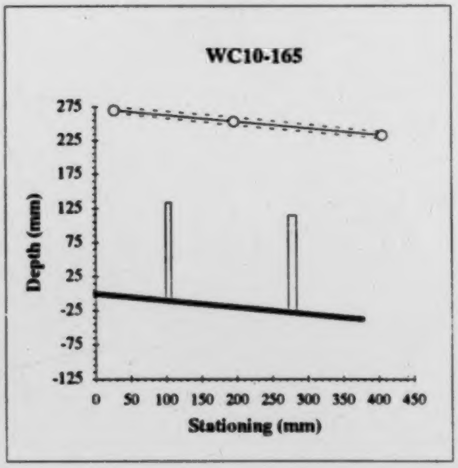
WC10-165
Depth (mm)
275
225
175
125
75
25
-25
-75
-125
0 50 100 150 200 250 300 350 400 450
Stationing (mm)

WC15 - (005 to 165 l/s)

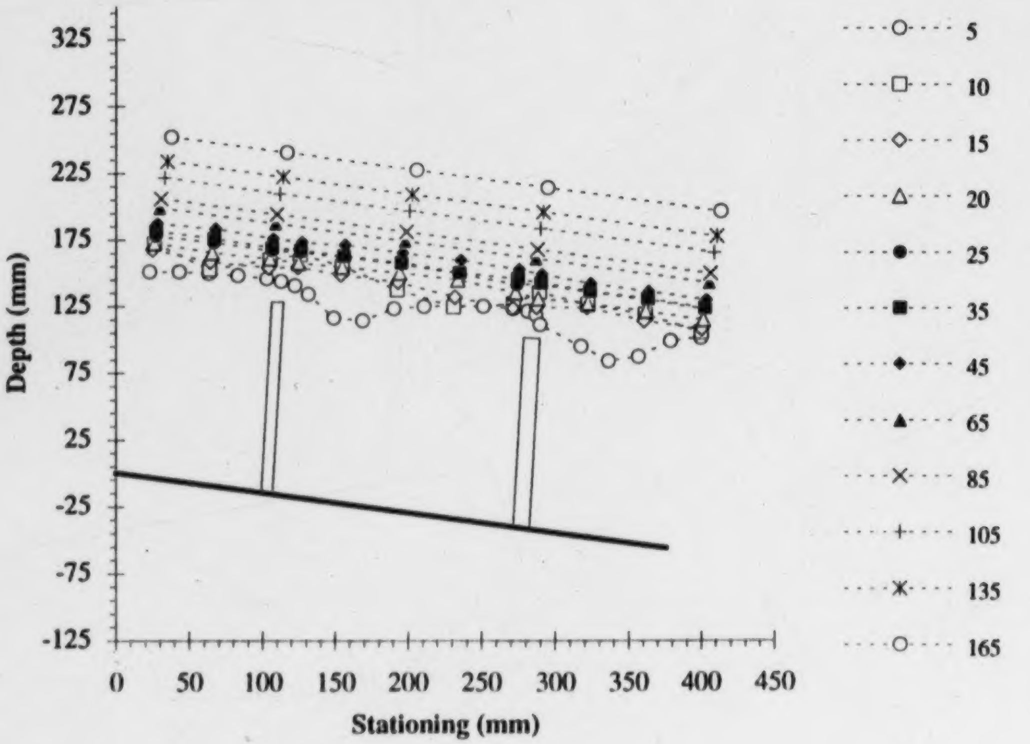

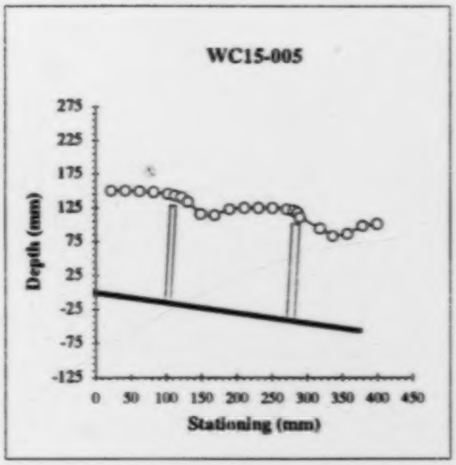
WC15-005

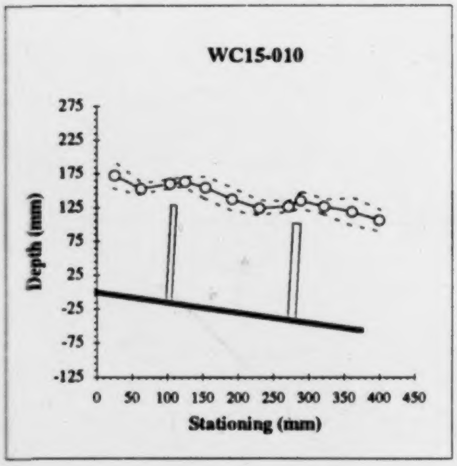
WC15-010

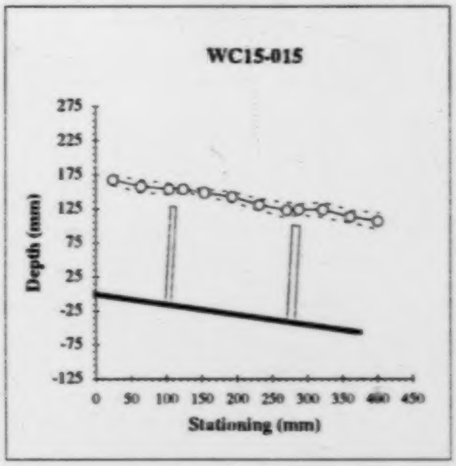
WC15-015

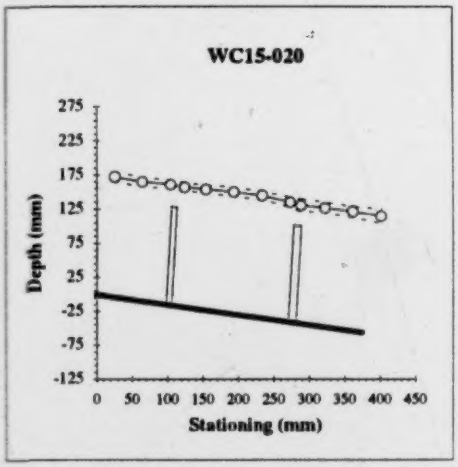
WC15-020

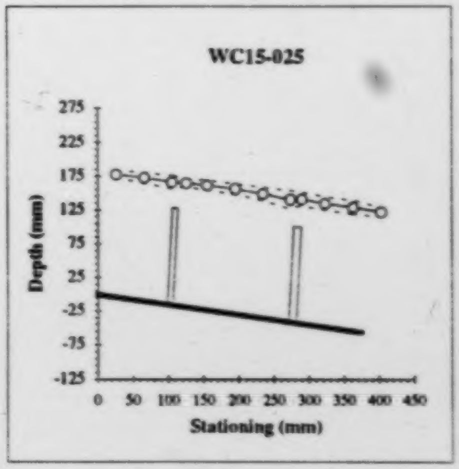
WC15-025

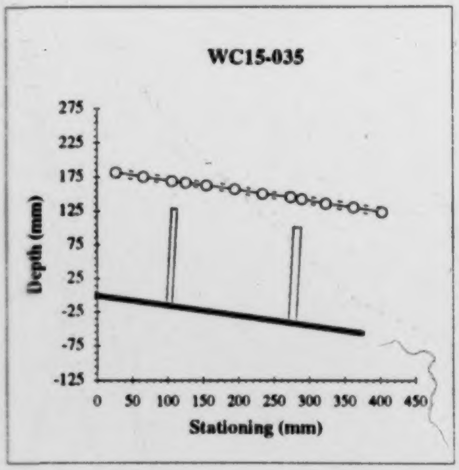
WC15-035

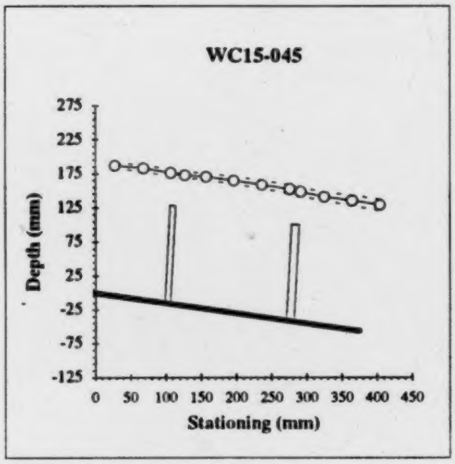
WC15-045

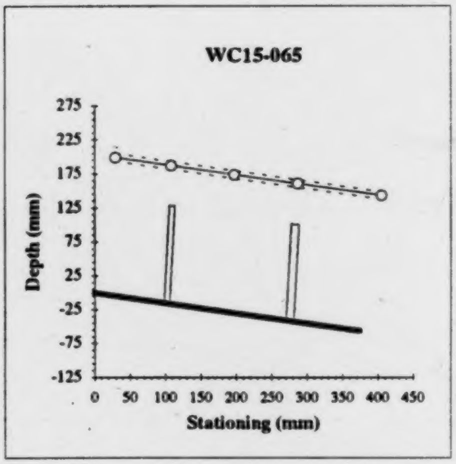
WC15-065

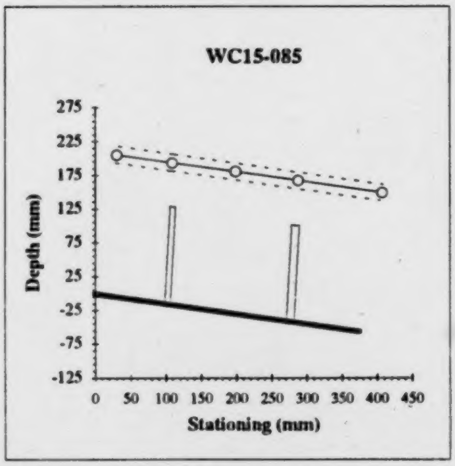
WC15-085

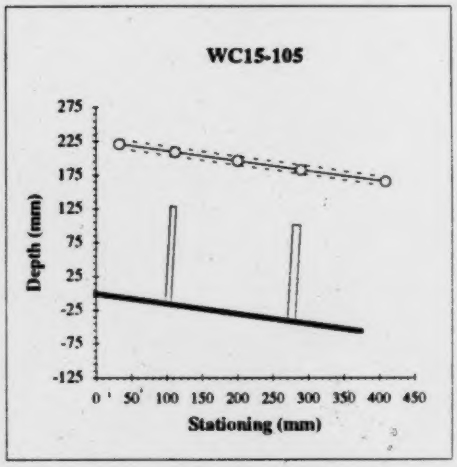
WC15-105

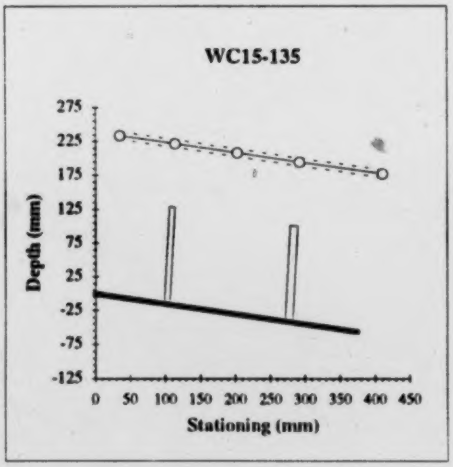
WC15-135

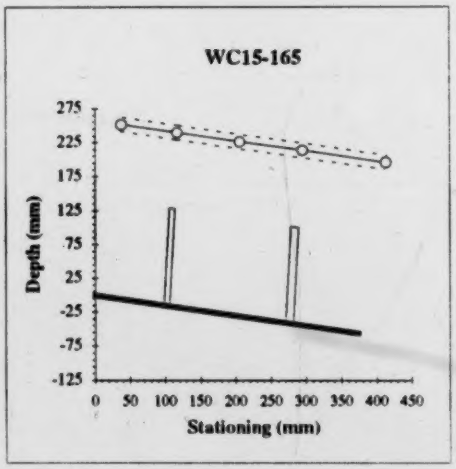
WC15-165

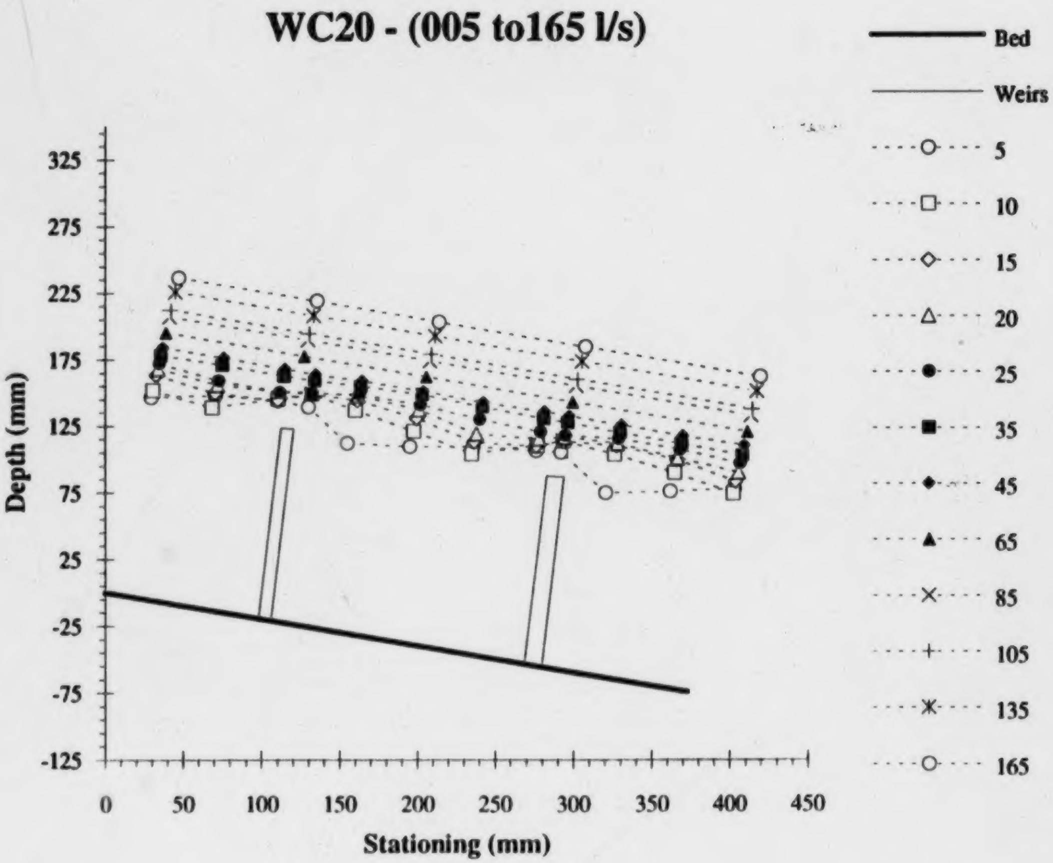
WC20 - (005 to165 l/s)
Depth (mm)
325
275
225
175
125
75
25
-25
-75
-125
0
50
100
150
200
250
300
350
400
450
Stationing (mm)
Bed
Weirs
5
10
15
20
25
35
45
65
85
105
135
165

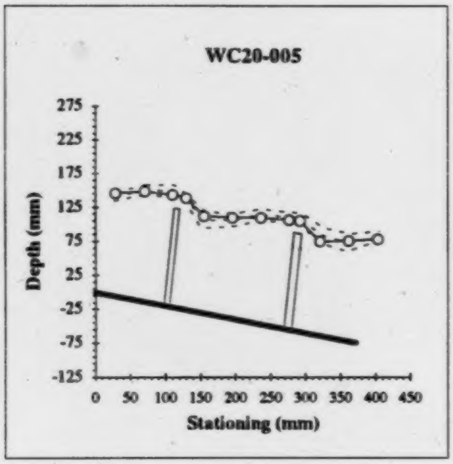
WC20-005
Depth (mm)
275
225
175
125
75
25
-25
-75
-125
0 50 100 150 200 250 300 350 400 450
Stationing (mm)

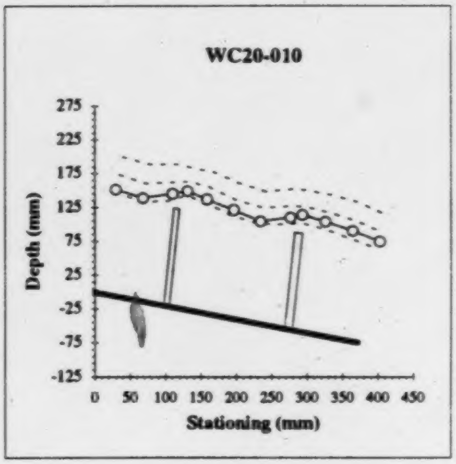
WC20-010
Depth (mm)
275
225
175
125
75
25
-25
-75
-125
0 50 100 150 200 250 300 350 400 450
Stationing (mm)

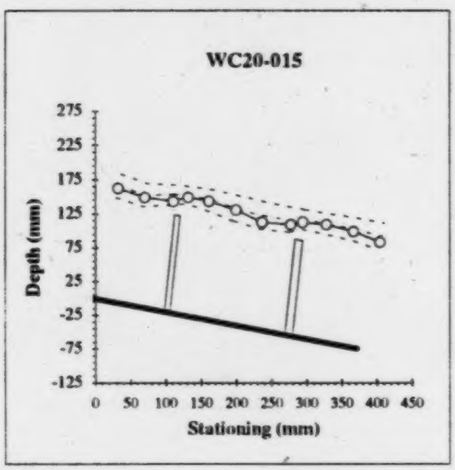
WC20-015
Depth (mm)
275
225
175
125
75
25
-25
-75
-125
0 50 100 150 200 250 300 350 400 450
Stationing (mm)

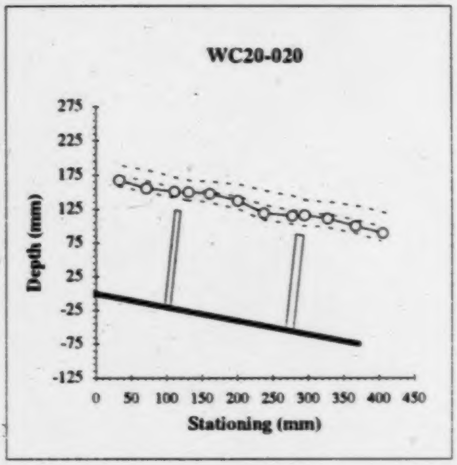
WC20-020
Depth (mm)
275
225
175
125
75
25
-25
-75
-125
0 50 100 150 200 250 300 350 400 450
Stationing (mm)

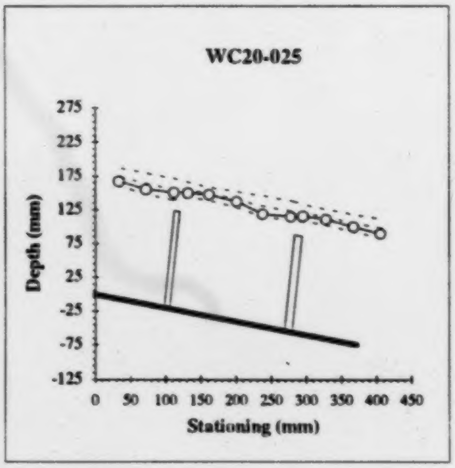
WC20-025
Depth (mm)
275
225
175
125
75
25
-25
-75
-125
0 50 100 150 200 250 300 350 400 450
Stationing (mm)

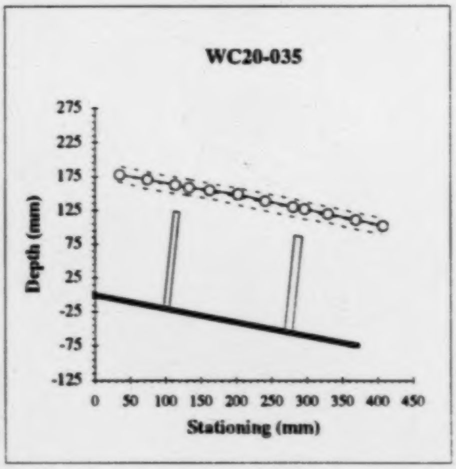
WC20-035
Depth (mm)
275
225
175
125
75
25
-25
-75
-125
0 50 100 150 200 250 300 350 400 450
Stationing (mm)

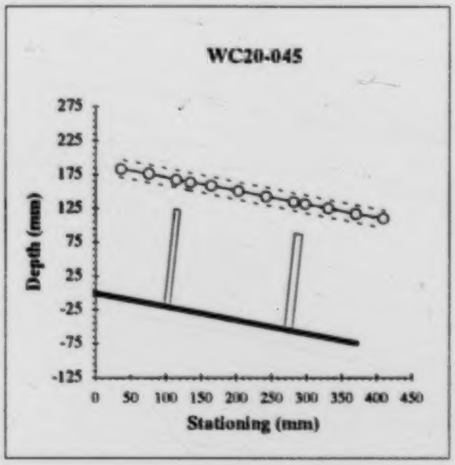
WC20-045
Depth (mm)
275
225
175
125
75
25
-25
-75
-125
0
50
100
150
200
250
300
350
400
450
Stationing (mm)

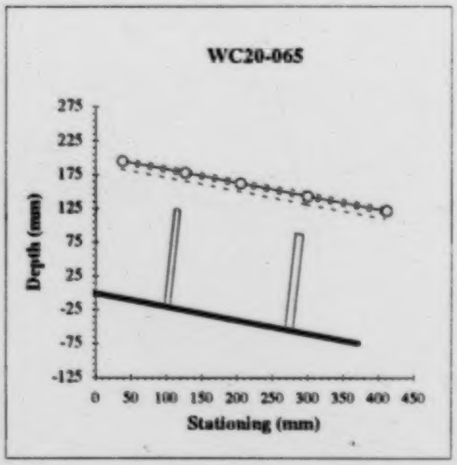
WC20-065
Depth (mm)
275
225
175
125
75
25
-25
-75
-125
0
50
100
150
200
250
300
350
400
450
Stationing (mm)

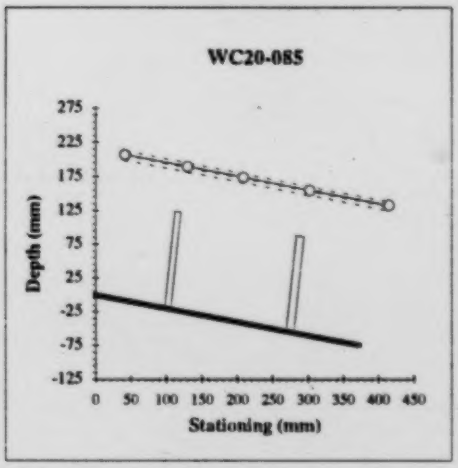
WC20-085
Depth (mm)
275
225
175
125
75
25
-25
-75
-125
0
50
100
150
200
250
300
350
400
450
Stationing (mm)

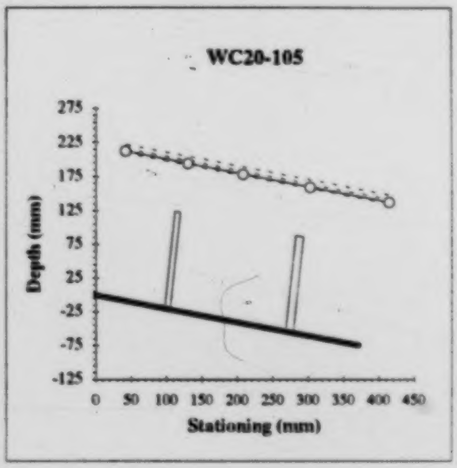
WC20-105
Depth (mm)
275
225
175
125
75
25
-25
-75
-125
0
50
100
150
200
250
300
350
400
450
Stationing (mm)

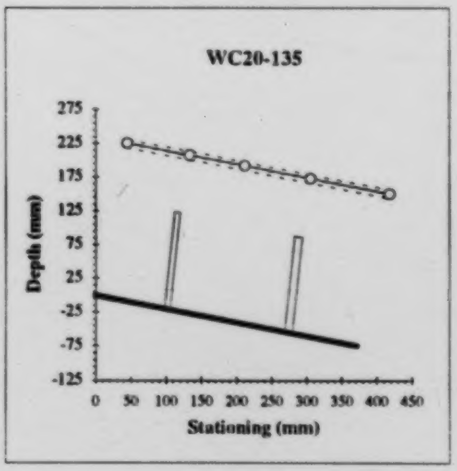
WC20-135
Depth (mm)
275
225
175
125
75
25
-25
-75
-125
0
50
100
150
200
250
300
350
400
450
Stationing (mm)

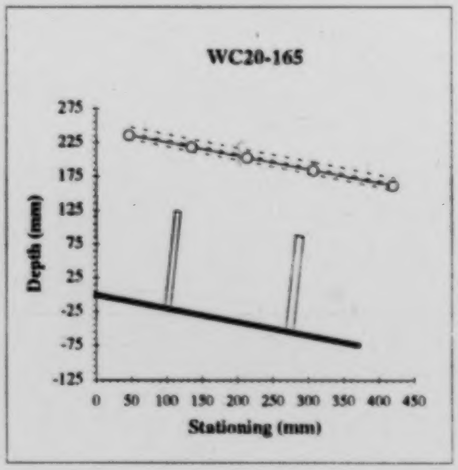
WC20-165
Depth (mm)
275
225
175
125
75
25
-25
-75
-125
0
50
100
150
200
250
300
350
400
450
Stationing (mm)

WC30 - (005 to165 l/s)

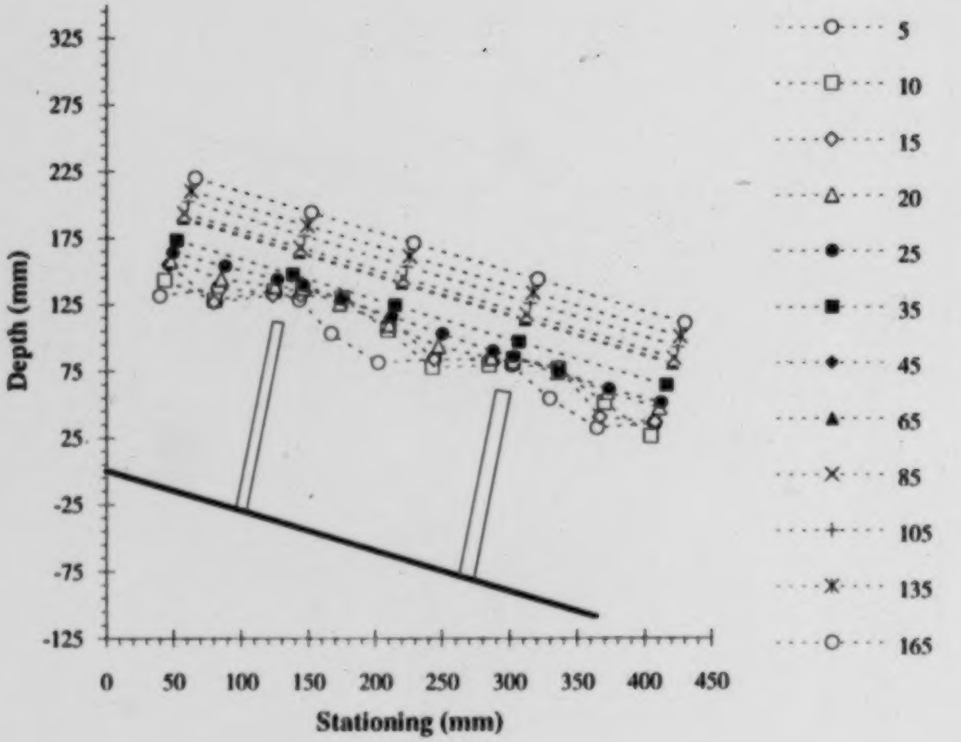

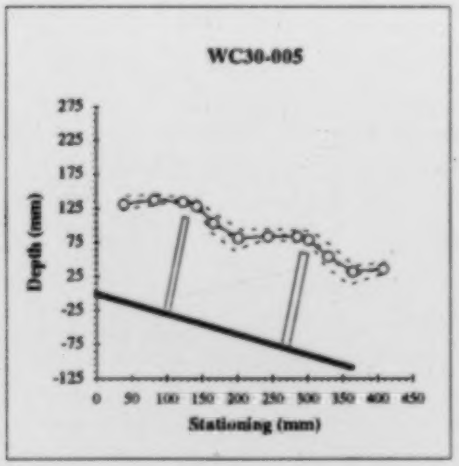
WC30-005

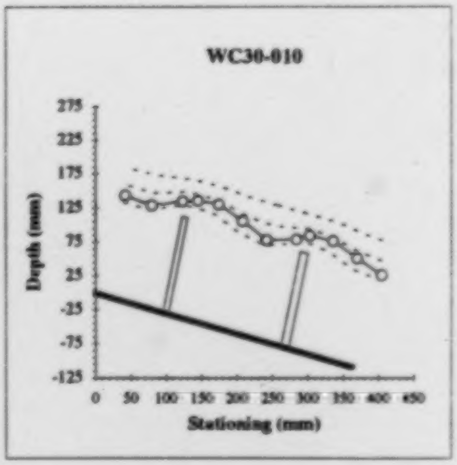
WC30-010

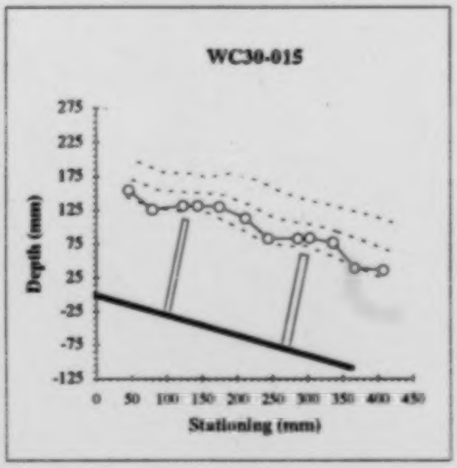
WC30-015

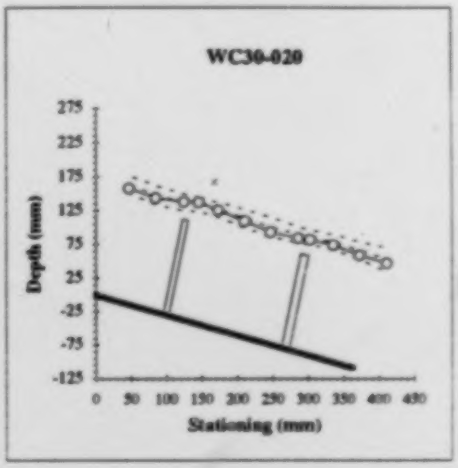
WC30-020

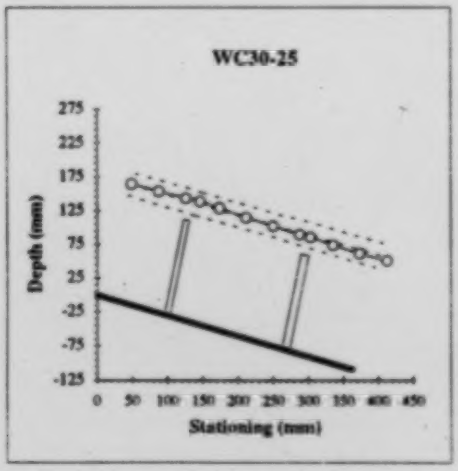
WC30-25

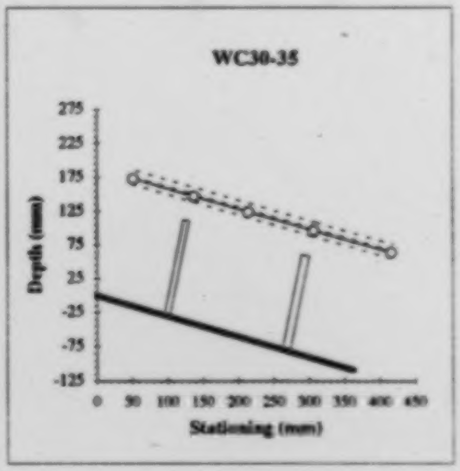
WC30-35

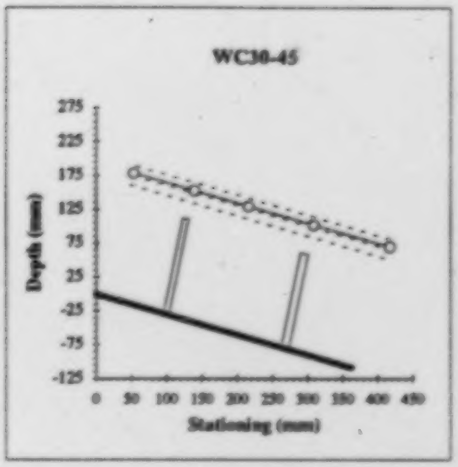
WC30-45
Depth (mm)
275
225
175
125
75
25
-25
-75
-125
0
50
100
150
200
250
300
350
400
450
Stationing (mm)

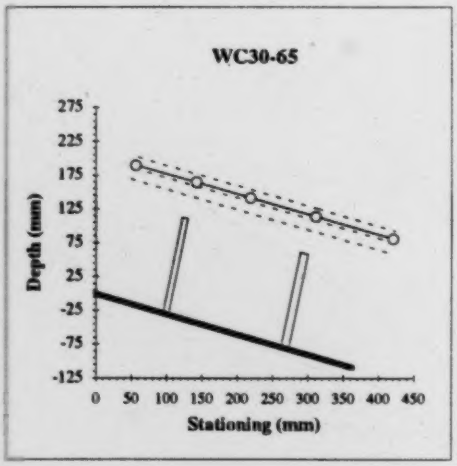
WC30-65
Depth (mm)
275
225
175
125
75
25
-25
-75
-125
0
50
100
150
200
250
300
350
400
450
Stationing (mm)

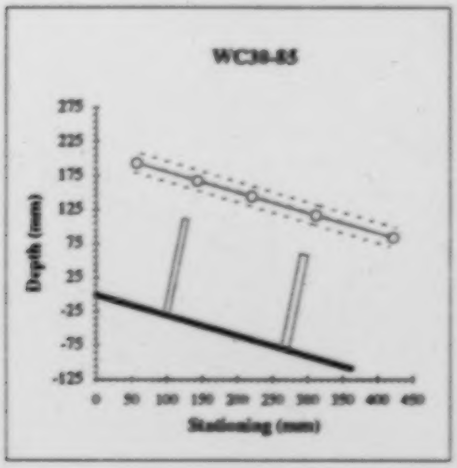
WC30-85
Depth (mm)
275
225
175
125
75
25
-25
-75
-125
0
50
100
150
200
250
300
350
400
450
Stationing (mm)

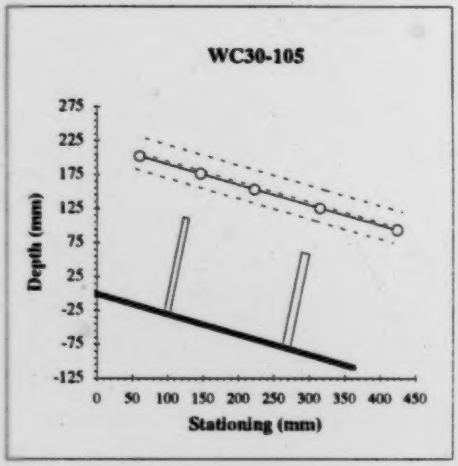
WC30-105
Depth (mm)
275
225
175
125
75
25
-25
-75
-125
0
50
100
150
200
250
300
350
400
450
Stationing (mm)

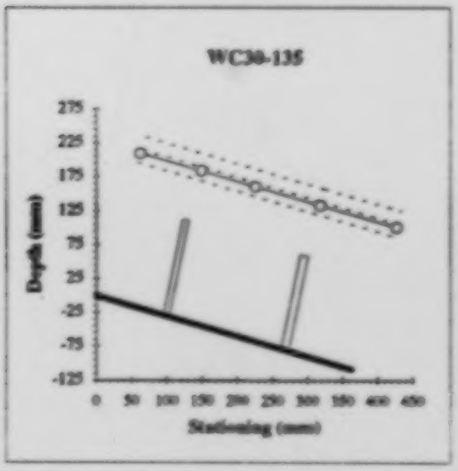
WC30-135
Depth (mm)
275
225
175
125
75
25
-25
-75
-125
0
50
100
150
200
250
300
350
400
450
Stationing (mm)

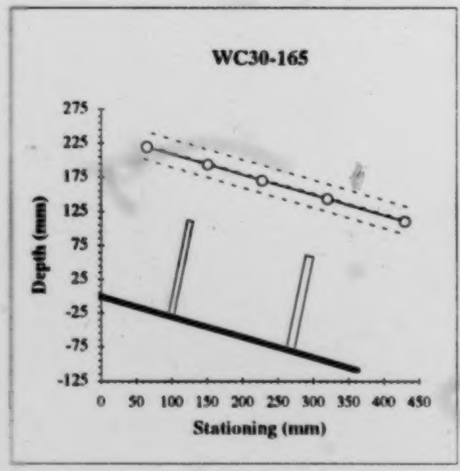
WC30-165
Depth (mm)
275
225
175
125
75
25
-25
-75
-125
0
50
100
150
200
250
300
350
400
450
Stationing (mm)

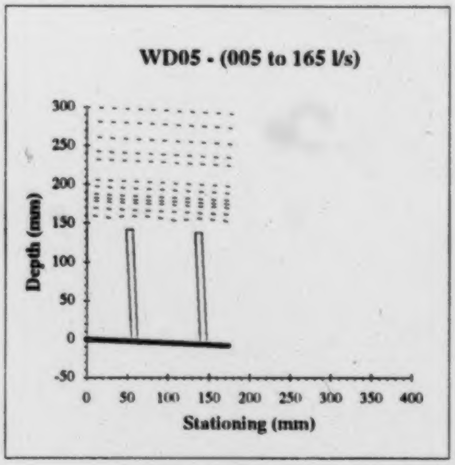

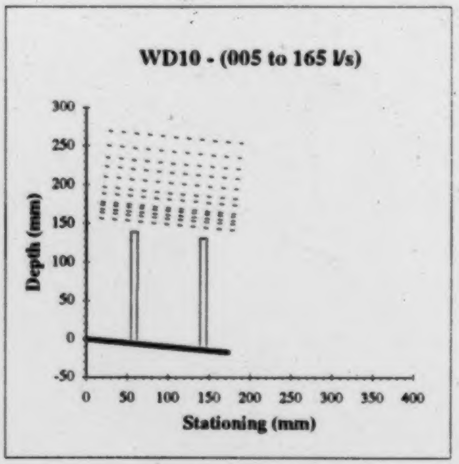

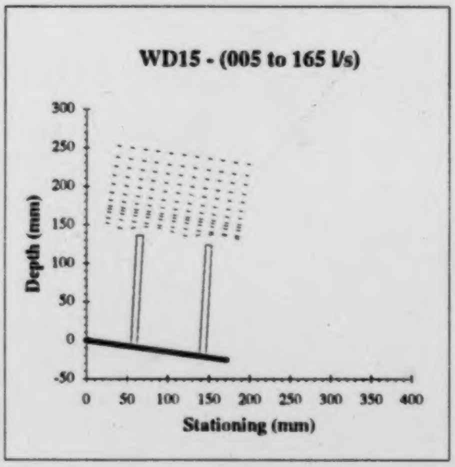

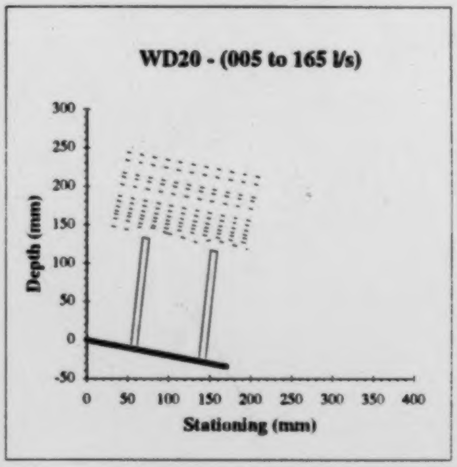

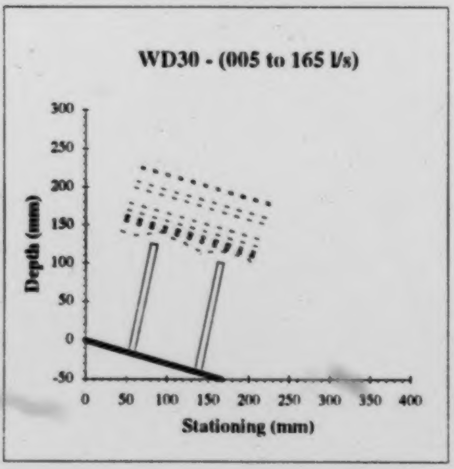

Water Surface Profiles

Full Weir Height

Class 'D' Weir Spacing

5 to 30 % Slope, 5 to 165 l/s

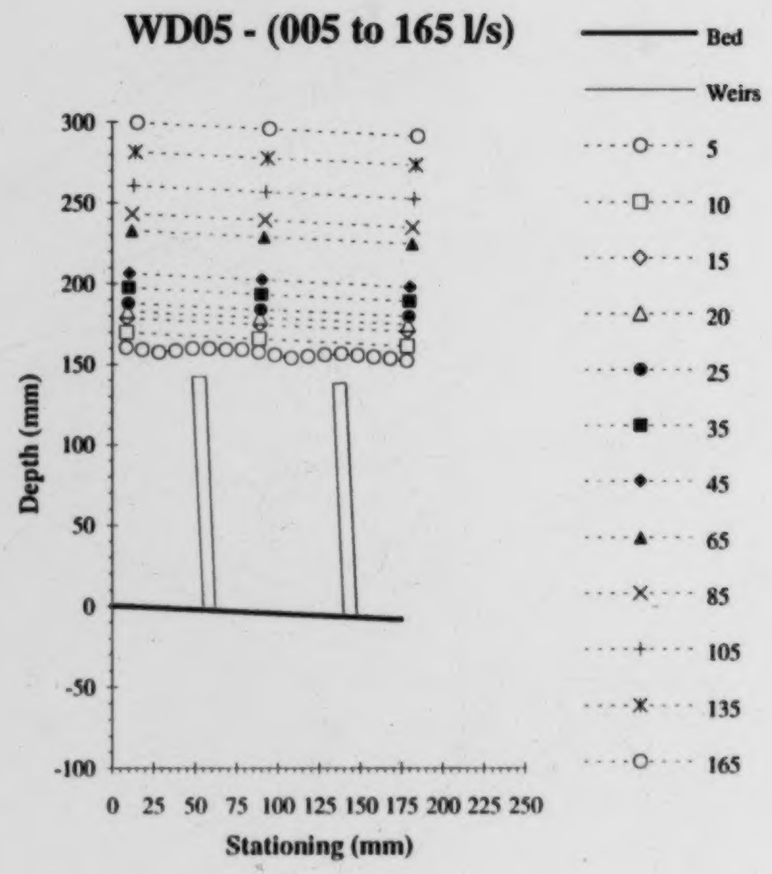
WD05 - (005 to 165 l/s)
Depth (mm)
300
250
200
150
100
50
0
-50
-100
0
25
50
75
100
125
150
175
200
225
250
Stationing (mm)
Bed
Weirs
5
10
15
20
25
35
45
65
85
105
135
165

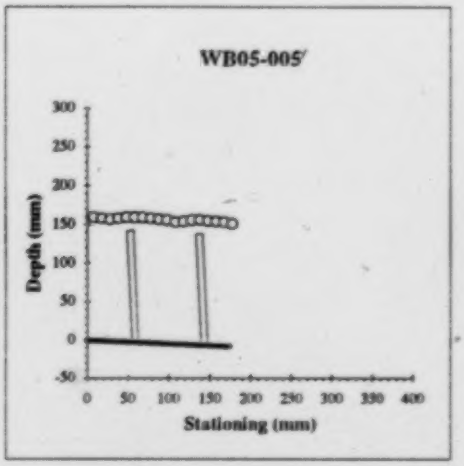
WB05-005

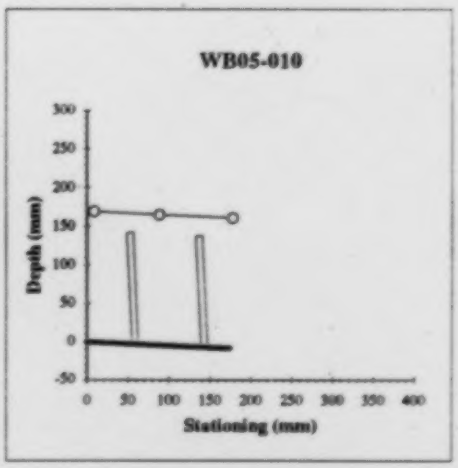
WB05-010

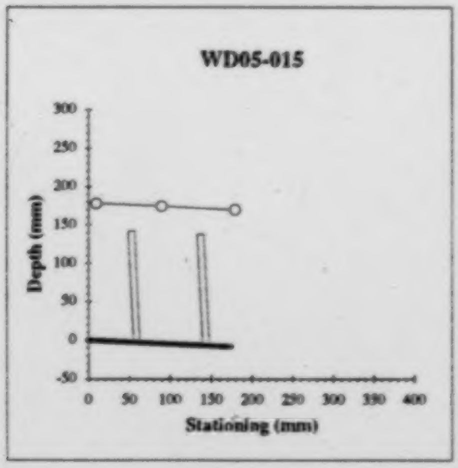
WD05-015

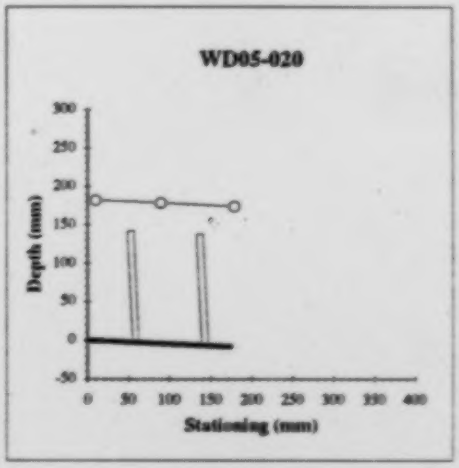
WD05-020

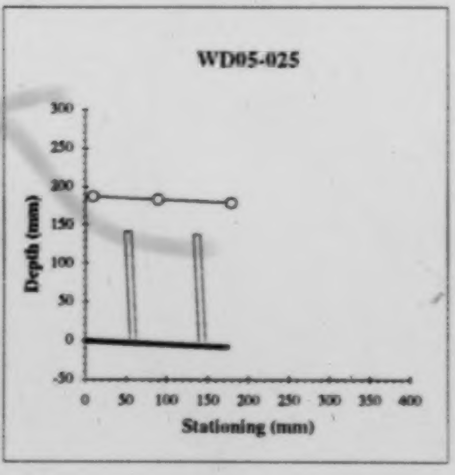
WD05-025

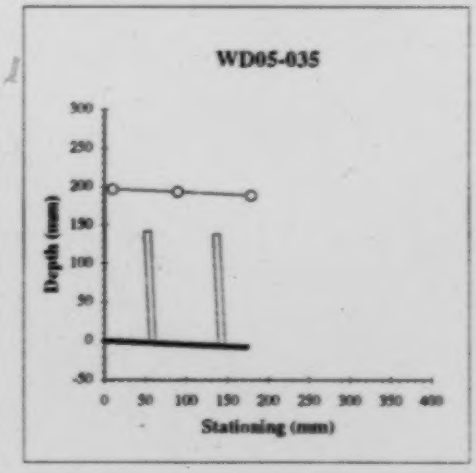
WD05-035

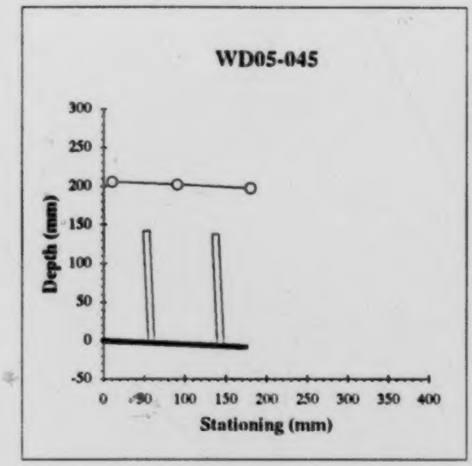
WD05-045

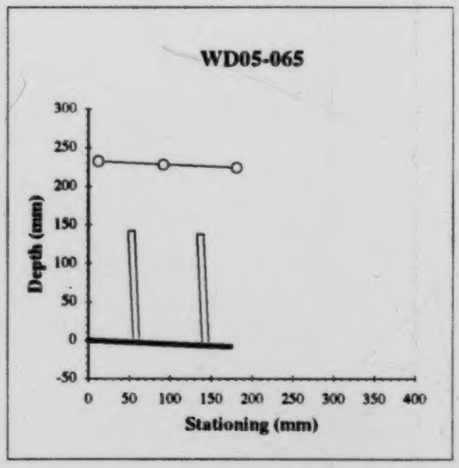
WD05-065

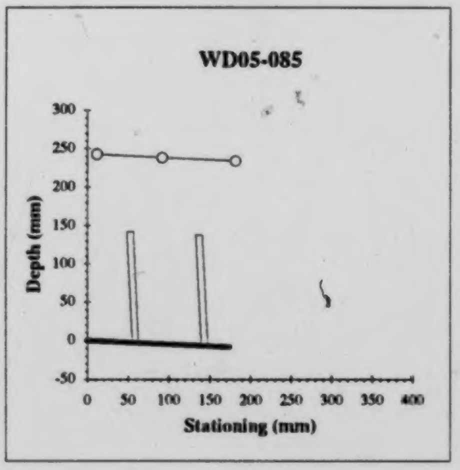
WD05-085

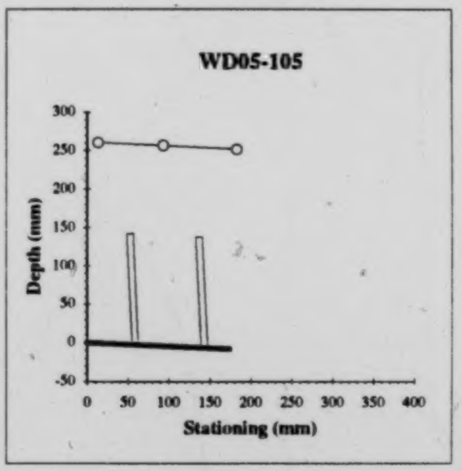
WD05-105

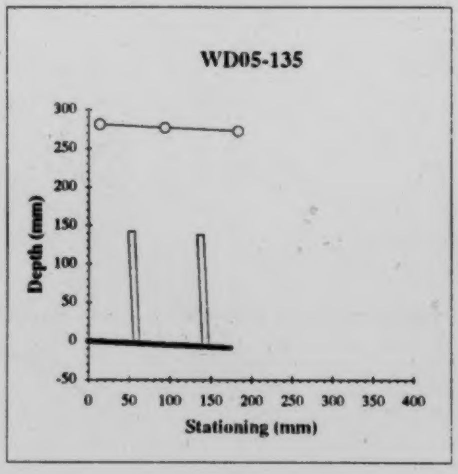
WD05-135

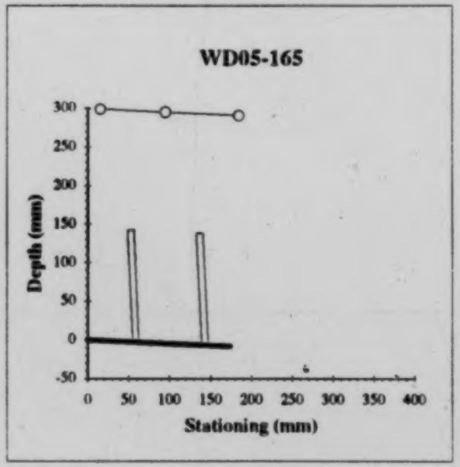
WD05-165

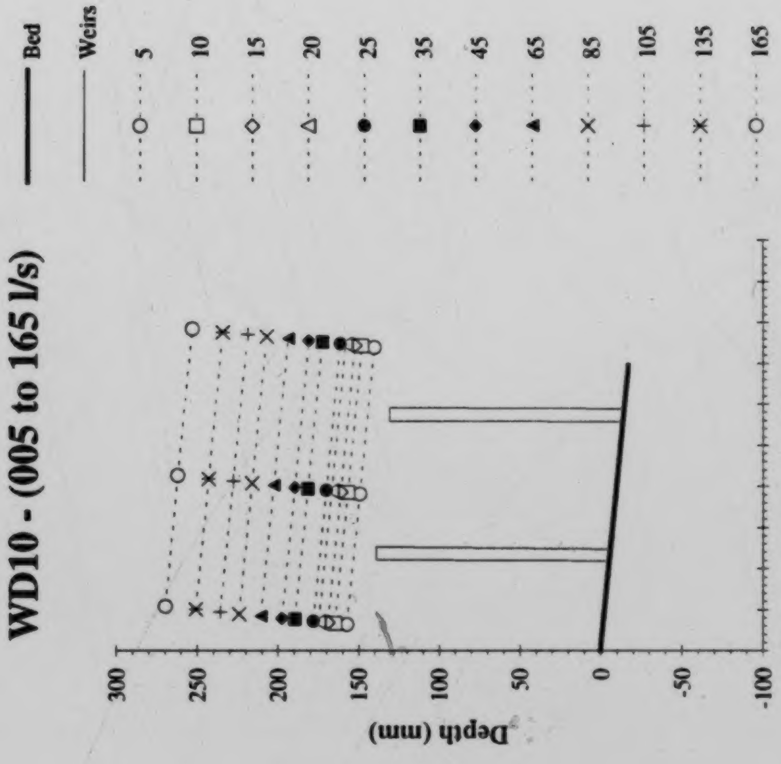

WD10 - (005 to 165 l/s)

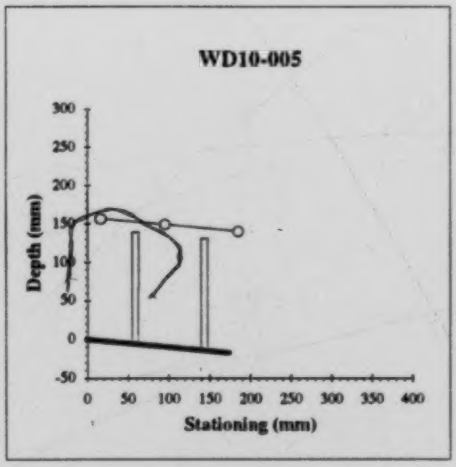
WD10-005
Depth (mm)
300
250
200
150
100
50
0
-50
0
50
100
150
200
250
300
350
400
Stationing (mm)

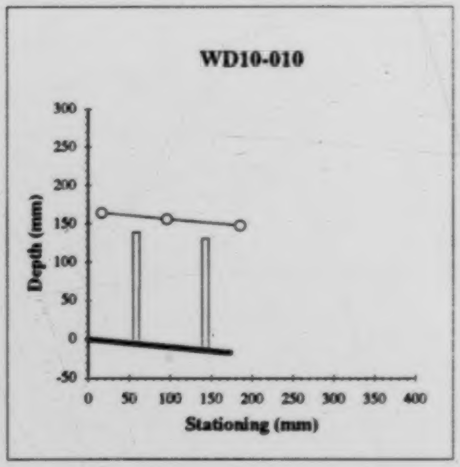
WD10-010
Depth (mm)
300
250
200
150
100
50
0
-50
0
50
100
150
200
250
300
350
400
Stationing (mm)

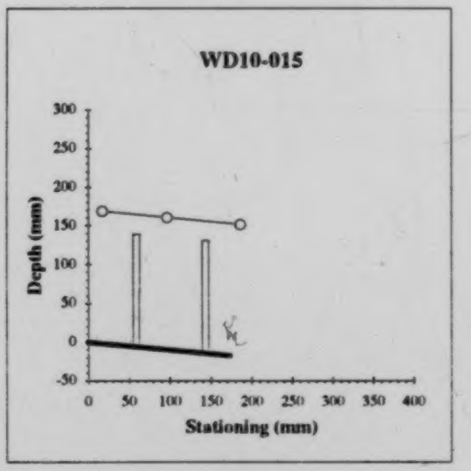
WD10-015
Depth (mm)
300
250
200
150
100
50
0
-50
0
50
100
150
200
250
300
350
400
Stationing (mm)

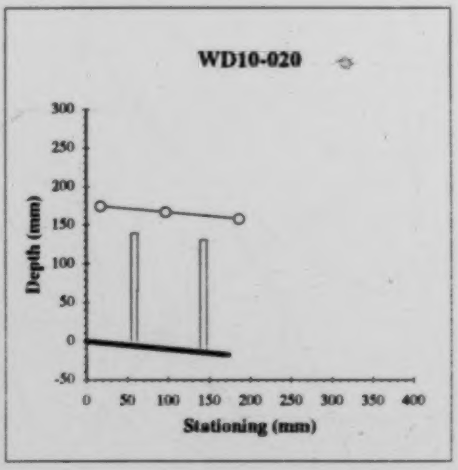
WD10-020
Depth (mm)
300
250
200
150
100
50
0
-50
0
50
100
150
200
250
300
350
400
Stationing (mm)

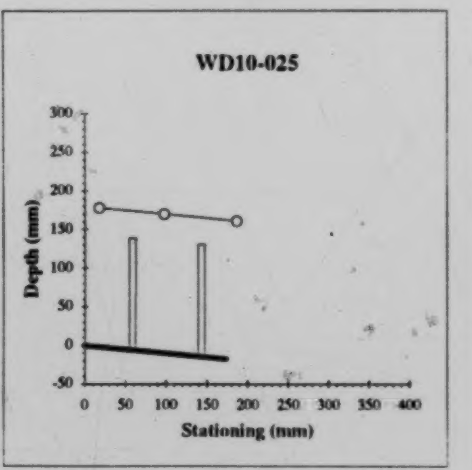
WD10-025
Depth (mm)
300
250
200
150
100
50
0
-50
0
50
100
150
200
250
300
350
400
Stationing (mm)

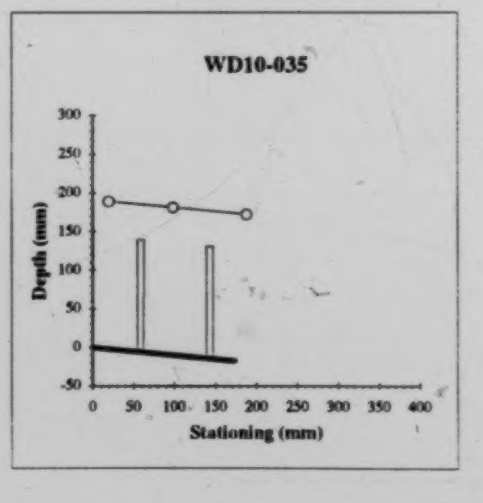
WD10-035
Depth (mm)
300
250
200
150
100
50
0
-50
0
50
100
150
200
250
300
350
400
Stationing (mm)

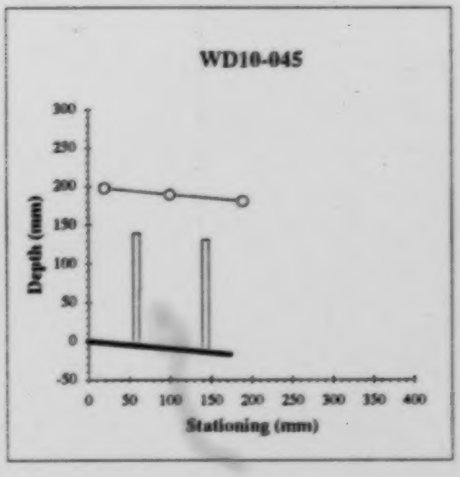
WD10-045

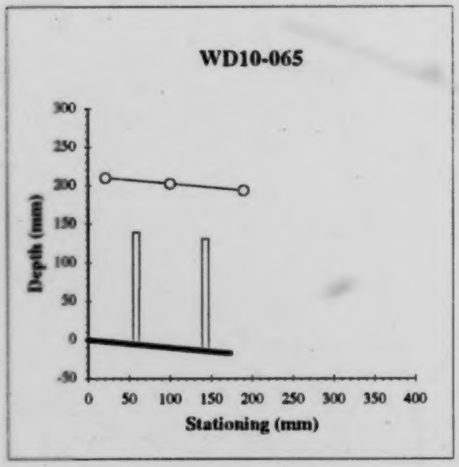
WD10-065

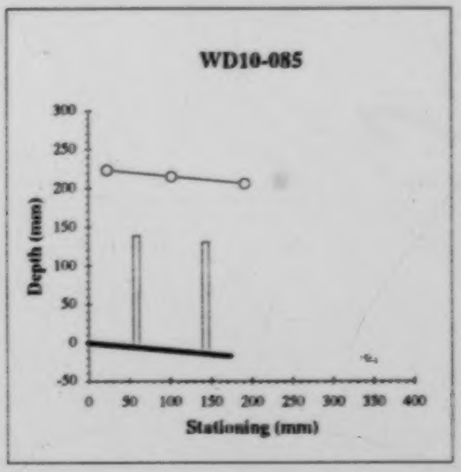
WD10-085

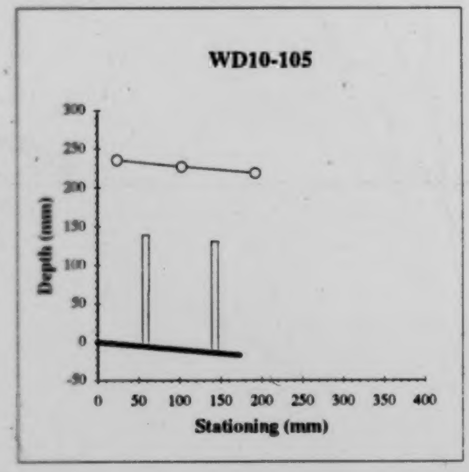
WD10-105

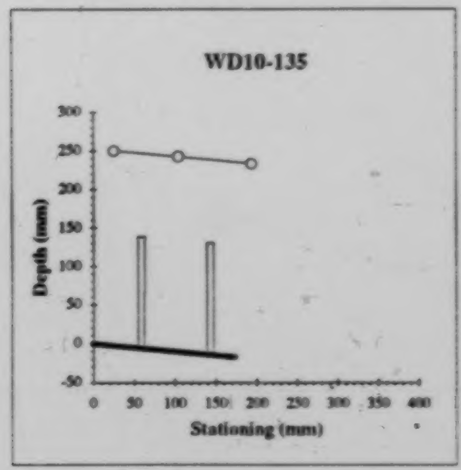
WD10-135

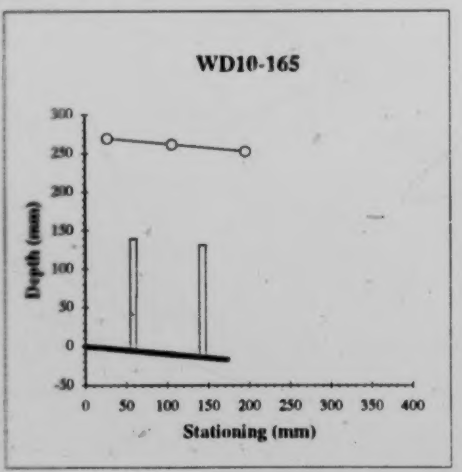
WD10-165

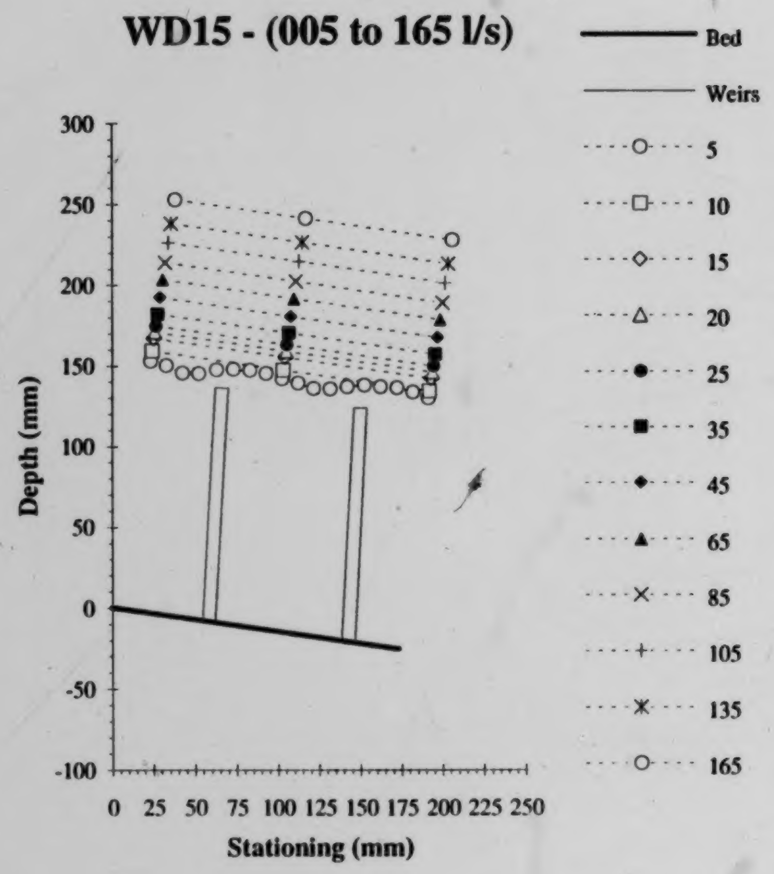
WD15 - (005 to 165 l/s)
Depth (mm)
300
250
200
150
100
50
0
-50
-100
0 25 50 75 100 125 150 175 200 225 250
Stationing (mm)
Bed
Weirs
5
10
15
20
25
35
45
65
85
105
135
165

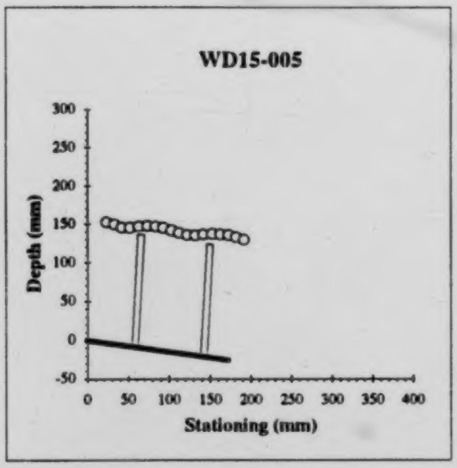
WD15-005
Depth (mm)
300
250
200
150
100
50
0
-50
0
50
100
150
200
250
300
350
400
Stationing (mm)

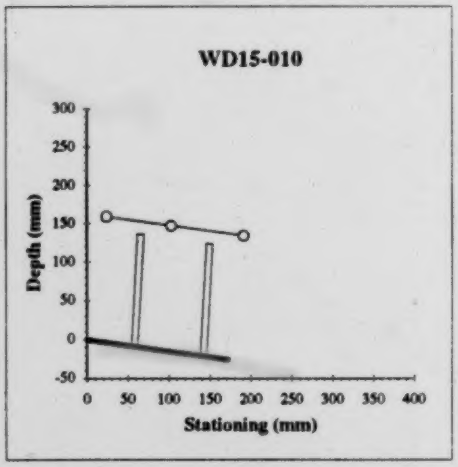
WD15-010
Depth (mm)
300
250
200
150
100
50
0
-50
0
50
100
150
200
250
300
350
400
Stationing (mm)

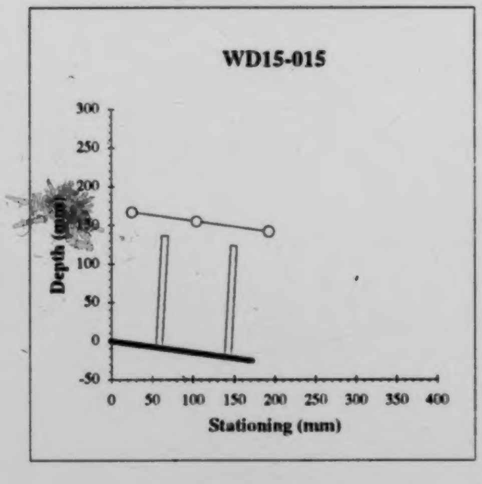
WD15-015
Depth (mm)
300
250
200
150
100
50
0
-50
0
50
100
150
200
250
300
350
400
Stationing (mm)

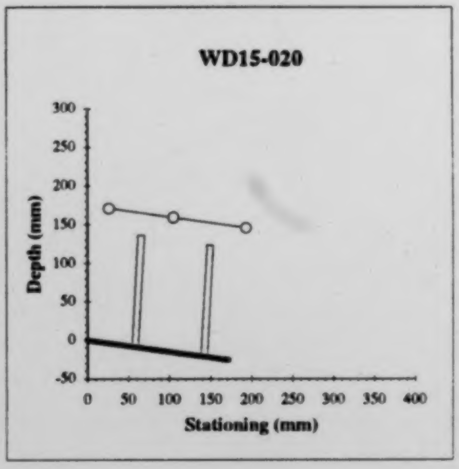
WD15-020
Depth (mm)
300
250
200
150
100
50
0
-50
0
50
100
150
200
250
300
350
400
Stationing (mm)

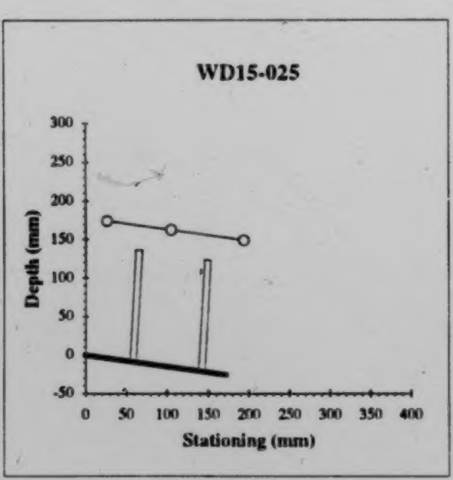
WD15-025
Depth (mm)
300
250
200
150
100
50
0
-50
0
50
100
150
200
250
300
350
400
Stationing (mm)

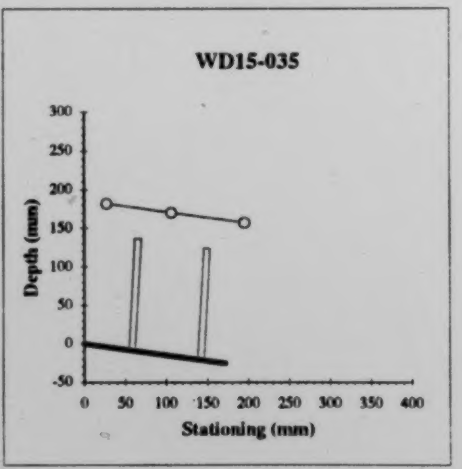
WD15-035
Depth (mm)
300
250
200
150
100
50
0
-50
0
50
100
150
200
250
300
350
400
Stationing (mm)

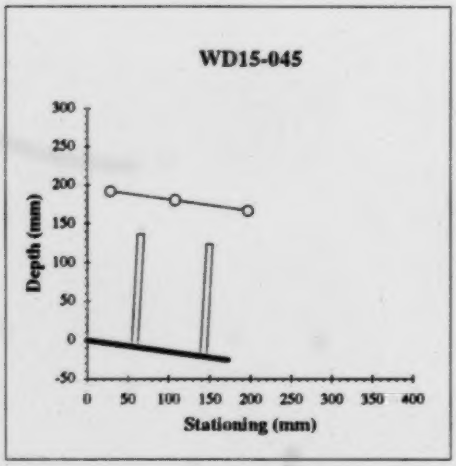
WD15-045
Depth (mm)
300
250
200
150
100
50
0
-50
0 50 100 150 200 250 300 350 400
Stationing (mm)

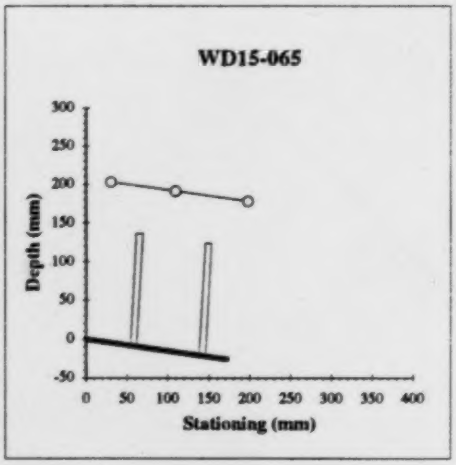
WD15-065
Depth (mm)
300
250
200
150
100
50
0
-50
0 50 100 150 200 250 300 350 400
Stationing (mm)

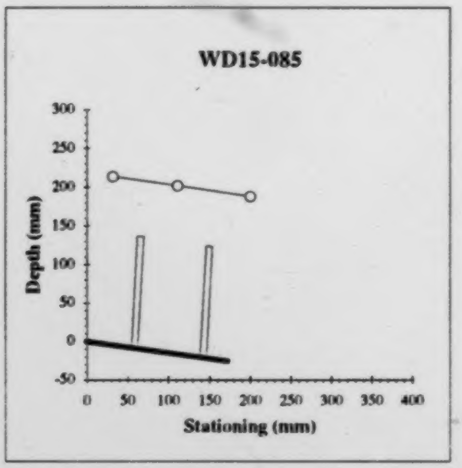
WD15-085
Depth (mm)
300
250
200
150
100
50
0
-50
0 50 100 150 200 250 300 350 400
Stationing (mm)

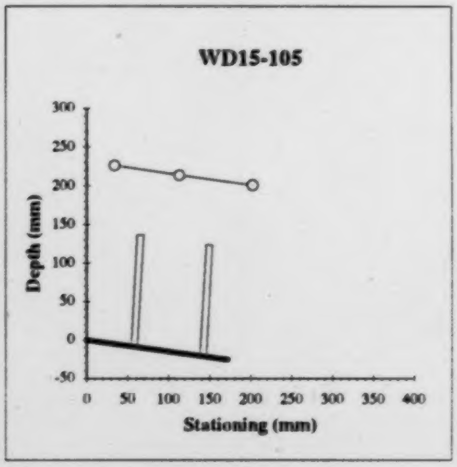
WD15-105
Depth (mm)
300
250
200
150
100
50
0
-50
0 50 100 150 200 250 300 350 400
Stationing (mm)

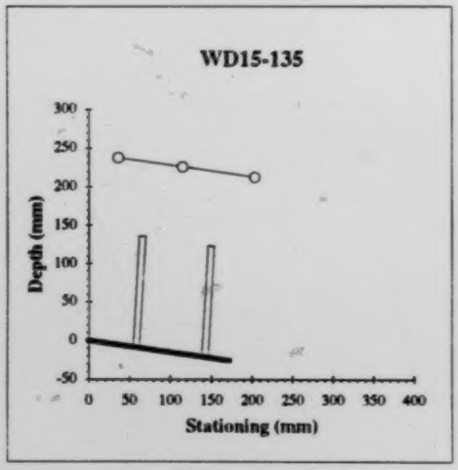
WD15-135
Depth (mm)
300
250
200
150
100
50
0
-50
0 50 100 150 200 250 300 350 400
Stationing (mm)

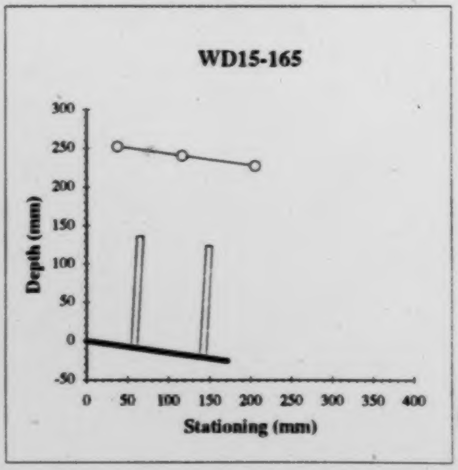
WD15-165
Depth (mm)
300
250
200
150
100
50
0
-50
0 50 100 150 200 250 300 350 400
Stationing (mm)

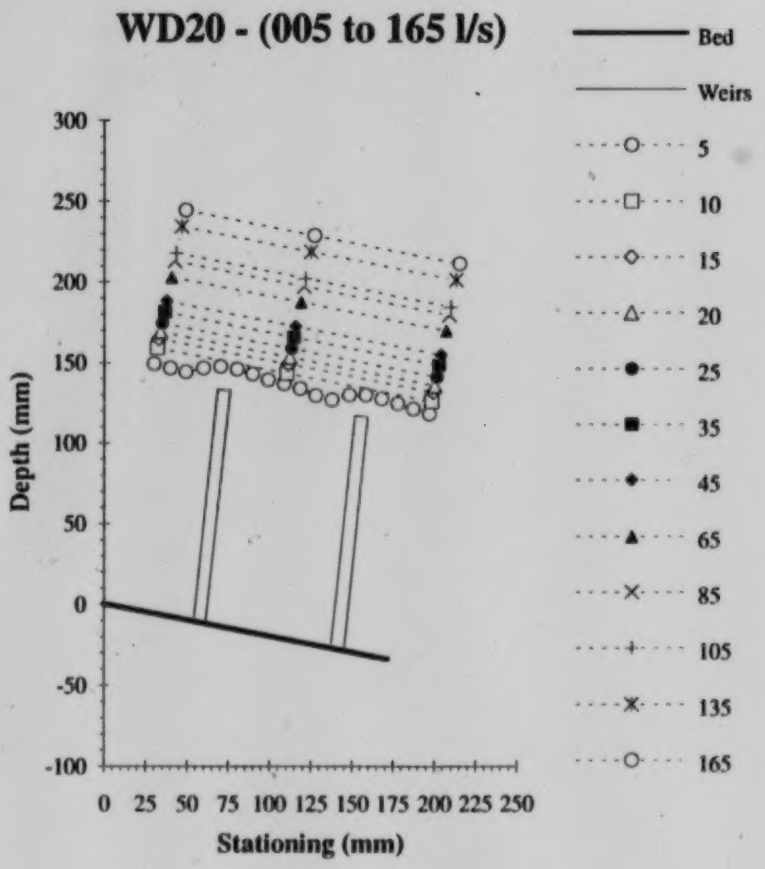
WD20 - (005 to 165 l/s)
Depth (mm)
300
250
200
150
100
50
0
-50
-100
Stationing (mm)
0
25
50
75
100
125
150
175
200
225
250
Bed
Weirs
5
10
15
20
25
35
45
65
85
105
135
165

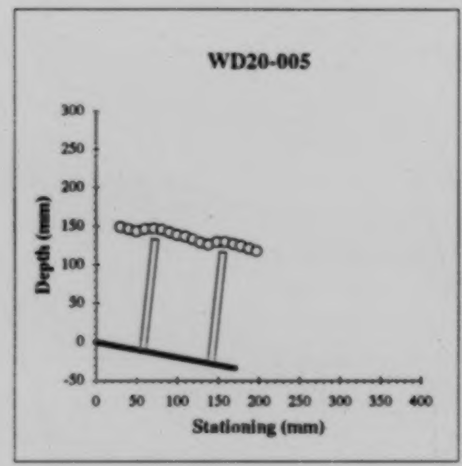
WD20-005
Depth (mm)
300
250
200
150
100
50
0
-50
0
50
100
150
200
250
300
350
400
Stationing (mm)

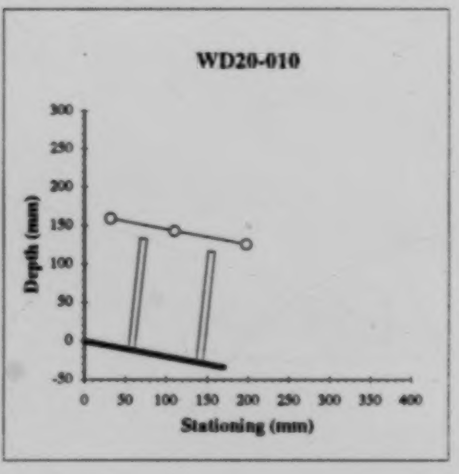
WD20-010
Depth (mm)
300
250
200
150
100
50
0
-50
0
50
100
150
200
250
300
350
400
Stationing (mm)

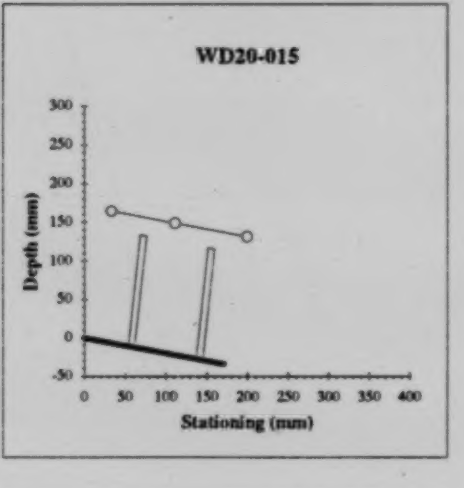
WD20-015
Depth (mm)
300
250
200
150
100
50
0
-50
0
50
100
150
200
250
300
350
400
Stationing (mm)

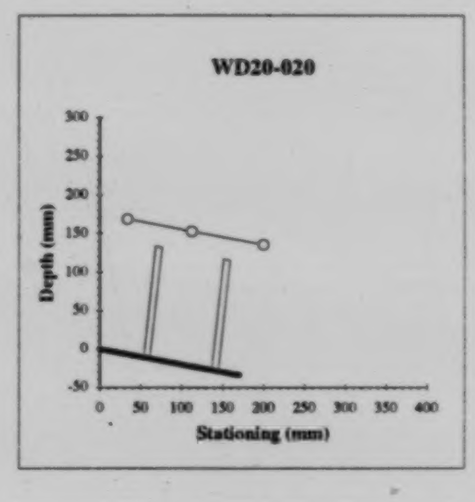
WD20-020
Depth (mm)
300
250
200
150
100
50
0
-50
0
50
100
150
200
250
300
350
400
Stationing (mm)

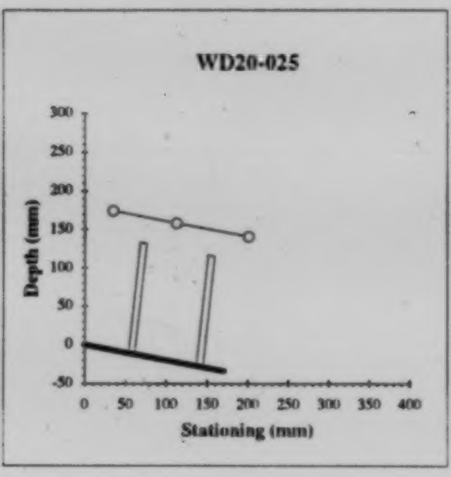
WD20-025
Depth (mm)
300
250
200
150
100
50
0
-50
0
50
100
150
200
250
300
350
400
Stationing (mm)

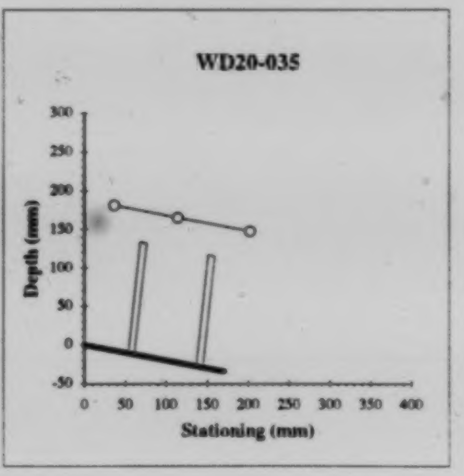
WD20-035
Depth (mm)
300
250
200
150
100
50
0
-50
0
50
100
150
200
250
300
350
400
Stationing (mm)

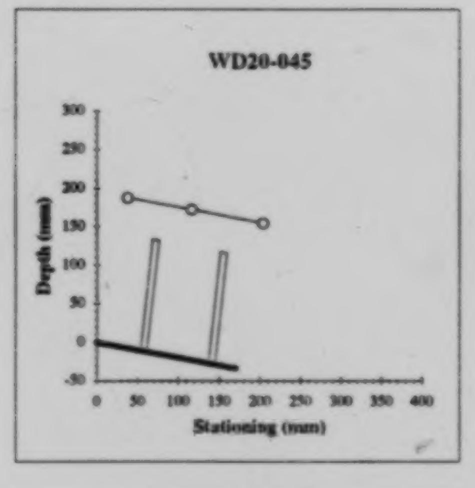
WD20-045

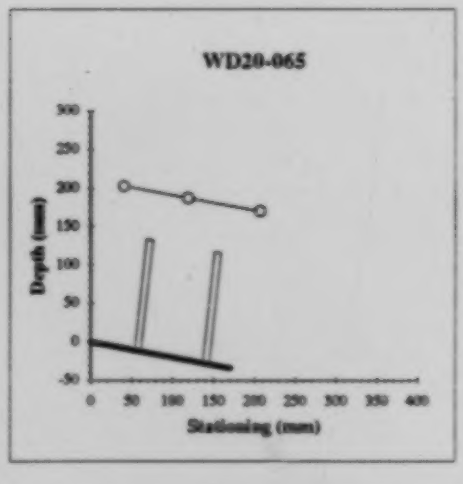
WD20-065

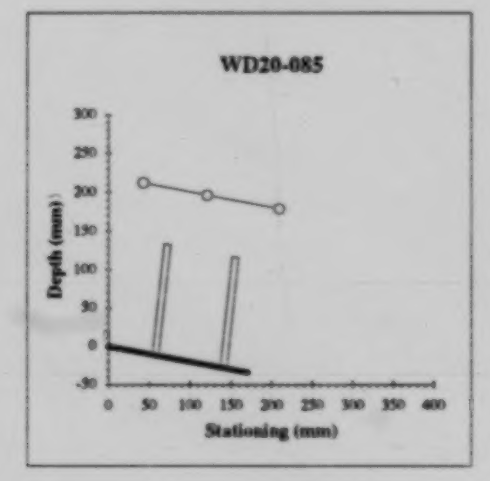
WD20-085

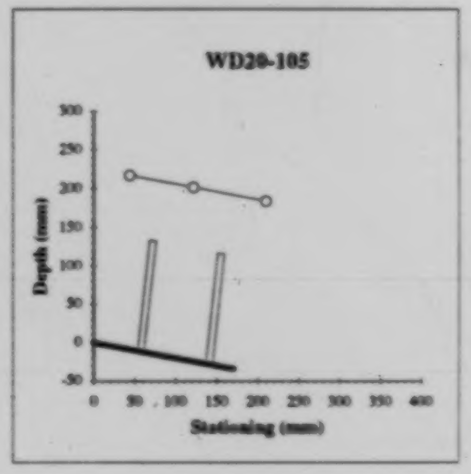
WD20-105

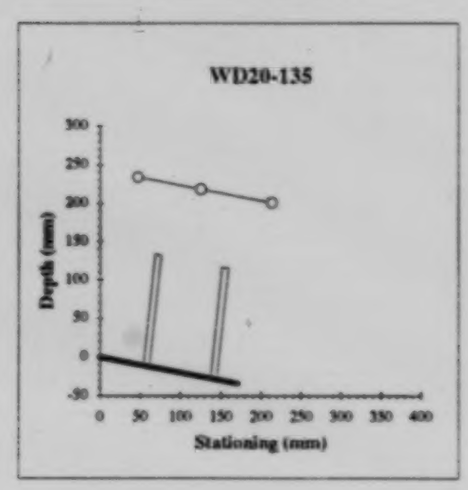
WD20-135

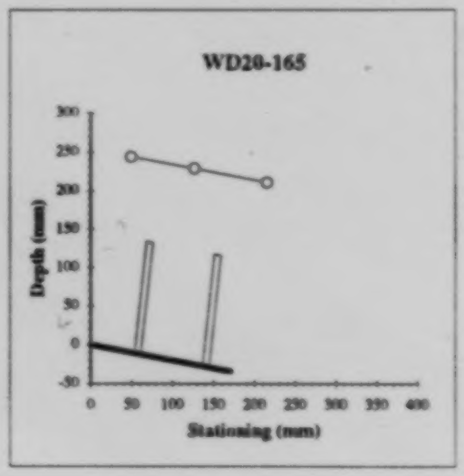
WD20-165

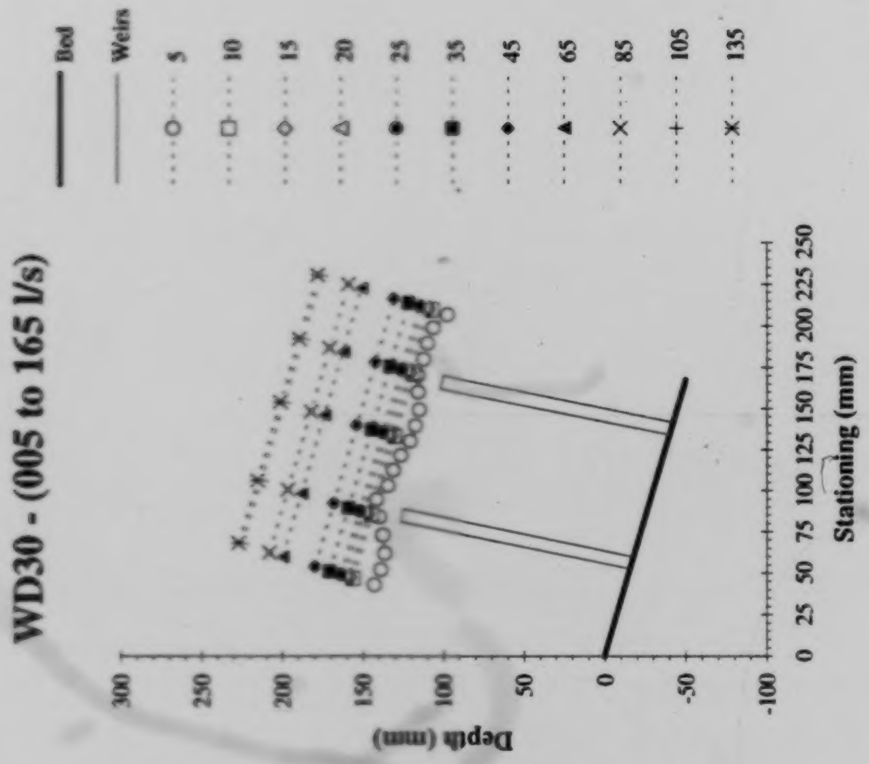
WD30 - (005 to 165 l/s)
Depth (mm)
300
250
200
150
100
50
0
-50
-100
Stationing (mm)
0
25
50
75
100
125
150
175
200
225
250
Bed
Weirs
5
10
15
20
25
35
45
65
85
105
135

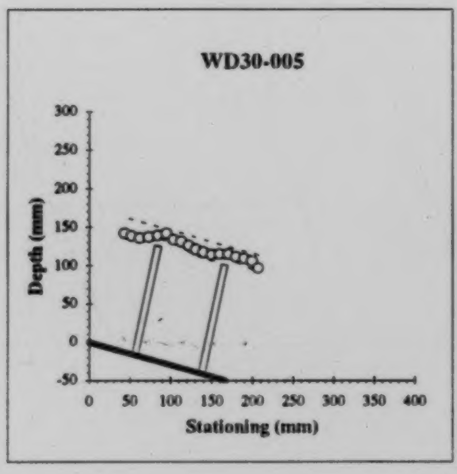
WD30-005

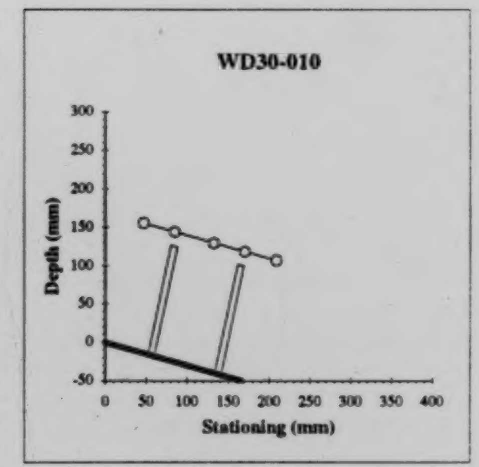
WD30-010

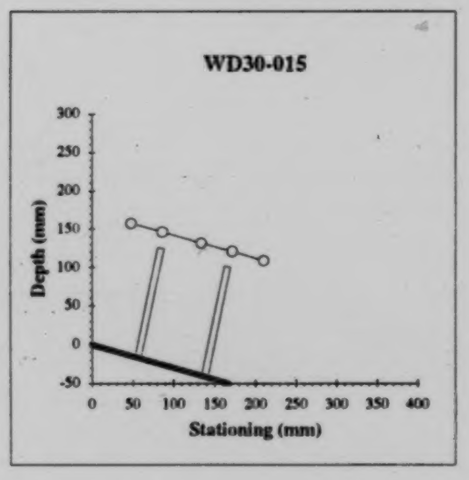
WD30-015

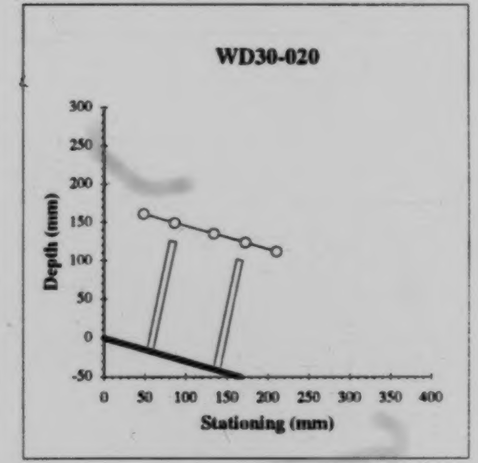
WD30-020

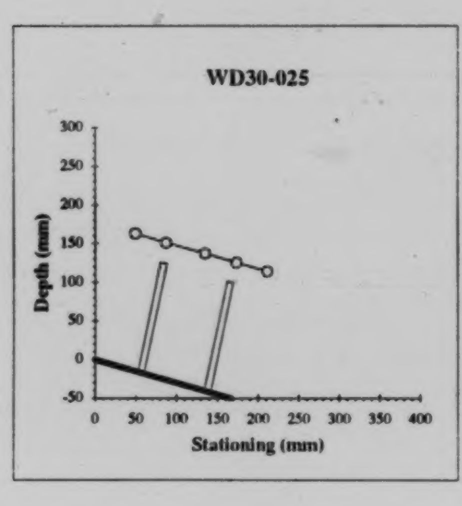
WD30-025

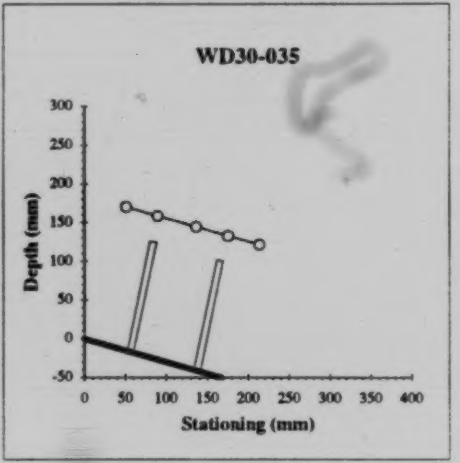
WD30-035

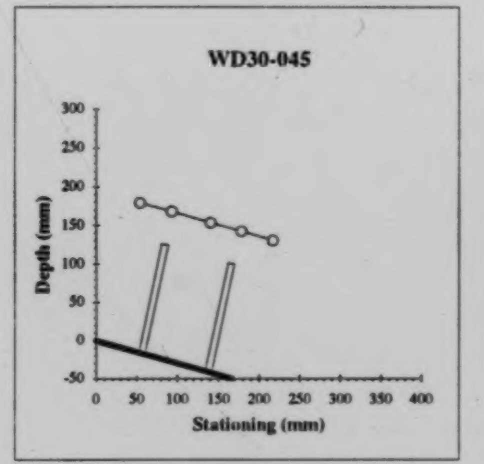
WD30-045
Depth (mm)
300
250
200
150
100
50
0
-50
0
50
100
150
200
250
300
350
400
Stationing (mm)

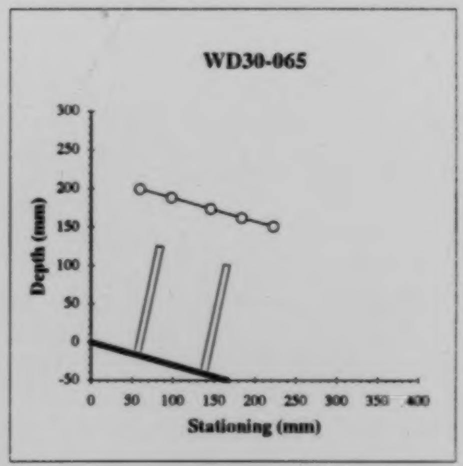
WD30-065
Depth (mm)
300
250
200
150
100
50
0
-50
0
50
100
150
200
250
300
350
400
Stationing (mm)

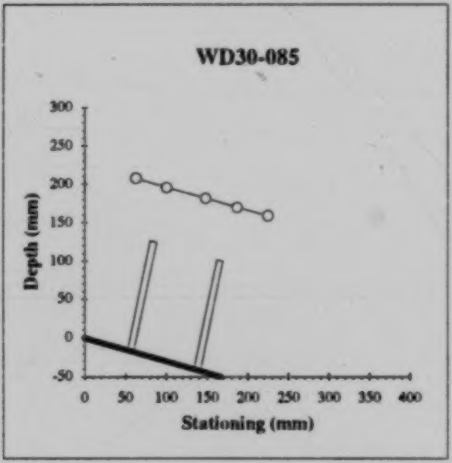
WD30-085
Depth (mm)
300
250
200
150
100
50
0
-50
0
50
100
150
200
250
300
350
400
Stationing (mm)

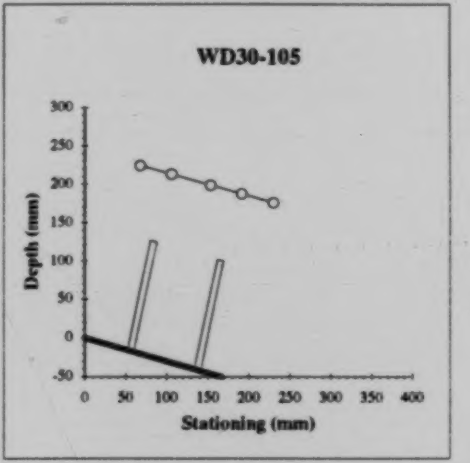
WD30-105
Depth (mm)
300
250
200
150
100
50
0
-50
0
50
100
150
200
250
300
350
400
Stationing (mm)

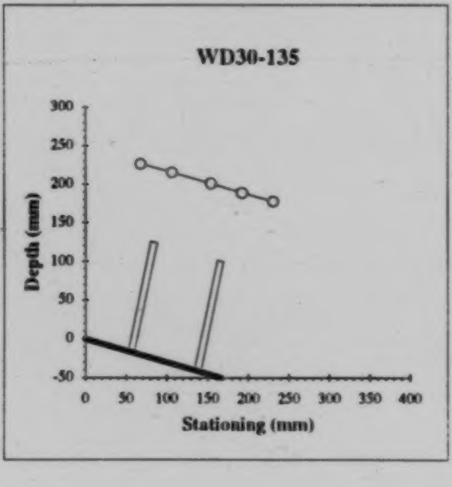
WD30-135
Depth (mm)
300
250
200
150
100
50
0
-50
0
50
100
150
200
250
300
350
400
Stationing (mm)

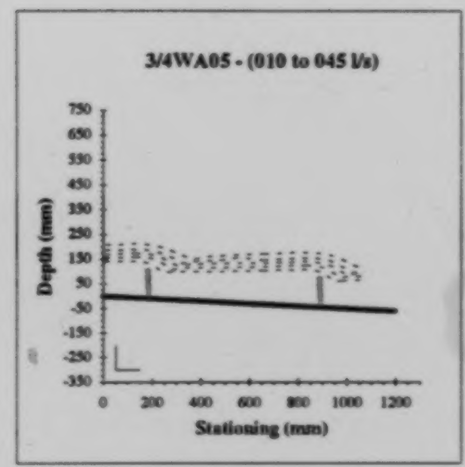
3/4WA05 - (010 to 045 l/s)

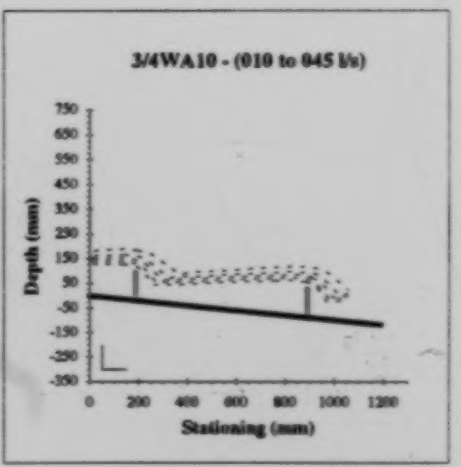
3/4WA10 - (010 to 045 l/s)

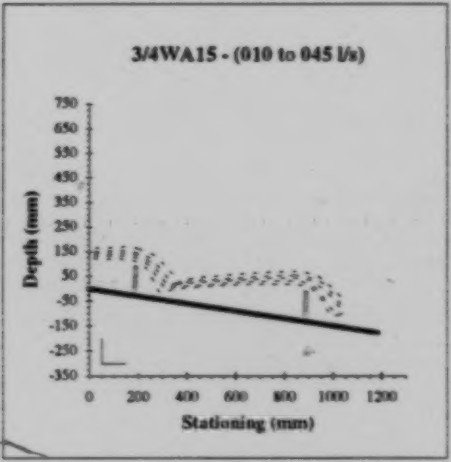
3/4WA15 - (010 to 045 l/s)

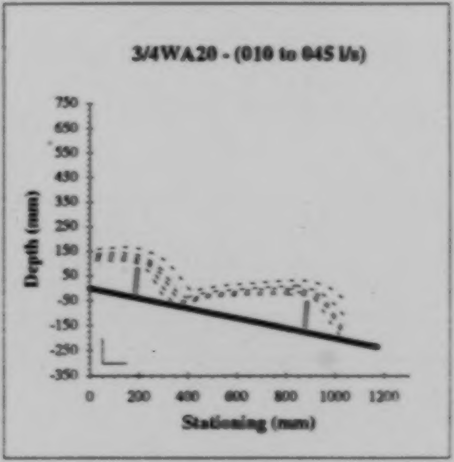
3/4WA20 - (010 to 045 l/s)

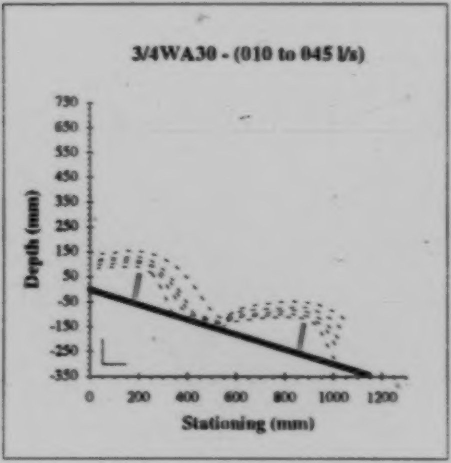
3/4WA30 - (010 to 045 l/s)

Water Surface Profiles

Three Quarter Weir Height

Class 'A' Weir Spacing

5 to 30 % Slope, 10 to 35 l/s

3/4WA05 - (010 to 045 l/s)

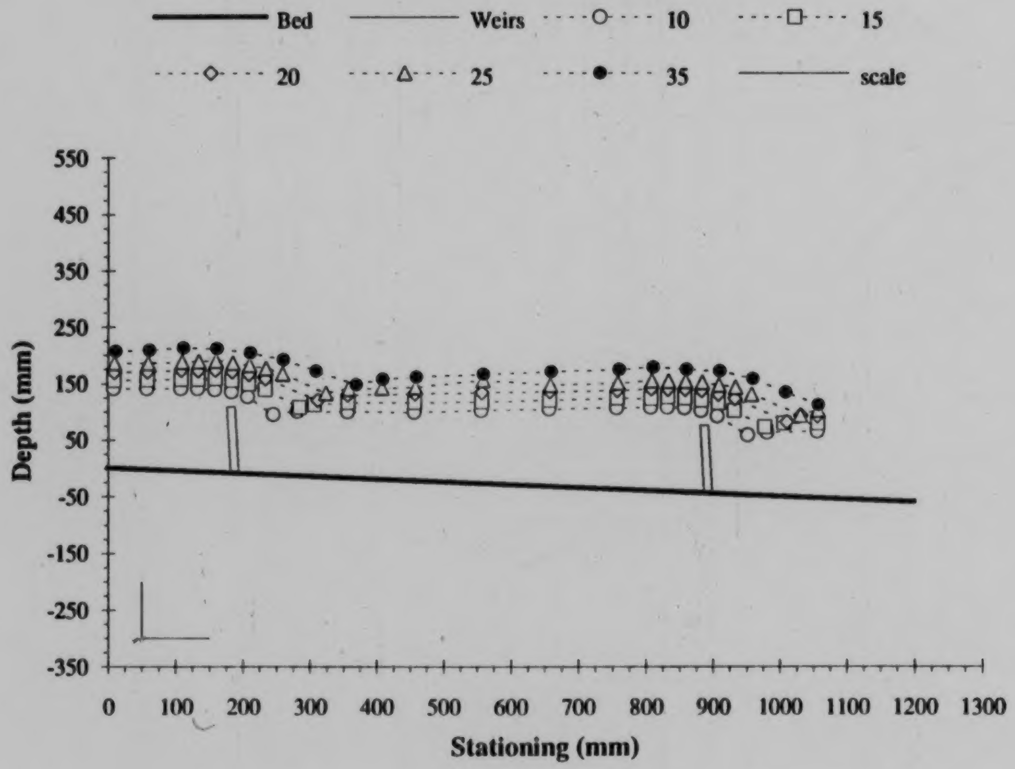

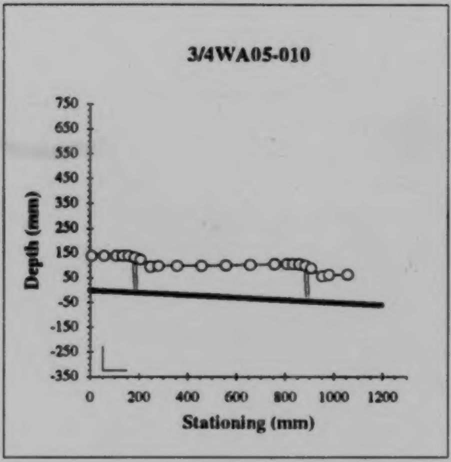

3/4WA05-010

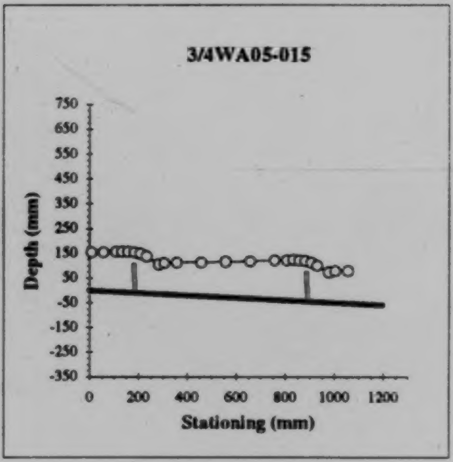

3/4WA05-015

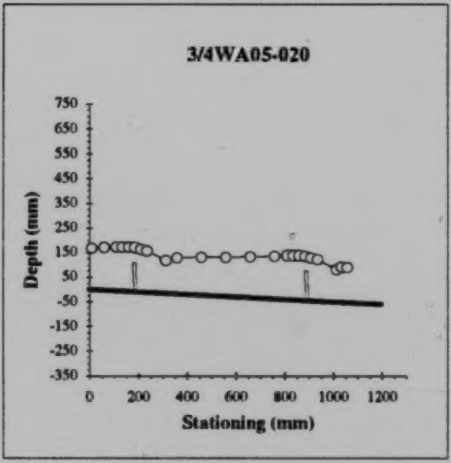

3/4WA05-020

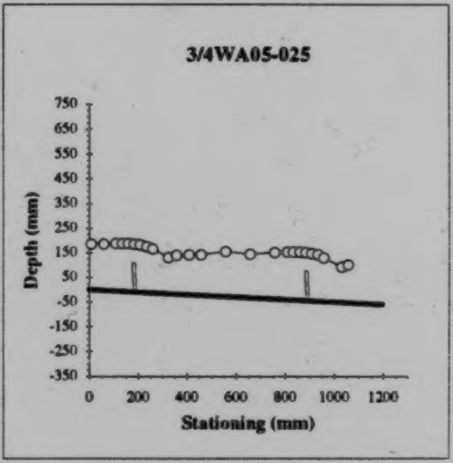

3/4WA05-025

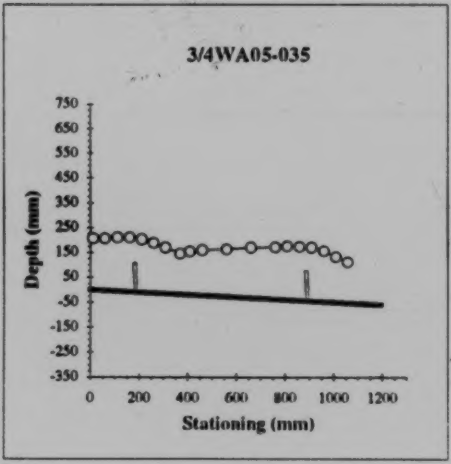

3/4WA05-035

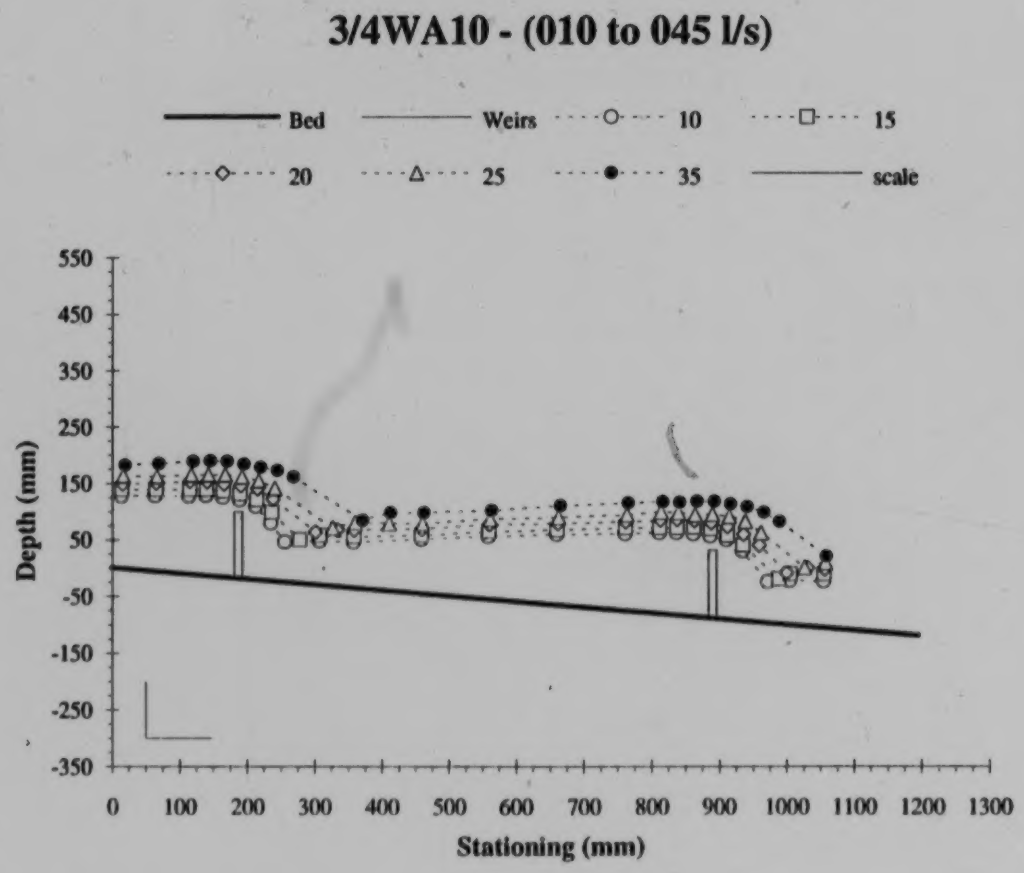
3/4WA10 - (010 to 045 l/s)
Bed
Weirs
10
15
20
25
35
scale
Depth (mm)
550
450
350
250
150
50
-50
-150
-250
-350
Stationing (mm)
0
100
200
300
400
500
600
700
800
900
1000
1100
1200
1300

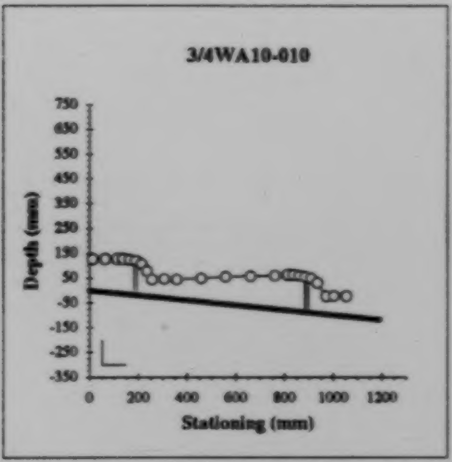
3/4WA10-010

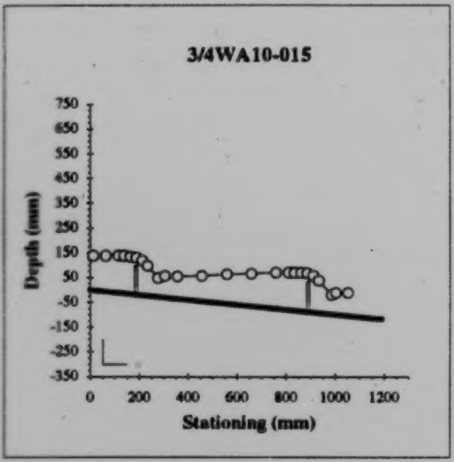
3/4WA10-015

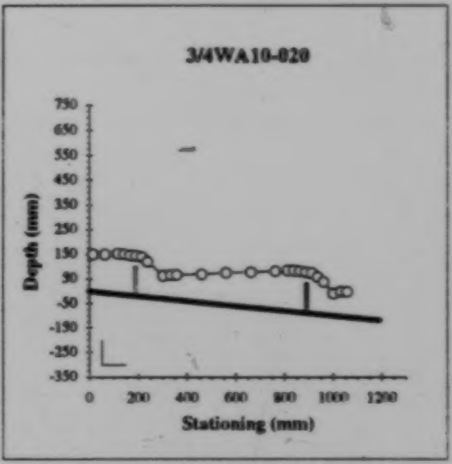
3/4WA10-020

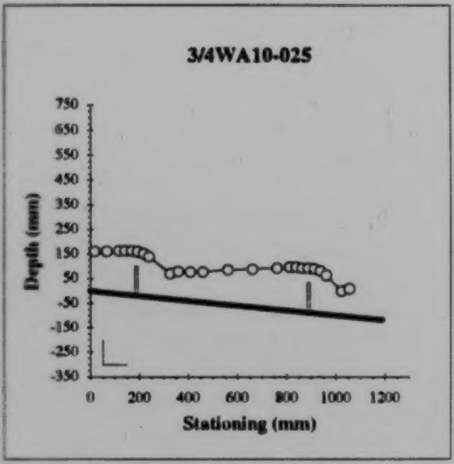
3/4WA10-025

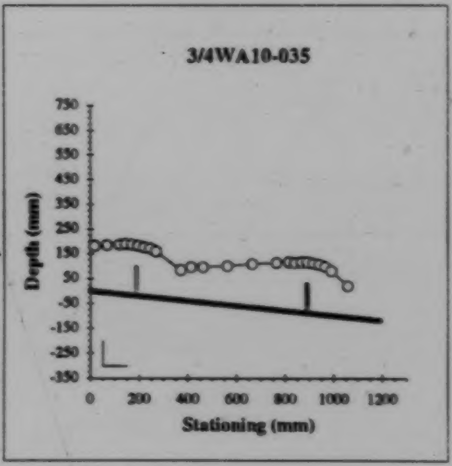
3/4WA10-035

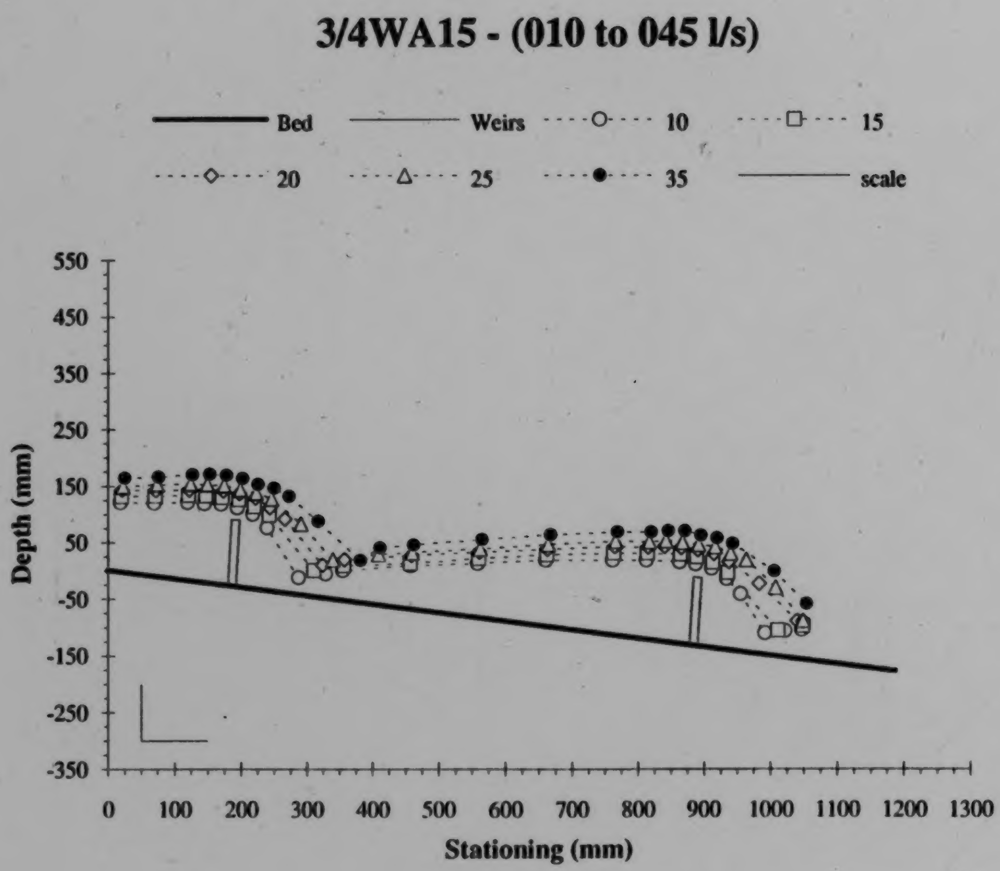
3/4WA15 - (010 to 045 l/s)
Bed
Weirs
10
15
20
25
35
scale
Depth (mm)
550
450
350
250
150
50
-50
-150
-250
-350
0
100
200
300
400
500
600
700
800
900
1000
1100
1200
1300
Stationing (mm)

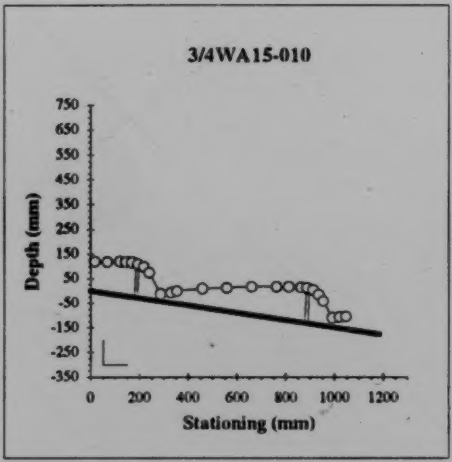
3/4WA15-010

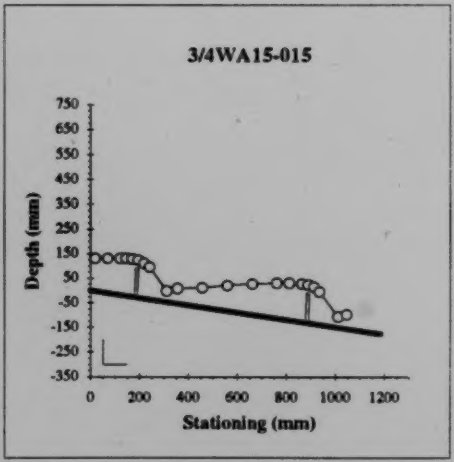
3/4WA15-015

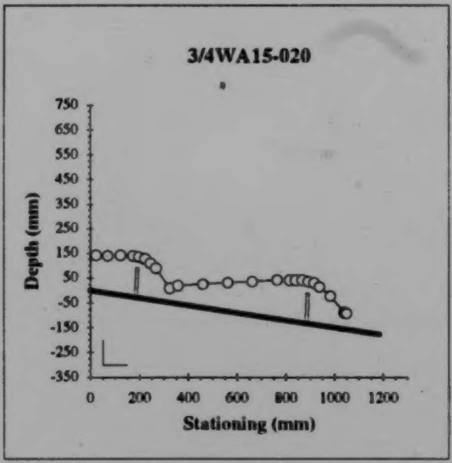
3/4WA15-020

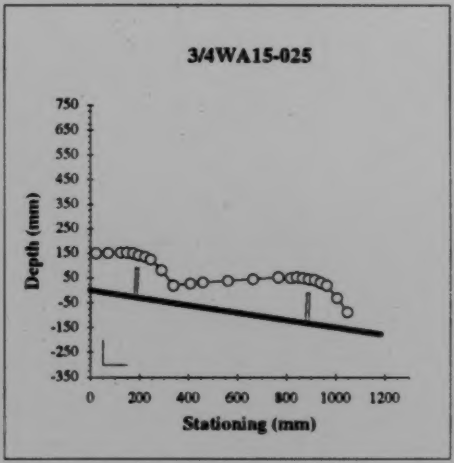
3/4WA15-025

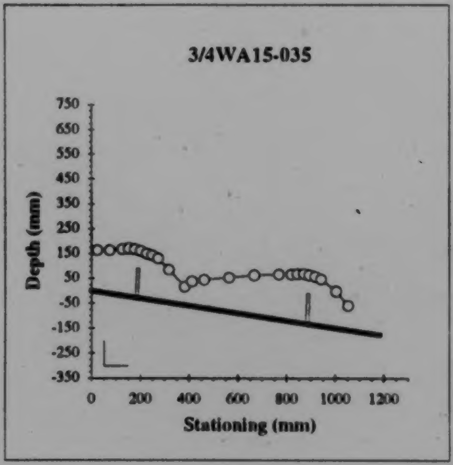
3/4WA15-035

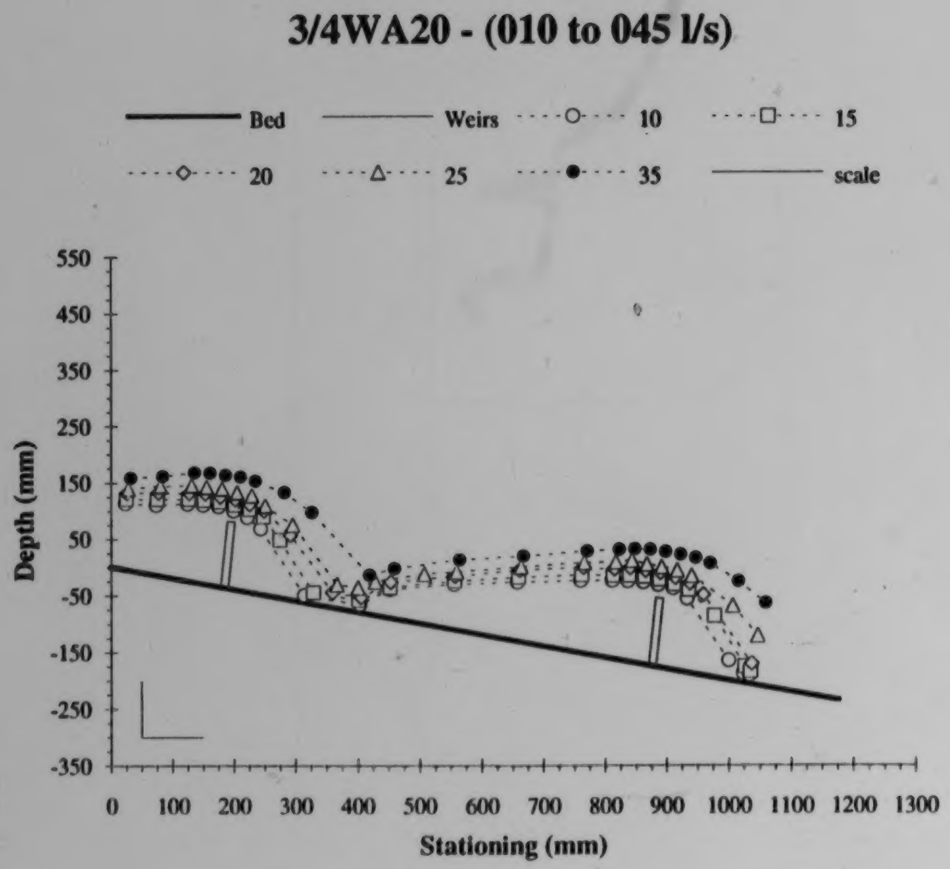
3/4WA20 - (010 to 045 l/s)
Bed
Weirs
10
15
20
25
35
scale
Depth (mm)
550
450
350
250
150
50
-50
-150
-250
-350
0
100
200
300
400
500
600
700
800
900
1000
1100
1200
1300
Stationing (mm)

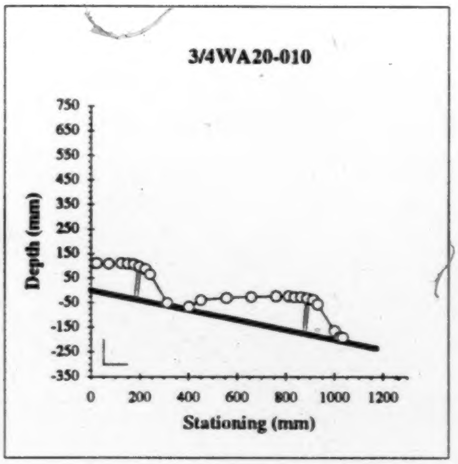
3/4WA20-010
Depth (mm)
750
650
550
450
350
250
150
50
-50
-150
-250
-350
0
200
400
600
800
1000
1200
Stationing (mm)

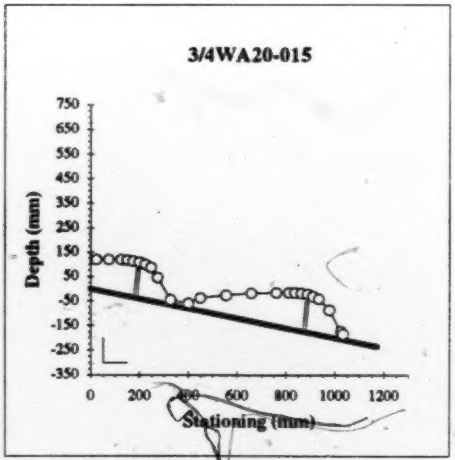
3/4WA20-015
Depth (mm)
750
650
550
450
350
250
150
50
-50
-150
-250
-350
0
200
400
600
800
1000
1200
Stationing (mm)

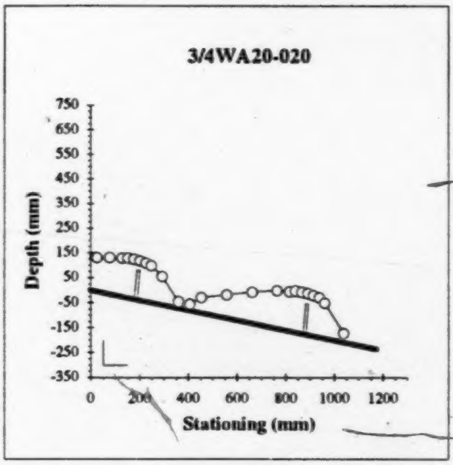
3/4WA20-020
Depth (mm)
750
650
550
450
350
250
150
50
-50
-150
-250
-350
0
200
400
600
800
1000
1200
Stationing (mm)

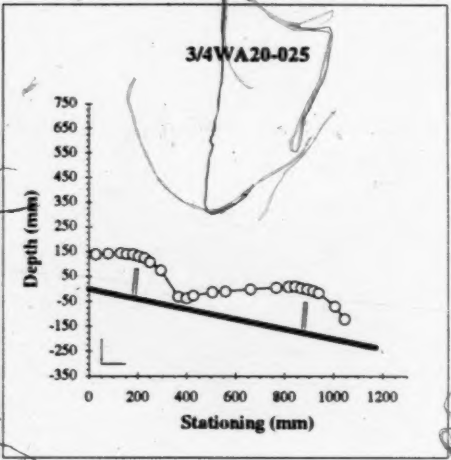
3/4WA20-025
Depth (mm)
750
650
550
450
350
250
150
50
-50
-150
-250
-350
0
200
400
600
800
1000
1200
Stationing (mm)

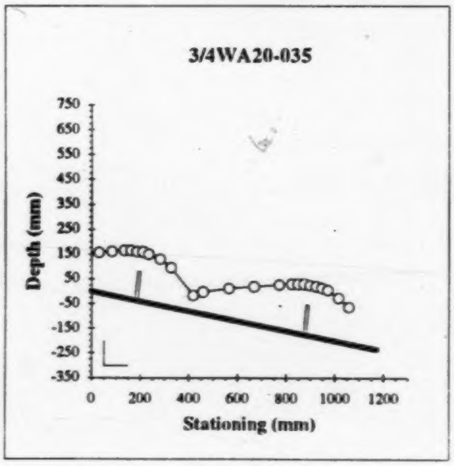
3/4WA20-035
Depth (mm)
750
650
550
450
350
250
150
50
-50
-150
-250
-350
0
200
400
600
800
1000
1200
Stationing (mm)

3/4WA30 - (010 to 045 l/s)

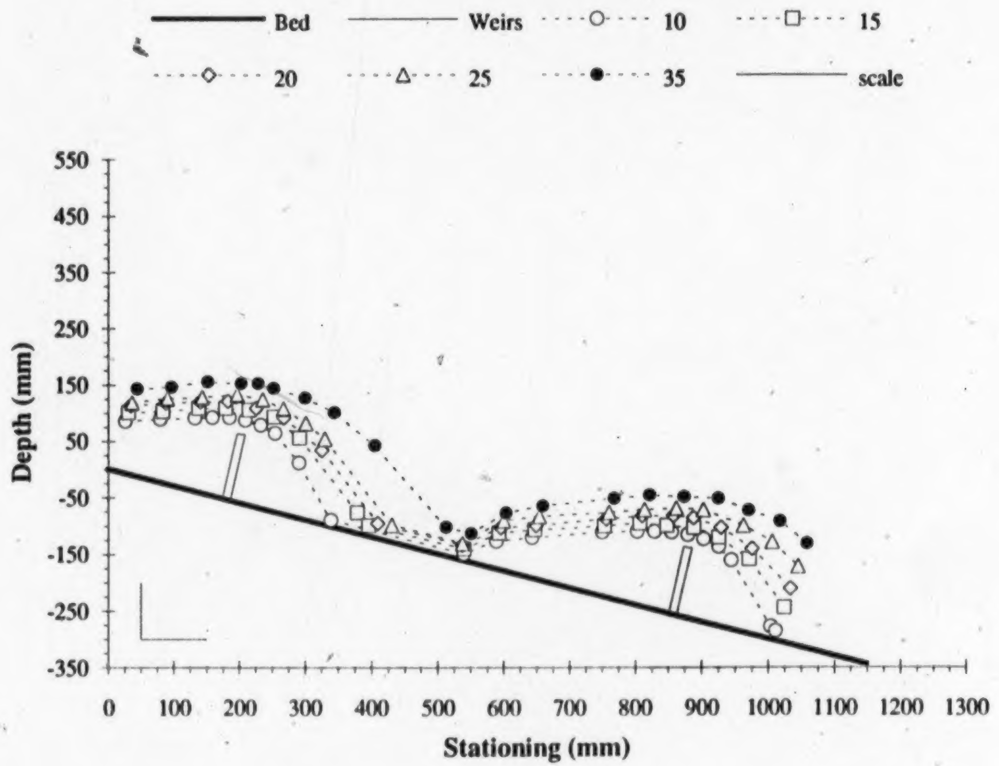

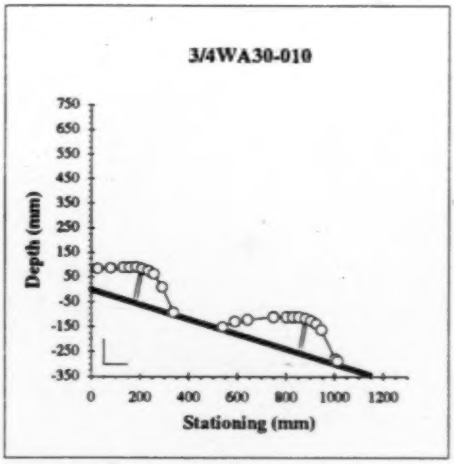
3/4WA30-010
Depth (mm)
750
650
550
450
350
250
150
50
-50
-150
-250
-350
0
200
400
600
800
1000
1200
Stationing (mm)

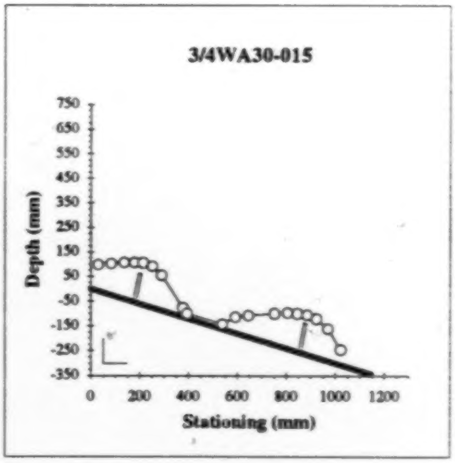
3/4WA30-015
Depth (mm)
750
650
550
450
350
250
150
50
-50
-150
-250
-350
0
200
400
600
800
1000
1200
Stationing (mm)

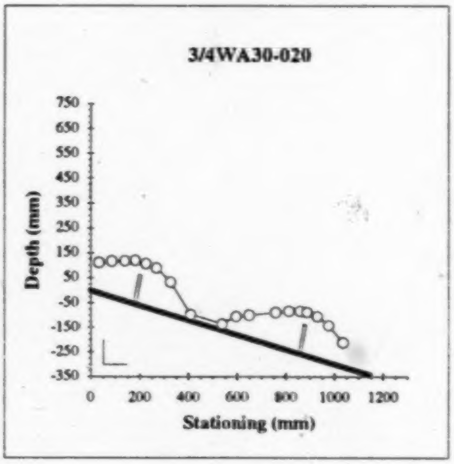
3/4WA30-020
Depth (mm)
750
650
550
450
350
250
150
50
-50
-150
-250
-350
0
200
400
600
800
1000
1200
Stationing (mm)

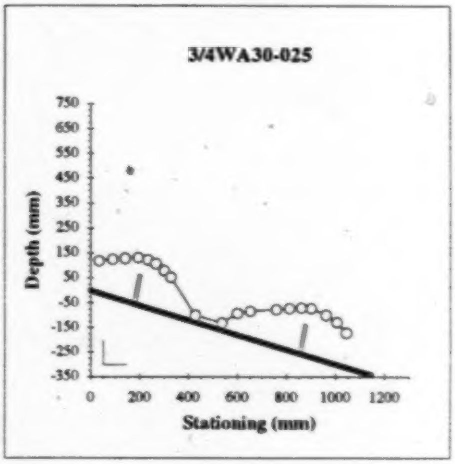
3/4WA30-025
Depth (mm)
750
650
550
450
350
250
150
50
-50
-150
-250
-350
0
200
400
600
800
1000
1200
Stationing (mm)

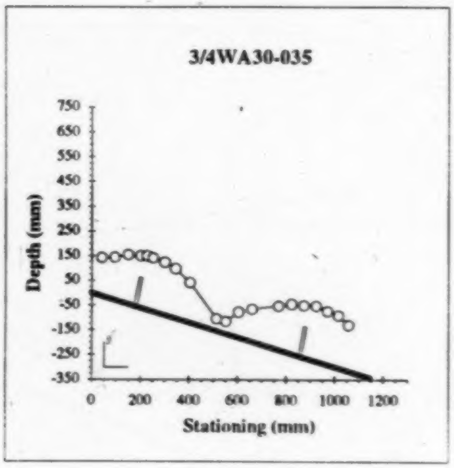
3/4WA30-035
Depth (mm)
750
650
550
450
350
250
150
50
-50
-150
-250
-350
0
200
400
600
800
1000
1200
Stationing (mm)

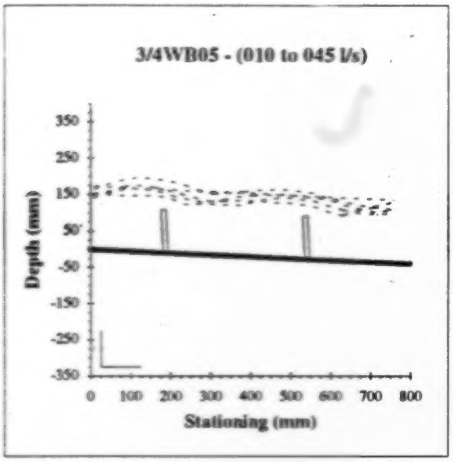

3/4WB05 - (010 to 045 l/s)

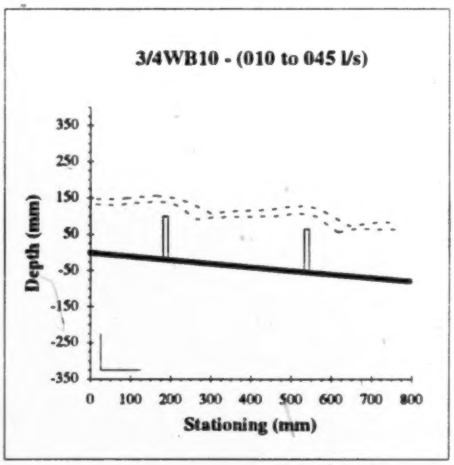

3/4WB10 - (010 to 045 l/s)

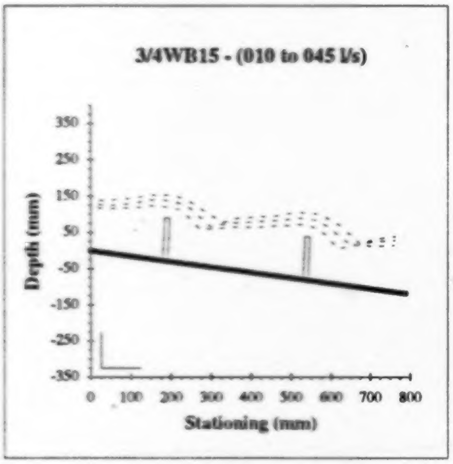

3/4WB15 - (010 to 045 l/s)

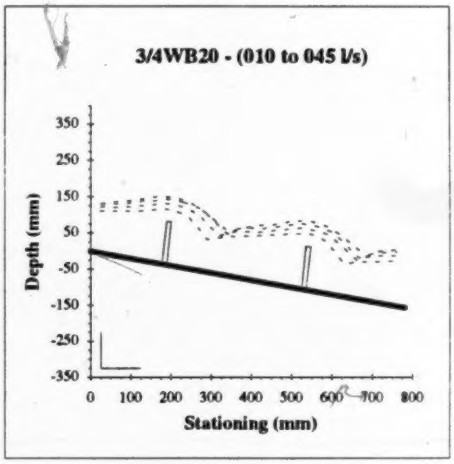

3/4WB20 - (010 to 045 l/s)

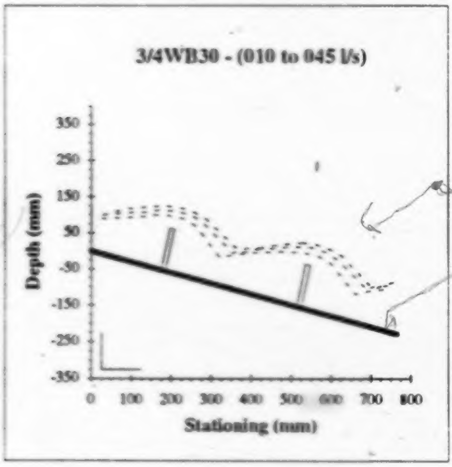

3/4WB30 - (010 to 045 l/s)

Water Surface Profiles

Three Quarter Weir Height

Class 'B' Weir Spacing

5 to 30 % Slope, 10 to 35 l/s

3/4WB05 - (010 to 045 l/s)

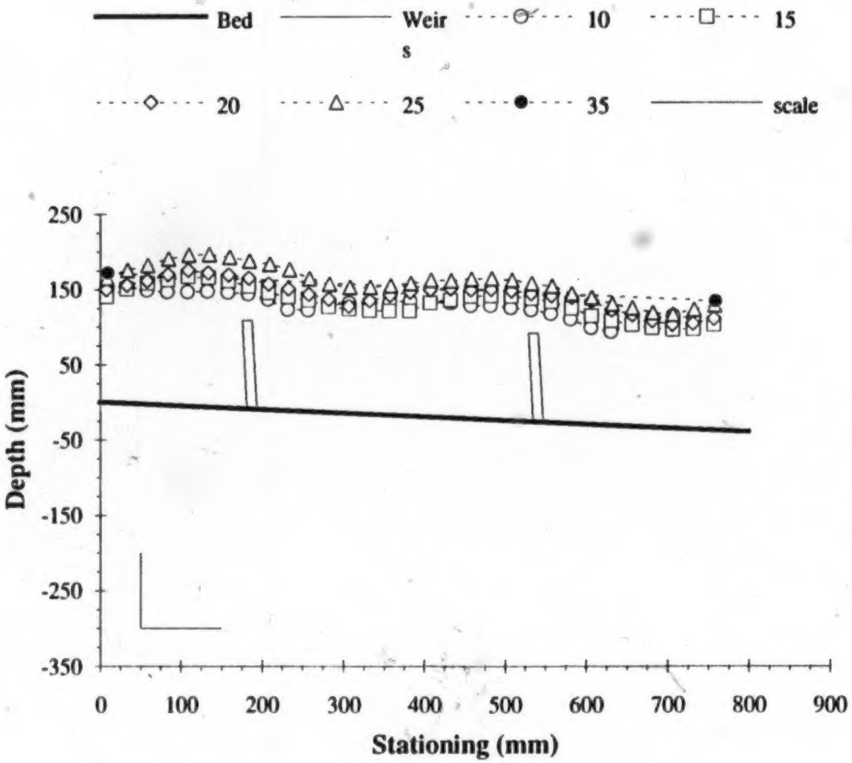

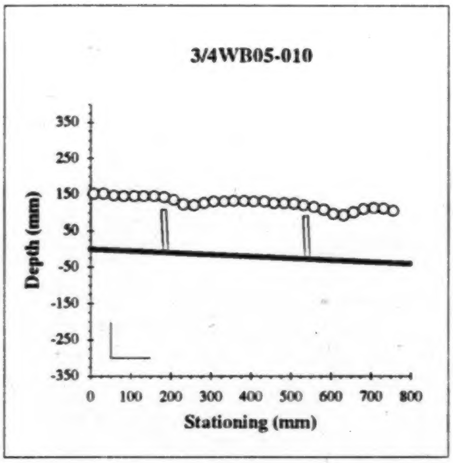

3/4WB05-010

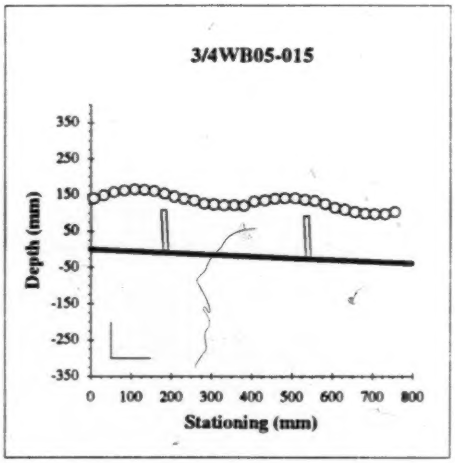

3/4WB05-015

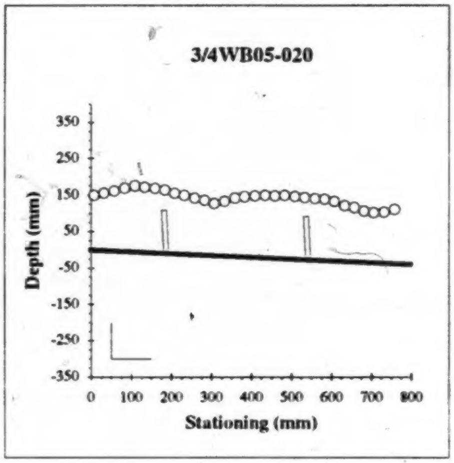

3/4WB05-020

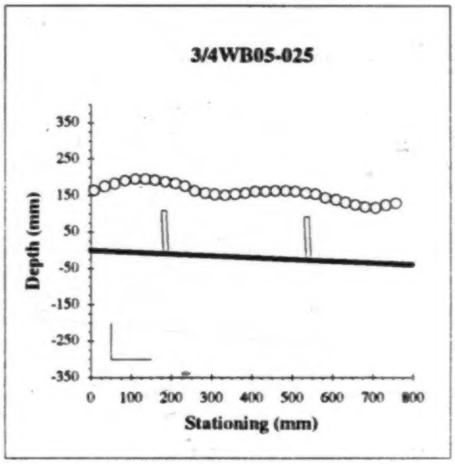

3/4WB05-025

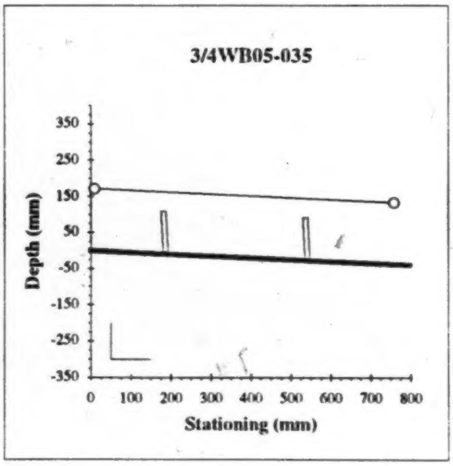

3/4WB05-035

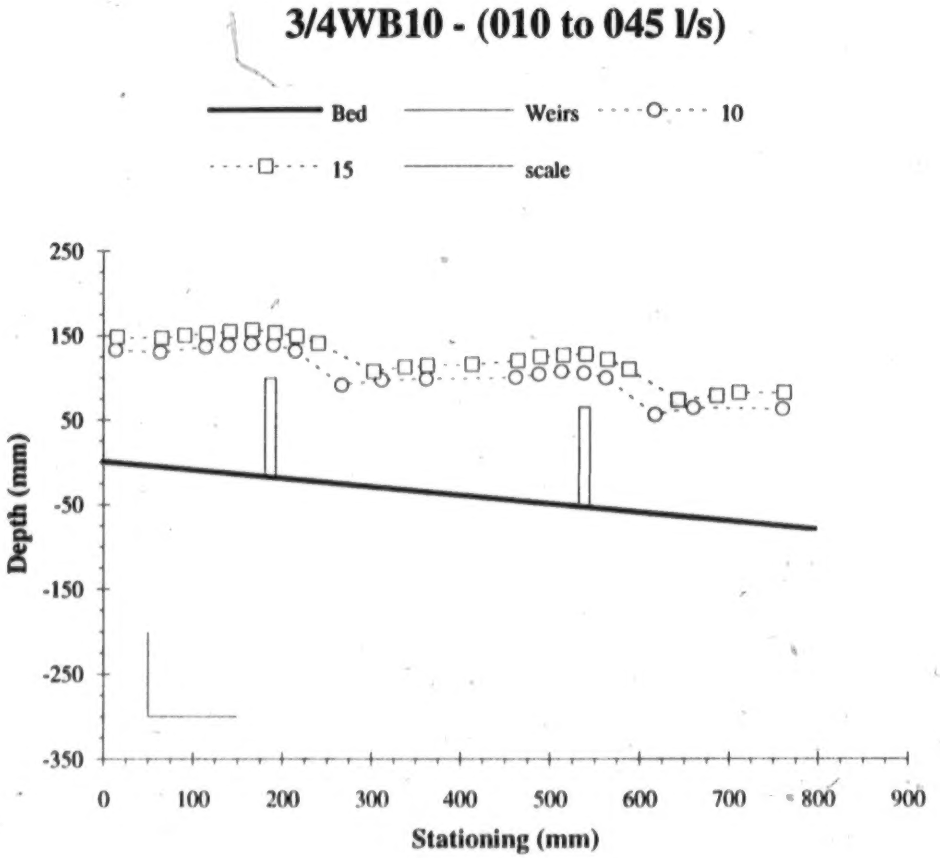
3/4WB10 - (010 to 045 l/s)
Bed
Weirs
10
15
scale
Depth (mm)
250
150
50
-50
-150
-250
-350
Stationing (mm)
0
100
200
300
400
500
600
700
800
900

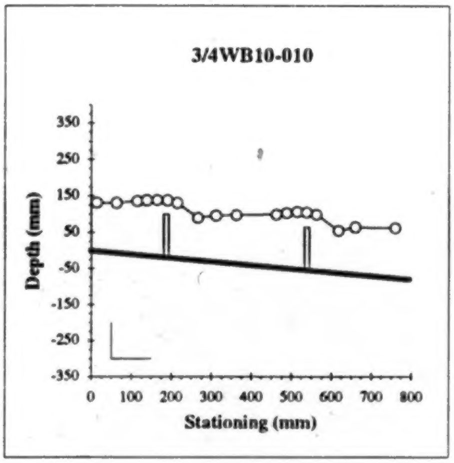
3/4WB10-010
Depth (mm)
350
250
150
50
-50
-150
-250
-350
0 100 200 300 400 500 600 700 800
Stationing (mm)

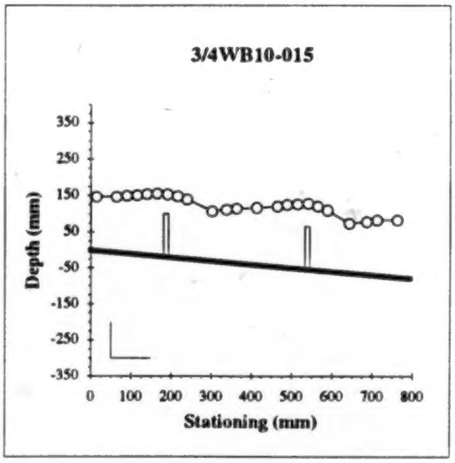
3/4WB10-015
Depth (mm)
350
250
150
50
-50
-150
-250
-350
0 100 200 300 400 500 600 700 800
Stationing (mm)

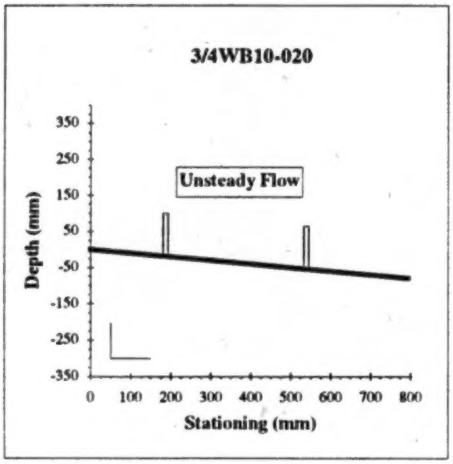
3/4WB10-020
Unsteady Flow
Depth (mm)
350
250
150
50
-50
-150
-250
-350
0 100 200 300 400 500 600 700 800
Stationing (mm)

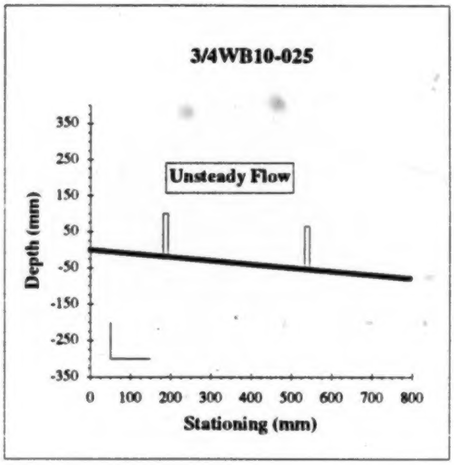
3/4WB10-025
Unsteady Flow
Depth (mm)
350
250
150
50
-50
-150
-250
-350
0 100 200 300 400 500 600 700 800
Stationing (mm)

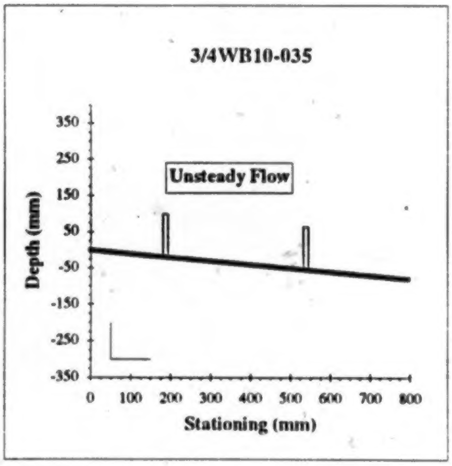
3/4WB10-035
Unsteady Flow
Depth (mm)
350
250
150
50
-50
-150
-250
-350
0 100 200 300 400 500 600 700 800
Stationing (mm)

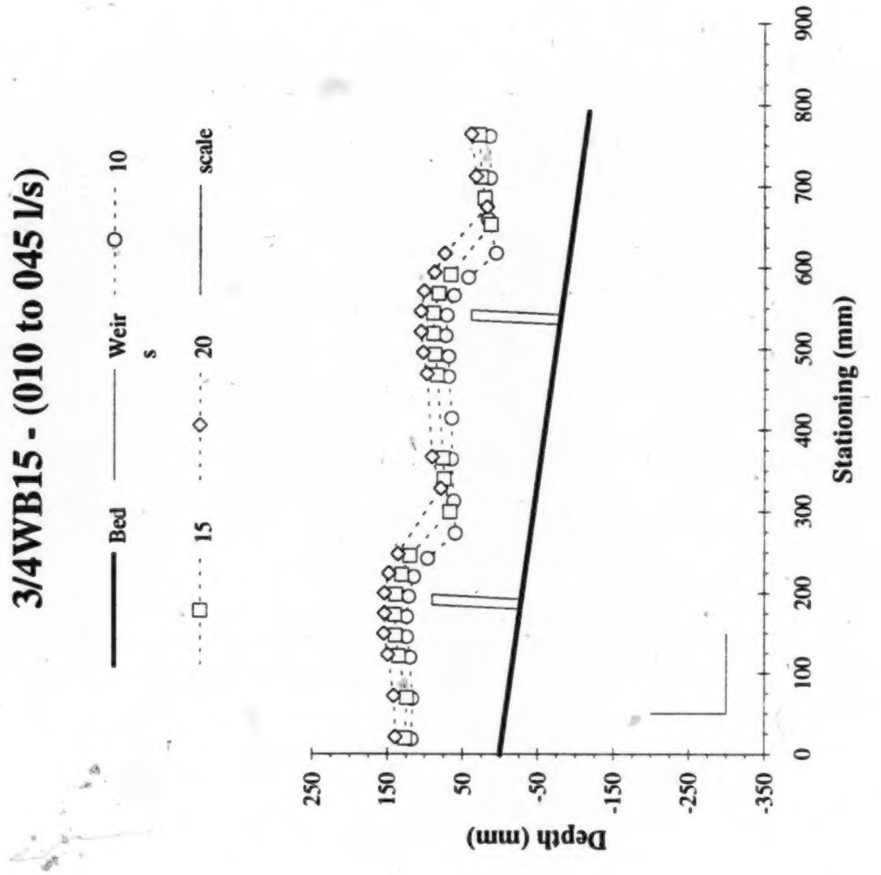

3/4WB15 - (010 to 045 l/s)

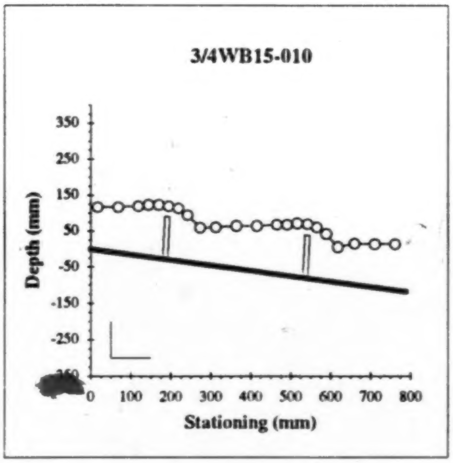
3/4WB15-010

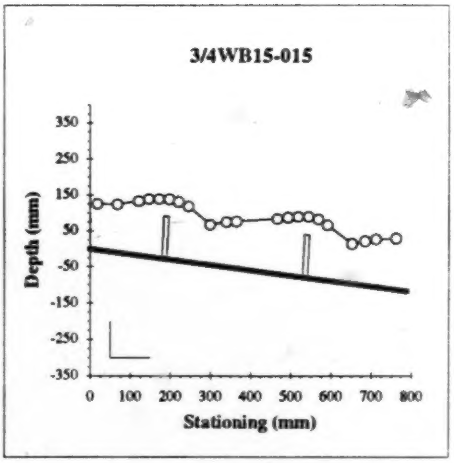
3/4WB15-015

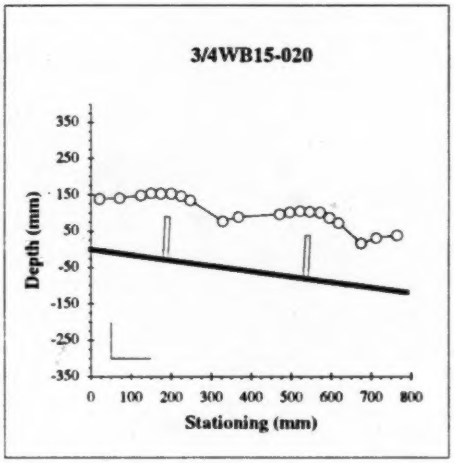
3/4WB15-020

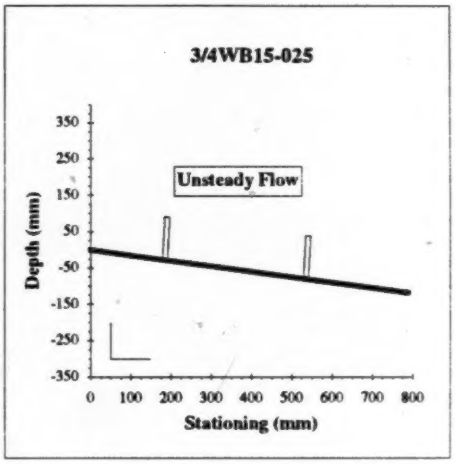
3/4WB15-025

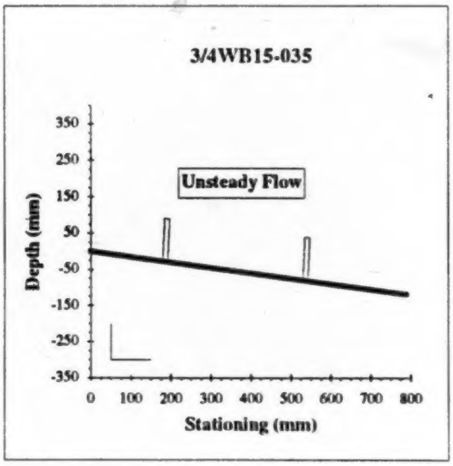
3/4WB15-035

3/4WB20 - (010 to 045 l/s)

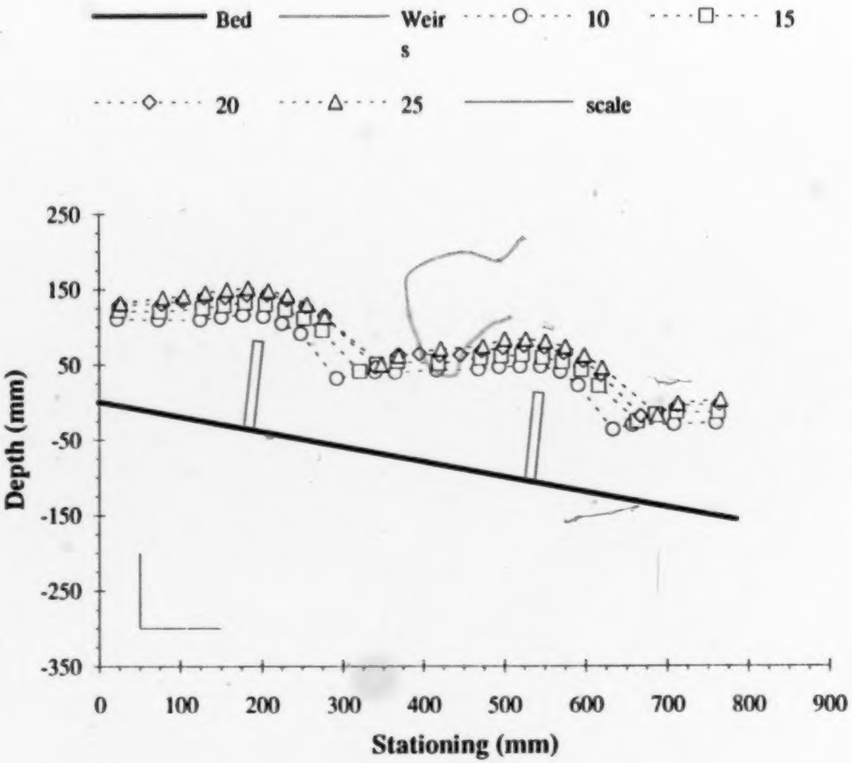

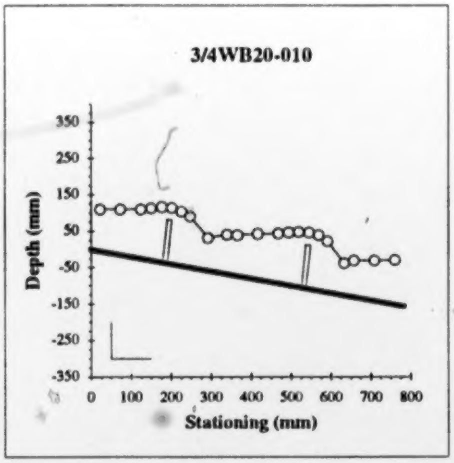
3/4WB20-010

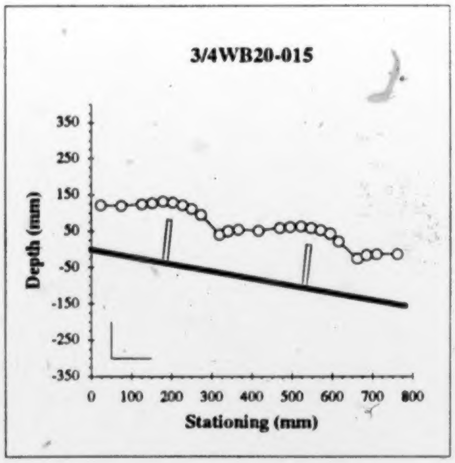
3/4WB20-015

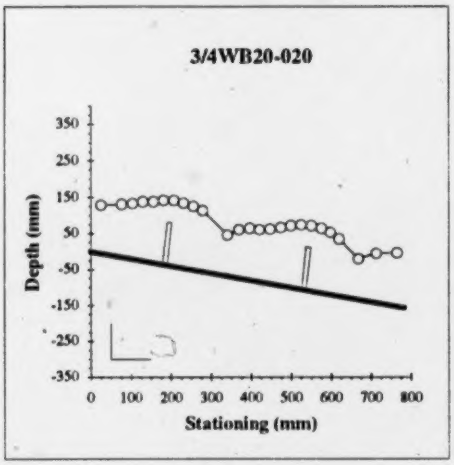
3/4WB20-020

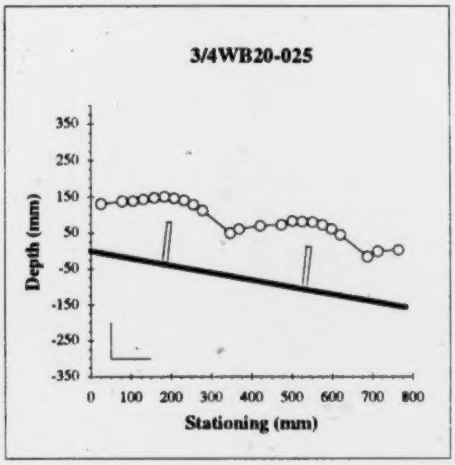
3/4WB20-025

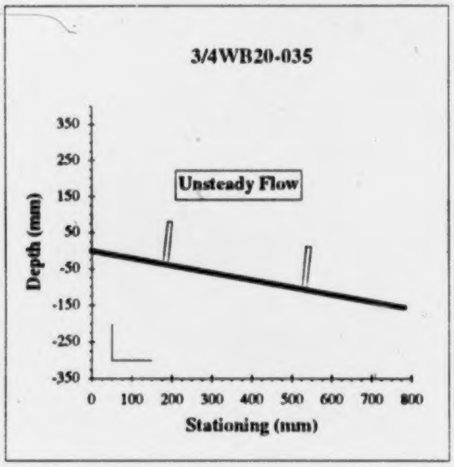
3/4WB20-035

3/4WB30 - (010 to 045 l/s)

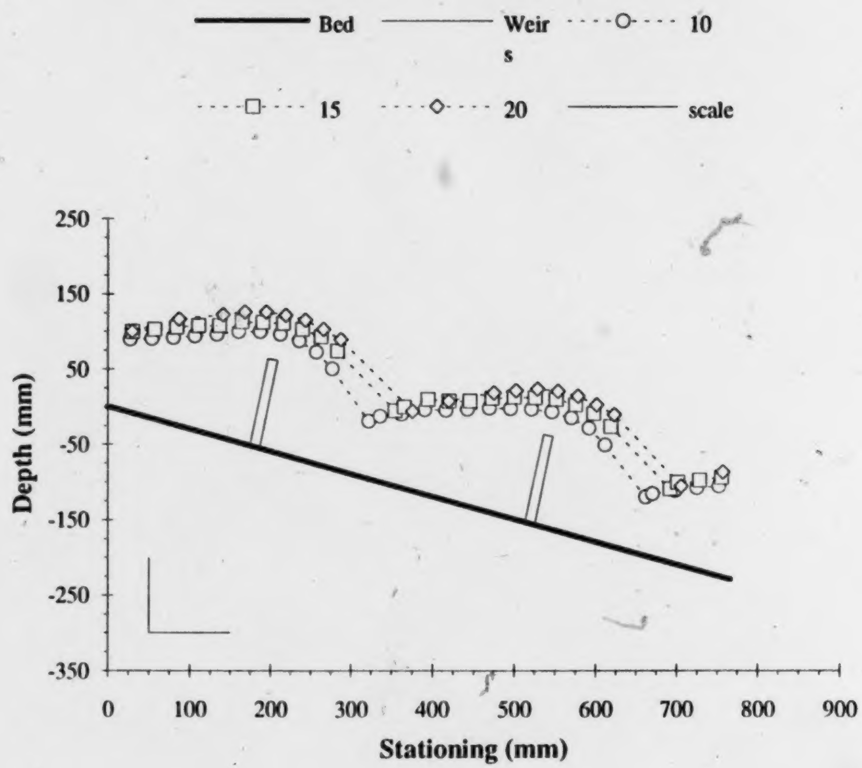

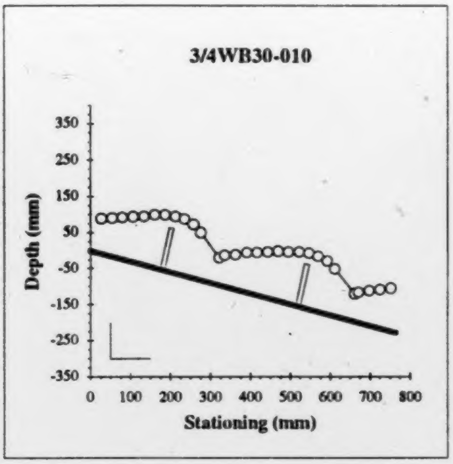
3/4WB30-010

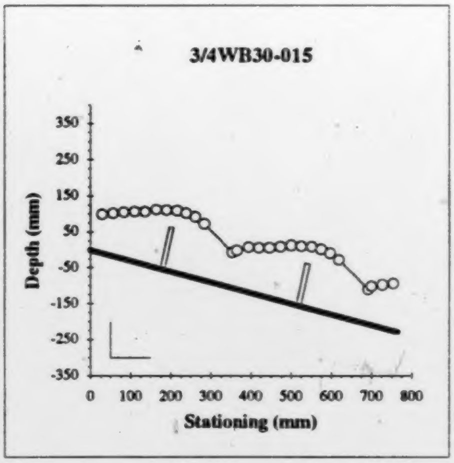
3/4WB30-015

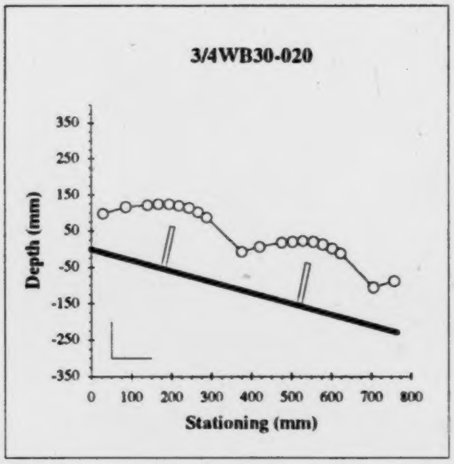
3/4WB30-020

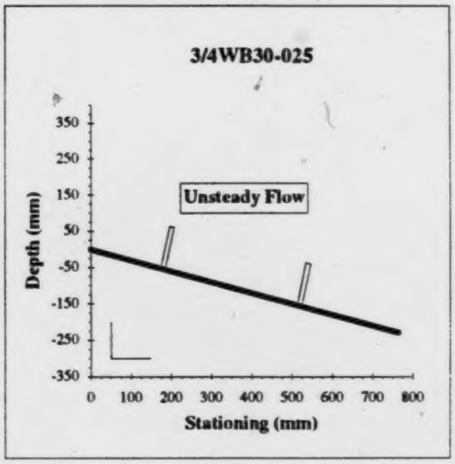
3/4WB30-025

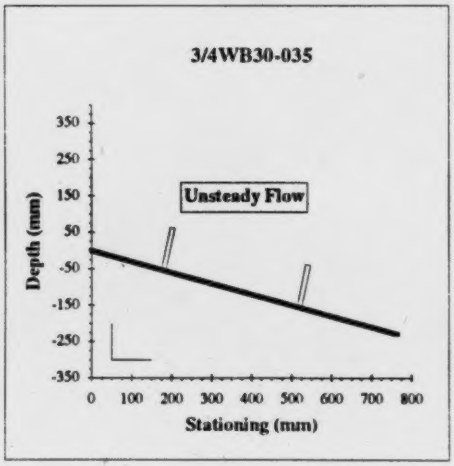
3/4WB30-035

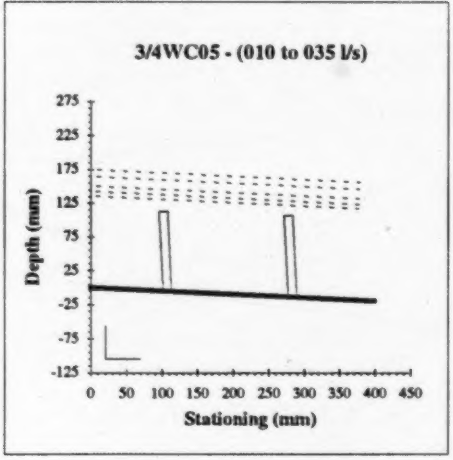
3/4WC05 - (010 to 035 l/s)

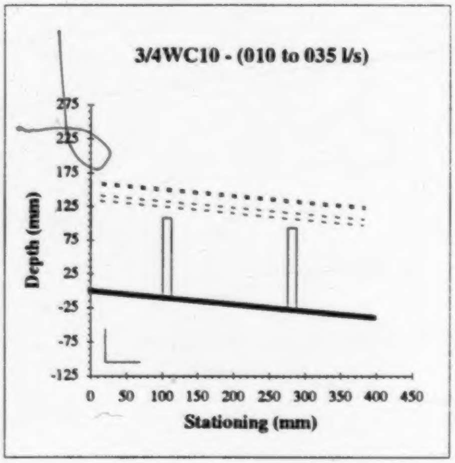
3/4WC10 - (010 to 035 l/s)

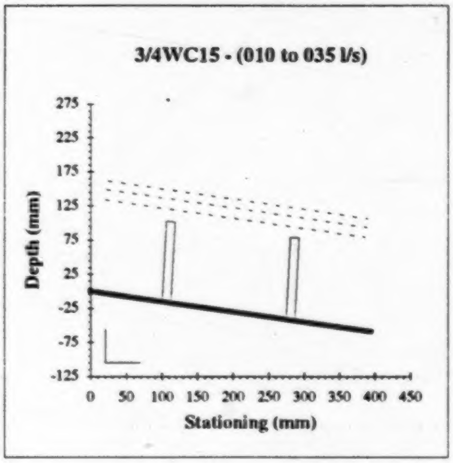
3/4WC15 - (010 to 035 l/s)

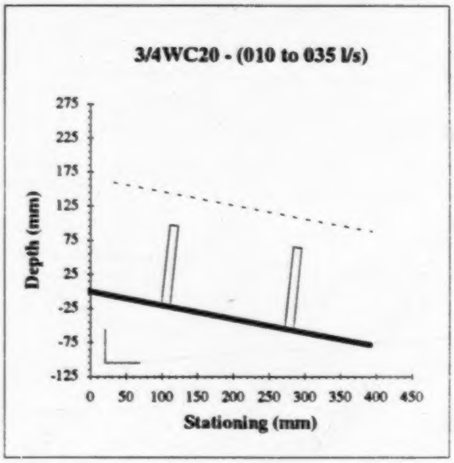
3/4WC20 - (010 to 035 l/s)

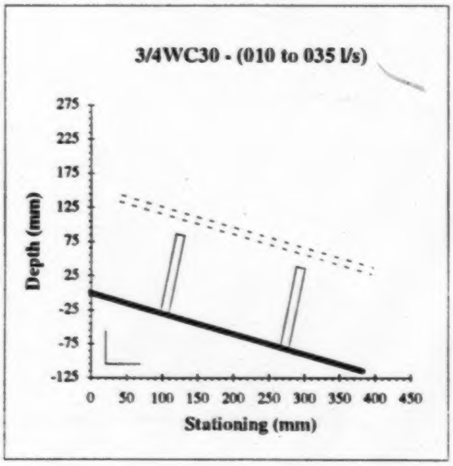
3/4WC30 - (010 to 035 l/s)

Water Surface Profiles

Three Quarter Weir Height

Class 'C' Weir Spacing

5 to 30 % Slope, 10 to 35 l/s

3/4WC05 - (010 to 035 l/s)

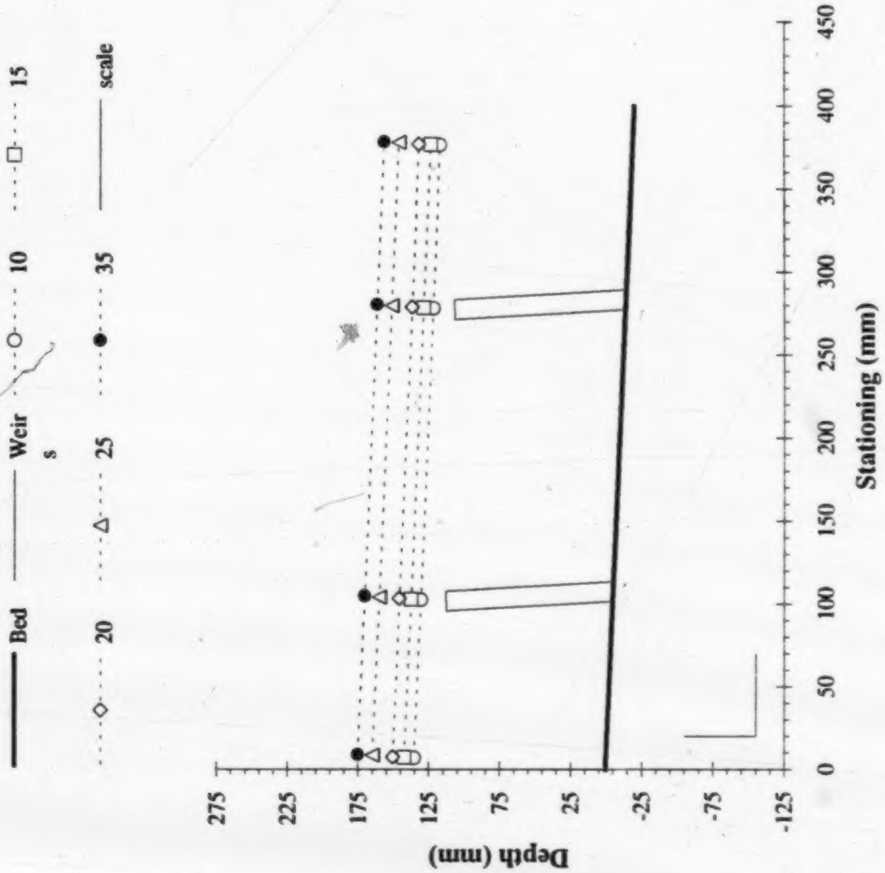

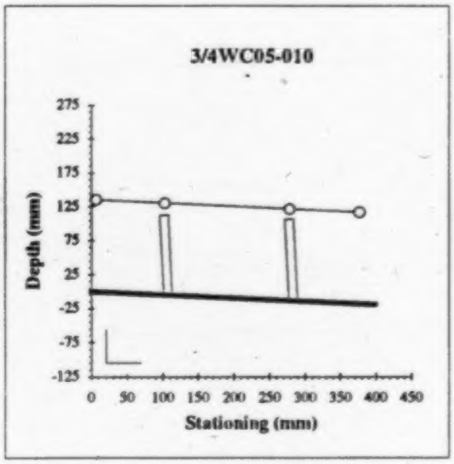

3/4WC05-010

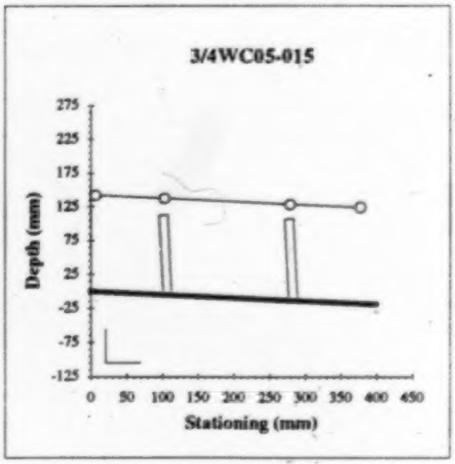

3/4WC05-015

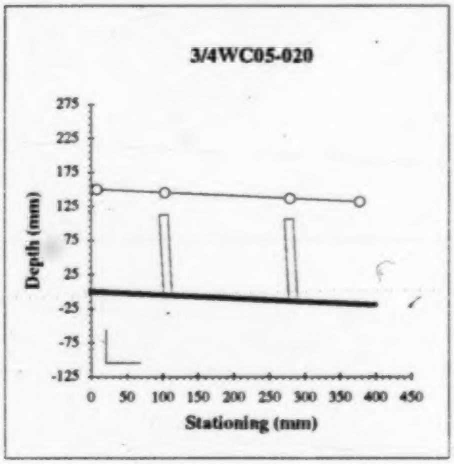

3/4WC05-020

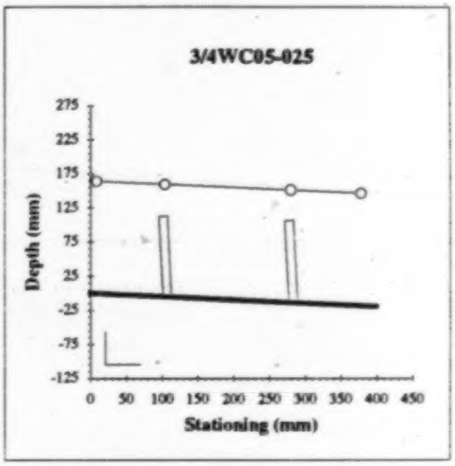

3/4WC05-025

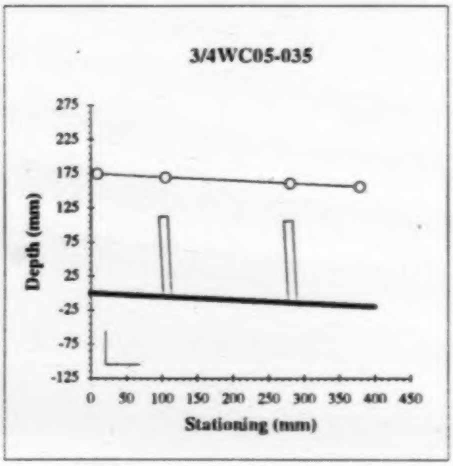

3/4WC05-035

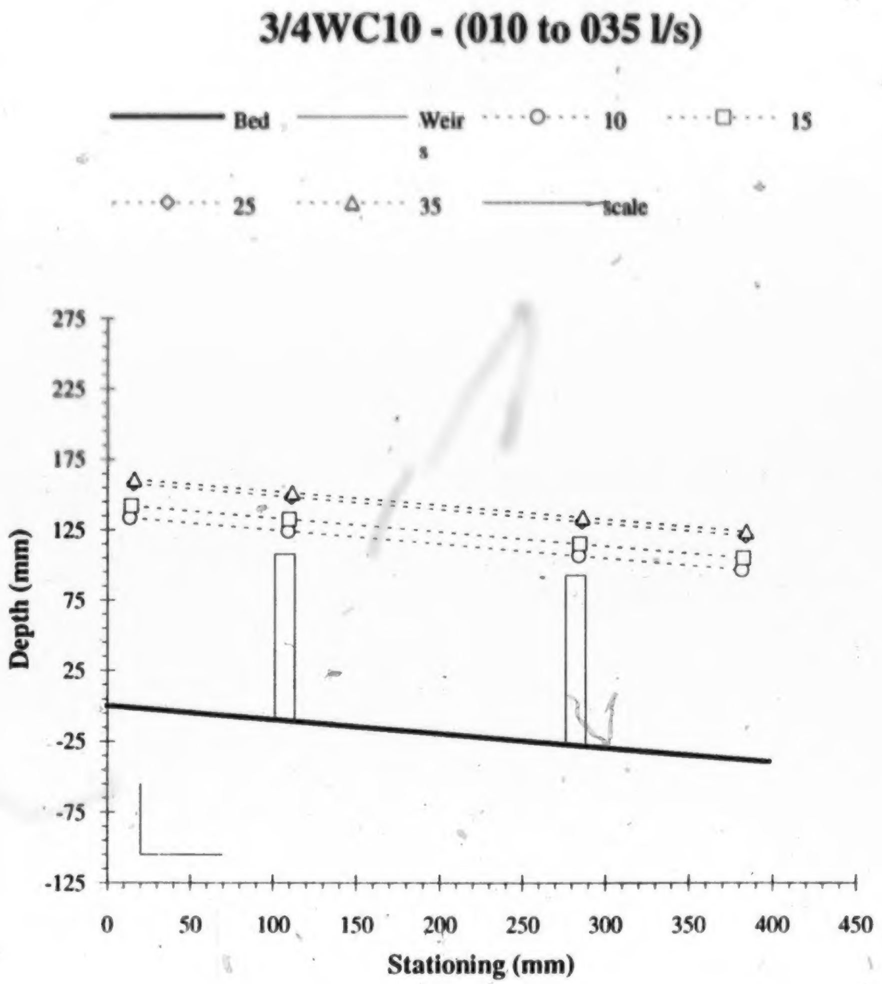

3/4WC10 - (010 to 035 l/s)

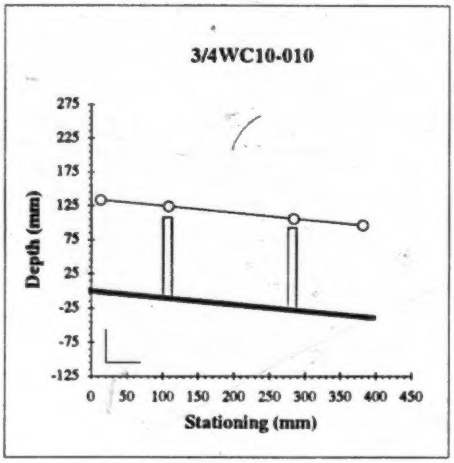
3/4WC10-010
Depth (mm)
275
225
175
125
75
25
-25
-75
-125
0 50 100 150 200 250 300 350 400 450
Stationing (mm)

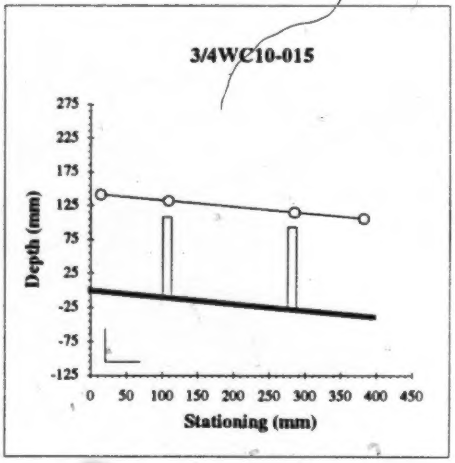
3/4WC10-015
Depth (mm)
275
225
175
125
75
25
-25
-75
-125
0 50 100 150 200 250 300 350 400 450
Stationing (mm)

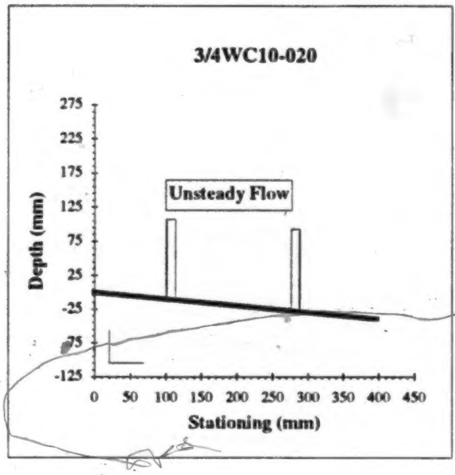
3/4WC10-020
Unsteady Flow
Depth (mm)
275
225
175
125
75
25
-25
-75
-125
0 50 100 150 200 250 300 350 400 450
Stationing (mm)

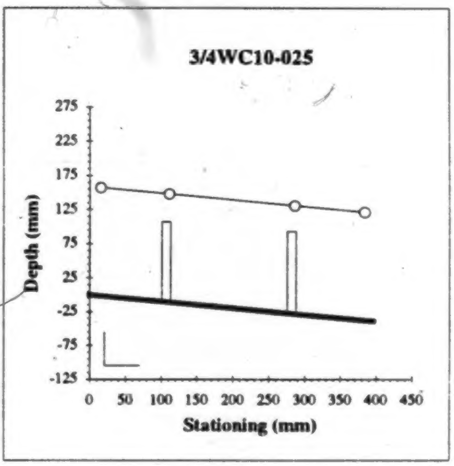
3/4WC10-025
Depth (mm)
275
225
175
125
75
25
-25
-75
-125
0 50 100 150 200 250 300 350 400 450
Stationing (mm)

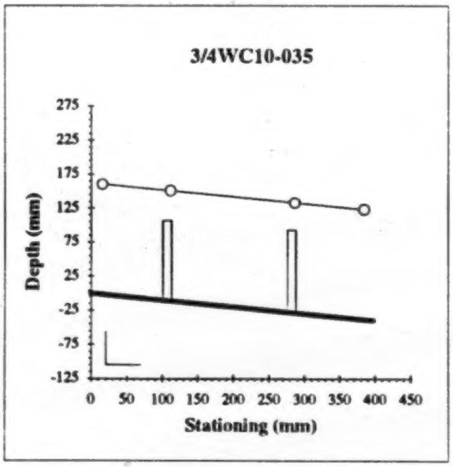
3/4WC10-035
Depth (mm)
275
225
175
125
75
25
-25
-75
-125
0 50 100 150 200 250 300 350 400 450
Stationing (mm)

3/4WC15 - (010 to 035 l/s)

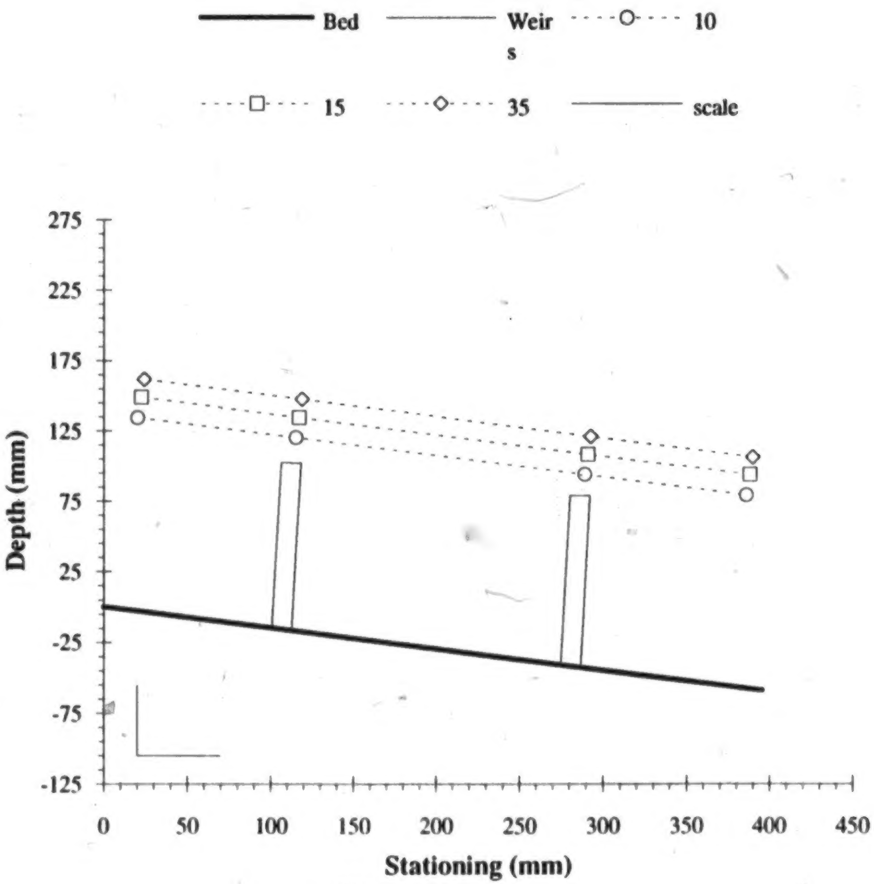

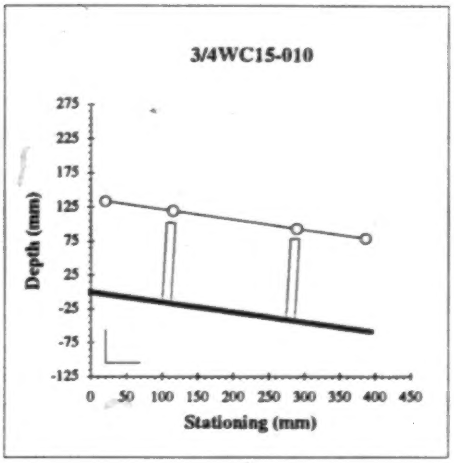
3/4WC15-010
Depth (mm)
275
225
175
125
75
25
-25
-75
-125
0 50 100 150 200 250 300 350 400 450
Stationing (mm)

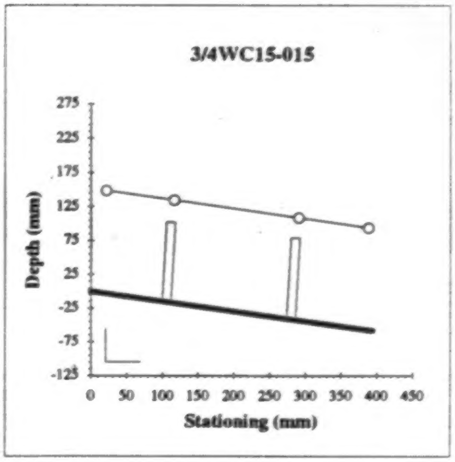
3/4WC15-015
Depth (mm)
275
225
175
125
75
25
-25
-75
-125
0 50 100 150 200 250 300 350 400 450
Stationing (mm)

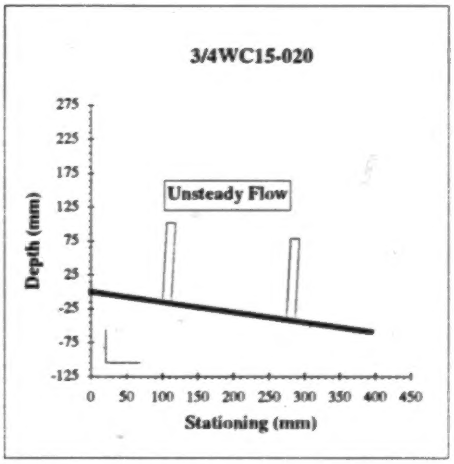
3/4WC15-020
Unsteady Flow
Depth (mm)
275
225
175
125
75
25
-25
-75
-125
0 50 100 150 200 250 300 350 400 450
Stationing (mm)

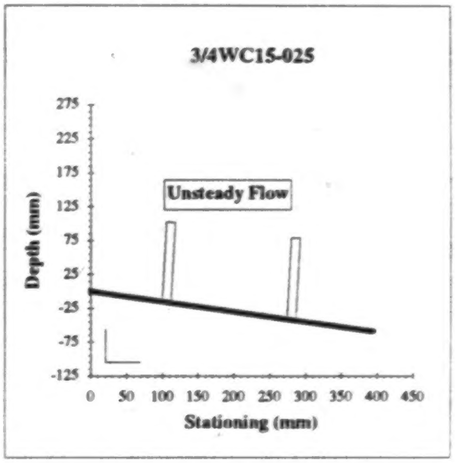
3/4WC15-025
Unsteady Flow
Depth (mm)
275
225
175
125
75
25
-25
-75
-125
0 50 100 150 200 250 300 350 400 450
Stationing (mm)

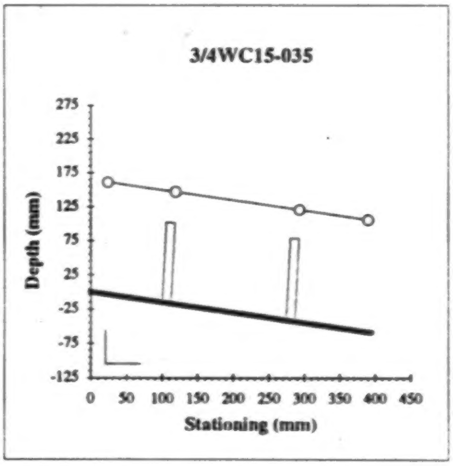
3/4WC15-035
Depth (mm)
275
225
175
125
75
25
-25
-75
-125
0 50 100 150 200 250 300 350 400 450
Stationing (mm)

3/4WC20 - (010 to 035 l/s)

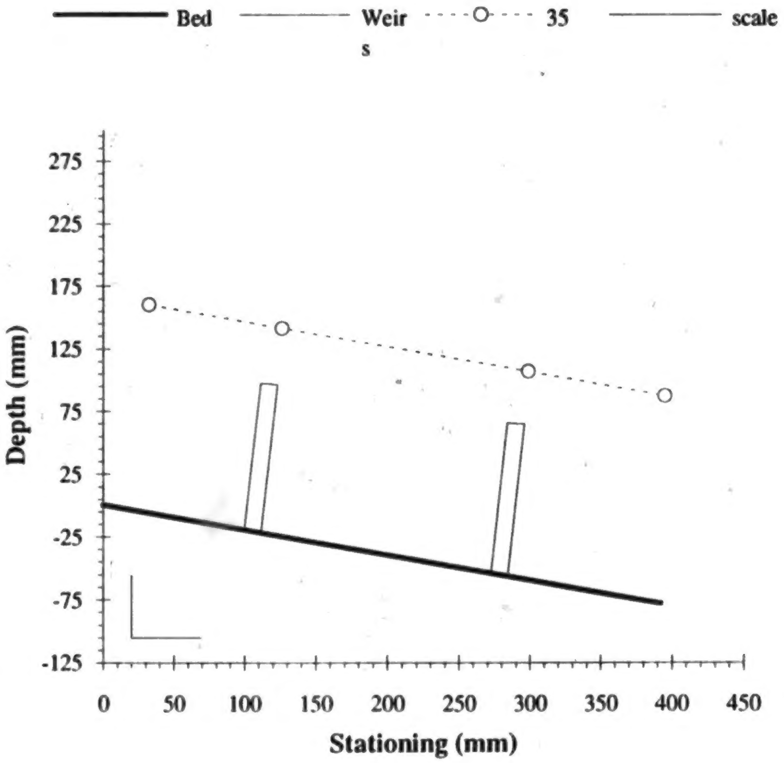

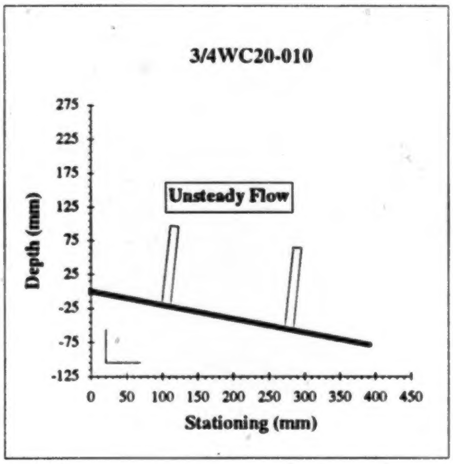
3/4WC20-010

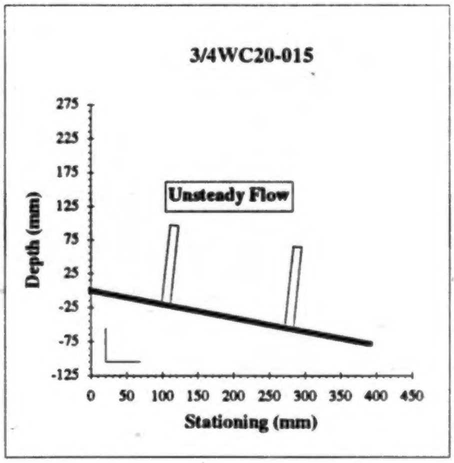
3/4WC20-015

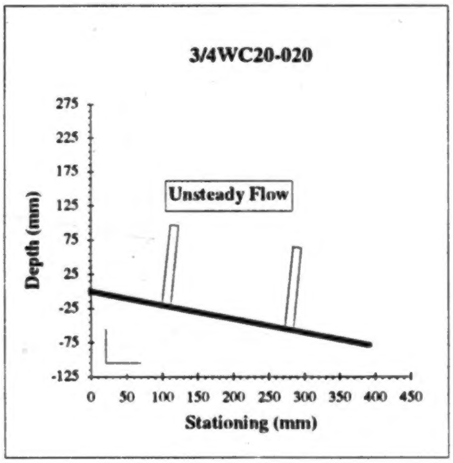
3/4WC20-020

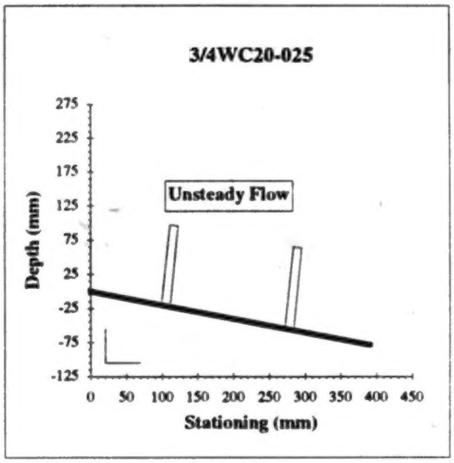
3/4WC20-025

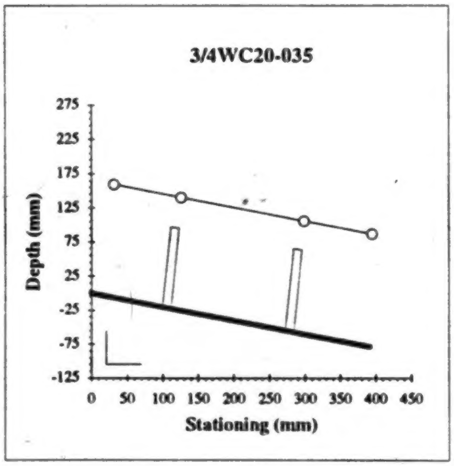
3/4WC20-035

3/4WC30 - (010 to 035 l/s)

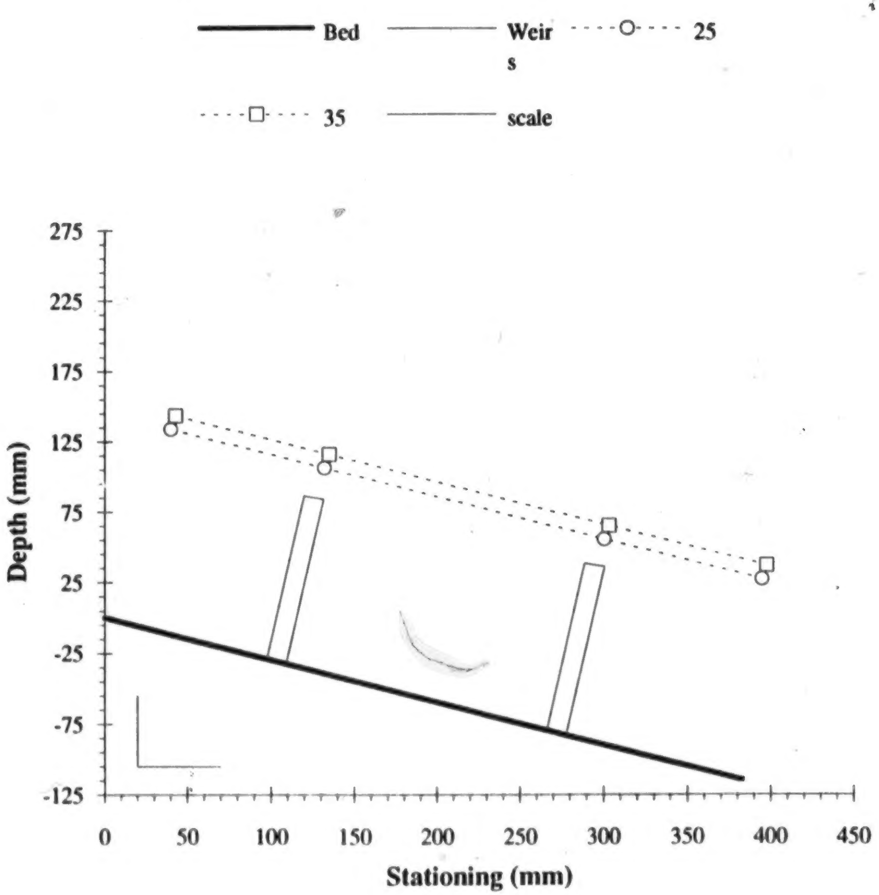

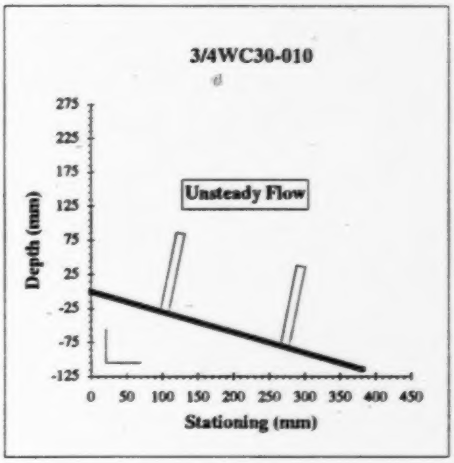
3/4WC30-010

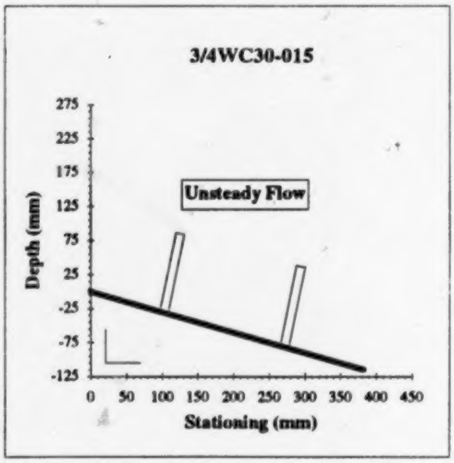
3/4WC30-015

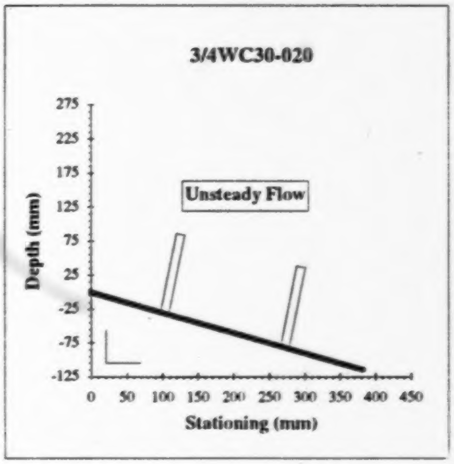
3/4WC30-020

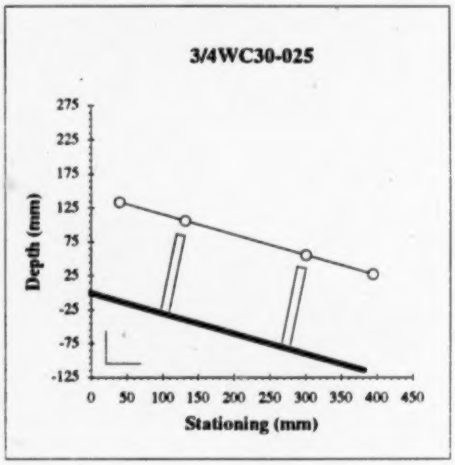
3/4WC30-025

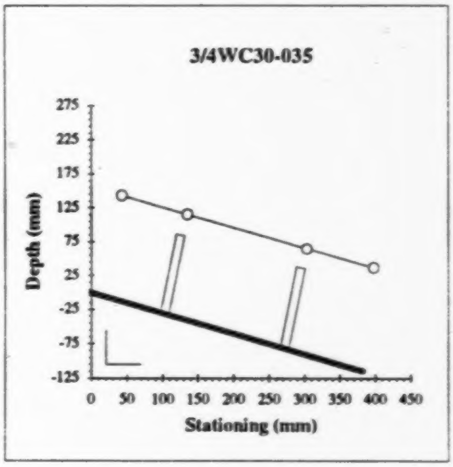
3/4WC30-035

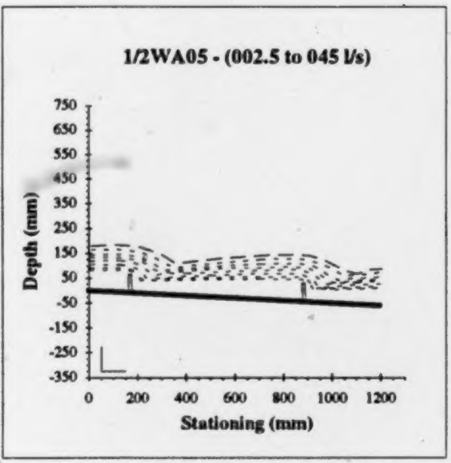

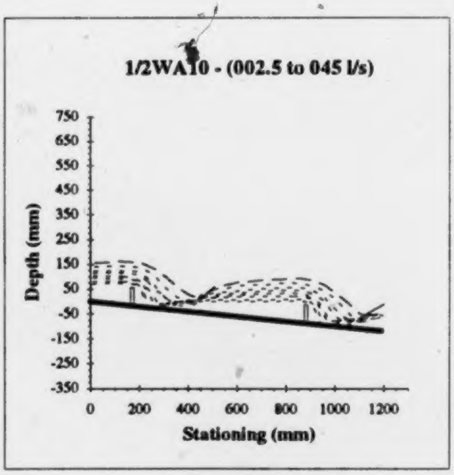

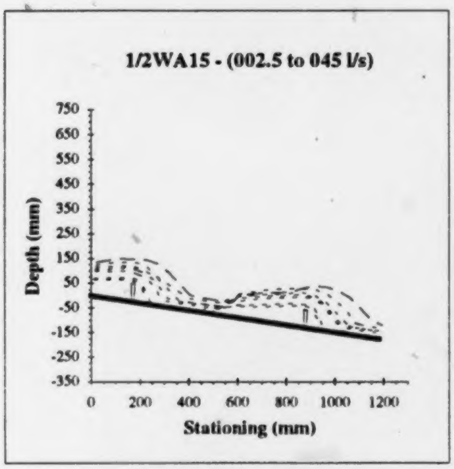

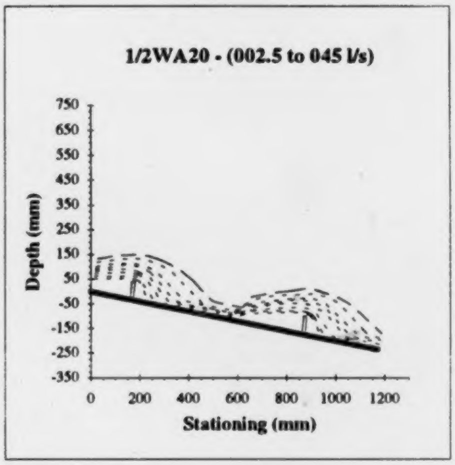

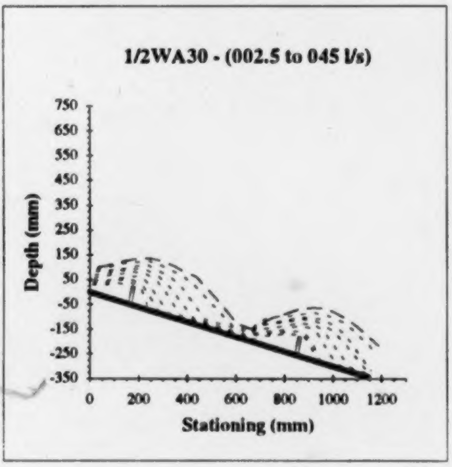

Water Surface Profiles

Half Weir Height

Class 'A' Weir Spacing

5 to 30 % Slope, 5 to 45 l/s

1/2WA05 - (002.5 to 045 l/s)

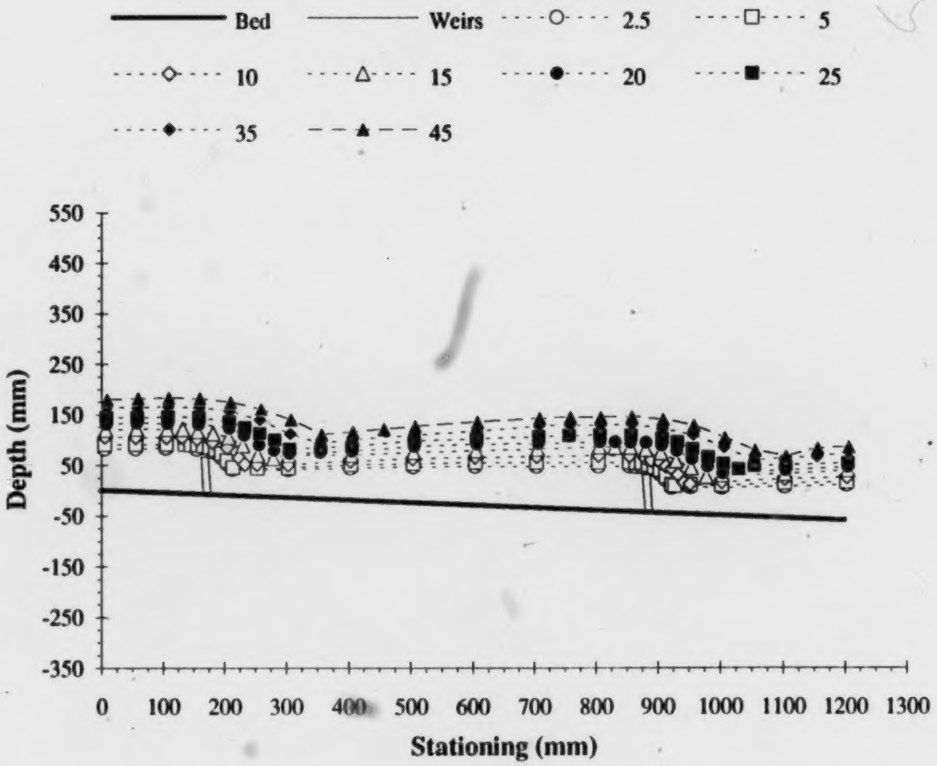

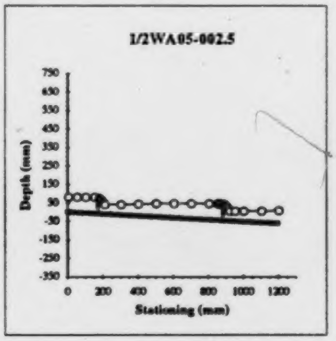
1/2WA05-002.5
Depth (mm)
750
650
550
450
350
250
150
50
-50
-150
-250
-350
0
200
400
600
800
1000
1200
Stationing (mm)

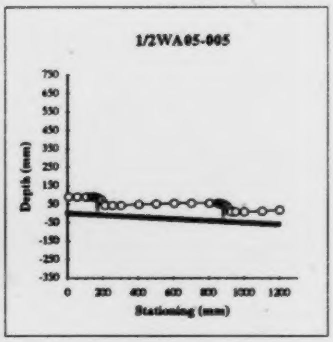
1/2WA05-005
Depth (mm)
750
650
550
450
350
250
150
50
-50
-150
-250
-350
0
200
400
600
800
1000
1200
Stationing (mm)

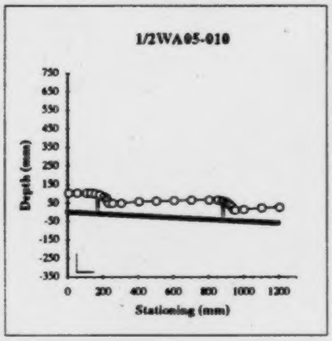
1/2WA05-010
Depth (mm)
750
650
550
450
350
250
150
50
-50
-150
-250
-350
0
200
400
600
800
1000
1200
Stationing (mm)

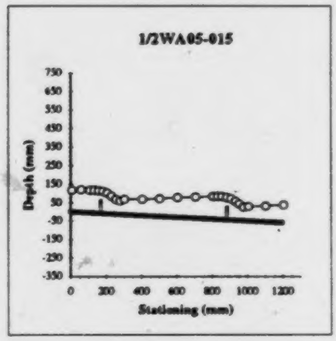
1/2WA05-015
Depth (mm)
750
650
550
450
350
250
150
50
-50
-150
-250
-350
0
200
400
600
800
1000
1200
Stationing (mm)

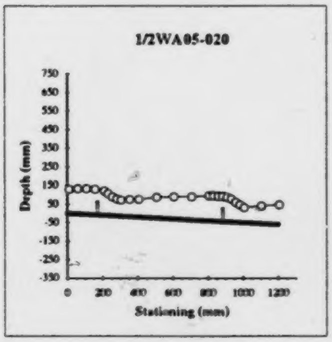
1/2WA05-020
Depth (mm)
750
650
550
450
350
250
150
50
-50
-150
-250
-350
0
200
400
600
800
1000
1200
Stationing (mm)

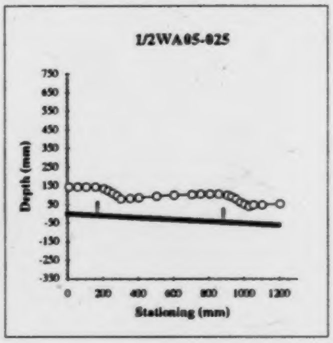
1/2WA05-025
Depth (mm)
750
650
550
450
350
250
150
50
-50
-150
-250
-350
0
200
400
600
800
1000
1200
Stationing (mm)

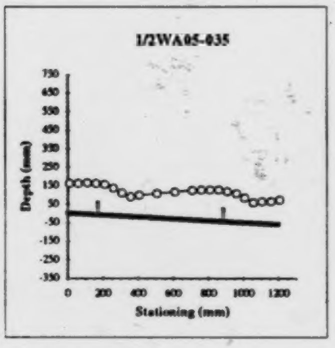
1/2WA05-035
Depth (mm)
750
650
550
450
350
250
150
50
-50
-150
-250
-350
0
200
400
600
800
1000
1200
Stationing (mm)

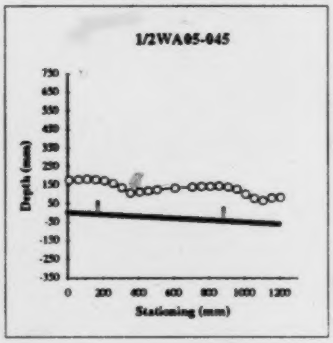
1/2WA05-045
Depth (mm)
750
650
550
450
350
250
150
50
-50
-150
-250
-350
0
200
400
600
800
1000
1200
Stationing (mm)

1/2WA10 - (002.5 to 045 l/s)

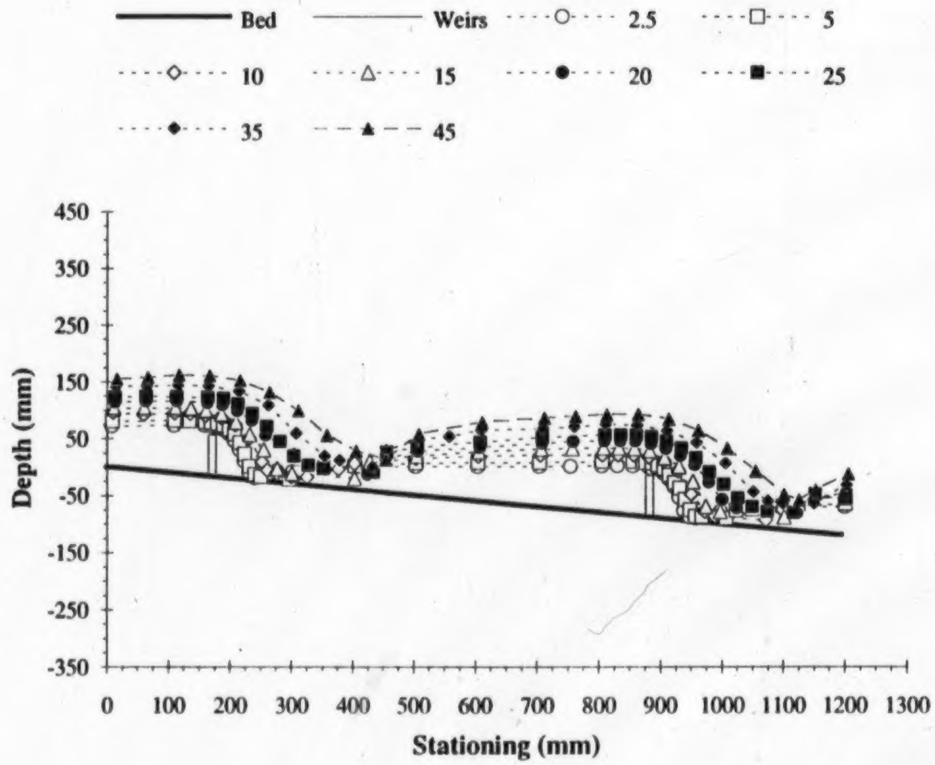

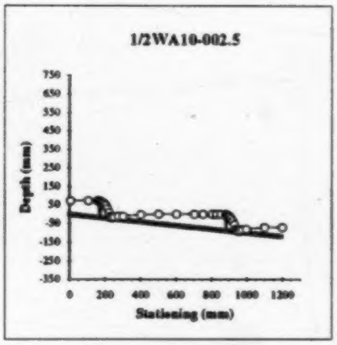
1/2WA10-002.5

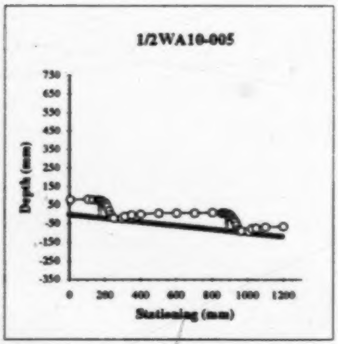
1/2WA10-005

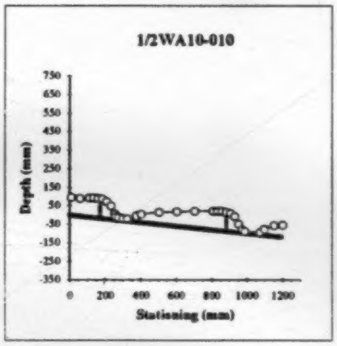
1/2WA10-010

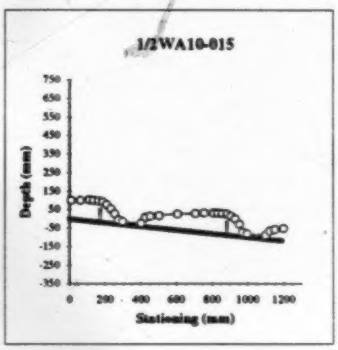
1/2WA10-015

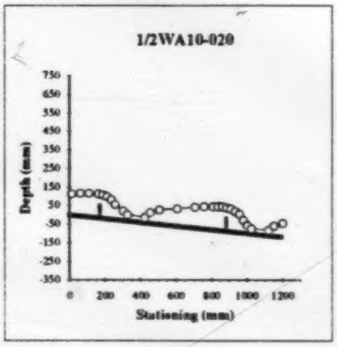
1/2WA10-020

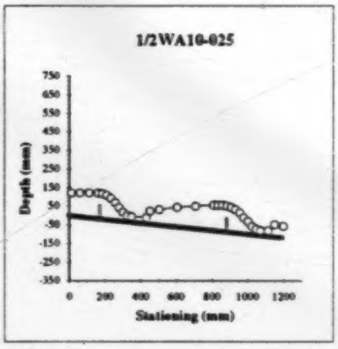
1/2WA10-025

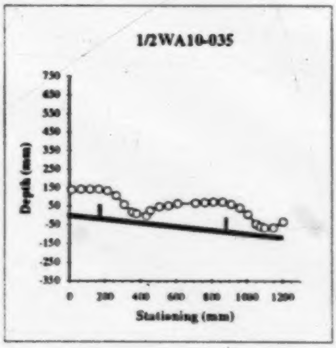
1/2WA10-035

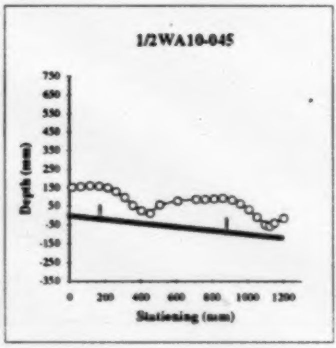
1/2WA10-045

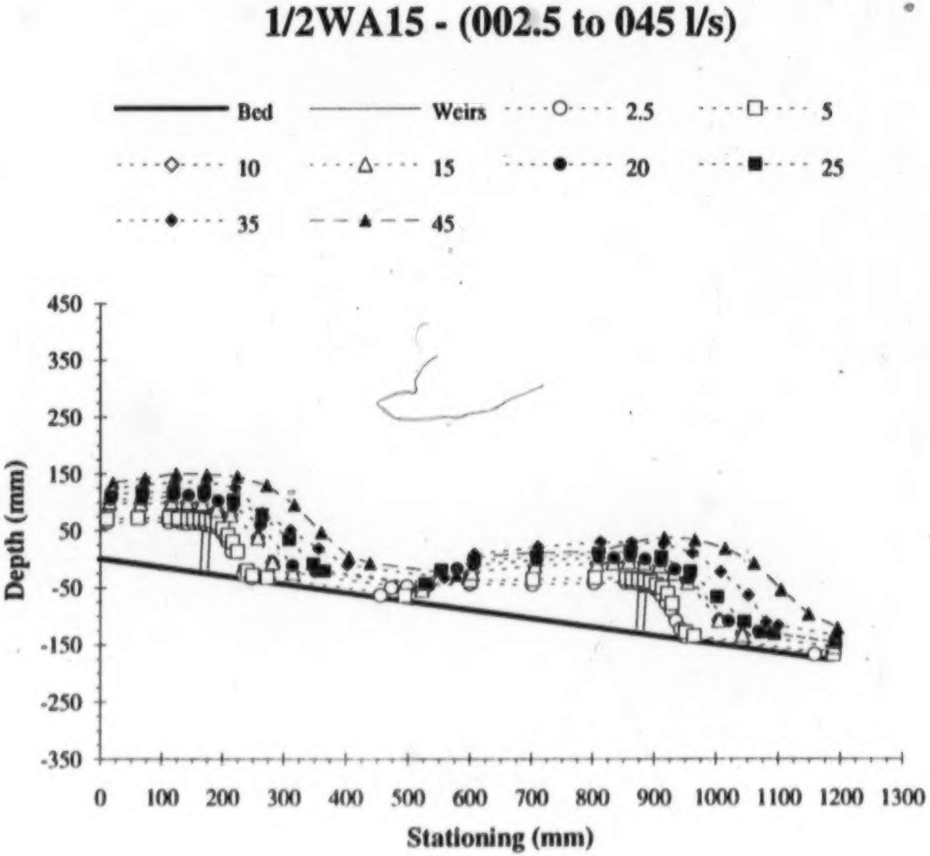
1/2WA15 - (002.5 to 045 l/s)
Bed
Weirs
2.5
5
10
15
20
25
35
45
Depth (mm)
450
350
250
150
50
-50
-150
-250
-350
0
100
200
300
400
500
600
700
800
900
1000
1100
1200
1300
Stationing (mm)

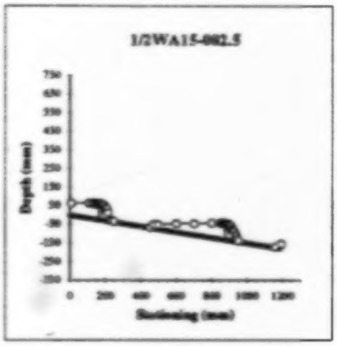
1/2WA15-002.5

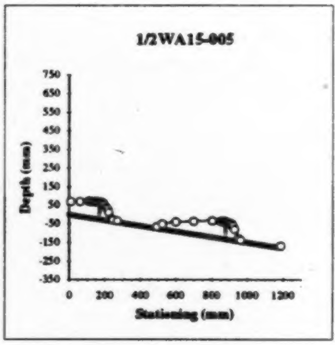
1/2WA15-005

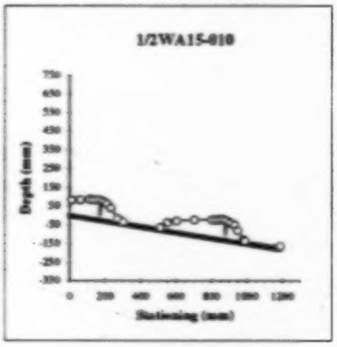
1/2WA15-010

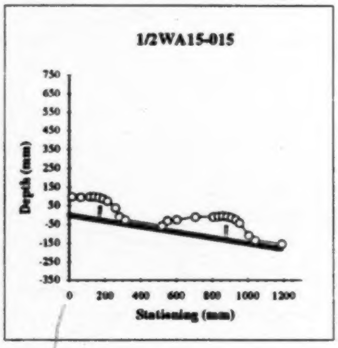
1/2WA15-015

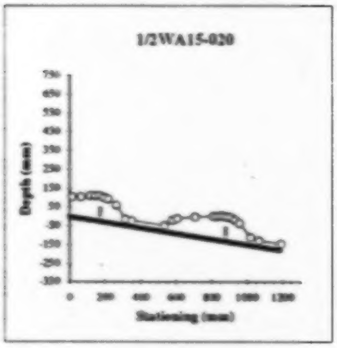
1/2WA15-020

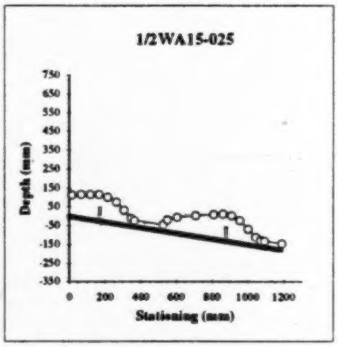
1/2WA15-025

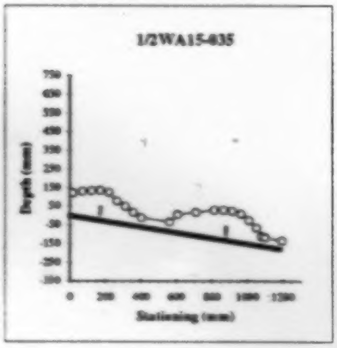
1/2WA15-035

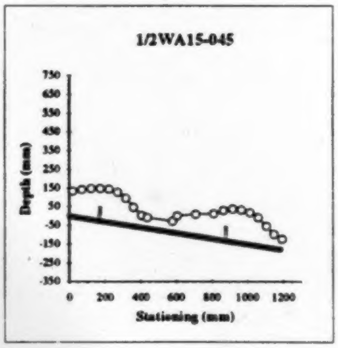
1/2WA15-045

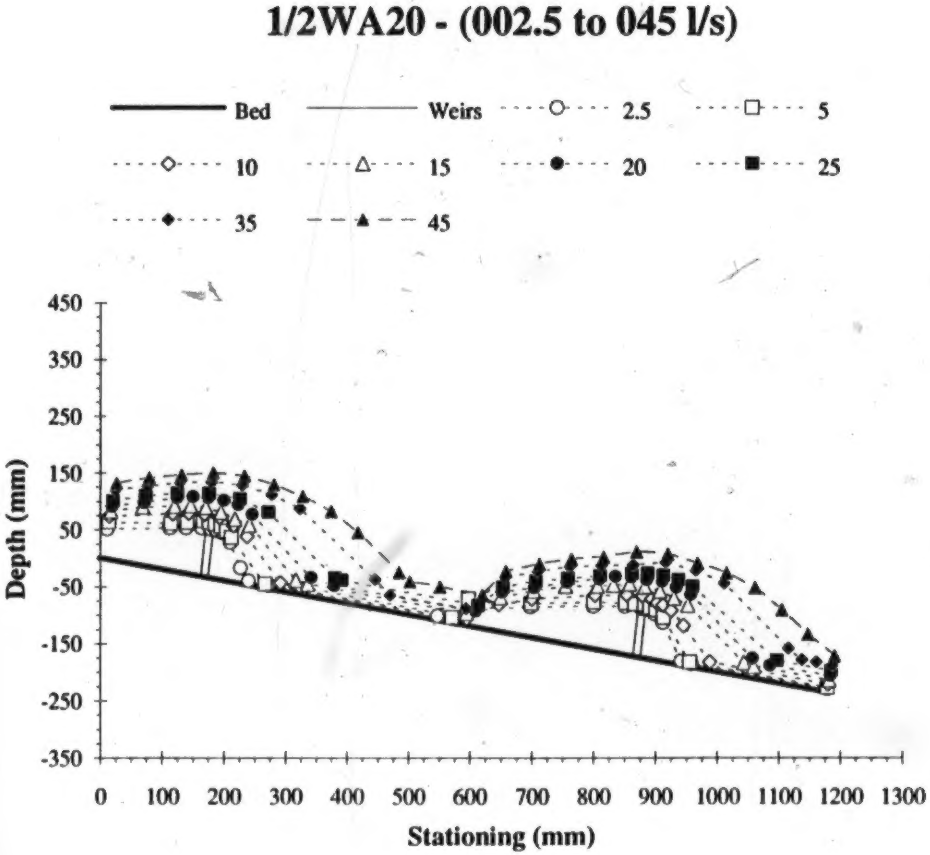
1/2WA20 - (002.5 to 045 l/s)
Bed
Weirs
2.5
5
10
15
20
25
35
45
Depth (mm)
450
350
250
150
50
-50
-150
-250
-350
0
100
200
300
400
500
600
700
800
900
1000
1100
1200
1300
Stationing (mm)

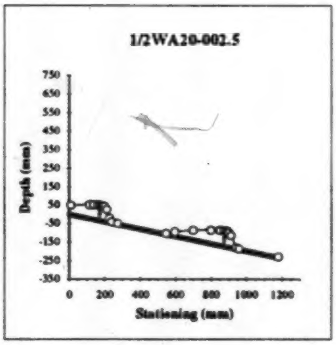
1/2WA20-002.5

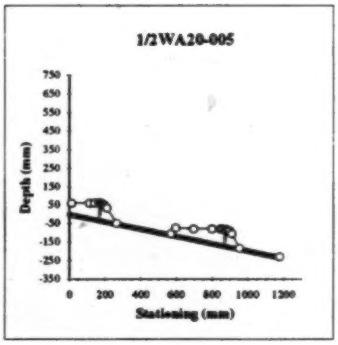
1/2WA20-005

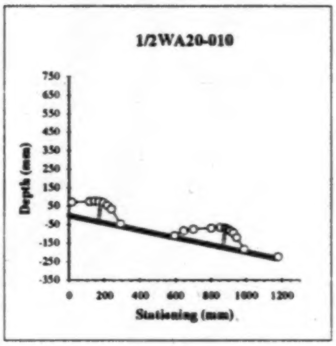
1/2WA20-010

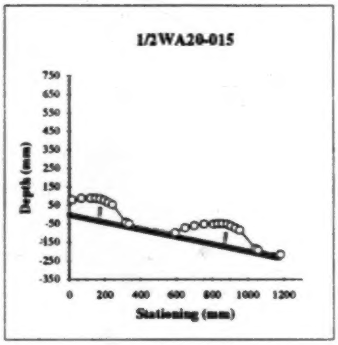
1/2WA20-015

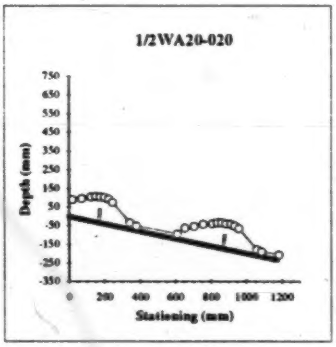
1/2WA20-020

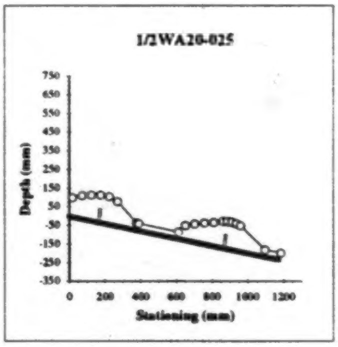
1/2WA20-025

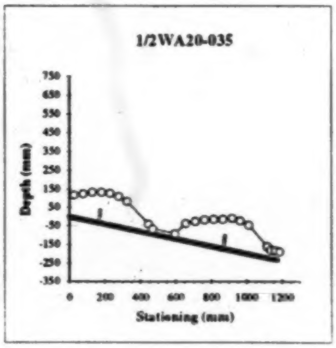
1/2WA20-035

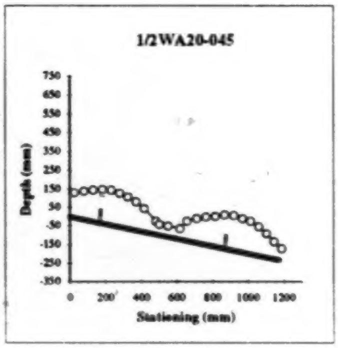
1/2WA20-045

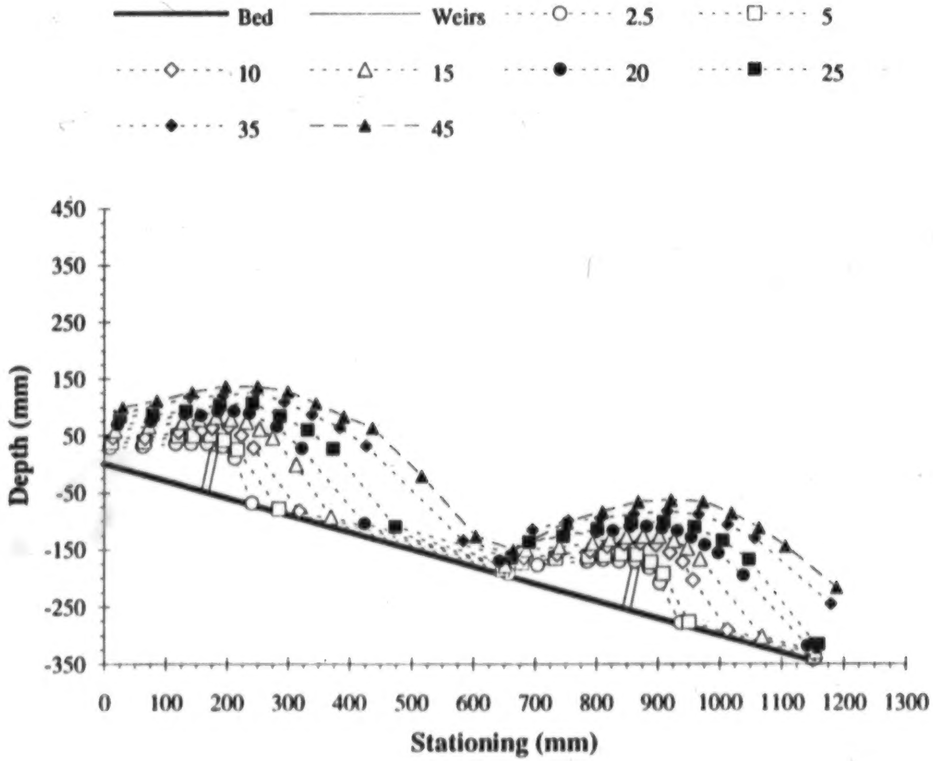

1/2WA30 - (002.5 to 045 l/s)

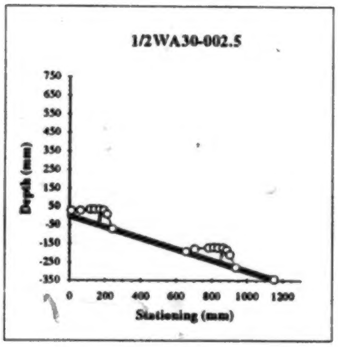

1/2WA30-002.5

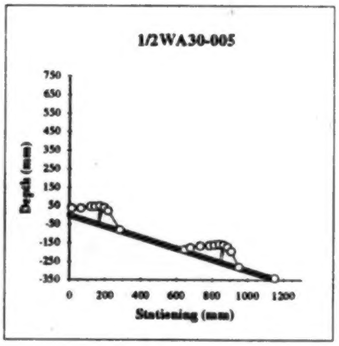

1/2WA30-005

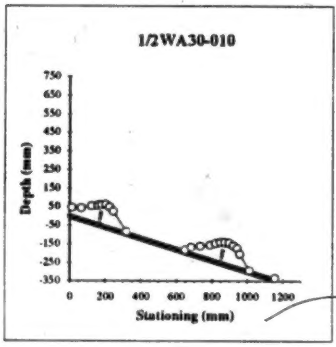

1/2WA30-010

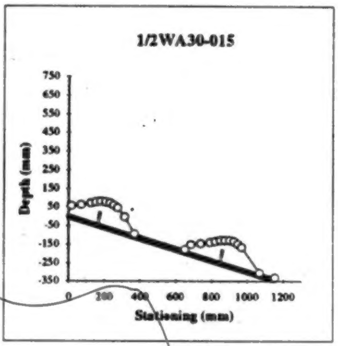

1/2WA30-015

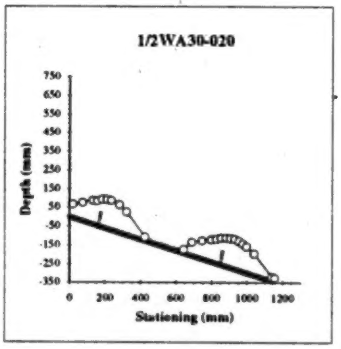

1/2WA30-020

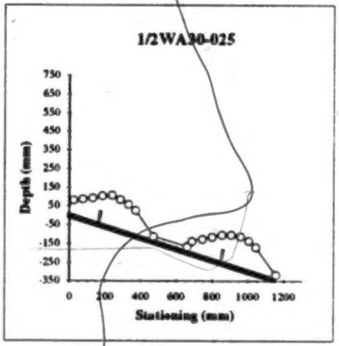

1/2WA30-025

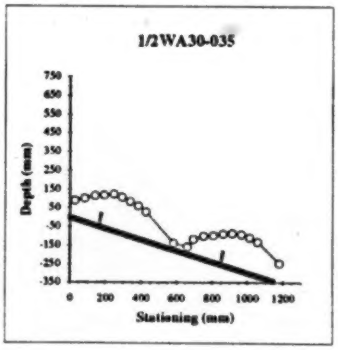

1/2WA30-035

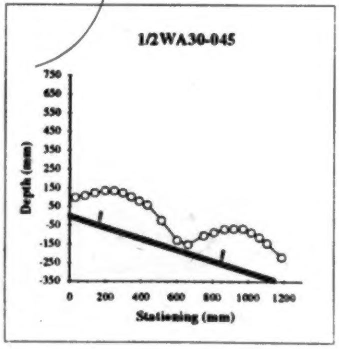

1/2WA30-045

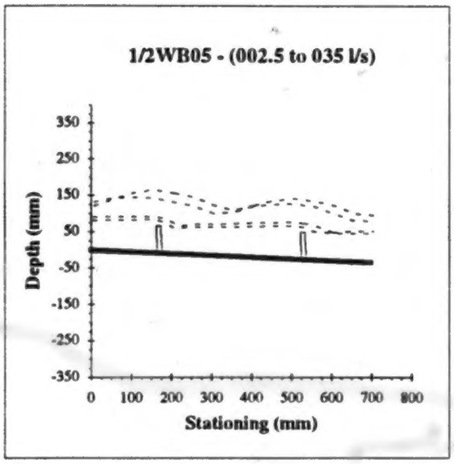

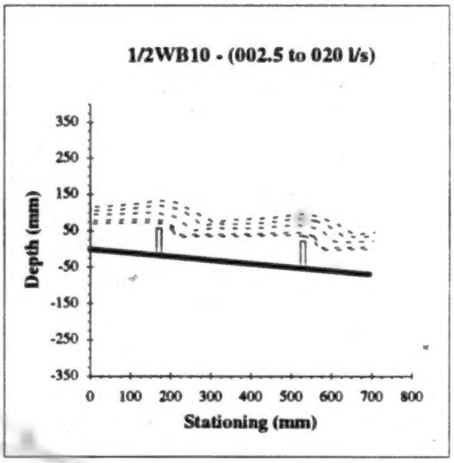

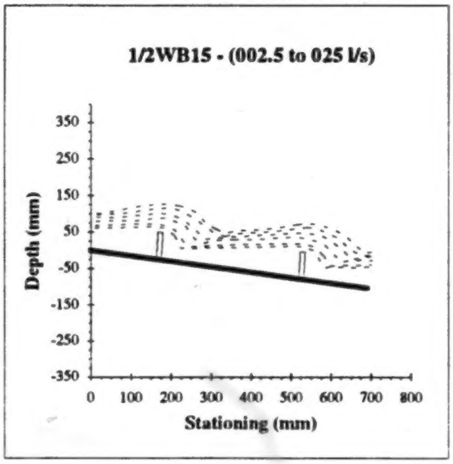

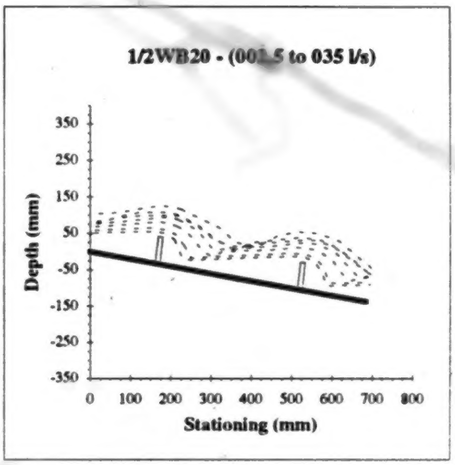

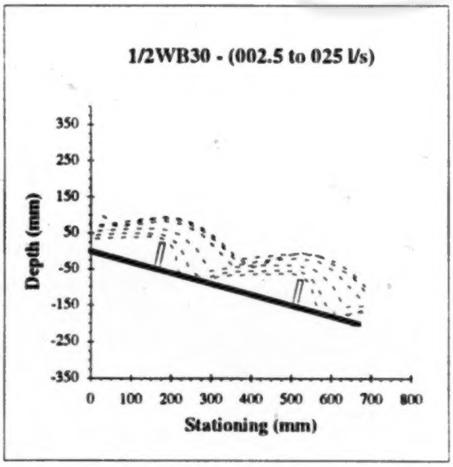

Water Surface Profiles

Half Weir Height

Class 'B' Weir Spacing

5 to 30 % Slope, 5 to 45 l/s

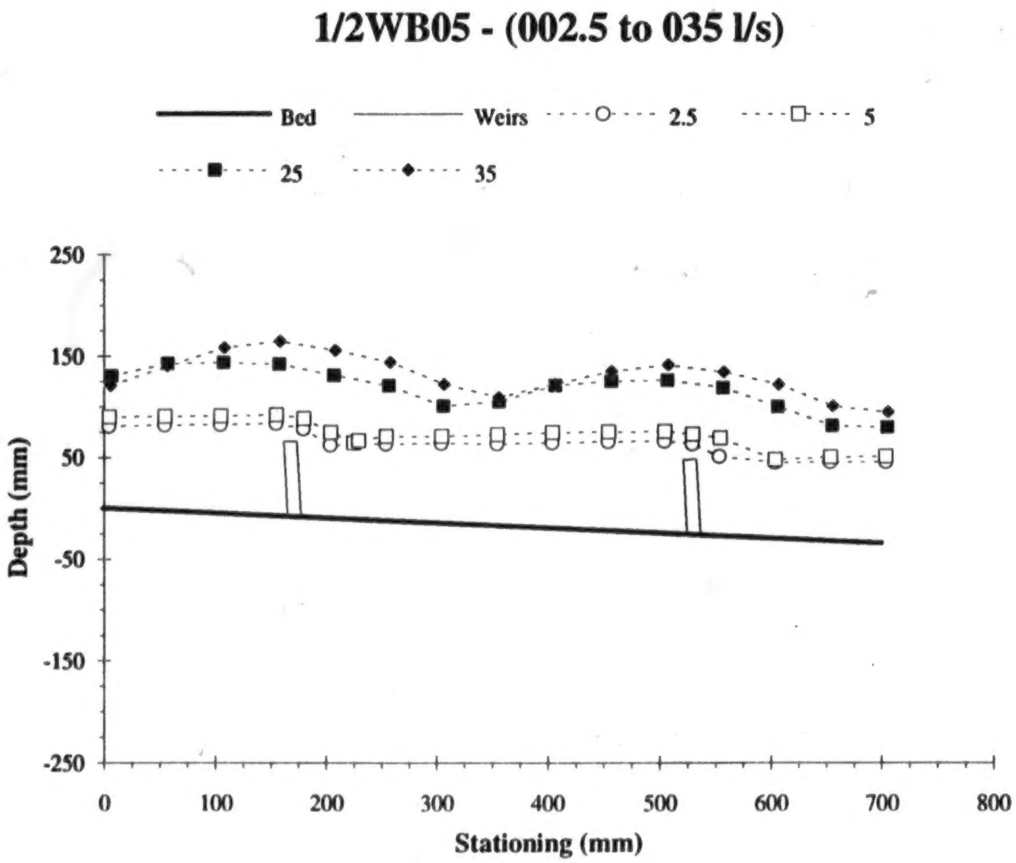
1/2WB05 - (002.5 to 035 l/s)
Bed
Weirs
2.5
5
25
35
Depth (mm)
250
150
50
-50
-150
-250
0
100
200
300
400
500
600
700
800
Stationing (mm)

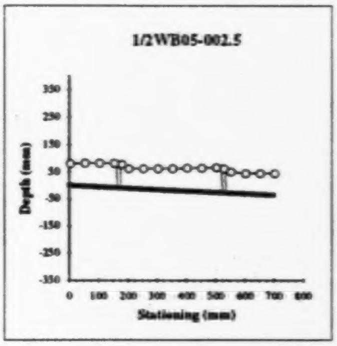
1/2WB05-002.5

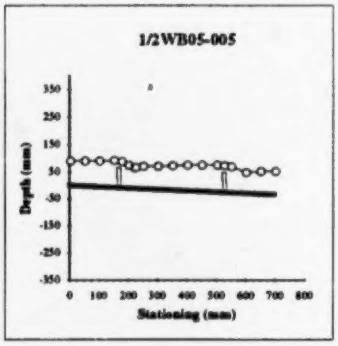
1/2WB05-005

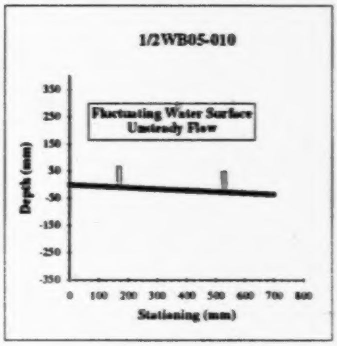
1/2WB05-010

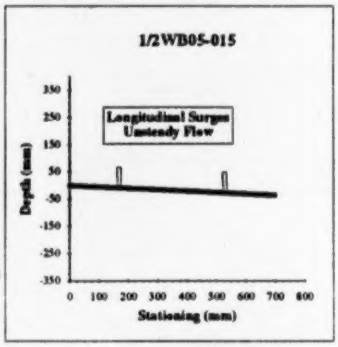
1/2WB05-015

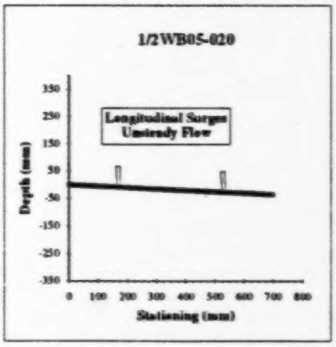
1/2WB05-020

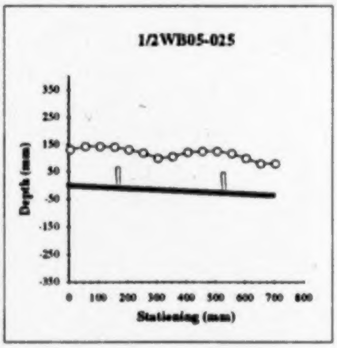
1/2WB05-025

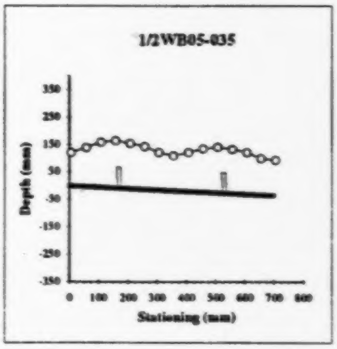
1/2WB05-035

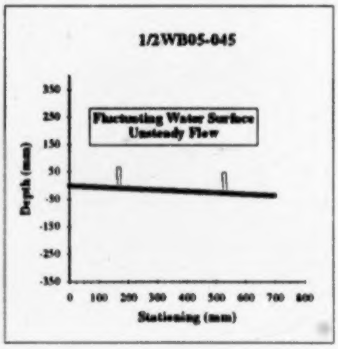
1/2WB05-045

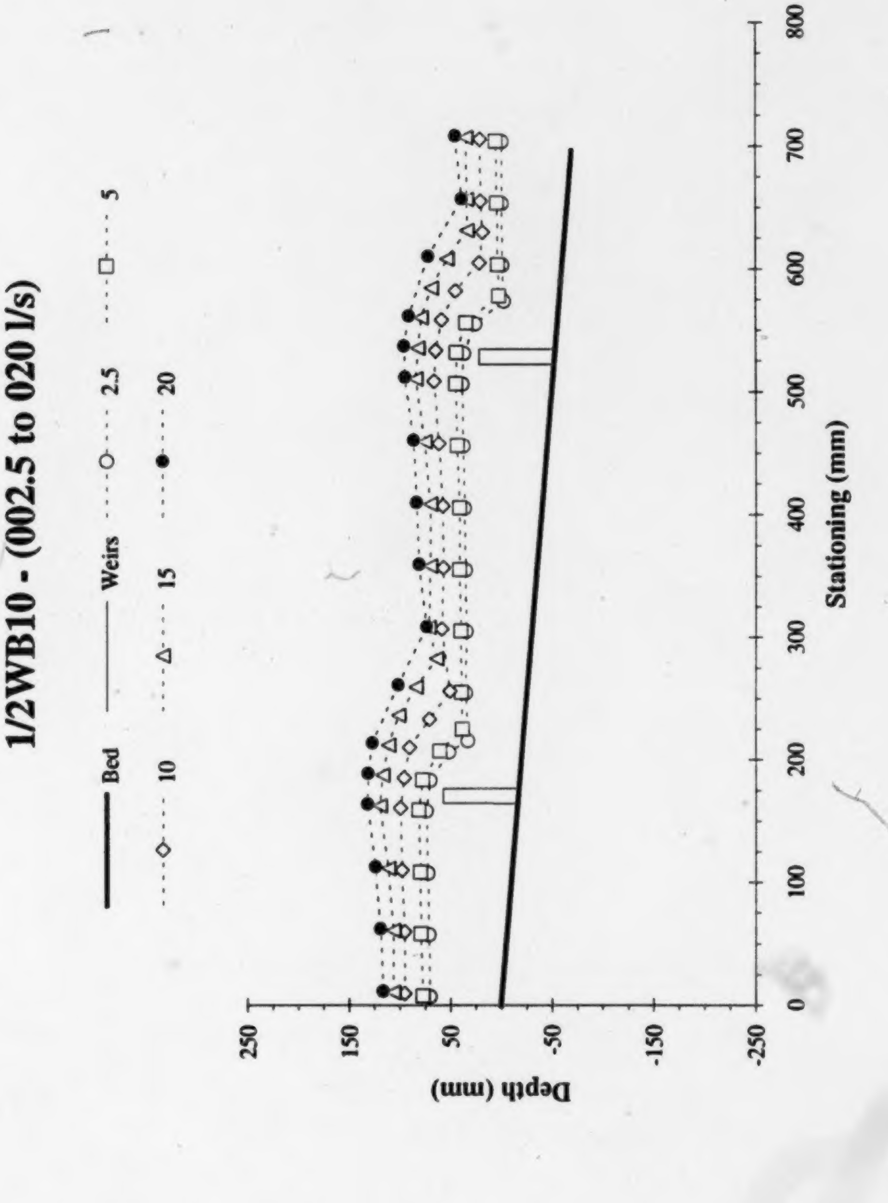
1/2WB10 - (002.5 to 020 l/s)
Bed
Weirs
2.5
5
10
15
20
Depth (mm)
250
150
50
-50
-150
-250
Stationing (mm)
0
100
200
300
400
500
600
700
800

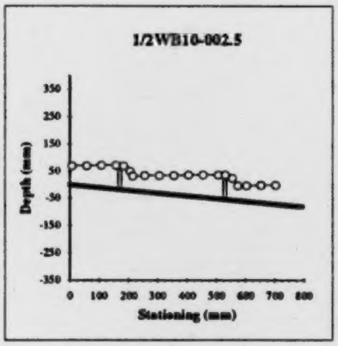
1/2WB10-002.5

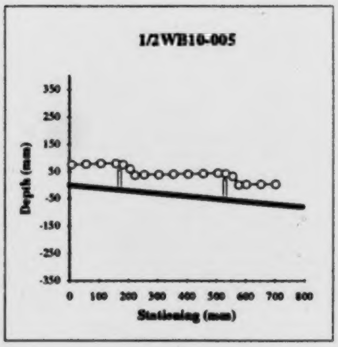
1/2WB10-005

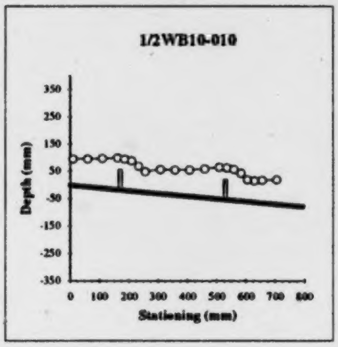
1/2WB10-010

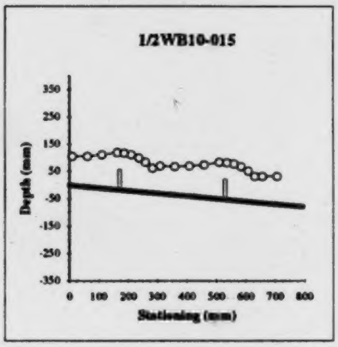
1/2WB10-015

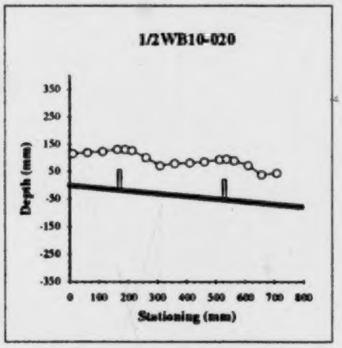
1/2WB10-020

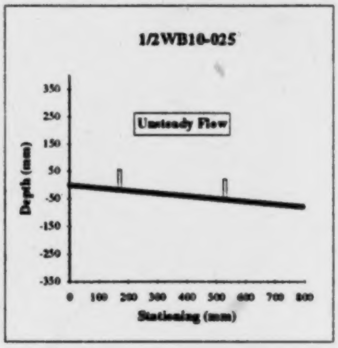
1/2WB10-025

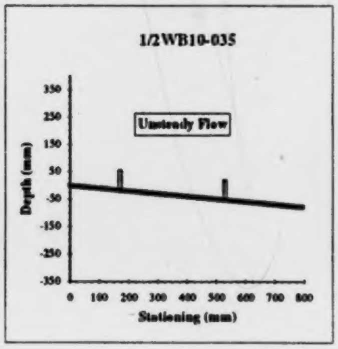
1/2WB10-035

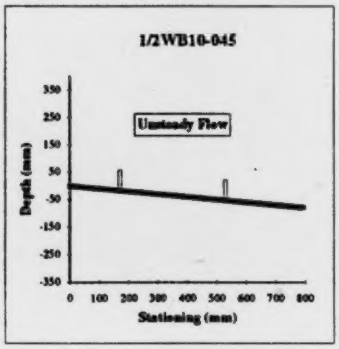
1/2WB10-045

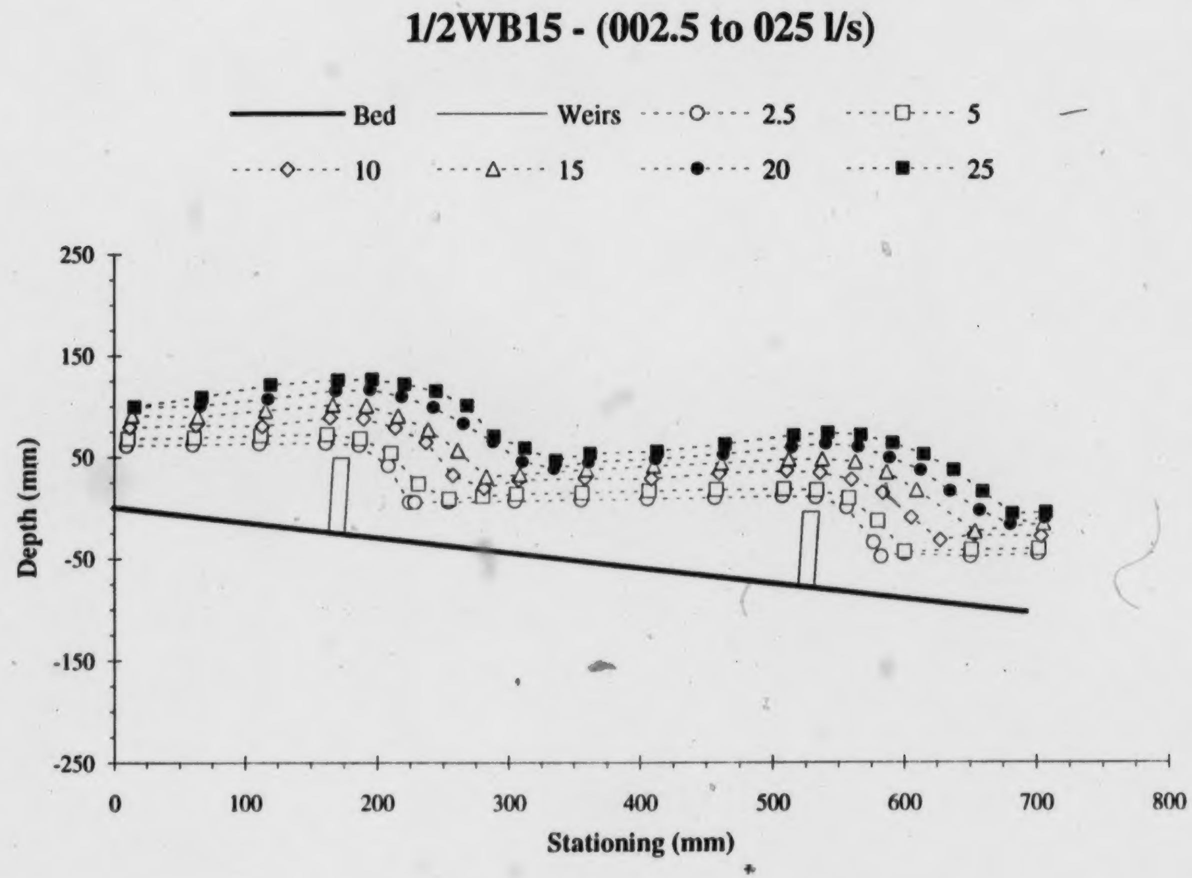

1/2WB15 - (002.5 to 025 l/s)

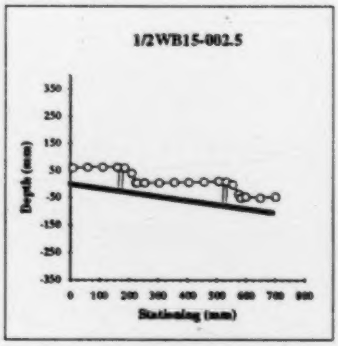
1/2WB15-002.5

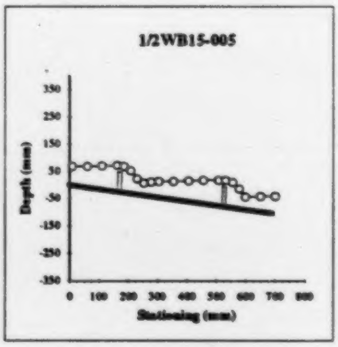
1/2WB15-005

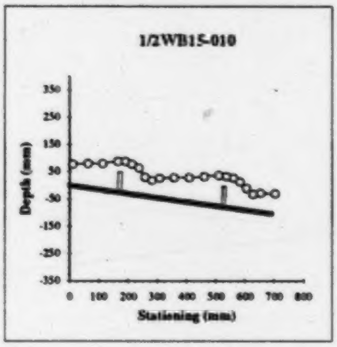
1/2WB15-010

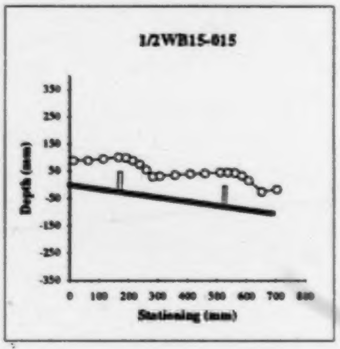
1/2WB15-015

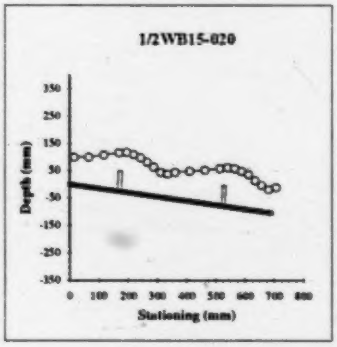
1/2WB15-020

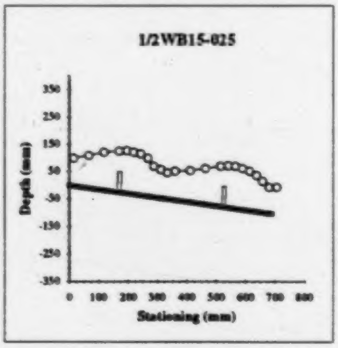
1/2WB15-025

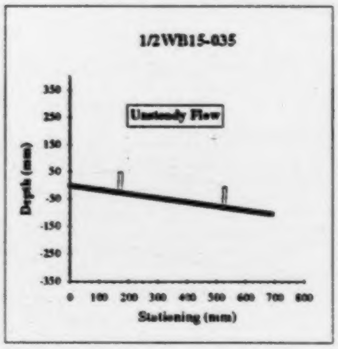
1/2WB15-035

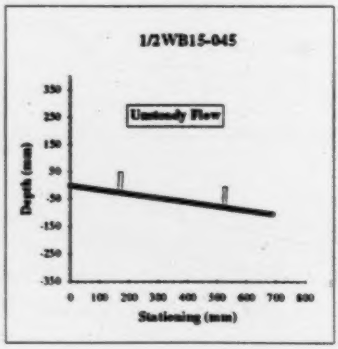
1/2WB15-045

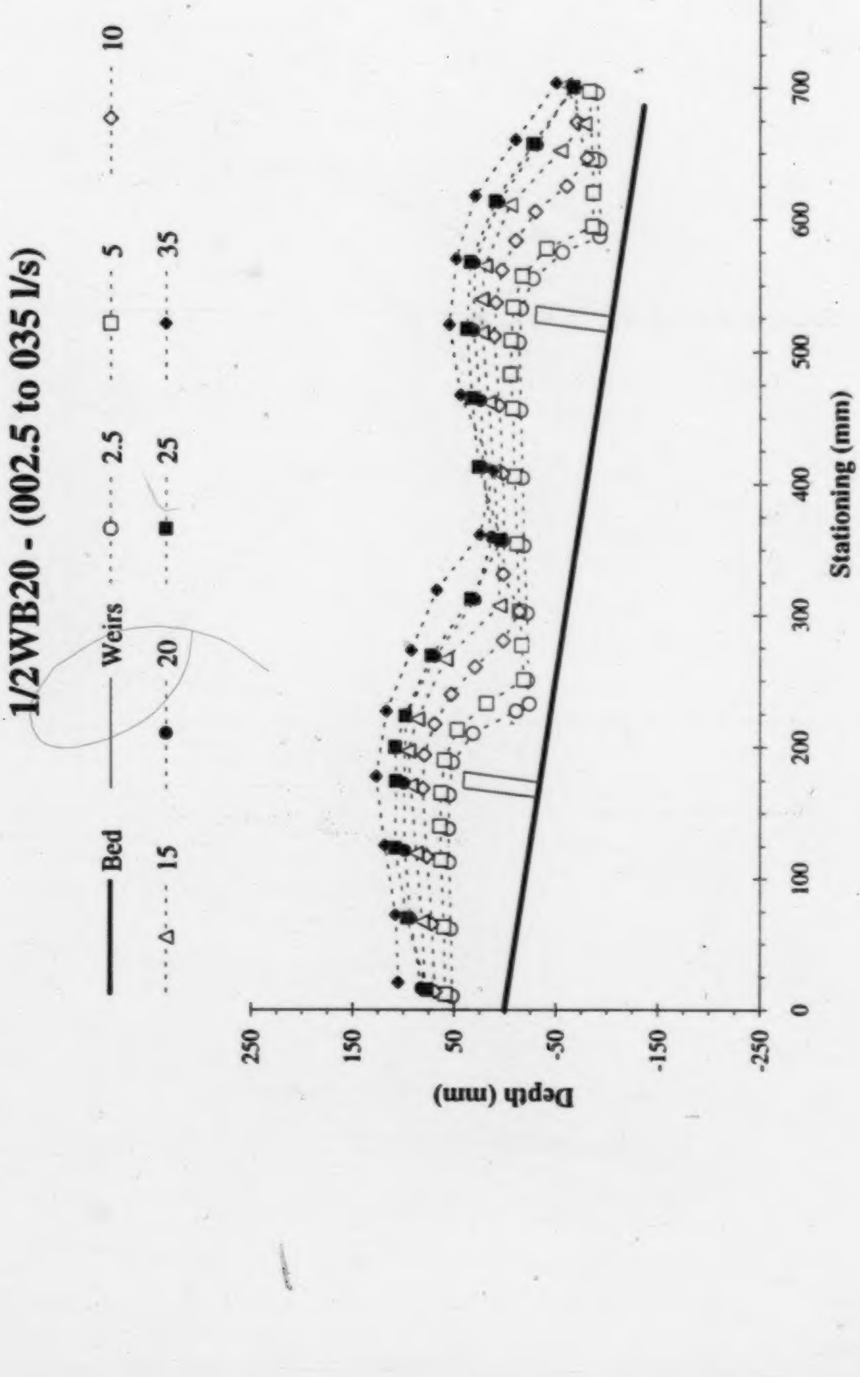
1/2WB20 - (002.5 to 035 l/s)
Bed
Weirs
2.5
5
10
15
20
25
35
Depth (mm)
250
150
50
-50
-150
-250
Stationing (mm)
0
100
200
300
400
500
600
700
800

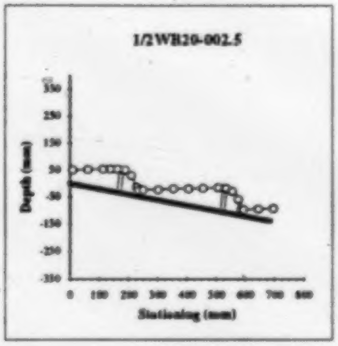
1/2WB20-002.5

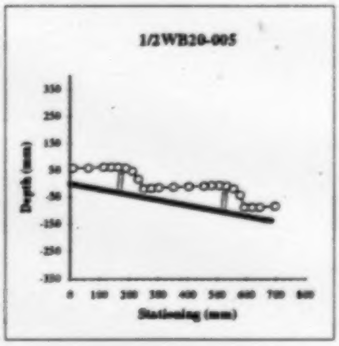
1/2WB20-005

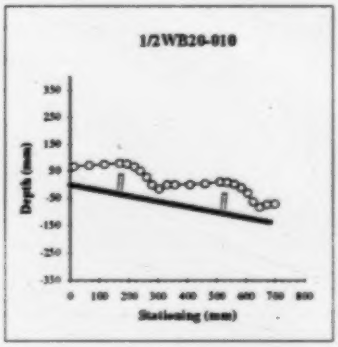
1/2WB20-010

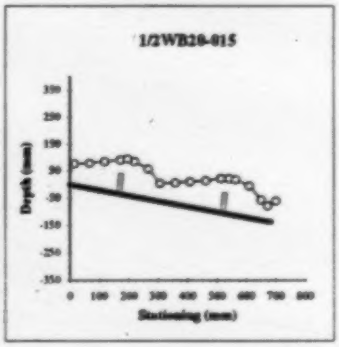
1/2WB20-015

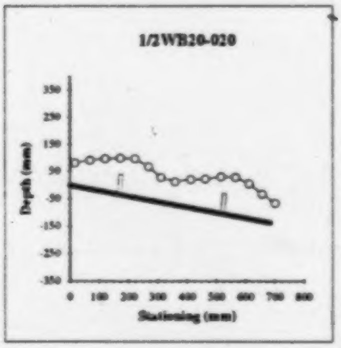
1/2WB20-020

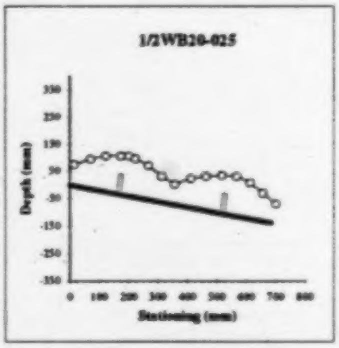
1/2WB20-025

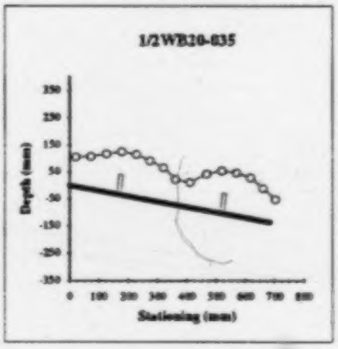
1/2WB20-035

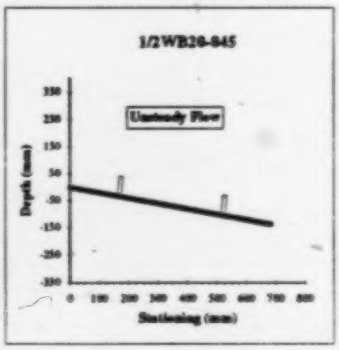
1/2WB20-045

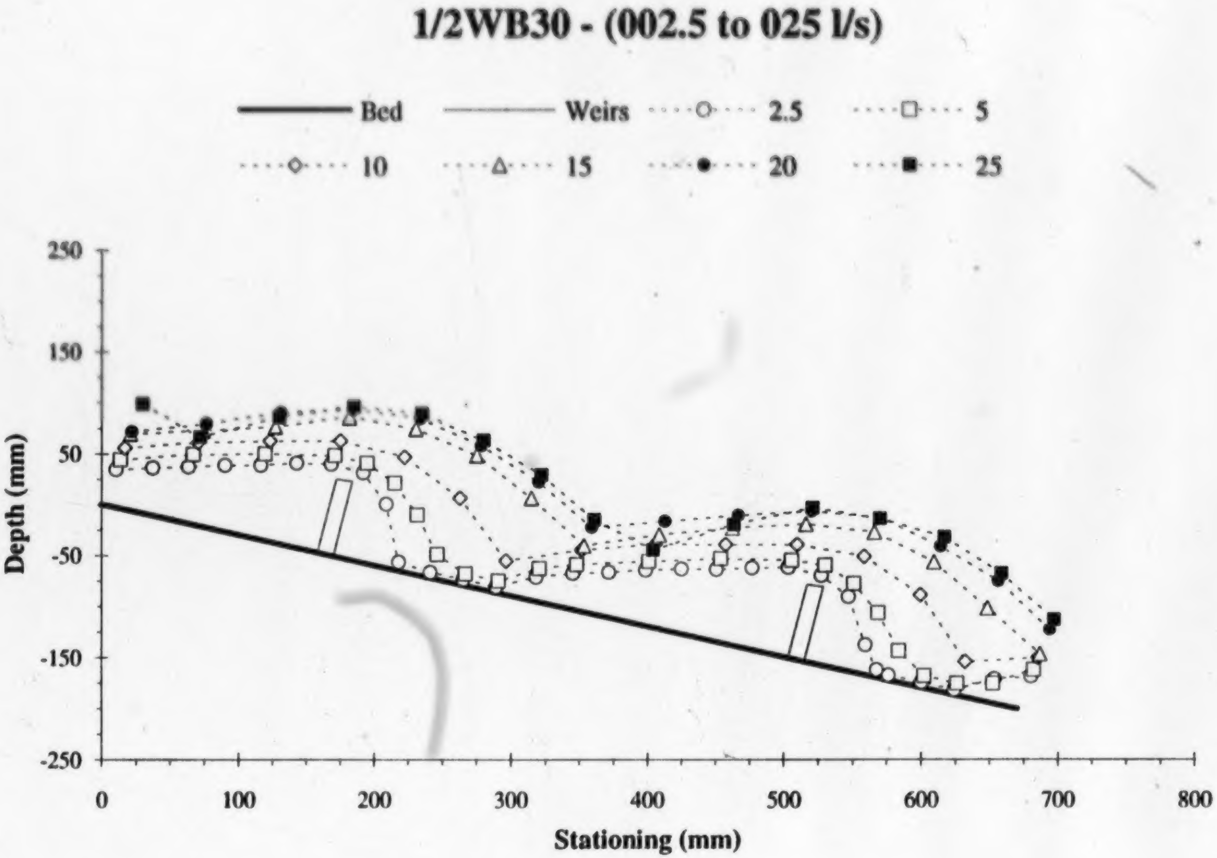
1/2WB30 - (002.5 to 025 l/s)
Bed
Weirs
2.5
5
10
15
20
25
Depth (mm)
250
150
50
-50
-150
-250
Stationing (mm)
0
100
200
300
400
500
600
700
800

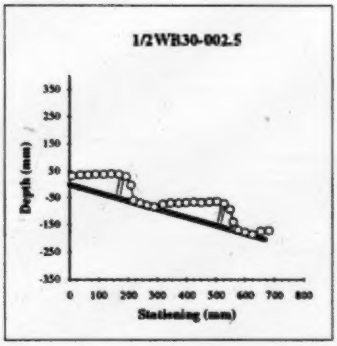
1/2WB30-002.5

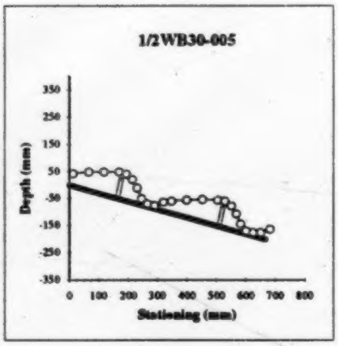
1/2WB30-005

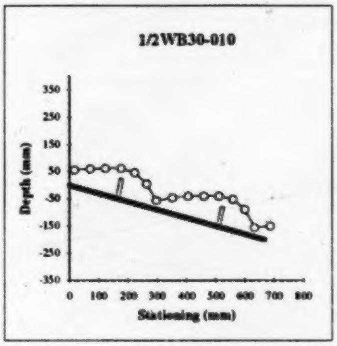
1/2WB30-010

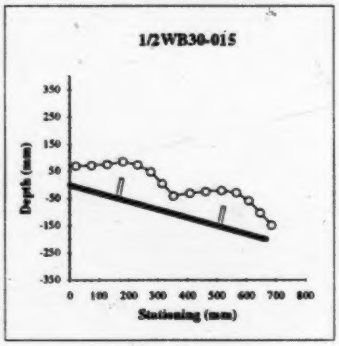
1/2WB30-015

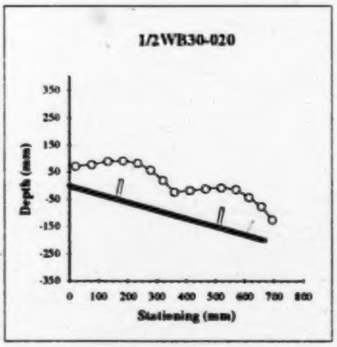
1/2WB30-020

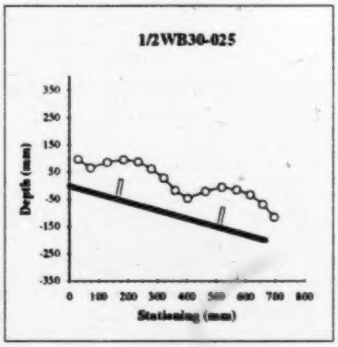
1/2WB30-025

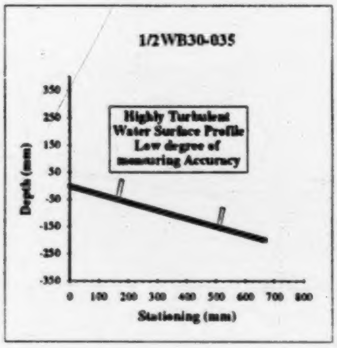
1/2WB30-035

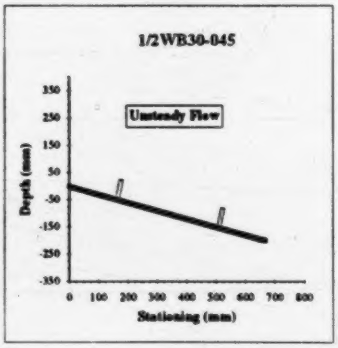
1/2WB30-045

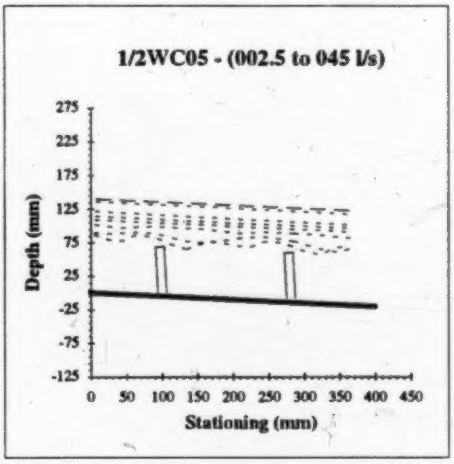
1/2WC05 - (002.5 to 045 l/s)

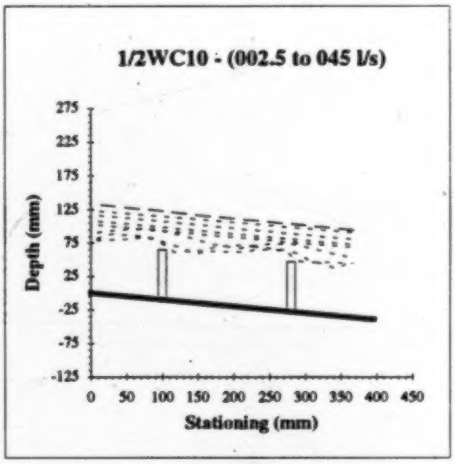
1/2WC10 - (002.5 to 045 l/s)

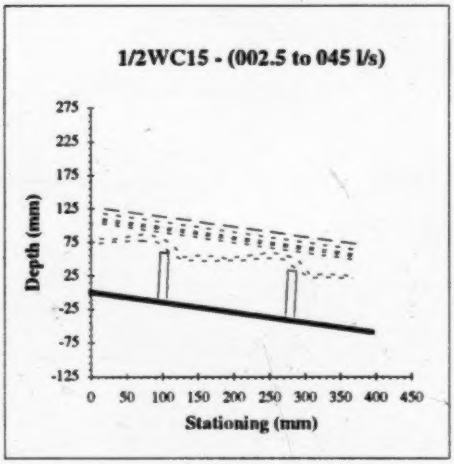
1/2WC15 - (002.5 to 045 l/s)

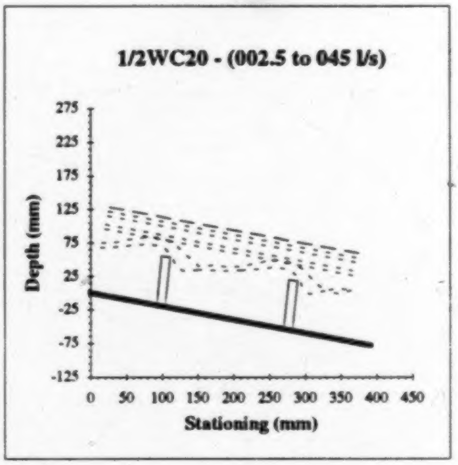
1/2WC20 - (002.5 to 045 l/s)

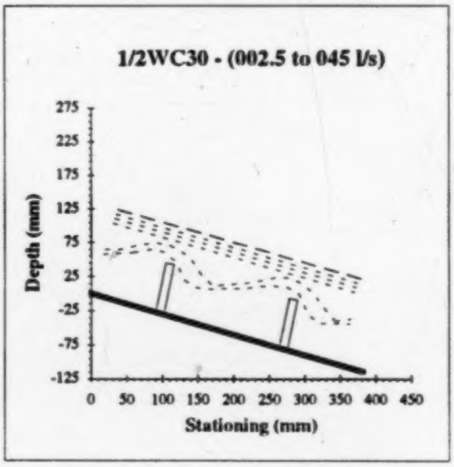
1/2WC30 - (002.5 to 045 l/s)

Water Surface Profiles

Half Weir Height

Class 'C' Weir Spacing

5 to 30 % Slope, 5 to 45 l/s

1/2WC05 - (002.5 to 045 l/s)

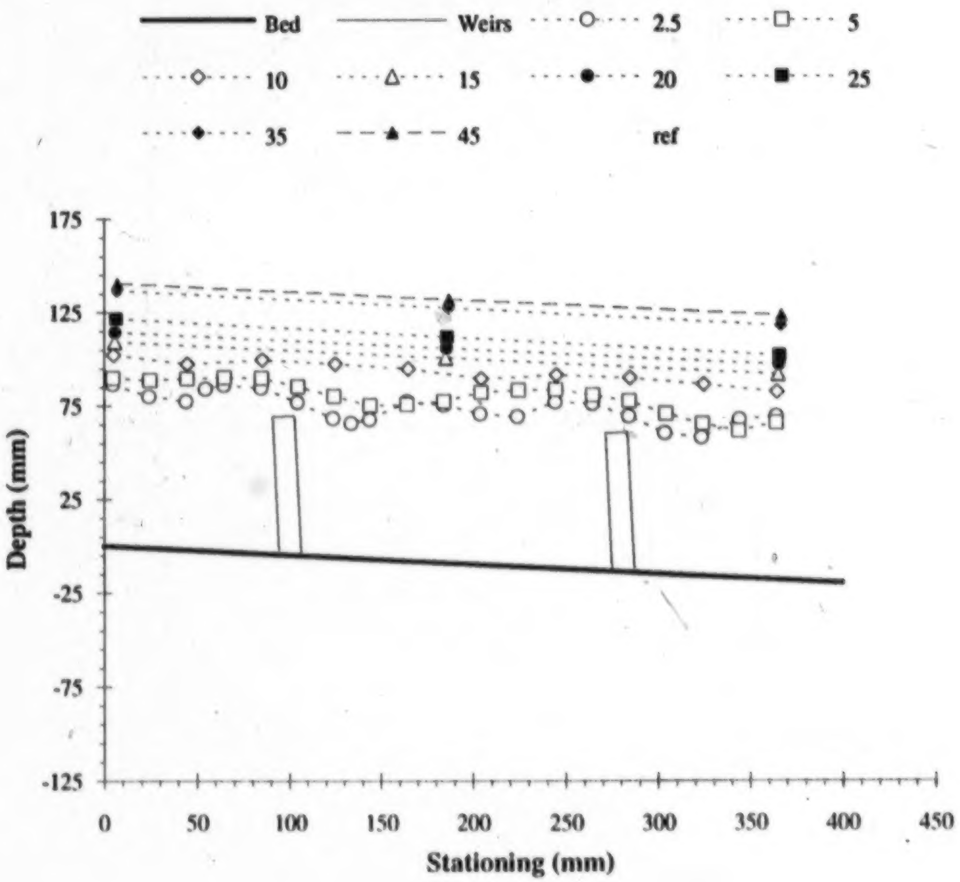

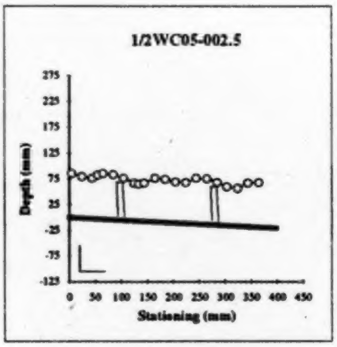
1/2WC05-002.5

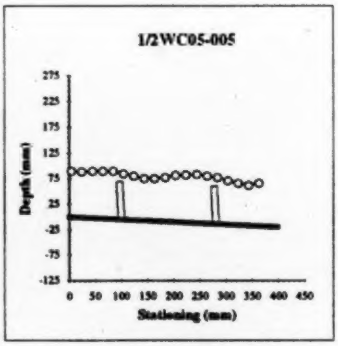
1/2WC05-005

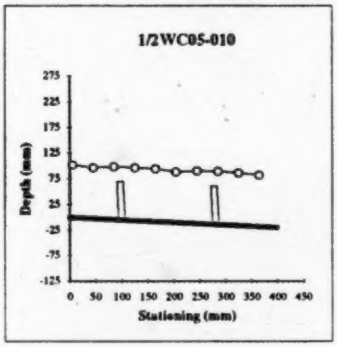
1/2WC05-010

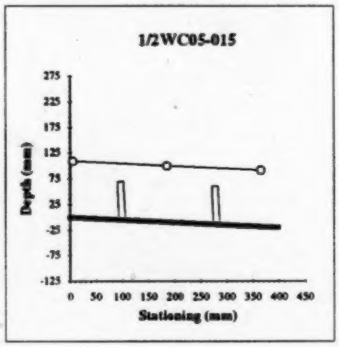
1/2WC05-015

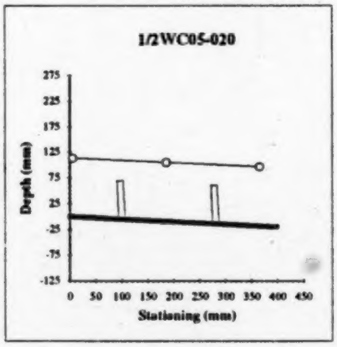
1/2WC05-020

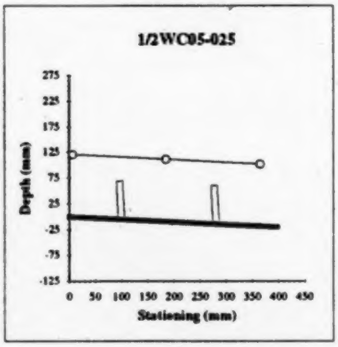
1/2WC05-025

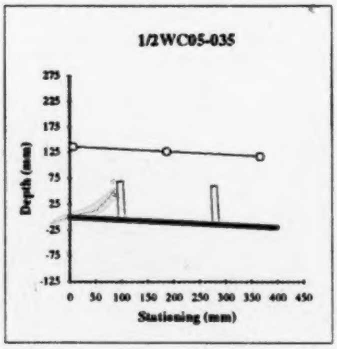
1/2WC05-035

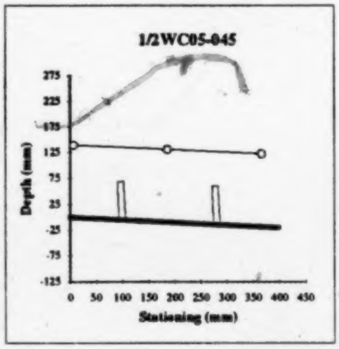
1/2WC05-045

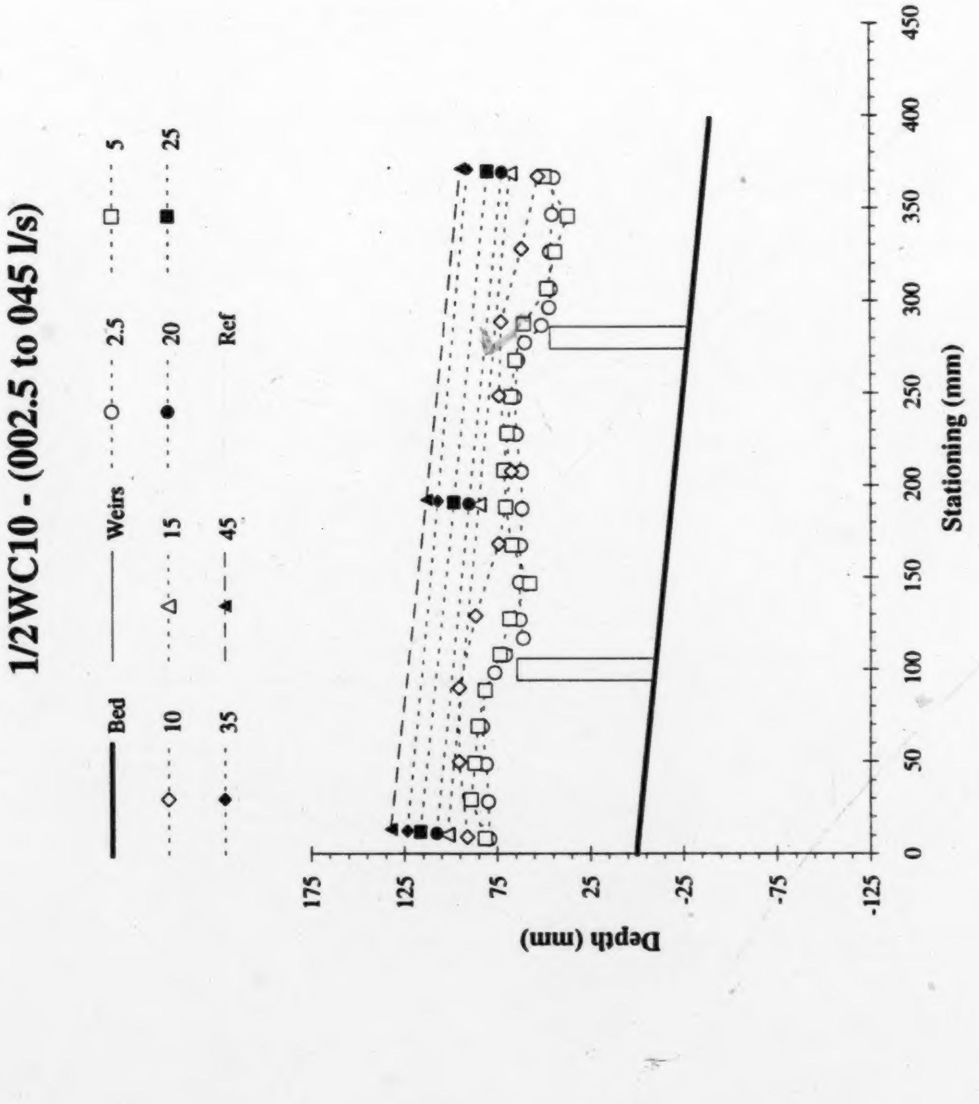
1/2WC10 - (002.5 to 045 l/s)
Bed
Weirs
2.5
5
10
15
20
25
35
45
Ref
Depth (mm)
175
125
75
25
-25
-75
-125
Stationing (mm)
0
50
100
150
200
250
300
350
400
450

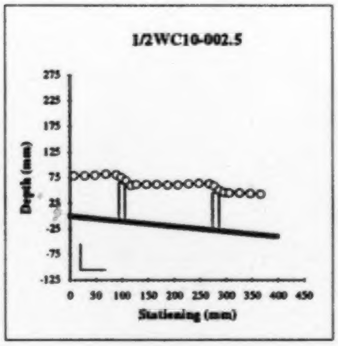
1/2WC10-002.5

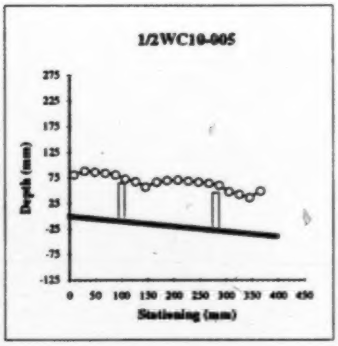
1/2WC10-005

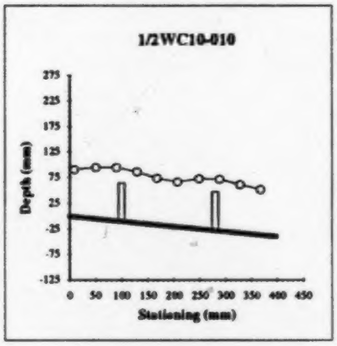
1/2WC10-010

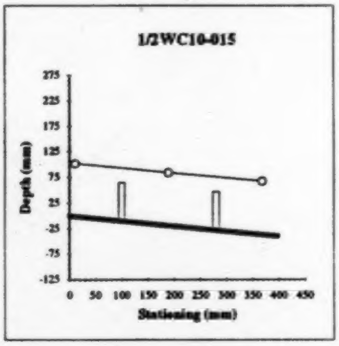
1/2WC10-015

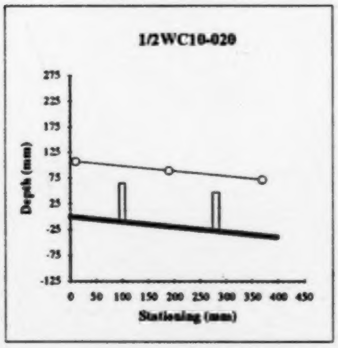
1/2WC10-020

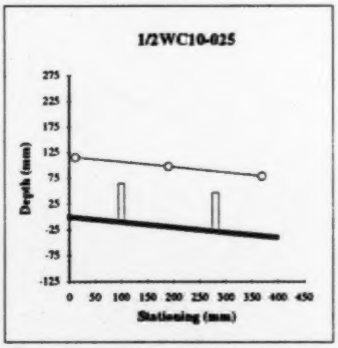
1/2WC10-025

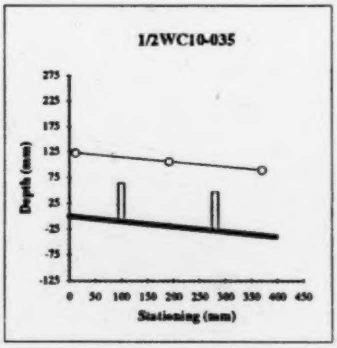
1/2WC10-035

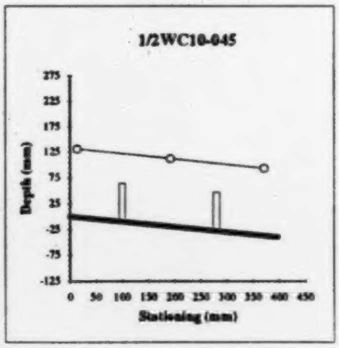
1/2WC10-045

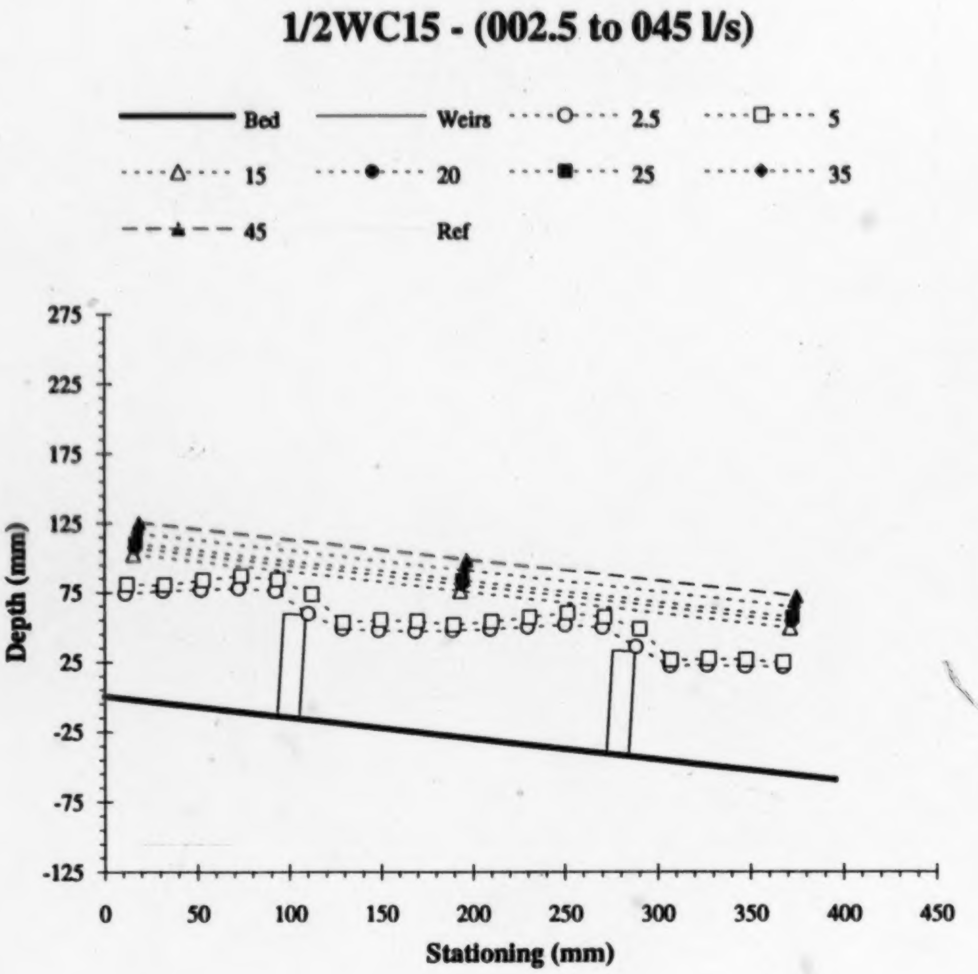
1/2WC15 - (002.5 to 045 l/s)
Bed
Weirs
2.5
5
15
20
25
35
45
Ref
275
225
175
125
75
25
-25
-75
-125
Depth (mm)
0
50
100
150
200
250
300
350
400
450
Stationing (mm)

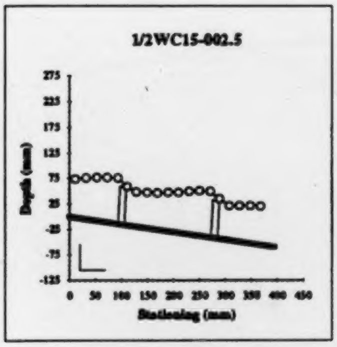
1/2WC15-002.5

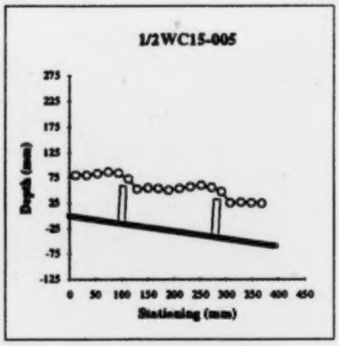
1/2WC15-005

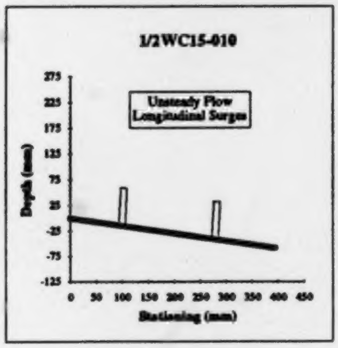
1/2WC15-010

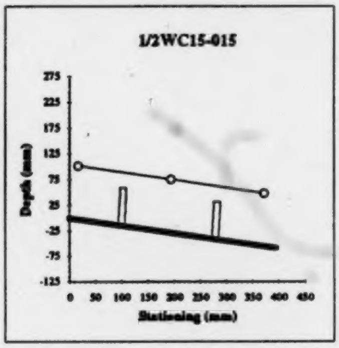
1/2WC15-015

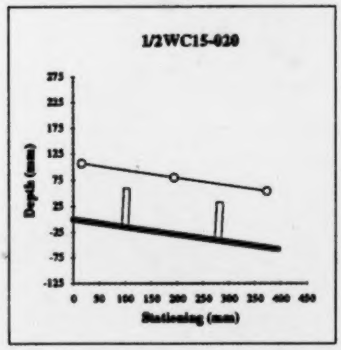
1/2WC15-020

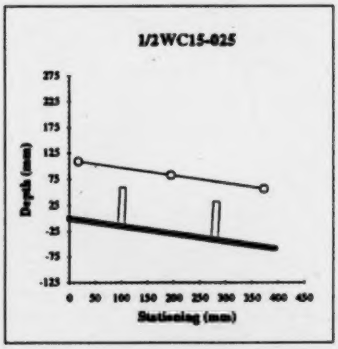
1/2WC15-025

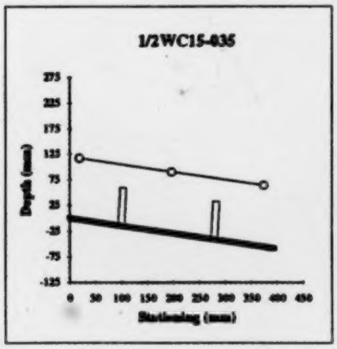
1/2WC15-035

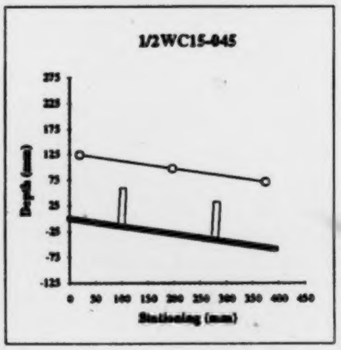
1/2WC15-045

1/2WC20 - (002.5 to 045 l/s)

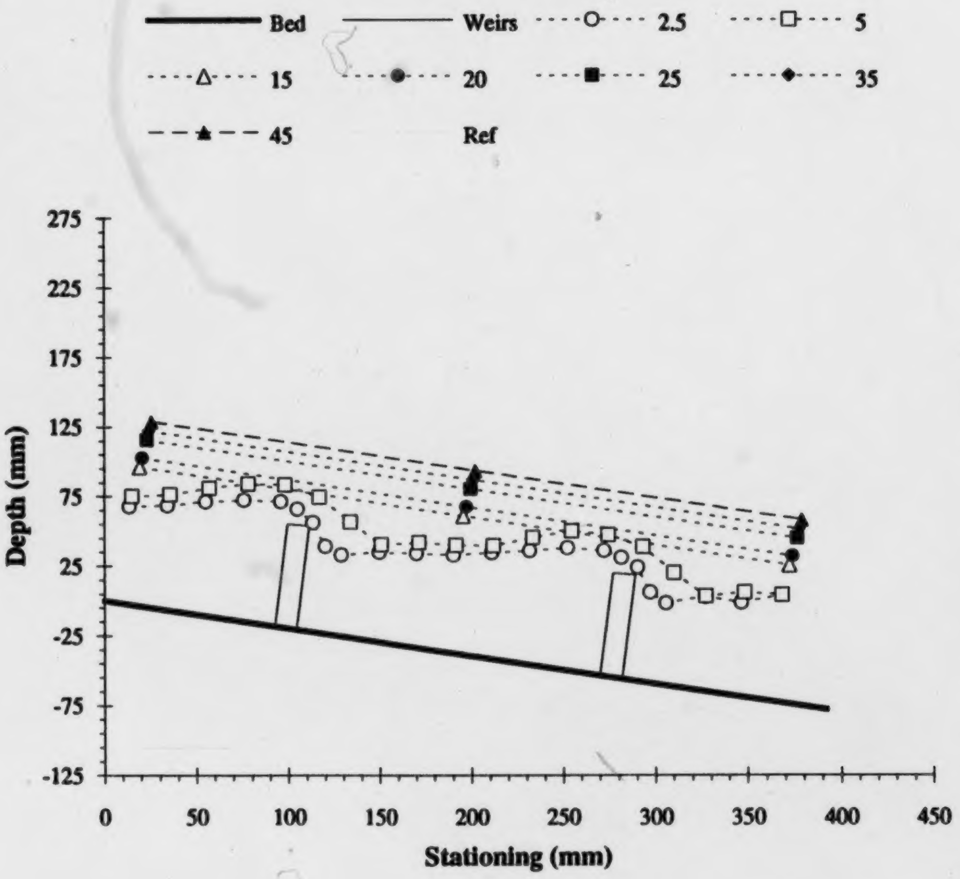

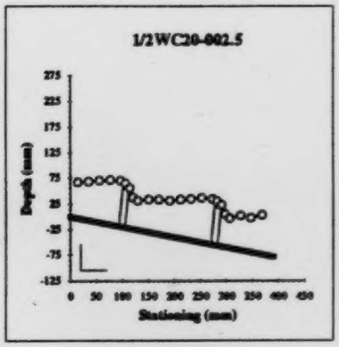
1/2WC20-002.5

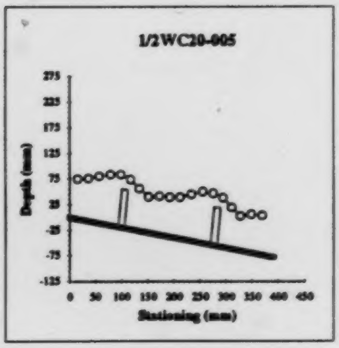
1/2WC20-005

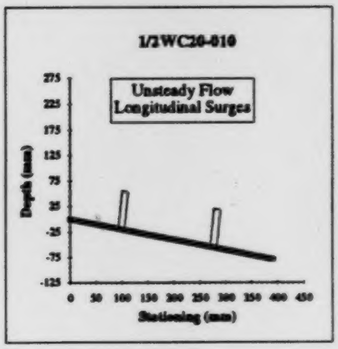
1/2WC20-010

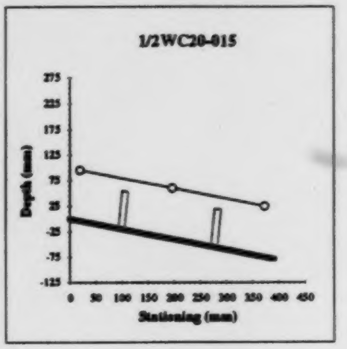
1/2WC20-015

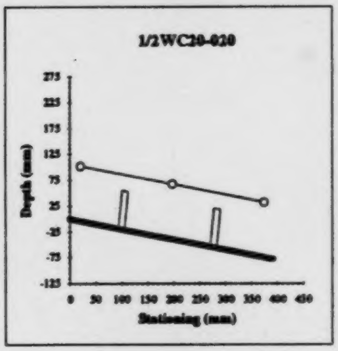
1/2WC20-020

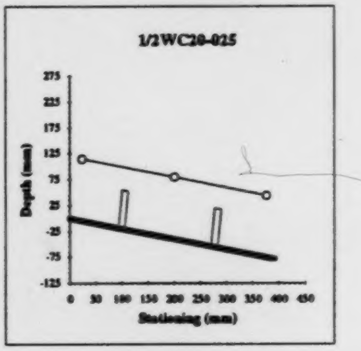
1/2WC20-025

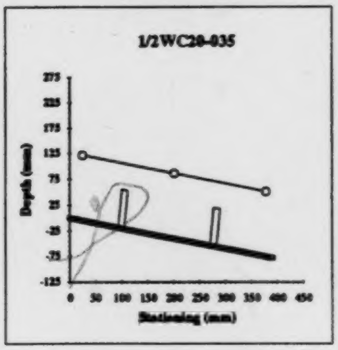
1/2WC20-035

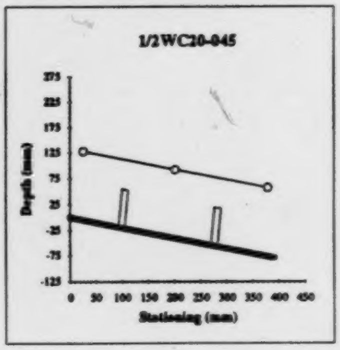
1/2WC20-045

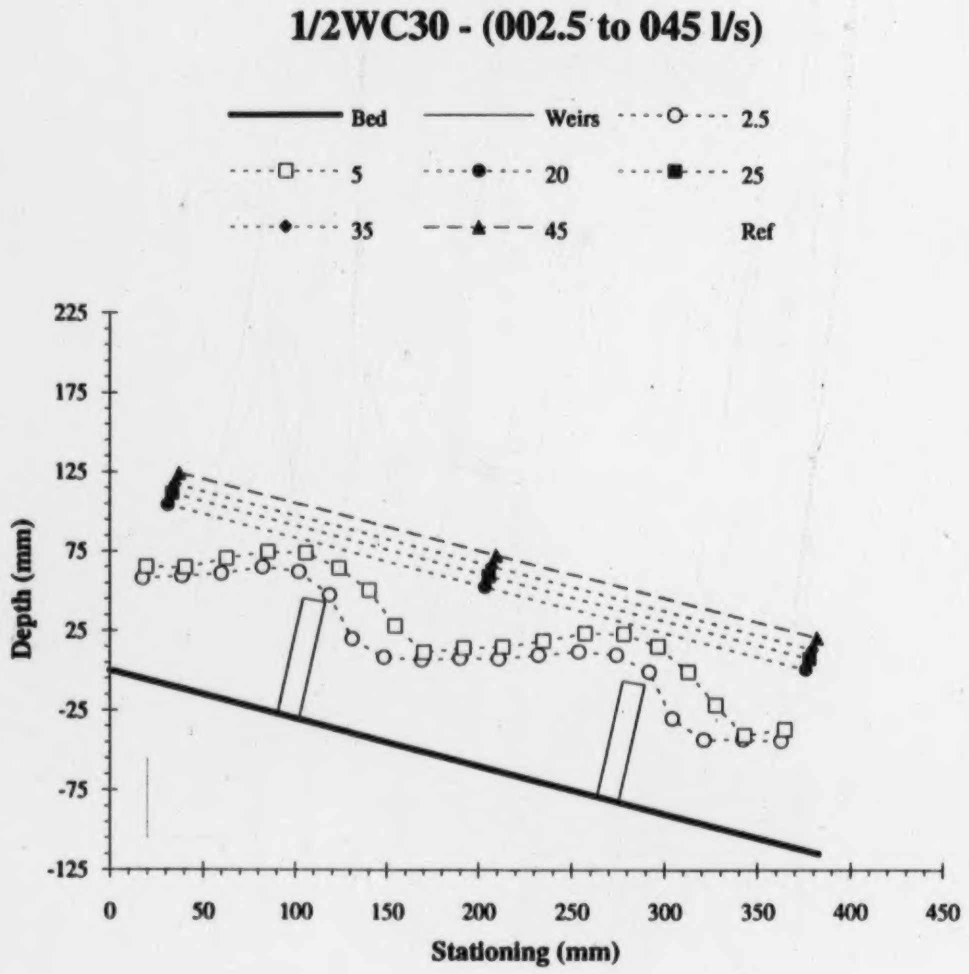
1/2WC30 - (002.5 to 045 l/s)
Bed
Weirs
2.5
5
20
25
35
45
Ref
Depth (mm)
225
175
125
75
25
-25
-75
-125
Stationing (mm)
0
50
100
150
200
250
300
350
400
450

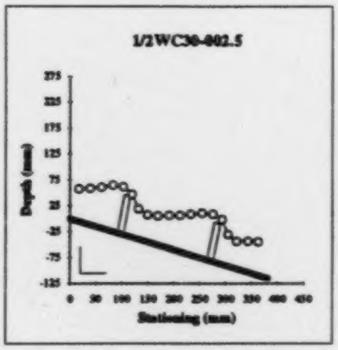
1/2WC30-002.5
Depth (mm)
275
225
175
125
75
25
-25
-75
-125
0 50 100 150 200 250 300 350 400 450
Stationing (mm)

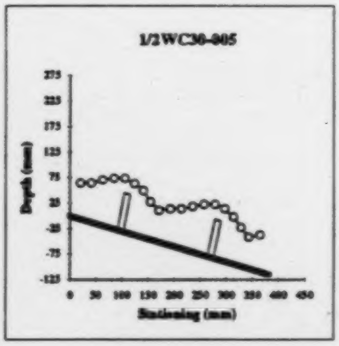
1/2WC30-005
Depth (mm)
275
225
175
125
75
25
-25
-75
-125
0 50 100 150 200 250 300 350 400 450
Stationing (mm)

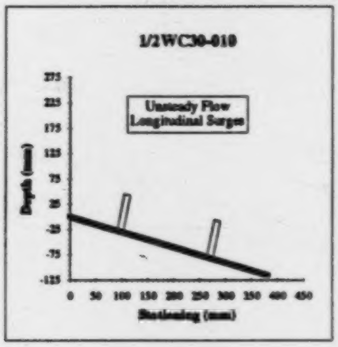
1/2WC30-010
Unsteady Flow
Longitudinal Surges
Depth (mm)
275
225
175
125
75
25
-25
-75
-125
0 50 100 150 200 250 300 350 400 450
Stationing (mm)

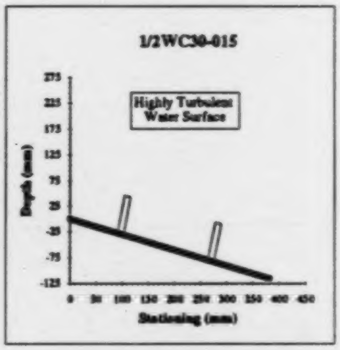
1/2WC30-015
Highly Turbulent
Water Surface
Depth (mm)
275
225
175
125
75
25
-25
-75
-125
0 50 100 150 200 250 300 350 400 450
Stationing (mm)

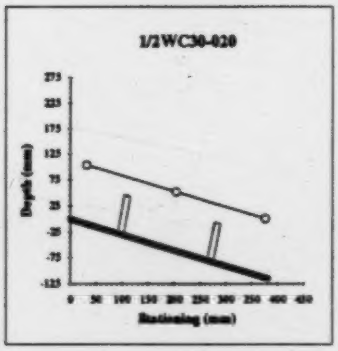
1/2WC30-020
Depth (mm)
275
225
175
125
75
25
-25
-75
-125
0 50 100 150 200 250 300 350 400 450
Stationing (mm)

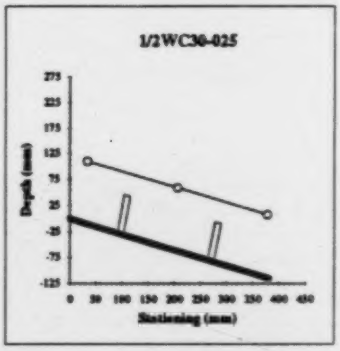
1/2WC30-025
Depth (mm)
275
225
175
125
75
25
-25
-75
-125
0 50 100 150 200 250 300 350 400 450
Stationing (mm)

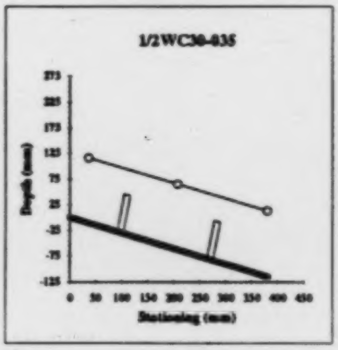
1/2WC30-035
Depth (mm)
275
225
175
125
75
25
-25
-75
-125
0 50 100 150 200 250 300 350 400 450
Stationing (mm)

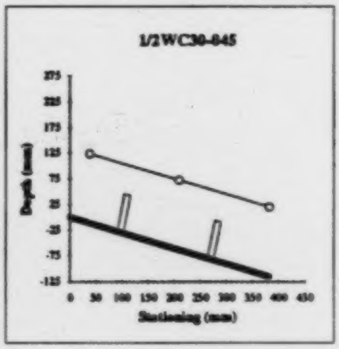
1/2WC30-045
Depth (mm)
275
225
175
125
75
25
-25
-75
-125
0 50 100 150 200 250 300 350 400 450
Stationing (mm)

APPENDIX B

Stability Observations

B.1 Full Weir Height

B.1.1 'A' Class Weir Spacing - 5, 10, 15, 20 & 30 % Slope

Stability Observations

Class: **WA05** (Full weir height, 'A' class weir spacing, 5% bed slope)

Discharge (l/s)	Steady or Unsteady	Type of Flow	Description / Additional Notes
0.5	Steady	Plunging	Surface tension effects controlled the flow. The nape could not be induced even with external assistance.
1	"	"	The nape did form with external assistance. No air entrainment.
2	"	"	The nape formed without external assistance. Very little air entrainment.
5	"	"	The surface was smooth and unbroken. Very little air entrainment. The nape was at the threshold of collapse.
10	"	"	The nape did not exist without assistance. The flow over the weir was descending at approximately 45° to the bed. This was observed by trace amounts of air entrainment and by utilizing a dye tracer.
15	"	"	More air entrainment than 10 l/s.
20	"	"	
25	Steady	Plunging -T	Although the flow was still classified as plunging, the c.c.w. roller was restricted to the top 50 mm and is very small. In addition, the roller now resembled a hydraulic jump rather than a rotating cell.
35	Unsteady	Trans. - B	There appeared to be some storage occurring which leads into a surge pattern. The flow pattern resembled some baffle like characteristics.
45	"	"	Similar to 35 l/s. No c.c.w. roller.
65	Steady	Baffle	Undoubtedly baffle flow
85	"	"	"
105	"	"	"
135	"	"	"
165	Not attempted due to violent nature.		

Stability Observations

Class: **WA10** (Full weir height, 'A' class weir spacing, 10% bed slope)

Discharge (l/s)	Steady or Unsteady	Type of Flow	Description / Additional Notes
0.5	Steady	Plunging	Surface tension effects controlled the flow. The nape could not be induced even with external assistance.
1	"	"	Surface tension effects. The nape would aerate if assisted.
2	"	"	The nape was self aerating.
5	"	"	Small concentrations of air entrainment. Surface was smooth, continuous and unbroken.
10	"	"	Excellent example of classical pool and weir flow. Larger concentrations of air entrainment. Very steady.
15	"	"	Steady plunging flow. Nape collapsed without external intervention.
20	Unsteady	Plunging	Same as 15 l/s. Slight longitudinal surge was present.
25	"	"	Same as 20 l/s. Fluctuations were larger because of vertically directed jet. The nape collapsed without external intervention.
35	Steady	Plunging	The flow has regained stability. The c.c.w. roller typical of plunging flow was restricted to the surface. The nape would not aerate even with external assistance.
45	"	"	High concentrations of air entrainment.
65	Steady	Plunging -T	High concentrations of air entrainment.
85	Steady	Baffle	The c.c.w. roller was very small. The flow exhibited characteristics that were related to baffle flow.
105	Unsteady	Baffle	The water surface profile changes between two main baffle flow patterns. No c.c.w. roller.
135	"	Baffle -S	The flow was highly turbulent. The flow shared baffle and streaming characteristics.
165	Not attempted due to violent nature.		

Stability Observations

Class: **WA15** (Full weir height, 'A' class weir spacing, 15% bed slope)

Discharge (l/s)	Steady or Unsteady	Type of Flow	Description / Additional Notes
0.5	Steady	Plunging	Surface tension effects controlled the flow.
1	"	"	The nape was not fully developed, for it collapsed shortly after it was induced. Threshold of a fully supported nape.
2	"	"	Fully aerated nape. Steady plunging flow. The surface was smooth and continuous.
5	"	"	Same as 2 l/s. Small % of air entrainment.
10	"	"	Same as 5 l/s. However, larger concentration of air entrainment.
15	Unsteady	Plunging	Same as 10 l/s. Appeared to be a longitudinal surge superimposed into this plunging flow.
20	Steady	Plunging	Nape was aerated. Small fluctuations were not large enough to consider the flow unsteady.
25	"	"	Same as 20 l/s.
35	"	"	Same as 25 l/s, but the nape was at a threshold of collapse.
45	"	"	The nape collapsed. It would regain positioning only if assisted. Again like other arrangements, the c.c.w. roller was forced to the surface section and it was reduced in size. Large concentrations of air entrainment.
65	Steady	Trans. - B	Streamline in tufting grid suggest baffle like flow. C.c.w. roller was very small.
85	Steady	Baffle	Definitely baffle flow.
105	Unsteady	Baffle	Flow increase has caused instabilities.
135	"	"	Same as 105 l/s.
165	Not attempted, for instability caused violent flow patterns.		

Stability Observations

Class: **WA20** (Full weir height, 'A' class weir spacing, 20% bed slope)

Discharge (l/s)	Steady or Unsteady	Type of Flow	Description / Additional Notes
0.5	Steady	Plunging	Surface tension effects dominated. 0% air entrainment. No supercritical bed flow as found in WA30-001.
1	"	"	Same as 0.5 l/s
2	"	"	Nape has formed and was fully aerated.
5	"	"	Overall steady in global perspective. There was a trace of a transverse wave.
10	"	"	Approximately 50 % of the entrained air was expelled before the flow reached the downstream weir.
15	"	"	Aerated nape. Steady plunging flow.
20	"	"	Relatively steady. Aerated nape. Almost fully air entrained flow.
25	Unsteady	plunging	Same as 20 l/s. There was a trace of a longitudinal surge.
35	"	"	Still plunging flow (c.c.w. roller was forced to the surface). There was a trace of a longitudinal surge.
45	"	"	There was a slight trace of a transverse wave which produced a serpentine like surface disturbance. The c.c.w. roller was smaller and restricted to the surface. This roller was confined from 1/2 weir length to 3/4 weir length.
65	Steady	Baffle	Threshold of collapsing of nape. There were some characteristics of baffle flow present.
85	"	"	The nape collapsed. There were some characteristics of baffle flow present.
105	Unsteady	Baffle	Unsteady Baffle / Weir flow.
135	"	"	Highly unsteady. Weirs switch flow patterns from one range to another.
165	Not attempted for instability caused violent flow patterns.		

Stability Observations

Class: **WA30** (Full weir height, 'A' class weir spacing, 30% bed slope)

Discharge (l/s)	Steady or Unsteady	Type of Flow	Description / Additional Notes
0.5	Steady	*Plunging*	The bed of the flume had supercritical flow (230 mm). No nape.
1	Unsteady	*Plunging*	The nape was not fully developed and was in a transition which induced surges. 230 mm of supercritical bed flow existed.
2	"	"	The nape had partially developed but the flow was unsteady due to the collapsing napes in the mid flume weirs. This ultimately produced longitudinal surges.
4	"	"	Surges persisted with supercritical bed flow. The nape was fully aerated.
5	"	"	Same as 4 l/s.
6	"	"	Same as 5 l/s. 230 mm of supercritical bed flow.
7	"	"	Almost steady but there was still noticeable surges. The impact of the nape on the bed was closely approaching the hydraulic jump.
8	"	"	Same as 7 l/s.
10	Steady	*Plunging*	The curved plunging jet almost reaches the hydraulic jump. Very small surges in the tail end of the flume.
12	"	"	Same as 10 l/s. Supercritical bed flow was approximately 50 mm long.
13	"	"	Same as 12 l/s. No noticeable surges.
14	"	"	Same as 13 l/s. Supercritical bed flow still existed.
15	"	"	Same as 14 l/s. Very little Supercritical bed flow existed.
20	Steady	Plunging	No supercritical bed flow. The plunging jet had sufficient approach velocity to allow for impact to occur in the downstream pool.
25	"	"	Nape was still well developed. High concentrations of entrained air.
35	"	"	
45	"	"	The c.c.w. roller located at the surface and centered between the weirs was smaller than before. Streamlines visible with the tufting grid suggest a baffle like flow.

Stability Observations

Class: **WA30** (Full weir height, 'A' class weir spacing, 30% bed slope)

Discharge (l/s)	Steady or Unsteady	Type of Flow	Description / Additional Notes
65	Steady	Baffle	The flow was definitely behaving as baffle flow.
85	"	"	Highly turbulent baffle flow.
105	Unsteady	Baffle	Surges crested the baffles / weirs thus rendering the system unsteady. First sign of collapse of the nape. It appeared to be a struggle to keep the nape aerated.
135	"	"	Unsteady. Uncontrollable baffle flow. Measurement of profile would be impossible.
165	Not attempted for the flume would overflow.		

B.1.2 'B' Class Weir Spacing - 5, 10, 15, 20 & 30 % Slope

Stability Observations

Class: **WB05** (Full weir height, 'B' class weir spacing, 5% bed slope)

Discharge (l/s)	**Steady or Unsteady**	**Type of Flow**	**Description / Additional Notes**
0.5	Unsteady	Plunging	The transverse wave increased in amplitude in the d/s section of flume. Relatively steady in first 11 weirs.
1	"	"	Same as 0.5 l/s, but only relatively steady in first 8 weirs.
1.5	"	"	A transverse wave has developed.
2	"	"	The flow was almost steady throughout the entire length of the flume. This flow marks the outer limits of true plunging flow. There were some fluctuations in the water surface in the tail end of the flume.
2.5	Steady	Plunging -T	The flow was completely steady.
3	"	"	
4	"	"	Slight transverse wave with a longitudinal surge in the very end of flume. This disturbance was suspected to be the result of the outlet, draw down conditions and different weir spaces.
5	"	"	
6	Steady	Transitional	
8	"	"	
10	"	"	

Note, the following information does not apply only for the WB05-010 class and discharge, but for other classes which share this similar regime. For this particular discharge, slope and weir spacing, a dye tracer was utilized in determining the flow patterns in one cell. It was observed that although the flow may be steadily supplied, the flow over any one weir does not necessarily behave this way. It was observed that the flow patterns for this arrangement were highly three dimensional and were not uniform across the width of the flume. A streaming jet which was confined to the centre of the flume crested the downstream weir. The flow pattern along the sides resembled a clockwise rotating cell which was essentially water impinged against the downstream weir and forced back upstream to the head of the cell. This flow along the sides then converges to the centre, where it was entrained into the streaming central jet and expelled downstream. The hydraulic jump did not span the flume along a straight line, but the jump formation resembled an arch or parabolic configuration with the apex of the curve near the upstream weir. This flow pattern can be best described as streaming flow along the centerline and plunging flow near the side walls. The streaming section encompassed up to one third the width of the flume.

Stability Observations

Class: **WB05** (Full weir height, 'B' class weir spacing, 5% bed slope)

Discharge (l/s)	**Steady or Unsteady**	**Type of Flow**	**Description / Additional Notes**
15	Steady	Transitional	The flow was globally steady, but between the weirs there was unsteady flow surges which were systems of the streaming flow and hydraulic jump. This variability occurs mainly in the centre where the plane jet or streaming flow forced the downstream jump to fluctuate in location.
20	Unsteady	Transitional	There were several flow patterns which exhibited in this arrangement. Generally the variability in the water surface was due to the streaming flow which collided with the downstream weir, thus caused a upward over flow motion downstream or a backwards flow pattern. Violent water surface.
25	Unsteady	Trans. -S	Threshold of streaming flow.
35	Unsteady	Streaming	There was 'boil' like flow patterns in the undulating streaming flow.
45	"	"	The surface was still not steady, but the streaming layer of water is more defined.
65	"	"	The water surface is highly turbulent, however, more steady than 45 l/s.
85	"	"	The streaming flow was visually more pronounced.
105	"	"	
135	Steady	Streaming	
165 "	"		

Stability Observations

Class: **WB10** (Full weir height, 'B' class weir spacing, 10% bed slope)

Discharge (l/s)	Steady or Unsteady	Type of Flow	Description / Additional Notes
0.5	Steady	Plunging	Steady in all but last few weirs where a small transverse wave action occurred. Maximum amplitude or deflection was approx. 5 mm. Surface tension effects were on d/s side of weir.
1	Unsteady	Plunging	Same as 0.5 l/s but transverse wave was evident in d/s 1/2 of the flume. Surface was still unbroken and continuous.
2	"	"	Upstream half of the flume was still steady. The transverse wave in the d/s section increased in amplitude. Still unbroken or continuous surface throughout.
2.5	"	"	Transverse wave was still in d/s section.
3	Steady	Plunging	There was no longer any transverse wave in the d/s section of the flume.
4	"	"	Steady throughout.
5	"	"	Classical plunging flow. The flow was steady and uniform across the weirs. The surface was continuous without any turbulent disturbances. There was a little air entrainment, however, it quickly escaped to the surface in the lower section of each pool.
6	"	"	
8	"	"	
10	Steady	Plunging -T	Variable flow patterns. The centre line exhibited a plunging type of flow, where the sides were clearly a transitional streaming flow pattern. There was no wave action. The surface was no longer continuously smooth, but now had a boiling like motion.
11	"	"	Same as 10 l/s. Plunging along centre line.
12	"	"	Returned to an uniform plunging flow pattern fully across the weir.
13	"	"	

Stability Observations

Class: **WB10** (Full weir height, 'B' class weir spacing, 10% bed slope)

Discharge (l/s)	**Steady or Unsteady**	**Type of Flow**	**Description / Additional Notes**
14	Unsteady	Plunging -T	Initial evidence of a longitudinal surge.
15	"	"	The c.c.w. roller was now restricted to a region near the surface. This roller no longer extends down to the bottom as in a typical plunging flow pattern. There were fluctuations between a streaming transitional flow and a plunging flow.
20	"	"	A longitudinal surge was evident. The hydraulic jump and c.c.w. roller which exists in a plunging flow condition was now positioned near the surface in the top last quarter of the pool.
25	Unsteady	Transitional	Longitudinal surge
35	Unsteady	Trans. - S	The center of the flume experienced a streaming flow pattern, where the flow along the edges resembled transitional flow.
45	"	"	Slowly changed to a more standard streaming flow, but still not fully uniform across the x-section.
65	"	"	Almost steady flow. The flow was not ideal parallel skimming flow in the streaming sense.
85	Steady	Streaming	Globally steady. Some variability in the surface.
105	"	"	There was some fluctuations in the surface. V-shaped streaming flow conditions were really predominant here. Although the flow in the entire flume was streaming, the centre line section was flowing faster than the sides. In addition, the water surface was higher along the edges.
135	"	"	The water surface was more uniform across the width of the flume.
165	Steady	Streaming	Fully developed and uniform steady streaming flow.

Stability Observations

Class: **WB15** (Full weir height, 'B' class weir spacing, 15% bed slope)

Discharge (l/s)	**Steady or Unsteady**	**Type of Flow**	**Description / Additional Notes**
0.5	Steady	Plunging	Unbroken smooth surface. Surface tension causes nape to collapse. No air entrainment.
1	"	"	Same as 0.5 l/s, except there was trace amounts of air entrainment.
2	"	"	The nape was fully supported and self aerating.
3	"	"	Same as 2 l/s
4	"	"	Same as 3 l/s
5	"	"	Barely noticeable transverse wave action.
6	"	"	Very small transverse waves. There was more air entrainment. The surface was less smooth and was now comprised of irregularities.
8	"	"	
10	"	"	Aerated nape was in the process of collapsing. Increased air entrainment.
14	"	"	Same as 10 l/s
15	Unsteady	Plunging	The flow was typically steady ,however, the transverse waves were producing different water elevations. Maximum deviation in the water surface was approx. 1 cm. The flow was comprised of two rollers, one c.w. in the bottom half and one c.c.w. in the top half. Overall steady
20	"	"	The longitudinal surges that developed do not develop until downstream of the first three weirs. The flow was steady in the first three pool and weirs.
25	Unsteady	Plunging - T	Same as 20 l/s but the longitudinal surge had increased in frequency.
35	Unsteady	Trans. - S	No longer any plunging flow (c.c.w. rotation). Starting of streaming flow. There appeared to be some transverse waves as well as longitudinal surges; however, the surface was very turbulent and it was difficult to detect any wave forms.

Stability Observations

Class: **WB15** (Full weir height, 'B' class weir spacing, 15% bed slope)

Discharge (l/s)	Steady or Unsteady	Type of Flow	Description / Additional Notes
45	Steady	Trans. - S	Highly turbulent surface. Large air entrainment.
65	"	"	The flow had not yet developed into the classical parallel streaming conditions.
85	"	"	Same as 65 l/s
105	Steady	Streaming	For 150 to 165 l/s, as the discharge increased, the surface became less turbulent.
135	"	"	
165	"	"	

Stability Observations

Class: **WB20** (Full weir height, 'B' class weir spacing, 20% bed slope)

Discharge (l/s)	Steady or Unsteady	Type of Flow	Description / Additional Notes
0.5	Steady	Plunging	Unbroken smooth surface. Surface tension caused the nape to collapse.
1	"	"	Slight fluctuation in elevation. This was due to the surface tension which caused temporal separation of the nape.
2	"	"	The nape was fully aerated. Small concentrations of air entrainment.
3	"	"	Same as 2 l/s.
4	"	"	Same as 3 l/s, except for more air entrainment.
5	"	"	Steady throughout upstream one half of the flume, however, a slight longitudinal surge developed in the tail end.
6	Unsteady	Plunging	Slight longitudinal surge is evident.
7	"	"	"
8	"	"	"
9	"	"	A very small transverse wave had developed.
10	"	"	A transverse wave was not constant. The amplitude of the wave varied rhythmically from a maximum to a minimum of zero.
12	"	"	Transverse wave was now more constant.
14	"	"	The transverse wave was still present, however, it was smaller in size.
15	Steady	Plunging	The transverse wave had been eliminated.
20	Unsteady	Plunging -T	There was very little c.c.w. circulating flow typical of plunging conditions. There was a longitudinal surge present in first few weirs for this flow arrangement. The nape was no longer self aerating and had collapsed.
25	Unsteady	Transitional	No more c.c.w. roller. The flow was typically plunging with a periodic longitudinal surge which induced a streaming or skimming flow. The flow appeared to be restricted in the first few weirs. This was where the head could be built up sufficiently enough to form the base of the streaming surge.

Stability Observations

Class: **WB20** (Full weir height, 'B' class weir spacing, 20% bed slope)

Discharge (l/s)	Steady or Unsteady	Type of Flow	Description / Additional Notes
35	Steady	Transitional	Surges have died down into a highly turbulent transitional flow. Some surges were still evident, however, they were not easily noticed.
45	Steady	Trans. -S	Starting to approach streaming flow. The unsteady flow was mainly due to water that was impinged against the d/s weirs.
65	Steady	Trans. -S	The flow in the centre of the flume more accurately resembles streaming flow, whereas the flow along the sides behaved more like a highly turbulent transitional flow.
85	"	"	The weir spacing did not lend to a smooth streaming flow as in a closely spaced arrangement (WD Class). The flow in some ways resembled a baffle flow.
105	"	"	The flow did not appear to be calming down. Similar to 85 l/s. Water levels were simply an approximation.
135	"	"	Starting to gain the parallel streaming flow characteristics.
165	Steady	Streaming	

Stability Observations

Class: **WB30** (Full weir height, 'B' class weir spacing, 30% bed slope)

Discharge (l/s)	Steady or Unsteady	Type of Flow	Description / Additional Notes
0.5	Steady	Plunging	Unbroken smooth surface. Surface tension causes the nape to collapse.
1	"	"	Threshold of fully aerated nap. The nape became aerated and then collapsed. This instability caused slight surges.
2	"	"	Nape was fully aerated.
3	"	"	Same as 2 l/s.
4	"	"	Same as 3 l/s, except for growth of surges in lower section of the flume.
5	"	"	Same as 4 l/s, except for longitudinal surges have become more noticeable. The period of return for the longitudinal surges were not constant but tend to build up and then dissipate.
6	"	"	The flow was steady in the upstream half of the flume. The longitudinal surges were only noticeable in the lower half of the flume.
8	Unsteady	Plunging	A transverse wave had evolved. It was significant only in the lower half of the flume.
10	"	"	The transverse wave was smaller than found in 8 l/s. The amplitude of transverse wave varied rhythmically from a maximum to a minimum of zero. The nape was aerated. Considerable volumes of air entrainment.
12	Steady	Plunging	The nape was aerated. Substantial air entrainment.
13	"	"	Same as 12 l/s. Classical plunging flow. No surges or waves.
14	"	"	Steady well behaved plunging flow. The c.c.w. roller was only in half of the pool. The nape was aerated.
15	Steady	Plunging	Negligible surges.

Stability Observations

Class: **WB30** (Full weir height, 'B' class weir spacing, 30% bed slope)

Discharge (l/s)	**Steady or Unsteady**	**Type of Flow**	**Description / Additional Notes**
20	Unsteady	Plunging -T	A longitudinal surge was present. Aerated nape remained always, even as surge passed over. The water level dropped to approximately one half the weir height (70 mm) after the surge passed, then regained a depth which produces a 10 mm head. The c.c.w. roller existed only after the surge passed and the pool started to fill.
25	Unsteady	Transitional	Longitudinal surges were smaller and less frequent. The nape was aerated but no c.c.w. roller existed. 100% c.w. roller. The flow was taking on baffle flow characteristics.
35	Unsteady	Trans. - Baffle	Longitudinal surges were evident. The nape had collapsed. Resembled baffle flow.
45	Unsteady	Trans. - B - S	
65	Unsteady	Trans. - S	The flow was still very turbulent This was due to the water which was impinged against the weirs and forced to take a upward trajectory. The flow over the weirs was not yet parallel to the bed.
85	Unsteady	Trans. - S	Still not the classical streaming flow and c.w. rotating pool, but close enough.
105	"	"	Same as 85 l/s.
135	Steady	Streaming	
165	"	"	

B.1.3 'C' Class Weir Spacing - 5, 10, 15, 20 & 30 % Slope

Stability Observations

Class: **WC05** (Full weir height, 'C' class weir spacing, 5% bed slope)

Discharge (l/s)	Steady or Unsteady	Type of Flow	Description / Additional Notes
1	Unsteady	Plunging	A transverse wave existed in d/s section of flume.
2	"	"	A transverse wave as before, however larger in size.
2.5	"	"	The amplitude of the transverse wave has decreased in size, almost steady flow.
3	Steady	Transitional	A transverse wave was not evident.
4	"	"	
5	"	"	
6	"	"	
8	"	"	
10	"	"	Steady u/s with some small amplitude transverse waves. Evidence of surges in lower end of flume. It appeared that streaming flow was initiating.
12	Unsteady	Streaming	Transverse waves and longitudinal surges developed in first 1/4 flume length; however, they were more pronounced in lower 1/3 l. Larger amplitude waves than previous.
14	"	"	Same as above. Unstable in lower 1/2. larger amplitude.
15	"	"	
16	"	"	Same as 14 l/s
20	Steady	Streaming	Transverse wave died out. Only a slight trace of existence.
25	"	"	Well developed streaming flow.
30	"	"	" [Note: as Q increases, the surface
35	"	"	" disturbances became smaller.]
45	"	"	"
55	"	"	Well developed steady streaming flow. Little air entrainment in the streaming flow.
65	"	"	"
85	"	"	" Little air entrainment.
105	"	"	Well developed streaming flow with higher concentrations of air entrainment.
135	"	"	Steady streaming flow. Flume arrangement was at its capacity .
165	"	"	Significant streaming flow.

Stability Observations

Class: **WC10** (Full weir height, 'C' class weir spacing, 10% bed slope)

Discharge (l/s)	Steady or Unsteady	Type of Flow	Description / Additional Notes
1	Unsteady	Plunging	The transverse wave left the d/s weirs exposed. The disturbance was chaotic at the tail of flume. 8th weir - small disturbances, 14th weir - disturbances increased, 20th weir - chaos reigned.
2	"	"	Upstream half of flume was almost steady. Region of rapid amplitude growth had moved d/s as in 1 l/s discharge case.
3	"	"	Amplitudes resonated and then dispersed.
4	Steady	Plunging	Steady, however, there were trace disturbances due to transverse waves in the tail end of the flume
5	"	"	Good steady plunging flow.
6	Steady	Transitional	
8	"	"	No longer counter clockwise rotation in cell.
8.5	Unsteady	Transitional	Transverse waves at tail end of flume were evident.
9	"	"	Transverse wave had developed.
10	"	"	Transverse and longitudinal waves had made the flow pattern unstable.
12	"	"	Chaos. Larger amplitude transverse waves exist.
14	"	"	Same as 12l/s. Amplitude increased.
16	"	"	Same as 14l/s. Amplitude is increased. Transverse waves start at 1/3 length of flume from the top.
18	"	"	Same as 16l/s. Longitudinal surges appeared with transverse waves. Only one wave form appears at a time. They appear to alternate.
20	Unsteady	Streaming	Longitudinal surges dominated. 33 surges per 60 seconds i.e..(33/60).
22	"	"	Almost steady streaming flow, except for longitudinal surges which now decreased in frequency. (10/60).
24	"	"	Same as 22 l/s. Less surges.

Stability Observations

Class: **WC10** (Full weir height, 'C' class weir spacing, 10% bed slope)

Discharge (l/s)	Steady or Unsteady	Type of Flow	Description / Additional Notes
26	Steady	Streaming	Very small longitudinal surges. Almost non existent.
28	"	"	Although considered steady streaming flow, the water surface was rather choppy. Rough water surface due to jet impingement on the weirs.
30	"	"	2 cm max. water surface deflections.
35	"	"	"
40	"	"	
45	"	"	
55	"	"	Low concentration of air entrainment. < 1%
65	"	"	
85	"	"	Little more air entrainment.
105	Steady	Streaming	Same air entrainment concentrations as for 85 l/s. Water surface was fairly uniform.
135	"	"	Flume arrangement introduced more air entrainment.
165	"	"	More air entrainment in vortex cells as well as in the streaming flow. Discernible separation line between c.w. rotating cells and streaming overflow. Surface was turbulent but uniform.

Stability Observations

Class: **WC15** (Full weir height, 'C' class weir spacing, 15% bed slope)

Discharge (l/s)	Steady or Unsteady	Type of Flow	Description / Additional Notes
1	Unsteady	Plunging	Downstream 1/2 of the flume was unsteady due to transverse waves but upstream 1/2 was steady
2	"	"	Almost steady. Slight transverse wave.
3	"	"	Reverted back to 1l/s condition
4	"	"	Transverse wave increased in amplitude in d/s 1/2
5	Steady	Plunging	
6	Steady	Transitional	Trace of longitudinal surge in tail end of flume.
7	"	"	Same as 6 l/s. Longitudinal surge was confined to tail end of flume. No disturbances in upper or central sections of the flume.
8	Unsteady	Transitional	Flow was more turbulent. Transverse waves and longitudinal surges merge.
10	"	"	Violent transverse waves.
12	Unsteady	Streaming	Transverse waves have produced a chaotic water surface.
14	"	"	Same as 12 l/s.
16	"	"	Same as 14 l/s. Transverse waves start in the top 1/4 of the flume
18	"	"	Longitudinal surges and transverse waves. Longitudinal surges stream clear over the weirs. Violent surface.
20	"	"	Longitudinal surges were more predominant than Transverse waves. Can start to discern a distinct streaming flow on top in the longitudinal surges.
22	"	"	Longitudinal surges.
25	"	"	Longitudinal surges were smaller than before.
28	Steady	Streaming	Globally steady with very small longitudinal surges.
30	"	"	
35	"	"	Distinct separation between cells and streaming flow.
40	"	"	Steady streaming flow.

Stability Observations

Class: **WC15** (Full weir height, 'C' class weir spacing, 15% bed slope)

Discharge (l/s)	Steady or Unsteady	Type of Flow	Description / Additional Notes
45	"	"	
55	"	"	Water surface fluctuations increase in d/s section of flume.
65	"	"	Water surface fluctuations decrease in d/s section of flume.
85	"	"	Same as 65 l/s
105	"	"	The air entrainment in vortex cells increased.
135	"	"	Increased air entrainment in streaming flow; however, increase was mostly noticed in the cells.
165	"	"	High air entrainment in both streaming and cell sections.

Stability Observations

Class: **WC20** (Full weir height, 'C' class weir spacing, 20% bed slope)

Discharge (l/s)	**Steady or Unsteady**	**Type of Flow**	**Description / Additional Notes**
1	Unsteady	Plunging	Slight surface disturbance.
1.5	"	"	Disturbance > 1 l/s.
2	"	"	Surface tension disturbances in the nape occur at the mid length of the flume. This disturbance causes the flow to spill over one weir into the following pool. This minor fluid displacement caused the water along the sides to rise then fall, thus, causing a peak or crest in the centre of the pool width. This induced crest exceeded the weir height and as a result was spilled over into the d/s pool.
2.5	"	"	This disturbance has diminished to less than 1 l/s. Isolated in the tail end of the flume.
3	Steady	Plunging	No wave action at all. Steady
3.5	Unsteady	Plunging	Initiation of longitudinal surge. Almost entirely steady.
4	"	"	Longitudinal surge has developed. Frequency of 8 in 60 seconds. (8/60)
5	Unsteady	Plunging-T	longitudinal surge. Frequency (13/60)
6	"	"	longitudinal surge. Frequency (17/60) Visible at 1/2 length of flume
7	"	"	Well developed longitudinal surge. Frequency (18/60)
8	"	"	Same as 7 l/s; however, frequency of surge has increased (26/60). Flow was very violent.
9	Unsteady	Transitional	The flow still exhibits plunging characteristics. Longitudinal surges and transverse waves were present. A streaming flow condition existed only when the longitudinal surge proceeds d/s.
10	"	"	The transverse wave appeared to develop from a isolated longitudinal surge in the head waters. As the longitudinal surge proceeded d/s to 1/4 the flume length, the transverse wave dominated and the wave amplitude increased. This flow was very peculiar for, the transitional wave crests which reach a maximum elevation at the sides, was only one distinct flow pattern. The centre line of the flume exhibited a steaming flow pattern. There appeared to be a flushing surge which built up enough head to induce a streaming flow condition.

Stability Observations

Class: **WC20** (Full weir height, 'C' class weir spacing, 20% bed slope)

Discharge (l/s)	Steady or Unsteady	Type of Flow	Description / Additional Notes
11	Unsteady	Transitional	Unsteady transverse wave.
15	Unsteady	Trans.- S	" More dynamic than 11 l/s
17.5	"	"	The longitudinal surge was initiated and the transverse wave was suppressed.
20	"	"	The longitudinal surge dominated. The transverse wave was very small. Highly dynamic wave surface. There appears to be streaming flow surges, which suggest the threshold of classical streaming flow.
25	"	"	Similar to 20 l/s. Frequency of return for longitudinal surge was 70 surge crests in 60 seconds (70/60).
30	"	"	Very turbulent surface. Longitudinal surges.
35	"	"	"
40	Steady	Streaming	Longitudinal surges were barely noticeable. Excellent separation between circulating cell and skimming flow.
45	"	"	Water surface seems to catapult droplets of water. i.e., percolating water surface.
55	"	"	Increased air entrainment.
65	"	"	Surface was still very turbulent.
85	"	"	Significant volumes of air entrainment and a turbulent water surface
105	"	"	"
135	"	"	" Considerable air entrainment due to inflow arrangement.
165	"	"	

Note:
Typically for the higher discharges, 65 l/s and on, it appeared that the air entrainment in the streaming flow was caused by the inflow arrangement and not totally due to the water-free surface mixing in the flume. Other arrangements which incorporate large inflow tanks will have different levels of air entrainment.

Stability Observations

Class: **WC30** (Full weir height, 'C' class weir spacing, 30% bed slope)

Discharge (l/s)	Steady or Unsteady	Type of Flow	Description / Additional Notes
1	Steady	Plunging	No visible waves. The nape was unstable. Surface tension effects have collapsed the nape.
2	"	"	Stable. Nape fully aerated.
3	"	"	Stable, with no visible waves.
3.5	"	"	Longitudinal surge was difficult to detect. Initiation was in d/s length of flume.
4	Unsteady	Plunging	Longitudinal surge was evident. Frequency was approx. equal to 10 in 60 sec. (10/60)
5	Unsteady	Plunging -T	Longitudinal surge was well developed. Frequency (13/60)
6	"	"	Longitudinal surge now stems from u/s 1/2 section. Large volume of air entrainment.
7	Unsteady	Transitional -S	Frequency of longitudinal surge has increased.. (28/60). Exhibited some transverse waves in the longitudinal surge section of flume.
8	"	"	Longitudinal surges seem to have an instantaneous period of return. i.e. converged. Fully aerated surface. Transverse waves have developed. Still some random separation between longitudinal surges.
9	"	"	Transverse waves were fully established. Longitudinal surges can not be detected.
10	"	"	Amplitude of transverse wave was greater than 9 l/s. Transverse wave propagated downstream from the u/s 1/4 of flume length.
11	"	"	Transverse wave was larger than for 10 l/s. Appears that the period was getting smaller.

Note that these transverse waves were not singular. A second mirrored wave created a superimposed wave crest in the centre of the flume. These Transverse wave crests which were serpentine in nature, were visually similar to waves in high velocity sheet flow However, these waves were distinctly different for they do not remain in one location relative to the weirs but move downstream within the surface flow.

Stability Observations

Class: **WC30** (Full weir height, 'C' class weir spacing, 30% bed slope)

Discharge (l/s)	**Steady or Unsteady**	**Type of Flow**	**Description / Additional Notes**
12	"	"	Again transverse waves were greater than prior discharge. Transverse wave dominates the flow; however, there may be a longitudinal surge meshed in.
14	"	"	Turbulent transverse wave. Chaos. It appeared that there were instances when the flow was forced up over one weir and into not the following pool but the next pool. The pools were rotating fully clockwise.
15	"	"	The water surface was not uniform across the width of the flume. Forming the basis of streaming flow.
20	"	"	Transverse waves were still evident, however, it did not appear to cause a large variance in the water surface. First real sign of the initiation of streaming flow.
21	"	"	Transverse wave was still evident.
22	"	"	Observe little signs of transverse wave.
25	Steady	Streaming	The transverse wave was difficult to detect, if at all. Small fluctuations in the water surface.
30	"	"	Possibility of some surges occurring.
35	"	"	Water surface was more or less uniform across the width. No noticeable wave forms.
40	"	"	Well developed streaming flow. High concentrations of air entrainment. Slight surface disturbances.
45	"	"	Surface disturbances were relatively the same.
55	"	"	High concentrations of air entrainment. Pools were rotating fully clockwise. Very small stagnation regions in the corners. The velocity in these cells were noticeably higher than any other slope for this weir spacing.
65	"	"	Well developed streaming flow.
85	"	"	Same as 65 l/s. A sharp line of separation existed between the rotating cell and the streaming surface flow.
105, 135 & 165	"	"	

B.1.4 'D' Class Weir Spacing - 5, 10, 15, 20 & 30 % Slope

Stability Observations

Class: **WD05** (Full weir height, 'D' class weir spacing, 5% bed slope)

Discharge (l/s)	Steady or Unsteady	Type of Flow	Description / Additional Notes
0.5	Unsteady	Transitional	There were transverse waves throughout the entire length of the flume.
1	"	"	Transverse waves remain throughout. Amplitude of transverse wave has increased. The flow was very violent.
2	"	"	The transverse waves were much smaller. The flow was almost steady in the upstream half of the flume.
3	Steady	Transitional	Flow was now steady.
4	"	"	There were no longitudinal surges or transverse waves evident throughout the flume.
5	Steady	Streaming	
6	"	"	The flow was steady in the upstream section of the flume. Some transverse wave disturbances were evident in the tail end of the flume. This was due to the 'C' class weir spacing in the tail end of the flume.
7	"	"	Steady streaming flow was well developed.
8	"	"	Steady streaming flow
10	"	"	
15	"	"	
20	"	"	
25	"	"	
35	"	"	
45	"	"	
65	"	"	
85	"	"	
105	"	"	
135	"	"	
165	Steady	Streaming	

Stability Observations

Class: **WD10** (Full weir height, 'D' class weir spacing, 10% bed slope)

Discharge (l/s)	**Steady or Unsteady**	**Type of Flow**	**Description / Additional Notes**
0.5	Unsteady	Transitional	Transverse waves were noticeable in the downstream 3/4 of the weir.
1	"	"	Transverse waves existed throughout. Amplitude of transverse wave has increased.
2	"	"	Same as 1 l/s.
3	"	"	Longitudinal surges and transverse waves were present. The longitudinal surges appeared to be more dominant.
3.5	"	"	Longitudinal surges and transverse waves.
4	"	"	There were no longitudinal surges but transverse waves existed throughout the flume.
5	Unsteady	Trans. - S	Transverse wave was still evident.
6	Steady	Trans. - S	
8	"	"	Approached the threshold of classical streaming flow.
10	Steady	Streaming	The flow can be confidently defined as steady streaming flow.
15	"	"	There were very small flushes or more specifically sheet surges.
20	"	"	Steady Streaming Flow.
25	"	"	
35	"	"	
45	"	"	
65	"	"	
85	"	"	
105	"	"	
135	"	"	
165	Steady	Streaming	

Stability Observations

Class: **WD15** (Full weir height, 'D' class weir spacing, 15% bed slope)

Discharge (l/s)	Steady or Unsteady	Type of Flow	Description / Additional Notes
0.5	Unsteady	Plunging	Steady plunging flow in upstream 3 /4 of the weirs. Transverse waves exist in the downstream section, or more specifically the last 12 weirs.
1	"	"	Transverse waves existed throughout.
2	"	"	Unsteady. Temporal. The transverse waves which exist in the entire flume grew in amplitude to a maximum point, then decrease in size and transform into a longitudinal surge. Essentially this action phases in and phases out. The longitudinal surge and the transverse wave disturbances did not exist together at once. Transitional discharge.
3	"	"	Longitudinal surges were only evident.
3.5	"	"	Same as 3 l/s.
3.8	"	"	Longitudinal surges acted as flushing sheets of water.
4	Steady	Trans. - S	There was an occasional surge, however, the flow can be considered steady. This flow depicts the threshold of streaming flow.
5	"	"	There were no longitudinal surges. Steady transitional streaming flow.
6	"	"	Same as 5 l/s
8	"	"	Same as 6 l/s
10	Steady	Streaming	The flow over the weirs can now be confidently defined as streaming flow.
15	"	"	
20	"	"	
25	"	"	
35	"	"	
45	"	"	
65	"	"	
85	"	"	
105	"	"	
135	"	"	
165	Steady	Streaming	

Stability Observations

Class: **WD20** (Full weir height, 'D' class weir spacing, 20% bed slope)

Discharge (l/s)	Steady or Unsteady	Type of Flow	Description / Additional Notes
0.5	Steady	Plunging	Steady plunging flow. Very steady.
0.6	Unsteady	Plunging	Steady throughout except for last 5 weirs where transverse waves appear.
1	Unsteady	Plunging	Of the 40 weirs in the flume, the first fourteen (1 to 14) the flow was steady plunging. The remainder (15 to 40) had a transverse wave present.
1.5	"	"	Transverse wave only in flume
1.8	"	"	Transverse wave convergence. Starting point of longitudinal waves
2	"	"	Longitudinal surge and transverse waves were both evident.
2.5	"	"	Longitudinal surge only.
4	Unsteady	Transitional	The longitudinal surge takes on the form of streaming flow. This was the initial stages of streaming flow.
5	Steady	Trans. -S	The flow was not fully developed as streaming flow. The flow was globally steady, however, an occasional longitudinal surge developed every minute. The flow did not exhibit the same flushing regime as WD30 did. This flow was not fully streaming, but it was a good approximation of the threshold of streaming flow.
6.	Steady	Streaming	Percolating water surface.
10	Unsteady	Streaming	There were traces of longitudinal surges. Generally in an overview, the flow could be considered steady.
15	Steady	Streaming	The longitudinal surges which were evident in 10l/s are far and few in between.
20	"	"	Well developed streaming flow.
25	"	"	
35	"	"	
45	"	"	
65	"	"	
85	"	"	
105	"	"	
135	"	"	
165	Steady	Streaming	

Stability Observations

Class: **WD30** (Full weir height, 'D' class weir spacing, 30% bed slope)

Discharge (l/s)	**Steady or Unsteady**	**Type of Flow**	**Description / Additional Notes**
0.5	Steady	Plunging	Nape was partially aerated. Surface tension effects were evident.
0.75	"	"	Steady except for tail end (last 2 weirs in the flume), where a slight transverse wave was noticeable. Overall steady.
0.9	Unsteady	Plunging	Transverse wave became predominant in d/s 1/2 of flume
1.0	"	"	The nape was fully aerated. The amplitudes of the transverse waves have increased in the d/s section of the flume. i.e. the lower 1/2. The transverse waves forced the flow to reach a maximum elevation at the sides and at the centre of the flume. When the wave formed this central peak, the flow was substantially higher than the mean pool height, and flow over the weir occurred. Because of this wave action, the water elevation in the centre of the flume did vary from approximately 50 mm below the crest of the weir, to 50 mm over the crest of the weir. This maximum and minimum did not occur simultaneously in every pool, however, it was offset to produce the elusion of a supercritical wave. Unlike supercritical waves however, the formation is not stationary, but steadily progresses downstream in a serpentine flow pattern.
1.5	"	"	Transverse wave
1.66	"	"	A longitudinal surge had developed with the transverse wave.
1.8	"	"	A longitudinal surge was dominant.
2	"	"	Longitudinal surge
2.5	"	"	A longitudinal surge was well developed.
3	"	"	"
4	"	"	Longitudinal surge has increased in frequency, almost to convergence. In other words, almost streaming flow condition.
5	Unsteady	Trans. - S	Same as 4.0 l/s. The longitudinal surge which flushes the system was well developed.
6	"	"	A longitudinal surge still exists. Streaming characteristics were evident.
8	"	"	Longitudinal surges. Basis of streaming flow.

Stability Observations

Class: **WD30** (Full weir height, 'D' class weir spacing, 30% bed slope)

Discharge (l/s)	Steady or Unsteady	Type of Flow	Description / Additional Notes
10	Unsteady	Streaming	Longitudinal waves that appeared to flush the system were still evident.
11.5	"	"	Surges which produce the flushing action were still produced. The flow appeared to be approaching a steady state.
14	Unsteady	Streaming	Surges were sill evident. The flow was streaming.
15	"	"	same as 14 l/s
20	"	"	Steaming. Almost steady.
25	"	"	Verge of steady streaming flow. Longitudinal surges could still be detected.
30	Steady	Streaming	Threshold of steady streaming flow.
35	"	"	Turbulent surface, however, steady streaming flow.
45	"	"	Same as 35 l/s
65	"	"	
85	"	"	
105	"	"	
135	"	"	
165	"	"	Steady streaming flow.

B.2 Half Weir Height

B.2.1 'A' Class Weir Spacing - 5, 10, 15, 20 & 30 % Slope

Stability Observations

Class: **1/2WA05** (Half weir height, 'A' class weir spacing, 5% bed slope)

Discharge (l/s)	Steady or Unsteady	Type of Flow	Description / Additional Notes
1	Steady	Plunging	Surface tension effects dominate. Non aerated nape.
1.5	"	"	"
2	"	"	Aerated nape. Steady weir flow.
2.5	"	"	"
3	"	"	"
4	"	"	"
5	"	"	Generally steady, however, a slight transverse wave was evident in the last two pools. (pools 6 & 7)
6	"	"	The nape was no longer aerated. Steady flow in first 4 pools, a slight longitudinal surge occurs in the following pools. This surge was not a large disturbance but can be described as an undular motion which propagated down through the downstream pools.
7	"	"	Same as for 6.0 l/s. Undular motion occurred in pools 5 through 7. Overall steady.
8	"	"	The undulating wave action described in previous recordings was now initiated in the third pool. This wave action was rather passive and possesses an amplitude of approximately 5 mm. In addition, three or four wave lengths may occur in one pool. Although this wave action did occur, this disturbance was quite small in comparison to the general flow pattern and steady plunging flow was a suitable classification.
9	"	"	Same as for 8.0 l/s.
10	"	"	The flow can be described as steady plunging and it was undoubtedly that case in the first three pools, however, the wave

Stability Observations

Class: **1/2WA05** (Half weir height, 'A' class weir spacing, 5% bed slope)

Discharge (l/s)	**Steady or Unsteady**	**Type of Flow**	**Description / Additional Notes**
			form which existed in the following pools was much more choppy. This violent water surface disturbance was highly noticeable in the seventh pool.
12	“	“	There was a slight reduction in the wave action noted in the previous discharges.
14	“	“	Only a slight surface disturbance existed.
15	“	“	
17.5	“	“	Almost no wave action.
20	“	“	
25	“	“	Steady plunging flow throughout the entire flume.
35	“	“	Steady plunging flow. Can recognize the onset of baffle like flow.
45	“	“	This flow pattern was still described as plunging for the point of surface bifurcation was upstream of the weir. Otherwise the visible flow streamlines, beneath the plunging flow water surface profile, resembled baffle flow.

Stability Observations

Class: **1/2WA10** (Half weir height, 'A' class weir spacing, 10% bed slope)

Discharge (l/s)	Steady or Unsteady	Type of Flow	Description / Additional Notes
0.5	Steady	*Plunging*	This plunging flow pattern has a section of supercritical bed flow. This section of free surface supercritical flow was not suitable for fish transport. In fact all of the discharges observed in this section exhibited supercritical flow. Surface tension effects did not allow for an aerated nape.
1	"	"	Same as 0.5 l/s.
1.5	"	"	Supercritical bed flow exists. The water surface had a non distinct broken wave pattern. This disturbance did temporarily cause aeration of the nape.
2	"	"	0.5 to 2.0 cm of supercritical bed flow exists.
2.5	"	"	Same as 2.0 l/s.
3	"	"	Supercritical bed flow exists. No visible longitudinal surges or transverse waves.
4	"	"	Supercritical bed flow now varies from 2 to 7 centimeters in length.
5	"	"	Same as 4.0 l/s.
6	"	"	Supercritical bed flow exists. No visible longitudinal surges or transverse waves.
7	"	"	Supercritical bed flow exists. The surface had a slight 'choppy' disturbance but was not structured as observed in a transverse wave.
8	"	"	Supercritical bed flow exists. A trace of a longitudinal surge was evident. This longitudinal surge was the result of the combined effects due to the supercritical flow and the fluctuating hydraulic jump.
9	"	"	10 cm of supercritical bed flow exists.
10	"	"	Same as 9.0 l/s.

Stability Observations

Class: **1/2WA10** (Half weir height, 'A' class weir spacing, 10% bed slope)

Discharge (l/s)	Steady or Unsteady	Type of Flow	Description / Additional Notes
12	"	"	Supercritical bed flow exists. No visible longitudinal surges or transverse waves.
14	"	"	Same as 12.0 l/s. Approximately 10 cm of supercritical bed flow existed.
15	"	"	Same as 14.0 l/s. Nape was in no longer fully aerated and continuous across the flume.
17.5	"	"	Nape no longer existed.
20	"	"	Section of supercritical flow.
25	"	"	Supercritical bed flow exists.
35	"	"	Supercritical bed flow exists.
45	"	"	This flow pattern was still described as plunging for the point of surface bifurcation was upstream of the weir. However, the onset of baffle flow was evident.

Stability Observations

Class: **1/2WA15** (Half weir height, 'A' class weir spacing, 15% bed slope)

Discharge (l/s)	**Steady or Unsteady**	**Type of Flow**	**Description / Additional Notes**
0.5	Steady	*Baffle*	This baffle flow pattern has a portion section of supercritical bed flow. The section of free surface supercritical flow was not suitable for fish transport. In fact, all of the discharges observed in this section exhibit supercritical flow. Surface tension effects did not allow for an aerated nape.
2.0	"	"	Supercritical bed flow. The water surface was rather 'choppy' and the deviations were in the order of 2 cm. The nape was aerated.
2.5	Unsteady	*Baffle*	The unsteady action between the supercritical flow and the hydraulic jump produced a minute longitudinal wave formation.
3.0	Steady	*Baffle*	Similarly to 2.5 l/s, the hydraulic jump and supercritical flow induced longitudinal waves. Overall or in a global picture, the flow can be described as steady with a slight variance due to this natural fluctuation. The supercritical bed flow was approximately 22 cm in length.
4.0	"	"	Same as 3.0 l/s. Supercritical bed flow was approximately 21 to 22 cm in length.
5.0	"	"	Same as previous.
6.0	"	"	No instabilities.
8.0	"	"	Nape was still self aerated. Supercritical range was approximately 22 cm.
10.0	"	"	Essentially the same as previous. The surface roller was very small. The point of surface bifurcation was close to the toe of the hydraulic jump. Onset of baffle flow with a superimposed hydraulic jump. There were some surge fluctuations attributed to the supercritical flow . These longitudinal surge fluctuations were very small and the flow could be considered steady.

Stability Observations

Class: **1/2WA15** (Half weir height, 'A' class weir spacing, 15% bed slope)

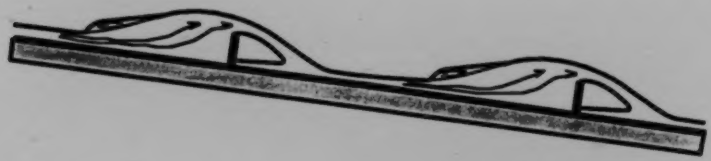

Discharge (l/s)	Steady or Unsteady	Type of Flow	Description / Additional Notes
12.5	“	“	Generally the same flow pattern as expressed in previous discharges. The supercritical jet was not totally diffused and as a result, it proceeded through the downstream pool in a continuous motion. The surface was still more or less horizontal and weir / baffle like flow occurred.
15.0	“	“	The flow was defiantly plunging; however, the flow characteristics were starting to resemble baffle flow rather than weir flow.
17.5	“	“	Surface roller was approximately 150 mm in length and 25 mm deep.
20.0	“	“	Nape was still aerated.
25.0	“	“	
35.0	“	“	Nape was still aerated. Large quantities of air entrained.
45.0	Steady	Baffle	Defiantly baffle flow. The nape collapsed.

Stability Observations

Class: **1/2WA20** (Half weir height, 'A' class weir spacing, 20% bed slope)

Discharge (l/s)	**Steady or Unsteady**	**Type of Flow**	**Description / Additional Notes**
1	Steady	Plunging	Non aerated nape. There was a slight longitudinal surge evident due to the instability of the hydraulic jump.
2	Unsteady	Plunging	Due to the instability of the nape, a slight transverse wave occurred. Subsequently the surface was quite broken and 'choppy'.
2.5	Unsteady	*Baffle*	Same as 2.0 l/s
3	Steady	*Baffle*	Still quite choppy but more stable.
4	"	"	Same as 3.0 l/s
5	"	"	The flow was steady, however, the water surface was not transversely uniform.
6	"	"	There was visual evidence that the streaming wall jet proceeded downstream, was partially diffused, and then was passed over the downstream weir.
8	"	"	The flow possessed more characteristics typical of baffle flow. The approach velocity from the jet entering the pool produced a fluctuation in the trajectory angle of the following downstream nape. This fluctuation causes the nape to increase and decrease in size and subsequently affected the downstream jet and pool.
10	"	"	
12.5	"	"	
15	"	"	The flow was highly three dimensional. Can discern side wall rollers as well as central flume streams.
17.5	"	"	
20	"	"	
25	"	"	Steady baffle flow. The nape for this flow and the previous discharge was fully aerated.

Stability Observations

Class: **1/2WA20** (Half weir height, 'A' class weir spacing, 20% bed slope)

Discharge (l/s)	Steady or Unsteady	Type of Flow	Description / Additional Notes
35	"	"	The nape was still self aerated. The hydraulic jump had been forced downstream to the lower 1/3 pool length. There was a slight longitudinal surge evident; however, it was not large enough to deem the flow as unsteady.
45	Steady	Baffle	The free surface supercritical flow had a maximum length of 100 mm. The nape remained aerated. The continuous streamlines in this flow were very pronounced and could be easily identified.

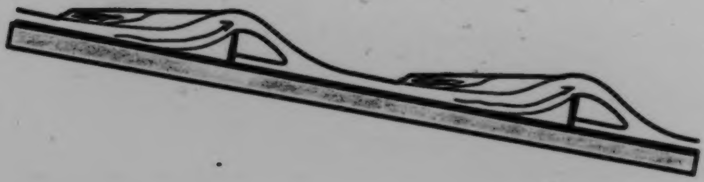

Stability Observations

Class: **1/2WA30** (Half weir height, 'A' class weir spacing, 30% bed slope)

Discharge (l/s)	Steady or Unsteady	Type of Flow	Description / Additional Notes
1	Unsteady	*Baffle*	The nape was unstable. This was the result of surface tension effects and the unsteady action of the hydraulic jump.
2	"	"	Same as 1.0 l/s.
2.5	"	"	Same as 2.0 l/s.
3.5	Steady	*Baffle*	The hydraulic jump continued to cause fluctuation; however, the nape was fully aerated and neither transverse waves or longitudinal surges were evident.
5	"	"	Same as 3.5 l/s.
7.5	"	"	The maximum water elevation was downstream of the following weir. Again the hydraulic jump caused fluctuation in the water surface, but these disturbances were not sufficiently large. 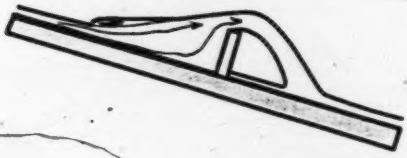
10	"	"	Considerable volumes of air entrainment. There was now evidence of vertical flow which resulted in boil like flow patterns.
15	"	"	The flow was much more turbulent, and as a result the water surface was broken and discontinuous. The large volumes of air entrainment had noticeably bulked up the flow volume. Two phase flow would adequately describe this situation.
20	"	"	With the increase in discharge, the location of the toe of the hydraulic jump has progressed downstream. This point was approximately located in the latter one quarter of the pool length.

Stability Observations

Class: **1/2WA30** (Half weir height, 'A' class weir spacing, 30% bed slope)

Discharge (l/s)	**Steady or Unsteady**	**Type of Flow**	**Description / Additional Notes**
25	Steady	*Baffle*	Note: The return flow which was formed by he impingement of the plunging jet on the bed, does not reach the downstream side of the upstream weir.

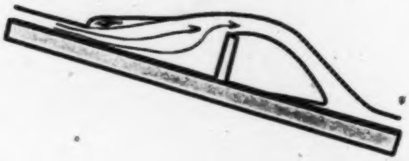

35	"	"	This flow undoubtedly could be classified as a baffle flow. The length of the streaming bed jet ranged from 5 mm to a maximum of 100 mm. This fluctuation did not suggest that the flow was unsteady, but rather a result of the fluctuating hydraulic jump.
45	"	"	The trajectory of the plunging jet was sufficiently large enough to cause the surface roller, found in the hydraulic jump, to be washed downstream. This wash out occurs periodically and the jump or roller quickly re-establishes.

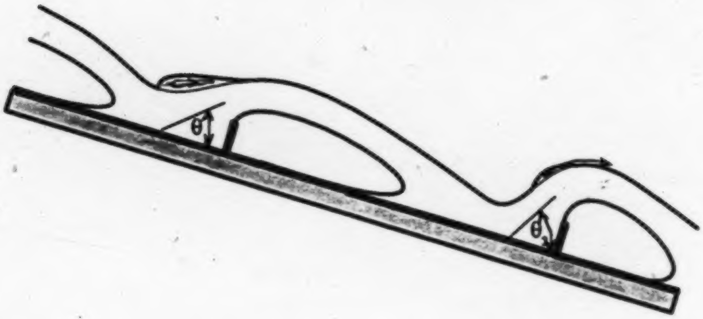

APPENDIX C

Pool and Weir Experiment Database

APPENDIX C: Pool and Weir Experimental Data

Dr. N. Rajaratnam
Mr. C. Katopodis
Mr. G. J. Sikora
T. Blench Hydraulics Laboratory
Department of Civil Engineering, Water Resources
University of Alberta

Flume Width = 560 mm

Weir Heights		
Type	Design (mm)	Actual (mm)
Full (1)	140	140.8
0.75	105	119.1
0.5	70	74.1

Weir Spacings (l)				
Type	Design (mm) / Actual (mm)			
	A	B	C	D
Full (1)	/ 685	/ 335	/ 166	/ 77
0.75	696 / 694	342 / 342	165 / 164	
0.5	696 / 703	342 / 348	165 / 169	-

Legend

P = Plunging Flow
Pt = Plunging Transitional Flow (slight deviation from plunging flow conditions)
T = Transitional Flow
tS = Transitional Streaming Flow (slight deviation from streaming flow conditions)
S = Streaming Flow
tB = Transitional Baffle Flow (flow is developing into baffle flow rather than streaming flow)
B = Baffle flow
B/S = Baffle Streaming Flow
P = Plunging Flow pattern which has a section of supercritical bed flow
B = Baffle Flow pattern which has a section of supercritical bed flow

h = Maximum head over weir (mm)
d = Depth of streaming flow (mm)
Italics indicate that the flow is not in a true plunging or streaming state
[96.05] indicates that the maximum head is downstream of the weir, i.e., baffle flow
** Signifies that there was more than one flow pattern present.
This was typically found in an unsteady flow

Experimental Arrangement	Weir Spacing (L) (mm)	Weir Height (p) (mm)	Slope (%)	Discharge (Qm) (l/s)	Stability d/dt	Type of Flow Pattern	Plunging Head (h) (mm)	Streaming Depth (d) (mm)
WA05-005	685	140.8	5	5	Steady	P	27.3	-
WA05-010	685	140.8	5	10	Steady	P	47.0	-
WA05-015	685	140.8	5	15	Steady	P	65.6	-
WA05-020	685	140.8	5	20	Steady	P	80.4	-
WA05-025	685	140.8	5	25	Steady	Pt	*100.0*	-
WA05-035	685	140.8	5	35	Unsteady	tB	-	-
WA05-045	685	140.8	5	45	Unsteady	tB	-	-
WA05-065	685	140.8	5	65	Steady	B	-	-
WA05-085	685	140.8	5	85	Steady	B	-	-
WA05-105	685	140.8	5	105	Steady	B	-	-
WA05-135	685	140.8	5	135	Steady	B	-	-
WA05-165	685	140.8	5	165	-	-	-	-
WA10-005	685	140.8	10	5	Steady	P	27.3	-
WA10-010	685	140.8	10	10	Steady	P	44.3	-
WA10-015	685	140.8	10	15	Steady	P	55.1	-

Experimental Arrangement	Weir Spacing (L) (mm)	Weir Height (p) (mm)	Slope (%)	Discharge (Qm) (l/s)	Stability d/dt	Type of Flow Pattern	Plunging Head (h) (mm)	Streaming Depth (d) (mm)
WA10-020	685	140.8	10	20	Unsteady	P	68.8	-
WA10-025	685	140.8	10	25	Unsteady	P	83.1	-
WA10-035	685	140.8	10	35	Steady	P	114.5	-
WA10-045	685	140.8	10	45	Steady	P	135.7	-
WA10-065	685	140.8	10	65	Steady	Pt	*168.8*	-
WA10-085	685	140.8	10	85	Steady	tB	-	-
WA10-105	685	140.8	10	105	Steady	tB	-	-
WA10-135	685	140.8	10	135	Steady	B/S	-	-
WA10-165	685	140.8	10	165	-	-	-	-
WA15-005	685	140.8	15	5	Steady	P	29.1	-
WA15-010	685	140.8	15	10	Steady	P	45.8	-
WA15-015	685	140.8	15	15	Unsteady	P	58.3	-
WA15-020	685	140.8	15	20	Steady	P	71.2	-
WA15-025	685	140.8	15	25	Steady	P	84.1	-
WA15-035	685	140.8	15	35	Steady	P	106.2	-
WA15-045	685	140.8	15	45	Steady	P	112.6	-
WA15-065	685	140.8	15	65	Steady	tB	-	-
WA15-085	685	140.8	15	85	Steady	B	-	-
WA15-105	685	140.8	15	105	Unsteady	B	-	-
WA15-135	685	140.8	15	135	Unsteady	B	-	-
WA15-165	685	140.8	15	165	-	-	-	-
WA20-005	685	140.8	20	5	Steady	P	28.1	-
WA20-010	685	140.8	20	10	Steady	P	45.4	-
WA20-015	685	140.8	20	15	Steady	P	67.2	-
WA20-020	685	140.8	20	20	Steady	P	73.6	-
WA20-025	685	140.8	20	25	Unsteady	P	82.4	-
WA20-035	685	140.8	20	35	Unsteady	P	107.3	-
WA20-045	685	140.8	20	45	Unsteady	P	130.1	-
WA20-065	685	140.8	20	65	Steady	tB	-	-
WA20-085	685	140.8	20	85	Steady	tB	-	-
WA20-105	685	140.8	20	105	Unsteady	tB	-	-
WA20-135	685	140.8	20	135	Unsteady	tB	-	-
WA20-165	685	140.8	20	165	-	-	-	-
WA30-005	685	140.8	30	5	Unsteady	P	27.1	-
WA30-010	685	140.8	30	10	Steady	P	42.9	-
WA30-015	685	140.8	30	15	Steady	P	73.9	-
WA30-020	685	140.8	30	20	Steady	P	75.6	-
WA30-025	685	140.8	30	25	Steady	P	90.5	-
WA30-035	685	140.8	30	35	Steady	P	114.1	-
WA30-045	685	140.8	30	45	Steady	P	139.2	-
WA30-065	685	140.8	30	65	Steady	tB	-	-
WA30-085	685	140.8	30	85	Steady	tB	-	-
WA30-105	685	140.8	30	105	Unsteady	tB	-	-
WA30-135	685	140.8	30	135	Unsteady	tB	-	-
WA30-165	685	140.8	30	165	-	-	-	-
WB05-005	335	140.8	5	5	Steady	Pt	*28.7*	-
WB05-010	335	140.8	5	10	Steady	T	-	-
WB05-015	335	140.8	5	15	Steady	T	-	-
WB05-020	335	140.8	5	20	Unsteady	T	-	-
WB05-025	335	140.8	5	25	Unsteady	tS	-	*62.6*
WB05-035	335	140.8	5	35	Unsteady	S	-	71.3
WB05-045	335	140.8	5	45	Unsteady	S	-	77.4
WB05-065	335	140.8	5	65	Unsteady	S	-	102.2
WB05-085	335	140.8	5	85	Unsteady	S	-	130.9
WB05-105	335	140.8	5	105	Unsteady	S	-	156.1
WB05-135	335	140.8	5	135	Steady	S	-	176.6
WB05-165	335	140.8	5	165	Steady	S	-	199.0

Experimental Arrangement	Weir Spacing (L) (mm)	Weir Height (p) (mm)	Slope (%)	Discharge (Qm) (l/s)	Stability d/dt	Type of Flow Pattern	Plunging Head (h) (mm)	Streaming Depth (d) (mm)
WB10-005	335	140.8	10	5	Steady	P	27.1	-
WB10-010	335	140.8	10	10	Steady	Pt	*49.2*	-
WB10-015	335	140.8	10	15	Unsteady	Pt	*54.7*	-
WB10-020	335	140.8	10	20	Unsteady	Pt	*59.4*	-
WB10-025	335	140.8	10	25	Unsteady	T	-	-
WB10-035	335	140.8	10	35	Unsteady	tS	-	*61.4*
WB10-045	335	140.8	10	45	Unsteady	tS	-	*67.0*
WB10-065	335	140.8	10	65	Unsteady	tS	-	*83.2*
WB10-085	335	140.8	10	85	Steady	S	-	108.8
WB10-105	335	140.8	10	105	Steady	S	-	120.4
WB10-135	335	140.8	10	135	Steady	S	-	145.7
WB10-165	335	140.8	10	165	Steady	S	-	151.7
WB15-005	335	140.8	15	5	Steady	P	31.0	-
WB15-010	335	140.8	15	10	Steady	P	45.4	-
WB15-015	335	140.8	15	15	Unsteady	P	64.1	-
WB15-020	335	140.8	15	20	Unsteady	P	59.1	-
WB15-025	335	140.8	15	25	Unsteady	Pt	*56.1*	-
WB15-035	335	140.8	15	35	Unsteady	tS	-	*61.4*
WB15-045	335	140.8	15	45	Steady	tS	-	*64.7*
WB15-065	335	140.8	15	65	Steady	tS	-	*85.0*
WB15-085	335	140.8	15	85	Steady	tS	-	*100.0*
WB15-105	335	140.8	15	105	Steady	S	-	116.8
WB15-135	335	140.8	15	135	Steady	S	-	129.5
WB15-165	335	140.8	15	165	Steady	S	-	149.1
WB20-005	335	140.8	20	5	Steady	P	31.6	-
WB20-010	335	140.8	20	10	Unsteady	P	48.1	-
WB20-015	335	140.8	20	15	Steady	P	61.2	-
WB20-020	335	140.8	20	20	Unsteady	Pt	*71.0*	-
WB20-025	335	140.8	20	25	Unsteady	T	-	-
WB20-035	335	140.8	20	35	Steady	T	-	-
WB20-045	335	140.8	20	45	Steady	tS	-	*61.0*
WB20-065	335	140.8	20	65	Steady	tS	-	*90.8*
WB20-085	335	140.8	20	85	Steady	tS	-	*102.0*
WB20-105	335	140.8	20	105	Steady	tS	-	*113.7*
WB20-135	335	140.8	20	135	Steady	tS	-	*134.4*
WB20-165	335	140.8	20	165	Steady	S	-	138.1
WB30-005	335	140.8	30	5	Steady	P	30.8	-
WB30-010	335	140.8	30	10	Unsteady	P	44.4	-
WB30-015	335	140.8	30	15	Steady	P	59.6	-
WB30-020	335	140.8	30	20	Unsteady	Pt	-	-
WB30-025	335	140.8	30	25	Unsteady	T	-	-
WB30-035	335	140.8	30	35	Unsteady	tB	-	-
WB30-045	335	140.8	30	45	Unsteady	tB/tS	-	**
WB30-065	335	140.8	30	65	Unsteady	tS	-	**
WB30-085	335	140.8	30	85	Unsteady	S	-	**
WB30-105	335	140.8	30	105	Unsteady	S	-	**
WB30-135	335	140.8	30	135	Steady	S	-	119.0
WB30-165	335	140.8	30	165	Steady	S	-	148.1
WC05-005	166	140.8	5	5	Steady	Pt	*21.0*	-
WC05-010	166	140.8	5	10	Steady	T	-	-
WC05-015	166	140.8	5	15	Unsteady	S	-	32.4
WC05-020	166	140.8	5	20	Steady	S	-	38.2
WC05-025	166	140.8	5	25	Steady	S	-	42.4
WC05-035	166	140.8	5	35	Steady	S	-	53.5
WC05-045	166	140.8	5	45	Steady	S	-	66.8
WC05-065	166	140.8	5	65	Steady	S	-	83.1
WC05-085	166	140.8	5	85	Steady	S	-	99.2

Experimental Arrangement	Weir Spacing (L) (mm)	Weir Height (p) (mm)	Slope (%)	Discharge (Qm) (l/s)	Stability d/dt	Type of Flow Pattern	Plunging Head (h) (mm)	Streaming Depth (d) (mm)
WC05-105	166	140.8	5	105	Steady	S	-	114.1
WC05-135	166	140.8	5	135	Steady	S	-	132.9
WC05-165	166	140.8	5	165	Steady	S	-	168.0
WC10-005	166	140.8	10	5	Steady	P	24.8	-
WC10-010	166	140.8	10	10	Unsteady	T	-	-
WC10-015	166	140.8	10	15	Unsteady	T	-	-
WC10-020	166	140.8	10	20	Unsteady	S	-	38.0
WC10-025	166	140.8	10	25	Unsteady	S	-	41.1
WC10-035	166	140.8	10	35	Steady	S	-	49.6
WC10-045	166	140.8	10	45	Steady	S	-	54.4
WC10-065	166	140.8	10	65	Steady	S	-	69.9
WC10-085	166	140.8	10	85	Steady	S	-	82.5
WC10-105	166	140.8	10	105	Steady	S	-	93.2
WC10-135	166	140.8	10	135	Steady	S	-	110.7
WC10-165	166	140.8	10	165	Steady	S	-	129.6
WC15-005	166	140.8	15	5	Steady	P	24.3	-
WC15-010	166	140.8	15	10	Unsteady	tS	-	*27.4*
WC15-015	166	140.8	15	15	Unsteady	S	-	24.5
WC15-020	166	140.8	15	20	Unsteady	S	-	32.5
WC15-025	166	140.8	15	25	Unsteady	S	-	39.9
WC15-035	166	140.8	15	35	Steady	S	-	41.4
WC15-045	166	140.8	15	45	Steady	S	-	48.8
WC15-065	166	140.8	15	65	Steady	S	-	58.8
WC15-085	166	140.8	15	85	Steady	S	-	65.7
WC15-105	166	140.8	15	105	Steady	S	-	81.5
WC15-135	166	140.8	15	135	Steady	S	-	94.0
WC15-165	166	140.8	15	165	Steady	S	-	112.6
WC20-005	166	140.8	20	5	Unsteady	Pt	22.9	-
WC20-010	166	140.8	20	10	Unsteady	T	-	-
WC20-015	166	140.8	20	15	Unsteady	tS	-	*24.0*
WC20-020	166	140.8	20	20	Unsteady	tS	-	*28.6*
WC20-025	166	140.8	20	25	Unsteady	tS	-	*32.2*
WC20-035	166	140.8	20	35	Unsteady	tS	-	*41.0*
WC20-045	166	140.8	20	45	Steady	S	-	45.3
WC20-065	166	140.8	20	65	Steady	S	-	56.5
WC20-085	166	140.8	20	85	Steady	S	-	68.7
WC20-105	166	140.8	20	105	Steady	S	-	73.9
WC20-135	166	140.8	20	135	Steady	S	-	87.6
WC20-165	166	140.8	20	165	Steady	S	-	98.6
WC30-005	166	140.8	30	5	Unsteady	Pt	*24.3*	-
WC30-010	166	140.8	30	10	Unsteady	tS	-	*20.4*
WC30-015	166	140.8	30	15	Unsteady	tS	-	*23.0*
WC30-020	166	140.8	30	20	Unsteady	tS	-	*23.7*
WC30-025	166	140.8	30	25	Steady	S	-	28.9
WC30-035	166	140.8	30	35	Steady	S	-	38.2
WC30-045	166	140.8	30	45	Steady	S	-	43.7
WC30-065	166	140.8	30	65	Steady	S	-	55.9
WC30-085	166	140.8	30	85	Steady	S	-	59.6
WC30-105	166	140.8	30	105	Steady	S	-	68.7
WC30-135	166	140.8	30	135	Steady	S	-	76.6
WC30-165	166	140.8	30	165	Steady	S	-	87.0
WD05-005	77	140.8	5	5	Steady	S	-	17.0
WD05-010	77	140.8	5	10	Steady	S	-	25.3
WD05-015	77	140.8	5	15	Steady	S	-	34.1
WD05-020	77	140.8	5	20	Steady	S	-	38.4
WD05-025	77	140.8	5	25	Steady	S	-	43.6
WD05-035	77	140.8	5	35	Steady	S	-	53.0

Experimental Arrangement	Weir Spacing (L) (mm)	Weir Height (p) (mm)	Slope (%)	Discharge (Qm) (l/s)	Stability d/dt	Type of Flow Pattern	Plunging Head (h) (mm)	Streaming Depth (d) (mm)
WD05-045	77	140.8	5	45	Steady	S	-	61.9
WD05-065	77	140.8	5	65	Steady	S	-	88.4
WD05-085	77	140.8	5	85	Steady	S	-	98.8
WD05-105	77	140.8	5	105	Steady	S	-	116.4
WD05-135	77	140.8	5	135	Steady	S	-	137.2
WD05-165	77	140.8	5	165	Steady	S	-	155.1
WD10-005	77	140.8	10	5	Unsteady	tS	-	*13.4*
WD10-010	77	140.8	10	10	Steady	S	-	21.0
WD10-015	77	140.8	10	15	Steady	S	-	25.3
WD10-020	77	140.8	10	20	Steady	S	-	31.1
WD10-025	77	140.8	10	25	Steady	S	-	34.4
WD10-035	77	140.8	10	35	Steady	S	-	45.8
WD10-045	77	140.8	10	45	Steady	S	-	54.0
WD10-065	77	140.8	10	65	Steady	S	-	67.1
WD10-085	77	140.8	10	85	Steady	S	-	80.5
WD10-105	77	140.8	10	105	Steady	S	-	92.4
WD10-135	77	140.8	10	135	Steady	S	-	107.6
WD10-165	77	140.8	10	165	Steady	S	-	126.5
WD15-005	77	140.8	15	5	Steady	tS	-	*11.7*
WD15-010	77	140.8	15	10	Steady	S	-	16.5
WD15-015	77	140.8	15	15	Steady	S	-	24.4
WD15-020	77	140.8	15	20	Steady	S	-	28.4
WD15-025	77	140.8	15	25	Steady	S	-	32.3
WD15-035	77	140.8	15	35	Steady	S	-	39.6
WD15-045	77	140.8	15	45	Steady	S	-	50.0
WD15-065	77	140.8	15	65	Steady	S	-	61.3
WD15-085	77	140.8	15	85	Steady	S	-	71.9
WD15-105	77	140.8	15	105	Steady	S	-	84.4
WD15-135	77	140.8	15	135	Steady	S	-	96.3
WD15-165	77	140.8	15	165	Steady	S	-	111.3
WD20-005	77	140.8	20	5	Steady	tS	-	*11.3*
WD20-010	77	140.8	20	10	Unsteady	S	-	17.7
WD20-015	77	140.8	20	15	Steady	S	-	23.5
WD20-020	77	140.8	20	20	Steady	S	-	27.7
WD20-025	77	140.8	20	25	Steady	S	-	33.2
WD20-035	77	140.8	20	35	Steady	S	-	40.5
WD20-045	77	140.8	20	45	Steady	S	-	47.2
WD20-065	77	140.8	20	65	Steady	S	-	62.5
WD20-085	77	140.8	20	85	Steady	S	-	72.5
WD20-105	77	140.8	20	105	Steady	S	-	77.7
WD20-135	77	140.8	20	135	Steady	S	-	94.5
WD20-165	77	140.8	20	165	Steady	S	-	104.9
WD30-005	77	140.8	30	5	Unsteady	tS	-	*12.4*
WD30-010	77	140.8	30	10	Unsteady	S	-	18.3
WD30-015	77	140.8	30	15	Unsteady	S	-	20.7
WD30-020	77	140.8	30	20	Unsteady	S	-	23.8
WD30-025	77	140.8	30	25	Unsteady	S	-	26.2
WD30-035	77	140.8	30	35	Steady	S	-	33.5
WD30-045	77	140.8	30	45	Steady	S	-	43.0
WD30-065	77	140.8	30	65	Steady	S	-	49.7
WD30-085	77	140.8	30	85	Steady	S	-	64.0
WD30-105	77	140.8	30	105	Steady	S	-	72.5
WD30-135	77	140.8	30	135	Steady	S	-	90.2
WD30-165	77	140.8	30	165	Steady	S	-	92.4

Experimental Arrangement	Weir Spacing (L) (mm)	Weir Height (p) (mm)	Slope (%)	Discharge (Qm) (l/s)	Stability d/dt	Type of Flow Pattern	Plunging Head (h) (mm)	Streaming Depth (d) (mm)
1/2 WEIR HEIGHT								
1/2WA05-002.5	703	74.1	5	2.5	Steady	P	16.3	-
1/2WA05-005	703	74.1	5	5	Steady	P	24.4	-
1/2WA05-010	703	74.1	5	10	Steady	P	37.4	-
1/2WA05-015	703	74.1	5	15	Steady	P	54.8	-
1/2WA05-020	703	74.1	5	20	Steady	P	64.8	-
1/2WA05-025	703	74.1	5	25	Steady	P	78.8	-
1/2WA05-035	703	74.1	5	35	Steady	P	98.6	-
1/2WA05-045	703	74.1	5	45	Steady	P	115.6	-
1/2WA10-002.5	703	74.1	10	2.5	Steady	*P*	*15.7*	-
1/2WA10-005	703	74.1	10	5	Steady	*P*	*23.3*	-
1/2WA10-010	703	74.1	10	10	Steady	*P*	*35.0*	-
1/2WA10-015	703	74.1	10	15	Steady	*P*	*47.6*	-
1/2WA10-020	703	74.1	10	20	Steady	*P*	*59.7*	-
1/2WA10-025	703	74.1	10	25	Steady	*P*	*70.3*	-
1/2WA10-035	703	74.1	10	35	Steady	*P*	*88.5*	-
1/2WA10-045	703	74.1	10	45	Steady	*P*	*106.9*	-
1/2WA15-002.5	703	74.1	15	2.5	Unsteady	*B*	*16.4*	-
1/2WA15-005	703	74.1	15	5	Steady	*B*	*23.0*	-
1/2WA15-010	703	74.1	15	10	Steady	*B*	*38.7*	-
1/2WA15-015	703	74.1	15	15	Steady	*B*	*52.8*	-
1/2WA15-020	703	74.1	15	20	Steady	*B*	*62.8*	-
1/2WA15-025	703	74.1	15	25	Steady	*B*	*70.3*	-
1/2WA15-035	703	74.1	15	35	Steady	*B*	*86.9*	-
1/2WA15-045	703	74.1	15	45	Steady	*B*	*[96.05]*	-
1/2WA20-002.5	703	74.1	20	2.5	Unsteady	*B*	*16.1*	-
1/2WA20-005	703	74.1	20	5	Steady	*B*	*22.1*	-
1/2WA20-010	703	74.1	20	10	Steady	*B*	*35.6*	-
1/2WA20-015	703	74.1	20	15	Steady	*B*	*55.0*	-
1/2WA20-020	703	74.1	20	20	Steady	*B*	*68.3*	-
1/2WA20-025	703	74.1	20	25	Steady	*B*	*[74.00]*	-
1/2WA20-035	703	74.1	20	35	Steady	*B*	*[93.01]*	-
1/2WA20-045	703	74.1	20	45	Steady	*B*	*111.8*	-
1/2WA30-002.5	703	74.1	30	2.5	Unsteady	*B*	*[27.12]*	-
1/2WA30-005	703	74.1	30	5	Steady	*B*	25.2	-
1/2WA30-010	703	74.1	30	10	Steady	*B*	*[43.75]*	-
1/2WA30-015	703	74.1	30	15	Steady	*B*	*[56.01]*	-
1/2WA30-020	703	74.1	30	20	Steady	*B*	*[73.82]*	-
1/2WA30-025	703	74.1	30	25	Steady	*B*	*[80.65]*	-
1/2WA30-035	703	74.1	30	35	Steady	*B*	*[99.63]*	-
1/2WA30-045	703	74.1	30	45	Steady	*B*	*[120.06]*	-
1/2WB05-002.5	348	74.1	5	2.5	Steady	P	17.6	-
1/2WB05-005	348	74.1	5	5	Steady	P	27.4	-
1/2WB05-010	348	74.1	5	10	Unsteady	Pt	-	-
1/2WB05-015	348	74.1	5	15	Unsteady	Pt	-	-
1/2WB05-020	348	74.1	5	20	Unsteady	tS	-	-
1/2WB05-025	348	74.1	5	25	Steady	tS	-	*62.0*
1/2WB05-035	348	74.1	5	35	Steady	tS	-	*76.1*
1/2WB05-045	348	74.1	5	45	Unsteady	tS	-	-
1/2WB10-002.5	348	74.1	10	2.5	Steady	P	16.6	-
1/2WB10-005	348	74.1	10	5	Steady	P	23.0	-
1/2WB10-010	348	74.1	10	10	Steady	P	44.6	-

Experimental Arrangement	Weir Spacing (L) (mm)	Weir Height (p) (mm)	Slope (%)	Discharge (Qm) (l/s)	Stability d/dt	Type of Flow Pattern	Plunging Head (h) (mm)	Streaming Depth (d) (mm)
1/2WB10-015	348	74.1	10	15	Steady	P	62.4	-
1/2WB10-020	348	74.1	10	20	Steady	Pt	*74.2*	-
1/2WB10-025	348	74.1	10	25	Unsteady	tB	-	-
1/2WB10-035	348	74.1	10	35	Unsteady	Bt	-	-
1/2WB10-045	348	74.1	10	45	Unsteady	tS	-	-
1/2WB15-002.5	348	74.1	15	2.5	Steady	P	15.9	-
1/2WB15-005	348	74.1	15	5	Steady	P	22.9	-
1/2WB15-010	348	74.1	15	10	Steady	P	40.9	-
1/2WB15-015	348	74.1	15	15	Steady	P	52.1	-
1/2WB15-020	348	74.1	15	20	Steady	Pt	*67.7*	-
1/2WB15-025	348	74.1	15	25	Steady	tB	*78.2*	-
[illegible]/2WB15-035	348	74.1	15	35	Unsteady	tS	-	-
1/2WB15-045	348	74.1	15	45	Unsteady	tS	-	-
1/2WB20-002.5	348	74.1	20	2.5	Steady	P	16.7	-
1/2WB20-005	348	74.1	20	5	Steady	P	25.4	-
1/2WB20-010	348	74.1	20	10	Steady	P	41.5	-
1/2WB20-015	348	74.1	20	15	Steady	P	53.7	-
1/2WB20-020	348	74.1	20	20	Steady	P	61.5	-
1/2WB20-025	348	74.1	20	25	Steady	Pt	*68.4*	-
1/2WB20-035	348	74.1	20	35	Unsteady	tB	*85.4*	-
1/2WB20-045	348	74.1	20	45	Unsteady	tS	-	-
1/2WB30-002.5	348	74.1	30	2.5	Unsteady	*P*	*19.1*	-
1/2WB30-005	348	74.1	30	5	Steady	*P*	*27.7*	-
1/2WB30-010	348	74.1	30	10	Steady	P	42.0	-
1/2WB30-015	348	74.1	30	15	Steady	tB	*61.8*	-
1/2WB30-020	348	74.1	30	20	Steady	tB	*74.6*	-
1/2WB30-025	348	74.1	30	25	Steady	tB	*77.5*	-
1/2WB30-035	348	74.1	30	35	Steady	tB	-	-
1/2WB30-045	348	74.1	30	45	Unsteady	tS	-	-
1/2WC05-002.5	169	74.1	5	2.5	Steady	T	-	-
1/2WC05-005	169	74.1	5	5	Steady	tS	-	*15.3*
1/2WC05-010	169	74.1	5	10	Steady	tS	-	*28.2*
1/2WC05-015	169	74.1	5	15	Steady	S	-	35.7
1/2WC05-020	169	74.1	5	20	Steady	S	-	40.8
1/2WC05-025	169	74.1	5	25	Steady	S	-	46.9
1/2WC05-035	169	74.1	5	35	Steady	S	-	62.4
1/2WC05-045	169	74.1	5	45	Steady	S	-	66.9
1/2WC10-002.5	169	74.1	10	2.5	Steady	P	18.9	-
1/2WC10-005	169	74.1	10	5	Steady	P	24.7	-
1/2WC10-010	169	74.1	10	10	Unsteady	tS	-	*19.4*
1/2WC10-015	169	74.1	10	15	Steady	S	-	29.1
1/2WC10-020	169	74.1	10	20	Steady	S	-	34.1
1/2WC10-025	169	74.1	10	25	Steady	S	-	42.5
1/2WC10-035	169	74.1	10	35	Steady	S	-	51.2
1/2WC10-045	169	74.1	10	45	Steady	S	-	57.6
1/2WC15-002.5	169	74.1	15	2.5	Steady	P	19.2	-
1/2WC15-005	169	74.1	15	5	Steady	P	28.0	-
1/2WC15-010	169	74.1	15	10	Unsteady	Pt	-	-
1/2WC15-015	169	74.1	15	15	Steady	tS	-	*29.9*
1/2WC15-020	169	74.1	15	20	Steady	S	-	34.4
1/2WC15-025	169	74.1	15	25	Steady	S	-	37.5
1/2WC15-035	169	74.1	15	35	Steady	S	-	45.1
1/2WC15-045	169	74.1	15	45	Steady	S	-	52.7
1/2WC20-002.5	169	74.1	20	2.5	Steady	P	19.5	-

Experimental Arrangement	Weir Spacing (L) (mm)	Weir Height (p) (mm)	Slope (%)	Discharge (Qm) (l/s)	Stability d/dt	Type of Flow Pattern	Plunging Head (h) (mm)	Streaming Depth (d) (mm)
1/2WC20-005	169	74.1	20	5	Steady	P	31.5	-
1/2WC20-010	169	74.1	20	10	Unsteady	T	-	-
1/2WC20-015	169	74.1	20	15	Steady	tS	-	*23.8*
1/2WC20-020	169	74.1	20	20	Steady	S	-	30.8
1/2WC20-025	169	74.1	20	25	Steady	S	-	43.6
1/2WC20-035	169	74.1	20	35	Steady	S	-	50.6
1/2WC20-045	169	74.1	20	45	Steady	S	-	57.3
1/2WC30-002.5	169	74.1	30	2.5	Steady	P	20.8	-
1/2WC30-005	169	74.1	30	5	Steady	P	32.2	-
1/2WC30-010	169	74.1	30	10	Unsteady	P	-	-
1/2WC30-015	169	74.1	30	15	Steady	T	-	
1/2WC30-020	169	74.1	30	20	Steady	tS	-	*34.8*
1/2WC30-025	169	74.1	30	25	Steady	tS	-	*42.1*
1/2WC30-035	169	74.1	30	35	Steady	S	-	48.2
1/2WC30-045	169	74.1	30	45	Steady	S	-	55.8
3/4 WEIR HEIGHT								
3/4WA05-010	694	119.1	5	10	Steady	P	31.8	-
3/4WA05-015	694	119.1	5	15	Steady	P	50.0	-
3/4WA05-020	694	119.1	5	20	Steady	P	63.8	-
3/4WA05-025	694	119.1	5	25	Steady	P	78.7	-
3/4WA05-035	694	119.1	5	30	Steady	P	102.1	-
3/4WA10-010	694	119.1	10	10	Steady	P	31.1	-
3/4WA10-015	694	119.1	10	15	Steady	P	39.9	-
3/4WA10-12	694	119.1	10	20	Steady	P	53.6	-
3/4WA10-13	694	119.1	10	25	Steady	P	66.7	-
3/4WA10-14	694	119.1	10	30	Steady	P	86.0	-
3/4WA15-010	694	119.1	15	10	Steady	P	30.5	-
3/4WA15-015	694	119.1	15	15	Steady	P	43.2	-
3/4WA15-020	694	119.1	15	20	Steady	P	53.9	-
3/4WA15-025	694	119.1	15	25	Steady	P	65.4	-
3/4WA15-035	694	119.1	15	30	Steady	P	82.0	-
3/4WA20-010	694	119.1	20	10	Steady	•P•	*31.2*	-
3/4WA20-015	694	119.1	20	15	Steady	•P•	*40.8*	-
3/4WA20-020	694	119.1	20	20	Steady	•P•	*54.5*	-
3/4WA20-025	694	119.1	20	25	Steady	•P•	*66.4*	-
3/4WA20-035	694	119.1	20	30	Steady	•P•	*86.5*	-
3/4WA30-010	694	119.1	30	10	Steady	•B•	*28.3*	-
3/4WA30-015	694	119.1	30	15	Steady	•B•	*42.8*	-
3/4WA30-020	694	119.1	30	20	Steady	•B•	*56.1*	-
3/4WA30-025	694	119.1	30	25	Steady	•B•	*69.2*	-
3/4WA30-035	694	119.1	30	30	Steady	•B•	*92.4*	-
3/4WB05-010	342	119.1	5	10	Steady	tS	-	30.0
3/4WB05-015	342	119.1	5	15	Steady	tS	-	35.0
3/4WB05-020	342	119.1	5	20	Steady	tS	-	46.0
3/4WB05-025	342	119.1	5	25	Steady	tS	-	64.0
3/4WB05-035	342	119.1	5	30	Steady	S	-	54.3
3/4WB10-010	342	119.1	10	10	Steady	P	42.1	-
3/4WB10-015	342	119.1	10	15	Unsteady	P	-	-
3/4WB10-020	342	119.1	10	20	Unsteady	Pt	-	-

Experimental Arrangement	Weir Spacing (L) (mm)	Weir Height (p) (mm)	Slope (%)	Discharge (Qm) (l/s)	Stability d/dt	Type of Flow Pattern	Plunging Head (h) (mm)	Streaming Depth (d) (mm)
3/4WB10-025	342	119.1	10	25	Unsteady	Pt	-	-
3/4WB10-035	342	119.1	10	30	Steady	tS	-	-
3/4WB15-010	342	119.1	15	10	Steady	P	34.0	-
3/4WB15-015	342	119.1	15	15	Steady	P	50.6	-
3/4WB15-020	342	119.1	15	20	Steady	P	66.8	-
3/4WB15-025	342	119.1	15	25	Unsteady	Pt	-	-
3/4WB15-035	342	119.1	15	30	Unsteady	tS	-	-
3/4WB20-010	342	119.1	20	10	Steady	P	35.5	-
3/4WB20-015	342	119.1	20	15	Steady	P	50.4	-
3/4WB20-020	342	119.1	20	20	Steady	P	62.1	-
3/4WB20-025	342	119.1	20	25	Unsteady	Pt	-	-
3/4WB20-035	342	119.1	20	30	Steady	tS	-	-
3/4WB30-010	342	119.1	30	10	Steady	P	36.7	-
3/4WB30-015	342	119.1	30	15	Steady	P	51.1	-
3/4WB30-020	342	119.1	30	20	Steady	P	62.0	-
3/4WB30-025	342	119.1	30	25	Unsteady	Pt	-	-
3/4WB30-035	342	119.1	30	30	Unsteady	tS	-	-
3/4WC05-010	164	119.1	5	10	Steady	tS	-	*16.6*
3/4WC05-015	164	119.1	5	15	Steady	S	-	23.3
3/4WC05-020	164	119.1	5	20	Steady	S	-	31.6
3/4WC05-025	164	119.1	5	25	Steady	S	-	45.9
3/4WC05-035	164	119.1	5	30	Steady	S	-	56.2
3/4WC10-010	164	119.1	10	10	Unsteady	tS	-	*15.1*
3/4WC10-015	164	119.1	10	15	Steady	tS	-	*23.6*
3/4WC10-020	164	119.1	10	20	Unsteady	tS	-	-
3/4WC10-025	164	119.1	10	25	Unsteady	tS	-	*39.5*
3/4WC10-035	164	119.1	10	30	Steady	S	-	42.5
3/4WC15-010	164	119.1	15	10	Unsteady	tS	-	*16.6*
3/4WC15-015	164	119.1	15	15	Unsteady	tS	-	*31.2*
3/4WC15-020	164	119.1	15	20	Unsteady	tS	-	-
3/4WC15-025	164	119.1	15	25	Unsteady	tS	-	-
3/4WC15-035	164	119.1	15	30	Steady	tS	-	*44.0*
3/4WC20-010	164	119.1	20	10	Unsteady	T	-	-
3/4WC20-015	164	119.1	20	15	Unsteady	tS	-	-
3/4WC20-020	164	119.1	20	20	Unsteady	tS	-	-
3/4WC20-025	164	119.1	20	25	Unsteady	tS	-	-
3/4WC20-035	164	119.1	20	30	Steady	S	-	44.0
3/4WC30-010	164	119.1	30	10	Steady	tS	-	-
3/4WC30-015	164	119.1	30	15	Steady	tS	-	-
3/4WC30-020	164	119.1	30	20	Steady	S	-	-
3/4WC30-025	164	119.1	30	25	Steady	S	-	30.0
3/4WC30-035	164	119.1	30	30	Steady	S	-	40.0